(12) INTERNATIONAL APPLICATION PUBLISHED UNDER THE PATENT COOPERATION TREATY (PCT)

(19) World Intellectual Property Organization
International Bureau

(43) International Publication Date
30 September 2021 (30.09.2021)

WIPO | PCT

(10) International Publication Number
WO 2021/195446 A2

(51) International Patent Classification:
C12N 15/11 (2006.01)

(21) International Application Number:
PCT/US2021/024254

(22) International Filing Date:
25 March 2021 (25.03.2021)

(25) Filing Language: English

(26) Publication Language: English

(30) Priority Data:

62/994,797	25 March 2020 (25.03.2020)	US
63/063,174	07 August 2020 (07.08.2020)	US
63/133,749	04 January 2021 (04.01.2021)	US

(71) Applicants: **PRESIDENT AND FELLOWS OF HARVARD COLLEGE** [US/US]; 17 Quincy St, Cambridge, MA 02138 (US). **UNIVERSITY OF MASSACHUSETTS** [US/US]; One Beacon Street, 31st Floor, Boston, MA (US).

(72) Inventors: **EGGAN, Kevin, C.**; 181 Essex Street, Boston, MA 02111 (US). **KLIM, Joseph, Robert**; 193 Webster Street, Apt. 1, Boston, MA 02128 (US). **BROWN, Robert, H., Jr.**; 16 Oakland Av, Needham, MA 02492 (US). **WATTS, Jonathan, K.**; 5 Brook Hill Dr, Worcester, MA 01609 (US).

(74) Agent: **WARREN, Lisa, M.**; Morse, Barnes-Brown & Pendleton, P.C., CityPoint, 480 Totten Pond Road, 4th Floor, Waltham, MA 02451 (US).

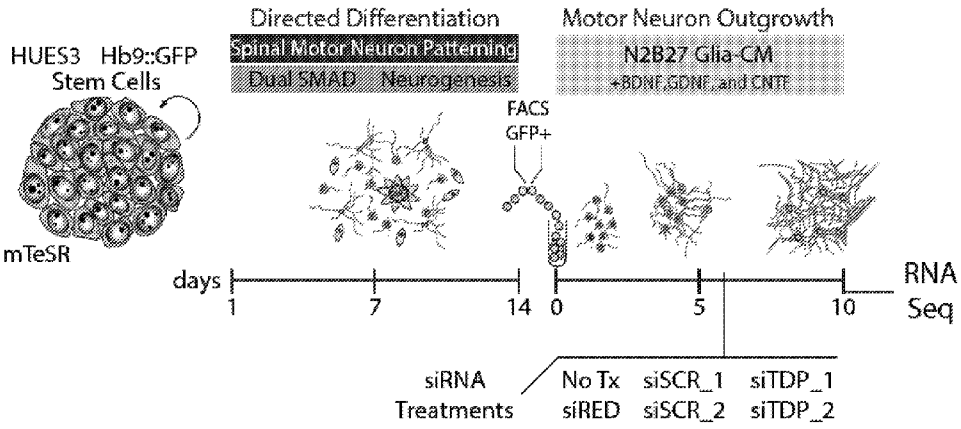
(81) Designated States *(unless otherwise indicated, for every kind of national protection available)*: AE, AG, AL, AM, AO, AT, AU, AZ, BA, BB, BG, BH, BN, BR, BW, BY, BZ, CA, CH, CL, CN, CO, CR, CU, CZ, DE, DJ, DK, DM, DO, DZ, EC, EE, EG, ES, FI, GB, GD, GE, GH, GM, GT, HN, HR, HU, ID, IL, IN, IR, IS, IT, JO, JP, KE, KG, KH, KN, KP, KR, KW, KZ, LA, LC, LK, LR, LS, LU, LY, MA, MD, ME, MG, MK, MN, MW, MX, MY, MZ, NA, NG, NI, NO, NZ, OM, PA, PE, PG, PH, PL, PT, QA, RO, RS, RU, RW, SA, SC, SD, SE, SG, SK, SL, ST, SV, SY, TH, TJ, TM, TN, TR, TT, TZ, UA, UG, US, UZ, VC, VN, WS, ZA, ZM, ZW.

(84) Designated States *(unless otherwise indicated, for every kind of regional protection available)*: ARIPO (BW, GH, GM, KE, LR, LS, MW, MZ, NA, RW, SD, SL, ST, SZ, TZ, UG, ZM, ZW), Eurasian (AM, AZ, BY, KG, KZ, RU, TJ, TM), European (AL, AT, BE, BG, CH, CY, CZ, DE, DK, EE, ES, FI, FR, GB, GR, HR, HU, IE, IS, IT, LT, LU, LV, MC, MK, MT, NL, NO, PL, PT, RO, RS, SE, SI, SK, SM, TR), OAPI (BF, BJ, CF, CG, CI, CM, GA, GN, GQ, GW, KM, ML, MR, NE, SN, TD, TG).

Published:
— *without international search report and to be republished upon receipt of that report (Rule 48.2(g))*

(54) Title: METHODS AND COMPOSITIONS FOR RESTORING STMN2 LEVELS

FIG. 1A



(57) Abstract: The disclosure relates to compositions and methods for treating a disease or condition associated with a TDP-pathology or a decline in TDP-43 functionality in neuronal cells in a subject, and for identifying candidate agents to suppress or prevent inclusion of an abortive or altered STMN2 RNA sequence.

WO 2021/195446 A2

METHODS AND COMPOSITIONS FOR RESTORING STMN2 LEVELS

RELATED APPLICATIONS

This application claims priority to U.S. Provisional Application No. 63/133,749, filed on January 4, 2021, U.S. Provisional Application No. 63/063,174, filed on August 7, 2020, and U.S. Provisional Application No. 62/994,797, filed on March 25, 2020. The entire teachings of the above applications are incorporated herein by reference.

BACKGROUND OF THE INVENTION

Amyotrophic lateral sclerosis (ALS) is a fatal neurodegenerative disease characterized by the selective loss of both upper and lower motor neurons (1). Patients with ALS experience progressive paralysis and develop difficulties in speaking, swallowing, and eventually breathing (2, 3) and usually succumb to the disease after 1-5 years from the time of diagnosis. Aside from two FDA approved drugs which modestly alter disease progression (4), treatment for ALS is limited to supportive care. ALS is now recognized to be on the same clinical and pathological spectrum as frontotemporal dementia (FTD), the most common cause of pre-senile dementia. FTD is characterized by behavioral changes, language impairment, and loss of executive functions (5) for which there is no effective treatment. Although the etiology of most ALS and FTD cases remains unknown, pathological findings and family-based linkage studies have demonstrated that there is overlap in molecular pathways involved in both diseases (1, 6).

SUMMARY OF THE INVENTION

TDP-43 is a predominantly nuclear DNA/RNA-binding protein with functional roles in transcriptional regulation, splicing, pre-microRNA processing, stress granule formation, and messenger RNA transport and stability. TDP-43 has been found to be a major constituent of inclusions in many sporadic cases of ALS and FTD. In response to aberrant expression of TDP-43, a decrease in STMN2 levels is seen. STMN2, also known as SCG10, is a regulator of microtubule stability and has been shown to encode a protein necessary for normal human motor neuron outgrowth and repair. Described herein are methods and compositions for restoring or increasing STMN2 levels.

Disclosed herein are antisense oligonucleotides that specifically bind an STMN2 mRNA, pre-mRNA, or nascent RNA sequence, thereby suppressing or preventing inclusion of an abortive or altered STMN2 RNA sequence. In some embodiments the antisense oligonucleotides do not bind to a polyadenylation site of the STMN2 RNA sequence. In some embodiments, the abortive or altered STMN2 RNA sequence occurs and increases in abundance when TDP-43 function declines or TDP-pathology occurs.

Also disclosed herein are antisense oligonucleotides that specifically bind an STMN2 mRNA, pre-mRNA, or nascent RNA sequence coding for a cryptic exon, thereby suppressing or preventing inclusion of a cryptic exon in STMN2 RNA, wherein the antisense oligonucleotide does not bind to a polyadenylation site of the STMN2 mRNA, pre-mRNA, or nascent RNA sequence.

Further disclosed herein are antisense oligonucleotides that specifically bind an STMN2 mRNA, pre-mRNA, or nascent RNA sequence, wherein the antisense oligonucleotide increases STMN2 protein expression.

In some embodiments, the antisense oligonucleotide is designed to target a 5' splice site, a 3' splice site, or a normal TDP-43 binding site. In some embodiments, the antisense oligonucleotide targets one or more splice sites. In some embodiments, the antisense oligonucleotide is designed to target a single stranded region located between the TDP-43 binding site and the polyadenylation site.

In some embodiments, the antisense oligonucleotide does not exhibit platelet toxicity.

Also disclosed herein are antisense oligonucleotides comprising a sequence selected from the group consisting of SEQ ID NOS: 37-85. In some aspects, the

antisense oligonucleotides comprising a sequence selected from the group consisting of SEQ ID NOS: 37-74. In some embodiments, the antisense oligonucleotide comprises a sequence selected from the group consisting of: SEQ ID NO: 40, SEQ ID NO: 47, SEQ ID NO: 48, SEQ ID NO: 49, SEQ ID NO: 50, SEQ ID NO: 52, SEQ ID NO: 53, SEQ ID NO: 54, SEQ ID NO: 56, and SEQ ID NO: 78, or more specifically the antisense oligonucleotide may comprise SEQ ID NO: 52. In certain embodiments, the antisense oligonucleotide comprises a sequence selected from the group consisting of SEQ ID NO: 53, SEQ ID NO: 72, and SEQ ID NO: 73, or more specifically the antisense oligonucleotide comprises SEQ ID NO: 73 or SEQ ID NO: 53.

Further disclosed herein are pharmaceutical compositions comprising one or more antisense oligonucleotides comprising a sequence selected from the group consisting of SEQ ID NOS: 37-85. In some embodiments, the one or more antisense oligonucleotides comprise a sequence selected from the group consisting of SEQ ID NOS: 37-74. In some embodiments, the one or more antisense oligonucleotides comprise a sequence selected from the group consisting of: SEQ ID NO: 40, SEQ ID NO: 47, SEQ ID NO: 48, SEQ ID NO: 49, SEQ ID NO: 50, SEQ ID NO: 52, SEQ ID NO: 53, SEQ ID NO: 54, SEQ ID NO: 56, and SEQ ID NO: 78, or more specifically the one or more antisense oligonucleotides may comprise SEQ ID NO: 52. In certain embodiments, the antisense oligonucleotide comprises a sequence selected from the group consisting of SEQ ID NO: 53, SEQ ID NO: 72, and SEQ ID NO: 73, or more specifically the antisense oligonucleotide comprises SEQ ID NO: 73 or SEQ ID NO: 53.

Disclosed herein are pharmaceutical compositions comprising a multimeric oligonucleotide. The multimeric oligonucleotide comprises one or more sequences selected from the group consisting of SEQ ID NOS: 37-85. In some embodiments, the multimeric oligonucleotide comprises two or more sequences selected from the group consisting of SEQ ID NOS: 37-85. The multimeric oligonucleotide may comprise multiple copies of a sequence, or alternatively may comprise single copies of multiple sequences.

In some embodiments, the antisense oligonucleotide suppresses or prevents inclusion of a cryptic exon in STMN2 RNA. In some embodiments, the antisense oligonucleotide specifically binds an STMN2 RNA, pre-mRNA, or nascent RNA sequence, e.g., coding for a cryptic exon. In some embodiments, the antisense oligonucleotide prevents or retards the degradation of STMN2 protein. In some

embodiments, the antisense oligonucleotide increases STMN2 protein. In some embodiments, the antisense oligonucleotide is designed to target a 5' splice site, a 3' splice site, or a normal TDP-43 binding site. In some embodiments, the antisense oligonucleotide is designed to target a single stranded region, e.g., a single stranded region located between the TDP-43 binding site and the polyadenylation site. In some embodiments, the antisense oligonucleotide is designed to target a site proximal to a cryptic splice site, a site proximal to a premature polyadenylation site, or a site located between a cryptic splice site and a premature polyadenylation site. In some embodiments, the antisense oligonucleotide binds to a target region within the cryptic exon that is unstructured. In some embodiments, the antisense oligonucleotide binds near or adjacent to the 5' splice site regulated by TDP-43. In some embodiments, the antisense oligonucleotide targets a region proximal to a predicted TDP-43 binding site. In some embodiments, the antisense oligonucleotide targets the TDP-43 normal binding site. In some embodiments, the antisense oligonucleotide targets one or more splice sites. In some embodiments, the antisense oligonucleotide suppresses cryptic splicing.

In some embodiments, a pharmaceutical composition comprises two or more antisense oligonucleotides, and in some aspects comprises three or more antisense oligonucleotides. In some embodiments, the two or more antisense oligonucleotides are covalently linked. In some embodiments, the one or more antisense oligonucleotides increase STMN2 protein expression.

In some embodiments, a pharmaceutical composition further comprises an agent for treating a neurodegenerative disease, an agent for treating a traumatic brain injury, or an agent for treating a proteasome-inhibitor induced neuropathy. In some embodiments, a pharmaceutical composition further comprises STMN2 as a gene therapy. In some embodiments, a pharmaceutical composition further comprises a JNK inhibitor.

Also disclosed herein are methods of treating or reducing the likelihood of a disease or condition associated with a decline in TAR DNA-binding protein 43 (TDP-43) functionality in neuronal cells in a subject in need thereof. The methods may include contacting the neuronal cells with an antisense oligonucleotide that corrects reduced levels of STMN2 protein, wherein the agent does not target a polyadenylation site of a target transcript.

Further disclosed herein are methods of treating or reducing the likelihood of a disease or condition associated with a decline in TAR DNA-binding protein 43 (TDP-43) functionality in neuronal cells in a subject in need thereof. The methods may include contacting the neuronal cells with an antisense oligonucleotide that increases STMN2 protein expression.

In some embodiments, the antisense oligonucleotide specifically binds an STMN2 RNA, pre-RNA, or nascent RNA sequence coding for a cryptic exon. In some embodiments, the antisense oligonucleotide is designed to target a 5' splice site, a 3' splice site, or a normal TDP-43 binding site. In some embodiments, the antisense oligonucleotide is designed to target a single stranded region, e.g., a single stranded region located between the TDP-43 binding site and the polyadenylation site. In some embodiments, the antisense oligonucleotide is designed to target a site proximal to a cryptic splice site, a site proximal to a premature polyadenylation site, or a site located between a cryptic splice site and a premature polyadenylation site. In some embodiments, the antisense oligonucleotide binds to a target region within the cryptic exon that is unstructured. In some embodiments, the antisense oligonucleotide binds near or adjacent to the 5' splice site regulated by TDP-43. In some embodiments, the antisense oligonucleotide targets a region proximal to a predicted TDP-43 binding site. In some embodiments, the antisense oligonucleotide is designed to target one or more splice sites. In some embodiments, the antisense oligonucleotide restores normal length or protein coding STMN2 pre-mRNA or mRNA.

In some embodiments, the subject exhibits improved neuronal outgrowth and repair. In some embodiments, the disease or condition is a neurodegenerative disease, e.g., amyotrophic lateral sclerosis (ALS), frontotemporal dementia (FTD), inclusion body myositis (IBM), Parkinson's disease, or Alzheimer's disease. In some embodiments, the disease or condition is a traumatic brain injury. In some embodiments, the disease or condition is a proteasome-inhibitor induced neuropathy. In some embodiments, the disease or condition is associated with mutant or reduced levels of TDP-43 in neuronal cells.

In some embodiments, the methods further comprise administering an effective amount of a second agent to the subject. In some embodiments, a second agent is administered to treat a neurodegenerative disease or a traumatic brain injury. In some embodiments, the second agent is STMN2, e.g., administered as a gene therapy.

Also disclosed herein are methods of treating or reducing the likelihood of a disease or condition associated with a decline in TAR DNA-binding protein 43 (TDP-43) functionality in neuronal cells in a subject in need thereof. The methods may include contacting the neuronal cells with an antisense oligonucleotide that corrects reduced levels of STMN2 protein, wherein the antisense oligonucleotide comprises a sequence selected from the group consisting of SEQ ID NOS: 37-85.

In some embodiments, the antisense oligonucleotide comprises a sequence selected from the group consisting of SEQ ID NOS: 37-74. In some embodiments, the antisense oligonucleotide comprises a sequence selected from the group consisting of SEQ ID NO: 40, SEQ ID NO: 47, SEQ ID NO: 48, SEQ ID NO: 49, SEQ ID NO: 50, SEQ ID NO: 52, SEQ ID NO: 53, SEQ ID NO: 54, SEQ ID NO: 56, and SEQ ID NO: 78, or more specifically the antisense oligonucleotide may comprise SEQ ID NO: 52. In certain embodiments, the antisense oligonucleotide comprises a sequence selected from the group consisting of SEQ ID NO: 53, SEQ ID NO: 72, and SEQ ID NO: 73, or more specifically the antisense oligonucleotide comprises SEQ ID NO: 73 or SEQ ID NO: 53.

Further disclosed herein are methods of reducing the likelihood of a disease or condition associated with a decline in TAR DNA-binding protein 43 (TDP-43) functionality in neuronal cells in a subject in need thereof. The methods may include contacting the neuronal cells with one or more antisense oligonucleotides that suppress or prevents inclusion of a cryptic exon in STMN2 RNA. In some embodiments, the one or more antisense oligonucleotides comprise a sequence selected from the group consisting of SEQ ID NOS: 37-85.

In some embodiments, the antisense oligonucleotide comprises a sequence selected from the group consisting of: SEQ ID NO: 40, SEQ ID NO: 47, SEQ ID NO: 48, SEQ ID NO: 49, SEQ ID NO: 50, SEQ ID NO: 52, SEQ ID NO: 53, SEQ ID NO: 54, SEQ ID NO: 56, and SEQ ID NO: 78, or more specifically comprises SEQ ID NO: 52. In certain embodiments, the antisense oligonucleotide comprises a sequence selected from the group consisting of SEQ ID NO: 53, SEQ ID NO: 72, and SEQ ID NO: 73, or more specifically the antisense oligonucleotide comprises SEQ ID NO: 73 or SEQ ID NO: 53.

In some embodiments, the antisense oligonucleotide specifically binds an STMN2 RNA, pre-RNA, or nascent RNA sequence coding for a cryptic exon. In some embodiments, the antisense oligonucleotide is designed to target a 5' splice site,

a 3' splice site, or a normal TDP-43 binding site. In some embodiments, the antisense oligonucleotide is designed to target a single stranded region, e.g., a single stranded region located between the TDP-43 binding site and the polyadenylation site. In some embodiments, the antisense oligonucleotides are designed to target a site proximal to a cryptic splice site, a site proximal to a premature polyadenylation site, or a site located between a cryptic splice site and a premature polyadenylation site. In some embodiments, the antisense oligonucleotides bind to a target region within the cryptic exon that is unstructured. In some embodiments, the antisense oligonucleotide binds near or adjacent to the 5' splice site regulated by TDP-43. In some embodiments, the antisense oligonucleotide targets a region proximal to a predicted TDP-43 binding site. In some embodiments, the antisense oligonucleotide targets the TDP-43 normal binding site.

In some embodiments, the disease or condition is selected from the group consisting of amyotrophic lateral sclerosis (ALS), frontotemporal dementia (FTD), inclusion body myositis (IBM), Parkinson's disease, and Alzheimer's disease. In some embodiments, the disease or condition is a traumatic brain injury. In some embodiments, the disease or condition is a proteasome-inhibitor induced neuropathy.

In some embodiments, the antisense oligonucleotide suppresses cryptic splicing. In some embodiments, the antisense oligonucleotide prevents or retards the degradation of STMN2 protein. In some embodiments, the subject exhibits improved neuronal outgrowth and repair.

In some embodiments, the methods further include administering an effective amount of a second agent to the subject. In some embodiments, the second agent is administered to treat a neurodegenerative disease or a traumatic brain injury.

Further disclosed herein are methods of treating or reducing the likelihood of a disease or condition associated with a decline in TAR DNA-binding protein 43 (TDP-43) functionality in neuronal cells in a subject in need thereof, comprising contacting the neuronal cells with a multimeric oligonucleotide that corrects reduced levels of STMN2 protein, wherein the multimeric oligonucleotide comprises two or more antisense oligonucleotides selected from the group consisting of SEQ ID NOS: 37-85. In some embodiments, the multimeric oligonucleotide comprises two or more antisense oligonucleotides selected from the group consisting of SEQ ID NOS: 37-74.

Also disclosed herein are antisense oligonucleotides that corrects reduced levels of STMN2 protein, wherein the antisense oligonucleotide is designed to target

an unstructured region within a cryptic exon. In some embodiments, the unstructured region within the cryptic exon is located between a cryptic splice site and a premature polyadenylation site.

Also disclosed herein are methods of detecting altered levels of STMN2 or ELAVL3 protein in a subject. The methods comprise obtaining a sample from the subject; and detecting whether the STMN2 or ELAVL3 protein levels are altered. In some embodiments, the subject has amyotrophic lateral sclerosis. In some embodiments, the detection of whether the STMN2 or ELAVL3 levels are altered comprises determining if the STMN2 or ELAVL3 levels are decreased (e.g., using an ELISA). In some embodiments, the sample is a biofluid sample (e.g., a CSF sample).

BRIEF DESCRIPTION OF THE DRAWINGS

The patent or application file contains at least one drawing executed in color. Copies of this patent or patent application publication with color drawings will be provided by the Office upon request and payment of the necessary fee.

FIGS. 1A-1F demonstrate RNA Sequencing of TDP-43 knockdown in hMNs. FIG. 1A provides a schematic showing hMN differentiation, purification, and RNAi strategy for TDP-43 knockdown in cultured MNs. FIG. 1B provides multidimensional scaling analysis for RNA-Seq data sets obtained from two biologically independent MN differentiation and siRNA transfection experiments based on 500 most differentially expressed genes. FIG. 1C provides a volcano plot showing statistically misregulated genes in hMNs treated with siTDP-43 compared to those treated with scrambled controls. Genes identified as significant (Benjamini-Hochberg adjusted P value cutoff of 0.05 and a log fold-change ratio cutoff of 0) after differential expression analysis are highlighted in yellow (for up-regulated/increased abundance genes) and in blue (for down-regulated/decreased abundance genes). FIG. 1D provides a scatter plot comparing TPM values for all genes expressed in MNs treated with control siRNAs versus the fold change in expression for those genes in cells treated with siTDP-43. FIGS. 1E and 1F show a subset of 11 genes initially identified as 'hits' (significantly up-regulated (FIG. 1E) or down-regulated (FIG. 1F)) in the TDP43 knockdown experiment were selected for validation by qRT-PCR. A total of 9 out 11 of these genes (including TDP-43) exhibited the predicted response to TDP-43 depletion when their expression was assayed by qRT-PCR (Unpaired t test, P value < 0.05).

FIGS. 2A-2J Demonstrate a familial ALS model. FIG. 2A provides a schematic of a strategy for assessing gene expression in iPS cell-derived hMNs expressing mutant TDP-43. FIG. 2B provides micrographs showing the morphology of neurons cultured for 10 days derived from the iPS cells of healthy controls (11a, 18a, 20b, 17a) and patients with mutations in TARDP (+/Q343R, +/G298S, +/A315T, and +/M337V). FIGS. 2C-2H provide qRT-PCR analysis of the genes consistently downregulated (FIGS. 2D-2F) or upregulated (FIG. 2C) after TDP-43 knockdown in neurons differentiated from the controls or TDP-43 patients. (Unpaired t test, P value < 0.05). FIG. 2I provides representative micrographs of control and patient neurons immunostained for TDP-43 (red), β-III tubulin (green) and counterstained with DAPI (blue). Scale bar, 100 μm. FIG. 2J provides Pearson's correlation analysis for TDP-43 immunostaining and DAPI fluorescence comparing control neurons to neurons with TDP-43 mutations. Dots represent individual cells. (Unpaired t test, P value < 0.05).

FIGS. 3A-3I demonstrate STMN2 regulation and localization. FIG. 3A provides qRT-PCR analysis for the STMN2 transcript in independent experiments using two different sets of primer pairs. (Unpaired t test, P value < 0.05). FIG. 3B provides immunoblot analysis for TDP-43 and STMN2 protein levels following partial depletion of TDP-43 by siRNA knockdown. Protein levels were normalized to GAPDH and are expressed relative to the levels in MNs treated with the siRED control. FIG. 3C provides qRT-PCR analysis for STMN2 transcript analysis in Hb9::GFP+ MNs treated with siRNAs targeting three ALS-linked genes (TDP-43, FUS, and C9ORF72). (Dunnett's multiple comparison test, Alpha value < 0.05). FIGS. 3D-3F show formaldehyde RNA immunoprecipitation was used to identify transcripts bound to TDP-43. After TDP-43 immunoprecipitation (FIG. 3D), qRT-PCR analysis was used to test for enrichment of TDP-43 transcripts (FIG. 3E) and STMN2 transcripts (FIG. 3F) relative to the sample input. FIG. 3G provides micrographs of Hb9::GFP+ MNs immunostained for TDP-43 (red), β-III tubulin (green) and counterstained with DAPI (blue). FIG. 3H provides micrographs of Hb9::GFP+ MNs co-cultured on glia immunostained for STMN2 (red) and MAP2 green and GOLGIN97 (green). FIG. 3I provides a micrograph of Hb9::GFP+ MNs day 3 after sorting immunostained for STMN2 (red), MAP2 (green) and counterstained with F-actin-binding protein phalloidin (white). Scale bar, 5 μm.

FIGS. 4A-4K demonstrate STMN2 Knockout. FIG. 4A provides a schematic of the knockout strategy using guide RNAs (gRNAs) targeting two constitutive exons, Exon 2 and 4, of the human *STMN2* gene. The intervening DNA segment (~18Kb) is targeted and deleted as a result of NHEJ (Non-homologous end joining) repair of the two double strand breaks (DSBs) introduced by the Cas9/gRNA nuclease complex. FIGS. 4B-4D show STMN2 knockout was confirmed in the HUES3 *Hb9::GFP* line by RT-PCR analysis of genomic DNA (FIG 4B), by immunoblot analysis (FIG. 4C), and by immunofluorescence (FIG. 4D). FIG 4E provides an experimental strategy used to assess the cellular effect of lacking STMN2 in hMNs. FIGS. 4F-4H show Sholl analysis of hMNs with and without STMN2 and in the absence (FIG. 4G) or presence (FIG. 4H) of a ROCK inhibitor (Y-27632, 10 μM) to stimulate neurite outgrowth. (Unpaired t test, P value < 0.05). FIG. 4I provides an experimental strategy used to assess the cellular effect of lacking STMN2 in hMNs after axonal injury. FIGS. 4J-4K show axonal regrowth after injury. Representative micrographs of hMNs in the microfluidics device prior to and after axotomy (FIG. 4J). Measurements of axonal regeneration after axotomy. (Unpaired t test, P value < 0.05).

FIGS. 5A-5G demonstrate a sporadic ALS model. FIG. 5A provides an experimental strategy used to assess the effect of proteasome inhibition on TDP-43 localization in human motor neurons. FIG. 5B shows Pearson's correlation analysis for TDP-43 immunostaining and DAPI fluorescence of cells treated with MG-132 (1 μM). (Dunnett's multiple comparison test, Alpha value < 0.05). FIG. 5C provides micrographs of HUES3 motor neurons untreated or treated with MG-132 and immunostained for TDP-43 (red), β-III tubulin (green) and counterstained with DAPI (blue). Scale bar, 100 μm. FIG. 5D provides immunoblot analysis of TDP-43 in detergent soluble (RIPA) and detergent-insoluble (UREA) fractions in neurons treated with MG-132 (Unpaired t test, P value < 0.05). FIG. 5E provides qRT-PCR analysis of STMN2 expression for motor neurons treated with MG-132 at the indicated concentrations and durations relative to DMSO control (Unpaired t test, P value < 0.05). FIG. 5F provides a diagram of RT-PCR detection strategy for STMN2 cryptic exon. FIG. 5G provides a tapestation analysis for the STMN2 cryptic exon in hMNs control cells treated with MG-132 (1 μM).

FIGS. 6A-6H demonstrates ALS patient data. FIGS. 6A-6C provides histologic analysis of human adult lumbar spinal cord from post-mortem samples collected from a subject with no evidence of spinal cord disease (control) (FIG. 6A)

or two patients diagnosed with sporadic ALS (FIGS. 6B-6C). Immunoreactivity to STMN2 was detected in the perinuclear region (indicated by arrows) of spinal motor neurons but not in the surrounding glial cells. STMN2 immunoreactivity in lumbar spinal motor neurons from control and ALS cases was scored as 'strong' [as indicated by arrows in control (FIG. 6A) and sporadic ALS (FIG. 6B)] or as 'absent' [as indicated by arrowheads in sporadic ALS (FIG. 6C)]. Scale bars, 50 μm. FIG. 6D show the percentage of lumbar spinal motor neurons with strong STMN2 immunoreactivity was significantly lower in ALS tissue samples (n= 3 controls and 3 ALS cases; approximately 40 MNs were scored for each subject; Two-tailed t-test, P value < 0.05). FIGS. 6E-6G show gene expression analysis for STMN2 from previously published data sets, Rabin et al 2009 (FIG. 6E), Highley et al 2014 (FIG. 6F), and D'Erchia et al. 2017 (Two-tailed t-test, P value < 0.05). FIG. 6H provides a molecular model of ALS pathogenesis.

FIGS. 7A-7I demonstrate production of differentiated human motor neurons. FIG. 7A shows hMN differentiation, purification, and culture strategy. FIG. 7B provides flow-cytometric analysis of differentiated HUES3 Hb9:GFP cells. Cells not treated with the RA and SHH pathway agonist were used as negative control for the gating of GFP expression. FIGS. 7C-7F provides micrographs and quantification of purified Hb9::GFP+ cells immunostained for HB9 and counterstained with DAPI (FIG. 7C) (Scale bar = 10 μm) or immunostained for ISL1 and the neuronal markers β-III tubulin and MAP2 (FIG. 7E) (Scale bar = 20 μm). FIGS. 7G-7J show differentiated MNs are electrophysiologically active as determined by whole-cell patch-clamp recordings. FIG. 7G show upon depolarization in voltage-clamp mode, cells exhibited fast inward currents followed slow outward currents, indicating the expression and opening of voltage-activated sodium and potassium channels, respectively. FIG. 7H shows in current-clamp mode, depolarization elicited repetitive action potential firing. FIG. 7I shows response to Kainate is consistent with the expression of functional receptors for excitatory glutamatergic transmitters.

FIGS. 8A-8E demonstrate TDP-43 knockdown in cultured hMNs. FIG. 8A provides RNAi strategy for TDP-43 knockdown in cultured MNs. FIG. 8B shows phase and red fluorescence micrographs of cultured hMNs 4 days after treatment with different siRNAs including scrambled siRNA conjugated to Alexa Fluor 555. FIG. 8C provides flow-cytometric analysis of hMNs after treatment with different siRNAs. FIG. 8D shows relative levels of TDP-43 mRNA in MNs exposed to different siRNAs

for 2, 4 or 6 days. Levels for each sample were normalized to GAPDH and expressed relative to the no transfection control. FIG. 8E provides immunoblot analysis of hMNs after RNAi treated with the indicated siRNAs. Each sample was normalized using GAPDH, and TDP-43 protein levels were calculated relative to the siSCR_555-treated control sample.

FIGS. 9A-9C demonstrate motor neuron RNA-Seq. FIG. 9A shows global transcriptional analysis of motor neurons treated as indicated represented as a heat map. Unsupervised clustering of expression profiles revealed that the samples segregated based on the batch on motor neuron production and analysis. FIG. 9B provides analysis of TDP-43 transcript abundance after RNA-Sequencing validated the knockdown (Benjamini-Hochberg adjusted P value cutoff of 0.05). FIG. 9C shows alteration in the splicing pattern of the *POLDIP3* gene was detected as result of TDP-43 knockdown, with siTDP43-treated cells showing significant reduction of isoform 1 and increased levels of spliced variant 2 (which lacks Exon3) (false discovery rate 'FDR'>0.05).

FIG. 10 demonstrates pluripotent stem cell genotyping sequencing chromatograms of Exon6 of *TARDBP* in the indicated iPS cell lines to confirm the heterozygous mutations in the patient lines.

FIGS. 11A-11F demonstrate neuronal cell sorting. FIG. 11A shows using a cell surface marker screen, antibodies enriched on GFP+ motor neurons (Quadrant 1) and GFP- cells (Quadrant 3) were identified. FIG. 11B shows after sorting for NCAM+ and EpCAM- cells, high content imaging was used to determine if the sorting method can deplete the cultures of mitotic cells (EdU+) and significantly enrich for motor neurons (Isl1+) and neurons (MAP2+). N= 6 different iPS cell lines. Statistical analysis was performed using a two-tailed Student's t test. FIGS. 11C-11D provides qRT-PCR analysis of cultures after sorting for the motor neuron marker ISL1 (FIG. 11C) and the neuronal marker βIII-tubulin (FIG. 11D) revealed enrichment and more homogenous cultures compared to unsorted cultures. FIG. 11E provides flow-cytometric analysis with phycoerythrin (PE)-conjugated antibodies to EpCAM (anti-epCAM–PE) and Alexa Fluor 700–conjugated antibodies to NCAM (anti-NCAM–AF700) of cultures differentiated from the indicated healthy controls (grey) and TDP-43 mutant lines (red). FIG. 11F shows the percentage of NCAM+ cells for the indicated lines from 4-6 independent differentiations. No significant difference was observed between mutant and control lines in terms of their ability to

generate NCAM+ cells. Statistical analysis was performed using a two-tailed Student's t test, P value < 0.05.

FIGS. 12A-12G demonstrate TDP-43 and STMN2 connections. FIGS. 12A-12C provide qRT-PCR validation of the downregulation of ALS genes upon siRNA treatments. Expression of TDP-43 (FIG. 12A), FUS (FIG. 12B), and C9ORF72 (FIG. 12C) was assessed for all the controls and each siRNA used (Unpaired t test, P value < 0.05). FIG. 12D provides a western blot analysis of STMN2 protein in different cell types along the motor neuron differentiation. FIG. 12E shows RNA-Seq expression levels for the Stathmin family in motor neurons treated with either siSCR (-) or siTDP-43 (+) oligos. Only STMN2 levels were altered after TDP-43 knockdown. FIGS. 12F-12G shows TDP-43 binding sites within the Stathmin family of genes (FIG. 12F) normalized to gene length (FIG. 12G). STMN2 has the greatest number of binding motifs.

FIGS. 13A-13H demonstrate STMN2 regulates neuronal outgrowth. CRISPR-mediated STMN2 knockout in the WA01 line was confirmed by RT-PCR analysis of genomic DNA (FIG. 13A), by immunoblot analysis (FIG. 13B), and by immunofluorescence (FIG. 13C). FIGS. 13D-13F provide Sholl analysis of hMNs with and without STMN2 and in the presence of a Y-27632 (10 μM), a ROCK inhibitor (FIG. 13F) (Unpaired t test, P value < 0.05). FIGS. 13G-13H shows axonal regrowth after injury. Representative micrographs of hMNs in the microfluidics device prior to and after axotomy (FIG. 13G). Analysis of axonal regrowth after axotomy (Unpaired t test, P value < 0.05) (FIG. 13H).

FIGS. 14A-14E demonstrate cell survival and proteasome activity assays. FIGS. 14A-14C shows Cell Titer Glo uses ATP from metabolically active cells to generate light. (FIG. 14A) shows a direct relationship exists between luminescence and the number of cells in culture over several orders of magnitude. FIG. 14B shows the assay can detect differences in neuronal survival in the absence of growth factors. N= 6 separate wells of neurons. (Unpaired t test, P value < 0.05). FIG. 14C shows MG-132 neuronal survival experimental outline. FIG. 14D shows dose response curve for motor neurons cultured with indicated concentrations of MG-132 for the indicated times. N= triplicate wells. Cells are viable after 1 day of treatment at all the concentrations tested and lower concentrations are tolerated for more extended periods of time. FIG. 14E shows following cleavage by the proteasome, the substrate for luciferase is liberated, which allows for quantitative measurement of proteasome

activity. Neurons treated with MG-132 show significantly decreased proteasome activity. N= 4 separate wells of neurons (Unpaired t test, P value < 0.05).

FIGS. 15A-15E demonstrate TDP-43 regulates cryptic exon splicing in hMNs (FIGS. 15A-15C). Visualization of the cryptic exons for PFKP (FIG. 15A), ELAVL3 (FIG. 15B), and STMN2 (FIG. 15C) for the cells treated with scrambled siRNAs or siRNAs targeting TDP-43 transcript. Read coverage and splice junctions are shown for alignment to the human HG19 genome. FIGS. 15D-15E provides diagram of RT-PCR detection strategy for STMN2 cryptic exon (FIG. 15D), and Sanger sequencing of the PCR product confirmed the splicing of STMN2 Exon 1 with the cryptic exon (FIG. 15E).

FIGS. 16A-16P provide cryptic STMN2 transcript qPCR data from patient cerebral spinal fluid (CSF) samples. FIGS. 16A-16D provide graphs summarizing the patient sample data of normalized cryptic STMN2 relative to healthy controls. FIGS. 16E-16M provide graphs providing details regarding individual patient samples. FIG. 16N provides a graph demonstrating survival duration following diagnosis. FIG. 16O provides a graph demonstrating age at death. FIG. 16P provides a graph demonstrating vital capacity.

FIGS. 17A-17C demonstrate an STMN2 multiplexed qPCR Assay. FIG. 17A shows Q-RT PCT assay for STMN2 in fluids. Experimental schemes are provided and STMN2 multiplexed TaqMan assay is shown to simultaneously detect cryptic STMN2, normal STMN2 transcript, and the housekeeping gene RNA18S5. RNA can be collected from CSF-derived exosomes and then converted into cDNA to assay for full and cryptic STMN2 transcripts, as well as control RNAs for normalization. FIG. 17B shows *in vitro* validation of the multiplexed assay in cells where TDP-43 levels were reduced using either an ASO or using siRNA. FIG. 17C shows the STMN2 multiplexed qPCR assay was used to probe cryptic STMN2 transcript levels in the cDNA samples generated from the MGH CSF samples. STMN2 cryptic splicing is significantly induced in ALS patients.

FIGS. 18A-18D demonstrate a sandwich ELISA for detecting STMN2 protein. FIG. 18A provides a schematic of the STMN2 sandwich ELISA. FIG. 18B demonstrates the sensitivity of the STMN2 ELISA to picogram quantities. FIG. 18C shows the sandwich ELISA was validated using recombinant STMN2 protein and is capable of detecting picogram levels of STMN2. FIG. 18D shows STMN2 levels are

reduced in patient cerebral spinal fluid (CSF) when assessed using the STMN2 ELISA.

FIG. 19 provides a chart demonstrating the genetics of ALS, with each gene being plotted against the year it was discovered. *See* Alsultan et al. *Degenerative Neurological and Neuromuscular Disease.* 2016, *6*, 49-64.

FIG. 20 demonstrates that TDP-43 is a multifunctional nucleic acid-binding protein. TDP-43 has been shown to play a role in various functions including RNA splicing, miRNA processing, autoregulation of its own transcript, RNA transport and stability, and stress granule formation. The transcripts TDP-43 regulates are highly species and cell type dependent. *See* Buratti and Baralle *Trends in Biochem. Sci..* 2012, 6, 237-247.

FIG. 21 provides a strategy for measuring transcriptional effects of TDP-43 depletion. The schematic demonstrates hMN differentiation, purification, and culture strategy. The strategy uses small molecules that mimic early development to convert stem cells into postmitotic neurons in 2 weeks. Various methods were developed to sort and study the neurons. siRNA technology combined with RNA sequencing was used to identify transcripts regulated by TDP-43.

FIG. 22 demonstrates TDP-43 binds to STMN2. ALS patient spinal cords were stained for STMN2 and decreased STMN2 protein in ALS patients was observed based on fold enrichment relative to PGK1 (fRIP). *See* Klim et al. *Nature Neuroscience* vol. 22, pages 167–179 (2019).

FIG. 23 shows splicing alterations after TDP-43 depletion. Differential exon usage analysis was performed on RNA-seq samples from motor neurons treated with siTDP. Splicing changes were observed in STMN2.

FIG. 24 demonstrates TDP-43 suppresses a cryptic exon in STMN2. The integrated genome viewer was used to look at where RNA seq reads were mapped to the human genome (top graph # of reads) and how the reads reconnected between the exons (splice track). The graphs show the number of reads mapped to areas of a gene.

FIG. 25 provides a STMN2 splicing defect summary. Under normal conditions STMN2 is transcribed with all 5 exons leading to an mRNA that is translated into a 20 kDa STMN2 protein. After TDP-43 perturbations, the cryptic exon intercepts the transcript so that only a 17 amino acid polypeptide could be translated.

FIG. 26 shows STMN2 is consistently decreased. The overlap of decreased transcripts down in 3 human RNA seq data sets (ALS patient data sets and siTDP43 stem cell motor neuron data set) were compared and STMN2 is the only transcript down in all three data sets.

FIG. 27 shows the STMN2 cryptic exon is present in ALS patient spinal cords. Read coverage and splice junctions are shown for alignment to the human HG19 genome. The reads mapped to the human genome in ALS patients was observed, and for 5 out of 6 patients reads mapped to and splicing went into the cryptic exon and none of the controls.

FIG. 28 shows TDP-43 depletion leads to neurite outgrowth and axonal regrowth defects. Representative micrographs of hMNs treated with indicated siRNAs and immunostained for β-III tubulin to perform Sholl analysis are provided. A Sholl analysis of hMNs after siRNA treatment is provided. Lines represent sample means and shading represents the s.e.m. with unpaired t-test between siTDP43 and siSCR, two sided, $P<0.05$.

FIG. 29 shows microfluidic devices for investigating axon regeneration. The microfluidic device includes a soma compartment (left panel) and axon compartment (right panel).

FIGS. 30A-30B demonstrate TDP-43 depletion leads to neurite outgrowth and axonal regrowth defects. FIG. 30A provides representative micrographs of hMNs in the microfluidics device after axotomy. Scale bars, 150 μM. FIG. 30B provides measurements of axonal regrowth and regeneration after axotomy (Unpaired t test, two sided, P value < 0.05 18h $\leq$0.0001, 24h $\leq$0.0001, 48$\leq$0.0001 and 72$\leq$0.0001).

FIG. 31 demonstrates STMN2 is a c-Jun N-terminal kinase (JNK) target in the axonal degeneration pathway. JNK1 is shown to bind to and phosphorylate STMN2, and phosphorylated STMN2 is rapidly degraded. *See* J. Eun Shin et al. *PNAS* 2012, *109*, E3696-3705.

FIG. 32 provides a strategy to determine if JNKi can rescue siTDP43 phenotypes. *See* Klim et al. *Nature Neuroscience* vol. 22, pages 167–179 (2019).

FIG. 33 shows a JNK inhibitor (SP600125) boosts STMN2 levels. STMN2 protein levels increased in neurons treated with JNKi and lower levels observed in cells treated with siTDP43 could be rescued.

FIG. 34 shows JNKi (SP600125) increases neurite outgrowth. Cells treated with JNKi exhibited increased neurite branching.

FIG. 35 shows JNKi (SP600125) increases neurite outgrowth. Sholl analysis confirmed that under all conditions JNKi increased neurite branching and regrowth following injury.

FIG. 36 shows JNKi increases axon regeneration. Microfluidic devices confirmed that under all conditions JNKi increased neurite branching and regrowth following injury.

FIG. 37 provides a model for proteasome inhibition. Disruptions to protein homeostasis lead to TDP-43 mislocalization and altered STMN2 levels, which disrupts axon biology.

FIGS. 38A-38B shows TDP-43 localization. TDP-43 is normally nuclear (FIG. 38A), but after compound washout, a loss of distinct nuclear TDP-43 staining was observed (FIG. 38B). No cytoplasmic aggregation was observed, only loss of nuclear TDP-43.

FIG. 39 shows TDP-43 mislocalization is reversible.

FIG. 40 shows STMN2 transcripts decreased after TDP-43 mislocalization. The decrease for STMN2 was even more pronounced than in cells expressing mutant TDP-43.

FIG. 41 provides a table summarizing recent ALS genes with their relative mutation frequencies in different ALS and FTD cohorts and associated pathways. Advances in WGS and WES have led to identification of genes carrying rare causal variants: TBK1, CHCHD10, TUBA4A, MATR3, CCNF, NEK1, C21orf2, ANXA11, and TIA1. TBK1 is shown as having the highest mutation frequencies of ALS-FTD (3-4%) in different cohorts. *See* Nguyen, et al., *Trends in Genetics*, 2018.

FIG. 42 shows Atg7 and TBK1 act at distinct times in autophagy. *See* Hansen, et, al,. *Nature Reviews Molecular Cell Biology*. 2018

FIG. 43 shows eliminating TBK1 shares similarities with, but is distinct from, blocking autophagy initiation.

FIG. 44 shows TBK1 knock out decreases functional TDP-43 and STMN2 levels while eliminating ATG7 has no effect. Loss of TBK1 induces TDP-43 pathology in motor neurons through autophagy-independent mechanisms.

FIG. 45 shows loss of TBK1 shows impaired axon regeneration after axon injury.

FIG. 46 shows proteasome inhibition induced TDP-43 mislocalization in TBK1 mutant motor neurons.

FIGS. 47A-47C demonstrate targeting STMN2 intron using CRISPR. A CRISPR strategy for targeting STMN2 is provided, as well as genotyping for STMN2 (FIGS. 47A-47B). FIG. 47C provides a table summarizing the CRISPR targeting strategy and genotyping for STMN2.

FIG. 48 demonstrates STMN2 mice are significantly smaller than Rosa26 control mice and show deficiencies in motor performance tasks with no signs of progression of these deficits over time.

FIG. 49 demonstrates STMN2 mice are significantly smaller than Rosa26 control mice and show deficiencies in motor performance tasks with no signs of progression of these deficits over time.

FIG. 50 demonstrates behavioral outcomes, as well as the total distance traveled in open field assays, appear to be similar between two mice cohorts.

FIG. 51 demonstrates STMN2 transcript levels are significantly reduced or no transcript is present in brain tissue from mutant cohort.

FIG. 52 provides Western Blot of brain tissue validating loss or significant reduction of STMN2 protein in mutant mice cohort.

FIG. 53 demonstrates STMN2 primarily localizes to ChAT+ motor neurons in the ventral horn of adult mice spinal cords.

FIG. 54 demonstrates a STMN2 cohort exhibits a significant decrease in the number of STMN2+/ChAT+ motor neurons on the ventral horn of the spinal cord.

FIG. 55 provides graphs showing the difference in organ or muscle weight between control and STMN2 mice. It is demonstrated that lower limb muscles are lighter in STMN2 mice (see two boxed graphs).

FIG. 56 provides pre- and post-synaptic staining of STMN2 gastrocnemius (GA) muscle and Rosa26 control gastrocnemius (GA) muscle. The staining suggests de-innervation in STMN2 -/- animals.

FIG. 57 demonstrates pre-and post-synaptic staining of STMN2 gastrocnemius (GA) muscle and Rosa26 control gastrocnemius (GA) muscle suggests de-innervation in STMN2 -/- animals.

FIG. 58 demonstrates neuromuscular junction (NMJ) morphology supports active de-innervation in gastrocnemius muscle of STMN2 mutants.

FIG. 59 demonstrates mutant TDP-43 does not display pathological mislocalization. Stains of control and ALS patient neurons for TDP-43 show that for both the control and ALS patient neurons TDP-43 was primarily nuclear.

FIG. 60 identifies different classes of proteasome inhibitors and provides their chemical structures.

FIG. 61 shows decreased expression of full length STMN2 in hMNs upon treatment with structurally distinct proteasome inhibitors.

FIG. 62 shows a PCR assay of hMNs treated with MG-132 or Bortezomib. Full length STMN2 was detected in all samples as a control. The presence of transcripts containing the STMN2 cryptic exon were specific to those cells treated with the proteasome inhibitors.

FIGS. 63A-63B demonstrate in vitro assay for TDP-43 binding to STMN2 RNA. Using genomic DNA, RNA containing the TDP-43 binding sites from the cryptic exon region of STMN2 was in vitro transcribed (FIG. 63A). The RNA was used to assess whether it could pull down IP TDP-43 protein from human neuronal protein lysates. The in vitro assay shows transcripts containing the cryptic exon region pulled down TDP-43 (FIG. 63B).

FIG. 64 shows an in vitro assay for TDP-43 binding to STMN2 RNA. RNA containing the 5' and 3' TDP-43 binding regions were in vitro transcribed similar that described in FIG. 63. Although both 5' and 3' transcripts can pull down some TDP-43, the enrichment is not as strong as the full cryptic exon.

FIG. 65 shows design of gRNAs for generation of targeted mutant cell line with no cryptic exon. A strategy was prepared to delete 105 nucleotides within the cryptic exon within STMN2 intron between exons 1 and 2. The deletion will eliminate the TDP-43 binding motif, but not affect the predicted poly-adenylation site.

FIG. 66 provides a confirmation of mutational status. TIDE analysis was used to analyze the mutational status of the clones and checked the sequence alignment to control cells to obtain a more precise view of the size and location of the deletions. One cell line contained a homozygous 105 nt deletion, which was consistent with the gel electrophoresis. The deletion eliminated the TDP-43 binding motif, but did not affect the predicted poly-adenylation site.

FIG. 67 shows TDP-43 binding site is a potential negative regulator of STMN2 expression. Three cell lines, HUES3, IG2 (Stmn2 KO), and CN7 (cryptic exon deletion) were treated with normal media or media + 1 uM MG132 for 24 hours to stress the cells. In HUES3 cells, the stressed condition had 52% STMN2 mRNA expression compared to the unstressed condition. In IG2 (Stmn2 KO) condition, unstressed cells had 13% expression, and when stressed, expression increased to 42%.

The expression levels in the CN7 (Cryptic Exon Deletion) cell line were significantly higher than the other two cell lines, with unstressed having 729% and stressed having 473% expression. It was shown that if several exons are knocked out the expression goes down, but if the TDP-43 binding site is removed, expression goes way up.

FIGS. 68A-68B demonstrate deletion of putative TDP-43 binding site leads to increased STMN2 protein levels. Consistent with the gene expression data, deletion of the TDP-43 binding region within the STMN2 cryptic exon causes increased protein expression.

FIGS. 69A-69B demonstrate the conservation of the STMN2 gene locus. FIG. 69A shows human *STMN2* is located on long arm of chromosome 8 and is transcribed as several isoforms generally including 5 canonical exons. The location of the cryptic exon is highlighted in orange. Conservation amongst 100 vertebrates along the locus reveals strong conservation at exons as well as some intronic regions. FIG. 69B shows a higher resolution genomic view at the *STMN2* cryptic exon (orange) with nucleotide resolution combined with multiple sequence alignment for 12 primates and 2 rodents. Salient features of the human gene and the extent of their conservation down the list of species are underlined including the splice acceptor site (teal), the putative coding region (yellow), the stop codon (red), the TDP-43 binding motifs (blue), and the poly-A signal (purple).

FIG. 70 demonstrates a multiplexed assay for detecting cryptic STMN2.

FIGS. 71A-71C demonstrate siTDP-43 and TDP-43 ASO induce STMN2 reduction and cryptic exon induction. Relative expression levels are shown for TARDBP (FIG. 71A), STMN2 Exons 3-4 (FIG. 71B), and Cryptic STMN2 (FIG. 71C) when treated with SCR ASO, TDP ASO or siTDP.

FIGS. 72A-72C show relative mRNA levels for TARDP (FIG. 72A), STMN2 (FIG. 72B), and cryptic STMN2 (FIG. 72C) after treatment with a scrambled ASO, TDP-43 ASO or SOD1 ASO over a time course of 6 days.

FIG. 73 demonstrates cryptic STMN2 expression. mRNA levels of cryptic STMN2 expression is shown after treatment with Scrambled ASO, TDP-43 ASO, SOD1 ASO, siTDP-43, and siRED. Each treatment was applied using NeuroPorter5, NeuroPorter1, RNAiMAX, or LipoFecamine, with RNAimax being the most effective.

FIG. 74 provides a schematic showing the strategy for testing STMN2 splice switching ASOs.

FIGS. 75A-75D provide schematics of ASO screening set up plate 1 (FIG. 75A), plate 2 (FIG. 75B), plate 3 (FIG. 75C), and plate 4 (FIG. 75D).

FIG. 76 provides results from ASO screening with comparable cDNA for all wells. The ASOs screened are STMN2 intron targeting ASOs.

FIG. 77 provides results from ASO screening showing ASOs near the splice junction suppress cryptic exon inclusion.

FIG. 78 provides the best hits from the ASO screen showing dose dependence or suppression to lowest concentration.

FIGS. 79A-79B demonstrate TDP-43 protein structure, pathogenic mutations, and function. FIG. 79A shows TDP-43 comprises six domains: an N-terminal region (aa 1–102) with a nuclear localization signal (NLS, aa 82–98); two RNA recognition motifs: RRM1 (aa 104–176) and RRM2 (aa 192–262); a nuclear export signal (NES, aa 239–250); a C-terminal region (aa 274–414), encompassing a prion-like glutamine/asparagine-rich (Q/N) domain (aa 345–366); and a glycine-rich region (aa 366–414). Forty-six dominant mutations have been identified in TDP-43 in sporadic and familial ALS patients and in rare FTLD patients, mostly lying in the C-terminal glycine-rich region. FIG. 79B shows salient TDP-43 functions are strongly implicated in disease pathogenesis. The most common motif identified for TDP-43 is (TG)n, which corresponds to the (UG)n RNA binding motif. Interaction with RNA allows TDP-43 to regulate pre-mRNA splicing to inhibit the inclusion of cryptic exons as well as influence polyadenylation site selection. Cytosolic roles for TDP-43 include transport of RNA along neuronal processes and response to stresses including those affecting proteostasis that can trigger TDP-43 nuclear efflux and localization to stress granules. A multitude of these basic molecular functions contribute to TDP-43 autoregulation including splicing and polyadenylation.

FIGS. 80A-80B demonstrate STMN2 protein structure and function. FIG. 80A shows STMN2 comprises two domains that can be further subdivided: 1) an N-terminal domain containing a conserved Golgi-specifying sequence and two palmitoylation sites enabling membrane insertion, and 2) a Stathmin-like domain containing two tubulin binding repeats (TBR1 and TBR2) that each bind tubulin, a proline rich domain (PRD) harboring two phosphorylation sites that can be modulated by JNK to potentially modulate the ability of STMN2 to interact with tubulin and promote STMN2 degradation, and a stathmin N-terminal domain (SLDN), which contain a peptide that inhibits tubulin polymerization. Identified posttranslational

modifications (PTMs) according to PhosphositePlus are marked along the protein structure. FIG. 80B shows the reported subcellular localization of STMN2 protein. STMN2 localizes to the golgi apparatus and is found in vesicles trafficked throughout dendrites and axons, and concentrates within growth cones of developing neurons as well as in regenerating axon tips after injury.

FIG. 81 provides a proposed model for TDP-43 regulation of STMN2. A pathological hallmark of ALS is the nuclear loss of TDP-43 and its aggregation. We propose a model of TDP-43 regulation of STMN2 where it binds to STMN2 pre-mRNA upon the intron between exons 1 and 2. Either reduction of TDP-43 levels or nuclear egress leads to early polyadenylation and splicing of a cryptic exon leading to a truncated STMN2 mRNA transcript. The blunted transcript encodes for a putative 17 amino acid polypeptide thus leading to reduced levels of STMN2 protein. Loss of STMN2 leads to reduced neurite outgrowth and axonal repair after injury.

FIG. 82 shows antisense oligonucleotides and their location in relation to the STMN2 sequence. The sequence, chemistry and alignment of ASOs to STMN2 locus is indicated. Salient features of the human gene highlighted including the splice acceptor site (teal), the putative coding region (yellow), the stop codon (red), the TDP-43 binding motifs (orange), and the poly-A signal (purple). ASOs highlighted in yellow had locked nucleic acid chemistry.

FIGS. 83A-83C examine the cryptic exon-containing region of STMN2 pre-mRNA. FIG. 83A provides the sequence of the cryptic exon-containing region of STMN2 pre-mRNA, with various salient features highlighted. FIGS. 83B-83C provide predicted RNA structures of the cryptic exon-containing region of STMN2 pre-mRNA, showing that the green highlighted region is partially unstructured and can adopt different binding interactions with similar energies.

FIGS. 84A-84D demonstrate patient specific induced pluripotent stem cell characterization. FIG. 84A provides a micrograph showing the undifferentiated patient iPS cells. FIG. 84B provides sequencing chromatogram of PCR product amplified from exon 8 of *TBK1* in the indicated iPS cell line confirming the heterozygous L306I non-pathological variant of no significance in the patient line. FIGS. 84C-84D provide micrographs showing the motor neurons differentiated from the patient iPS cells.

FIGS. 85A-85B demonstrate decreased nuclear TDP-43 observed in patient neurons. FIG. 85A provides representative micrographs of control and patient

neurons immunostained for TDP-43 (red), β-III tubulin (green) and counterstained with DAPI (blue) marking the nucleus. Scale bar, 100 μm. FIG. 85B provides Pearson's correlation analysis for TDP-43 immunostaining and DAPI fluorescence comparing control neurons to the patients. Dots represent individual cells and are displayed as mean with s.d. for at least 25 cells from n= 4 control and 1 patient lines (unpaired t test, two-sided, $P< 0.05$).

FIGS. 86A-86C demonstrate patient motor neurons produce truncated STMN2 in response to TDP-43 depletion. RNA levels analyzed by qRT-PCR analysis after TDP-43 knockdown by siTARDBP in motor neurons differentiated from patients iPS cells. FIG. 86A shows RNA levels of TDP-43. FIG. 86B shows RNA levels of full-length STMN2. FIG. 86C shows RNA levels of cryptic STMN2 compared to control (siCTRL).

FIGS. 87A-87C demonstrate patient STMN2 locus sequencing. FIG. 87A shows the sequencing results of PCR product amplified from the first intron of *STMN2* in the patient iPS cell line aligned to the reference sequence. FIG. 87B identifies one mismatch between the patient and the reference sequence consisting of a common single nucleotide variant (SNP). FIG. 87C provides a sequencing chromatogram of PCR product-amplified from the ASO-targeted region of first intron of *STMN2* confirms no heterozygous at this locus and highlights the match for the ASOs.

FIGS. 88A-88B demonstrate levels of cryptic and full length STMN2 RNA with SJ+94 ASO (SEQ ID NO: 73) in patient motor neurons. FIG. 88A shows cryptic STMN2 RNA levels. FIG. 88B shows full-length STMN2 RNA levels after TDP-43 reduction by siTARDP in patient's motor neurons. Neurons were cultured from left to right with 30, 3, 0.3, or 0.03 nM of the STMN2-targeting ASO (SJ+94) or a non-targeting control ASO (NTC).

FIG. 89 demonstrates full length STMN2 RNA is increased by ASO SJ+94 after its suppression due to nuclear depletion of TDP43 in patient's motor neurons. qRT-PCR analysis of full-length STMN2 after proteasome inhibition with MG-132 (1 μM) in patient's neurons, which induces nuclear depletion of the TDP-43, leads to decreased STMN2 expression. Full length STMN2 RNA is increased by ASO SJ+94 under these conditions when compared to those treated with a non-targeting control ASO (NTC).

FIGS. 90 demonstrates immunoblot analysis for STMN2 protein levels following reduction of TDP-43 by siRNA. Protein input was normalized by BCA and STMN2 levels are expressed relative to the levels in hMNs treated with control siRNAs. Data are displayed as mean with s.d. of technical replicates from $n = 3$ independent experiments (unpaired t test, two-sided, $P<0.05$).

FIGS. 91A-91E demonstrate outgrowth deficits following TDP-43 depletion can be rescued by STMN2 ASO SJ +94 in patient's motor neurons. FIG. 91A outlines the experimental strategy used to assess the cellular effect of STMN2 restoration in hMNs after axonal injury. FIG. 91B provides representative micrographs of patient's motor neurons in the microfluidics devices 18 hours after axotomy. Fields highlighted by red rectangles from NTC and SJ +94 are enlarged in the images (i) and (ii) respectively. FIG. 91C shows length of individual neurites displayed as dots along with the mean and standard deviation. (unpaired t test, two-sided). FIG. 91D provides representative micrographs of patient's motor neurons in the microfluidics devices 18 hours after axotomy. Fields highlighted by red rectangles from NTC and SJ-1 are enlarged in the images (i) and (ii) respectively. FIG. 91C shows lengths of individual neurites displayed as dots along with the mean and standard deviation. (unpaired t test, two-sided).

FIG. 92 demonstrates neurite outgrowth deficits following TDP-43 depletion can be rescued by STMN2 ASOs SJ-1, SJ+94, and SJ+101. Individual neurites are displayed as dots.

FIG. 93 demonstrates STMN2 can be restored in TDP-43 depleted neurons by STMN2 ASOs SJ-1, SJ+94, and SJ+101.

FIG. 94 demonstrates cry STMN2 can be reduced in TDP-43 depleted neurons by STMN2 ASOs SJ-1, SJ+94, and SJ+101.

FIGS. 95A-95B demonstrate levels of cryptic and full length STMN2 RNA with SJ-1 ASO in patient motor neurons. FIG. 95A shows cryptic STMN2 RNA levels. FIG. 95B shows full-length STMN2 RNA levels after TDP-43 reduction by siTARDBP (siTDP-43) in patient's motor neurons. Neurons were cultured from left to right with 30, 3, 0.3, or 0.03 nM of the STMN2-targeting ASO (SJ -1) or a non-targeting control ASO (NTC).

FIG. 96 demonstrates full length STMN2 RNA is increased by ASO SJ-1 after its suppression due to nuclear mis-localization of TDP3 in patient's motor neurons: qRT-PCR analysis of full-length STMN2 after proteasome inhibition with MG-132 (1

μM) in patient's neurons, which induces nuclear mis-localization of TDP-43, leads to decreased STMN2 expression. Full-length STMN2 RNA is increased by ASO SJ-1 under these conditions when compared to those treated with a non-targeting control ASO (NTC).

FIG. 97 demonstrates STMN2 protein levels measured by Western Blot in patient's motor neurons following reduction of TDP-43 by siRNA. Protein loading was normalized by total protein content and STMN2 levels are expressed relative to the levels in hMNs treated with control siCTRLs. Data are displayed as mean with s.d. of technical replicates from $n = 3$ independent experiments. The p values for the increase in STMN2 levels induced by SJ-1, SJ+94 and SJ+101 as compared to the non-targetting controls (NTC) are indicated above each result. The increase is significant in each case (unpaired t test, two-sided, $P < 0.05$).

DETAILED DESCRIPTION OF THE INVENTION

Mislocalization or depletion of the RNA-binding protein TDP-43 results in decreased expression of STMN2, which encodes a microtubule regulator. STMN2 is essential for normal axonal outgrowth and regeneration. Decreased TDP-43 function causes an abortive or altered STMN2 RNA sequence which results in reduced STMN2 protein expression. STMN2 may be a promising therapeutic target and biomarker of disease risk (e.g., neurodegenerative diseases).

Work described herein relates to compositions and methods for suppressing or preventing the inclusion of a cryptic exon in STMN2 mRNA. The inclusion of a cryptic exon in STMN2 mRNA may lead to a truncated transcript and protein. In some aspects the inclusion of the cryptic exon leads to early polyadenylation. STMN2 expression may be restored through suppression of a cryptic splicing form of STMN2 that occurs when TDP-43 becomes sequestered or is reduced in functionality, such as by blocking the occurrence or accumulation of the cryptic form and converting it back to or restoring functional STMN2 RNA (e.g., by administration of an antisense oligonucleotide). In addition, work described herein relates to compositions and methods for increasing protein synthesis of STMN2, i.e., increasing STMN2 protein expression.

Agents and Pharmaceutical Compositions

The disclosure contemplates agents (e.g., antisense oligonucleotides) that specifically bind an STMN2 mRNA, pre-mRNA, or nascent RNA sequence that occurs and increases in abundance when TDP-43 function declines or TDP-pathology occurs, thereby suppressing or preventing inclusion of an abortive or altered STMN2 RNA sequence. In some aspects, agents prevent degradation of STMN2 protein. In some aspects, agents restore STMN2 protein levels. In some aspects, an agent suppresses or prevents inclusion of a cryptic exon in STMN2 RNA. In certain aspects an agent specifically binds an STMN2 mRNA, pre-mRNA, or nascent RNA sequence coding for a cryptic exon.

In some aspects, the disclosure further contemplates agents (e.g., antisense oligonucleotides) that specifically bind an ELAVL3 mRNA, pre-mRNA, or nascent RNA sequence. ELAVL3 may be downregulated when TDP-43 function declines or TDP-pathology occurs. In some aspects, an agent suppresses or prevents cryptic splicing of ELAVL3.

In some embodiments, the agent (e.g., an antisense oligonucleotide) binds to an STMN2 RNA sequence (e.g., an abortive or altered STMN2 RNA sequence). In some aspects the binding of an agent to a short abortive or altered STMN2 RNA sequence results in continued production by the RNA polymerase. For example, the agent may directly suppress premature transcriptional termination at the polyadenylation site of the cryptic exon or may mimic the activity of TDP-43 binding at its target site, thereby altering transcriptional termination at the cryptic exon. In some aspects, the agent suppresses or prevents inclusion of a cryptic exon in STMN2 RNA. In some aspects the agent prevents degradation of STMN2 protein. In some aspects the agent increases STMN2 levels (e.g., through exon skipping). In some aspects the agent restores normal length or protein coding STMN2 RNA (e.g., pre-mRNA or mRNA). In some aspects the agent increases the amount or activity of STMN2 RNA. In some aspects the agent increases protein expression of STMN2.

The terms “increased” or “increase” are used herein to generally mean an increase by a statically significant amount; for the avoidance of any doubt, the terms “increased”, or “increase” means an increase of at least 10% as compared to a reference level, for example an increase of at least about 20%, or at least about 30%, or at least about 40%, or at least about 50%, or at least about 60%, or at least about 70%, or at least about 80%, or at least about 90%, or up to and including a 100% increase or any increase between 10-100% as compared to a reference level, or at

least about a 2-fold, or at least about a 3-fold, or at least about a 4-fold, or at least about a 5-fold, or at least about a 10-fold increase, or any increase between 2-fold and 10-fold or greater as compared to a reference level.

In some aspects the agent increases the amount or activity of STMN2 RNA by at least about 2-fold, at least about 3-fold, at least about 4-fold, at least about 5-fold, at least about 6-fold, at least about 7-fold, at least about 8-fold, at least about 9-fold, or at least about 10-fold. In some aspects the agent increases STMN2 protein expression by at least about 2-fold, at least about 3-fold, at least about 4-fold, at least about 5-fold, at least about 6-fold, at least about 7-fold, at least about 8-fold, at least about 9-fold, or at least about 10-fold.

In some embodiments an agent (e.g., an antisense oligonucleotide) targets one or more sites, for example, a 5' splice site, a 3' splice site, a normal binding site, and/or a polyadenylation site of the STMN2 transcript. In some aspects an agent targets one or more sites for example a site proximal to a 5' splice site, a site proximal to a 3' splice site, a site proximal to a normal binding site, and/or a site proximal to a polyadenylation of the STMN2 transcript. In certain embodiments an agent targets one or more sites including a 5' splice site regulated by TDP-43, a TDP-43 normal binding site, and/or a cryptic polyadenylation site. In some embodiments, an agent targets a single stranded site. In certain embodiments, an agent targets a single stranded region located between the TDP-43 binding site and the polyadenylation site. In some embodiments, the agent targets a site proximal to a cryptic splice site. In some embodiments, the agent targets a site proximal to a premature polyadenylation site. In some embodiments, the agent targets a region located between the cryptic splice site and the premature polyadenylation site. In some embodiments the agent does not target or bind to the polyadenylation site. In some embodiments the agent does not target or bind to the polyadenylation site of the STMN2 transcript. In some embodiments the agent does not target or bind to the cryptic polyadenylation site. In some aspects an agent targets and promotes the splicing of STMN2 Exon 2 to Exon 1.

STMN2 Exon 1 may have a sequence of:

AGCTCCTAGGAAGCTTCAGGGCTTAAAGCTCCACTCTACTTGGACTGTACT
ATCAGGCCCCCAAAATGGGGGGAGCCGACAGGGAAGGACTGATTTCCATT
TCAAACTGCATTCTGGTACTTTGTACTCCAGCACCATTGGCCGATCAATAT
TTAATGCTTGGAGATTCTGACTCTGCGGGAGTCATGTCAGGGGACCTTGG
GAGCCAATCTGCTTGAGCTTCTGAGTGATAATTATTCATGGGCTCCTGCCT

CTTGCTCTTTCTCTAGCACGGTCCCACTCTGCAGACTCAGTGCCTTATTCA
GTCTTCTCTCTCGCTCTCTCCGCTGCTGTAGCCGGACCCTTTGCCTTCGCCA
CTGCTCAGCGTCTGCACATCCCTACAATGGCTAAAACAGCAATGGGACTC
GGCAGAAGACCTTCGAGAGAAAGGTAGAAAATAAGAATTTGGCTCTCTGT
GTGAGCATGTGTGCGTGTGTGCGAGAGAGAGAGACAGACAGCCTGCCTAA
GAAGAAATGAATGTGAATGCGGCTTGTGGCACAGTTGACAAGGATGATAA
ATCAATAATGCAAGCTTACTATCATTTATGAATAGC (SEQ ID NO: 1).

STMN2 Exon 2 may have a sequence of:
CCTACAAGGAAAAAATGAAGGAGCTGTCCATGCTGTCACTGATCTGCTCT
TGCTTTTACCCGGAACCTCGCAACATCAACATCTATACTTACGATGG (SEQ ID NO: 2).

A cryptic exon may have a sequence of:
GACTCGGCAGAAGACCTTCGAGAGAAAGGTAGAAAATAAGAATTTGGCT
CTCTGTGTGAGCATGTGTGCGTGTGTGCGAGAGAGAGAGACAGACAGCCT
GCCTAAGAAGAAATGAATGTGAATGCGGCTTGTGGCACAGTTGACAAGGA
TGATAAATCAATAATGCAAGCTTACTATCATTTATGAATAGC (SEQ ID NO: 3).

Exemplary types of agents that can be used include small organic or inorganic molecules; saccharines; oligosaccharides; polysaccharides; a biological macromolecule selected from the group consisting of peptides, proteins, peptide analogs and derivatives; peptidomimetics; nucleic acids selected from the group consisting of siRNAs, shRNAs, antisense RNAs, ribozymes, and aptamers; an extract made from biological materials selected from the group consisting of bacteria, plants, fungi, animal cells, and animal tissues; naturally occurring or synthetic compositions; antibodies; and any combination thereof.

In some embodiments the agent is an oligonucleotide, protein, or a small molecule. In some embodiments the agent comprises one or more oligonucleotides. In some aspects the oligonucleotide is a splice-switching oligonucleotide. In certain aspects the oligonucleotide is an antisense oligonucleotide (ASO). In some embodiments the agent is not an antisense oligonucleotide. In some embodiments the agent is a small molecule (e.g., Branaplam (Novartis) or Risdiplam (Roche)) capable of binding to the target site (e.g., the STMN2 transcript) and shifting the metabolism of the target.

In some embodiments the agent is an oligonucleotide, protein, or a small molecule. In some embodiments the agent comprises one or more oligonucleotides. Agents comprising multiple oligonucleotides may be considered multimeric compounds. In some aspects the agent comprises one or more copies of an oligonucleotide. In some aspects the agent comprises one or more copies of multiple oligonucleotides. In some aspects, multiple oligonucleotides may be covalently linked. In some aspects the oligonucleotide is a splice-switching oligonucleotide. In certain aspects the oligonucleotide is an antisense oligonucleotide (ASO). In some embodiments the agent is a small molecule (e.g., Branaplam (Novartis) or Risdiplam (Roche)) capable of binding to the target site (e.g., the STMN2 transcript) and shifting the metabolism of the target. In some aspects the agent does not exhibit toxicity, e.g., platelet toxicity.

An agent may target one or more of a 5' splice site, a 3' splice site, a normal binding site, or a polyadenylation site. In some aspects an agent targets one or more of a site proximal to a 5' splice site, a site proximal to a 3' splice site, a site proximal to a normal binding site, and/or a site proximal to a polyadenylation of the STMN2 transcript. In some embodiments, the agent targets a site proximal to a cryptic splice site. In some embodiments, the agent targets a site proximal to a premature polyadenylation site. In some embodiments, the agent targets a single stranded region of the STMN2 transcript. In some embodiments, the agent targets a single stranded region located between the TDP-43 binding site and the polyadenylation site. In some embodiments, the agent targets a region located between the cryptic splice site and the premature polyadenylation site. In some aspects the polyadenylation site is the polyadenylation site of the STMN2 transcript. In some aspects the polyadenylation site is the polyadenylation site of the cryptic exon (e.g., is a cryptic polyadenylation site). In some embodiments an agent does not target a 5' splice site (e.g., a TDP-43 5' splice site). In some embodiments an agent does not target a normal binding site (e.g., a normal TDP-43 binding site). In some embodiments an agent does not target a polyadenylation site (e.g., a cryptic polyadenylation site). In some aspects, a

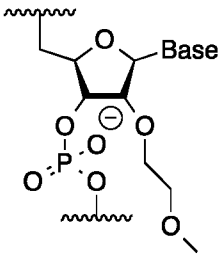
In certain embodiments an antisense oligonucleotide may target one or more of a 5' splice site, a 3' splice site, a normal binding site, or a polyadenylation site. In some embodiments an antisense oligonucleotide does not target a 5' splice site (e.g., a TDP-43 5' splice site). In certain aspects an antisense oligonucleotide targets one or more of a site proximal to a 5' splice site, a site proximal to a 3' splice site, a site

proximal to a normal binding site, and/or a site proximal to a polyadenylation of the STMN2 transcript. In some embodiments an antisense oligonucleotide targets a single stranded region of the STMN2 transcript. In certain embodiments, the antisense oligonucleotide targets a single stranded region located between the TDP-43 binding site and the polyadenylation site. In some embodiments, the antisense oligonucleotide targets a site proximal to a cryptic splice site, e.g., targets a site -1 of a cryptic splice site. In some embodiments, the antisense oligonucleotide targets a site proximal to a premature polyadenylation site. In some embodiments, the antisense oligonucleotide targets a region located between the cryptic splice site and the premature polyadenylation site. In some aspects, the antisense oligonucleotide targets a region +90 to +105, or more specifically +94 or +101, relative to a cryptic splice junction. In some embodiments an antisense oligonucleotide does not target a normal binding site (e.g., a normal TDP-43 binding site). In some embodiments an antisense oligonucleotide does not target a polyadenylation site (e.g., a cryptic polyadenylation site).

In certain embodiments an antisense oligonucleotide comprises a sequence selected from the group consisting of SEQ ID NOS: 37-85. In some embodiments an antisense oligonucleotide comprises a sequence selected from the group consisting of SEQ ID NOS: 37-74. In some aspects, the antisense oligonucleotide comprises a sequence selected from the group consisting of: SEQ ID NO: 40, SEQ ID NO: 47, SEQ ID NO: 48, SEQ ID NO: 49, SEQ ID NO:50, SEQ ID NO: 52, SEQ ID NO: 53, SEQ ID NO: 54, SEQ ID NO: 56, and SEQ ID NO: 78. In certain aspects, the antisense oligonucleotide comprises SEQ ID NO: 52. In some embodiments, the antisense oligonucleotide comprises a sequence selected from the group consisting of SEQ ID NO: 53, SEQ ID NO: 72, and SEQ ID NO: 73. In one embodiment, the antisense oligonucleotide comprises SEQ ID NO: 73. In one embodiment, the antisense oligonucleotide comprises SEQ ID NO: 53. In one embodiment, the antisense oligonucleotide comprises SEQ ID NO: 72.

Table 1 provides a listing of exemplary antisense oligonucleotides, and in some instances, the corresponding target site within the STMN2 intron. The underlined bases within SEQ ID NOS: 93-108 represent bases flanking the cryptic splice site. The underlined bases within SEQ ID NOS: 112-114 represent the binding site of TDP-43 protein. The oligonucleotides described herein were synthesized with multiple chemical modifications. For example, the antisense oligonucleotides of SEQ

ID NOS: 37-74 were made fully modified with MOE sugars having the following structure:



and phosphorothioate linkages. Additional modifications may also be tested.

Table 1: Oligonucleotides

Name	Oligo sequence	Target site
SJ-24	TATGAATATAATTTTAAA (SEQ ID NO: 37)	TTTAAAATTATATTCATA (SEQ ID NO: 91)
SJ-20	GCAATATGAATATAATTT (SEQ ID NO: 38)	AAATTATATTCATATTGC (SEQ ID NO: 92)
SJ-18	CTGCAATATGAATATAAT (SEQ ID NO: 39)	ATTATATTCATATTGCAG (SEQ ID NO: 93)
SJ-16	TC CTGCAATATGAATATA (SEQ ID NO: 40)	TATATTCATATTGCAG GA (SEQ ID NO: 94)
SJ-14	AGTC CTGCAATATGAATA (SEQ ID NO: 41)	TATTCATATTGCAG GACT (SEQ ID NO: 95)
SJ-13	GAGTC CTGCAATATGAAT (SEQ ID NO: 42)	ATTCATATTGCAG GACTC (SEQ ID NO: 96)
SJ-12	CGAGTC CTGCAATATGAA (SEQ ID NO: 43)	TTCATATTGCAG GACTCG (SEQ ID NO: 97)
SJ-10	GCCGAGTC CTGCAATATG (SEQ ID NO: 44)	CATATTGCAG GACTCGGC (SEQ ID NO: 98)
SJ-9	TGCCGAGTC CTGCAATAT (SEQ ID NO: 45)	ATATTGCAG GACTCGGCA (SEQ ID NO: 99)
SJ-8	CTGCCGAGTC CTGCAATA (SEQ ID NO: 46)	TATTGCAG GACTCGGCAG (SEQ ID NO: 100)
SJ-7	TCTGCCGAGTC CTGCAAT (SEQ ID NO: 47)	ATTGCAG GACTCGGCAGA (SEQ ID NO: 101)
SJ-6	TTCTGCCGAGTC CTGCAA (SEQ ID NO: 48)	TTGCAG GACTCGGCAGAA (SEQ ID NO: 102)
SJ-5	CTTCTGCCGAGTC CTGCA (SEQ ID NO: 49)	TGCAG GACTCGGCAGAAG (SEQ ID NO: 103)
SJ-4	TCTTCTGCCGAGTC CTGC (SEQ ID NO: 50)	GCAG GACTCGGCAGAAGA (SEQ ID NO: 104)
SJ-3	GTCTTCTGCCGAGTC CTG (SEQ ID NO: 51)	CAG GACTCGGCAGAAGAC (SEQ ID NO: 105)
SJ-2	GGTCTTCTGCCGAGTC CT (SEQ ID NO: 52)	AG GACTCGGCAGAAGACC (SEQ ID NO: 106)
SJ-1	AGGTCTTCTGCCGAGTC C (SEQ ID NO: 53)	G GACTCGGCAGAAGACCT (SEQ ID NO: 107)
SJ+1	AAGGTCTTCTGCCGAGTC	GACTCGGCAGAAGACCTT

	(SEQ ID NO: 54)	(SEQ ID NO: 108)
SJ+3	CGAAGGTCTTCTGCCGAG (SEQ ID NO: 55)	CTCGGCAGAAGACCTTCG (SEQ ID NO: 109)
SJ+6	TCTCGAAGGTCTTCTGCC (SEQ ID NO: 56)	GGCAGAAGACCTTCGAGA (SEQ ID NO: 110)
SJ+25	ATTCTTATTTTCTACCTTT (SEQ ID NO: 57)	AAAGGTAGAAAATAAGAAT (SEQ ID NO: 111)
SJ+45	CATGCTCACACAGAGAGCCA (SEQ ID NO: 58)	TGGCTCTCTGTGTGAGCATG (SEQ ID NO: 112)
SJ+47	CACATGCTCACACAGAGAGC (SEQ ID NO: 59)	GCTCTCTGTGTGAGCATGTG (SEQ ID NO: 113)
SJ+53	CACACACGCACACATGCTCACACA (SEQ ID NO: 60)	TGTGTGAGCATGTGTGCGTGTGTG (SEQ ID NO: 114)
SJ+2	GAAGGTCTTCTGCCGAGT (SEQ ID NO: 61)	
SJ+4	TCGAAGGTCTTCTGCCGA (SEQ ID NO: 62)	
SJ+5	CTCGAAGGTCTTCTGCCG (SEQ ID NO: 63)	
SJ-2 (17)	GTCTTCTGCCGAGTCCT (SEQ ID NO: 64)	
SJ-2 (19)	AGGTCTTCTGCCGAGTCCT (SEQ ID NO: 65)	
SJ-2 (20)	AAGGTCTTCTGCCGAGTCCT (SEQ ID NO: 66)	
SJ+189	TTTAATTTCTTCAGTATTGC (SEQ ID NO: 67)	
SJ+168	TATTCATAAATGATAGTAAGC (SEQ ID NO: 68)	
SJ+184	TTTAATTTCTTCAGTATTGCTATTC (SEQ ID NO: 69)	
SJ+159	ATAAATGATAGTAAGCTTGCATTAT (SEQ ID NO: 70)	
SJ+206	GAGACAGCAATCTTTTGTTTT (SEQ ID NO: 71)	
SJ+101	TTCACATTCATTTCTTCTTAG (SEQ ID NO: 72)	
SJ+94 (20)	CATTTCTTCTTAGGCAGGCT (SEQ ID NO: 73)	
SJ+94 (28)	TTCACATTCATTTCTTCTTAGGCAGGCT (SEQ ID NO: 74)	
LNA-SJ-16	T+CCT+GCA+ATA+TGA+ATA+TA (SEQ ID NO: 75)	
LNA-SJ-13	G+AGT+CCT+GCA+ATA+TGA+AT (SEQ ID NO: 76)	
LNA-SJ-10	G+CCG+AGT+CCT+GCA+ATA+TG (SEQ ID NO: 77)	
LNA-SJ-8	C+TGC+CGA+GTC+CTG+CAA+TA (SEQ ID NO: 78)	

LNA-SJ-6	T+TCT+GCC+GAG+TCC+TGC+AA (SEQ ID NO: 79)	
LNA-SJ-4	T+CTT+CTG+CCG+AGT+CCT+GC (SEQ ID NO: 80)	
LNA-SJ-2	G+GTC+TTC+TGC+CGA+GTC+CT (SEQ ID NO: 81)	
LNA-SJ+6	T+CTC+GAA+GGT+CTT+CTG+CC (SEQ ID NO: 82)	
LNA SJ+189	+T+TTAAT+TTCTTCAG+TAT+TG+C (SEQ ID NO: 83)	
LNA SJ+168	+TA+TTCATAAA+TGA+TAG+TAAG+C (SEQ ID NO: 84)	
LNA SJ+206	GAGA+CAG+CAAT+CTT+TTGTTT+T (SEQ ID NO: 85)	
nusinersen	TCACTTTCATAATGCTGG (SEQ ID NO: 86)	
NTC	CCTATAGGACTATCCAGGAA (SEQ ID NO: 87)	
tofersen	CAGGATACATTTCTACAGCT (SEQ ID NO: 88)	
TDP-43 ASO	AAGGCTTCATATTGTACTTT (SEQ ID NO: 89)	
NC5	GCGACTATACGCGCAATATG (SEQ ID NO: 90)	

Oligonucleotides (e.g., antisense oligonucleotides) may be designed to bind mRNA regions that prevent ribosomal assembly at the 5' cap, prevent polyadenylation during mRNA maturation, or affect splicing events (Bennett and Swayze, *Annu. Rev. Phamacol. Toxicol.*, 2010; Watts and Corey, *J. Pathol.*, 2012; Kole et al., *Nat. Rev. Drug Discov.*, 2012; Saleh et al, *In Exon Skipping: Methods and Protocols*, 2012, each incorporated herein by reference). In some aspects, an oligonucleotide (e.g., an antisense oligonucleotide) is designed to target one or more sites including, for example, the 5' TDP-3 splice site or the TDP-43 normal binding site. In some aspects, the oligonucleotide targets one or more splice sites. In some aspects, the oligonucleotide targets one or more of the 5' splice site regulated by TDP-43 or the TDP-43 normal binding site. In some aspects, an antisense oligonucleotide is designed to not target a polyadenylation site (e.g., a cryptic polyadenylation site). In some aspects, the oligonucleotide targets an unstructured region located between the cryptic splice site and the polyadenylation site (see FIG. 83).

Antisense oligonucleotides are small sequences of DNA (e.g., about 8-50 base pairs in length) able to target RNA transcripts by Watson-Crick base pairing, resulting in reduced or modified protein expression. Oligonucleotides are composed of a phosphate backbone and sugar rings. In some embodiments oligonucleotides are unmodified. In other embodiments oligonucleotides include one or more modifications, e.g., to improve solubility, binding, potency, and/or stability of the antisense oligonucleotide. Modified oligonucleotides may comprise at least one modification relative to unmodified RNA or DNA. In some embodiments, oligonucleotides are modified to include internucleoside linkage modifications, sugar modifications, and/or nucleobase modifications. Examples of such modifications are known to those of skill in the art.

In some embodiments the oligonucleotide is modified by the substitution of at least one nucleotide with a modified nucleotide, such that in vivo stability is enhanced as compared to a corresponding unmodified oligonucleotide. In some aspects, the modified nucleotide is a sugar-modified nucleotide. In another aspect, the modified nucleotide is a nucleobase-modified nucleotide.

In some embodiments, oligonucleotides, may contain at least one modified nucleotide analogue. The nucleotide analogues may be located at positions where the target-specific activity, e.g., the splice site selection modulating activity is not substantially affected, e.g., in a region at the 5′-end and/or the 3′-end of the oligonucleotide molecule. In some aspects, the ends may be stabilized by incorporating modified nucleotide analogues.

In some aspects preferred nucleotide analogues include sugar- and/or backbone-modified ribonucleotides (i.e., include modifications to the phosphate-sugar backbone). For example, the phosphodiester linkages of a ribonucleotide may be modified to include at least one of a nitrogen or sulfur heteroatom. In preferred backbone-modified ribonucleotides the phosphoester group connecting to adjacent ribonucleotides is replaced by a modified group, e.g., of phosphothioate group. In preferred sugar-modified ribonucleotides, the 2′ OH-group is replaced by a group selected from H, OR, R, halo, SH, SR, NH2, NHR, NR2 or ON, wherein R is C1-C6 alkyl, alkenyl or alkynyl and halo is F, Cl, Br or I.

In some embodiments, modified oligonucleotides comprise one or more modified nucleosides comprising a modified sugar moiety. In some embodiments, modified oligonucleotides comprise one or more modified nucleosides comprising a

modified nucleobase. In some embodiments, modified oligonucleotides comprise one or more modified internucleoside linkages. In certain embodiments, modified oligonucleotides comprise at least two of: one or more modified nucleosides comprising a modified sugar moiety, one or more modified nucleosides comprise a modified nucleobase, and one or more modified internucleoside linkages. In certain embodiments, modified oligonucleotides comprise one or more modified nucleosides comprising a modified sugar moiety, one or more modified nucleosides comprise a modified nucleobase, and one or more modified internucleoside linkages.

Sugar modifications

In some embodiments, modified sugar moieties are non-bicyclic modified sugar moieties. In some embodiments, modified sugar moieties are bicyclic or tricyclic sugar moieties. In some embodiments, modified sugar moieties are sugar surrogates. Such sugar surrogates may comprise one or more substitutions corresponding to those of other types of modified sugar moieties.

In some embodiments, modified sugar moieties are non-bicyclic modified sugar moieties comprising a furanosyl ring with one or more substituent groups none of which bridges two atoms of the furanosyl ring to form a bicyclic structure. Such non bridging substituents may be at any position of the furanosyl, including but not limited to substituents at the 2', 4', and/or 5' positions. In certain embodiments one or more non-bridging substituent of non-bicyclic modified sugar moieties is branched.

In some embodiments, modified sugar moieties comprise a substituent that bridges two atoms of the furanosyl ring to form a second ring, resulting in a bicyclic sugar moiety. In some aspects the bicyclic sugar moiety comprises a bridge between the 4' and 2' furanose ring atoms.

In some aspects bicyclic sugar moieties and nucleosides incorporating such bicyclic sugar moieties are further defined by isomeric configurations. In some embodiments, an LNA nucleoside is in the α-L configuration. In some embodiments, an LNA nucleoside is in the β-D configuration.

In some embodiments an oligonucleotide modification includes Locked Nucleic Acids (LNAs) in which the 2′-hydroxyl group is linked to the 3′ or 4′ carbon atom of the sugar ring thereby forming a bicyclic sugar moiety. The linkage is preferably a methelyne (—CH2—)n group bridging the 2′ oxygen atom and the 4′ carbon atom wherein n is 1 or 2. LNAs and preparation thereof are described in WO

98/39352 and WO 99/14226, the entire contents of which are incorporated by reference herein.

In some embodiments, modified sugar moieties comprise one or more non-bridging sugar substituent and one or more bridging sugar substituent (e.g., 5'-substituted and 4'-2' bridged sugars).

In some embodiments, modified sugar moieties are sugar surrogates. In some aspects the oxygen atom of the sugar moiety is replaced, e.g., with a sulfur, carbon, or nitrogen atom. In some aspects such modified sugar moieties also comprise bridging and/or non-bridging substituents as described herein. In some aspects sugar surrogates comprise rings having other than 5 atoms. In certain aspects a sugar surrogate comprises a six-membered tetrahydropyran (THP). In some aspects sugar surrogates comprise acyclic moieties.

Nucleobase modifications

Modified oligonucleotides may comprise one or more nucleosides comprising an unmodified nucleobase. In some embodiments modified oligonucleotides comprise one or more nucleosides comprising a modified nucleobase. In some embodiments, modified oligonucleotides comprise one or more nucleosides that does not comprise a nucleobase.

In certain embodiments, modified nucleobases are selected from: 5-substituted pyrimidines, 6-azapyrimidines, alkyl or alkynyl substituted pyrimidines, alkyl substituted purines, and N-2, N-6 and 0-6 substituted purines. In certain embodiments, modified nucleobases are selected from: 2-aminopropyladenine, 5 -hydroxymethyl cytosine, xanthine, hypoxanthine, 2-aminoadenine, 6-N-methylguanine, 6-N-methyladenine, 2-propyladenine , 2-thiouracil, 2-thiothymine and 2-thiocytosine, 5-propynyl (-C°C-C]¾) uracil, 5-propynylcytosine, 6-azouracil, 6-azocytosine, 6-azothymine, 5-ribosyluracil (pseudouracil), 4-thiouracil, 8-halo, 8-amino, 8-thiol, 8-thioalkyl, 8-hydroxyl, 8-aza and other 8-substituted purines, 5-halo, particularly 5-bromo, 5-trifluoromethyl, 5-halouracil, and 5-halocytosine, 7-methylguanine, 7-methyladenine, 2-F-adenine, 2-aminoadenine, 7-deazaguanine, 7-deazaadenine, 3-deazaguanine, 3-deazaadenine, 6-N-benzoyladenine, 2-N-isobutyrylguanine, 4-N-benzoylcytosine, 4-N-benzoyluracil, 5-methyl 4-N-benzoylcytosine, 5-methyl 4-N-benzoyluracil, universal bases, hydrophobic bases, promiscuous bases, size-expanded bases, and fluorinated bases. Further modified nucleobases include tricyclic pyrimidines, such as l,3-diazaphenoxazine-2-one, l,3-diazaphenothiazine-2-one and 9-

(2-aminoethoxy)-l,3-diazaphenoxazine-2-one (G-clamp). Modified nucleobases may also include those in which the purine or pyrimidine base is replaced with other heterocycles, for example 7-deaza-adenine, 7-deazaguanosine, 2-aminopyridine and 2-pyridone.

Also preferred are nucleobase-modified ribonucleotides, i.e., ribonucleotides, containing at least one non-naturally occurring nucleobase instead of a naturally occurring nucleobase. Examples of modified nucleobases include, but are not limited to, uridine and/or cytidine modifications at the 5-position, e.g., 5-(2-amino)propyl uridine, 5-bromo uridine; adenosine and/or guanosines modified at the 8 position, e.g., 8-bromo guanosine; deaza nucleotides, e.g., 7-deaza-adenosine; O- and N-alkylated nucleotides, e.g., N6-methyl adenosine. Oligonucleotide reagents of the invention also may be modified with chemical moieties that improve the in vivo pharmacological properties of the oligonucleotide reagents.

Internucleoside modifications

In some embodiments, nucleosides of modified oligonucleotides are linked together using any internucleoside linkage. The two main classes of internucleoside linking groups are defined by the presence or absence of a phosphorous atom. Representative phosphorus-containing internucleoside linkages include but are not limited to phosphates, which contain a phosphodiester bond ("P=O") (also referred to as unmodified or naturally occurring linkages), phosphotriesters, methylphosphonates, phosphoramidates, and phosphorothioates ("P=S"), and phosphorodithioates ("HS-P=S"). Representative non-phosphorus containing internucleoside linking groups include but are not limited to methylenemethylimino (-CH_2-N(CH_3)-O-CH_2-), thiodiester, thionocarbamate (-O-C(=O)(NH)-S-); siloxane (-O-SiH_2-O-); and N,N'-dimethylhydrazine (-CH_2-N(CH_3)-N(CH_3)-). Modified internucleoside linkages, compared to naturally occurring phosphate linkages, can be used to alter, typically increase, nuclease resistance of the oligonucleotide. In certain embodiments, internucleoside linkages having a chiral atom can be prepared as a racemic mixture, or as separate enantiomers. Methods of preparation of phosphorous-containing and non-phosphorous-containing internucleoside linkages are well known to those skilled in the art.

Additional modifications are known by those of skill in the art and examples can be found in WO 2019/241648, US 10,307,434, US 9,045,518, and US 10,266,822, each of which is incorporated herein by reference.

Oligonucleotides may be of any size and/or chemical composition sufficient to target the abortive or altered STMN2 RNA. In some embodiments, an oligonucleotide is between about 5-300 nucleotides or modified nucleotides. In some aspects an oligonucleotide is between about 10-100, 15-85, 20-70, 25-55, or 30-40 nucleotides or modified nucleotides. In certain aspects an oligonucleotide is between about 15-35, 15-20, 20-25, 25-30, or 30-35 nucleotides or modified nucleotides.

In some embodiments, an oligonucleotide and the target RNA sequence (e.g., the abortive or altered STMN2 RNA) have 100% sequence complementarity. In some aspects an oligonucleotide may comprise sequence variations, e.g., insertions, deletions, and single point mutations, relative to the target sequence. In some embodiments, an oligonucleotide has at least 70% sequence identity or complementarity to the target RNA (e.g., STMN2 mRNA, pre-mRNA, or nascent RNA). In certain embodiments, an oligonucleotide has at least 70%, 75%, 80%, 85%, 90%, 95%, 97%, 99%, or 100% sequence identity to the target sequence.

An antisense oligonucleotide targeting the abortive or altered STMN2 RNA sequence (e.g., STMN2 mRNA, pre-mRNA, or nascent RNA sequence) may be designed by any methods known to those of skill in the art. In certain aspects one or more oligonucleotides are synthesized.

In some embodiments, STMN2 is administered as a gene therapy. In some embodiments STMN2 is administered in combination with an agent described herein.

In some embodiments an agent is an inhibitor of c-Jun N-terminal kinase (JNK). In some aspects a JNK inhibitor is selected from the group consisting of small organic or inorganic molecules; saccharines; oligosaccharides; polysaccharides; a biological macromolecule selected from the group consisting of peptides, proteins, peptide analogs and derivatives; peptidomimetics; nucleic acids selected from the group consisting of siRNAs, shRNAs, antisense RNAs, ribozymes, and aptamers; an extract made from biological materials selected from the group consisting of bacteria, plants, fungi, animal cells, and animal tissues; naturally occurring or synthetic compositions; antibodies; and any combination thereof. In certain aspects the agent is a small molecule inhibitor, an oligonucleotide (e.g., designed to reduce expression of JNK), or a gene therapy (e.g., designed to inhibit JNK). In some aspects inhibition of JNK restores or increases STMN2 protein levels. In certain embodiments the agent is an oligonucleotide (e.g., an antisense oligonucleotide) targeting JNK.

The disclosure further contemplates pharmaceutical compositions comprising the agent (e.g., the antisense oligonucleotide) that binds an abortive or altered STMN2 RNA sequence. In some embodiments, the pharmaceutical composition comprises the agent that binds an STMN2 mRNA, pre-mRNA, or nascent RNA sequence coding for a cryptic exon. In some embodiments pharmaceutical compositions comprise the agent that prevents degradation of an STMN2 protein. In some embodiments pharmaceutical compositions comprise the agent that increases expression of STMN2 protein, e.g., activates STMN2 protein expression. In some aspects the composition comprises an oligonucleotide, protein, or small molecule. In some embodiments the composition comprises an oligonucleotide (e.g., an antisense oligonucleotide), wherein the oligonucleotide specifically binds an STMN2 mRNA, pre-mRNA, or nascent RNA sequence coding for a cryptic exon. In some aspects the agent (e.g., the antisense oligonucleotide) suppresses or prevents inclusion of a cryptic exon in STMN2 RNA. In some aspects the agent suppresses cryptic splicing.

In some embodiments, a pharmaceutical composition comprises an agent (e.g., an antisense oligonucleotide) that targets one or more sites, e.g., one or more splice sites, binding sites, or polyadenylation sites. In some embodiments, a pharmaceutical composition comprises an agent that targets one or more splice sites (e.g., 5' splice site regulated by TDP-43). In some embodiments, a pharmaceutical composition comprises an agent that targets a normal binding site (e.g., a TDP-43 normal binding site). In some embodiments, a pharmaceutical composition comprises an agent that targets a polyadenylation site (e.g., a cryptic polyadenylation site). In some embodiments, a pharmaceutical composition comprises an agent that targets a site proximal to a cryptic splice site or a site proximal to a polyadenylation site (e.g., a premature polyadenylation site). In some embodiments, a pharmaceutical composition comprises an agent that targets a site located between a cryptic splice site and a polyadenylation site. In some embodiments, a pharmaceutical composition comprises an agent that does not target one or more splice sites (e.g., 5' splice site regulated by TDP-43). In some embodiments, a pharmaceutical composition comprises an agent that does not target a normal binding site (e.g., a TDP-43 normal binding site). In some embodiments, a pharmaceutical composition comprises an agent that does not target a polyadenylation site (e.g., a cryptic polyadenylation site).

In some aspects a pharmaceutical composition comprises a multimeric compound, e.g., a compound comprising two or more antisense oligonucleotides. The

two or more antisense oligonucleotides may comprise two or more antisense oligonucleotides having the same sequence, or alternatively, may comprise two or more antisense oligonucleotides having different sequences. In some aspects, the two or more antisense oligonucleotides are covalently linked. In some aspects, a pharmaceutical composition comprises two or more antisense oligonucleotides. The two more antisense oligonucleotides may comprise a combination of multiple copies of the same antisense oligonucleotide and/or individual copies of multiple different antisense oligonucleotides.

In certain embodiments a pharmaceutical composition comprises an antisense oligonucleotide comprising a sequence selected from the group consisting of SEQ ID NOS: 37-85. In some embodiments, a pharmaceutical composition comprises an antisense oligonucleotide comprises a sequence selected from the group consisting of SEQ ID NOS: 37-74. In some aspects, the pharmaceutical composition comprises an antisense oligonucleotide comprising a sequence selected from the group consisting of: SEQ ID NO: 40, SEQ ID NO: 47, SEQ ID NO: 48, SEQ ID NO: 49, SEQ ID NO: 50, SEQ ID NO: 52, SEQ ID NO: 53, SEQ ID NO: 54, SEQ ID NO: 56, and SEQ ID NO: 78. In certain aspects, the pharmaceutical composition comprises antisense oligonucleotide comprising SEQ ID NO: 52. In some embodiments, the pharmaceutical composition comprises an antisense oligonucleotide comprising a sequence selected from the group consisting of SEQ ID NO: 53, SEQ ID NO: 72, and SEQ ID NO: 73. In certain embodiments, the pharmaceutical composition comprises an antisense oligonucleotide comprising SEQ ID NO: 73.

In some embodiments a pharmaceutical composition comprises an effective amount of an agent (e.g., an antisense oligonucleotide) that binds an STMN2 mRNA sequence coding for a cryptic exon and an effective amount of a second agent. In some aspects the second agent is an agent that treats or inhibits a neurodegenerative disorder. In some aspects the second agent is an agent that treats or inhibits a traumatic brain injury. In some aspects the second agent is an agent that treats or inhibits a proteasome inhibitor induced neuropathy.

In some embodiments a pharmaceutical composition comprises an effective amount of an agent (e.g., an antisense oligonucleotide) that binds to an abortive or altered STMN2 RNA sequence and an effective amount of STMN2 (e.g., administered as a gene therapy).

In some embodiments a pharmaceutical composition comprises an effective amount of a first agent (e.g., an antisense oligonucleotide) that binds to an abortive or altered STMN2 RNA sequence and a second agent that inhibits JNK.

In some embodiments a pharmaceutical composition comprises an effective amount of an agent (e.g., an antisense oligonucleotide) that binds an STMN2 mRNA, pre-mRNA, or nascent RNA sequence coding for a cryptic exon, an effective amount of a second agent, and a pharmaceutically acceptable carrier, diluent, or excipient.

The compositions comprising the agent (e.g., the antisense oligonucleotide) that binds to an abortive or altered STMN2 RNA sequence can be used for treating a disease or condition associated with a decline in TDP-43 function or a TDP-pathology. In some aspects the compositions comprising the agent (e.g., the antisense oligonucleotide) that binds to an abortive or altered STMN2 RNA sequence can be used for treating a disease or condition associated with mutant or reduced levels of STMN2 protein (e.g., in neuronal cells) as described herein.

Methods of Treatment

The disclosure contemplates various methods of treatment utilizing compositions comprising an agent (e.g., antisense oligonucleotide) that restores normal length or protein coding STMN2 RNA. In some aspects, an agent (e.g., an antisense oligonucleotide) specifically binds a STMN2 mRNA, pre-mRNA, or nascent RNA sequence that occurs and increases in abundance when TDP-43 function declines or TDP-pathology occurs, thereby suppressing or preventing inclusion of an abortive or altered STMN2 RNA sequence. In some aspects, the agent restores expression of a normal full-length or protein coding STMN2 RNA. In some aspects an agent suppresses or prevents inclusion of a cryptic exon in STMN2 RNA. In some aspects, an agent activates protein expression of STMN2.

In some aspects, the disclosure contemplates the treatment of any disease or condition in which the disease is associated with a decline in TDP-43 function or a TDP-pathology. In some embodiments, the inventions disclosed herein relate to methods of treating mutant or reduced levels of TDP-43 in neuronal cells (e.g., a disease or condition having a TDP-43 associated pathology). In some embodiments, the inventions disclosed herein relate to methods of treating TDP-43 associated dementias (e.g., ALS, FTD, Alzheimer's, Parkinson's, or TBI).

In some embodiments, the inventions disclosed herein relate to methods of treating a disease or condition associated with mutant, increased, or reduced levels of TDP-43. In some embodiments, the inventions disclosed herein relate to methods of treating a disease or condition associated with mislocalized TDP-43. In some embodiments the inventions disclosed herein relate to methods of treating a disease or condition associated with mutant or reduced levels of STMN2 protein and/or mislocalization of STMN2 protein. In some embodiments, the inventions disclosed herein relate to methods of treating a disease or condition associated with proteasome-inhibitor induced neuropathies (e.g., neuropathies occurring as a result of reduced amounts of functional nuclear TDP-43). In some embodiments, the inventions disclosed herein relate to methods of treating neurodegenerative disorders. In some embodiments, the inventions disclosed herein relate to methods of treating disorders or conditions associated with or occurring as a result of a TBI (e.g., a concussion).

In some aspects mutant or reduced levels of TDP-43 (e.g., nuclear TDP-43) results in mutant or reduced levels of STMN2 protein. Mislocalization of TDP-43 may result in increased levels of TDP-43 in the cytosol, but decreased levels of nuclear TDP-43. In addition, STMN2 levels may be decreased as a result of mutations in TDP-43. In some aspects mutant or increased levels of TDP-43 (e.g., nuclear TDP-43) results in mutant or reduced levels of STMN2 protein.

In some aspects methods of treatment comprise increasing levels of and/or preventing degradation or retardation of STMN2 protein. In some aspects methods of treatment comprise correcting mutant or reduced levels of STMN2 protein. In some aspects methods of treating comprise increasing the amount or activity of STMN2 RNA. In some aspects methods of treating comprise increasing the amount of STMN2 protein, e.g., increasing activation of protein expression. In some aspects methods of treatment comprise suppressing or preventing inclusion of a cryptic exon in STMN2 RNA (e.g., STMN2 mRNA). In some aspects methods of treatment comprise rescuing neurite outgrowth and axon regeneration.

In some embodiments methods of treatment comprise administering an effective amount of an agent (e.g., an antisense oligonucleotide) to a subject, wherein the agent prevents degradation of STMN2 protein. In some embodiments methods of treatment comprise administering an effective amount of an agent to a subject, wherein the agent restores normal length or protein coding STMN2 RNA. In some embodiments methods of treatment comprise administering an effective amount of an

agent to a subject, wherein the agent binds to an abortive or altered STMN2 RNA sequence. In some embodiments methods of treatment comprise administering an effective amount of an agent to a subject, wherein the agent suppresses or prevents inclusion of a cryptic exon in STMN2 RNA (e.g., in neuronal cells). In some aspects the agent increases STMN2 levels through exon skipping. In some aspects the agent is an oligonucleotide, protein, or small molecule. For example, the agent may be an oligonucleotide (e.g., an antisense oligonucleotide) that specifically binds an STMN2 mRNA, pre-mRNA or nascent RNA sequence coding for the cryptic exon.

In certain embodiments, methods of treatment comprise administering an effective amount an antisense oligonucleotide to a subject, wherein the antisense oligonucleotide comprises a sequence selected from the group consisting of SEQ ID NOs: 37-85. In some aspects, methods of treatment comprise administering an effective amount an antisense oligonucleotide to a subject, wherein the antisense oligonucleotide comprises a sequence selected from the group consisting of SEQ ID NOs: 37-74. In some embodiments, methods of treatment comprise administering an effective amount of an antisense oligonucleotide to a subject, wherein the antisense oligonucleotide comprises a sequence selected from the group consisting of SEQ ID NO: 40, SEQ ID NO: 47, SEQ ID NO: 48, SEQ ID NO: 49, SEQ ID NO: 50, SEQ ID NO: 52, SEQ ID NO: 53, SEQ ID NO: 54, SEQ ID NO: 56, and SEQ ID NO: 78. In some embodiments, methods of treatment comprise administering an effective amount of an antisense oligonucleotide to a subject, wherein the antisense oligonucleotide comprises SEQ ID NO: 52. In some embodiments, methods of treatment comprise administering an effective amount of an antisense oligonucleotide to a subject, wherein the antisense oligonucleotide comprises a sequence selected from the group consisting of SEQ ID NO: 53, SEQ ID NO: 72, and SEQ ID NO: 73. In some embodiments, methods of treatment comprise administering an effective amount of an antisense oligonucleotide to a subject, wherein the antisense oligonucleotide comprises SEQ ID NO: 73. In some embodiments, methods of treating a neurodegenerative disease or disorder (e.g., ALS, FTD, Alzheimer's, Parkinson's, or TBI) comprises administering to a subject an antisense oligonucleotide comprising a sequence selected from the group consisting of SEQ ID NOS: 37-85, or alternatively from the group consisting of SEQ ID NOS: 37-74. In some embodiments, methods of treating a neurodegenerative disease or disorder (e.g., ALS, FTD, Alzheimer's, Parkinson's, or TBI) comprises administering to a subject an antisense

oligonucleotide comprising a sequence selected from the group consisting of SEQ ID NO: 40, SEQ ID NO: 47, SEQ ID NO: 48, SEQ ID NO: 49, SEQ ID NO: 50, SEQ ID NO: 52, SEQ ID NO: 53, SEQ ID NO: 54, SEQ ID NO: 56, and SEQ ID NO: 78. In some embodiments, methods of treating a neurodegenerative disease or disorder (e.g., ALS, FTD, Alzheimer's, Parkinson's, or TBI) comprises administering to a subject an antisense oligonucleotide comprising SEQ ID NO: 52. In some embodiments, methods of treating a neurodegenerative disease or disorder (e.g., ALS, FTD, Alzheimer's, Parkinson's, or TBI) comprises administering to a subject an antisense oligonucleotide comprising a sequence selected from the group consisting of SEQ ID NO: 53, SEQ ID NO: 72, and SEQ ID NO: 73. In some embodiments, methods of treating a neurodegenerative disease or disorder (e.g., ALS, FTD, Alzheimer's, Parkinson's, or TBI) comprises administering to a subject an antisense oligonucleotide comprising SEQ ID NO: 73. In some embodiments, the methods of treatment include administering a second agent.

In some embodiments an agent (e.g., an antisense oligonucleotide) is administered (e.g., *in vitro* or *in vivo*) in an amount effective for increasing and/or restoring STMN2 protein levels.

In some aspects the agent (e.g., the antisense oligonucleotide) suppresses cryptic splicing. In some embodiments a subject treated with an agent that suppresses or prevents inclusion of a cryptic exon in STMN2 RNA exhibits improved neuronal (e.g., motor axon) outgrowth and/or repair. In some aspects the agent prevents degradation of STMN2 protein. In some aspects an agent improves symptoms of a neurodegenerative disease including ataxia, neuropathy, synaptic dysfunction, deficit in cognition, and/or decreased longevity.

In some embodiments inclusion of a cryptic exon in STMN2 RNA is suppressed or prevented using genome editing (e.g., CRISPR/Cas).

As used herein, "treat," "treatment," "treating," or "amelioration" when used in reference to a disease, disorder or medical condition, refers to therapeutic treatments for a condition, wherein the object is to reverse, alleviate, ameliorate, inhibit, slow down or stop the progression or severity of a symptom or condition. The term "treating" includes reducing or alleviating at least one adverse effect or symptom of a condition. Treatment is generally "effective" if one or more symptoms or clinical markers are reduced. Alternatively, treatment is "effective" if the progression of a condition is reduced or halted. That is, "treatment" includes not just the improvement

of symptoms or markers, but also a cessation or at least slowing of progress or worsening of symptoms that would be expected in the absence of treatment. Beneficial or desired clinical results include, but are not limited to, alleviation of one or more symptom(s), diminishment of extent of the deficit, stabilized *(i.e.,* not worsening) state of, for example, a neurodegenerative disorder, delay or slowing progression of a neurodegenerative disorder, and an increased lifespan as compared to that expected in the absence of treatment.

"Neurodegenerative disorder" refers to a disease condition involving neural loss mediated or characterized at least partially by at least one of deterioration of neural stem cells and/or progenitor cells. Non-limiting examples of neurodegenerative disorders include polyglutamine expansion disorders (e.g., HD, dentatorubropallidoluysian atrophy, Kennedy's disease (also referred to as spinobulbar muscular atrophy), and spinocerebellar ataxia (e.g., type 1, type 2, type 3 (also referred to as Machado-Joseph disease), type 6, type 7, and type 17)), other trinucleotide repeat expansion disorders (e.g., fragile X syndrome, fragile XE mental retardation, Friedreich's ataxia, myotonic dystrophy, spinocerebellar ataxia type 8, and spinocerebellar ataxia type 12), Alexander disease, Alper's disease, Alzheimer disease, amyotrophic lateral sclerosis (ALS), ataxia telangiectasia, Batten disease (also referred to as Spielmeyer-Vogt-Sjogren-Batten disease), Canavan disease, Cockayne syndrome, corticobasal degeneration, Creutzfeldt-Jakob disease, Guillain-Barré syndrome, ischemia stroke, Krabbe disease, kuru, Lewy body dementia, multiple sclerosis, multiple system atrophy, non-Huntingtonian type of Chorea, Parkinson's disease, Pelizaeus-Merzbacher disease, Pick's disease, primary lateral sclerosis, progressive supranuclear palsy, Refsum's disease, Sandhoff disease, Schilder's disease, spinal cord injury, spinal muscular atrophy (SMA), SteeleRichardson-Olszewski disease, frontotemperal dementia (FTD), and Tabes dorsalis. In some contexts neurodegenerative disorders encompass neurological injuries or damages to the CNS or PNS associated with physical injury (e.g., head trauma, mild to severe traumatic brain injury (TBI), diffuse axonal injury, cerebral contusion, acute brain swelling, and the like).

In some embodiments the neurodegenerative disorder is a disorder that is associated with mutant or reduced levels of TDP-43 in neuronal cells. In some embodiments the neurodegenerative disorder is a disorder that is associated with mutant or reduced levels of STMN2 protein and/or mislocalization of STMN2

protein. In some embodiments the neurodegenerative disorder is selected from the group consisting of amyotrophic lateral sclerosis (ALS), frontotemporal dementia (FTD), frontotemporal lobar degeneration (FTLD), Alzheimer's disease, Parkinson's disease, Inclusion Body Myositis (IBM) and combinations thereof. In some aspects the neurodegenerative disorder is ALS. In some aspects the neurodegenerative disorder is ALS in combination with FTD and/or FTLD. In some aspects the neurodegenerative disorder is Alzheimer's. In some aspects the neurodegenerative disorder is Parkinson's.

"Proteasome-inhibitor induced neuropathy" is used herein to refer to a disorder or condition that occurs as a result of a reduced amount of functional nuclear TDP-43. The nuclear TDP-43 may be decreased in overall levels, or the decreased levels may occur as a result of an increase in cytoplasmic aggregation of TDP-43, which induces evacuation of nuclear TDP-43. In some aspects, proteasome inhibition leads to decreased expression of STMN2.

"Traumatic brain injury" or "TBI" refers to an intracranial injury that occurs when an external force injures the brain. TBIs may be classified based on their severity (e.g., mild, moderate, or severe), mechanism (e.g., closed or penetrating head injury), or other features (e.g., location). A TBI can result in physical, cognitive, social, emotional, and behavioral symptoms. Conditions associated with TBI include concussions. TBIs and conditions associated with a TBI have been associated with TDP-43 pathology. In some aspects, alterations in STMN2 occur in a TBI or a condition associated therewith.

In some embodiments the traumatic brain injury is, or results in, a disorder that is associated with mutant levels of TDP-43 in neuronal cells. In some embodiments the traumatic brain injury is, or results in, a disorder that is associated with mutant or reduced levels of STMN2 protein and/or mislocalization of STMN2 protein. In some embodiments the severity of a traumatic brain injury is measured based on the decrease of functional TDP-43 in neuronal cells. In some embodiments the severity of a concussion is measured based on the decrease of functional TDP-43 in neuronal cells.

For administration to a subject, the agents disclosed herein can be provided in pharmaceutically acceptable compositions. These pharmaceutically acceptable compositions comprise a therapeutically-effective amount of one or more of the agents, formulated together with one or more pharmaceutically acceptable carriers

(additives) and/or diluents. The pharmaceutical compositions of the present invention can be specially formulated for administration in solid or liquid form, including those adapted for the following: (1) oral administration, for example, drenches (aqueous or non-aqueous solutions or suspensions), gavages, lozenges, dragees, capsules, pills, tablets (e.g., those targeted for buccal, sublingual, and systemic absorption), boluses, powders, granules, pastes for application to the tongue; (2) parenteral administration, for example, by subcutaneous, intramuscular, intrathecal, intercranially, intravenous or epidural injection as, for example, a sterile solution or suspension, or sustained-release formulation; (3) topical application, for example, as a cream, ointment, or a controlled-release patch or spray applied to the skin; (4) intravaginally or intrarectally, for example, as a pessary, cream or foam; (5) sublingually; (6) ocularly; (7) transdermally; (8) transmucosally; or (9) nasally. Additionally, agents can be implanted into a patient or injected using a drug delivery system. (See, for example, Urquhart, et al., Ann. Rev. Pharmacol. Toxicol. 24: 199-236 (1984); Lewis, ed. "Controlled Release of Pesticides and Pharmaceuticals" (Plenum Press, New York, 1981); U.S. Pat. No. 3,773,919; and U.S. Pat. No. 35 3,270,960, content of all of which is herein incorporated by reference.)

As used herein, the term "pharmaceutically acceptable" refers to those agents, materials, compositions, and/or dosage forms which are, within the scope of sound medical judgment, suitable for use in contact with the tissues of human beings and animals without excessive toxicity, irritation, allergic response, or other problem or complication, commensurate with a reasonable benefit/risk ratio.

As used herein, the term "pharmaceutically-acceptable carrier" means a pharmaceutically-acceptable material, composition or vehicle, such as a liquid or solid filler, diluent, excipient, manufacturing aid (e.g., lubricant, talc magnesium, calcium or zinc stearate, or steric acid), or solvent encapsulating material, involved in carrying or transporting the subject agent from one organ, or portion of the body, to another organ, or portion of the body. Each carrier must be "acceptable" in the sense of being compatible with the other ingredients of the formulation and not injurious to the subject. Some examples of materials which can serve as pharmaceutically-acceptable carriers include: (1) sugars, such as lactose, glucose and sucrose; (2) starches, such as corn starch and potato starch; (3) cellulose, and its derivatives, such as sodium carboxymethyl cellulose, methylcellulose, ethyl cellulose, microcrystalline cellulose and cellulose acetate; (4) powdered tragacanth; (5) malt; (6) gelatin; (7) lubricating

agents, such as magnesium stearate, sodium lauryl sulfate and talc; (8) excipients, such as cocoa butter and suppository waxes; (9) oils, such as peanut oil, cottonseed oil, safflower oil, sesame oil, olive oil, corn oil and soybean oil; (10) glycols, such as propylene glycol; (11) polyols, such as glycerin, sorbitol, mannitol and polyethylene glycol (PEG); (12) esters, such as ethyl oleate and ethyl laurate; (13) agar; (14) buffering agents, such as magnesium hydroxide and aluminum hydroxide; (15) alginic acid; (16) pyrogen-free water; (17) isotonic saline; (18) Ringer's solution; (19) ethyl alcohol; (20) pH buffered solutions; (21) polyesters, polycarbonates and/or polyanhydrides; (22) bulking agents, such as polypeptides and amino acids (23) serum component, such as serum albumin, HDL and LDL; (22) C_2-C_{12} alcohols, such as ethanol; and (23) other non-toxic compatible substances employed in pharmaceutical formulations. Wetting agents, coloring agents, release agents, coating agents, sweetening agents, flavoring agents, perfuming agents, preservative and antioxidants can also be present in the formulation. The terms such as "excipient", "carrier", "pharmaceutically acceptable carrier" or the like are used interchangeably herein.

The phrase "therapeutically-effective amount" as used herein means that amount of an agent, material, or composition comprising an agent described herein which is effective for producing some desired therapeutic effect in at least a sub-population of cells in an animal at a reasonable benefit/risk ratio applicable to any medical treatment. For example, an amount of an agent administered to a subject that is sufficient to produce a statistically significant, measurable increase in TDP-43 function.

The determination of a therapeutically effective amount of the agents and compositions disclosed herein is well within the capability of those skilled in the art. Generally, a therapeutically effective amount can vary with the subject's history, age, condition, sex, and the administration of other pharmaceutically active agents.

As used herein, the term "administer" refers to the placement of an agent or composition into a subject (e.g., a subject in need) by a method or route which results in at least partial localization of the agent or composition at a desired site such that desired effect is produced. Routes of administration suitable for the methods of the invention include both local and systemic routes of administration. Generally, local administration results in more of the administered agents being delivered to a specific location as compared to the entire body of the subject, whereas, systemic

administration results in delivery of the agents to essentially the entire body of the subject.

The compositions and agents disclosed herein can be administered by any appropriate route known in the art including, but not limited to, oral or parenteral routes, including intravenous, intramuscular, subcutaneous, transdermal, airway (aerosol), pulmonary, nasal, rectal, and topical (including buccal and sublingual) administration. Exemplary modes of administration include, but are not limited to, injection, infusion, instillation, inhalation, or ingestion. "Injection" includes, without limitation, intravenous, intramuscular, intraarterial, intrathecal, intraventricular, intracranial, intracapsular, intraorbital, intracardiac, intradermal, intraperitoneal, transtracheal, subcutaneous, subcuticular, intraarticular, sub capsular, subarachnoid, intraspinal, intracerebro spinal, and intrasternal injection and infusion. In preferred embodiments of the aspects described herein, the compositions are administered by intravenous infusion or injection.

As used herein, a "subject" means a human or animal (e.g., a mammal). Usually the animal is a vertebrate such as a primate, rodent, domestic animal or game animal. Primates include chimpanzees, cynomologous monkeys, spider monkeys, and macaques, e.g., Rhesus. Domestic and game animals include cows, horses, pigs, deer, bison, buffalo, feline species, e.g., domestic cat, canine species, e.g., dog, fox, wolf, avian species, e.g., chicken, emu, ostrich, and fish, e.g., trout, catfish and salmon. Patient or subject includes any subset of the foregoing, e.g., all of the above, but excluding one or more groups or species such as humans, primates or rodents. In certain embodiments of the aspects described herein, the subject is a mammal, e.g., a primate, e.g., a human. The terms, "patient" and "subject" are used interchangeably herein. A subject can be male or female. In some embodiments the subject suffers from a disease or condition associated with mutant or reduced levels of TDP-43 (e.g., in neuronal cells).

Screening Methods

The disclosure contemplates methods of screening one or more test agents (e.g., one or more antisense oligonucleotides) to identify candidate agents for treating or reducing the likelihood of a disease or condition associated with a TDP-pathology. In some aspects, a disease or condition is associated with mutant or reduced levels of TDP-43 (e.g., in neuronal cells). The disclosure further contemplates methods of

screening one or more test agents to identify candidate agents for treating or reducing the likelihood of a disease or condition associated with either mutant or reduced levels of STMN2 protein.

In some embodiments the method comprises providing a neuronal cell having reduced TDP-43 levels; contacting the cell with the one or more test agents; determining if the contacted cell has an increased level of STMN2 protein; and identifying the test agent as a candidate agent if the contacted cell has an increased level of STMN2 protein. In some aspects the step of determining if the contacted cell has increased level of STMN2 protein comprises measuring STMN2 protein levels in the contacted cell. In some aspects STMN2 protein level is measured using an ELISA (e.g., a sandwich ELISA), dot blot, and/or Western blot. In some aspects the step of determining if the contacted cell has increased level of STMN2 protein comprises assessing the morphology or function of the contacted cell. For example, neurons lacking STMN2 may have an altered morphology from that of neurons having STMN2. In some aspects the morphology or function of the contacted cell is assessed using immunoblotting and/or immunocytochemistry. In some aspects the contacted cell may further be assessed to determine if it expresses full-length STMN2 RNA. STMN2 RNA expression may be measured using qRT-PCR.

In some embodiments the method comprises providing a neuronal cell having mutant TDP-43 levels; contacting the cell with the one or more test agents; determining if the contacted cell has an increased level of STMN2 protein; and identifying the test agent as a candidate agent if the contacted cell has an increased level of STMN2 protein. In some aspects the step of determining if the contacted cell has increased level of STMN2 protein comprises measuring STMN2 protein levels in the contacted cell. In some aspects STMN2 protein level is measured using an ELISA, dot blot, and/or Western blot. In some aspects the step of determining if the contacted cell has increased level of STMN2 protein comprises assessing the morphology or function of the contacted cell. For example, neurons lacking STMN2 or having a reduced amount of STMN2 may have an altered morphology from that of neurons having normal levels of STMN2 (i.e., levels of STMN2 from a control sample). In some aspects the morphology or function of the contacted cell is assessed using immunoblotting and/or immunocytochemistry. In some aspects the contacted cell may further be assessed to determine if it expresses full-length STMN2 RNA. STMN2 RNA expression may be measured using qRT-PCR.

In some embodiments the method comprises providing a neuronal cell having reduced TDP-43 levels; contacting the cell with the one or more test agents; and determining if the contacted cell has cryptic exons in STMN2 RNA. The contacted cell may be assessed using FISH RNA, or RT-PCT, qPCR, qRT-PCR, or RNA sequencing to identify whether there is a cryptic exon in the STMN2 RNA. In some embodiments the method comprises providing a neuronal cell having reduced TDP-43 levels; contacting the cell with the one or more test agents; and determining if the contacted cell expresses full length STMN2 RNA. The contacted cell may be assessed using RNA FISH or RT-PCT, qPCR, qRT-PCR, or RNA sequencing.

In some embodiments the method comprises providing a neuronal cell having mutant TDP-43 levels; contacting the cell with the one or more test agents; and determining if the contacted cell has cryptic exons in STMN2 RNA. The contacted cell may be assessed using FISH RNA or RT-PCT, qPCR or RNA sequencing to identify whether there is a cryptic exon in the STMN2 RNA. In some embodiments the method comprises providing a neuronal cell having mutant TDP-43 levels; contacting the cell with the one or more test agents; and determining if the contacted cell expresses full length STMN2 RNA. The contacted cell may be assessed using RNA FISH or RT-PCT, qPCR, qRT-PCR, or RNA sequencing.

Biomarkers

In some aspects the disclosure contemplates the use of STMN2 and/or ELAVL3 as a biomarker for a disease or condition associated with a decline in TDP-43 functionality (e.g., a disease or condition having a substantial TDP-43-associated pathology). In some aspects STMN2 and/or ELAVL3 may act as a biomarker for the presence of a disease or condition. In other aspects STMN2 and/or ELAVL3 may act as a biomarker for monitoring the progression of a disease or condition. In some aspects STMN2 and/or ELAVL3 protein levels are assessed. In some aspects STMN2 and/or ELAVL3 transcript levels are assessed.

In some embodiments, a disease or condition is associated with mutant or reduced levels of TDP-43 in neuronal cells. In some embodiments, a disease or condition is associated with mutant or increased levels of TDP-43 in neuronal cells. In some embodiments the disease or condition is a neurodegenerative disease (e.g., amyotrophic lateral sclerosis (ALS), Alzheimer's disease, Parkinson's disease, or

frontotemperal dementia (FTD)). In some embodiments the disease or condition is associated with or occurs as a result of a traumatic brain injury.

In some aspects a method for detecting a disease or condition associated with a decline in TDP-43 functionality comprises obtaining a sample from a subject and assessing the sample to determine if it exhibits either mutant or reduced levels of STMN2 and/or ELAVL3 protein. In some embodiments the STMN2 and/or ELAVL3 protein levels are measured using any method known to those of skill in the art, including immunoblot, immunocytochemistry, dot blot, and/or ELISA. In certain aspects STMN2 and/or ELAVL3 protein levels are measured using ELISA. In some aspects a method for detecting a disease or condition associated with a decline in TDP-43 functionality comprises obtaining a sample from a subject and assessing the sample to determine if it exhibits reduced levels of STMN2 and/or ELAVL3 transcript. In some embodiments the STMN2 and/or ELAVL3 transcript levels are measured using any method known to those of skill in the art, including RNA FISH, RT-PCR, qPCR, or RNA sequencing. In certain aspects STMN2 and/or ELAVL3 transcript levels are measured using qRT-PCR. Reduced levels of STMN2 and/or ELAVL3 protein and/or transcript may be an indication of a decline in TDP-43 functionality as a result of a disease or disorder. In some aspects the progression of a disease or condition associated with a decline in TDP-43 functionality is assessed by analyzing multiple samples from a subject over an extended period of time to monitor the levels of STMN2 and/or ELAVL3 protein and/or transcript (e.g., in response to a treatment protocol).

In some aspects a method for detecting a neurodegenerative disease (e.g., ALS, FTD, Parkinson's, Alzheimer's) in a subject comprises obtaining a sample (e.g., a biofluid sample) from the subject suffering, and determining if the sample contains altered levels of STMN2 and/or ELAVL3 protein. In certain aspects the determination is made using ELISA. In some aspects a method for detecting a neurodegenerative disease (e.g., ALS, FTD, Parkinson's, Alzheimer's) in a subject comprises obtaining a sample (e.g., a biofluid sample) from the subject suffering, and determining if the sample contains reduced levels of STMN2 and/or ELAVL3 transcript. The screening of the sample may be performed using RNA FISH, RT-PCR, qPCR, or RNA sequencing. In certain aspects STMN2 and/or ELAVL3 transcript levels are measured using qRT-PCR. Reduced levels of STMN2 and/or

ELAVL3 protein and/or transcript may be an indication of a decline in TDP-43 functionality as a result of a neurodegenerative disease or disorder.

In some aspects a method for detecting a traumatic brain injury (TBI) in a subject comprises obtaining a sample (e.g., a biofluid sample) from the subject, and determining if the sample contains altered levels of STMN2 and/or ELAVL3 protein. In certain aspects the determination is made using ELISA. In some aspects a method for detecting a traumatic brain injury (TBI) in a subject comprises obtaining a sample (e.g., a biofluid sample) from the subject, and screening the sample for reduced levels of STMN2 and/or ELAVL3 transcript. The screening of the sample may be performed using RNA FISH, RT-PCR, qPCR, or RNA sequencing. In certain aspects STMN2 and/or ELAVL3 transcript levels are measured using qRT-PCR. Reduced levels of STMN2 and/or ELAVL3 protein and/or transcript may be an indication of a decline in TDP-43 functionality as a result of a TBI.

In some aspects the disclosure contemplates the use of cryptic variants of STMN2 as a biomarker for a disease or condition associated with a decline in TDP-43 functionality (e.g., a disease or condition having a substantial TDP-43-associated pathology). In some embodiments the disease or condition is a neurodegenerative disease (e.g., ALS, FTD, Alzheimer's, Parkinson's). In some embodiments the disease or condition is associated with or is a result of a traumatic brain injury.

In some aspects a method for detecting a disease or condition associated with a decline in TDP-43 functionality comprises obtaining a sample from a subject and assessing the sample to determine if it includes a cryptic variant of STMN2. In some embodiments the STMN2 transcript is assessed using RNA FISH, RT-PCR, qPCR, or RNA sequencing. In certain aspects an STMN2 transcript is measured using qRT-PCR. The presence of a cryptic variant of STMN2 may be an indication of a decline in TDP-43 functionality.

In some aspects a method for detecting a neurodegenerative disease comprises obtaining a sample (e.g., a biofluid sample) from the subject, and screening the sample for a cryptic variant of STMN2. The screening of the sample may be performed using PCR. The presence of a cryptic variant of STMN2 may be an indication of a decline in TDP-43 functionality as a result of a neurodegenerative disease or disorder.

In some aspects a method for detecting a TBI comprises obtaining a sample (e.g., a biofluid sample) from the subject, and screening the sample for a cryptic

variant of STMN2. The screening of the sample may be performed using PCR. The presence of a cryptic variant of STMN2 may be an indication of a decline in TDP-43 functionality as a result of a traumatic brain injury.

EXAMPLES:

Example 1:

In a landmark finding, TDP-43 (TAR DNA-binding protein 43) was discovered to be a major constituent of ubiquitin-positive inclusions in many sporadic cases of ALS and a substantial subset of FTD (7). TDP-43 is a predominantly nuclear DNA/RNA binding protein (8) with functional roles in transcriptional regulation (9), splicing (10, 11), pre-miRNA processing (12), stress granule formation (13, 14), and mRNA transport and stability (15, 16). Subsequently, autosomal-dominant, apparently causative mutations in *TARDBP* were identified in both ALS and FTD families, linking genetics and pathology with neurodegeneration (17-21). Thus, elucidating the role that TDP-43 mislocalization and mutation play in disease is essential to understanding both sporadic and familial ALS.

Whether neurodegeneration associated with TDP-43 pathology is the result of loss-of-function mechanisms, toxic gain-of-function mechanisms, or a combination of both, remains unclear (22). Early studies showed that overexpression of both wildtype and mutant TDP-43 led to its aggregation and loss of nuclear localization (22). While these studies along with the autosomal dominant inheritance pattern of *TARDBP* mutations would seemingly support a gain-of-function view, the loss of nuclear TDP-43, generally associated with its aggregation, suggests its normal functions might also be impaired. Subsequent findings revealed that TDP-43 depletion in the developing embryo or post-mitotic motor neurons can have profound consequences (23-27).

Given the myriad roles TDP-43 plays in neuronal RNA metabolism, a key question has become: what are the RNA substrates that are misregulated upon TDP-43 mislocalization, and how do they contribute to motor neuropathy? Early efforts to answer this question utilized cross-linking and immunoprecipitation with RNA sequencing (RNA-seq) of whole brain homogenates from either patients or mice subjected to *TARDBP* knockdown (11, 28). These resulting discoveries led to a general understanding that many transcripts are regulated by TDP-43 with a preference towards lengthy RNAs containing UG repeats and long introns; however, the prominence of glial RNAs in the brain homogenates sequenced in these

experiments limited insights into the specific neuronal targets of TDP-43. As a result, few clear connections between the TDP-43 target RNAs and mechanisms of motor neuron degeneration could be forged.

To identify substrates that when misregulated contribute to neuronal degeneration, the identity of RNAs regulated by TDP-43 in purified human motor neurons was sought. Because the vulnerable motor neurons in living ALS patients are fundamentally inaccessible for isolation and experimental perturbation, directed differentiation approaches have been developed for guiding human pluripotent stem cells into motor neurons (hMNs) to study ALS and other neurodegenerative conditions *in vitro* (29-31). Here, RNA-seq of hMNs was performed after TDP-43 knockdown to identify transcripts whose abundance are positively or negatively regulated by TDP-43's deficit. In total, 885 transcripts were identified for which TDP-43 is needed to maintain normal RNA levels. Although misregulation of any number of these targets may play subtle roles in motor neuron degeneration, it was noted that one of the most abundant transcripts in motor neurons, encoding *STMN2*, was particularly sensitive to a decline in *TARDBP,* but not *FUS* or *C9ORF72* activities. Additionally, it was determined that *STMN2* levels were also decreased in hMNs expressing mutant TDP-43 and in hMNs whose proteasomes were pharmacologically inhibited, which has been shown to induce cytoplasmic accumulation and aggregation of TDP-43 in rodent neurons (32). It was further shown that *STMN2,* a known regulator of microtubule stability, encodes a protein that is necessary for normal human motor neuron outgrowth and repair. Importantly, loss of STMN2 function as a result of loss of TDP-43 activity is likely to be of functional relevance to people with ALS as its expression was also found to be reproducibly decreased in the motor neurons of ALS patients.

Results

Differentiation and purification of human motor neurons (hMNs)

In order to produce hMNs, the human embryonic stem cell line HUES3 *Hb9::GFP* (33, 34) was differentiated into GFP+ hMNs under adherent culture conditions (35, 36) using a modified 14-day strategy (FIG. 7A). This approach relies on neural induction through small molecule inhibition of SMAD signaling, accelerated neural differentiation through FGF and NOTCH signaling inhibition, and MN patterning through the activation of retinoic acid (RA) and Sonic Hedgehog

signaling pathways (FIG. 7A). On day 14 of differentiation, cultures comprising ~18-20% GFP+ cells were routinely obtained (FIG. 7B). 2 days following fluorescent activated cell sorting (FACS), >95% of the resulting cells expressed the transcription factors HB9 (FIGS. 7C-7D). After another 8 days, cultures were composed of neurons expressing the transcription factor Islet-1(80%) as well as the pan-neuronal cytoskeletal proteins b-III tubulin (97%) and microtubule associated protein 2 (MAP2) (90%) (FIGS. 7E-7F). Whole-cell patch-clamp recordings following FACS and 10 days of culture in glia-conditioned medium supplemented with neurotrophic factors revealed that these purified hMNs were electrophysiologically active (FIGS 7G-7I). Upon depolarization, hMNs exhibited initial fast inward currents followed by slow outward currents, consistent with the expression of functional voltage-activated sodium and potassium channels, respectively (FIG. 7G). In addition, hMNs fired repetitive action potentials (FIG. 7H), and responded to Kainate, an excitatory neurotransmitter (FIG. 7I). Taken together, these data demonstrated these purified hMN cultures had expected functional properties.

RNA-Seq of hMNs with reduced levels of TDP-43

Reduced nuclear TDP-43 observed in ALS is emerging as potential cellular mechanism that may contribute to downstream neurodegenerative events (7, 37). It was therefore desired to identify the specific RNAs regulated by TDP-43 in purified hMN populations through a combination of knock-down and RNA-Seq approaches. Using a short interfering RNA conjugated to Alexa Fluor 555, transfection conditions were first validated to achieve high levels of siRNA delivery (~94.6%) into the hMNs (FIGS. 8A-8C). *TDP-43* RNAi was then carried out in purified hMNs using two distinct siRNAs targeting the *TDP-43* transcript (siTDP43), two control siRNAs with scrambled sequences that do not target any specific gene (siSCR and siSCR_555), and at three different time points after siRNA delivery (2, 4 and 6 days) (FIG. 8A). After siRNA transfection, total RNA and protein were isolated from the neurons. qRT-PCR assays validated the downregulation of *TDP-43* mRNA levels at all the time points for MNs treated with siTDP43s, but not in those with the scrambled controls, with maximum knockdown occurring 4 days after siRNA transfection (FIG. 8D). Furthermore, depletion of TDP-43 was also confirmed at the protein level by immunoblot assays, with siTDP43-treated MNs showing a 54-65% reduction in TDP-43 levels (FIG. 8E).

To capture global changes in gene expression in response to partial loss of TDP-43 in hMNs, RNA-Seq libraries were prepared from siRNA treated cells (FIG. 1A). After next-generation sequencing, expression data was obtained for each gene annotated as the number of transcripts per million (TPMs). Initial unsupervised hierarchical clustering revealed a transcriptional effect based on the batch of MN production (Experiment 1 vs. Experiment 2). (FIG. 9A) Subsequent principle component analyses of the RNA-Seq samples focused on the 500 most differentially expressed genes then segregated the samples based on siTDP-43 treatment (pc1), indicating that reduction of TDP-43 levels resulted in reliable transcriptional differences, followed by the batch of MN production (pc2) (FIG. 1B) Inspection of TPM values for *TDP-43* transcripts confirmed that its abundance was significantly reduced only in MNs treated with siTDP43 (FIG. 9B). Differential gene expression analysis was then performed using DESeq2 suite of bioinformatics tools (38), which at a false discovery rate (FDR) of 5%, identified a total of 885 statistically differentially expressed genes in hMNs after TDP-43 knockdown (FIGS. 1C-1D). In these cells, TPM values were significantly higher for 392 genes ('upregulated'), and significantly lower for 493 genes ('downregulated') compared to those values in MNs treated with the scrambled sequence siRNA controls (FIGS. 1C-1D).

In addition to altering total transcriptional levels of hundreds of genes in the mammalian CNS (11), reduced levels of TDP-43 can also influence gene splicing (11, 39-42). Although global analysis of splicing variants traditionally involves splicing-sensitive exon arrays (11, 39), the development of computational approaches for isoform deconvolution of RNA-Seq reads is rapidly evolving (43-45). A limited examination of the data with the bioinformatics algorithm 'Cuffdiff 2' (45) was indeed able to detect the *POLDIP3* gene as the top candidate for differential splicing with two significant isoform-switching events (FIG. 9C), which has previously been associated with deficits in TDP-43 function both *in vitro* and *in vivo* (42,46).

Of the 885 genes identified as significantly misregulated after TDP-43 knockdown, a candidate subset was selected for further validation. First, genes with enriched neuronal expression (*STMN2* (47,48), *ELAVL3* (49)), and association with neurodevelopment and neurological disorders (*RCAN1* (50), *NAT8L* (51)) were considered. In addition, genes with reasonable expression levels (TPM $\geq$ 5) and high fold changes as 'positive controls' (*SELPLG*, *NAT8L*) were considered, as it was hypothesized that these candidates would be more robust and likely to validate. RNA

was then obtained from independent biological replicates after TDP-43 knockdown and the relative expression levels for 11 candidate genes, including *TARDBP*, was determined by qRT-PCR. Notably, differential gene expression for 9/11 of these genes was confirmed in cells treated with either siTDP-43 relative to those treated with scrambled control (FIGS. 1E-1F). These results indicate reproducible expression differences among the genes selected and validate the findings from RNA-Seq analysis.

STMN2 levels are downregulated in hMNs expressing mutant TDP-43

It was next asked if any of the RNAs with altered abundances after TDP-43 depletion were also perturbed by expression of mutant forms of TDP-43 that cause ALS. To this end, the putative TDP-43 target RNAs that displayed reproducibly altered expression after TDP-43 knockdown in patient iPS cell-derived motor neurons harboring pathogenic mutations in *TARDBP* were investigated (FIG. 10). Based on previous experience with pluripotent stem cells, it was known that directed differentiation approaches tend to yield heterogeneous cultures making quantitative, comparative analyses challenging (52). Furthermore, the presence of mitotic progenitor cells is especially troublesome because they can overtake the cultures and skew results. To overcome these barriers, an unbiased FACS-based immunoprofiling analysis was performed (53) on the differentiated HUES3 *Hb9::GFP* cell line using 242 antibodies against cell surface markers to identify signatures enriched on the GFP+ and GFPcells (FIG. 11A). By sorting for NCAM+/EpCAM- cells, it was determined that the cultures could be rid of proliferating, Edu^+ cells and normalize the number of MAP2+/Islet-1+ neurons across a large number of induced pluripotent stem cell differentiations (FIGS. 11B-11D). Using this cell surface signature, 5 control iPSC lines (11a, 15b, 17a, 18a, and 20b) and 4 iPSC lines with distinct TDP-43 mutations (36a (Q343R), 47d (G298S), CS (M337V), and RB20 (A325T)) were differentiated and the resulting MNs were FACS purified. As anticipated, each iPS cell line exhibited its own propensity to differentiate into $NCAM^+$ MNs (FIGS. 11E-11F). After sorting, however, homogenous neuronal cultures for all iPSC lines were obtained (FIG. 2B).

After 10 days of further neuronal culture, total RNA from these FACS-purified MNs were collected and qRT-PCR was performed to investigate levels of the gene products most reproducibly impacted by TDP-43 depletion (*ALOX5AP*, *STMN2*,

ELAVL3, and *RCAN1*). For two of the genes (*STMN2* and *ELAVL3*), a significant decrease in transcript levels was observed (FIGS. 2C-2F). Consistent with the TDP-43 depletion experiments, significant changes to the abundance of the closely related *STMN1* RNA were not observed, suggesting a specific relationship between TDP-43 and *STMN2* (FIG. 2H, FIG. 12E). Additionally, significant differences in *TDP-43* transcript levels between mutant and control neurons were not observed (FIG. 2G). Together, these data imply that the presence of pathogenic point mutations in TDP-43 can alter *STMN2* and *ELAVL3* mRNA levels without affecting its own levels.

How ALS-associated mutations might hamper TDP-43's ability to regulate target transcripts was subsequently explored. Previous studies have reported that hMNs derived from iPSC lines expressing mutant TDP-43 recapitulate some aspects of TDP-43 pathology including its accumulation in both soluble and insoluble cell protein extracts (54, 55) as well as cytoplasmic mislocalization (56). Because decreased nuclear TDP-43 in mutant neurons could mimic the partial loss induced by the siRNAs, signs of TDP-43 mislocalization were tested for using immunofluorescence. In both control and mutant neurons, however, primarily nuclear staining for TDP-43 was observed (FIG. 2I). Pearson's correlation coefficient analysis supported these observations and revealed a strong correlation between TDP-43 immunostaining and DNA counterstain for both mutant and control neurons (FIG. 2J). These results are consistent with some TDP-43 iPS disease modeling studies (56), yet inconsistent with others (54), and raises the possibility that additional cellular perturbations could be required to induce TDP-43 mislocalization (57). Collectively, the data suggest that a subset of genes affected after TDP-43 depletion are also altered in neurons expressing mutant TDP-43, and that these changes precede the hallmark cytoplasmic aggregation of TDP-43. Thus, at least through the lens of these limited number of transcripts, the data suggest that mutations in TDP-43 can contribute in part to a loss-of-function transcriptional phenotype.

STMN2 levels are regulated by TDP-43 in hMNs

It was intriguing to see that transcripts for Stathmin-like 2 (*STMN2*) were decreased in both neurons expressing mutant TDP-43 and after TDP-43 depletion. STMN2 is one of four proteins (STMN1, STMN2, SCLIP/STMN3, and RB3/STMN4) belonging to the Stathmin family of microtubule-binding proteins with functional roles in neuronal cytoskeletal regulation and axonal regeneration pathways

(47,48,58-62). In humans, *STMN1* and *STMN3* genes exhibit ubiquitous expression, whereas STMN2 and STMN4 are enriched in CNS tissues (63). Considering the growing evidence for the relevance of cytoskeletal pathways in ALS (64-66) and its enrichment within the CNS, it was decided to focus on further characterizing the relationship between STMN2 and TDP-43.

First, it was examined if the significant downregulation of the *STMN2* transcripts also resulted in reduced levels of STMN2 protein. In independent RNAi experiments, qRT-PCR was performed with two different sets of primer pairs binding the *STMN2* mRNA and found significant downregulation (~50-60%) in siTDP43-treated hMNs relative to controls (FIG. 3A). Immunoblot assays were then carried out on hMN protein lysates and found that STMN2 protein levels were also reduced in siTDP-43-treated hMNs (FIG. 3B).

It was then considered whether downregulation of two other ALS-linked genes, *FUS* or *C9ORF72* (5,67), would also change *STMN2* levels in hMNs. FUS protein, structurally similar to TDP-43, is also involved in RNA metabolism (68), and FUS variants have been detected in familial ALS and FTD cases (69). The function of C9ORF72 is an active area of research, but large repeat expansions in the intronic regions of *C9ORF72* are responsible for a substantial number of familial and sporadic ALS and FTD cases (70-72). Following induction of RNAi targeting *TDP-43*, *FUS*, or *C9ORF72*, significant downregulation of the respective siRNA-targeted genes by qRT-PCR was found. (FIGS. 12A-12C). Downregulation of *TDP-43* did not alter expression levels of *FUS* or *C9ORF72*, and reduced expression of either *FUS* or *C9ORF72* showed no effect on the other ALS-linked genes (FIGS. 12A-12C). Although knockdown of *TDP-43* again reduced levels of *STMN2*, it was not the case for *FUS* or *C9ORF72* (FIG. 3C). Importantly, these results demonstrate that *STMN2* downregulation is not a consequence of RNAi induction, but instead a specific molecular mechanism in response to partial loss of TDP-43.

Through highly conserved RNA recognition motifs (73), TDP-43 can bind to RNA molecules to regulate them. To determine whether TDP-43 associates directly with *STMN2* RNA, which has many canonical TDP-43 binding motifs (FIGS. 12F-12G), conditions for TDP-43 immunoprecipitation were developed (FIG. 3D) and subsequently formaldehyde RNA immunoprecipitation (fRIP) was performed. After reversing the cross-linking, quantitative qRT-PCR was performed to detect bound RNA molecules. Amplification from *TDP-43* RNA transcripts was looked for,

because this auto-regulation is well established (11), as well as *STMN2* transcripts. In both cases, enrichment after TDP-43 pull down was observed, but not for an IgG control or when a different ALS-associated protein, SOD-1, was pulled down (FIGS. 3E-3F). Together, the results indicate that TDP-43 associates directly with *STMN2* mRNA, and that reduced TDP-43 levels lead to reduced STMN2 levels.

STMN2 function in hMNs

The function of STMN2 in hMNs was explored next. First, expression of STMN2 was examined across the differentiation process that yields MNs (FIG. 12D). Supporting previous expression studies (62, 63, 74), it was found that STMN2 protein is selectively expressed in differentiated neurons, as it could not be detected in stem cells or in neuronal progenitors (FIG. 12D). Immunocytochemistry was then used to probe the subcellular localization of STMN2 and found that it localized to discrete cytoplasmic puncta present at neurite tips with particular enrichment in the perinuclear region (FIG. 3G). It was determined that this region corresponds to the Golgi apparatus using a human-specific antibody against the Golgi-associated protein GOLGIN97, (FIG. 3H), substantiating the prediction of STMN2 N-terminus as the target of palmitoylation for vesicle trafficking and membrane binding (75). STMN2 is also predicted to function at the growth cone during neurite extension and injury (47). When hMNs were stained just after differentiation and sorting, strong staining of STMN2 was observed at the interface between microtubules and F-actin bundles, components defining the growth cone (FIG. 3I). These findings support a role for STMN2 microtubule dynamics at the growth cone. Together, the data indicate that STMN2 could function in cytoskeletal defects and altered axonal transport pathways implicated in ALS pathogenesis (76).

To explore the cellular consequences of decreased STMN2 levels in hMNs, *STMN2* knock-out stem cells were generated. Specifically, a CRISPR/Cas9-mediated genome editing strategy was used (FIG. 4A) to generate a large deletion in the human *STMN2* locus in two hES cell lines (WA01 and HUES3 *Hb9::GFP*). After carrying out a primary PCR screen to identify clones harboring the 18kb deletion in the *STMN2* gene (FIG. 4B), protein knockout in differentiated hMNs was confirmed by both immunoblotting and immunocytochemistry (FIGS. 4C-4D). As expected, it was found that when compared to the parental *STMN2+/+* lines, the hMNs derived from the candidate deletion clones exhibited the complete absence of STMN2 staining.

Given the reported role of STMN2 in regulating axonal growth by promoting the dynamic instability of microtubules (77), phenotypic assays were carried out characterizing neurite outgrowth in the *STMN2-/-* hMNs. After 7 days in culture, sorted hMNs were fixed and stained for β-III-tubulin to label the neuronal processes (FIG. 4E). Sholl analysis, which quantifies the number of intersections at a given interval from the center of the soma (78), revealed significantly reduced neurite extension in the $STMN2^{-/-}$ lines compared to the $STMN2^{+/+}$ (FIGS. 4F-4G). Separately, neurons were cultured in the presence of a ROCK inhibitor, Y-27632, which has been shown to increase neurite extension. The difference in neurite outgrowth was even more striking in these experiments with the molecule enhancing the outgrowth of the $STMN^{+/+}$ line but not the $STMN^{-/-}$ line, which suggests a role for STMN2 in this signaling cascade (FIG. 4H). Similar results were observed for the WA01 cell line (FIG. 13).

It was next asked if STMN2 functions not only in neuronal outgrowth, but also in neuronal repair after injury. To test these hypothesis, sorted hMNs were plated into a microfluidic device that permits the independent culture of axons from neuronal cell bodies (79) (FIG. 4I). Cells cultured for 7 days in the soma compartment of the device extended axons through the microchannels into the axon chamber (FIG. 4J). Repeated vacuum aspiration and reperfusion of the axon chamber was performed until axons were cut effectively without disturbing cell bodies in the soma compartment. Neurite length was then measured from the microchannel across a time course to assess axonal repair after injury. The analysis revealed significantly reduced regrowth in the $STMN2^{-/-}$ lines compared to the $STMN2^{+/+}$ for all time points measured (FIG. 4K). Similar results were observed for the WA01 cell line (FIG. 13). Together, these data indicate that reducing levels of STMN2 can have measurable phenotypic effects on the growth and complexity of neuronal processes in hMNs as well as repair after axotomy.

Proteasome function regulates TDP-43 localization and STMN2 levels

A previous study established that proteasome inhibition in hMNs could trigger accumulation of mutant SOD-1 (31). It was, therefore, examined whether MG-132-mediated proteasome inhibition affected TDP-43 localization in hMNs as a potential model of sporadic ALS. First, the range and timing of small molecule treatment that could inhibit the proteasome without inducing overt cellular toxicity was established

(FIGS. 14A-14D). It was determined that neurons could withstand an overnight 1 μM treatment, which decreases proteasome activity to less than 10% of normal activity (FIG. 14E). Then a pulse-chase experiment was performed to determine the consequences of proteasome inhibition on TDP-43 localization (FIG. 5A). Strikingly, using the Pearson's correlation coefficient analysis as described above, it was observed that TDP-43 staining in the nucleus was greatly diminished after 24 hour 1 μM pulse of MG-132 (FIGS. 5B-5C). Notably, following washout, it was found that TDP-43 staining became indistinguishable to unchallenged neurons after 4 days (FIGS. 5B-5C). Thus, proteasome inhibition in hMNs induces a TDP-43 mislocalization that is reversible. These findings are analogous with stress condition studies on primary cortical and hippocampal neurons, where proteasome inhibition also caused loss of TDP-43 nuclear staining (32).

To determine what happened to TDP-43 after proteasome inhibition, TDP-43 levels were examined by immunoblot analysis in both the detergent-soluble and detergent-insoluble fractions. In the soluble lysates obtained from control neurons treated with a low dose of MG-132 (FIG. 5A), significantly decreased TDP-43 levels (FIG. 5D) were found. The UREA, or insoluble, fraction was probed and it was discovered that proteasome inhibition triggers TDP-43 to become insoluble (FIG. 5D). Finally, *STMN2* levels in neurons treated with either a short-term high dose or a long-term low dose of MG-132 were probed. In both cases, significant decreases were observed in *STMN2* mRNA levels (FIG. 5E). Together, these data connect protein homeostasis with TDP-43 localization and STMN2 levels.

TDP-43 suppresses appearance of cryptic exons in hMNs

TDP-43 plays an important role in the nucleus regulating RNA splicing, and recent studies highlight its ability to suppress non-conserved or cryptic exons to maintain intron integrity (80). When cryptic exons are included in RNA transcripts, in many cases, their inclusion can affect normal levels of the gene product by disrupting its translation or by promoting nonsense-mediated decay (80). Interestingly, no overlap in the genes regulated by TDP-43 cryptic exon suppression has been observed between mouse and man (80). The sequencing data was examined for evidence of cryptic exons in genes observed to be reproducibly regulated by TDP-43 in human cancer cells (81). Reads mapping to cryptic exons in 9 of these 95 genes were found, including *PFKP,* which was consistently down-regulated in the RNA-Seq experiment

(FIG. 15A, FIG. 3C). Based on this observation, the RNA-Seq reads mapping to the other genes consistently misregulated in hMNs after TDP-43 depletion were also scrutinized. Strong evidence was found for the inclusion of cryptic exons in both *ELAVL3* and *STMN2* (FIGS. 15B-15C). It was then asked if cryptic exon inclusion could be contributing to decreased *STMN2* levels in hMNs after proteasome inhibition. To accomplish this goal, an RT-PCR assay was developed to detect transcripts containing the cryptic exon (FIG. 5F). Only hMNs treated with the proteasome inhibitor had detectable levels of the expected PCR product (FIG. 5G), and Sanger sequencing of the PCR product confirmed the anticipated splice junction (FIGS. 15D-15E). Together the data suggest that the mechanism for *STMN2* down-regulation is similar for both TDP-43 depletion and mislocalization.

STMN2 is expressed in human adult primary spinal MNs and is altered in ALS

Finally, it was sought to test if the *in vitro* findings were relevant to ALS patient motor neurons *in vivo*. To this end, immunohistochemistry was used of human adult spinal cord tissues to investigate STMN2 expression in control and ALS patients. It was predicted that levels of STMN2 protein would be altered in post-mortem spinal MNs from sporadic ALS cases, which typically manifest pathological loss of nuclear TDP-43 staining and accumulation of cytoplasmic TDP-43 immunoreactive inclusions (7, 37). Similar to what was observed in stem cell derived hMNs, strong STMN2 immunoreactivity was present in the cytoplasmic region of human adult lumbar spinal MNs, but absent in the surrounding glial cells (FIGS. 6A-6C). The percentage of MNs exhibiting strong STMN2 immunoreactivity in lumbar spinal cord tissue sections in 3 control cases (no evidence of spinal cord disease) and in 3 ALS cases was determined. Consistent with the hypothesis, it was found that the percentage of lumbar MNs with clear immunoreactivity to the STMN2 antibody was significantly reduced in tissue samples collected from sporadic ALS cases (FIG. 6D). The results are further supported by several independent expression studies of ALS postmortem samples. Three studies have performed laser dissection of motor neuron from ALS patients to perform expression studies (82-84). This data was interrogated and decreased *STMN2* transcript levels were observed for the ALS patient samples relative to control samples (FIGS. 6E-6F).

Discussion

The studies suggest that the abundance of hundreds of transcripts is likely regulated by TDP-43 in human motor neurons, including several RNAs that have surfaced previously in the context of studying ALS. For instance, the findings suggest that *BDNF* expression could in part be regulated by TDP-43, which is of note given that decreased expression of this neurotrophin has been observed previously (85). *MMP9* has previously been shown in the *SOD1* ALS mouse model to define populations of motor neurons most sensitive to degeneration (86). The studies suggest that reduced TDP-43 function might more widely induce expression of this factor, which could sensitize motor neurons to degeneration. Further interrogation of the transcripts that were identified here may provide insights into how perturbations to TDP-43 lead to motor neuron dysfunction.

An important outstanding question has been, what are the mechanistic consequences of familial mutations in TDP-43 and how do their effects relate to the events that occur when TDP-43 becomes pathologically relocalized in patients with sporadic disease. The identification of motor neuron transcripts regulated by TDP-43 provided an opportunity to explore the potential impact of differing manipulations to TDP-43 relevant to both familial and sporadic disease. First, it was asked whether a subset of the target RNAs identified as reduced after TDP-43 depletion displayed significant expression changes in motor neurons produced from patients with TDP-43 mutations. Interestingly, modest but significant changes were found in the expression of the RNA binding protein ELAVL3 and the microtubule regulator STMN2, but not other putative targets identified. Thus, reduced expression of target RNAs is considered as a TDP-43 phenotype, patient mutations displayed partial loss-of-function effects.

Upon over-expression, it has previously been shown that mutant TDP-43 is prone to aggregation (22). Some studies have also suggested that mutant TDP-43 is similarly prone to aggregation when expressed at native levels in patient specific motor neurons (54, 56, 57). To determine whether aggregation or loss of nuclear mutant TDP-43 could be contributing to decreased expression of *STMN2* and *ELAVL3* in the experiments, TDP-43 was carefully monitored in these patient motor neurons, but no such defect was identified. Although it cannot be ruled out that modest nuclear TDP-43 loss or insolubility that were below the range of detection are responsible for the observed decline in *STMN2* and *ELAVL3* expression, the findings are consistent with the notion that mutant protein might simply have reduced affinity or ability to

process certain substrates. Further biochemical experiments beyond the scope of this study will likely be required to discern these potential hypotheses.

It is believed that if larger scale aggregation, or nuclear loss of mutant TDP-43 were occurring in familial patient motor neurons it would be detectable. It was found that proteasome inhibition induced dramatic nuclear loss of TDP-43, along with its insoluble accumulation. The inspiration to perform this manipulation occurred after discovering that proteasome inhibition led to an accumulation of insoluble SOD1 in motor neurons from *SOD1* ALS patient-specific stem cells but not in control motor neurons harboring only normal SOD1 (31). Interestingly, and as apparently observed by others in distinct contexts (32), proteasome inhibition caused loss of nuclear TDP-43 and its insoluble accumulation regardless of whether in a control of disease genotype. This result was captivating as it suggested that disrupted proteostasis induced by any number of ALS implicated mutations or events could be upstream of the most common histopathological finding in sporadic ALS. The findings further the thought that TDP-43 re-localization to the cytoplasm may initially provide a protective and adaptive response to disrupted proteostasis (87). However, it may be that the biochemical nature of this response and the liquid crystal conversion that these complexes can undergo causes a transient response to become a pathological state that chronically depletes motor neurons of important RNAs regulated by TDP-43 (88). The finding that TDP-43 targets are depleted from motor neurons following proteasome inhibition is consistent with that model.

Although it was found that hundreds of RNAs were impacted by TDP-43 depletion, it was noted that not all transcripts seemed to be equally affected by alterations in TDP-43, with a modest number, including those encoding STMN2, ELAVL3 being particularly sensitive. This observation raises an important question with substantial therapeutic implications: Are the primary effects of TDP-43 pathology in patients and the role that it might play in motor neuropathy and degeneration propagated through a small number of target RNAs? If so, understanding the functions of these key TDP-43 targets, the mechanisms by which they become disrupted and whether they can be restored could be significant as it might spotlight a pathway downstream of TDP-43 pathology for restoring motor neuron functionality. Given the established functions of STMN orthologs and the magnitude of the effect of TDP-43 depletion on *STMN2* levels, it was wondered if it might be such a target.

The Stathmin family of proteins are recognized regulators of microtubule stability and have been demonstrated to regulate motor axon biology in the fly (77). Gene editing was used to determine if STMN2 has an important function in human stem cell derived motor neurons and it was found that both motor axon outgrowth and repair were significantly impaired in the absence of this protein. Although hMNs generated *in vitro* share many molecular and functional properties with *bona fide* MNs (29), the *in vivo* validation of discoveries from stem cell-based models of ALS is a critical test of their relevance to disease mechanisms and therapeutic strategies (89). Human adult spinal cord tissues were therefore used to provide *in vivo* evidence corroborating the finding that *STMN2* levels are altered in ALS. The likely mechanism for reduced expression of *STMN2* was the emergence of a cryptic exon. Properly targeted antisense oligonucleotides may suppress this splicing event and restore *STMN2* expression.

Materials and Methods

Cell culture and Differentiation of hESCs and hiPSCs into MNs

Pluripotent stem cells were grown with mTeSR1 medium (Stem Cell Technologies) on tissue culture dishes coated with Matrigel™ (BD Biosciences), and maintained in 5% CO2 incubators at 37ºC. Stem cells were passaged as small aggregates of cells after 1 mM EDTA treatment. 10 μM ROCK inhibitor (Sigma, Y-27632) was added to the cultures for 16-24 hours after dissociation to prevent cell death. MN differentiation was carried out using a modified protocol based on adherent culture conditions in combination with dual inhibition of SMAD signaling, inhibition of NOTCH and FGF signaling, and patterning by retinoic acid and SHH signaling. In brief, ES cells were dissociated to single cells using accutase™ (Stem Cell Technologies) and plated at a density of 80,000 cells/cm^2 on matrigel-coated culture plates with mTeSR1 medium (Stem Cell Technologies) supplemented with ROCK inhibitor (10μM Y-27632, Sigma). When cells reached 100% confluency, medium was changed to differentiation medium (1/2 Neurobasal (Life Technologies™) 1/2 DMEM-F12 (Life Technologies™) supplemented with 1x B-27 supplement (Gibco®), 1x N-2 supplement (Gibco®), 1x Gibco® GlutaMAX™ (Life Technologies™) and 100μM non-essential amino-acids (NEAA)). This time point was defined as day 0 (d0) of motor neuron differentiation. Treatment with small molecules was carried out as follows: 10μM SB431542 (Custom Synthesis), 100nM

LDN-193189 (Custom Synthesis), 1μM retinoic acid (Sigma) and 1μM Smoothend agonist (Custom Synthesis) on d0-d5; 5μM DAPT (Custom Synthesis), 4μM SU-5402 (Custom Synthesis), 1μM retinoic acid (Sigma) and 1μM Smoothend agonist (Custom Synthesis) on d6-d14.

Fluorescent Activated Cell Sorting (FACS) of GFP+ MNs

On d14, differentiated cultures were dissociated to single cells using accutase™ treatment for 1 hour inside a 5% CO2 / 37ºC incubator. Repeated (10-20 times) but gentle pipetting with a 1000μL Pipetman® was used to achieve a single cell preparation. Cells were spun down, washed 1x with PBS and resuspended in sorting buffer (1x cation-free PBS 15mM HEPES at pH 7 (Gibco®), 1% BSA (Gibco®), 1x penicillin-streptomycin (Gibco®), 1 mM EDTA, and DAPI (1μg/mL). Cells were passed through a 45μm filter immediately before FACS analysis and purification. The BD FACS Aria II cell sorter was routinely used to purify *Hb9::*GFP$^+$ cells into collection tubes containing MN medium (Neurobasal (Life Technologies™), 1x N-2 supplement (Gibco®), B-27 supplement (Gibco®), GlutaMax and NEAA) with 10μM ROCK inhibitor (Sigma, Y-27632) and 10ng/mL of neurotrophic factors GDNF, BDNF and CNTF (R&D). DAPI signal was used to resolve cell viability, and differentiated cells not exposed to MN patterning molecules (RA and SAG) were used as negative controls to gate for green fluorescence. For lines not containing the *Hb9::*GFP reporter, single cell sunspensions were incubated with antibodies against NCAM (BD Bioscience, BDB557919, 1:200) and EpCAM (BD Bioscience, BDB347198, 1:50) for 25 minutes in sorting buffer, then washed once with PBS 1x and resuspended in sorting buffer. For RNA-Seq experiments, 200,000 GFP$^+$ cells per well were plated in 24-well tissue culture dishes precoated with matrigel. MN medium supplemented with 10 ng/mL of each GDNF, BDNF and CNTF (R&D Systems) was used to feed and mature the purified MNs. RNA-Seq experiments and most downstream assays were carried with d10 purified MNs (10 days in culture after FACS) grown plates coated with 0,1 mg/ml poly-Dlysine (Invitrogen) and 5 μg/ml laminin (Sigma-Aldrich) at a concentration of around 130000 cells/cm^2.

RNAi

RNAi in cultures of purified GFP$^+$ MNs was induced with Silencer® Select siRNAs (Life Technologies™) targeting the *TDP-43* mRNA or with a non-targeting

siRNA control with scrambled sequence that is not predicted to bind to any human transcripts. Lyophilized siRNAs were resuspended in nuclease-free water and stored at -20oC as 20μM stocks until ready to use. For transfection, siRNAs were diluted in Optimem (Gibco®) and mixed with RNAiMAX (Invitrogen) according to manufacturer's instructions. After 30 min incubation, the mix was added drop-wise to the MN cultures, so that the final siRNA concentration in each well was 60nM in 1:1 Optimem:MN medium (Neurobasal (Life TechnologiesTM, N2 supplement (Gibco®), B-27 supplement (Gibco®), GlutaMax and NEAA) and 10ng/mL of each GDNF, BDNF and CNTF (R&D). 12-16 hours posttransfection media was changed. RNA-Seq experiments and validation assays were carried with material collected 4 days after transfection.

Immunocytochemistry

For immunofluorescence, cells were fixed with ice-cold 4% PFA for 15 minutes at 4°C, permeabilized with 0.2% Triton-X in 1x PBS for 45 minutes and blocked with 10% donkey serum in 1x PBS-T (0.1% Tween-20) for 1 hour. Cells were then incubated overnight at 4°C with primary antibody (diluted in blocking solution). At least 4 washes (5 min incubation each) with 1xPBS-T were carried out, before incubating the cells with secondary antibodies for 1 hour at room temperature (diluted in blocking solution). Nuclei were stained with DAPI. The following antibodies were used in this study: Hb9 (1:100, DSHB, MNR2 81.5C10-c), TUJ1 (1:1000, Sigma, T2200), MAP2 (1:10000, Abcam ab5392), Ki67 (1:400, Abcam, ab833), GFP (1:500, Life Technologies™, A10262), Islet1 (1:500, Abcam ab20670), TDP-43 (1:500, ProteinTech Group), STMN2 (1:4000, Novus), AlexaFluor™ 647-Phalloidin (1:200,). Secondary antibodies used (488, 555, 594, and 647) were AlexaFluor™ (1:1000, Life Technologies™) and DyLight (1:500, Jackson ImmunoResearch Laboratories). Micrographs were analyzed using FIJI software to determine the correlation coefficient.

Immunoblot Assays

For analysis of TDP-43 and STMN2 protein expression levels, d10 MNs were lysed in RIPA buffer (150mM Sodium Chloride; 1% Triton X-100; 0.5% sodium deoxycholate; 0.1% SDS; 50 mM Tris pH 8.0) containing protease and phosphatase inhibitors (Roche) for 20 min on ice, and centrifuged at high speed. 200μL of RIPA

buffer per well of 24-well culture were routinely used, which yielded ~20µg of total protein as determined by BCA (Thermo Scientific). After two washes with RIPA buffer, insoluble pellets were resuspended in 200 µl of UREA buffer (Bio-Rad). For immunoblot assays 2-3µg of total protein were separated by SDS-PAGE (BioRad), transferred to PDVF membranes (BioRad) and probed with antibodies against TDP-43 (1:1000, ProteinTech Group), GAPDH (1:1000, Millipore) and STMN2 (1:3000, Novus). Insoluble pellets were loaded based on protein concentration of correspondent RIPA-soluble counterparts. The same PDVF membrane was immunoassayed 2-3 times using Restore™ PLUS Western Blot Stripping Buffer (Thermo Scientific). GAPDH levels were used to normalized each sample, and LiCor software was used to quantitate protein band signal.

RNA preparation, qRT-PCR and RNA sequencing

Total RNA was isolated from d10 MNs for RNA-Seq experiments and validation assays using Trizol LS (Invitrogen) according to manufacturer's instructions. 500µL were added per well of the 24-well cultures. A total of 300-1000ng of total RNA was used to synthesize cDNA by reverse transcription according to the iSCRIPT kit (Bio-rad). Quantitative RT-PCR (qRT-PCR) was then performed using SYBR green (Bio-Rad) and the iCycler system (Bio-rad). Quantitative levels for all genes assayed were normalized using *GAPDH* expression. Normalized expression was displayed relative to the relevant control sample (mostly sired treated MNs or cells with 1x TDP-43 levels). For comparison between patient line, normalized expression was displayed relative to the average of pooled data points. All primer sequences are available upon request. For next-generation RNA sequencing (RNA-Seq), at least two technical replicas per siRNA sample or AAVS1-TDP43 genotype were included in the analyses. After RNA extraction, samples with RNA integrity numbers (RIN) above 7.5, determined by a bioAnalyzer, were used for library preparation. In brief, RNA sequencing libraries were generated from ~250ng of total RNA using the illumina TruSeq RNA kit v2, according to the manufacturer's directions. Libraries were sequenced at the Harvard Bauer Core Sequencing facility on a HiSeq 2000 platform. All FASTQ files were analyzed using the bcbioRNASeq workflow and toolchain (90). The FASTQ files were aligned to the GRCh37/hg19 reference genome. Differential expression testing was performed using DESeq2 suite of bioinformatics tools (38). The Cuffdiff module of Cufflinks was used to identify

differential splicing. Salmon was used to generate the counts and tximport to load them at gene level (91,92). All p-values are then corrected for multiple comparisons using the method of Benjamini and Hochberg (93).

Electrophysiology recordings

GFP+ MNs were plated at a density of 5,000 cells/cm^2 on poly-D-lysine/laminin-coated coverslips and cultured for 10 days in MN medium, conditioned for 2-3 days by mouse glial cells and supplemented with 10ng/mL of each GDNF, BDNF and CNTF (R&D Systems). Electrophysiology recordings were carried out as previously reported (31,94). Briefly, whole-cell voltage-clamp or current-clamp recordings were made using a Multiclamp 700B (Molecular Devices) at room temperature (21-23C). Data were digitized with a Digidata 1440A A/D interface and recorded using pCLAMP 10_software (Molecular Devices). Data were sampled at 20 kHz and low-pass filtered at 2 kHz. Patch pipettes were pulled from borosilicate glass capillaries on a Sutter Instruments P-97 puller and had resistances of 2-4 MW. The pipette capacitance was reduced by wrapping the shank with Parafilm and compensated for using the amplifier circuitry. Series resistance was typically 5-10 MW, always less than 15 MW, and compensated by at least 80%. Linear leakage currents were digitally subtracted using a P/4 protocol. Voltages were elicited from a holding potential of -80 mV to test potentials ranging from -80 mV to 30 mV in 10 mV increments. The intracellular solution was a potassium-based solution and contained K gluconate, 135; $MgCl_2$, 2; KCl, 6; HEPES, 10; Mg ATP, 5; 0.5 (pH 7.4 with KOH). The extracellular was sodium-based and contained NaCl, 135; KCl, 5; $CaCl_2$, 2; $MgCl_2$, 1; glucose, 10; HEPES, 10, pH 7.4 with NaOH). Kainate was purchased from Sigma.

Formaldehyde RNA Immunoprecipitation

1 well of a 6 well plate of hMNs (2 million cells) were crosslinked and processed according to the MagnaRIP instructions (Millipore). The following antibodies were used in this study: SOD1 (Cell Signaling Technologies), TDP-43 (FL9, gift of D. Cleveland), and mouse IgG, (cell signaling technology). Each RIP RNA fractions' Ct value was normalized to the Input RNA fraction Ct value for the same qPCR Assay to account for RNA sample preparation differences. To calculate the dCt [normalized RIP], Ct[RIP] – (Ct[Input] – log2 (Input Dilution Factor)) was

determined, where the dilution factor was 100 or 1%. To determine the fold enrichment, the ddCt by dCt[normalized RIP] – dCt[normalized IgG] then fold enrichment = 2^-ddCt was calculated.

STMN2 knockout generation

STMN2 guide RNAs were designed using the following web resources: CHOPCHOP (chopchop.rc.fas.harvard.edu) from the Schier Lab (95). Guides were cloned into a vector containing the human U6 promotor (custom synthesis Broad Institute, Cambridge) followed by the cloning site available by cleavage with BbsI, as well as ampicillin resistance. To perform the cloning, all the gRNAs were modified before ordering. The following modifications were used in order to generate overhangs compatible with a BbsI sticky end: if the 5' nucleotide of the sense strand was not a G, this nucleotide was removed and substituted with a G; for the reverse complement strand, the most 3' nucleotide was removed and substituted with a C, while AAAC was added to the 5' end. The resulting modified STMN2 gRNA sequences were used for Cas9 nuclease genome editing: guide 1: 5' CACCGTATAGATGTTGATGTTGCG 3' (Exon 2) (SEQ ID NO: 4), guide 2: 5' CACCTGAAACAATTGGCAGAGAAG 3' (Exon 3) (SEQ ID NO: 5), guide 3: 5' CACCAGTCCTTCAGAAGGCTTTGG 3' (Exon 4) (SEQ ID NO: 6). Cloning was performed by first annealing and phosphorylating both the gRNAs in PCR tubes. 1 µL of both the strands at a concentration of 100 µM was added to 1 µL of T4 PNK (New England Biolabs), 1 µL of T4 ligation buffer and 6 µL of H2O. The tubes were placed in the thermocycler and incubated at 37ºC for 30 mins, followed by 5 mins at 95ºC and a slow ramp down to 25ºC at a rate of 5ºC/minute. The annealed oligos were subsequently diluted 1:100 and 2 µL was added to the ligation reaction containing 2 µL of the 100 µM pUC6 vector, 2 µL of NEB buffer 2.1, 1 µL of 10mM DTT, 1 µL of 10mM ATP, 1 µL of BbsI (New England Biolabs), 0.5 µL of T7 ligase (New England Biolabs) and 10.5 µL of H2O. This solution was incubated in a thermocycler with the following cycle, 37ºC for 5 minutes followed by 21ºC for 5 minutes, repeated a total of 6 times. The vectors were subsequently cloned in OneShot Top10 (ThermoFisher Scientific) cells and plated on LB-ampicilin agar plates and incubated overnight on 37ºC. The vectors were isolated using the Qiagen MIDIprep kit (Qiagen) and measured DNA concentration using the nanodrop. Proper cloning was verified by sequencing the vectors by Genewiz using the M13F(-21) primer.

Stem cell transfection was performed using the Neon Transfection System (ThermoFisher Scientific) with the 100 µL kit (ThermoFisher Scientific). Prior to the transfection, stem cells were incubated in mTeSR1 containing 10µM Rock inhibitor for 1 hour. Cells were subsequently dissociated by adding accutase and incubating for 5 min at 37ºC. Cells were counted using the Countess and resuspended in R medium at a concentration of $2,5*10^6$ cells/mL. The cell solution was then added to a tube containing 1 µg of each vector containing the guide and 1.5 µg of the pSpCas9n(BB)-2A-Puro (PX462) V2.0, a gift from Feng Zhang (Addgene). The electroporated cells were immediately released in pre-incubated 37ºC mTeSR medium containing 10µM of Rock inhibitor in a 10-cm dish when transfected with the puromycin resistant vector. 24 hours after transfection with the Puromycin resistant vector, selection was started. Medium was aspirated and replaced with mTESR1 medium containing different concentrations of Puromycin: 1µg/µL, 2µg/µL and 4 µg/µL. After an additional 24 hours, the medium was aspirated and replaced with mTeSR1 medium. Cells were cultured for 10 days before colony picking the cells into a 24-well plate for expansion.

Genomic DNA was extracted from puromycin-selected colonies using the Qiagen DNeasy Blood and Tissue kit (Qiagen) and PCR screened to confirm the presence of the intended deletion in the STMN2 gene. PCR products were analyzed after electrophoresis on a 1% Agarose Gel. In brief, the targeted sequence was PCR amplified by a pair of primers external to the deletion, designed to produce a 1100 bp deletion-band in order to detect deleted clones. Sequences of the primers used are as follows: OUT_FWD, 5' GCAAAGGAGTCTACCTGGCA 3' (SEQ ID NO: 7) and OUT_REV, 5' GGAAGGGTGACTGACTGCTC 3' (SEQ ID NO: 8). Knockout lines were further confirmed using immunoblot analysis.

Neurite outgrowth assay

Individual Tuj1-positive neurons used for Sholl analyses were randomly selected and imaged using a Nikon Eclipse TE300 with a 40× objective. The neurites were traced using the ImageJ (NIH) plugin NeuronJ (78), and Sholl analysis was performed using the Sholl tool of Fiji (96), quantifying the number of intersections at 10-µm intervals from the cell body. Statistical analysis was performed by comparing the number of intersections of KO clones with the parental WT line for each 10-µm

interval using Prism 6 (Graph Pad, La Jolla, CA, USA). Significance was assessed by a standard Student's t-test, with a p value of $p<0.05$ considered as significant.

Axotomy

Sorted motor neurons were cultured in standard neuron microfluidic devices (SND150, XONA Microfluidics) mounted on glass coverslips coated with 0.1 mg/ml poly-D-lysine (Sigma-Aldrich) and 5 μg/ml laminin (Invitrogen) at a concentration of around 250,000 neurons/device. Axotomy was performed at day 7 of culture by repeated vacuum aspiration and reperfusion of the axon chamber until axons were cut effectively without disturbing cell bodies in the soma compartment.

TDP-43 and STMN2 immunohistochemical analyses

Post-mortem samples from 3 sporadic ALS cases and 3 controls (no evidence of spinal cord disease) were gathered from the Massachusetts Alzheimer's Disease Research Center (ADRC) in accordance with Partners and Harvard IRB protocols. Histologic analysis of TDP-43 immunoreactivity (rabbit polyclonal, ProteinTech Group) was performed to confirm the diagnosis. For STMN2 analyses, sections of formalin fixed lumbar spinal cord were stained using standard immunohistochemical procedure with the exception that citrate buffer antigen retrieval was performed before blocking. Briefly, samples were rehydrated, rinsed with water, blocked in 3% hydrogen peroxide then normal serum, incubated with primary STMN2 rabbit-derived antibody (1:100 dilution, Novus), followed by incubation with the appropriate secondary antibody (anti-rabbit IgG conjugated to horseradish peroxidase 1:200), and exposure to ABC Vectastain kit and DAB peroxidase substrate, and briefly counterstained with hematoxylin before mounting. Multiple levels were examined for each sample.

STMN2 splicing analysis

Total RNA was isolated from neurons using RNeasy Mini Kit (Qiagen) according to manufacturer's instructions. A total of 300-1000ng of total RNA was used to synthesize cDNA by reverse transcription according to the iSCRIPT kit (Bio-rad). RT-PCR was then performed using one cryptic exon-specific primer and then analyzed using the Agilent 2200 Tapestation.

Statistical analysis

Statistical significance for qRT-PCR assays and STMN2 immunohistochemical analyses was assessed using a 2-tail unpaired Student's *t*-test, with a p value of *p<0.05 considered as significant. Type II Error was controlled at the customary level of 0.05.

References

1. Pasinelli, P. & Brown, R. H. Molecular biology of amyotrophic lateral sclerosis: insights from genetics. *Nat. Rev. Neurosci.* 7, 710–723 (2006).

2. Rowland, L. P. & Shneider, N. A. Amyotrophic lateral sclerosis. *New England Journal of Medicine* 344, 1688–1700 (2001).

3. Ravits, J. *et al.* Deciphering amyotrophic lateral sclerosis: What phenotype, neuropathology and genetics are telling us about pathogenesis. *Amyotroph Lateral Scler Frontotemporal Degener* 14, 5–18 (2013).

4. Miller, R. G., Mitchell, J. D. & Moore, D. H. Riluzole for amyotrophic lateral sclerosis (ALS)/motor neuron disease (MND). *Cochrane Database Syst Rev* 3, CD001447 (2012).

5. Ling, S.-C., Polymenidou, M. & Cleveland, D. W. Converging mechanisms in ALS and FTD: disrupted RNA and protein homeostasis. *Neuron* 79, 416–438 (2013).

6. Dion, P. A., Daoud, H. & Rouleau, G. A. Genetics of motor neuron disorders: new insights into pathogenic mechanisms. *Nat. Rev. Genet.* 10, 769–782 (2009).

7. Neumann, M. *et al.* Ubiquitinated TDP-43 in frontotemporal lobar degeneration and amyotrophic lateral sclerosis. *Science* 314, 130–133 (2006).

8. Chen-Plotkin, A. S., Lee, V. M.-Y. & Trojanowski, J. Q. TAR DNA-binding protein 43 in neurodegenerative disease. *Nature Reviews Neurology* 6, 211–220 (2010).

9. Ignatius, S. H., Wu, F., Harrich, D., GarciaMartinez, L. F. & Gaynor, R. B. Cloning and Characterization of a Novel Cellular Protein, Tdp-43, That Binds to Human-Immunodeficiency-Virus Type-1 Tar Dna-Sequence Motifs. *J Virol* 69, 3584–3596 (1995).

10. Buratti, E. *et al.* Nuclear factor TDP-43 and SR proteins promote in vitro and in vivo CFTR exon 9 skipping. *EMBO J* 20, 1774–1784 (2001).

11. Polymenidou, M. *et al.* Long pre-mRNA depletion and RNA missplicing contribute to neuronal vulnerability from loss of TDP-43. *Nat Neurosci* 14, 459–468 (2011).

12. Kawahara, Y. & Mieda-Sato, A. TDP-43 promotes microRNA biogenesis as a component of the Drosha and Dicer complexes. *P Natl Acad Sci Usa* 109, 3347–3352 (2012).

13. Liu-Yesucevitz, L. *et al.* Tar DNA Binding Protein-43 (TDP-43) Associates with Stress Granules: Analysis of Cultured Cells and Pathological Brain Tissue. *PLoS ONE* 5, (2010).

14. Parker, S. J. *et al.* Endogenous TDP-43 localized to stress granules can subsequently form protein aggregates. *Neurochem. Int.* 60, 415–424 (2012).

15. Alami, N. H. *et al.* Axonal transport of TDP-43 mRNA granules is impaired by ALS-causing mutations. *Neuron* 81, 536–543 (2014).

16. Volkening, K., Leystra-Lantz, C., Yang, W., Jaffee, H. & Strong, M. J. Tar DNA binding protein of 43 kDa (TDP-43), 14-3-3 proteins and copper/zinc superoxide dismutase (SOD1) interact to modulate NFL mRNA stability. Implications for altered RNA processing in amyotrophic lateral sclerosis (ALS). *Brain Research* 1305, 168–182 (2009).

17. Benajiba, L. *et al.* TARDBP mutations in motoneuron disease with frontotemporal lobar degeneration. *Ann Neurol.* 65, 470–473 (2009).

18. Rutherford, N. J. *et al.* Novel Mutations in TARDBP(TDP-43) in Patients with Familial Amyotrophic Lateral Sclerosis. *PLoS Genet* 4, (2008).

19. Sreedharan, J. *et al.* TDP-43 mutations in familial and sporadic amyotrophic lateral sclerosis. *Science* 319, 1668–1672 (2008).

20. Van Deerlin, V. M. *et al.* TARDBP mutations in amyotrophic lateral sclerosis with TDP-43 neuropathology: a genetic and histopathological analysis. *The Lancet Neurology* 7, 409–416 (2008).

21. Yokoseki, A. *et al.* TDP-43 mutation in familial amyotrophic lateral sclerosis. *Ann Neurol.* 63, 538–542 (2008).

22. Lee, E. B., Lee, V. M.-Y. & Trojanowski, J. Q. Gains or losses: molecular mechanisms of TDP43-mediated neurodegeneration. *Nat. Rev. Neurosci.* 13, 38–50 (2012).

23. Kraemer, B. C. *et al.* Loss of murine TDP-43 disrupts motor function and plays an essential role in embryogenesis. *Acta Neuropathol* 119, 409–419 (2010).

24. Sephton, C. F. *et al.* TDP-43 is a developmentally regulated protein essential for early embryonic development. *J. Biol. Chem.* 285, 6826–6834 (2010).

25. Wu, L.-S., Cheng, W.-C. & Shen, C.-K. J. Targeted depletion of TDP-43 expression in the spinal cord motor neurons leads to the development of amyotrophic lateral sclerosis-like phenotypes in mice. *J. Biol. Chem.* 287, 27335–27344 (2012).

26. Yang, C. *et al.* Partial loss of TDP-43 function causes phenotypes of amyotrophic lateral sclerosis. *Proc. Natl. Acad. Sci. U.S.A.* 111, E1121–9 (2014).

27. Iguchi, Y. *et al.* Loss of TDP-43 causes age-dependent progressive motor neuron degeneration. *Brain* 136, 1371–1382 (2013).

28. Tollervey, J. R. *et al.* Characterizing the RNA targets and position-dependent splicing regulation by TDP-43. *Nat Neurosci* 14, 452–458 (2011).

29. Davis-Dusenbery, B. N., Williams, L. A., Klim, J. R. & Eggan, K. How to make spinal motor neurons. *Development* 141, 491–501 (2014).

30. Han, S. S. W., Williams, L. A. & Eggan, K. C. Constructing and deconstructing stem cell models of neurological disease. *Neuron* 70, 626–644 (2011).

31. Kiskinis, E. *et al.* Pathways disrupted in human ALS motor neurons identified through genetic correction of mutant SOD1. *Cell Stem Cell* 14, 781–795 (2014).

32. van Eersel, J. *et al.* Cytoplasmic accumulation and aggregation of TDP-43 upon proteasome inhibition in cultured neurons. *PLoS ONE* 6, e22850 (2011).

33. Di Giorgio, F. P., Boulting, G. L., Bobrowicz, S. & Eggan, K. C. Human Embryonic Stem Cell-Derived Motor Neurons Are Sensitive to the Toxic Effect of Glial Cells Carrying an ALS-Causing Mutation. *Stem Cell* 3, 637–648 (2008).

34. Amoroso, M. W. *et al.* Accelerated high-yield generation of limb-innervating motor neurons from human stem cells. *J Neurosci* 33, 574–586 (2013).

35. Chambers, S. M. *et al.* Highly efficient neural conversion of human ES and iPS cells by dual inhibition of SMAD signaling. *Nat Biotechnol* 27, 275–280 (2009).

36. Chambers, S. M. *et al.* Combined small-molecule inhibition accelerates developmental timing and converts human pluripotent stem cells into nociceptors. *Nat Biotechnol* 30, 715–720 (2012).

37. Mackenzie, I. R. A. *et al.* Pathological TDP-43 distinguishes sporadic amyotrophic lateral sclerosis from amyotrophic lateral sclerosis with SOD1 mutations. *Ann Neurol.* 61, 427–434 (2007).

38. Love, M. I., Huber, W. & Anders, S. Moderated estimation of fold change and dispersion for RNA-seq data with DESeq2. *Genome Biology* 15, 550 (2014).

39. Arnold, E. S. *et al.* ALS-linked TDP-43 mutations produce aberrant RNA splicing and adult-onset motor neuron disease without aggregation or loss of nuclear TDP-43. *Proc. Natl. Acad. Sci. U.S.A.* 110, E736–45 (2013).

40. Fiesel, F. C., Weber, S. S., Supper, J., Zell, A. & Kahle, P. J. TDP-43 regulates global translational yield by splicing of exon junction complex component SKAR. *Nucleic Acids Res* 40, 2668–2682 (2012).

41. Prudencio, M. *et al.* Misregulation of human sortilin splicing leads to the generation of a nonfunctional progranulin receptor. *P Natl Acad Sci Usa* 109, 21510–21515 (2012).

42. Yang, C. *et al.* Partial loss of TDP-43 function causes phenotypes of amyotrophic lateral sclerosis. *Proc. Natl. Acad. Sci. U.S.A.* 111, E1121–9 (2014).

43. Bernard, E., Jacob, L., Mairal, J. & Vert, J.-P. Efficient RNA isoform identification and quantification from RNA-Seq data with network flows. *Bioinformatics* 30, 2447–2455 (2014).

44. Bryant, D. W., Priest, H. D. & Mockler, T. C. Detection and quantification of alternative splicing variants using RNA-seq. *Methods Mol Biol* 883, 97–110 (2012).

45. Trapnell, C. *et al.* Differential analysis of gene regulation at transcript resolution with RNA-seq. *Nat Biotechnol* 31, 46–53 (2013).

46. Shiga, A. *et al.* Alteration of POLDIP3 Splicing Associated with Loss of Function of TDP-43 in Tissues Affected with ALS. *PLoS ONE* 7, (2012).

47. Grenningloh, G., Soehrman, S., Bondallaz, P., Ruchti, E. & Cadas, H. Role of the microtubule destabilizing proteins SCG10 and stathmin in neuronal growth. *J. Neurobiol.* 58, 60–69 (2004).

48. Shin, J. E., Geisler, S. & DiAntonio, A. Dynamic regulation of SCG10 in regenerating axons after injury. *Exp Neurol* 252, 1–11 (2014).

49. Kasashima, K., Sakashita, E., Saito, K. & Sakamoto, H. Complex formation of the neuron-specific ELAV-like hu RNA-binding proteins. *Nucleic Acids Res* 30, 4519–4526 (2002).

50. Martin, K. R. *et al.* Over-expression of RCAN1 causes Down syndrome-like hippocampal deficits that alter learning and memory. *Human Molecular Genetics* 21, 3025–3041 (2012).

51. Ariyannur, P. S. *et al.* Methamphetamine-induced neuronal protein NAT8L is the NAA biosynthetic enzyme: implications for specialized acetyl coenzyme A metabolism in the CNS. *Brain Research* 1335, 1–13 (2010).

52. Boulting, G. L. *et al.* A functionally characterized test set of human induced pluripotent stem cells. *Nat Biotechnol* 29, 279–286 (2011).

53. Yuan, S. H. *et al.* Cell-surface marker signatures for the isolation of neural stem cells, glia and neurons derived from human pluripotent stem cells. *PLoS ONE* 6, e17540 (2011).

54. Egawa, N. *et al.* Drug Screening for ALS Using Patient-Specific Induced Pluripotent Stem Cells. *Sci Transl Med* 4, 145ra104–145ra104 (2012).

55. Serio, A. *et al.* Astrocyte pathology and the absence of non-cell autonomy in an induced pluripotent stem cell model of TDP-43 proteinopathy. *Proc. Natl. Acad. Sci. U.S.A.* 110, 4697–4702 (2013).

56. Bilican, B. *et al.* Mutant induced pluripotent stem cell lines recapitulate aspects of TDP-43 proteinopathies and reveal cell-specific vulnerability. *Proc. Natl. Acad. Sci. U.S.A.* 109, 5803–5808 (2012).

57. Zhang, Z. *et al.* Downregulation of MicroRNA-9 in iPSC-Derived Neurons of FTD/ALS Patients with TDP-43 Mutations. *PLoS ONE* 8, e76055 (2013).

58. Mason, M., Lieberman, A. R., Grenningloh, G. & Anderson, P. N. Transcriptional upregulation of SCG10 and CAP-23 is correlated with regeneration of the axons of peripheral and central neurons in vivo. *Mol Cell Neurosci* 20, 595–615 (2002).

59. Morii, H., Shiraishi-Yamaguchi, Y. & Mori, N. SCG10, a microtubule destabilizing factor, stimulates the neurite outgrowth by modulating microtubule dynamics in rat hippocampal primary cultured neurons. *J. Neurobiol.* 66, 1101–1114 (2006).

60. Shin, J. E. *et al.* SCG10 is a JNK target in the axonal degeneration pathway. *P Natl Acad Sci Usa* 109, E3696–E3705 (2012).

61. Sobczak, A. *et al.* Calmyrin1 binds to SCG10 protein (stathmin2) to modulate neurite outgrowth. *Biochim Biophys Acta* 1813, 1025–1037 (2011).

62. Stein, R., Mori, N., Matthews, K., Lo, L. C. & Anderson, D. J. The NGF-inducible SCG10 mRNA encodes a novel membrane-bound protein present in growth cones and abundant in developing neurons. *Neuron* 1, 463–476 (1988).

63. Bieche, I. *et al.* Expression of stathmin family genes in human tissues: non-neural-restricted expression for SCLIP. *Genomics* 81, 400–410 (2003).

64. Smith, B. N. *et al.* Exome-wide rare variant analysis identifies TUBA4A mutations associated with familial ALS. *Neuron* 84, 324–331 (2014).

65. Wu, C.-H. *et al.* Mutations in the profilin 1 gene cause familial amyotrophic lateral sclerosis. *Nature* 488, 499–503 (2012).

66. Nicolas, A. *et al.* Genome-wide Analyses Identify KIF5A as a Novel ALS Gene. *Neuron* 97, 1268–1283.e6 (2018).

67. Guerreiro, R., Bras, J. & Hardy, J. SnapShot: Genetics of ALS and FTD. *Cell* 160, 798–U485 (2015).

68. Lagier-Tourenne, C. *et al.* Divergent roles of ALS-linked proteins FUS/TLS and TDP-43 intersect in processing long pre-mRNAs. *Nat Neurosci* 15, 1488–1497 (2012).

69. Lattante, S., Rouleau, G. A. & Kabashi, E. TARDBP and FUS Mutations Associated with Amyotrophic Lateral Sclerosis: Summary and Update. *Hum. Mutat.* 34, 812–826 (2013).

70. DeJesus-Hernandez, M. *et al.* Expanded GGGGCC hexanucleotide repeat in noncoding region of C9ORF72 causes chromosome 9p-linked FTD and ALS. *Neuron* 72, 245–256 (2011).

71. Renton, A. E., Chiò, A. & Traynor, B. J. State of play in amyotrophic lateral sclerosis genetics. *Nat Neurosci* 17, 17–23 (2014).

72. Renton, A. E. *et al.* A Hexanucleotide Repeat Expansion in C9ORF72 Is the Cause of Chromosome 9p21-Linked ALS-FTD. *Neuron* 72, 257–268 (2011).

73. Buratti, E. & Baralle, F. E. Multiple roles of TDP-43 in gene expression, splicing regulation, and human disease. *Front Biosci* 13, 867–878 (2008).

74. Sugiura, Y. & Mori, N. SCG10 expresses growth-associated manner in developing rat brain, but shows a different pattern to p19/stathmin or GAP-43. *Brain Res. Dev. Brain Res.* 90, 73–91 (1995).

75. Levy, A. D. *et al.* Subcellular Golgi localization of stathmin family proteins is promoted by a specific set of DHHC palmitoyl transferases. *Mol Biol Cell* 22, 1930–1942 (2011).

76. Taylor, J. P., Brown, R. H. & Cleveland, D. W. Decoding ALS: from genes to mechanism. *Nature* 539, 197–206 (2016).

77. Chauvin, S. & Sobel, A. Neuronal stathmins: A family of phosphoproteins cooperating for neuronal development, plasticity and regeneration. *Progress in Neurobiology* 126, 1–18 (2015).

78. Meijering, E. *et al.* Design and validation of a tool for neurite tracing and analysis in fluorescence microscopy images. *Cytometry Part A* 58A, 167–176 (2004).

79. Taylor, A. M. *et al.* A microfluidic culture platform for CNS axonal injury, regeneration and transport. *Nat Methods* 2, 599–605 (2005).

80. Ling, J. P., Pletnikova, O., Troncoso, J. C. & Wong, P. C. TDP-43 repression of nonconserved cryptic exons is compromised in ALS-FTD. *Science* 349, 650–655 (2015).

81. Humphrey, J., Emmett, W., Fratta, P., Isaacs, A. M. & Plagnol, V. Quantitative analysis of cryptic splicing associated with TDP-43 depletion. *BMC Med Genomics* 10, 38 (2017).

82. Rabin, S. J. *et al.* Sporadic ALS has compartment-specific aberrant exon splicing and altered cell–matrix adhesion biology. *Human Molecular Genetics* 19, 313–328 (2009).

83. Highley, J. R. *et al.* Loss of nuclear TDP-43 in amyotrophic lateral sclerosis (ALS) causes altered expression of splicing machinery and widespread dysregulation of RNA splicing in motor neurones. *Neuropathology and Applied Neurobiology* 40, 670–685 (2014).

84. D'Erchia, A. M. *et al.* Massive transcriptome sequencing of human spinal cord tissues provides new insights into motor neuron degeneration in ALS. *Sci Rep* 7, 10046 (2017).

85. Henriques, A., Pitzer, C. & Schneider, A. Neurotrophic growth factors for the treatment of amyotrophic lateral sclerosis: where do we stand? *Front Neurosci* 4, 32 (2010).

86. Kaplan, A. *et al.* Neuronal Matrix Metalloproteinase-9 Is a Determinant of Selective Neurodegeneration. *Neuron* 81, 333–348 (2014).

87. Markmiller, S. *et al.* Context-Dependent and Disease-Specific Diversity in Protein Interactions within Stress Granules. *Cell* 172, 590–604.e13 (2018).

88. Taylor, J. P., Brown, R. H. & Cleveland, D. W. Decoding ALS: from genes to mechanism. *Nature* 539, 197–206 (2016).

89. de Boer, A. S. *et al.* Genetic validation of a therapeutic target in a mouse model of ALS. *Sci Transl Med* 6, 248ra104–248ra104 (2014).

90. Steinbaugh, M. J. *et al.* bcbioRNASeq: R package for bcbio RNA-seq analysis. *F1000Research* 6, 1976 (2017).

91. Patro, R., Duggal, G., Love, M. I., Irizarry, R. A. & Kingsford, C. Salmon provides fast and bias-aware quantification of transcript expression. *Nat Methods* 14, 417–419 (2017).

92. Soneson, C., Love, M. I. & Robinson, M. D. Differential analyses for RNA-seq: transcript-level estimates improve gene-level inferences. *F1000Research* 4, 1521 (2016).

93. Benjamini, Y. & Hochberg, Y. Controlling the False Discovery Rate: A Practical and Powerful Approach to Multiple Testing. *http://www.jstor.org/stable/2346101* 1, 289–300 (1995).

94. Son, E. Y. *et al.* Conversion of mouse and human fibroblasts into functional spinal motor neurons. *Cell Stem Cell* 9, 205–218 (2011).

95. Labun, K., Montague, T. G., Gagnon, J. A., Thyme, S. B. & Valen, E. CHOPCHOP v2: a web tool for the next generation of CRISPR genome engineering. *Nucleic Acids Res* 44, W272–W276 (2016).

96. Ferreira, T. A. *et al.* Neuronal morphometry directly from bitmap images. *Nat Methods* 11, 982–984 (2014).

Example 2:

Recently the identity of mRNA transcripts regulated by the RNA binding protein TDP-43 in human motor neurons was reported. *See* Klim, J.R., et al., ALS-implicated protein TDP-43 sustains levels of STMN2, a mediator of motor neuron growth and repair. *Nat Neurosci*, 2019. 22(2): p. 167-179. Although TDP-43 regulates hundreds of transcripts in human motor neurons, one of the transcripts most affected by TDP-43 depletion was *STMN2*. STMN2 is a protein involved in microtubule assembly and is one of the most abundant transcripts expressed by a neuron. In depth analysis of the data revealed that TDP-43 suppresses a cryptic exon in the *STMN2* transcript. The inclusion of this cryptic exon prevents the full-length form from being expressed leading to drastically decreased levels of STMN2 protein. Knockdown of TDP-43 in cell culture, as well as post-mortem tissue from patients exhibiting TDP-43 pathology, display altered *STMN2* splicing. The cryptic exon-containing transcript contains its own stop and start sites and therefore potentially encodes for a 17 amino acid peptide. This change in human models was validated in RNA sequencing data from post-mortem spinal cord. Therefore, it was considered whether the cryptic *STMN2* transcript or the peptide it encodes could serve as a CSF/fluid biomarker for people developing or with ALS or other patients exhibiting TDP-43 proteinopathies (e.g., Parkinson's, traumatic brain injury, Alzheimer's).

FIGS. 17A-17C show RNA can be readily collected from CSF-derived exosomes and then converted into cDNA to assay for full and cryptic *STMN2* transcripts as well as control RNAs for normalization (FIG. 17A). The TaqMan Q-RT-PCR assay was validated to show that it simultaneously detects both the full and cryptic *STMN2* transcripts using TDP-43 knockdown approaches in human neurons. *STMN2* transcripts are normalized to the house keeping ribosomal subunit *RNA18S5.* TDP-43 levels were reduced in cultured human neurons using either an antisense oligonucleotide (ASO) to deplete cells of TDP-43 or an siRNAs to induce TDP-43 knockdown. In both conditions, a strong induction of the cryptic exon relative to a control was identified (FIG. 17B). Using the validated multiplexed qPCR assay, next RNA was isolated from CSF-derived exosomes using 300ul patient samples to

determine the levels of cryptic *STMN2* (n=7 healthy controls, n = 2 disease mimics and n = 9 ALS patients). Relative to control samples, most ALS samples demonstrated above average levels of the *STMN2* cryptic exon, with several samples showing levels orders of magnitude higher (FIG. 17C). Note that even in this modest set of samples that the increase in cryptic exon expression in ALS patients was highly significant ($P<0.005$). It is further notable that the two individuals who had non-ALS motor neuron disease (mimics) showed control levels of splicing. Finally, there is an interesting "texture" to the patient data with some patients showing high levels of expression and others more normal levels. It is hypothesized that patients with lower levels may either be earlier in their disease or have non-TDP-43 disease.

The most common pathological hallmark in ALS is the cytoplasmic accumulation and nuclear clearance of TDP-43. Many groups and companies are interested in developing therapeutics that rescue these changes in TDP-43 localization and function. However, to date, there are no biomarkers that could be used in a living person to monitor TDP-43 dysfunction or its rescue. The assay described here could be used in exactly this way. Furthermore, there is interest in *STMN2* and its cryptic splicing itself as a target in ALS. The assay will allow for target engagement to be directly measured in patients during clinical studies.

Example 3

Background on the Patient

The patient is currently a 40 year old male whose ALS symptoms first began in April 2017 with weakness in the left hand. The weakness progressively worsened and spread to involve bilateral hand and arm atrophy. Around May 2018, the patient developed progressively worsening leg spasticity, weakness and atrophy, and dysarthria. The diagnosis of ALS was established clinically in November 2017, and confirmed by EMG studies in March 2018. There is no family history of ALS; comprehensive exome and genome scans have not disclosed any mutations documented to cause ALS such as mutations in the C9ORF72 or SOD1 genes.

The patient takes three FDA-approved ALS therapies: riluzole, edaravone, and Nuedexta. Additionally, the patient was treated with autologous mesenchymal stem cells in South Korea in June and November 2019. Despite the foregoing therapies, the patient's clinical course and the ALSFRS trajectory have accelerated.

Project Rationale

Stathmin2 (STMN2) is a 179 amino acid protein expressed exclusively in the CNS (and particularly prominently in spinal motor neurons) that controls stability of microtubules. Studied for years as SCG10 (superior cervical ganglion 10), STMN2 is essential for axon regrowth after injury. Strikingly, in 2019 two important papers independently documented that the function of stathmin2 is suppressed in many cases of sporadic ALS, as well as in ALS arising from mutations in genes encoding TDP43 and C9ORF72 (1, 2). These findings were recently independently confirmed by a third lab (3).

Importantly, these studies identified STMN2, one of the most abundant transcripts in human motor neurons, as a central TDP-43 interacting RNA. They also each provided support for a mechanism in sporadic ALS in which disruptions to protein homeostasis resulting from aging, environmental exposure, injury or ALS/FTD-causing mutations leading to TDP43 mislocalization, aggregation, and altered RNA metabolism – a pathology that is present in nearly all sporadic ALS cases. While the abundance of many transcripts changes due to loss of TDP-43 function, the precipitous loss of STMN2 after TDP-43 knockdown or loss of function provides compelling evidence linking STMN2 to TDP-43 pathology and the disruption of mechanisms protecting the axon and preventing neuropathy.

In light of this impressive recent literature, tissue was sampled from the patient, and culture conditions were developed for modeling impacts on his motor neurons. A series of studies directed at this pathway and the patient's cells were undertaken to study the mechanism of TDP-43 regulation of STMN2 in which TDP-43 binds to STMN2 pre-mRNA on the intron between exons 1 and 2. Either reduction of TDP-43 levels or nuclear egress leads to the same outcome for STMN2: early polyadenylation and splicing of a cryptic exon leading to a truncated STMN2 mRNA transcript at the cost of full-length transcript (FIG. 81). It thus appears that TDP-43 regulation of STMN2 has the potential to serve as a disease biomarker or even a therapeutic target for splice-switching antisense oligonucleotides given the success of nusinersen for spinal muscular atrophy.

After extensive screening, a panel of three ASOs were identified, with one (SJ+94) that: (i) effectively corrects TDP-43-induced STMN2 mis-splicing in the patient's motor neurons and (ii) is non-toxic. Further analysis was also performed of the other two ASOs in the panel.

Patient's motor neurons have less nuclear TDP-43 when compared to healthy individuals

The scientific discoveries that ultimately led to the ASOs in the panel, including SJ+94 and SJ-1, are that (1) sporadic ALS patients have mis-localization of TDP-43, i.e., less nuclear TDP-43 when compared to healthy individual, and (2) this mis-localization of TDP-43 causes mis-splicing of STMN2, leading to truncated, cryptic STMN2 in sporadic ALS patients which is a driver of the progression of their disease.

Cells were reprogramed from cells donated by the patient to generate induced pluripotent stem cells (iPSC) MGH 138 (FIG. 84A). Using sequence analysis, the genotype of the stem cell line (MGH 138) was confirmed to be the patient's (FIG. 84B). With this confirmation stem cell-derived motor neurons (hMNs) were generated from the patient's iPS cells (FIGS. 84C-84D). The patient's motor neurons were then used for all the in vitro proof of concept tests described herein.

Once the patient's motor neurons were generated, it was determined to ascertain whether there is any difference in the nuclear TDP-43 in the patient's motor neurons versus healthy controls. As discussed above, loss of nuclear TDP-43, which can manifest as cytoplasmic mis-localization, is a pathological hallmark of sporadic ALS based on multiple analyses of post-mortem CNS tissues. Though far more difficult to detect in motor neurons than post-mortem tissue, at least one previous study has reported that iPSC-derived neurons from ALS patients can recapitulate TDP-43 pathology, including its cytoplasmic mis-localization.

Neurons were isolated from the patient's iPS cells as well as five healthy control iPSC lines. Immunocytochemistry was used to probe the subcellular localization of TDP-43 in the neurons (FIG. 85A). In the control neurons, primarily nuclear TDP-43 staining was observed using Pearson's coefficient analysis, which revealed a strong correlation between TDP-43 immunostaining and the DNA counterstain (FIG. 85B). In contrast, the patient's iPS cell-derived neurons displayed a diminished correlation between TDP-43 and the nuclear stain indicating lower levels of nuclear TDP-43 in the patient's motor neurons compared to control confirming TDP-43 pathology in the patient (FIG. 85B).

Patient specific *in vitro* model

Over the last two years three independent published studies have shown that depletion of nuclear TDP-43 in sporadic ALS patients causes truncation of STMN2. These studies however have involved post-mortem tissue of sporadic ALS patients. Thus, the patient's motor neurons were studied to see if the patient's STMN2 is similarly regulated by TDP-43. Therefore, while it has been demonstrated that the nuclear TDP-43 level in the patient's motor neurons was reduced when compared to non-ALS controls, it was then further reduced in an *in vitro* cell assay in order to more clearly assess the efficacy, if any, of the potential ASO's in suppressing cryptic STMN2 in the patient's motor neurons. This approach was required because definitive corroboration that TDP-43 and STMN2 are dysfunctional requires detailed analysis and dissection of CNS tissue, which is not an option for any living ALS patient. Moreover, this *in vitro* approach is fully consistent with the *in vivo* TDP-43 pathology (loss of functional TDP-43) in the patient with sporadic ALS.

To test whether the patient's STMN2 is regulated by TDP-43 the patient's motor neurons were treated with siTARDBP RNA, to reduce TDP-43 levels. Quantitative reverse transcription–polymerase chain reaction (qRT-PCR) was performed to measure TDP-43 mRNA levels and it was confirmed that TDP-43 mRNA levels had been reduced in the patient's motor neurons relative to those exposed to a nontargeting siRNA (siCTRL) (FIG. 86A). It was further confirmed that the TDP-43 depletion in the patient's motor neurons caused a decrease in STMN2 full length transcript and strong induction of the truncated (mis-spliced) form of STMN2 RNA (FIGS. 86B-86C).

These results thus confirmed that the patient's STMN2 is regulated by TDP-43. Moreover, it was established that depletion of TDP-43 levels in the patient's motor neurons directly causes mis-splicing of STMN2 leading to truncated, cryptic STMN2 mRNA transcript at the cost of full-length transcript. With these results, it was then assessed whether the pathological effects in the patient's motor neurons would be amenable to therapeutic modulation using antisense oligonucleotides—the pharmacological approach used for nusinersen, eteplirsen, mipomersen, milasen and jacifusen.

Design and screen of ASOs

To ensure that ASOs that were designed matched the patient's genetic signature, the region around the STMN2 cryptic exon – the intronic region that is

retained upon TDP-43 dysfunction - was PCR-amplified from genomic DNA extracted from the patient's iPS cells. The region was focused on as it was hypothesized that defects in STMN2 transcription could be rescued by targeting ASOs to the RNA region from the cryptic splice site to the cryptic polyadenylation site, and which includes the TDP-43 binding site. The PCR product was then Sanger sequenced and confirmed that the targeted region was a perfect match between the patient's sequence and the reference genome (FIG. 87A, FIG. 87C).

ASOs targeting this region were designed and synthesized in order to attempt to correct the splicing defects observed in STMN2 transcript of the patient's motor neurons. In particular, several ASOs were designed to be complementary to a region of the pre-mRNA that is predicted to be unstructured and thus potentially accessible for ASO binding (this region is from bases 94 to 121 after the cryptic splice site). These ASOs were synthesized using two different chemistries (2'-O-methoxyethyl RNA (MOE), as well as chimeras of MOE with locked nucleic acid; all sequences contained phosphorothioate linkages) and were tiled along the intron ranging from just 5' of the cryptic exon to the 3' polyadenylation site (FIG. 82). Because the compounds do not contain DNA, it was expected that these targeted ASOs would bind to the transcript and act sterically to promote proper STMN2 splicing.

In total, 51 ASOs were screened in the patient's motor neurons for their ability to (1) suppress the generation of truncated STMN2 transcript as well as (2) restore the full-length STMN2 transcript. ASO SJ+94 and ASO SJ-1 were selected as candidates after iterative screening experiments described below based upon their ability to both suppress cryptic splicing of STMN2 and restore full length STMN2 RNA in the patient's motor neurons (the latter in two different experiments), boost STMN2 protein levels in the patient's motor neurons and promote axonal regrowth in the patient's motor neurons—creating the potential for a real clinical benefit.

In the first experiment the patient's motor neurons were treated with siTARDBP, the patient's motor neurons were then cultured with the various ASOs over a range of concentrations (ranging from 30nM to 0.03nM) before extracting total RNA. Extracted RNA was used to synthesize cDNA by reverse transcription. qRT-PCR was used to assess levels for both truncated and full-length STMN2 RNAs normalized using RNA18S5 expression. While a number of ASOs showed promising results, ASO SJ+94's results stood out as it was able in a dose dependent manner to both (i) suppress cryptic splicing (FIG. 88A) and (ii) restore full length STMN2 RNA

relative to a non-targeting control ASO-NTC (FIG. 88B) in the patient's motor neurons. In addition, ASO SJ-1's results was both effective and safe in (i) suppressing cryptic splicing (FIG. 95A) and (ii) restoring full length STMN2 RNA relative to a non-targeting control ASO-NTC (FIG. 95B) in the patient's motor neurons.

Summary of efficacy of ASOs

It was established that ASO (SJ+94) and ASO (SJ-1) suppressed cryptic splicing of STMN2 and restored full length STMN2 RNA in the patient's motor neurons when there is a reduction in nuclear TDP-43. It was then assessed to see if it would prove efficacious in a different experimental paradigm when TDP-43 was mis-localized. Post-mortem tissue studies have shown that TDP-43 mis-localization and its aggregation in cytoplasm is a hallmark of sporadic ALS. Several groups have reported cytoplasmic aggregation of TDP-43 akin to that observed in post-mortem tissue of sporadic ALS patients occurs in response to pharmacological inhibition of the proteasome (1, 4). This mis-localization of TDP-43 has also been shown to cause altered expression of its transcripts including STMN2.

Proteasome inhibition (MG-132 (1 uM)) in the patient's neurons, which induces nuclear depletion of TDP-43, led to decreased STMN2 expression (FIG. 89). Indeed, the patient's motor neurons treated with ASO SJ+94 maintained significantly higher levels of full length STMN2 RNA (p value 0.0024) than those treated with a non-targeting control ASO (NTC) (FIG. 89). In addition, the patient's motor neurons treated with ASO SJ-1 maintained significantly higher levels of full-length STMN2 RNA (30% higher) than those treated with a non-targeting control ASO (NTC)-- which translates to a p value of 0.0003 (FIG. 96).

After establishing and validating that the STMN2 ASOs could affect transcript levels, it was sought to determine if they could also rescue diminished protein levels observed after TDP-43 reduction. The patient's motor neurons were treated with siRNAs and either a nontargeting ASO (NTC) or one of the lead compounds from the screen (FIG. 90, FIG. 97). As a positive control, the patient's motor neurons were cultured with SP600125, an established JNK inhibitor (JNKi) that has previously been demonstrated to boost STMN2 protein levels (1, 5). Subsequent immunoblot analysis showed STMN2 protein levels were decreased after the loss of nuclear TDP-43 by siTDP and increased after JNK inhibition (FIG. 90). Unlike the cells treated with the

non-targeting control ASO (NTC), restoration of STMN2 to the levels of the siRNA controls for the lead candidates was observed. These collective results demonstrated that the ASOs tested prevent processing of the nascent STMN2 RNA transcript into the truncated form in favor of the full-length transcript to restore protein levels back to normal.

Summary of efficacy of ASOs on axonal regeneration

It was previously demonstrated that TDP-43 depletion leads to reduced axonal regrowth after injury (1). A similar phenotype was observed in hMNs with reduced levels of STMN2 or completely lacking STMN2, which could be rescued through restoration of STMN2 or post-translational stabilization of STMN2 (1, 2). These results strongly implicate STMN2 in the motor neuropathy observed in ALS.
To test if ASO SJ+94 could rescue axonal regrowth after TDP-43 depletion and injury, the patient's motor neurons were cultured in microfluidic devices that permitted axon growth into a chamber distinct from the neuronal cell bodies (FIG. 91A). Neurons cultured for 7 days in the soma compartment of the device extended axons through the microchannels into the axon chamber. Neurons were treated with siTARDBP and ASO SJ+94 before severing axons without disturbing cell bodies in the soma compartment. The axon extension was then measured from the microchannel to assess regrowth after injury (FIG. 91B, FIG. 91D). The analysis revealed significantly increased regrowth with ASO SJ+94 relative to the non-targeting control ASO (FIG. 91C). The analysis additionally revealed significantly increased regrowth with ASO SJ-1 relative to the non-targeting control ASO (FIG. 91E) with mean values of 243um and 176um respectively (p value 0.0014).

References

1. Klim JR, Williams LA, Limone F, Guerra San Juan I, Davis-Dusenbery BN, Mordes DA, Burberry A, Steinbaugh MJ, Gamage KK, Kirchner R, Moccia R, Cassel SH, Chen K, Wainger BJ, Woolf CJ, Eggan K. ALS-implicated protein TDP-43 sustains levels of STMN2, a mediator of motor neuron growth and repair. Nat Neurosci. 2019;22(2):167-79. Epub 2019/01/16. doi: 10.1038/s41593-018-0300-4. PubMed PMID: 30643292.

2. Melamed Z, Lopez-Erauskin J, Baughn MW, Zhang O, Drenner K, Sun Y, Freyermuth F, McMahon MA, Beccari MS, Artates JW, Ohkubo T, Rodriguez M, Lin N, Wu D, Bennett CF, Rigo F, Da Cruz S, Ravits J, Lagier-Tourenne C, Cleveland DW. Premature polyadenylation-mediated loss of stathmin-2 is a hallmark of TDP-43-dependent neurodegeneration. Nat Neurosci. 2019;22(2):180-90. Epub 2019/01/16. doi: 10.1038/s41593-018-0293-z. PubMed PMID: 30643298; PMCID: PMC6348009.

3. Prudencio M, Humphrey J, Pickles S, Brown AL, Hill SE, Kachergus J, Shi J, Heckman M, Spiegel M, Cook C, Song Y, Yue M, Daughrity L, Carlomagno Y, Jansen-West K, Fernandez De Castro C, DeTure M, Koga S, Wang YC, Sivakumar P, Bodo C, Candalija A, Talbot K, Selvaraj BT, Burr K, Chandran S, Newcombe J, Lashley T, Hubbard I, Catalano D, Kim D, Propp N, Fennessey S, Fagegaltier D, Phatnani H, Secrier M, Fisher EM, Oskarsson B, van Blitterswijk M, Rademakers R, Graff-Radford NR, Boeve B, Knopman DS, Petersen R, Josephs K, Thompson EA, Raj T, Ward ME, Dickson D, Gendron TF, Fratta P, Petrucelli L. Truncated stathmin-2 is a marker of TDP-43 pathology in frontotemporal dementia. J Clin Invest. 2020. Epub 2020/08/14. doi: 10.1172/JCI139741. PubMed PMID: 32790644.

4. van Eersel J, Ke YD, Gladbach A, Bi M, Gotz J, Kril JJ, Ittner LM. Cytoplasmic accumulation and aggregation of TDP-43 upon proteasome inhibition in cultured neurons. PLoS One. 2011;6(7):e22850. Epub 2011/08/11. doi: 10.1371/journal.pone.0022850. PubMed PMID: 21829535; PMCID: PMC3146516.

5. Shin JE, Miller BR, Babetto E, Cho Y, Sasaki Y, Qayum S, Russler EV, Cavalli V, Milbrandt J, DiAntonio A. SCG10 is a JNK target in the axonal degeneration pathway. Proc Natl Acad Sci U S A. 2012;109(52):E3696-705. Epub 2012/11/29. doi: 10.1073/pnas.1216204109. PubMed PMID: 23188802; PMCID: PMC3535671.

***

Those skilled in the art will recognize, or be able to ascertain using no more than routine experimentation, many equivalents to the specific embodiments described herein. The scope of the present invention is not intended to be limited to the Description or the details set forth therein. Articles such as "a", "an" and "the" may mean one or more than one unless indicated to the contrary or otherwise evident from the context. Claims or descriptions that include "or" or "and/or" between one or more members of a group are considered satisfied if one, more than one, or all of the group members are present in, employed in, or otherwise relevant to a given product or process unless indicated to the contrary or otherwise evident from the context. The invention includes embodiments in which exactly one member of the group is present in, employed in, or otherwise relevant to a given product or process. The invention includes embodiments in which more than one, or all of the group members are present in, employed in, or otherwise relevant to a given product or process. Furthermore, it is to be understood that the invention encompasses all variations, combinations, and permutations in which one or more limitations, elements, clauses, descriptive terms, etc., from one or more of the claims (whether original or subsequently added claims) is introduced into another claim (whether original or subsequently added). For example, any claim that is dependent on another claim can be modified to include one or more element(s), feature(s), or limitation(s) found in any other claim, e.g., any other claim that is dependent on the same base claim. Any one or more claims can be modified to explicitly exclude any one or more embodiment(s), element(s), feature(s), etc. For example, any particular sideroflexin, sideroflexin modulator, cell type, cancer type, etc., can be excluded from any one or more claims.

It should be understood that (i) any method of classification, prediction, treatment selection, treatment, etc., can include a step of providing a sample, e.g., a sample obtained from a subject in need of classification, prediction, treatment selection, treatment, for cancer, e.g., a cancer sample obtained from the subject; (ii) any method of classification, prediction, treatment selection, treatment,, etc., can include a step of providing a subject in need of such classification, prediction, treatment selection, treatment, or treatment for cancer.

Where the claims recite a method, certain aspects of the invention provide a product, e.g., a kit, agent, or composition, suitable for performing the method.

Where elements are presented as lists, e.g., in Markush group format, each subgroup of the elements is also disclosed, and any element(s) can be removed from the group. For purposes of conciseness only some of these embodiments have been specifically recited herein, but the present disclosure encompasses all such embodiments. It should also be understood that, in general, where the invention, or aspects of the invention, is/are referred to as comprising particular elements, features, etc., certain embodiments of the invention or aspects of the invention consist, or consist essentially of, such elements, features, etc.

Where numerical ranges are mentioned herein, the invention includes embodiments in which the endpoints are included, embodiments in which both endpoints are excluded, and embodiments in which one endpoint is included and the other is excluded. It should be assumed that both endpoints are included unless indicated otherwise. Furthermore, unless otherwise indicated or otherwise evident from the context and understanding of one of ordinary skill in the art, values that are expressed as ranges can assume any specific value or subrange within the stated ranges in different embodiments of the invention, to the tenth of the unit of the lower limit of the range, unless the context clearly dictates otherwise. Where phrases such as "less than X", "greater than X", or "at least X" is used (where X is a number or percentage), it should be understood that any reasonable value can be selected as the lower or upper limit of the range. It is also understood that where a list of numerical values is stated herein (whether or not prefaced by "at least"), the invention includes embodiments that relate to any intervening value or range defined by any two values in the list, and that the lowest value may be taken as a minimum and the greatest value may be taken as a maximum. Furthermore, where a list of numbers, e.g., percentages, is prefaced by "at least", the term applies to each number in the list. For any embodiment of the invention in which a numerical value is prefaced by "about" or "approximately", the invention includes an embodiment in which the exact value is recited. For any embodiment of the invention in which a numerical value is not prefaced by "about" or "approximately", the invention includes an embodiment in which the value is prefaced by "about" or "approximately". "Approximately" or "about" generally includes numbers that fall within a range of 1% or in some embodiments 5% or in some embodiments 10% of a number in either direction (greater than or less than the number) unless otherwise stated or otherwise evident

from the context (e.g., where such number would impermissibly exceed 100% of a possible value).

It should be understood that, unless clearly indicated to the contrary, in any methods claimed herein that include more than one act, the order of the acts of the method is not necessarily limited to the order in which the acts of the method are recited, but the disclosure encompasses embodiments in which the order is so limited. In some embodiments a method may be performed by an individual or entity. In some embodiments steps of a method may be performed by two or more individuals or entities such that a method is collectively performed. In some embodiments a method may be performed at least in part by requesting or authorizing another individual or entity to perform one, more than one, or all steps of a method. In some embodiments a method comprises requesting two or more entities or individuals to each perform at least one step of a method. In some embodiments performance of two or more steps is coordinated so that a method is collectively performed. It should also be understood that unless otherwise indicated or evident from the context, any product or composition described herein may be considered "isolated". It should also be understood that, where applicable, unless otherwise indicated or evident from the context, any method or step of a method that may be amenable to being performed mentally or as a mental step or using a writing implement such as a pen or pencil, and a surface suitable for writing on, such as paper, may be expressly indicated as being performed at least in part, substantially, or entirely, by a machine, e.g., a computer, device (apparatus), or system, which may, in some embodiments, be specially adapted or designed to be capable of performing such method or step or a portion thereof.

Section headings used herein are not to be construed as limiting in any way. It is expressly contemplated that subject matter presented under any section heading may be applicable to any aspect or embodiment described herein.

Embodiments or aspects herein may be directed to any agent, composition, article, kit, and/or method described herein. It is contemplated that any one or more embodiments or aspects can be freely combined with any one or more other embodiments or aspects whenever appropriate. For example, any combination of two or more agents, compositions, articles, kits, and/or methods that are not mutually inconsistent, is provided. It will be understood that any description or exemplification of a term anywhere herein may be applied wherever such term appears herein (e.g., in

any aspect or embodiment in which such term is relevant) unless indicated or clearly evident otherwise.

CLAIMS

What is claimed is:

1. An antisense oligonucleotide that specifically binds an STMN2 mRNA, pre-mRNA, or nascent RNA sequence, wherein the antisense oligonucleotide increases STMN2 protein expression.

2. An antisense oligonucleotide that specifically binds an STMN2 mRNA, pre-mRNA, or nascent RNA sequence, thereby suppressing or preventing inclusion of an abortive or altered STMN2 RNA sequence, wherein the antisense oligonucleotide does not bind to a polyadenylation site of the STMN2 RNA sequence.

3. The antisense oligonucleotide of claim 1, wherein the abortive or altered STMN2 RNA sequence occurs and increases in abundance when TDP-43 function declines or TDP-pathology occurs.

4. An antisense oligonucleotide that specifically binds an STMN2 mRNA, pre-mRNA, or nascent RNA sequence coding for a cryptic exon, thereby suppressing or preventing inclusion of a cryptic exon in STMN2 RNA, wherein the antisense oligonucleotide does not bind to a polyadenylation site of the STMN2 mRNA, pre-mRNA, or nascent RNA sequence.

5. The antisense oligonucleotide of any one of claims 1-4, wherein the antisense oligonucleotide is designed to target a 5' splice site, a 3' splice site, or a normal TDP-43 binding site.

6. The antisense oligonucleotide of any one of claims 1-4, wherein the antisense oligonucleotide is designed to target a single stranded region.

7. The antisense oligonucleotide of claim 6, wherein the antisense oligonucleotide is designed to target a single stranded region located between the TDP-43 binding site and the polyadenylation site.

8. The antisense oligonucleotide of any one of claims 1-7, wherein the antisense oligonucleotide targets one or more splice sites.

9. An antisense oligonucleotide comprising a sequence selected from the group consisting of SEQ ID NOS: 37-85.

10. The antisense oligonucleotide of claim 9, wherein the antisense oligonucleotide comprises a sequence selected from the group consisting of SEQ ID NOS: 37-74.

11. The antisense oligonucleotide of claim 9, wherein the antisense oligonucleotide comprises a sequence selected from the group consisting of: SEQ ID NO: 40, SEQ ID NO: 47, SEQ ID NO: 48, SEQ ID NO: 49, SEQ ID NO: 50, SEQ ID NO: 52, SEQ ID NO: 53, SEQ ID NO: 54, SEQ ID NO: 56, and SEQ ID NO: 78.

12. The antisense oligonucleotide of claim 9, wherein the antisense oligonucleotide comprises SEQ ID NO: 52.

13. The antisense oligonucleotide of claim 9, wherein the antisense oligonucleotide comprises a sequence selected from the group consisting of: SEQ ID NO: 53, SEQ ID NO: 72, and SEQ ID NO: 73.

14. The antisense oligonucleotide of claim 9, wherein the antisense oligonucleotide comprises SEQ ID NO: 73

15. The antisense oligonucleotide of claim 9, wherein the antisense oligonucleotide comprises SEQ ID NO: 53.

16. The antisense oligonucleotide of claim 9, wherein the antisense oligonucleotide suppresses or prevents inclusion of a cryptic exon in STMN2 RNA.

17. The antisense oligonucleotide of claim 9, wherein the antisense oligonucleotide specifically binds an STMN2 RNA, pre-mRNA, or nascent RNA sequence coding for a cryptic exon.

18. The antisense oligonucleotide of claim 9, wherein the antisense oligonucleotide increases STMN2 protein.

19. The antisense oligonucleotide of claim 9, wherein the antisense oligonucleotide is designed to target a 5’ splice site, a 3’ splice site, or a normal TDP-43 binding site.

20. The antisense oligonucleotide of claim 9, wherein the antisense oligonucleotide is designed to target a site proximal to a cryptic splice site, a site proximal to a premature polyadenylation site, or a site located between a cryptic splice site and a premature polyadenylation site.

21. The antisense oligonucleotide of claim 9, wherein the antisense oligonucleotide is designed to target a single stranded region.

22. The antisense oligonucleotide of claim 9, wherein the antisense oligonucleotide is designed to target a single stranded region located between the TDP-43 binding site and the polyadenylation site.

23. The antisense oligonucleotide of claim 9, wherein the antisense oligonucleotide binds to a target region within the cryptic exon that is unstructured.

24. The antisense oligonucleotide of claim 9, wherein the antisense oligonucleotide binds near or adjacent to the 5' splice site regulated by TDP-43.

25. The antisense oligonucleotide of claim 9, wherein the antisense oligonucleotide targets a region proximal to a predicted TDP-43 binding site.

26. The antisense oligonucleotide of claim 9, wherein the antisense oligonucleotide targets the TDP-43 normal binding site.

27. A pharmaceutical composition comprising one or more antisense oligonucleotides comprising a sequence selected from the group consisting of SEQ ID NOS: 37-85.

28. The pharmaceutical composition of claim 27, wherein the one or more antisense oligonucleotides comprise a sequence selected from the group consisting of SEQ ID NOS: 37-74.

29. The pharmaceutical composition of claim 27, wherein the one or more antisense oligonucleotides comprise a sequence selected from the group consisting of: SEQ ID NO: 40, SEQ ID NO: 47, SEQ ID NO: 48, SEQ ID NO: 49, SEQ ID NO: 50, SEQ ID NO: 52, SEQ ID NO: 53, SEQ ID NO: 54, SEQ ID NO: 56, and SEQ ID NO: 78.

30. The pharmaceutical composition of claim 27, wherein the one or more antisense oligonucleotides comprise SEQ ID NO: 52.

31. The pharmaceutical composition of claim 27, wherein the one or more antisense oligonucleotides comprise a sequence selected from the group consisting of: SEQ ID NO: 53, SEQ ID NO: 72, and SEQ ID NO: 73.

32. The pharmaceutical composition of claim 27, wherein the one or more antisense oligonucleotides comprise SEQ ID NO: 73.

33. The pharmaceutical composition of claim 27, wherein the one or more antisense oligonucleotides comprise SEQ ID NO: 53.

34. The pharmaceutical composition of claim 27, wherein the composition comprises two or more antisense oligonucleotides.

35. The pharmaceutical composition of claim 27, wherein the two or more antisense oligonucleotides are covalently linked.

36. The pharmaceutical composition of claim 27, wherein the composition comprises three or more antisense oligonucleotides.

37. The pharmaceutical composition of claim 27, wherein the one or more antisense oligonucleotides increase STMN2 protein expression.

38. The pharmaceutical composition of claim 27, wherein the one or more antisense oligonucleotides are designed to target a 5' splice site, a 3' splice site, or a normal TDP-43 binding site.

39. The pharmaceutical composition of claim 27, wherein the one or more antisense oligonucleotides are designed to target a site proximal to a cryptic splice site, a site proximal to a premature polyadenylation site, or a site located between a cryptic splice site and a premature polyadenylation site.

40. The pharmaceutical composition of claim 27, wherein the one or more antisense oligonucleotides are designed to target a single stranded region.

41. The pharmaceutical composition of claim 27, wherein the one or more antisense oligonucleotides are designed to target a single stranded region located between the TDP-43 binding site and the polyadenylation site.

42. The pharmaceutical composition of claim 27, wherein the one or more antisense oligonucleotides bind to a target region within the cryptic exon that is unstructured.

43. The pharmaceutical composition of claim 27, wherein the one or more antisense oligonucleotides bind near or adjacent to the 5' splice site regulated by TDP-43.

44. The pharmaceutical composition of claim 27, wherein the one or more antisense oligonucleotides target a region proximal to a predicted TDP-43 binding site.

45. The pharmaceutical composition of claim 27, wherein the antisense oligonucleotide targets the TDP-43 normal binding site.

46. The pharmaceutical composition of claim 27, wherein the one or more antisense oligonucleotides target one or more splice sites.

47. The pharmaceutical composition of claim 27, wherein the one or more antisense oligonucleotides specifically bind an STMN2 mRNA, pre-mRNA, or nascent RNA sequence, thereby suppressing or preventing inclusion of an abortive or altered STMN2 RNA sequence.

48. The pharmaceutical composition of claim 27, wherein the one or more antisense oligonucleotides specifically bind an STMN2 mRNA, pre-mRNA, or nascent RNA sequence coding for a cryptic exon.

49. The pharmaceutical composition of claim 27, wherein the one or more antisense oligonucleotides suppress or prevent inclusion of a cryptic exon in STMN2 RNA.

50. The pharmaceutical composition of claim 27, wherein the one or more antisense oligonucleotides suppress cryptic splicing.

51. The pharmaceutical composition of claim 27, further comprising an agent for treating a neurodegenerative disease.

52. The pharmaceutical composition of claim 27, further comprising an agent for treating a traumatic brain injury.

53. The pharmaceutical composition of claim 27, further comprising an agent for treating a proteasome-inhibitor induced neuropathy.

54. The pharmaceutical composition of claim 27, further comprising STMN2 as a gene therapy.

55. The pharmaceutical composition of claim 27, further comprising a JNK inhibitor.

56. A pharmaceutical composition comprising a multimeric oligonucleotide, wherein the multimeric oligonucleotide comprises one or more sequences selected from the group consisting of SEQ ID NOS: 37-85.

57. The pharmaceutical composition of claim 56, wherein the multimeric oligonucleotide comprises two or more sequences selected from the group consisting of SEQ ID NOS: 37-85.

58. A method of treating or reducing the likelihood of a disease or condition associated with a decline in TAR DNA-binding protein 43 (TDP-43) functionality in neuronal cells in a subject in need thereof, comprising contacting the neuronal cells with an antisense oligonucleotide that corrects reduced levels of STMN2 protein, wherein the agent does not target a polyadenylation site of a target transcript.

59. A method of treating or reducing the likelihood of a disease or condition associated with a decline in TAR DNA-binding protein 43 (TDP-43) functionality in neuronal cells in a subject in need thereof, comprising contacting the neuronal cells with an antisense oligonucleotide that increases STMN2 protein expression.

60. The method of claim 59, wherein the antisense oligonucleotide specifically binds an STMN2 RNA, pre-RNA, or nascent RNA sequence coding for a cryptic exon.

61. The method of claim 59, wherein the antisense oligonucleotide is designed to target a 5' splice site, a 3' splice site, or a normal TDP-43 binding site.

62. The method of claim 59, wherein the antisense oligonucleotide is designed to target a site proximal to a cryptic splice site, a site proximal to a premature polyadenylation site, or a site located between a cryptic splice site and a premature polyadenylation site.

63. The method of claim 59, wherein the antisense oligonucleotide is designed to target a single stranded region.

64. The method of claim 59, wherein the antisense oligonucleotide is designed to target a single stranded region located between the TDP-43 binding site and the polyadenylation site.

65. The method of claim 59, wherein the antisense oligonucleotide binds to a target region within the cryptic exon that is unstructured.

66. The method of claim 59, wherein the antisense oligonucleotide binds near or adjacent to the 5' splice site regulated by TDP-43.

67. The method of claim 59, wherein the antisense oligonucleotide targets a region proximal to a predicted TDP-43 binding site.

68. The method of claim 59, wherein the antisense oligonucleotide is designed to target one or more splice sites.

69. The method of claim 59, wherein the antisense oligonucleotide restores normal length or protein coding STMN2 pre-mRNA or mRNA.

70. The method of claim 59, wherein the subject exhibits improved neuronal outgrowth and repair.

71. The method of claim 59, wherein the disease or condition is a neurodegenerative disease.

72. The method of claim 59, wherein the disease or condition is selected from the group consisting of amyotrophic lateral sclerosis (ALS), frontotemporal dementia (FTD), inclusion body myositis (IBM), Parkinson's disease, and Alzheimer's disease.

73. The method of claim 59, wherein the disease or condition is a traumatic brain injury.

74. The method of claim 59, wherein the disease or condition is a proteasome-inhibitor induced neuropathy.

75. The method of claim 59, wherein the disease or condition is associated with mutant or reduced levels of TDP-43 in neuronal cells.

76. The method of claim 59, further comprising administering an effective amount of a second agent to the subject.

77. The method of claim 76, wherein the second agent is administered to treat a neurodegenerative disease.

78. The method of claim 76, wherein the second agent is administered to treat a traumatic brain injury.

79. The method of claim 76, wherein the second agent is STMN2 administered as a gene therapy.

80. A method of treating or reducing the likelihood of a disease or condition associated with a decline in TAR DNA-binding protein 43 (TDP-43) functionality in neuronal cells in a subject in need thereof, comprising contacting the neuronal cells with one or more antisense oligonucleotides that correct reduced levels of STMN2 protein, wherein the one or more antisense oligonucleotides comprise a sequence selected from the group consisting of SEQ ID NOS: 37-85.

81. The method of claim 80, wherein the one or more antisense oligonucleotides comprise a sequence selected from the group consisting of SEQ ID NOS: 37-74.

82. The method of claim 80, wherein the one or more antisense oligonucleotides comprise a sequence selected from the group consisting of SEQ ID NO: 40, SEQ ID NO: 47, SEQ ID NO: 48, SEQ ID NO: 49, SEQ ID NO: 50, SEQ ID NO: 52, SEQ ID NO: 53, SEQ ID NO: 54, SEQ ID NO: 56, and SEQ ID NO: 78.

83. The method of claim 80, wherein the one or more antisense oligonucleotides comprise SEQ ID NO: 52.

84. The method of claim 80, wherein the one or more antisense oligonucleotides comprise a sequence selected from the group consisting of SEQ ID NO: 53, SEQ ID NO: 72, and SEQ ID NO: 73.

85. The method of claim 80, wherein the one or more antisense oligonucleotides comprise SEQ ID NO: 73.

86. The method of claim 80, wherein the one or more antisense oligonucleotides comprise SEQ ID NO: 53.

87. A method of treating or reducing the likelihood of a disease or condition associated with a decline in TAR DNA-binding protein 43 (TDP-43) functionality in neuronal cells in a subject in need thereof, comprising contacting the neuronal cells with one or more antisense oligonucleotides that suppress or prevents inclusion of a cryptic exon in STMN2 RNA, wherein the one or more antisense oligonucleotides comprise a sequence selected from the group consisting of SEQ ID NOS: 37-85.

88. The method of claim 87, wherein the one or more antisense oligonucleotides comprise a sequence selected from the group consisting of SEQ ID NOS: 37-74.

89. The method of claim 87, wherein the one or more antisense oligonucleotides comprise a sequence selected from the group consisting of: SEQ ID NO: 40, SEQ ID NO: 47, SEQ ID NO: 48, SEQ ID NO: 49, SEQ ID NO: 50, SEQ ID NO: 52, SEQ ID NO: 53, SEQ ID NO: 54, SEQ ID NO: 56, and SEQ ID NO: 78.

90. The method of claim 87, wherein the one or more antisense oligonucleotides comprise SEQ ID NO: 52.

91. The method of claim 87, wherein the one or more antisense oligonucleotides comprise a sequence selected from the group consisting of: SEQ ID NO: 53, SEQ ID NO: 72, and SEQ ID NO: 73.

92. The method of claim 87, wherein the one or more antisense oligonucleotides comprise SEQ ID NO: 73.

93. The method of claim 87, wherein the one or more antisense oligonucleotides comprise SEQ ID NO: 53.

94. The method of claim 87, wherein the one or more antisense oligonucleotides specifically bind an STMN2 RNA, pre-RNA, or nascent RNA sequence coding for a cryptic exon.

95. The method of claim 87, wherein the one or more antisense oligonucleotides are designed to target a 5' splice site, a 3' splice site, or a normal TDP-43 binding site.

96. The method of claim 87, wherein the one or more antisense oligonucleotides are designed to target a site proximal to a cryptic splice site, a site proximal to a premature polyadenylation site, or a site located between a cryptic splice site and a premature polyadenylation site.

97. The method of claim 87, wherein the one or more antisense oligonucleotides are designed to target a single stranded region.

98. The method of claim 87, wherein the one or more antisense oligonucleotides are designed to target a single stranded region located between the TDP-43 binding site and the polyadenylation site.

99. The method of claim 87, wherein the one or more antisense oligonucleotides bind to a target region within the cryptic exon that is unstructured.

100. The method of claim 87, wherein the one or more antisense oligonucleotides bind near or adjacent to the 5' splice site regulated by TDP-43.

101. The method of claim 87, wherein the one or more antisense oligonucleotides target a region proximal to a predicted TDP-43 binding site.

102. The method of claim 87, wherein the one or more antisense oligonucleotides target the TDP-43 normal binding site.

103. The method of claim 87, wherein the disease or condition is selected from the group consisting of amyotrophic lateral sclerosis (ALS), frontotemporal dementia (FTD), inclusion body myositis (IBM), Parkinson's disease, and Alzheimer's disease.

104. The method of claim 87, wherein the disease or condition is a traumatic brain injury.

105. The method of claim 87, wherein the disease or condition is a proteasome-inhibitor induced neuropathy.

106. The method of claim 87, wherein the antisense oligonucleotide suppresses cryptic splicing.

107. The method of claim 87, wherein the antisense oligonucleotide increases STMN2 protein expression.

108. The method of claim 87, wherein the subject exhibits improved neuronal outgrowth and repair.

109. The method of claim 87, further comprising administering an effective amount of a second agent to the subject.

110. The method of claim 109, wherein the second agent is administered to treat a neurodegenerative disease.

111. The method of claim 109, wherein the second agent is administered to treat a traumatic brain injury.

112. A method of treating or reducing the likelihood of a disease or condition associated with a decline in TAR DNA-binding protein 43 (TDP-43) functionality in neuronal cells in a subject in need thereof, comprising contacting the neuronal cells with a multimeric oligonucleotide that corrects reduced levels of STMN2 protein, wherein the multimeric oligonucleotide comprises two or more antisense oligonucleotides selected from the group consisting of SEQ ID NOS: 37-85.

113. The method of claim 112, wherein the multimeric oligonucleotide comprises two or more antisense oligonucleotides selected from the group consisting of SEQ ID NOS: 37-74.

114. An antisense oligonucleotide that corrects reduced levels of STMN2 protein, wherein the antisense oligonucleotide is designed to target an unstructured region within a cryptic exon.

115. The antisense oligonucleotide of claim 114, wherein the unstructured region within the cryptic exon is located between a cryptic splice site and a premature polyadenylation site.

116. A method of detecting altered levels of STMN2 or ELAVL3 protein in a subject comprising obtaining a sample from the subject; and detecting whether the STMN2 or ELAVL3 protein levels are altered.

117. The method of claim 116, wherein the subject has amyotrophic lateral sclerosis.

118. The method of claim 116, wherein the subject has a traumatic brain injury.

119. The method of any one of claims 116-118, wherein the detection of whether the STMN2 or ELAVL3 levels are altered comprises determining if the STMN2 or ELAVL3 levels are decreased compared to a reference sample.

120. The method of any one of claims 113-119, wherein the detection of whether the STMN2 of ELAVL3 levels are altered comprises using an ELISA.

121. The method of any one of claims 113-120, wherein the sample is a biofluid sample.

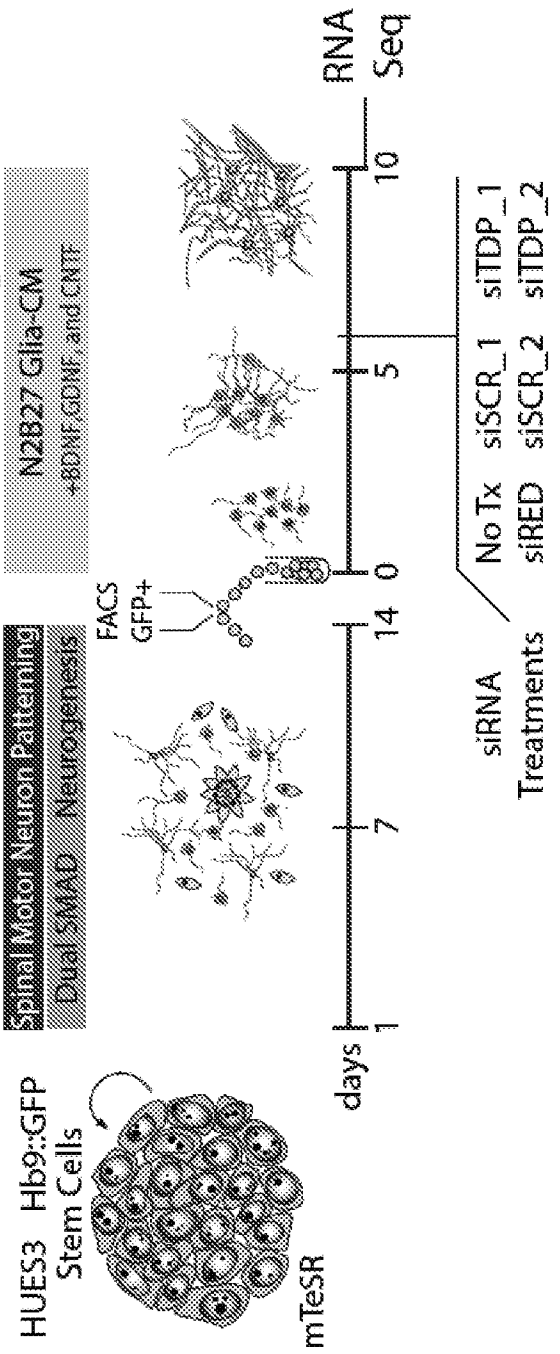

HUES3 Hb9::GFP Stem Cells
mTeSR
Directed Differentiation
Spinal Motor Neuron Patterning
Dual SMAD Neurogenesis
days
1
7
14
FACS
GFP+
0
5
10
RNA Seq
Motor Neuron Outgrowth
N2B27 Glia-CM
+BDNF,GDNF, and CNTF
siRNA Treatments
No Tx
siRED
siSCR_1
siSCR_2
siTDP_1
siTDP_2

FIG. 1A

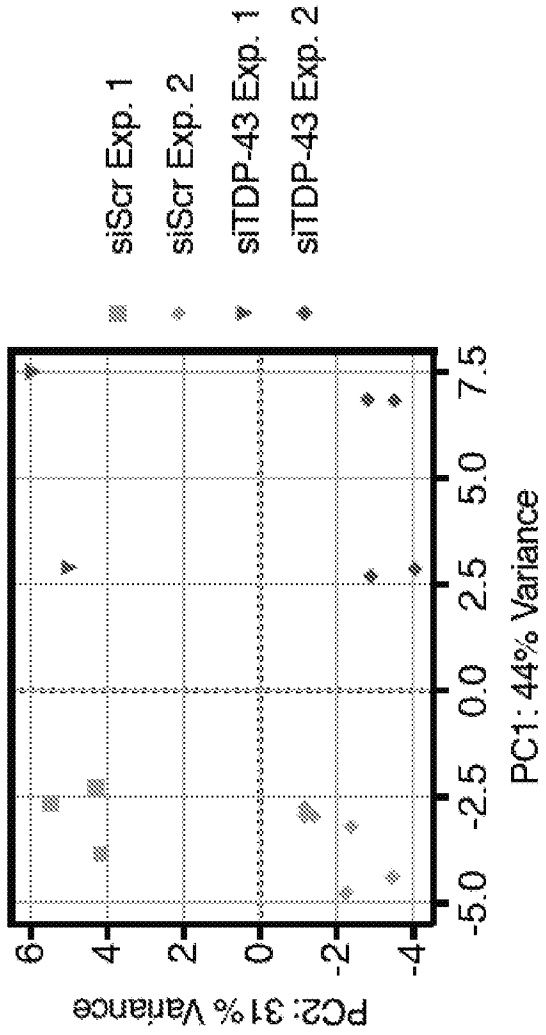

siScr Exp. 1
siScr Exp. 2
siTDP-43 Exp. 1
siTDP-43 Exp. 2
PC2: 31% Variance
PC1: 44% Variance
6
4
2
0
-2
-4
-5.0
-2.5
0.0
2.5
5.0
7.5

FIG. 1B

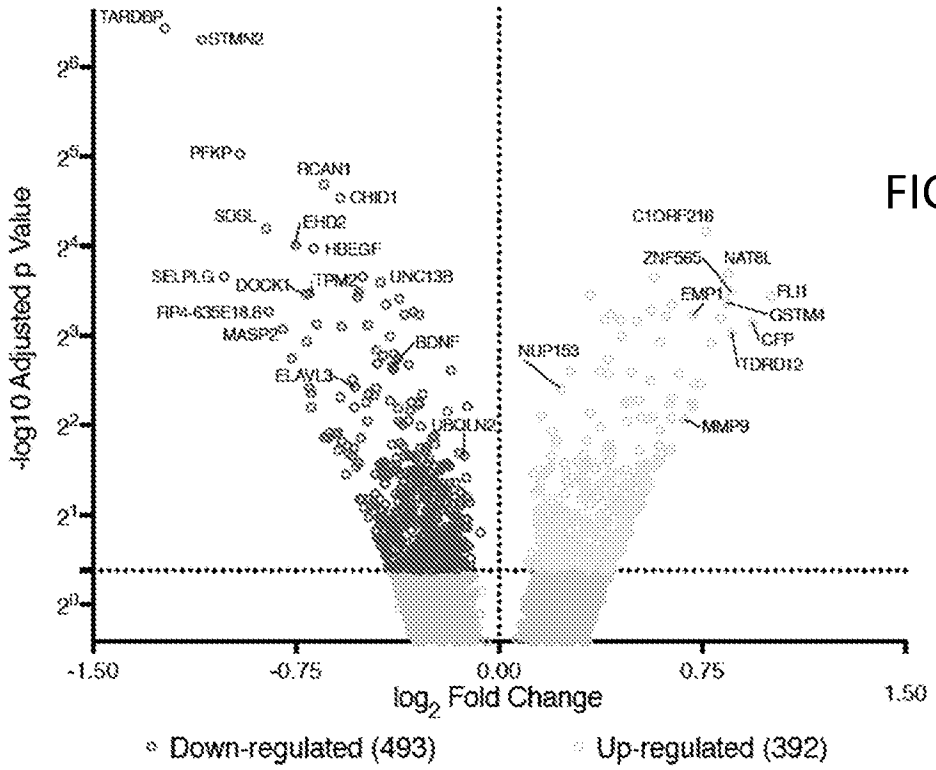

TARDBP
STMN2
PFKP
RCAN1
CHD1
SDSL
EHD2
HBEGF
SELPLG
DOCK1
TPM2
UNC13B
RPA-635E18.6
MASP2
BDNF
ELAVL3
UBQLN2
C1ORF216
ZNF565
NAT8L
EMP1
FLI1
GSTM4
CFP
TDRD12
NUP153
MMP9
-log10 Adjusted p Value
log2 Fold Change
Down-regulated (493)
Up-regulated (392)

FIG. 1C

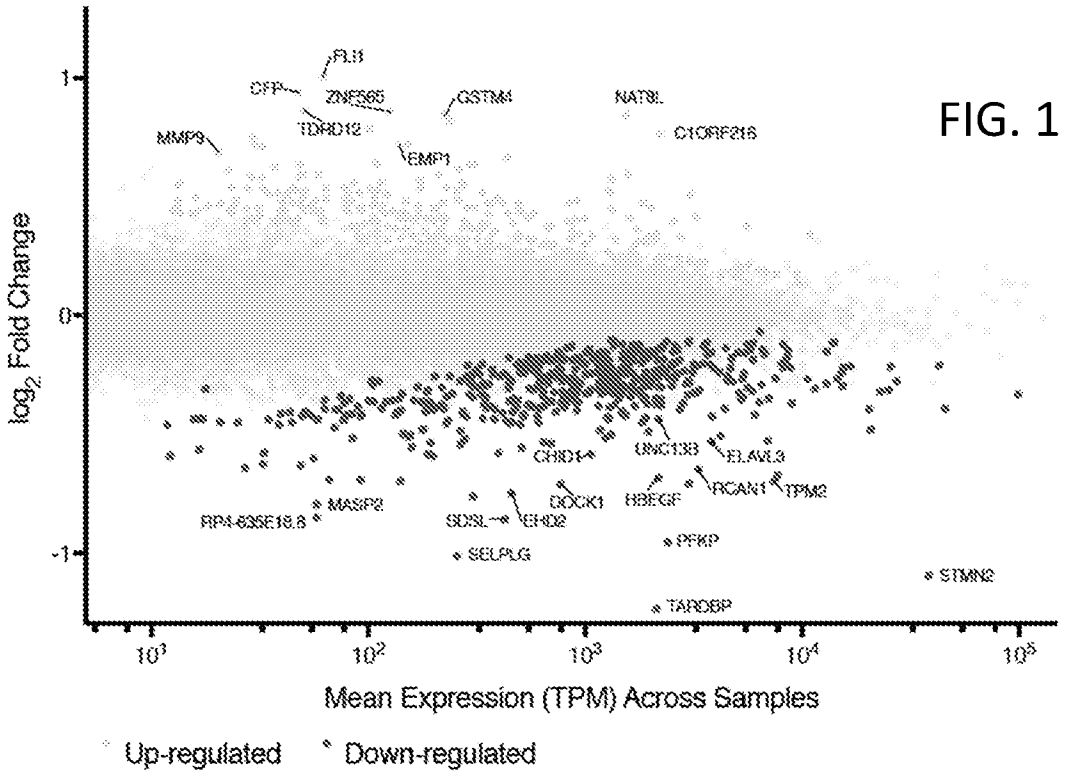

FLI1
CFP
ZNF565
GSTM4
NAT8L
TDRD12
C1ORF216
MMP9
EMP1
UNC13B
ELAVL3
CHD1
RCAN1
TPM2
DOCK1
HBEGF
MASP2
RPA-635E18.6
SDSL
EHD2
PFKP
SELPLG
STMN2
TARDBP
log2 Fold Change
Mean Expression (TPM) Across Samples
Up-regulated
Down-regulated

FIG. 1D

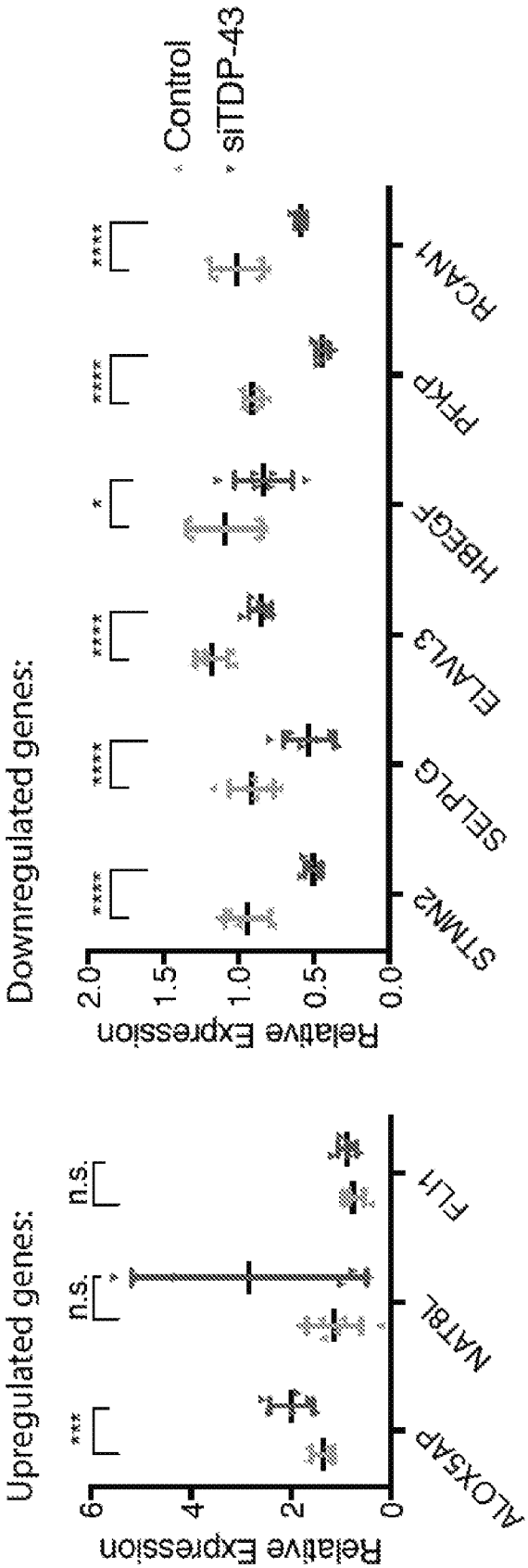

Upregulated genes:
Relative Expression
0
2
4
6
***
n.s.
*
n.s.
ALOX5AP
NAT8L
FLI1
Downregulated genes:
Relative Expression
0.0
0.5
1.0
1.5
2.0
****
****
****
*
****
****
STMN2
SELPLG
ELAVL3
HBEGF
PFKP
RCAN1
Control
siTDP-43

FIG. 1E

FIG. 1F

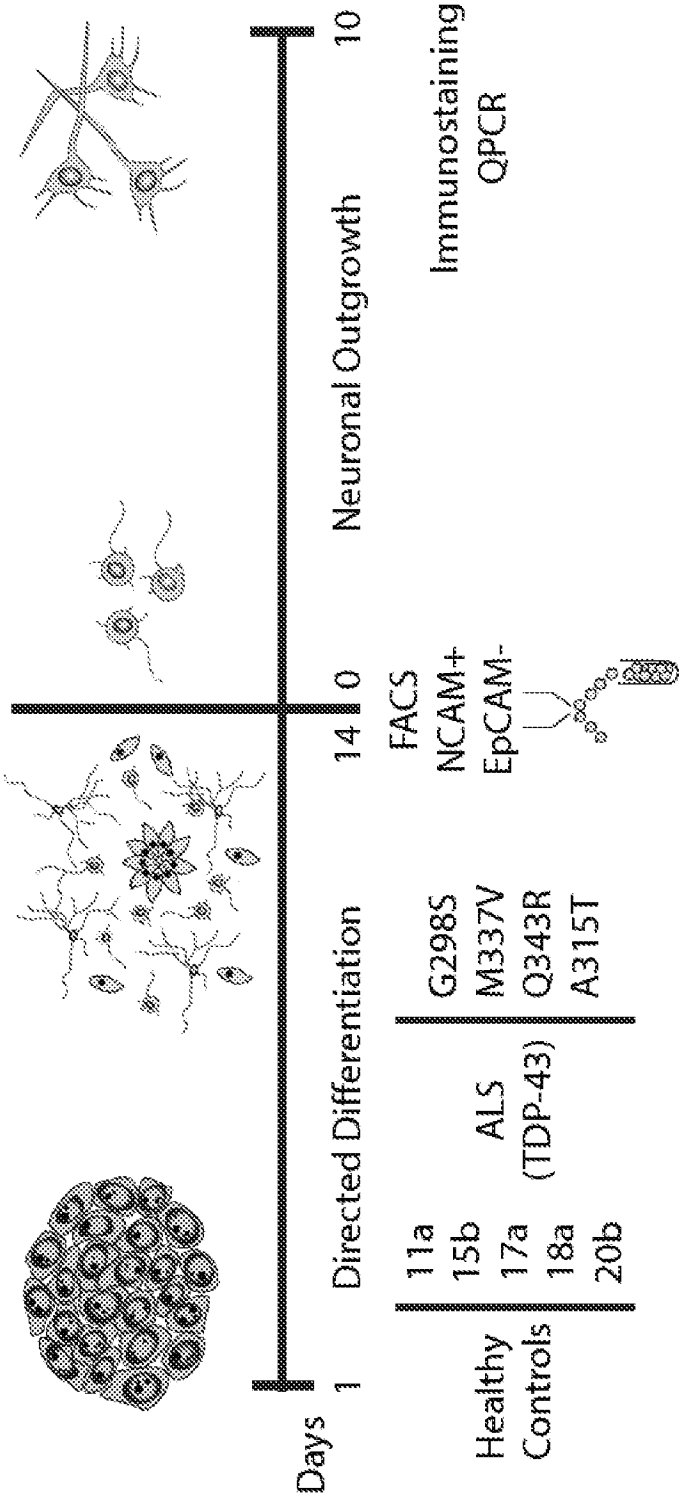

Days
1
Directed Differentiation
14
0
Neuronal Outgrowth
10
Healthy Controls
11a
15b
ALS (TDP-43)
17a
18a
20b
G298S
M337V
Q343R
A315T
FACS
NCAM+
EpCAM-
Immunostaining
QPCR

FIG. 2A

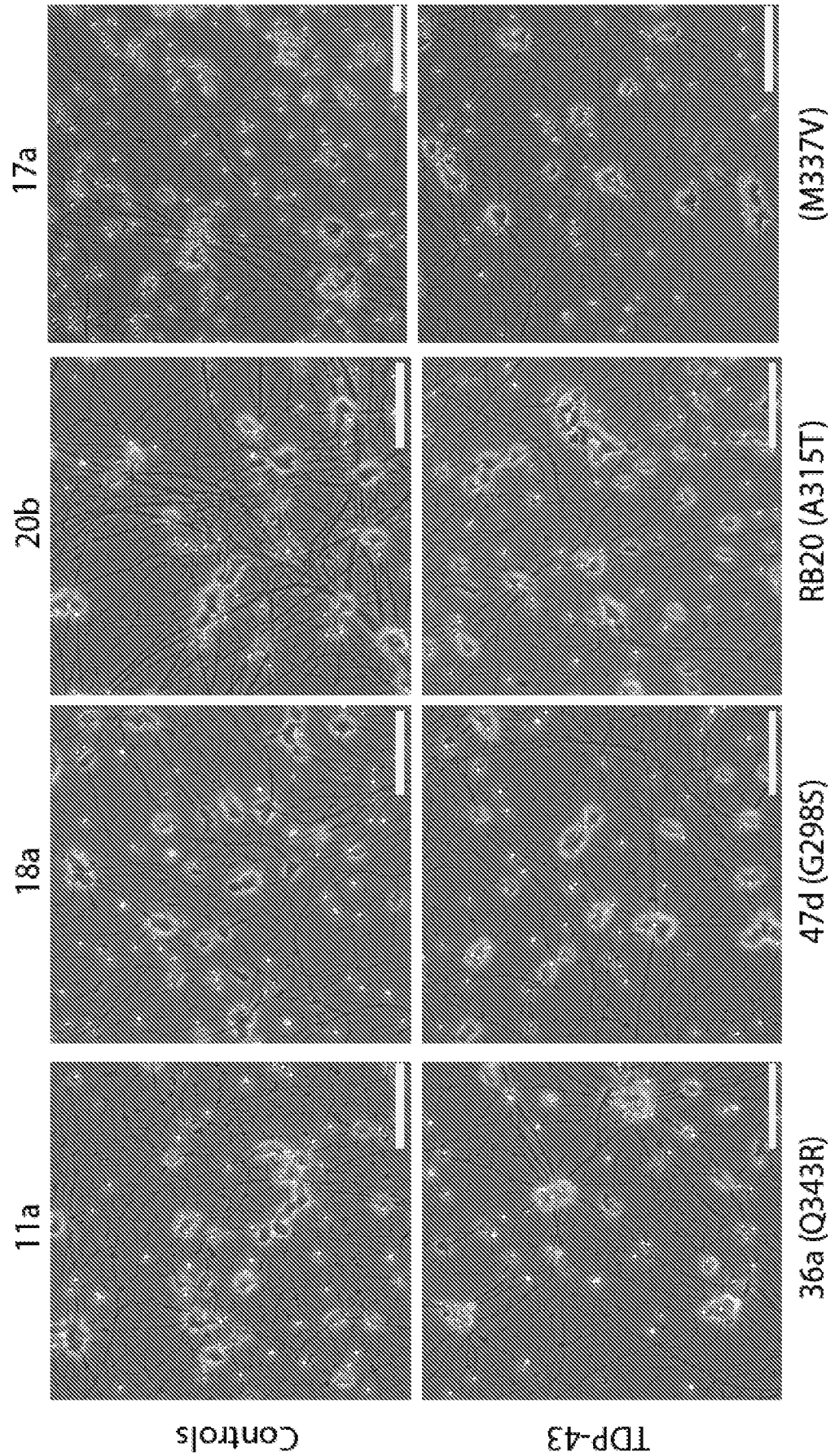

11a
18a
20b
17a
Controls
TDP-43
36a (Q343R)
47d (G298S)
RB20 (A315T)
(M337V)

FIG. 2B

FIG. 2C

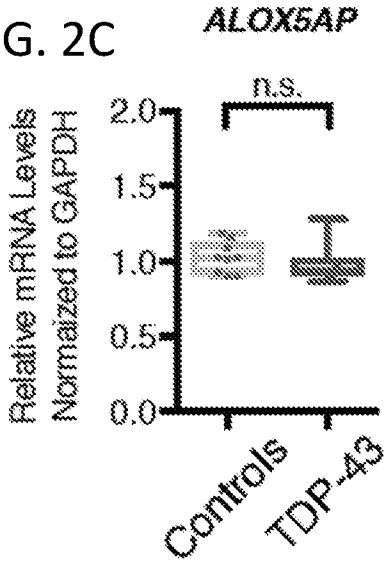


FIG. 2D

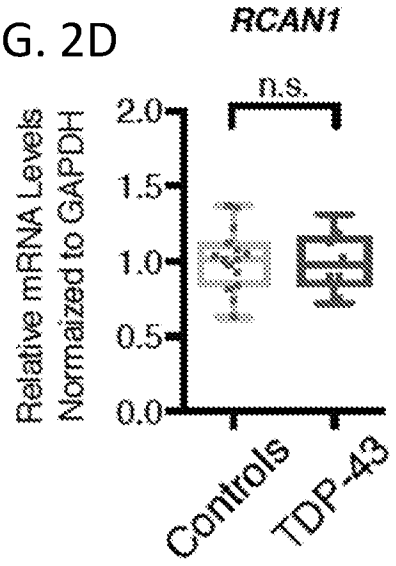


FIG. 2E

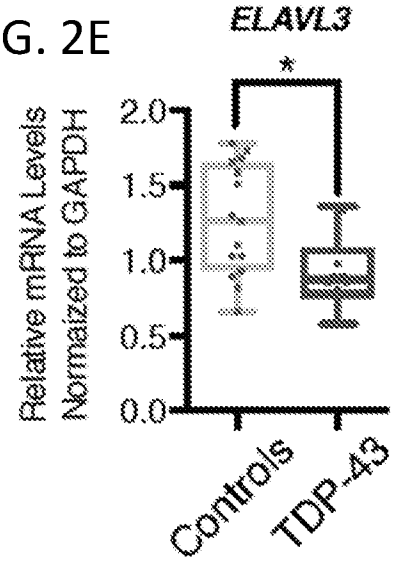


FIG. 2F

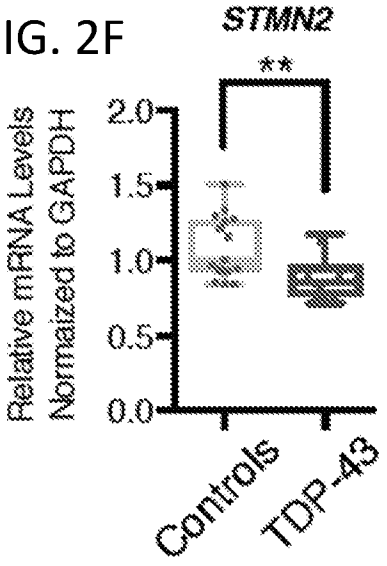


FIG. 2G

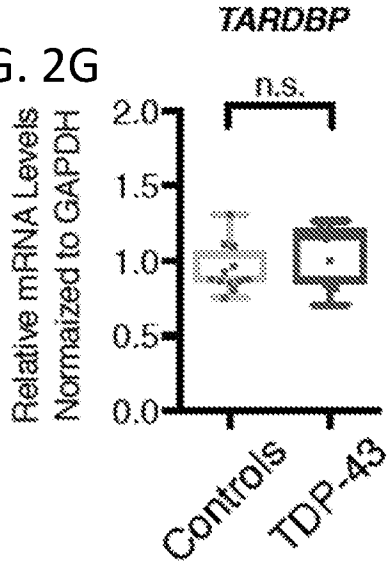
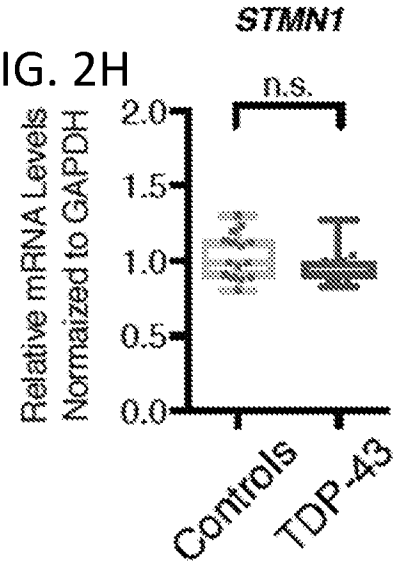


FIG. 2H



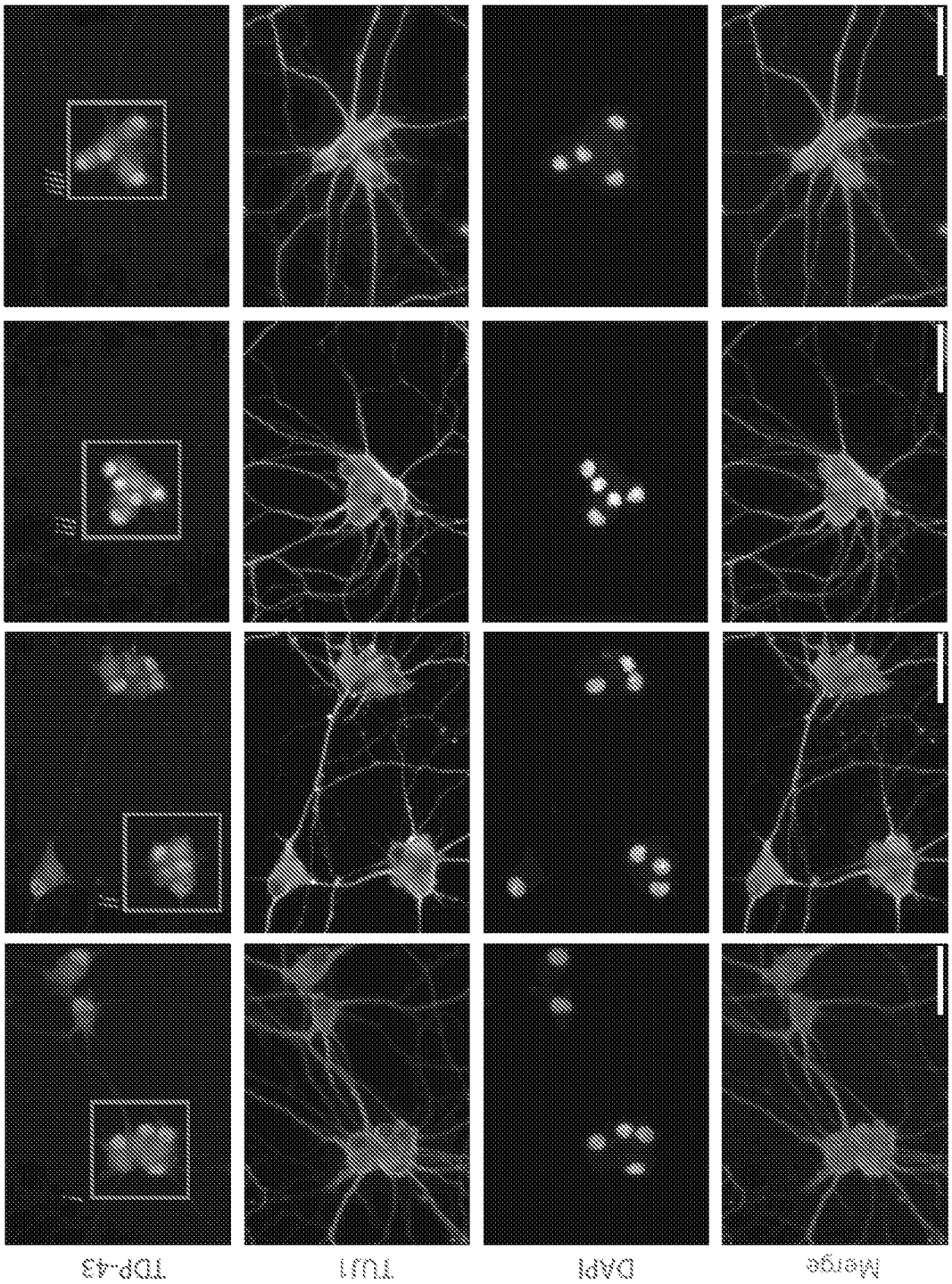


FIG. 2I

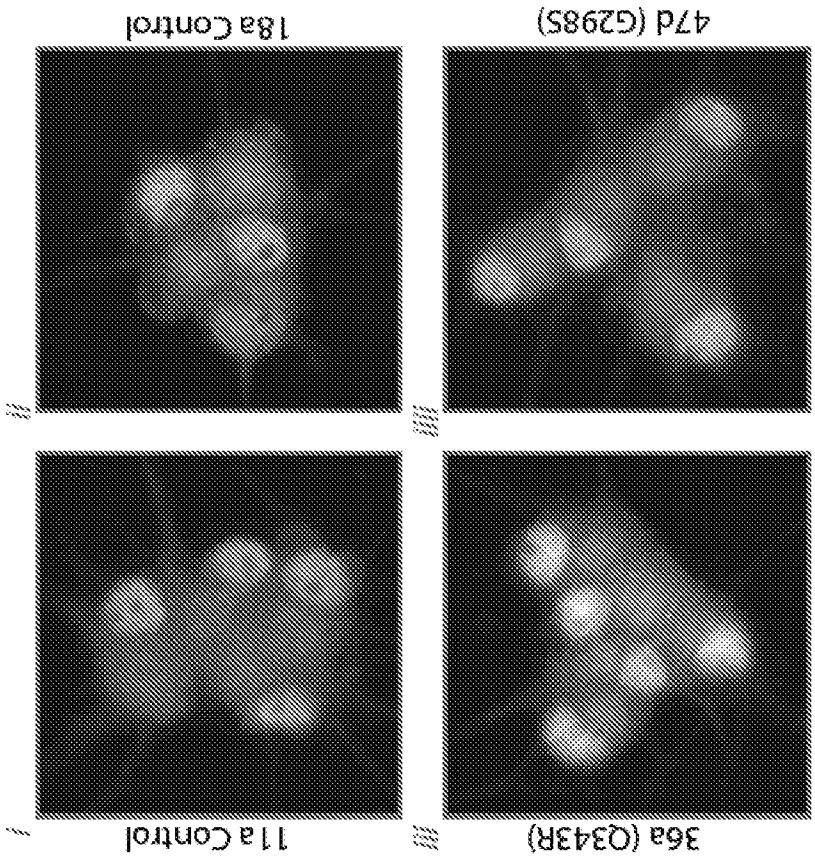


FIG. 2I cont.

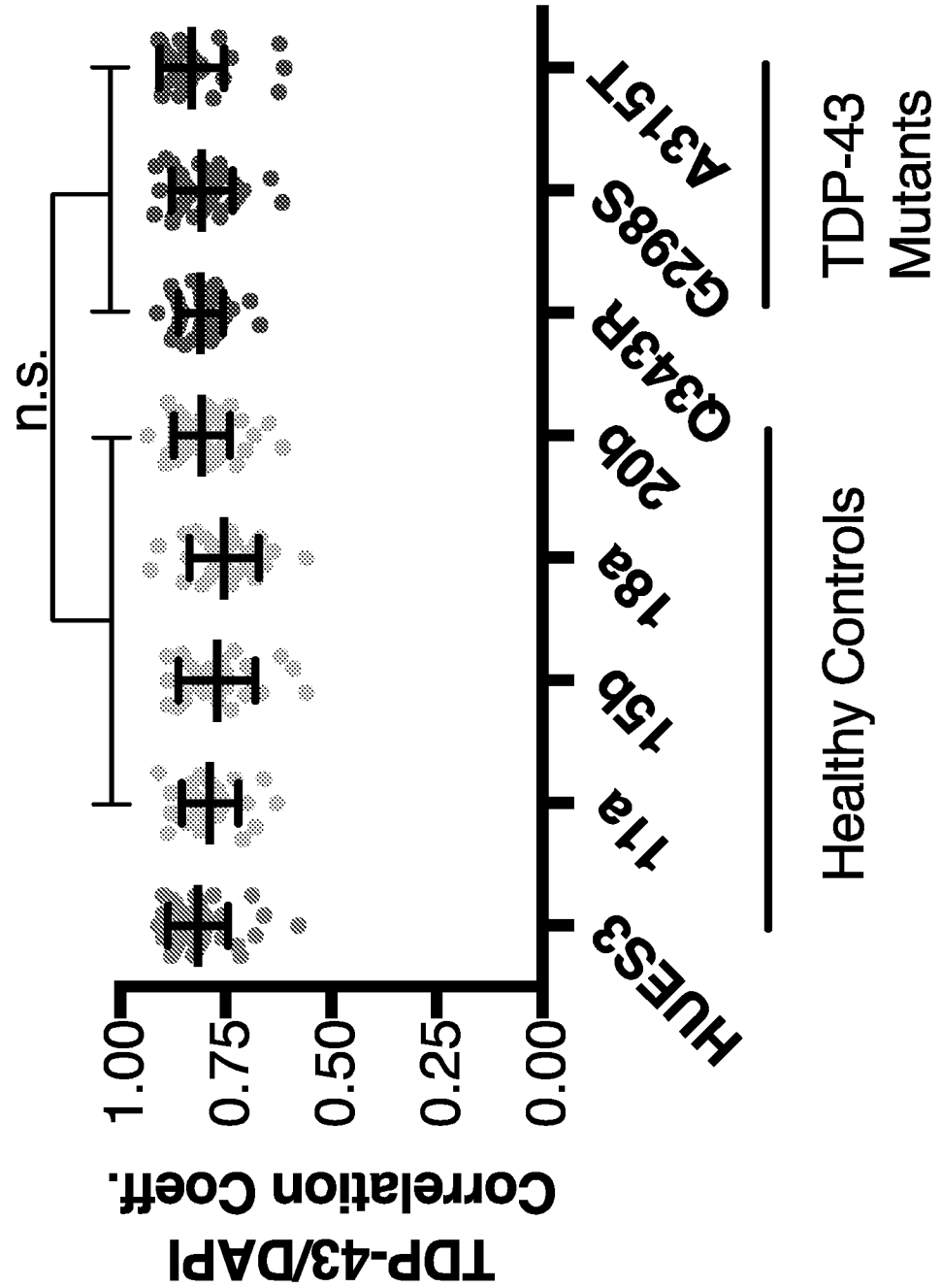

TDP-43/DAPI
Correlation Coeff.
1.00
0.75
0.50
0.25
0.00
n.s.
HUES3
11a
15b
18a
20b
Q343R
G298S
A315T
Healthy Controls
TDP-43
Mutants

FIG. 2J

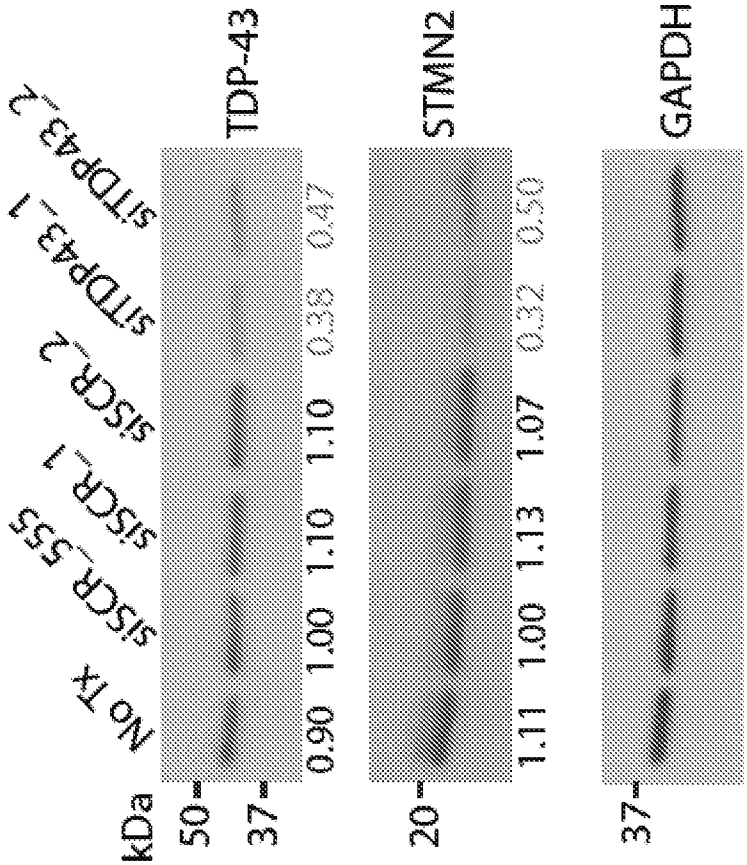

No Tx
siSCR_555
siSCR_1
siSCR_2
siTDP43_1
siTDP43_2
kDa
50
37
20
37
TDP-43
STMN2
GAPDH
0.90 1.00 1.10 1.10 0.38 0.47
1.11 1.00 1.13 1.07 0.32 0.50

FIG. 3B

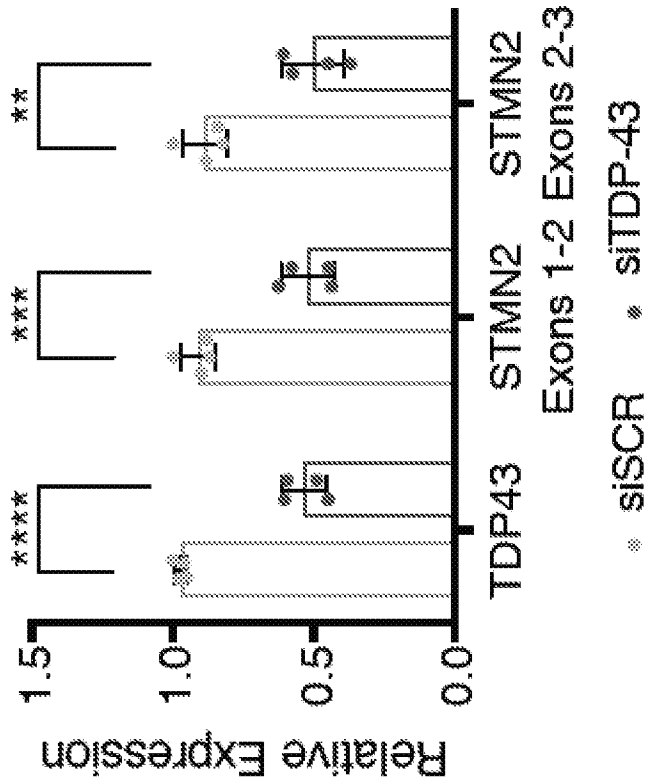

Relative Expression
1.5
1.0
0.5
0.0
****
***
**
TDP43
STMN2
STMN2
Exons 1-2 Exons 2-3
siSCR
siTDP-43

FIG. 3A

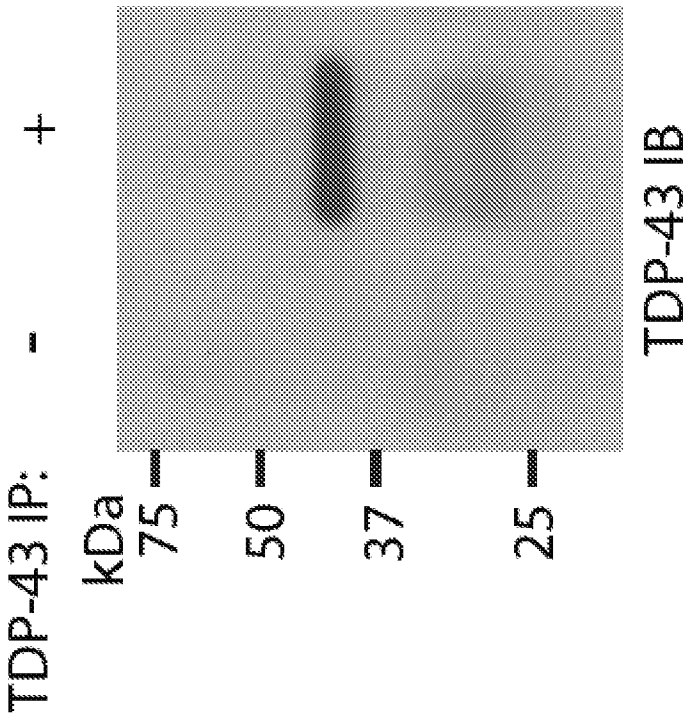

TDP-43 IP:
-
+
kDa
75
50
37
25
TDP-43 IB

FIG. 3D

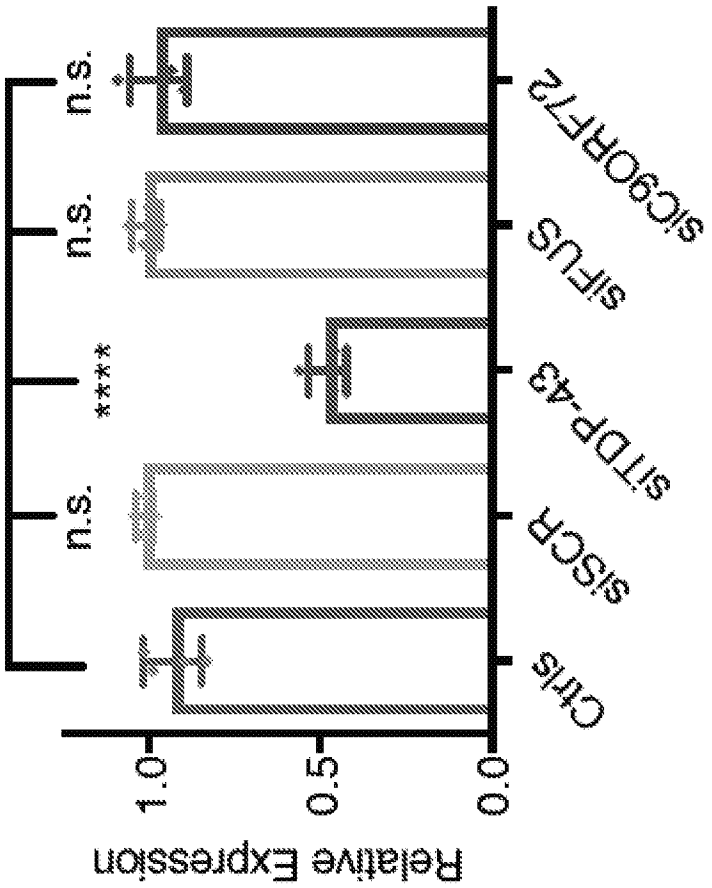

Relative Expression
1.0
0.5
0.0
Ctrls
siSCR
siTDP-43
siFUS
siC9ORF72
n.s.
****
n.s.
n.s.

FIG. 3C

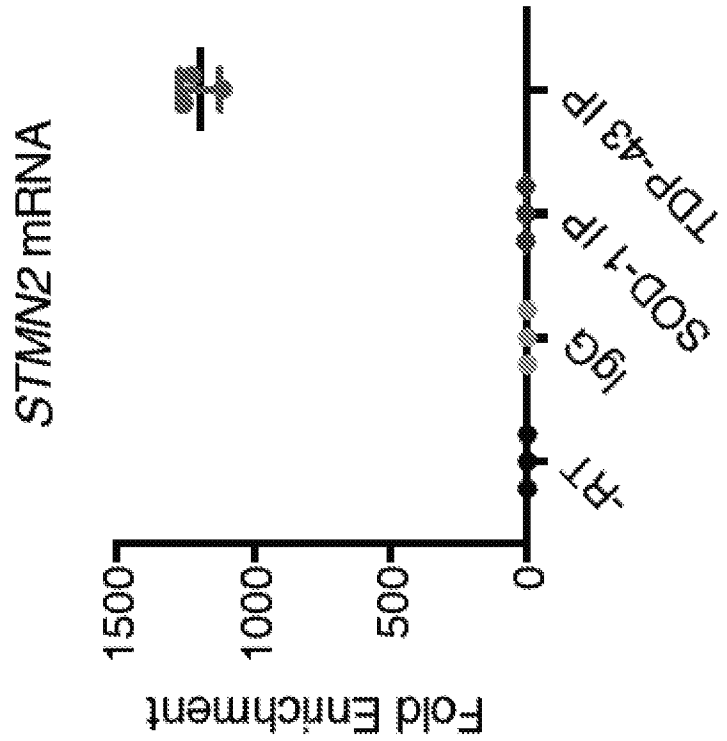

STMN2 mRNA
Fold Enrichment
1500
1000
500
0
RT
IgG
SOD-1 IP
TDP-43 IP

FIG. 3F

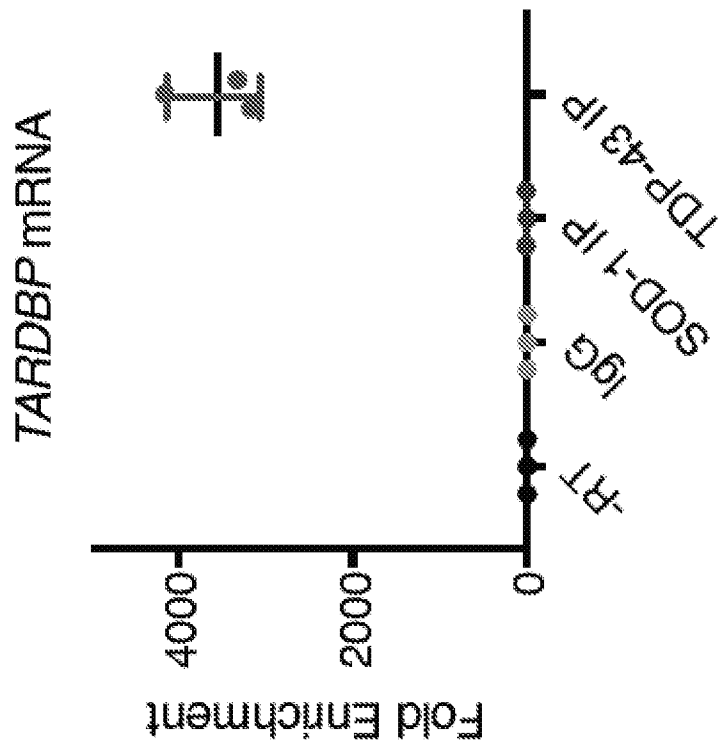

TARDBP mRNA
Fold Enrichment
4000
2000
0
RT
IgG
SOD-1 IP
TDP-43 IP

FIG. 3E

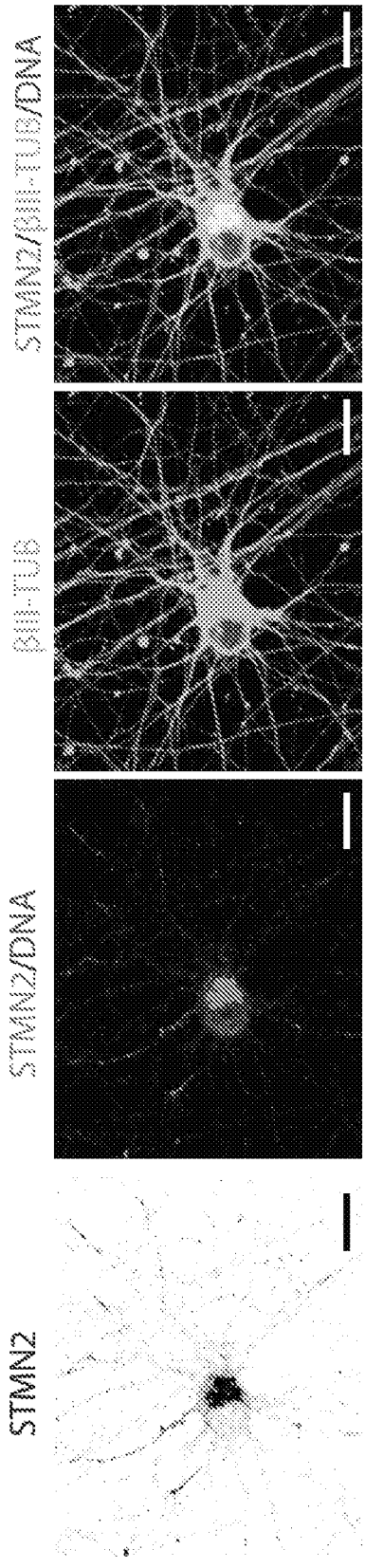

STMN2
STMN2/DNA
βIII-TUB
STMN2/βIII-TUB/DNA

FIG. 3G

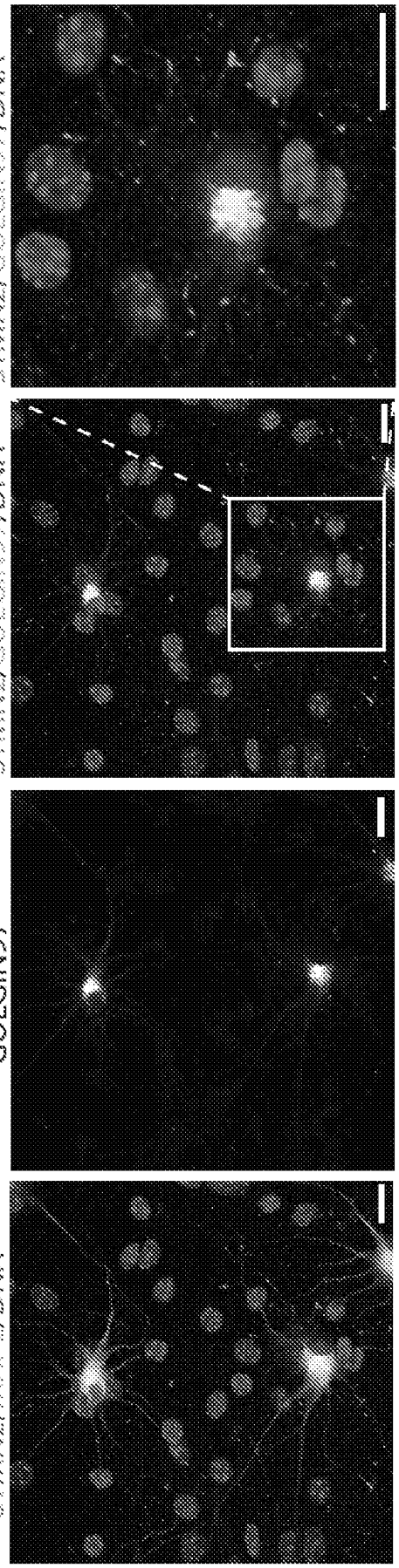

STMN2/MAP2/DNA
GOLGIN97
STMN2/GOLGIN97/DNA
STMN2/GOLGIN97/DNA

FIG. 3H

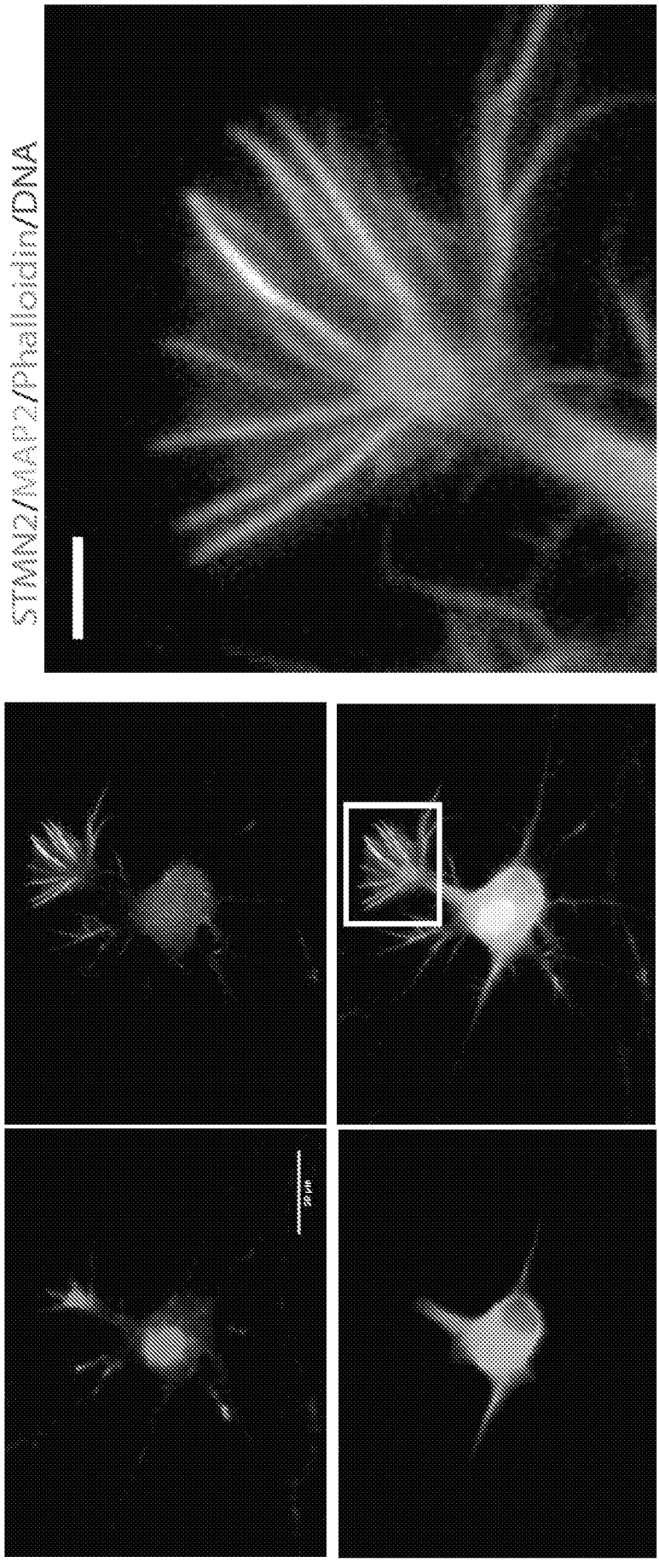


FIG. 3I

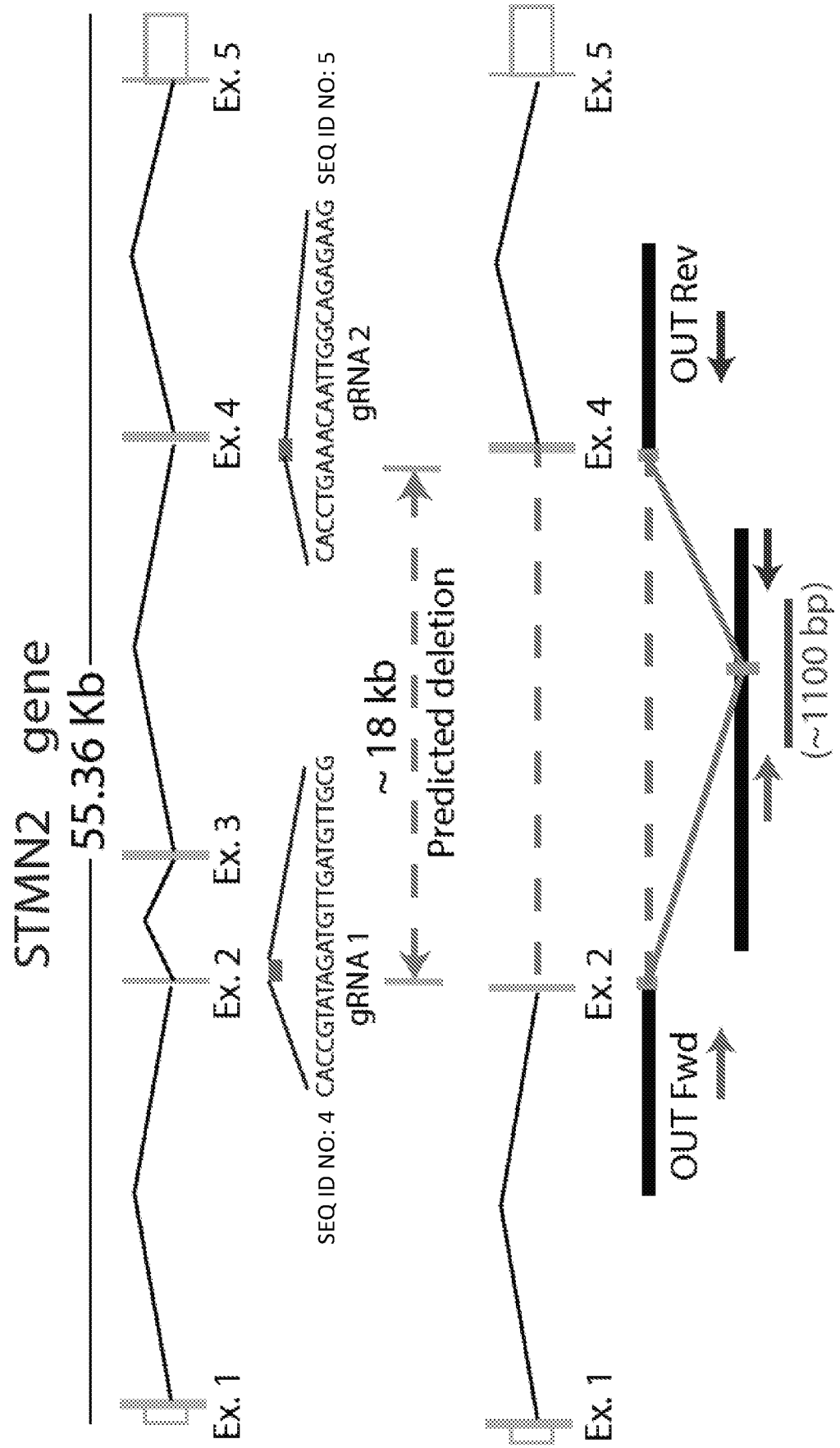

STMN2 gene
55.36 Kb
Ex. 1
Ex. 2
Ex. 3
Ex. 4
Ex. 5
SEQ ID NO: 4 CACCGTATAGATGTTGATGTTGCG
gRNA 1
~ 18 kb
Predicted deletion
CACCTGAAACAATTGGCAGAGAAG SEQ ID NO: 5
gRNA 2
OUT Fwd
OUT Rev
(~1100 bp)

FIG. 4A

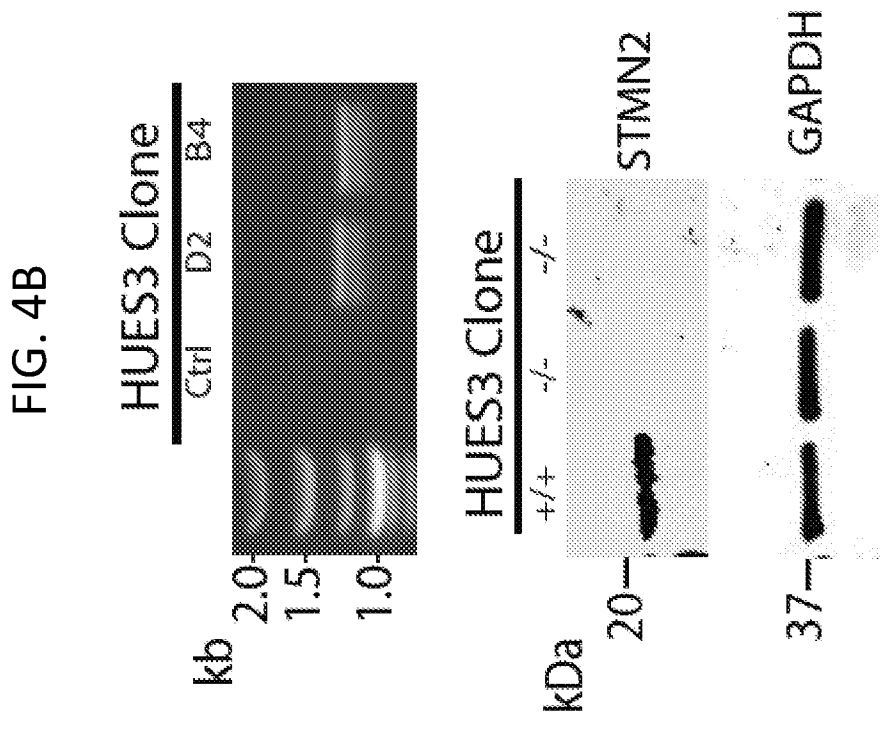


FIG. 4B

FIG. 4C

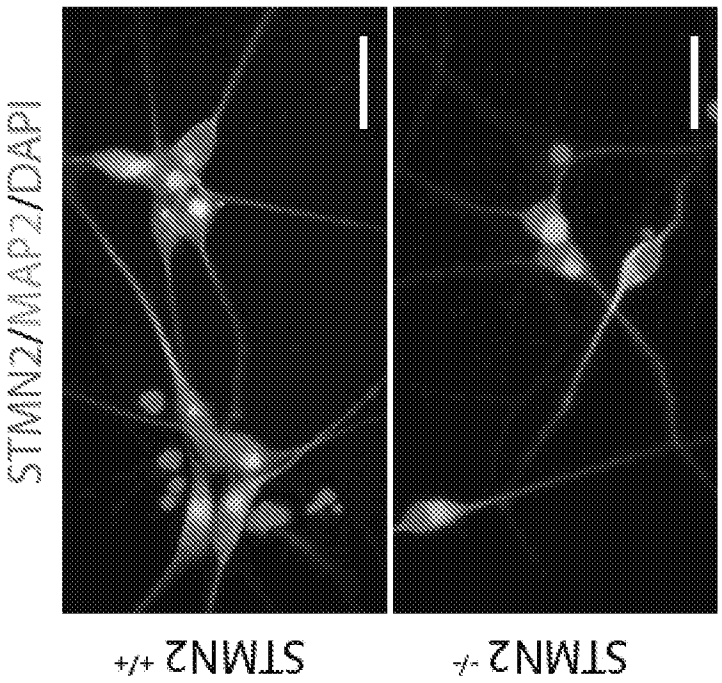


FIG. 4D

FIG. 4E

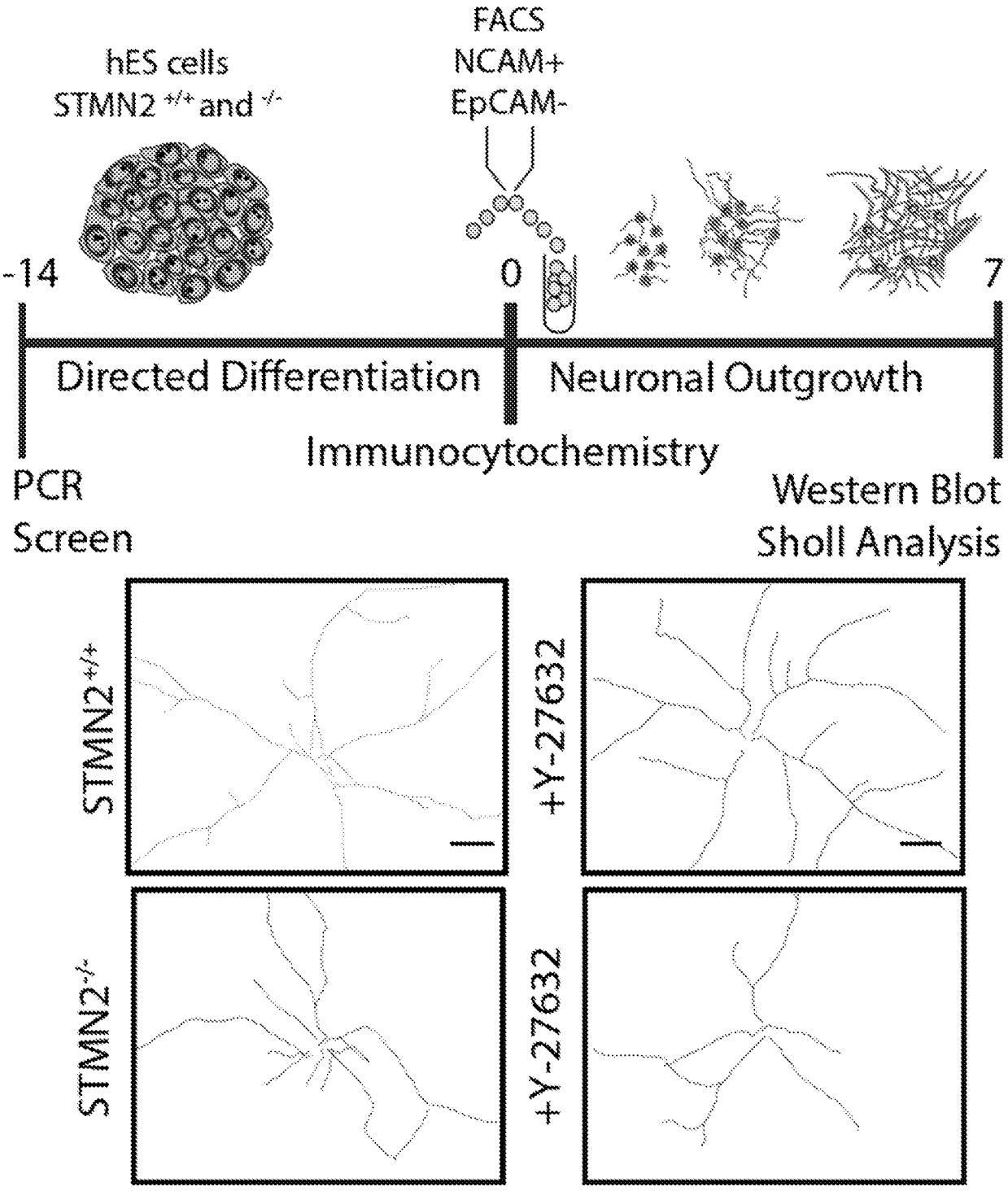
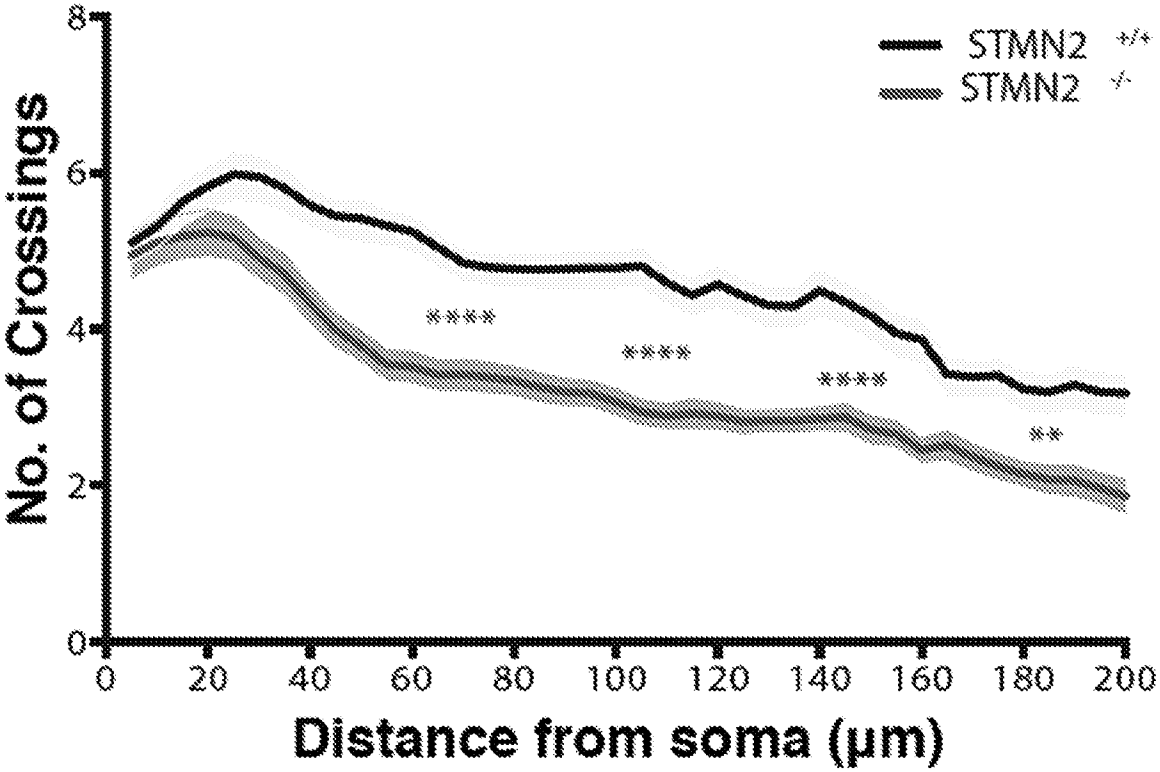

hES cells
STMN2 +/+ and -/-
FACS
NCAM+
EpCAM-
-14
0
7
Directed Differentiation
Neuronal Outgrowth
Immunocytochemistry
PCR
Screen
Western Blot
Sholl Analysis
STMN2+/+
+Y-27632
STMN2-/-
+Y-27632

FIG. 4F

FIG. 4G


STMN2 +/+
STMN2 -/-
No. of Crossings
0
2
4
6
8
****
****
****
**
0 20 40 60 80 100 120 140 160 180 200
Distance from soma (µm)

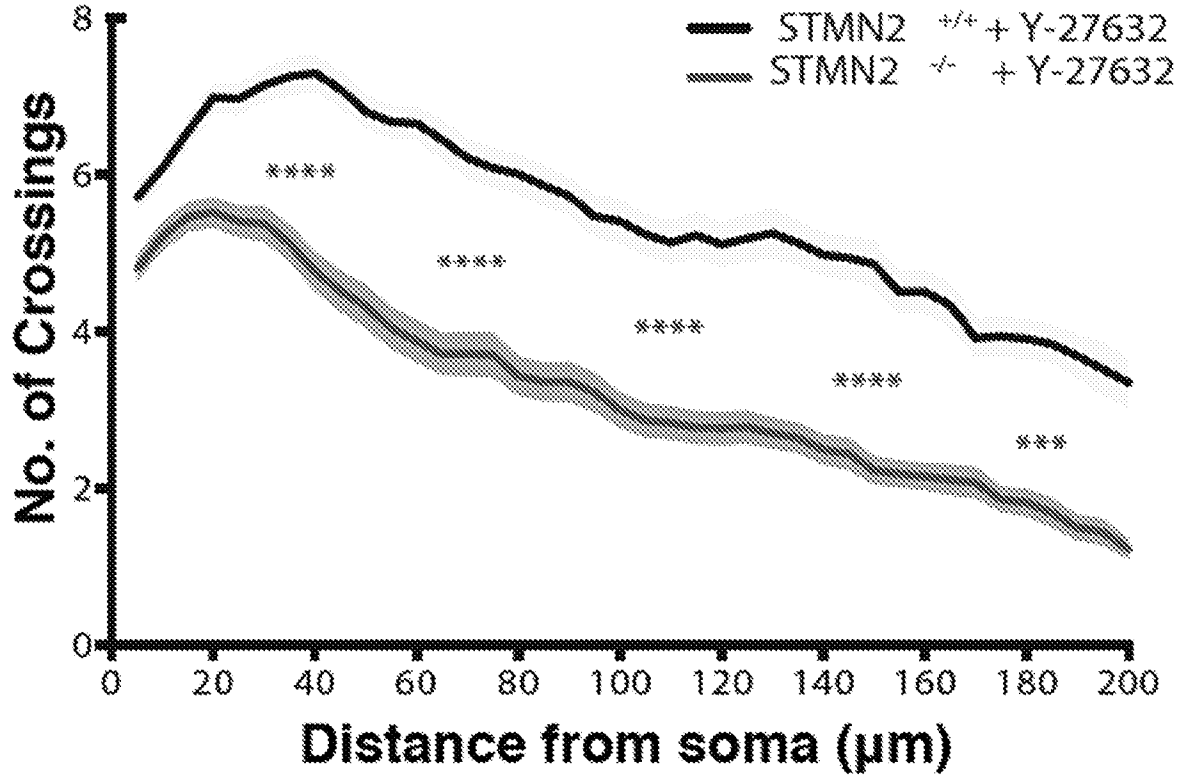
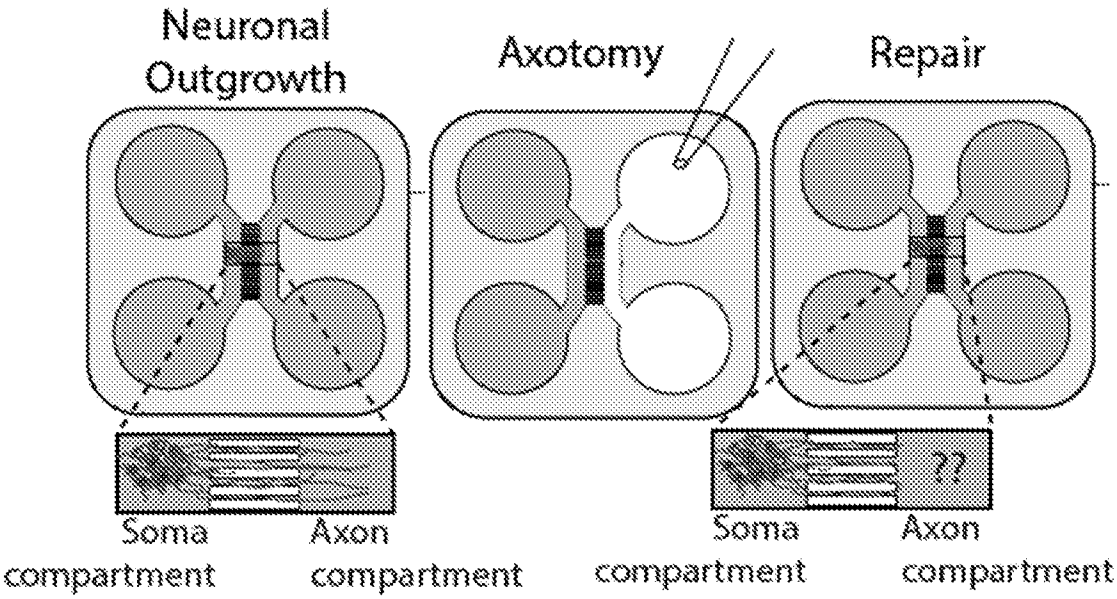

STMN2 +/+ + Y-27632
STMN2 -/- + Y-27632
No. of Crossings
0
2
4
6
8
****
****
****
****
***
0 20 40 60 80 100 120 140 160 180 200
Distance from soma (µm)

FIG. 4H

FIG. 4I


Neuronal Outgrowth
Axotomy
Repair
??
Soma compartment
Axon compartment
Soma compartment
Axon compartment

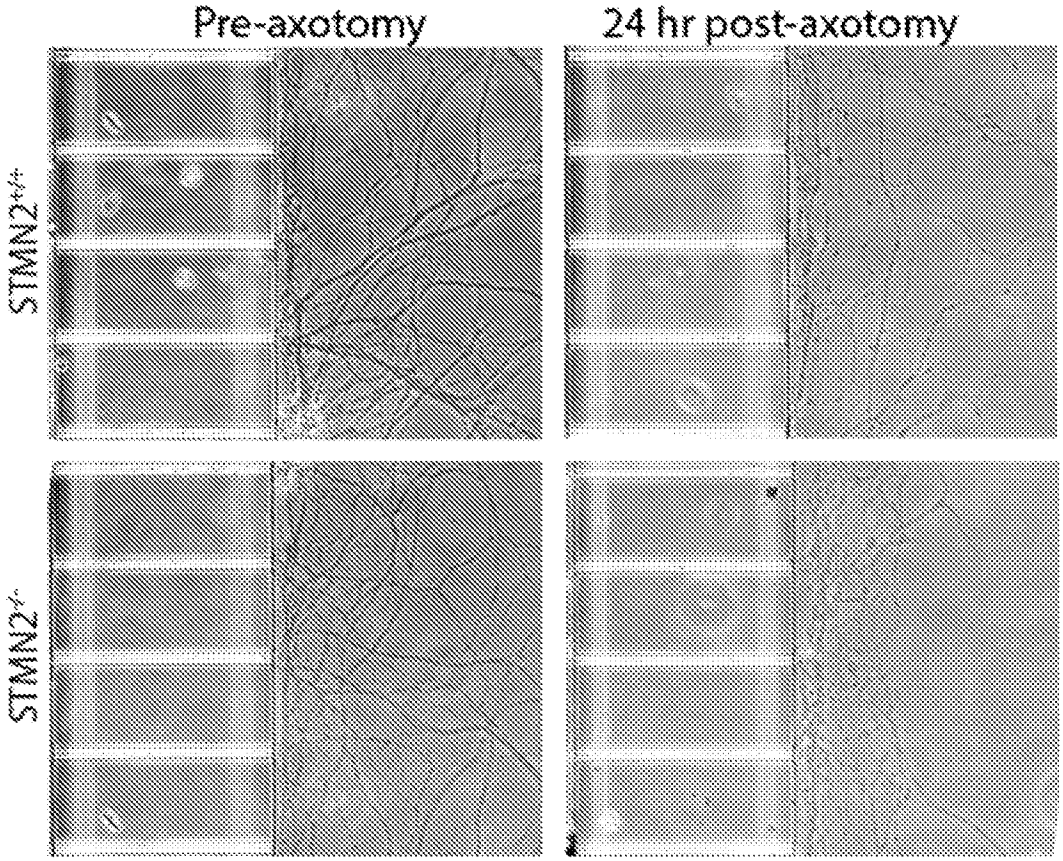

Pre-axotomy
24 hr post-axotomy
STMN2+/+
STMN2-/-

FIG. 4J

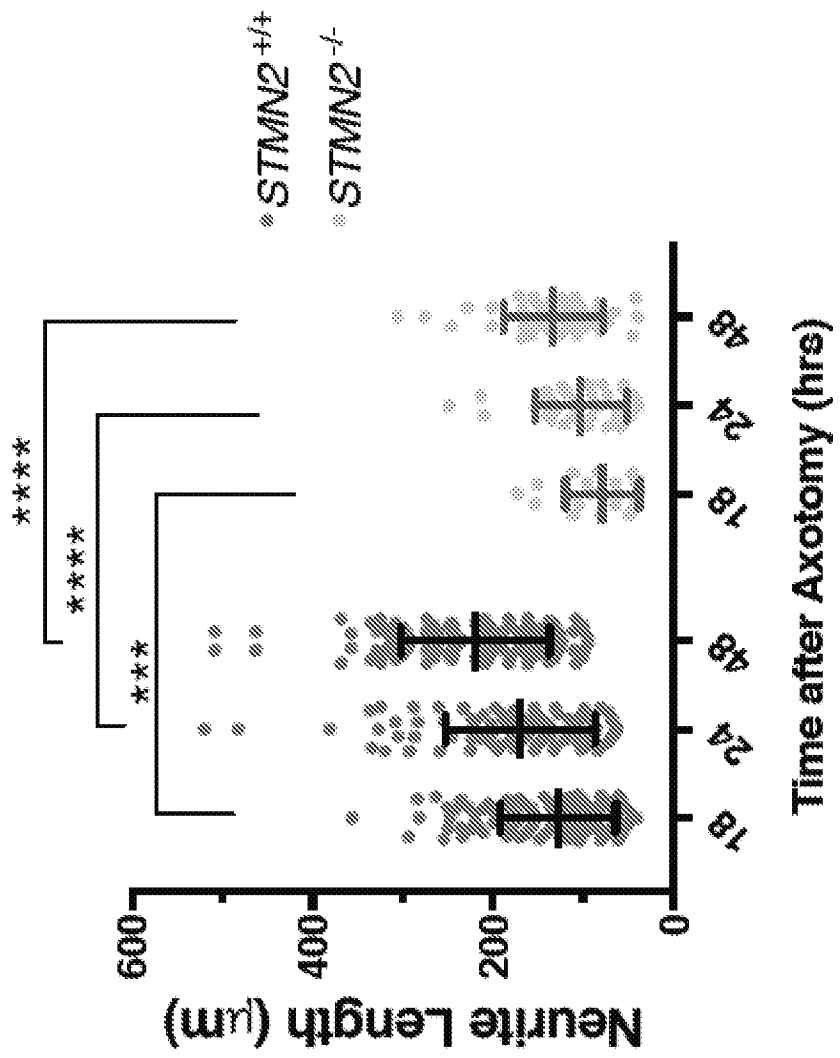

STMN2+/+
STMN2-/-
****
****
***
Neurite Length (μm)
600
400
200
0
1h
24
48
1h
24
48
Time after Axotomy (hrs)

FIG. 4K

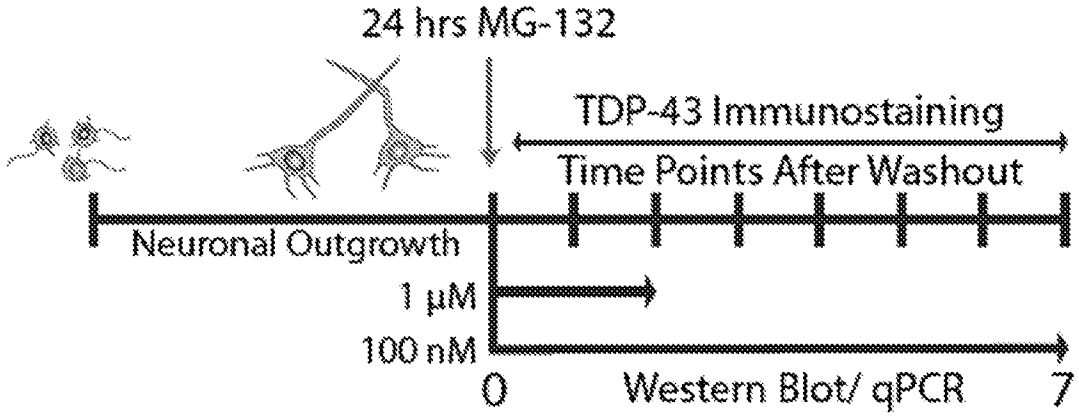

24 hrs MG-132
TDP-43 Immunostaining
Time Points After Washout
Neuronal Outgrowth
1 µM
100 nM
0
Western Blot/ qPCR
7

FIG. 5A

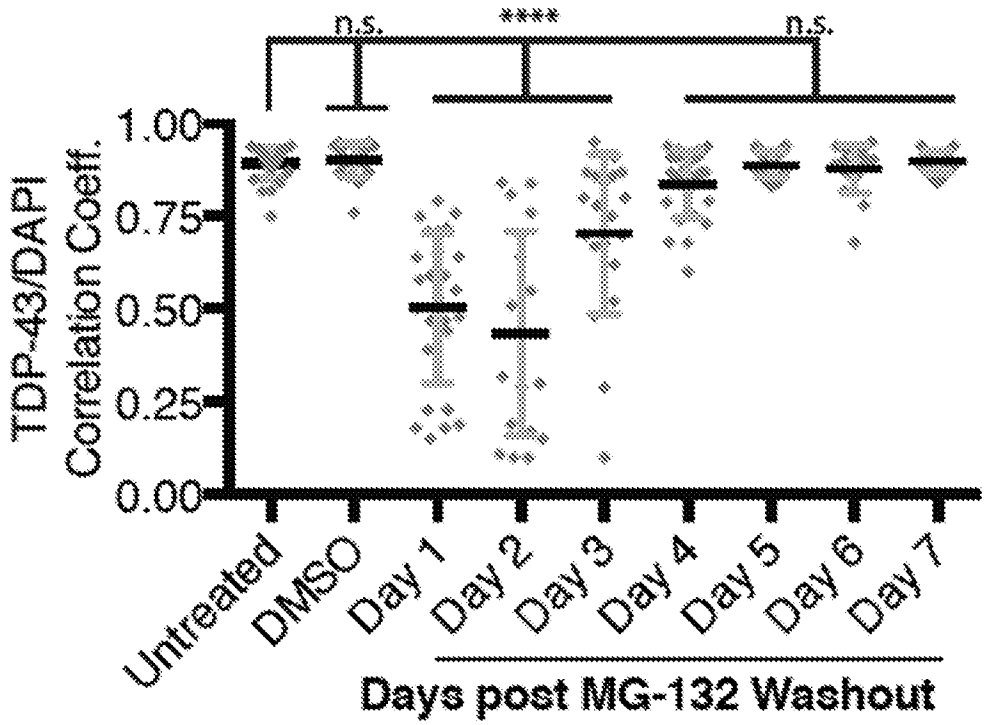

n.s.
****
n.s.
TDP-43/DAPI
Correlation Coeff.
1.00
0.75
0.50
0.25
0.00
Untreated
DMSO
Day 1
Day 2
Day 3
Day 4
Day 5
Day 6
Day 7
Days post MG-132 Washout

FIG. 5B

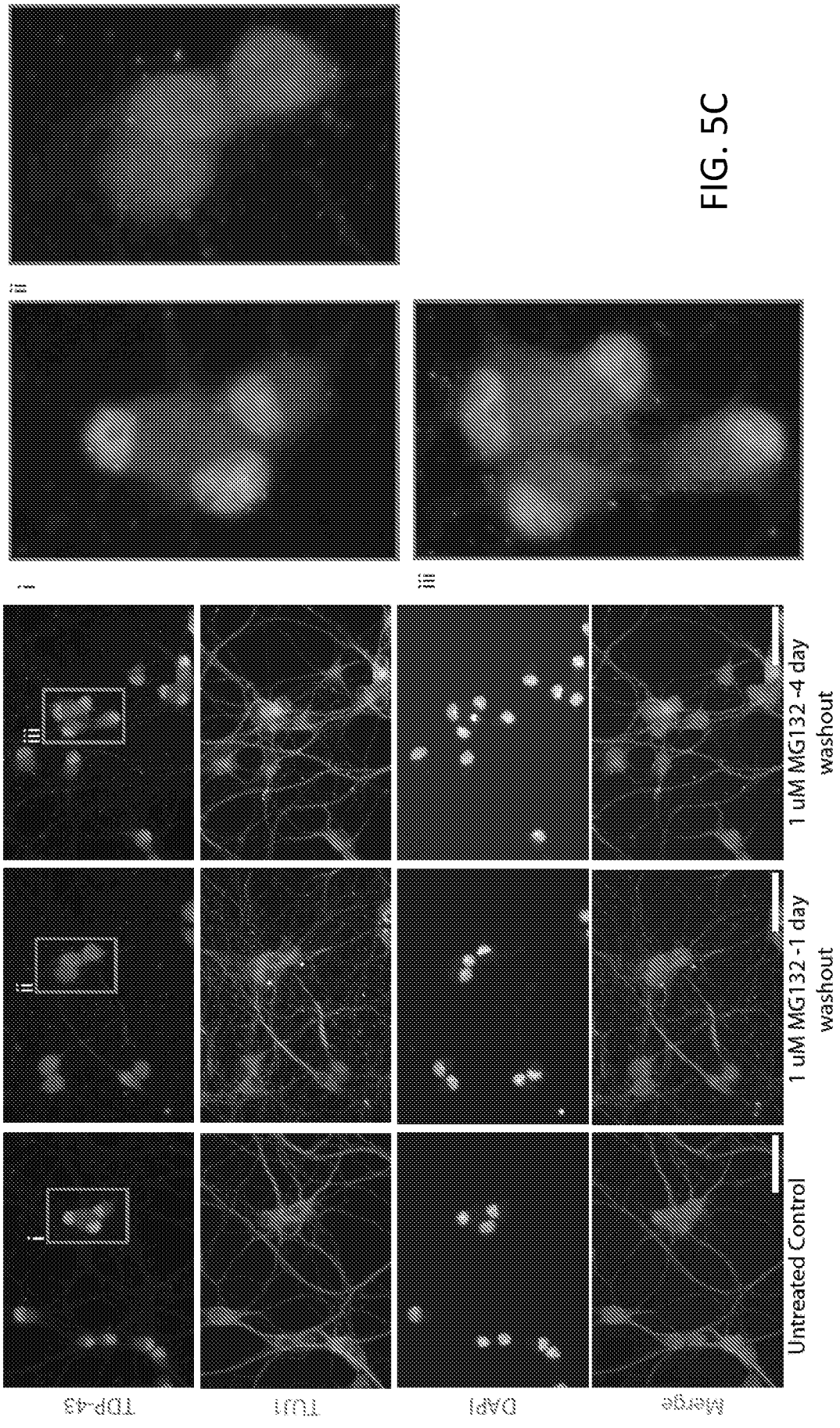
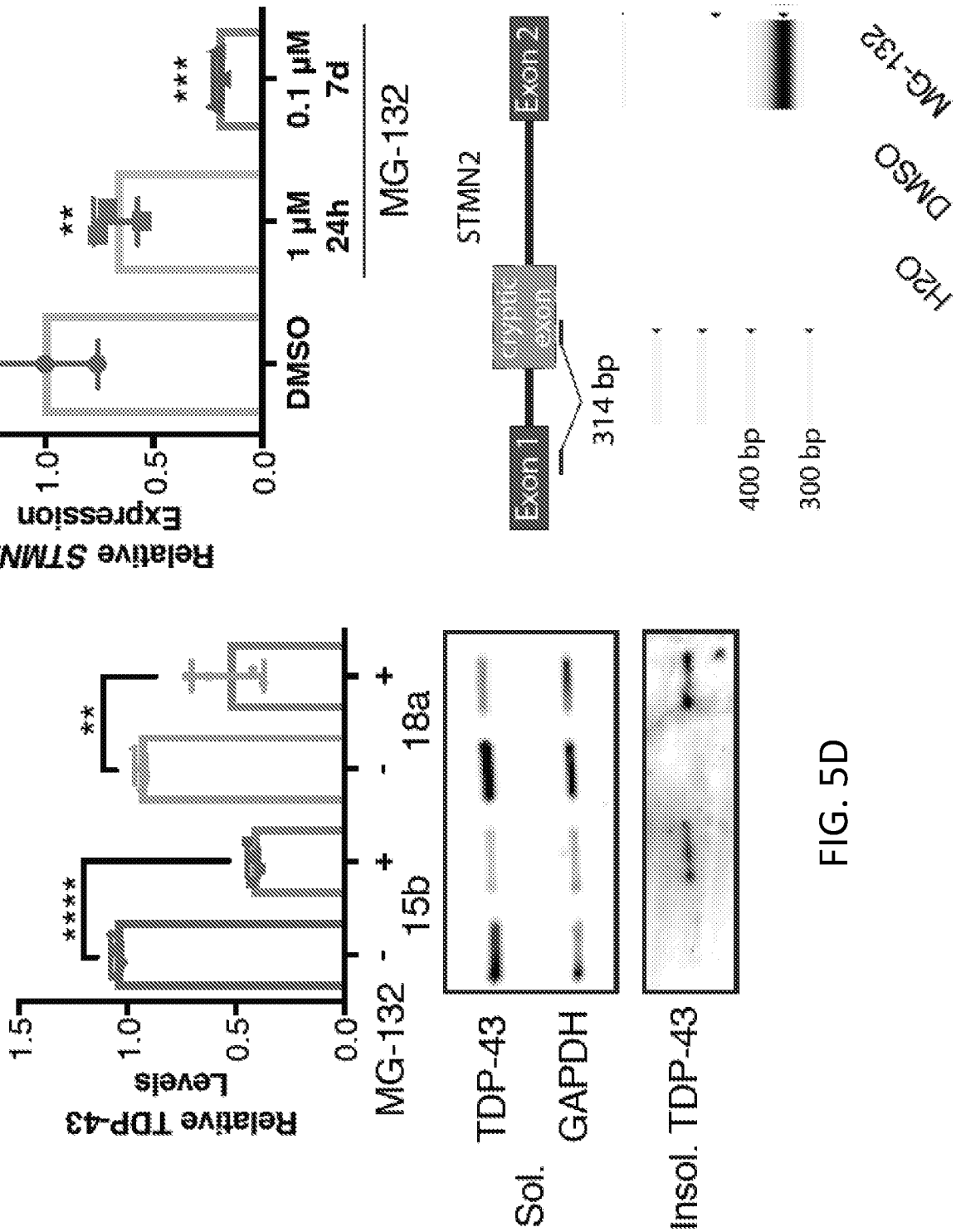

TDP-43
TUJ1
DAPI
Merge
Untreated Control
1 uM MG132 -1 day washout
1 uM MG132 -4 day washout
i
ii
iii

FIG. 5C


FIG. 5E
Relative STMN2 Expression
1.5
1.0
0.5
0.0
DMSO
1 µM
0.1 µM
24h
7d
MG-132
**
***
FIG. 5F
STMN2
Exon1
Exon2
314 bp
FIG. 5G
H2O
DMSO
MG-132
400 bp
300 bp
Relative TDP-43 Levels
****
**
MG-132 - + - +
15b 18a
Sol.
TDP-43
GAPDH
Insol. TDP-43
FIG. 5D

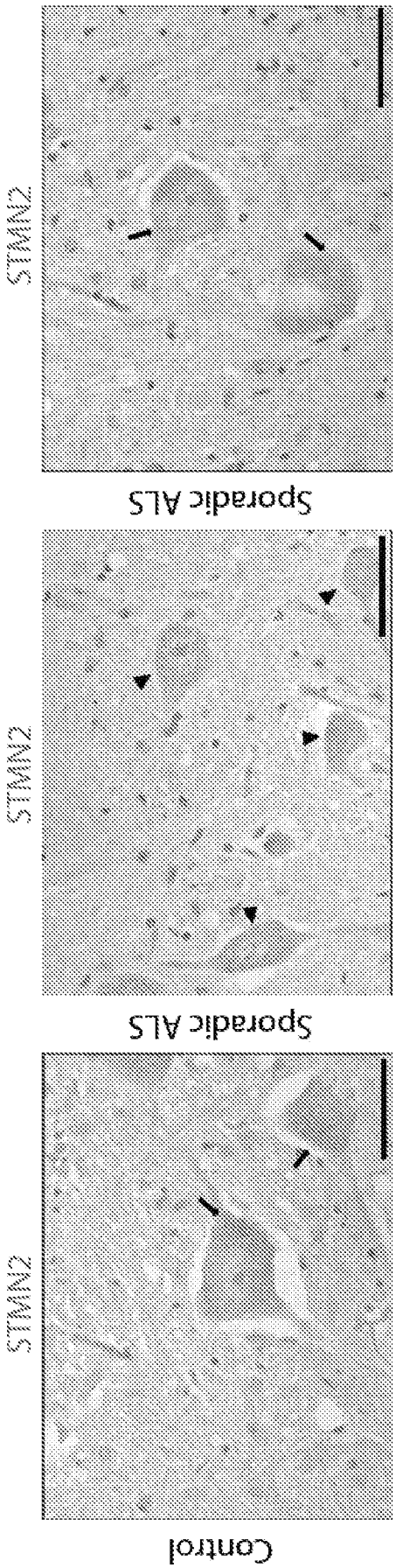


FIG. 6A

FIG. 6B

FIG. 6C

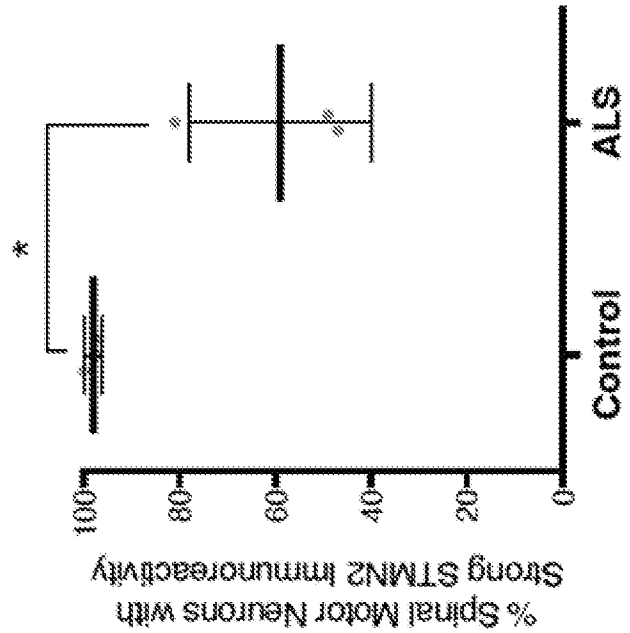


FIG. 6D

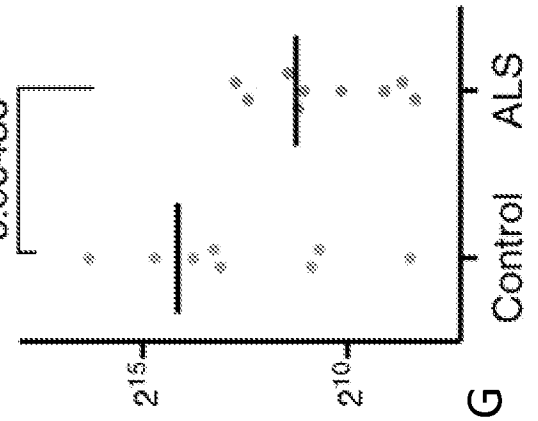


FIG. 6G

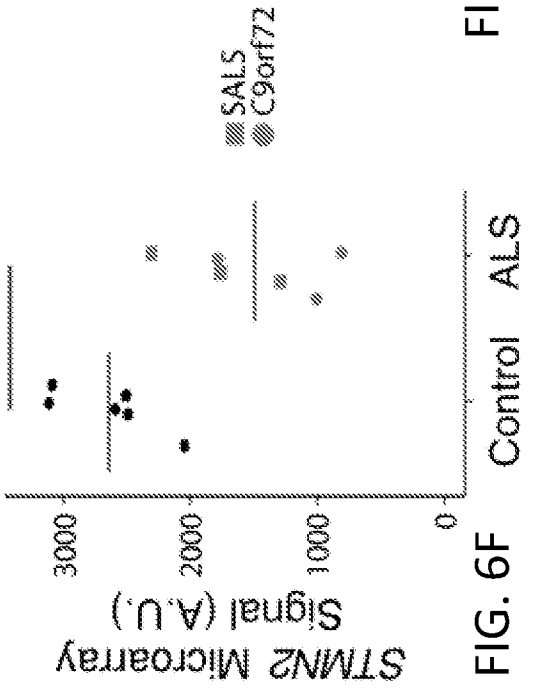


FIG. 6F

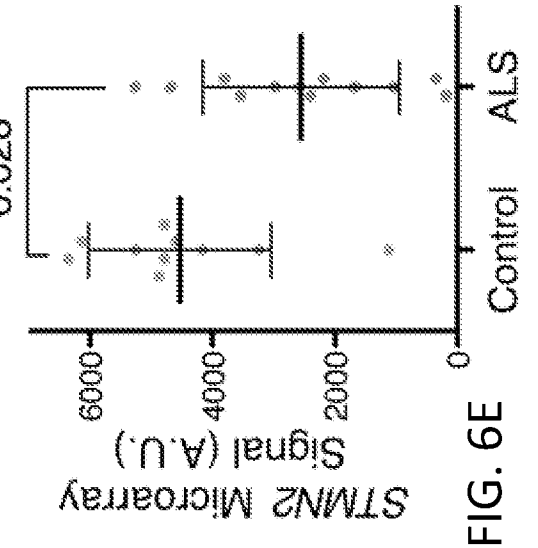


FIG. 6E

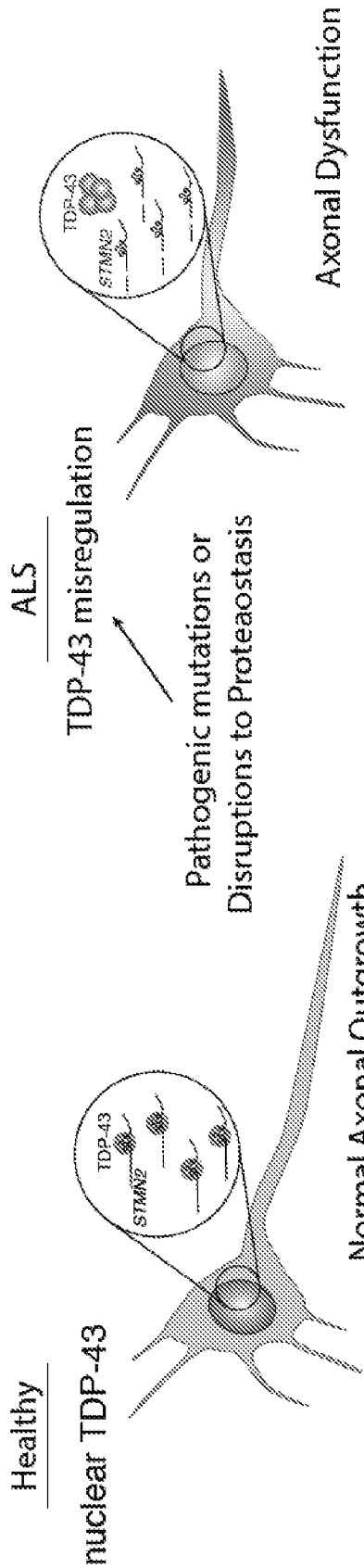

Healthy
nuclear TDP-43
TDP-43
STMN2
Normal Axonal Outgrowth
Pathogenic mutations or
Disruptions to Proteaostasis
ALS
TDP-43 misregulation
TDP-43
STMN2
Axonal Dysfunction

FIG. 6H

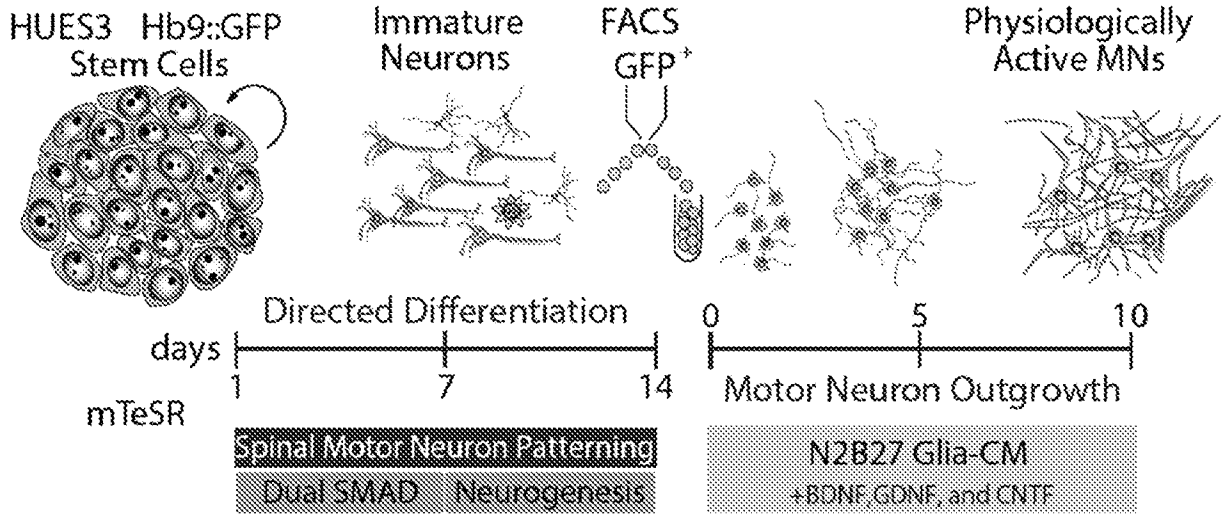

HUES3 Hb9::GFP
Stem Cells
Immature
Neurons
FACS
GFP+
Physiologically
Active MNs
Directed Differentiation
days
1
7
14
mTeSR
Spinal Motor Neuron Patterning
Dual SMAD Neurogenesis
0
5
10
Motor Neuron Outgrowth
N2B27 Glia-CM
+BDNF,GDNF, and CNTF

FIG. 7A

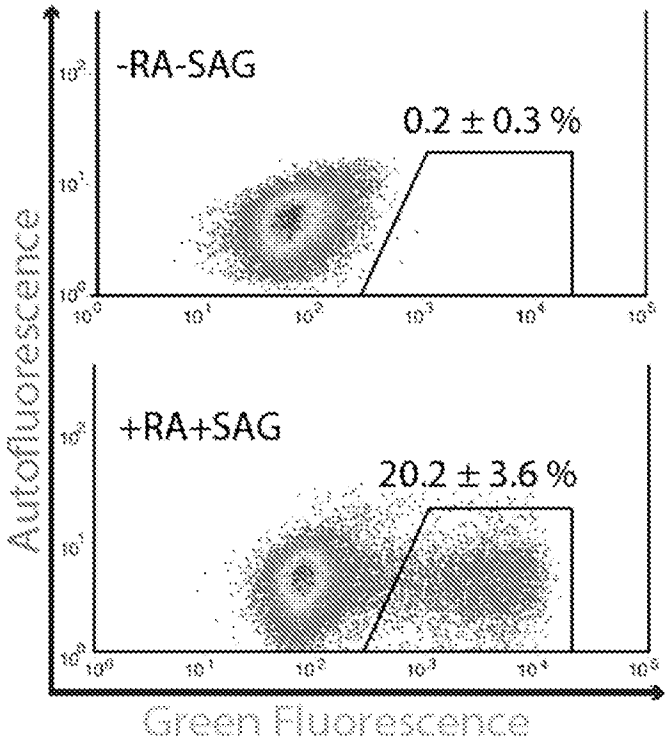
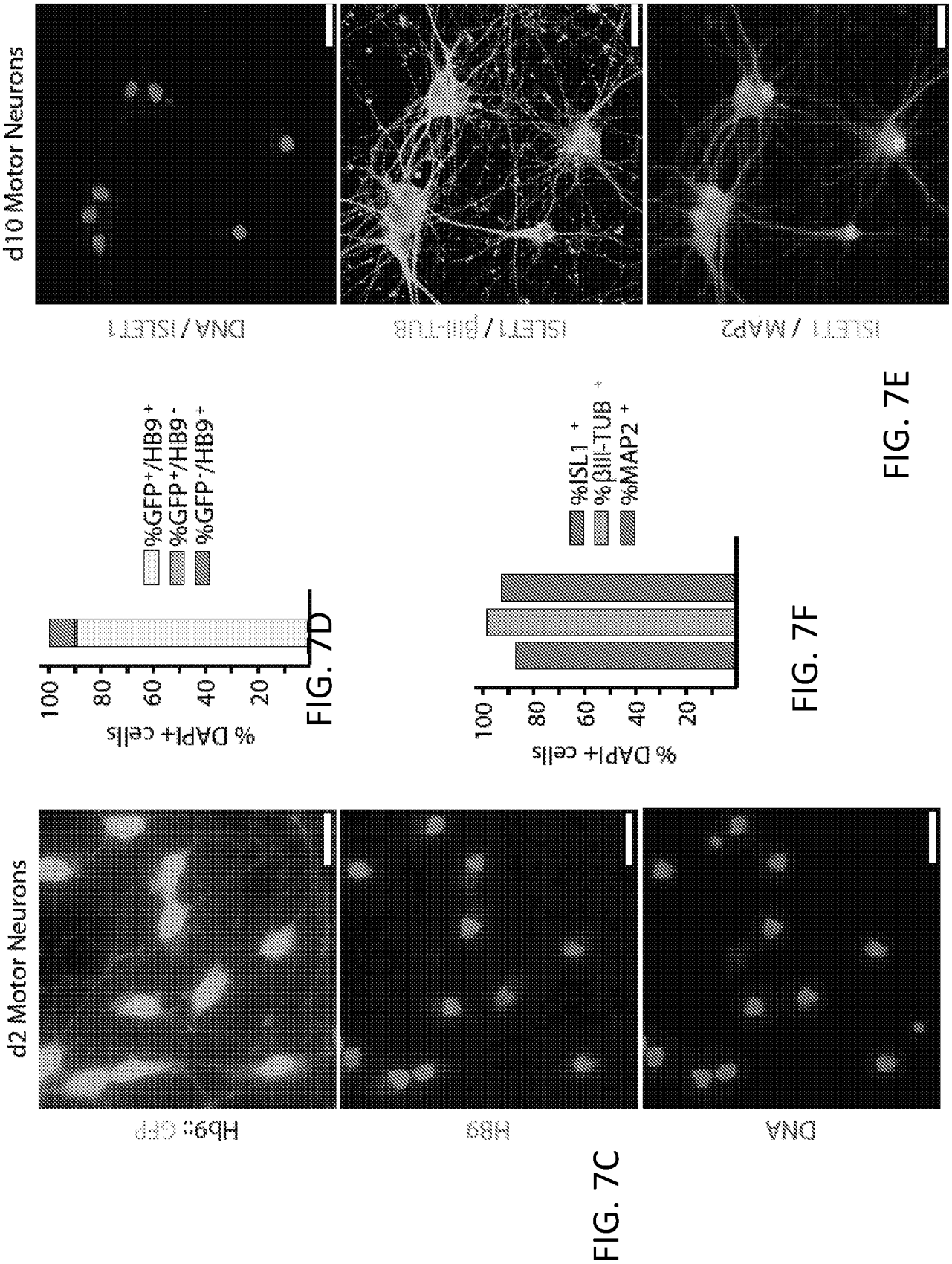

-RA-SAG
0.2 ± 0.3 %
+RA+SAG
20.2 ± 3.6 %
Autofluorescence
Green Fluorescence

FIG. 7B


d2 Motor Neurons
Hb9::GFP
H&9
DNA
FIG. 7C
% DAPI+ cells
100
80
60
40
20
%GFP+/HB9+
%GFP+/HB9-
%GFP-/HB9+
FIG. 7D
% DAPI+ cells
100
80
60
40
20
%ISL1+
%βIII-TUB+
%MAP2+
FIG. 7F
d10 Motor Neurons
DNA / ISLET1
ISLET1 / βIII-TUB
ISLET1 / MAP2
FIG. 7E

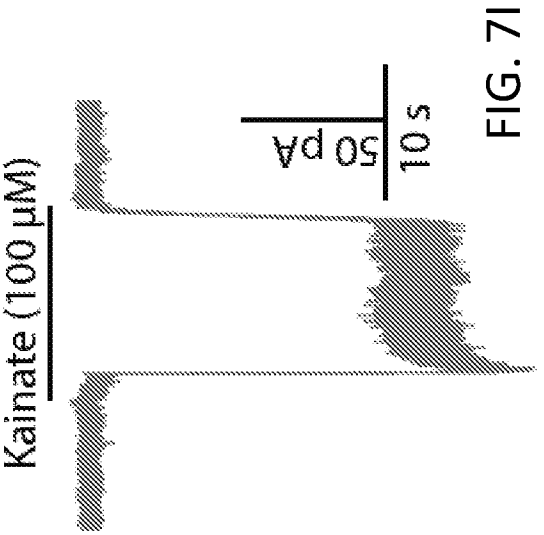


FIG. 7I

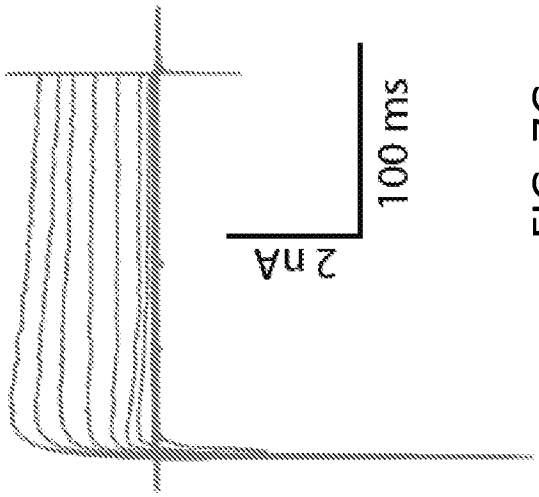


FIG. 7G

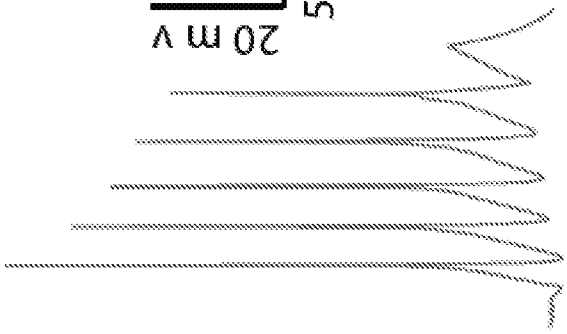


FIG. 7H

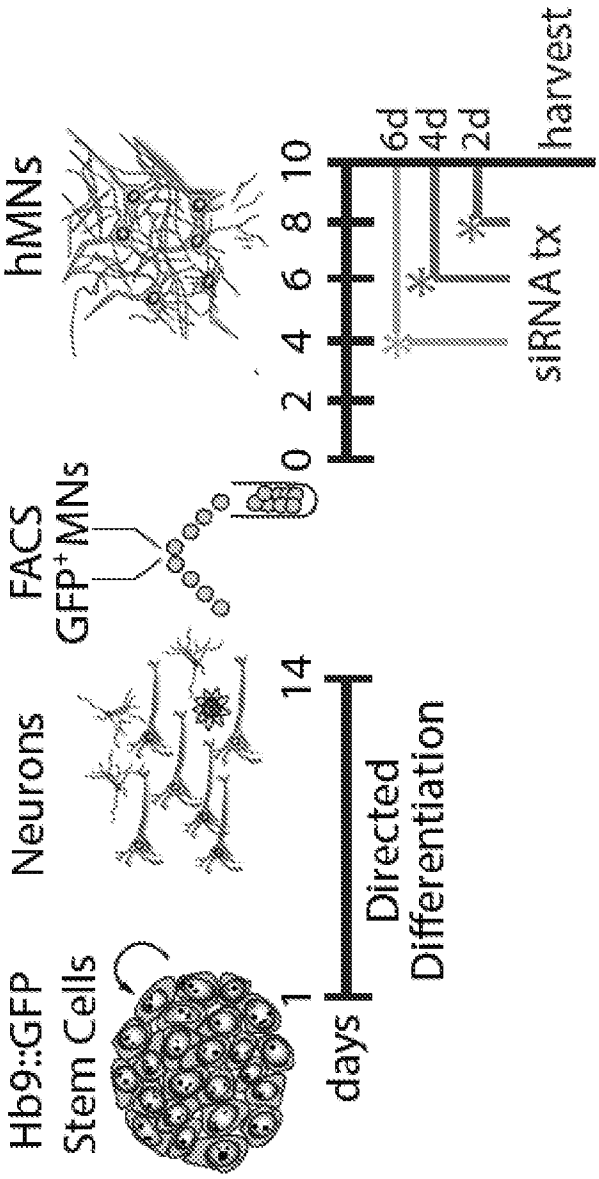

Hb9::GFP
Stem Cells
Neurons
FACS
GFP+MNs
hMNs
1
14
days
Directed
Differentiation
0
2
4
6
8
10
6d
4d
2d
siRNA tx
harvest

FIG. 8A

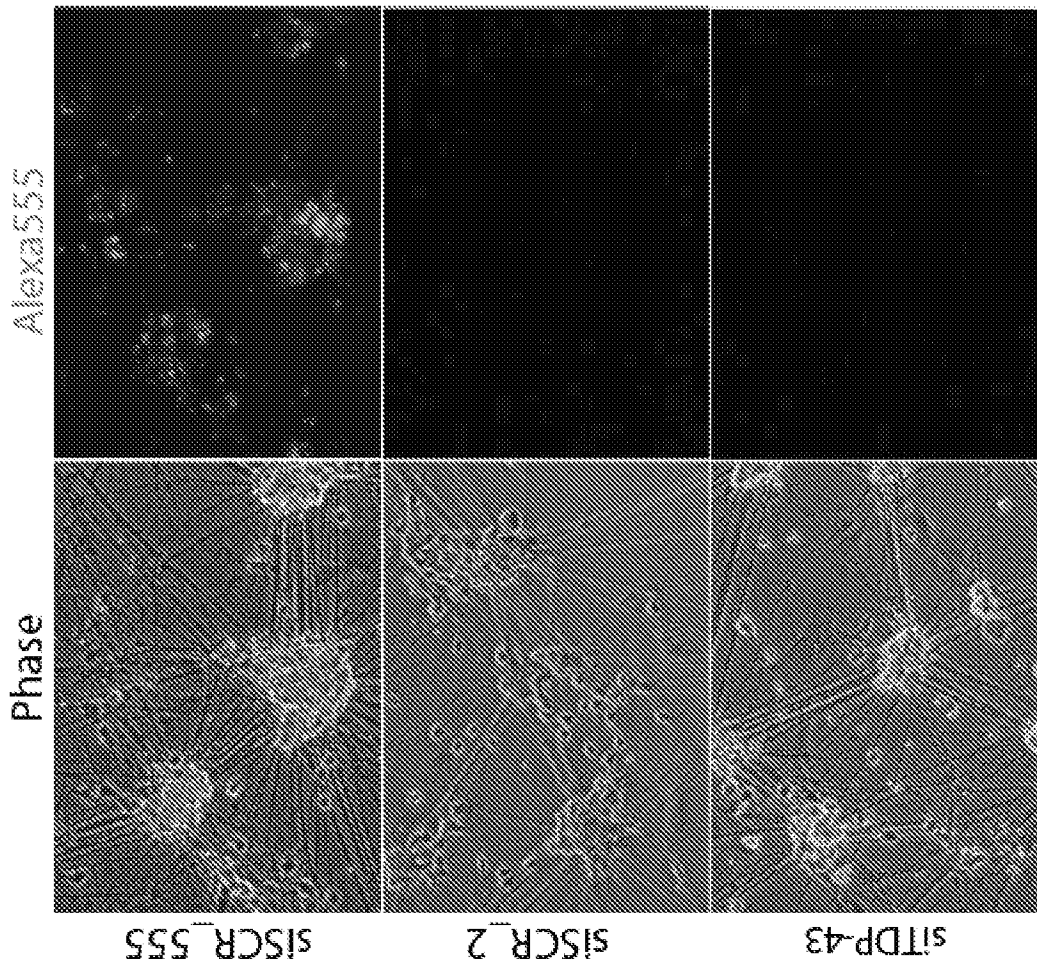


FIG. 8B

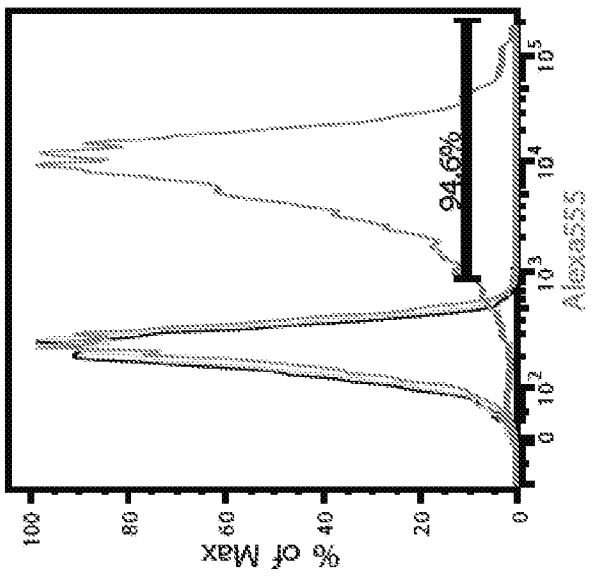


FIG. 8C

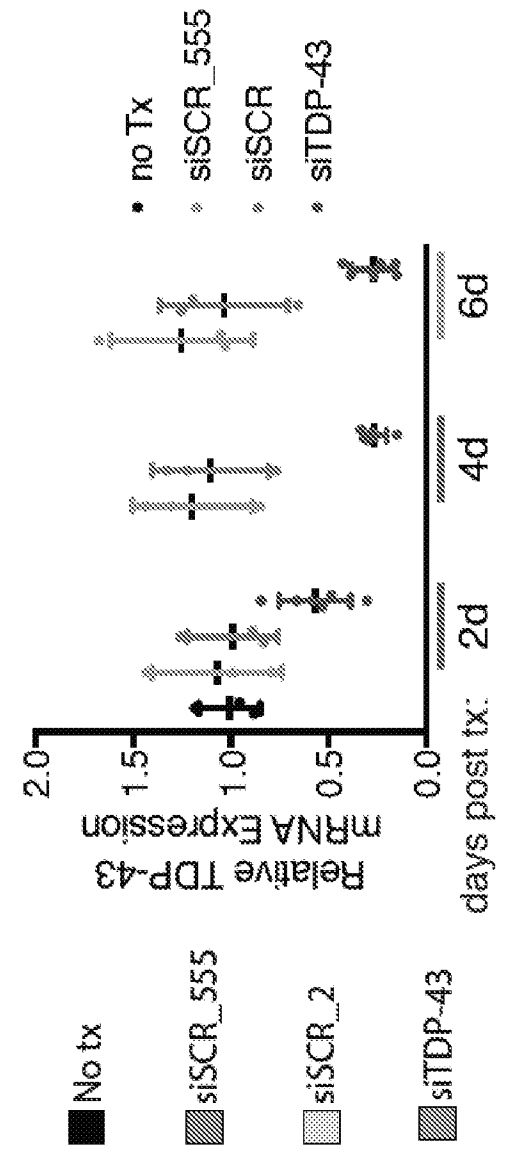


FIG. 8D

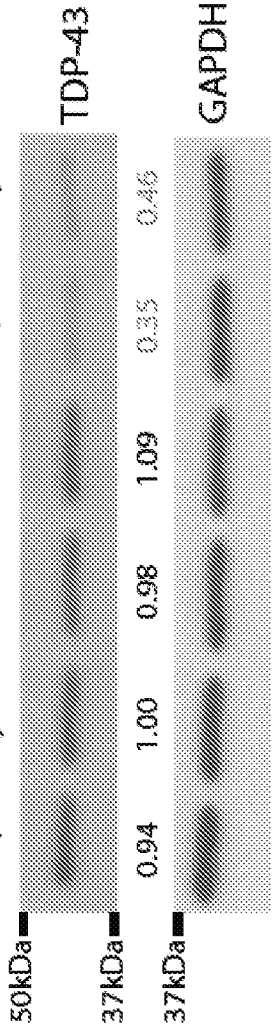


FIG. 8E

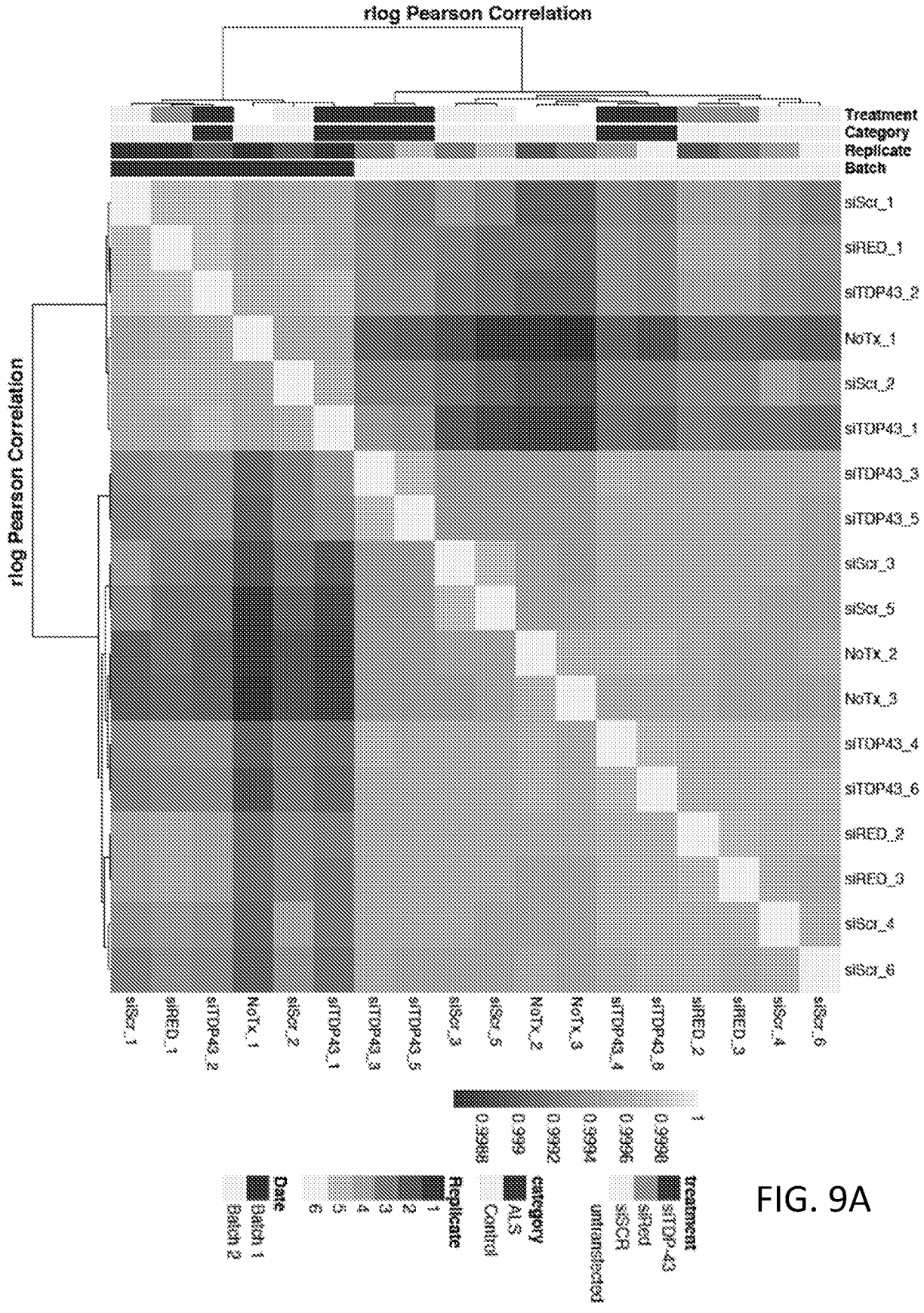

rlog Pearson Correlation
rlog Pearson Correlation
Treatment
Category
Replicate
Batch
siScr_1
siRED_1
siTDP43_2
NoTx_1
siScr_2
siTDP43_1
siTDP43_3
siTDP43_5
siScr_3
siScr_5
NoTx_2
NoTx_3
siTDP43_4
siTDP43_6
siRED_2
siRED_3
siScr_4
siScr_6
1
0.9998
0.9996
0.9994
0.9992
0.999
0.9988
treatment
siTDP-43
siRed
siSCR
untransfected
category
ALS
Control
Replicate
1
2
3
4
5
6
Date
Batch 1
Batch 2

FIG. 9A

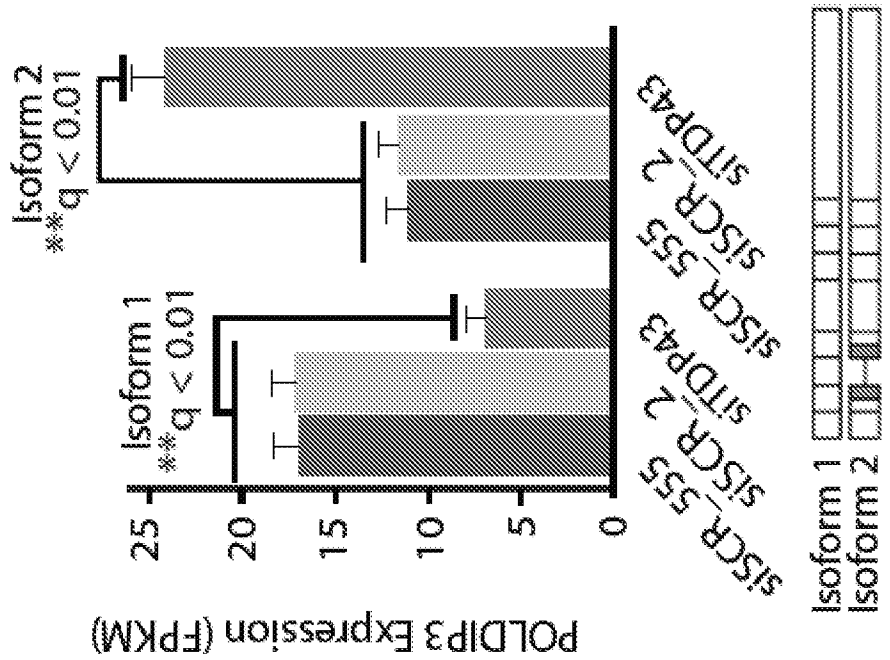

POLDIP3 Expression (FPKM)
25
20
15
10
5
0
siSCR_555
siSCR_2
siTDP43
siSCR_555
siSCR_2
siTDP43
Isoform 1
**q < 0.01
Isoform 2
**q < 0.01
Isoform 1
Isoform 2

FIG. 9C

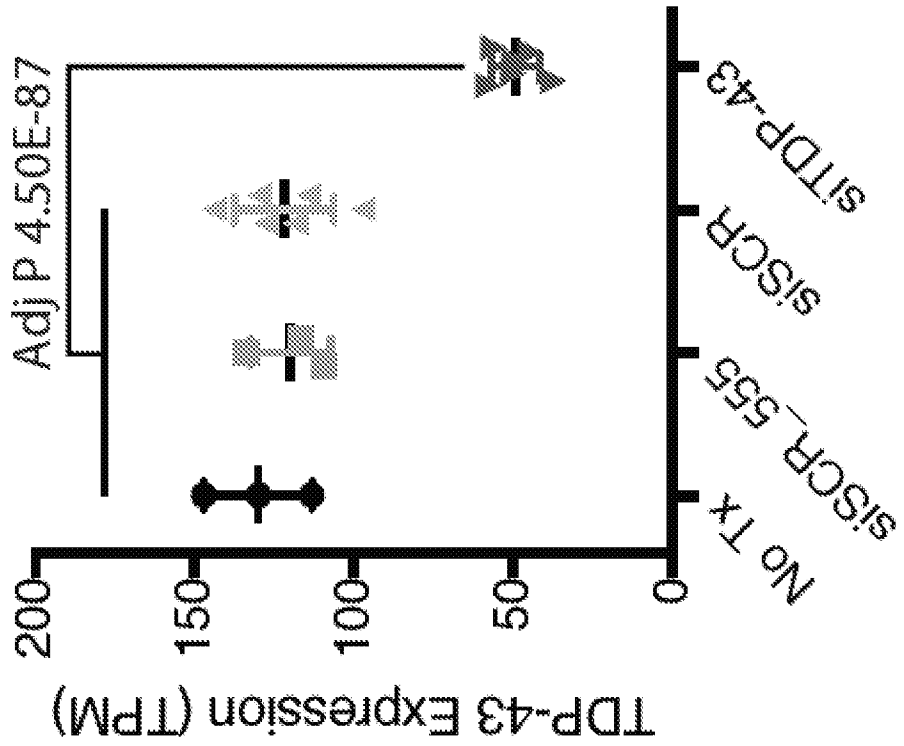

TDP-43 Expression (TPM)
200
150
100
50
0
Adj P 4.50E-87
No Tx
siSCR_555
siSCR
siTDP-43

FIG. 9B

FIG. 10

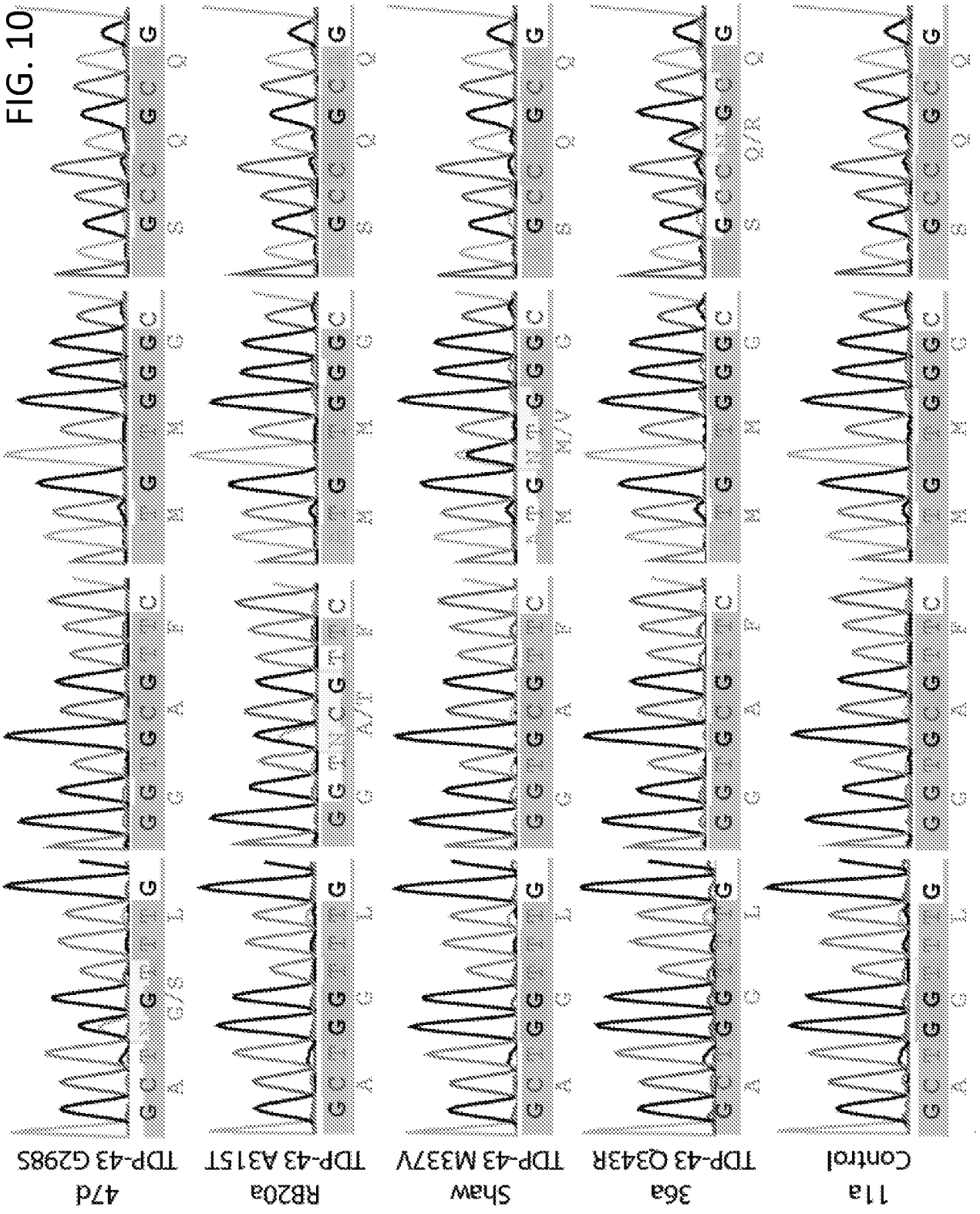
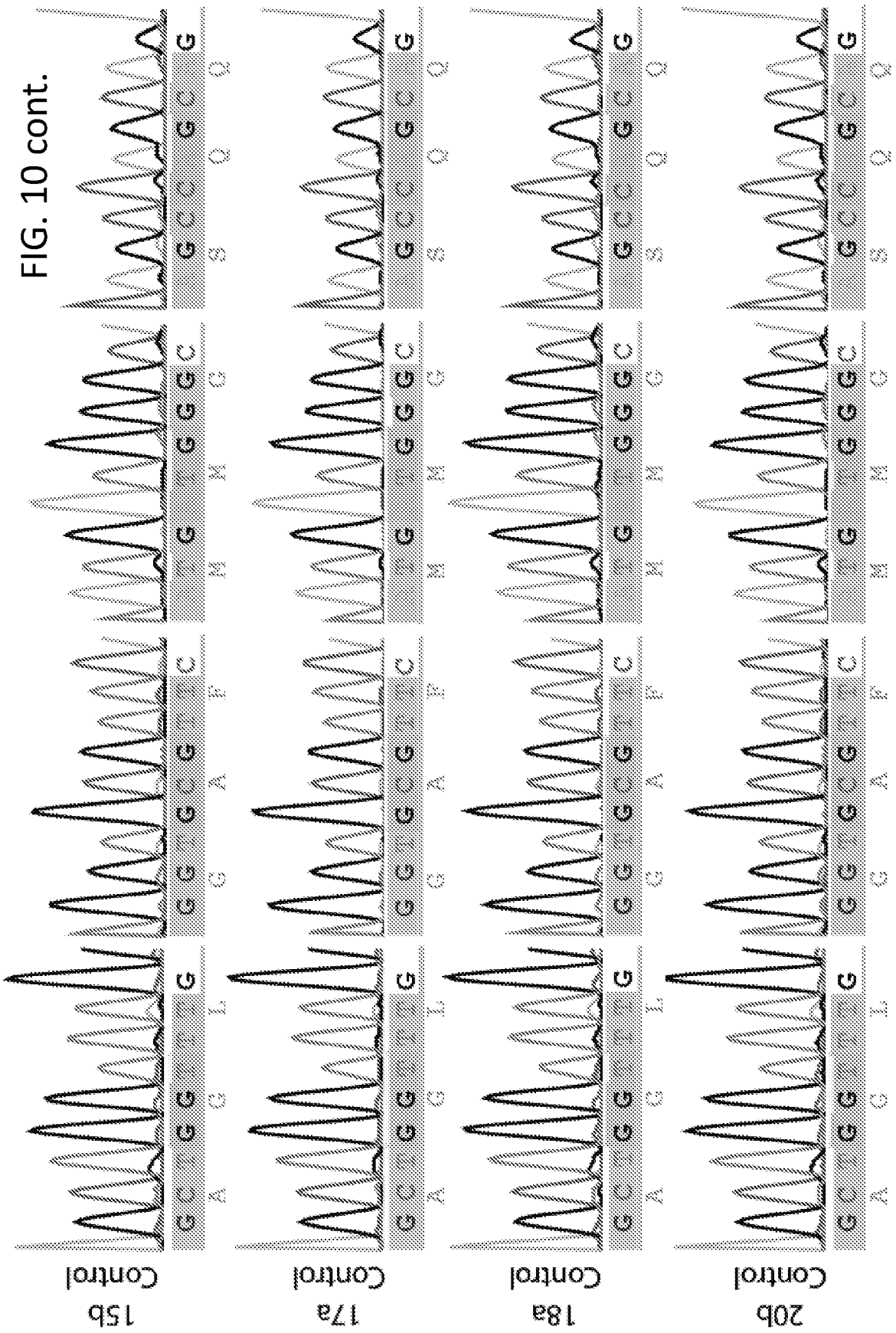

11a
Control
36a
TDP-43 Q343R
Shaw
TDP-43 M337V
RB20a
TDP-43 A315T
47d
TDP-43 G298S

FIG. 10 cont.



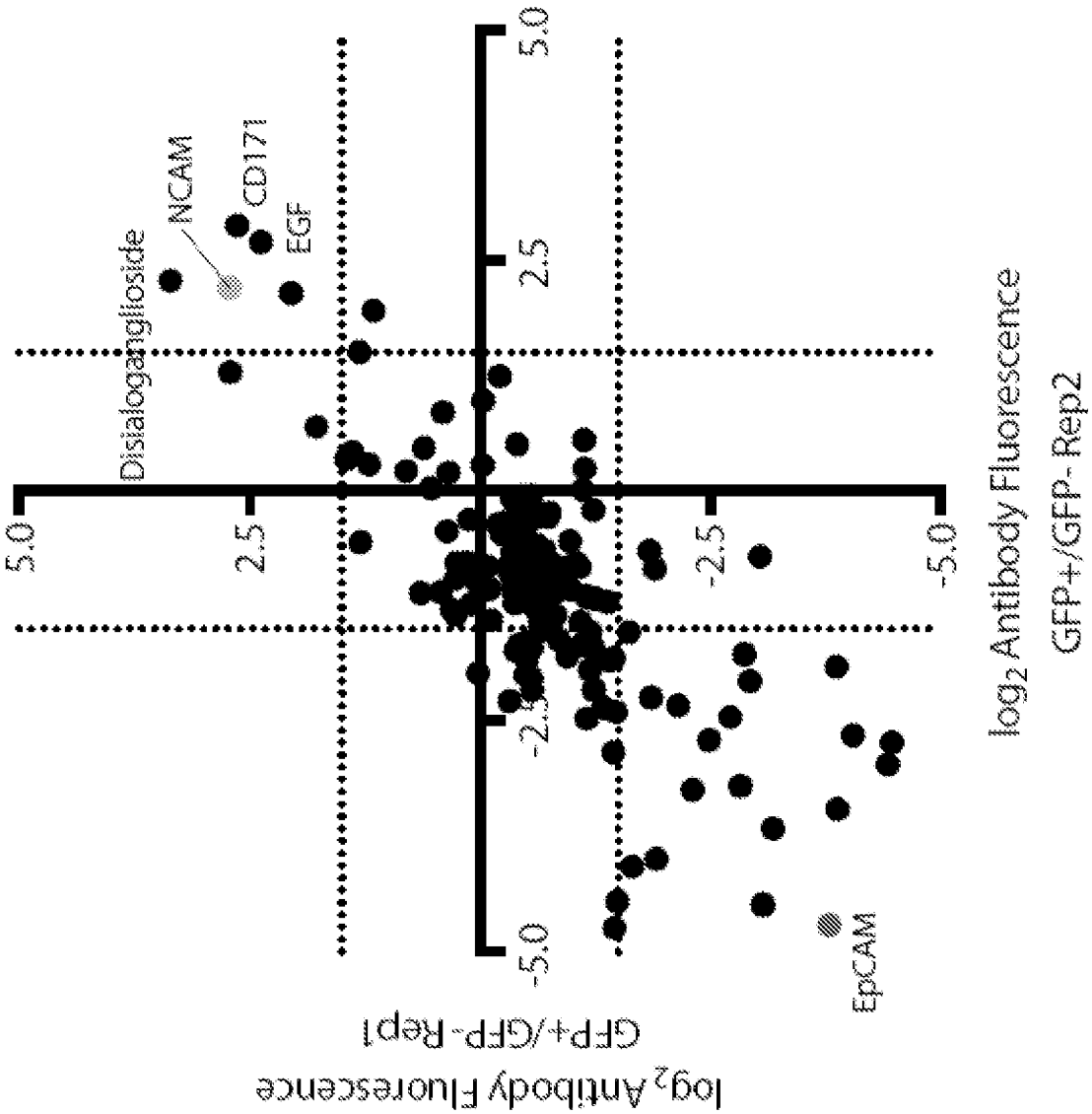

Disialoganglioside
NCAM
CD171
EGF
EpCAM
5.0
2.5
-2.5
-5.0
log2 Antibody Fluorescence
GFP+/GFP- Rep2
log2 Antibody Fluorescence
GFP+/GFP- Rep1

FIG. 11A

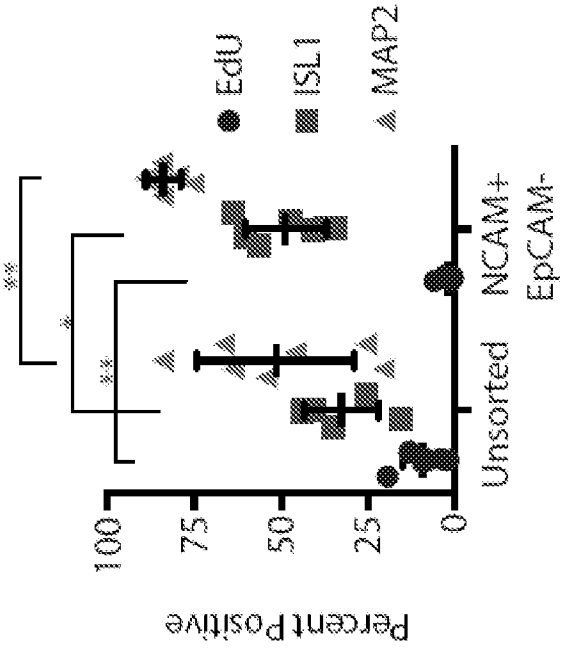


FIG. 11B

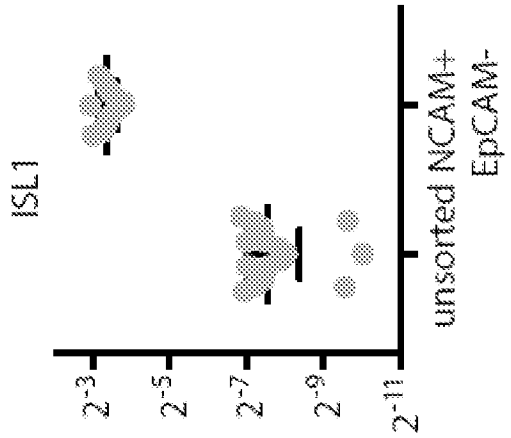


FIG. 11C

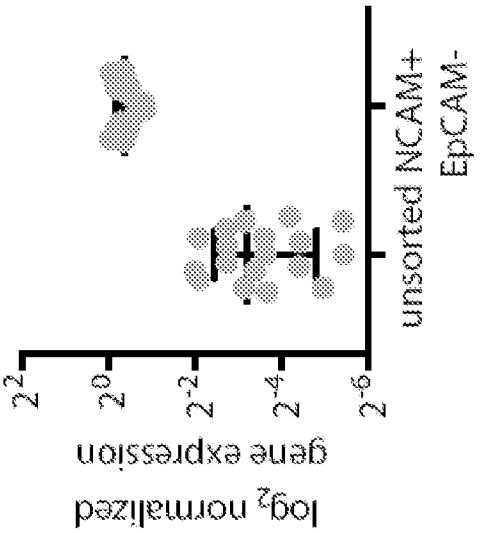


FIG. 11D

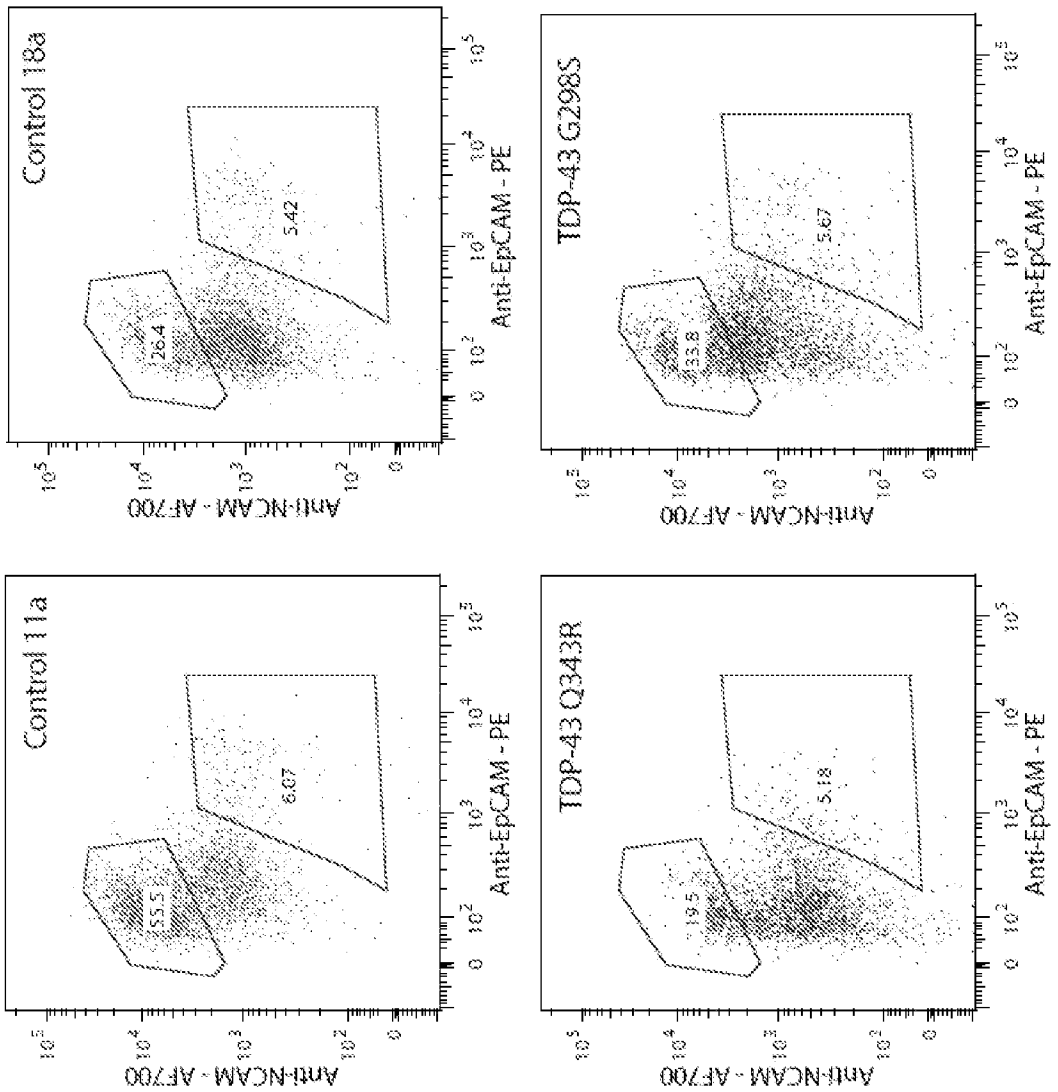

Control 18a
26.4
5.42
Anti-NCAM - AF700
Anti-EpCAM - PE
TDP-43 G298S
23.8
5.67
Anti-NCAM - AF700
Anti-EpCAM - PE
Control 11a
15.5
6.07
Anti-NCAM - AF700
Anti-EpCAM - PE
TDP-43 Q343R
19.5
5.18
Anti-NCAM - AF700
Anti-EpCAM - PE

FIG. 11E

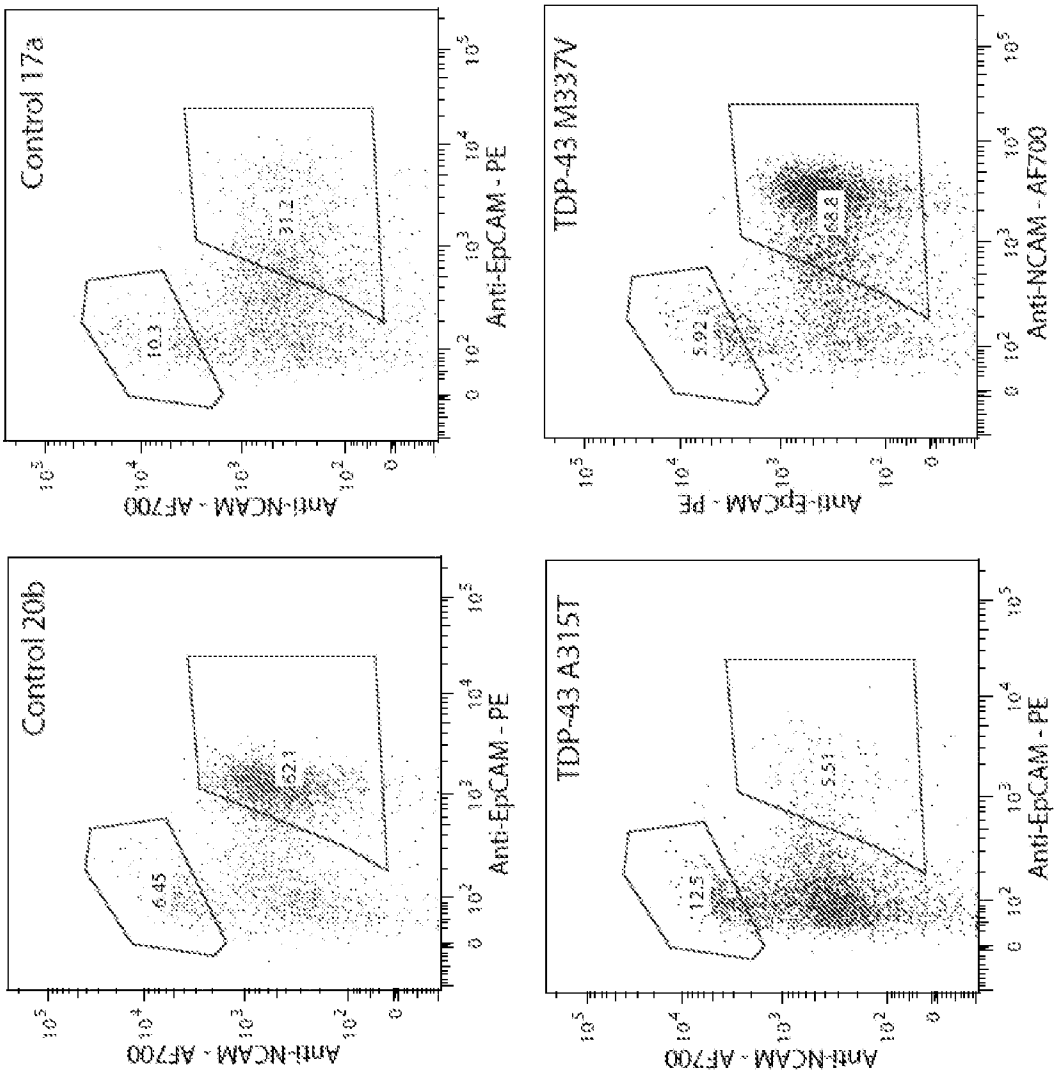

Control 17a
Control 20b
TDP-43 M337V
TDP-43 A315T
Anti-NCAM - AF700
Anti-EpCAM - PE
10.3
31.2
6.45
62.1
5.92
68.8
12.5
5.51

FIG. 11E cont.

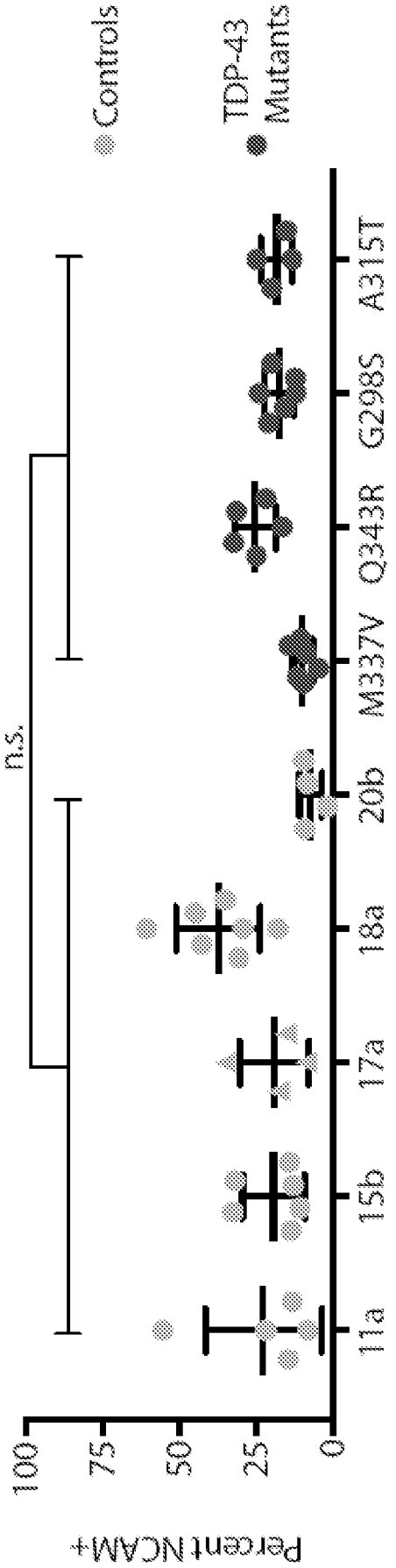

Controls
TDP-43 Mutants
n.s.
Percent NCAM+
100
75
50
25
0
11a
15b
17a
18a
20b
M337V
Q343R
G298S
A315T

FIG. 11F

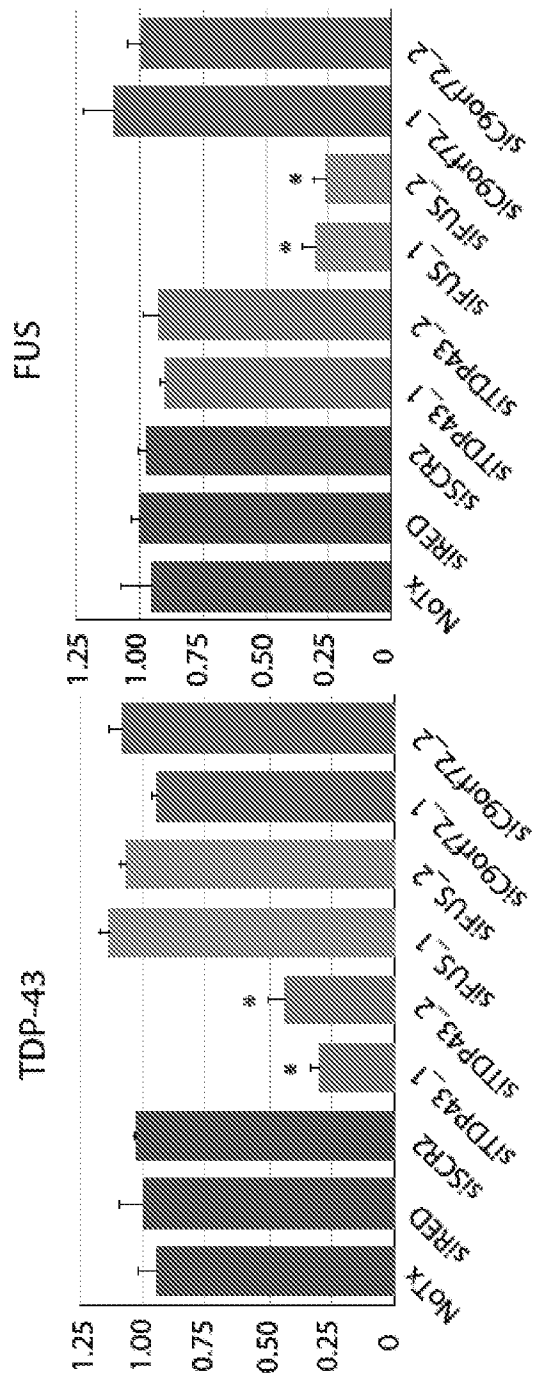


FIG. 12A

FIG. 12B

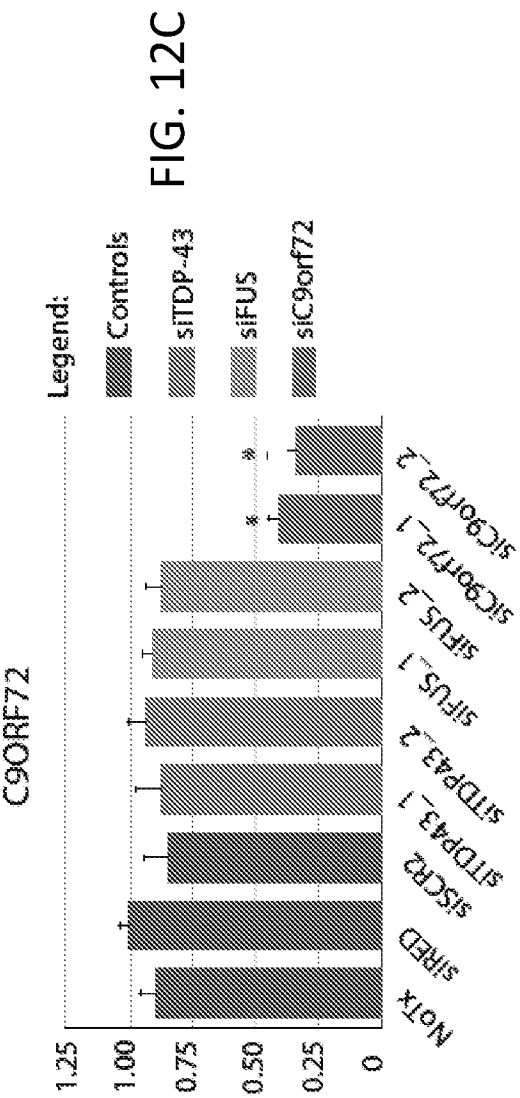


FIG. 12C

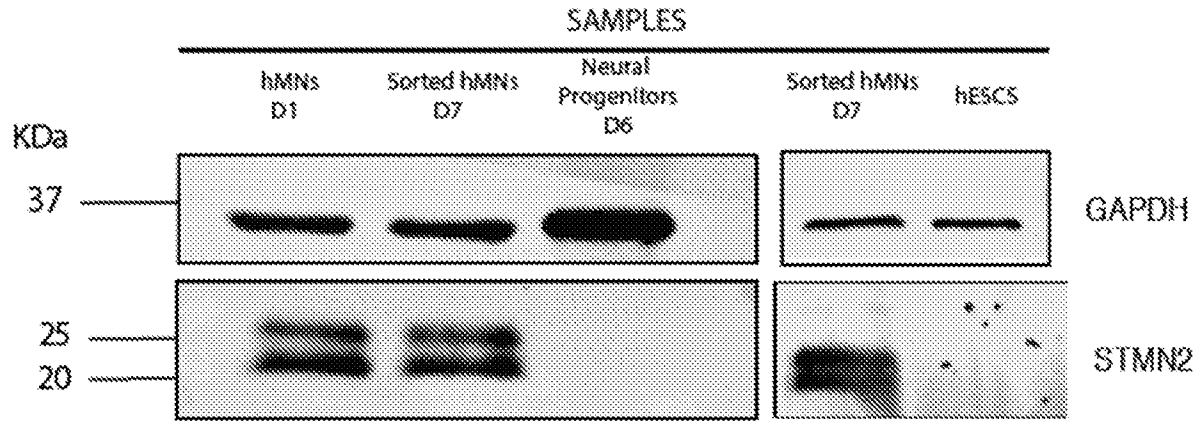


FIG. 12D

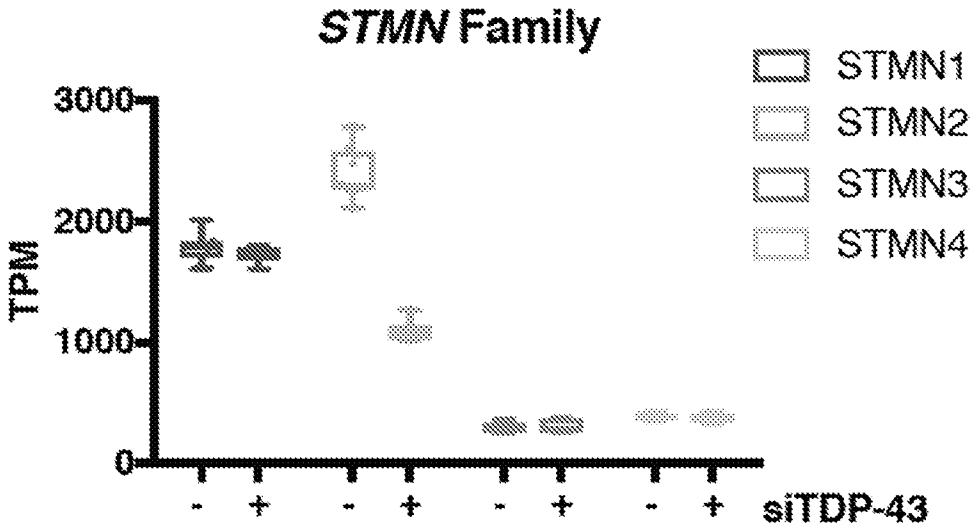


FIG. 12E

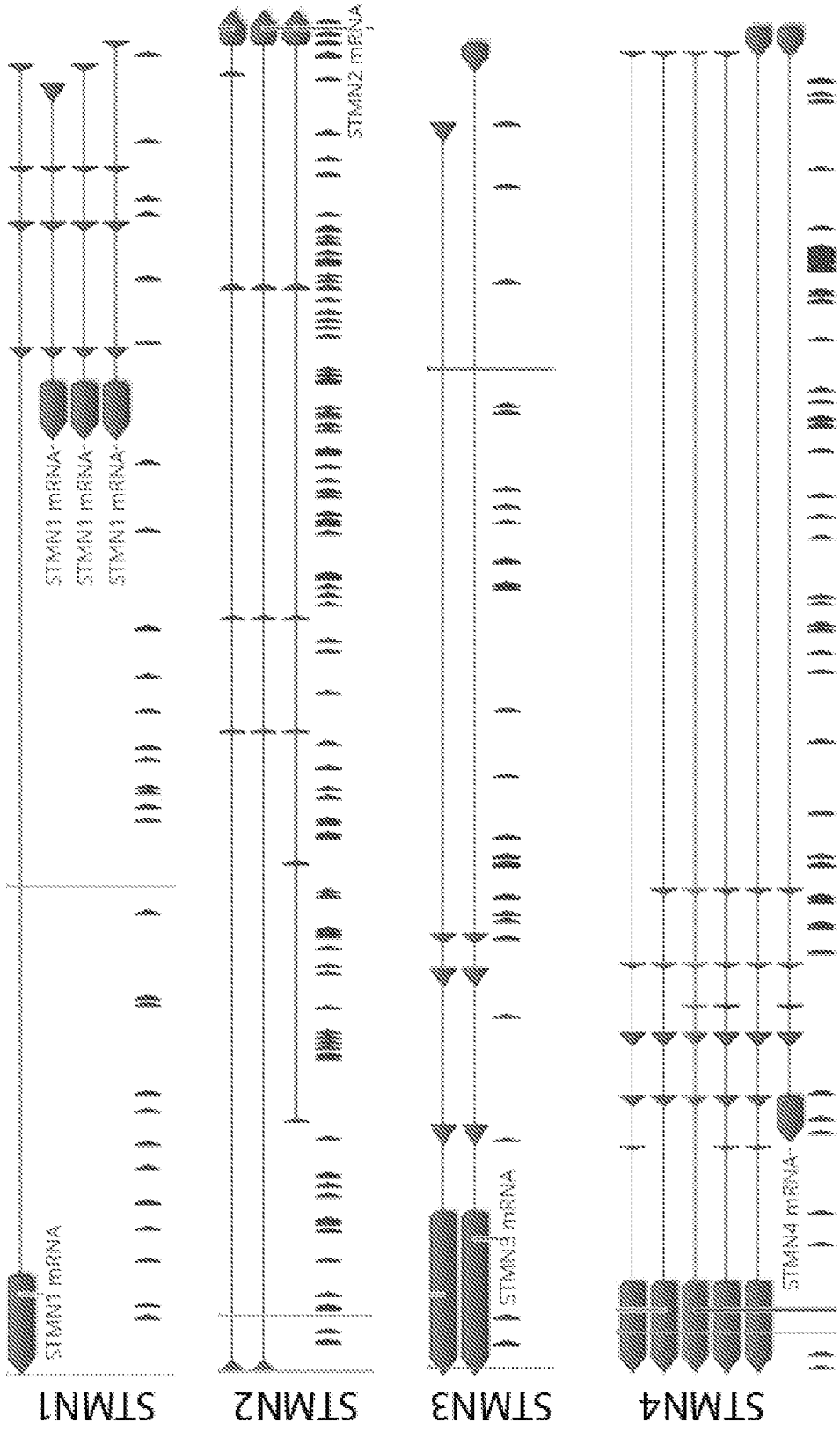

STMN1
STMN1 mRNA
STMN1 mRNA
STMN1 mRNA
STMN1 mRNA
STMN2
STMN2 mRNA
STMN3
STMN3 mRNA
STMN4
STMN4 mRNA

FIG. 12F

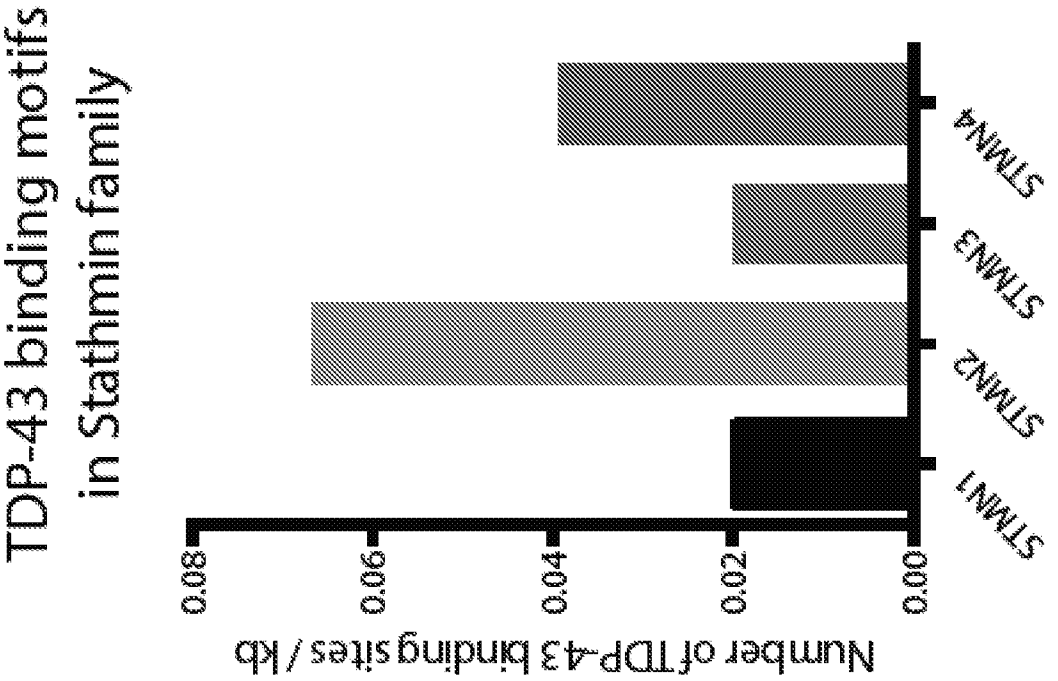

TDP-43 binding motifs
in Stathmin family
Number of TDP-43 binding sites / kb
0.00
0.02
0.04
0.06
0.08
STMN1
STMN2
STMN3
STMN4

FIG. 12G

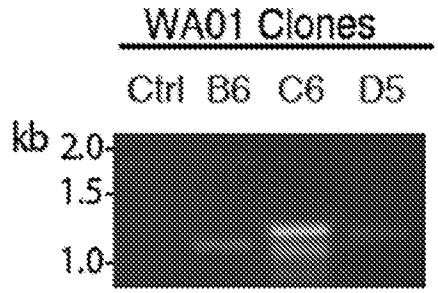


FIG. 13A

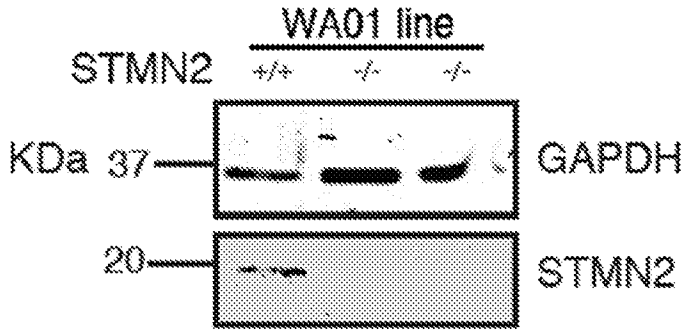


FIG. 13B

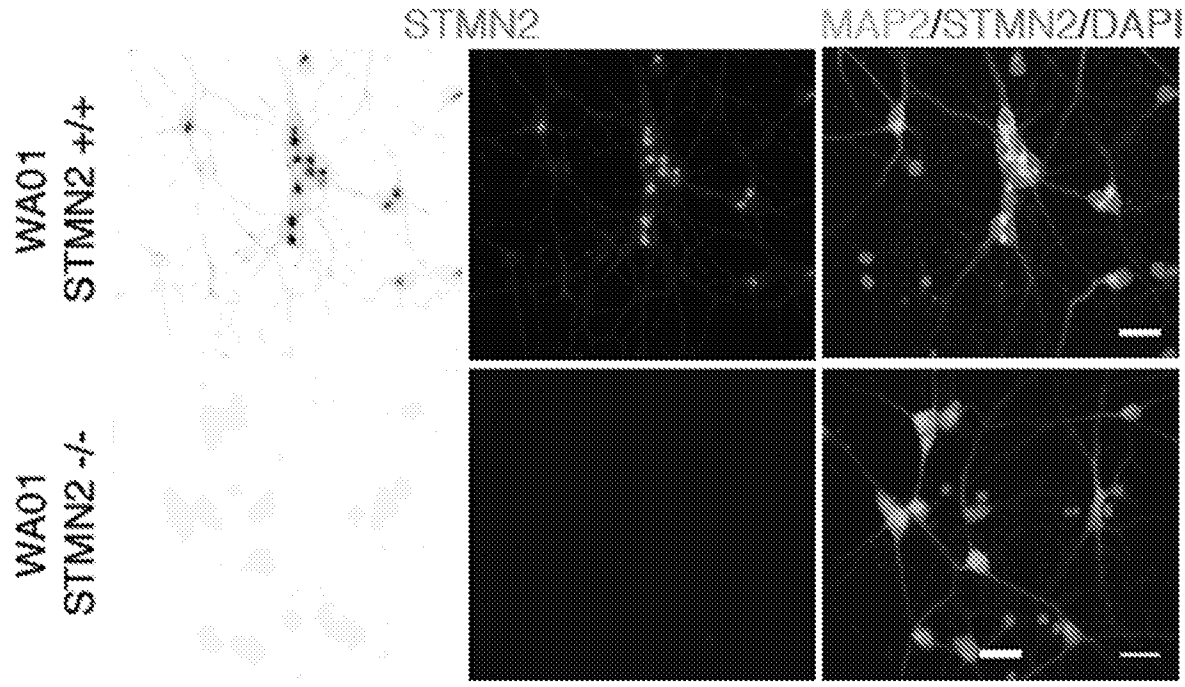


FIG. 13C

FIG. 13E

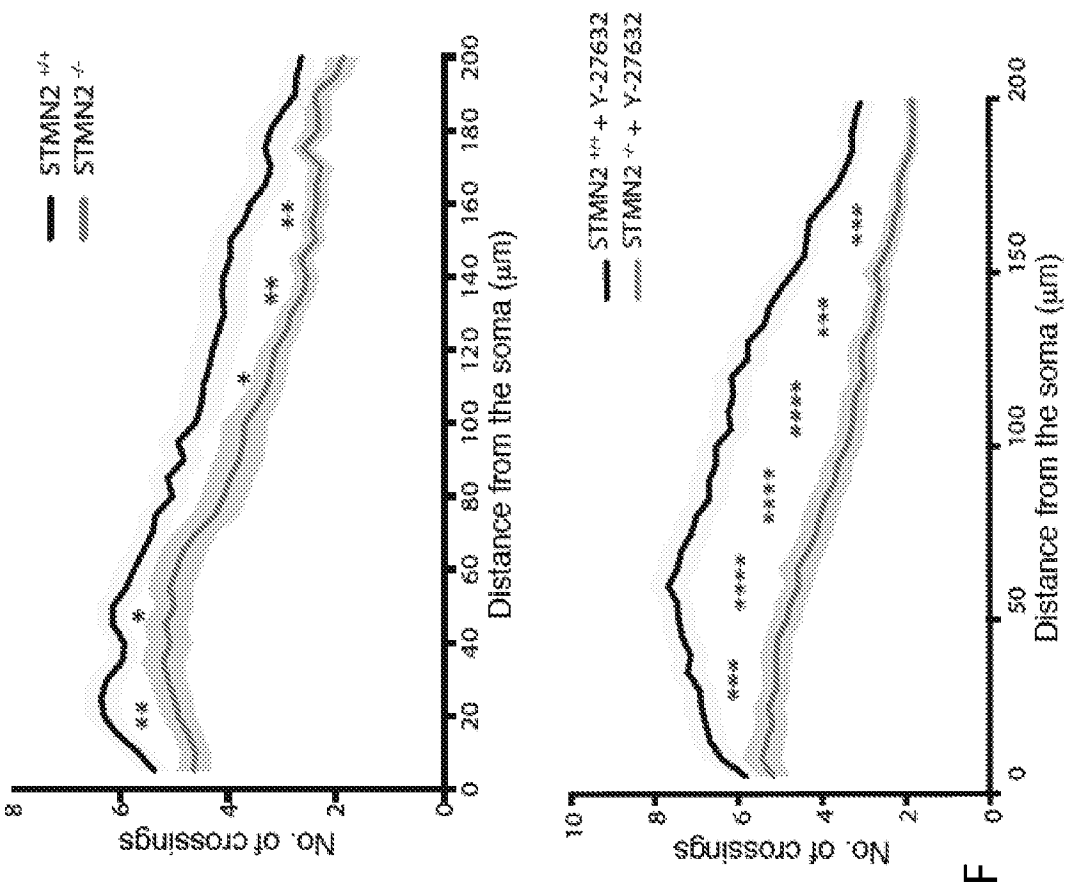


FIG. 13F

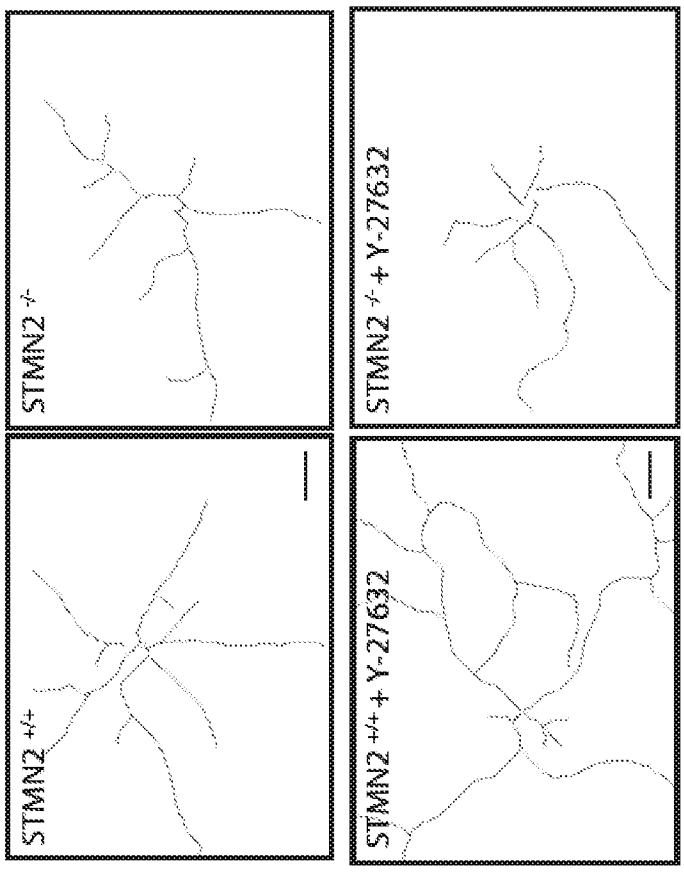


FIG. 13D

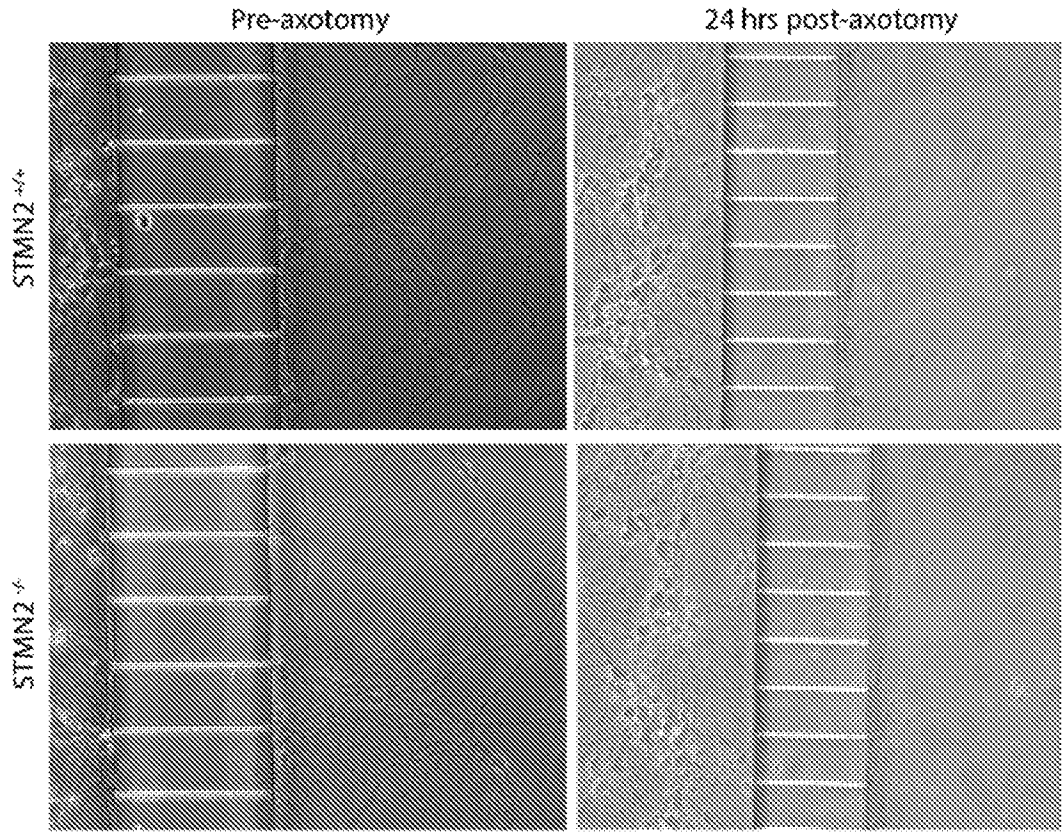


FIG. 13G

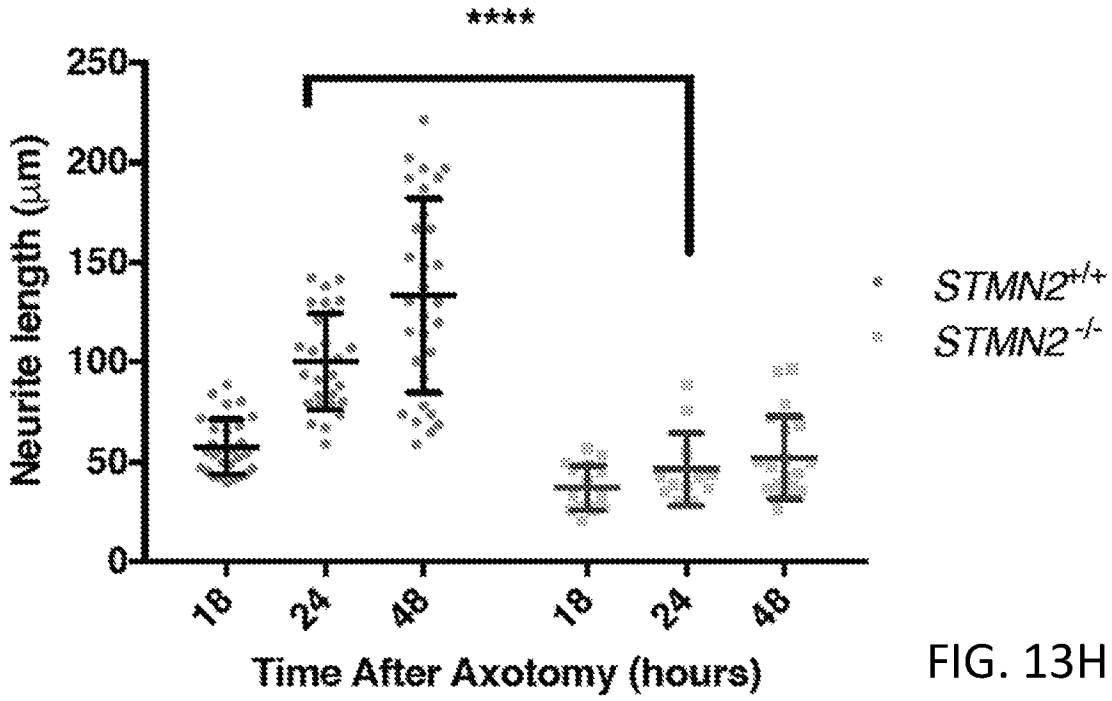


FIG. 13H

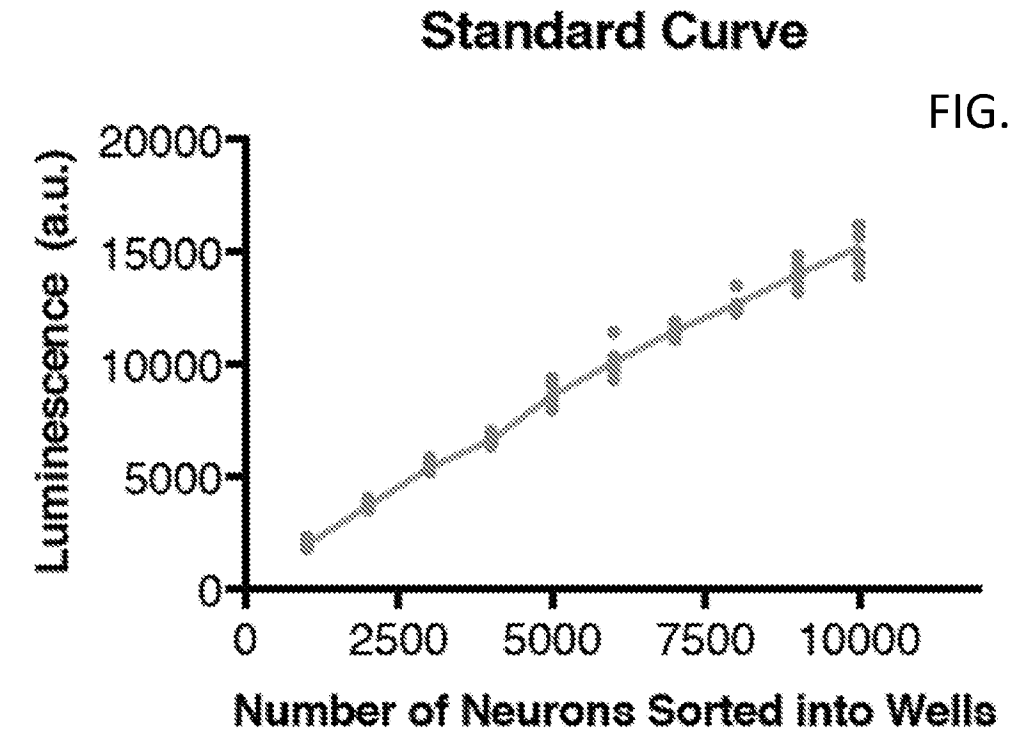


FIG. 14A

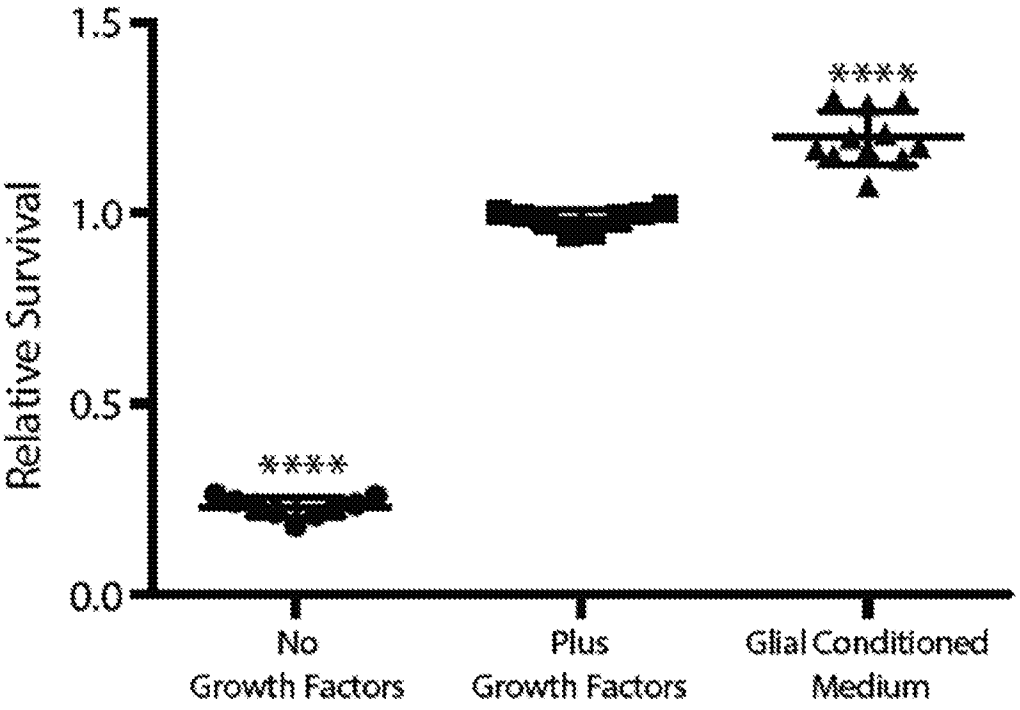


FIG. 14B

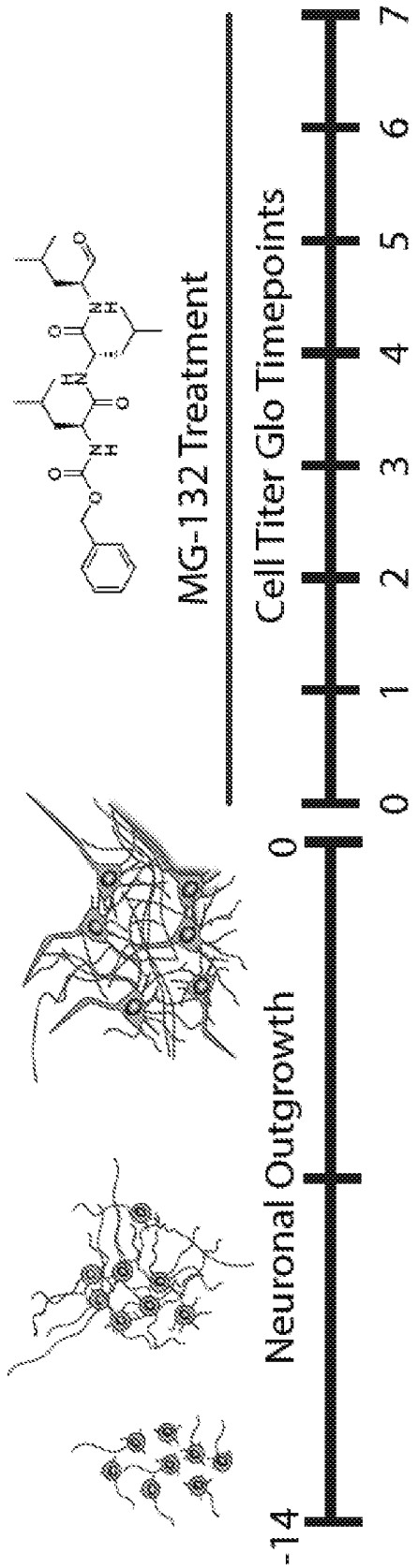

Neuronal Outgrowth
-14
0
MG-132 Treatment
Cell Titer Glo Timepoints
0
1
2
3
4
5
6
7

FIG. 14C

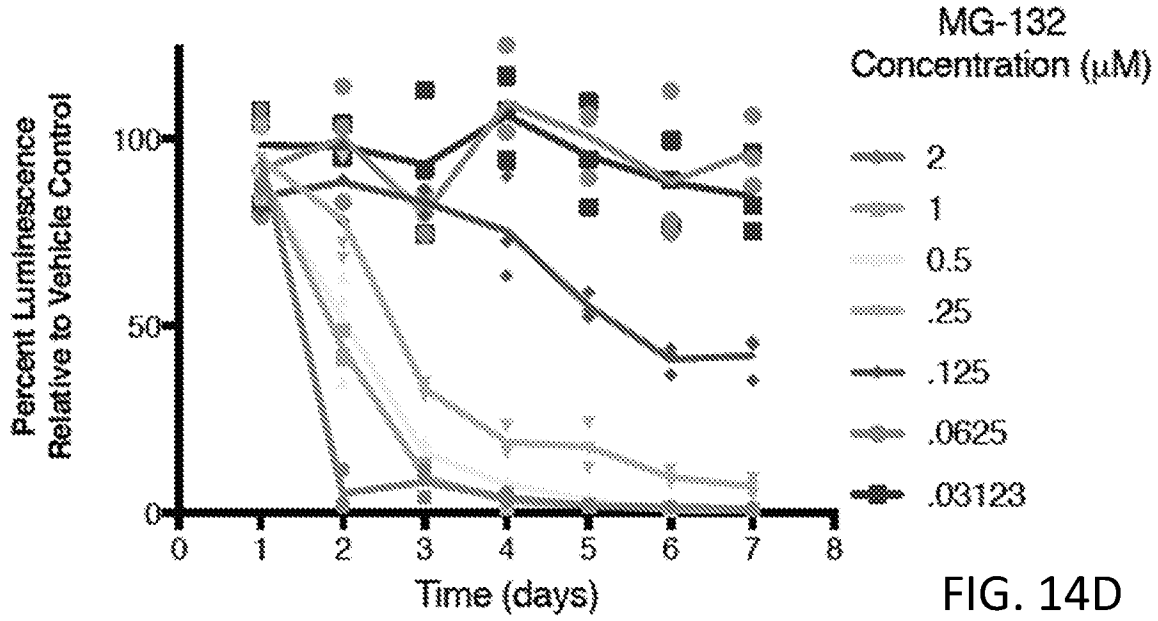


FIG. 14D

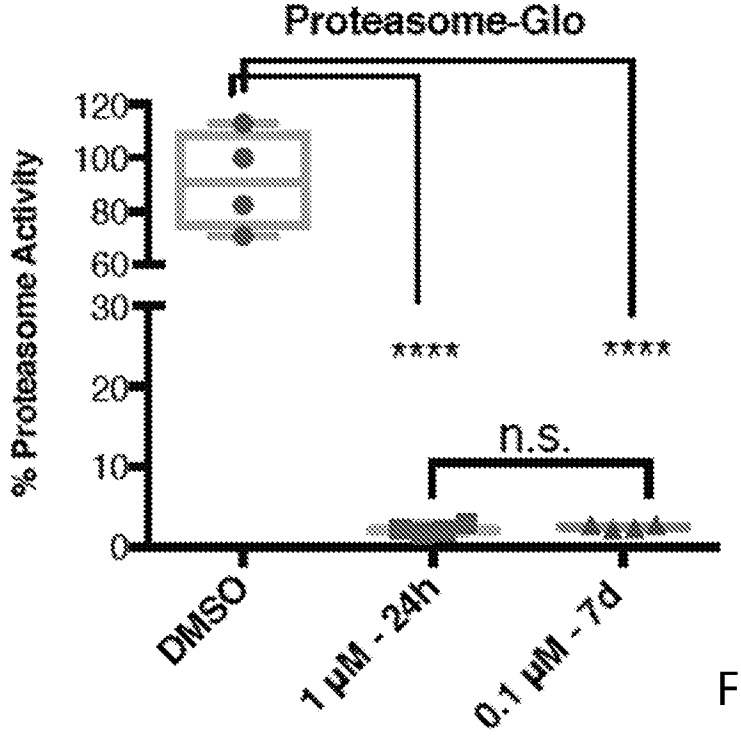


FIG. 14E

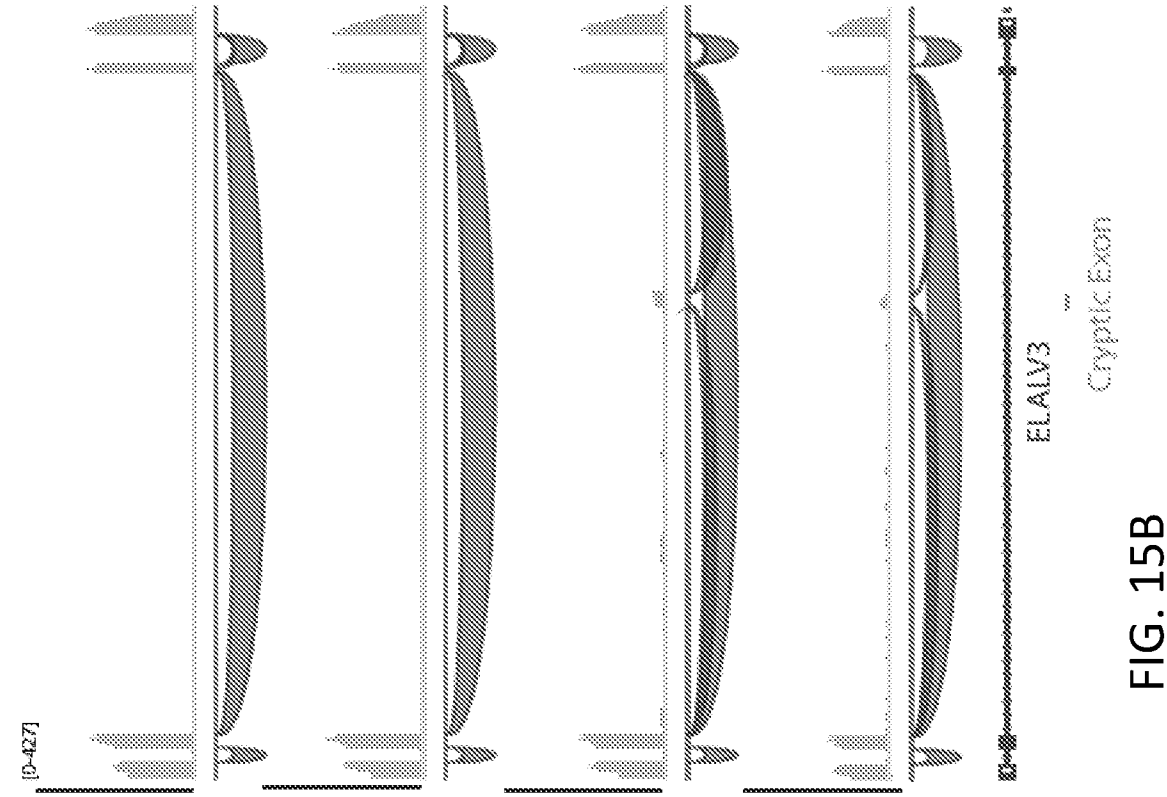


FIG. 15B

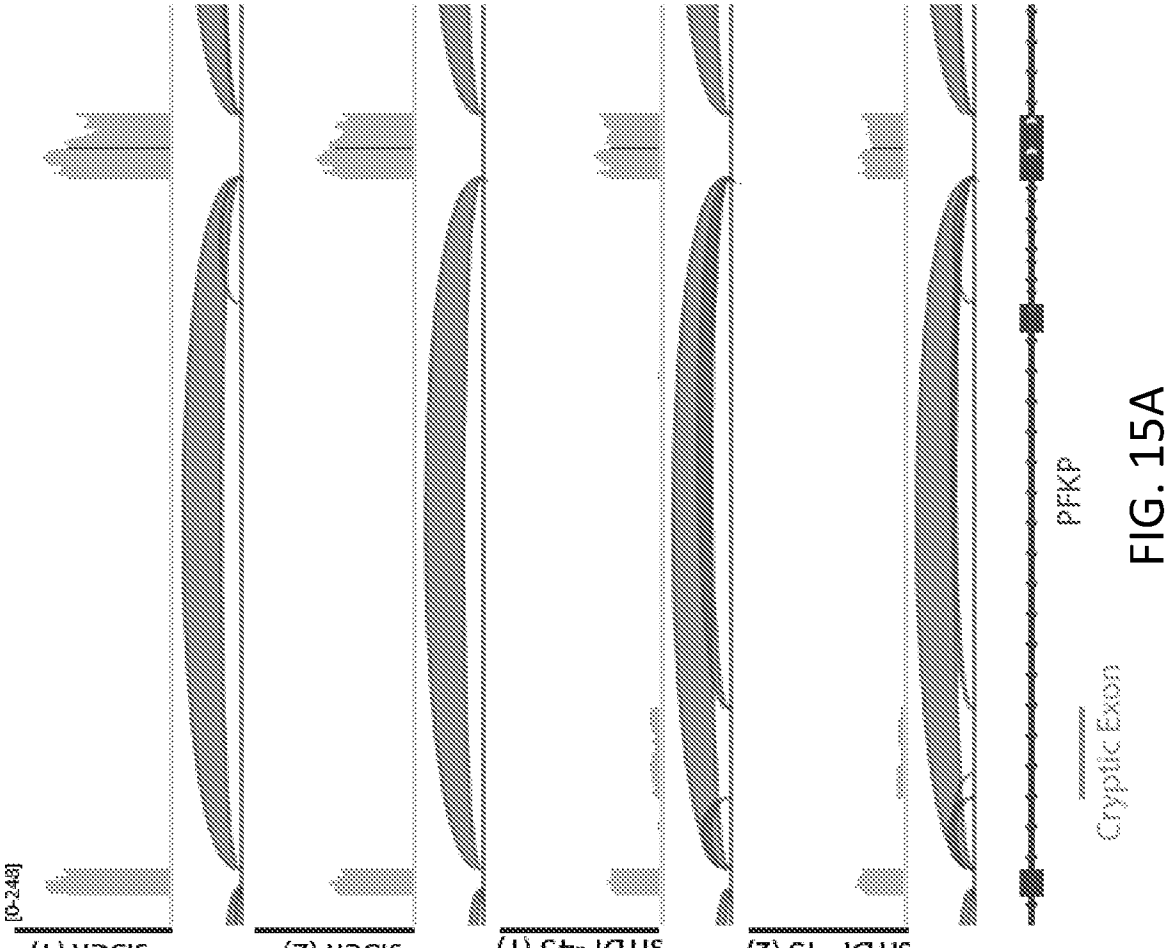


FIG. 15A

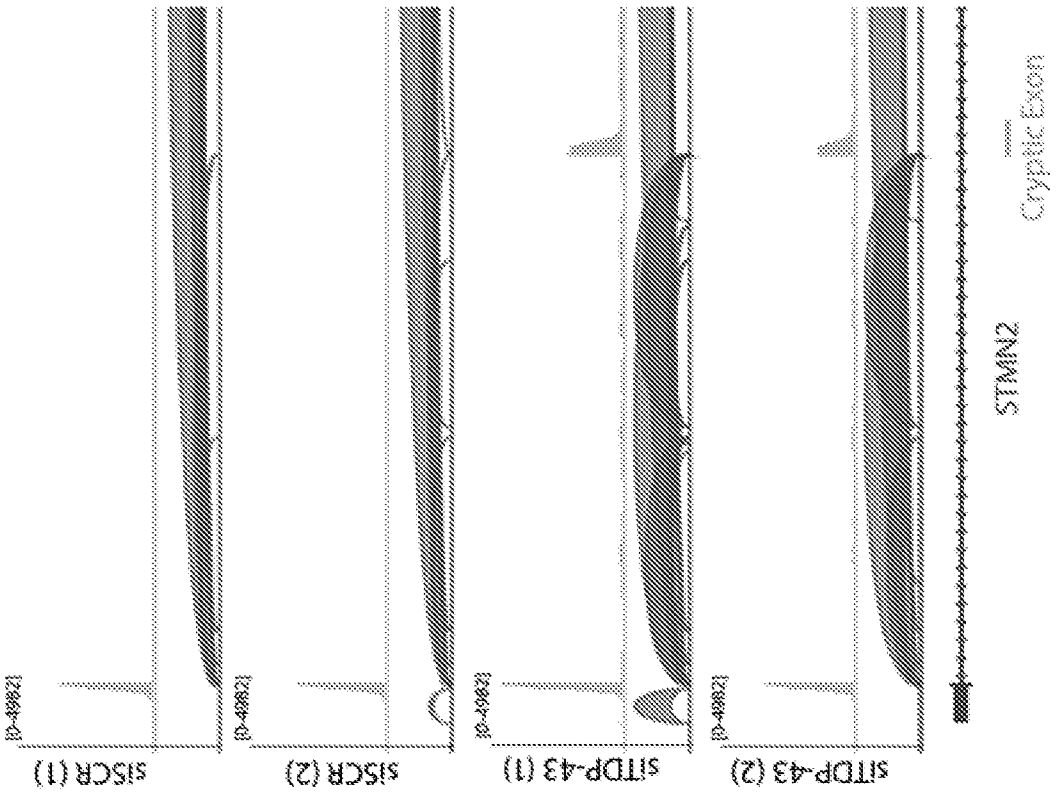


FIG. 15C

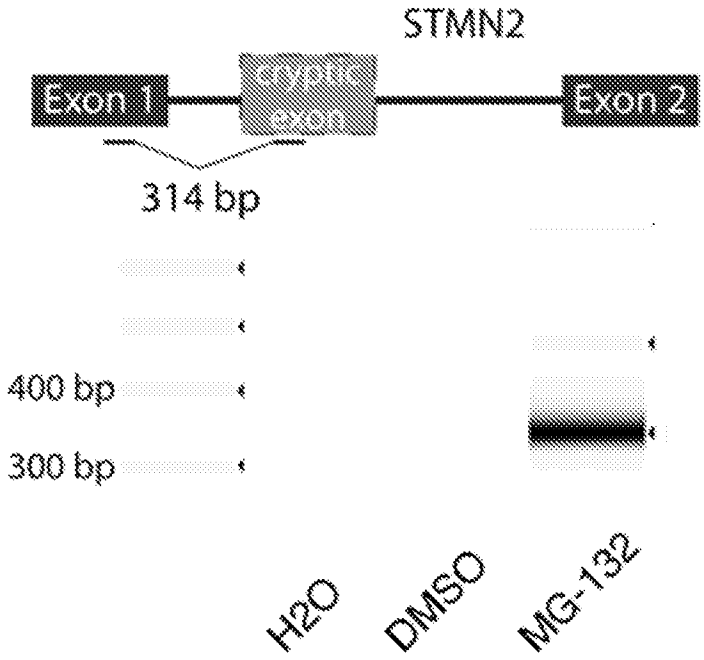


FIG. 15D

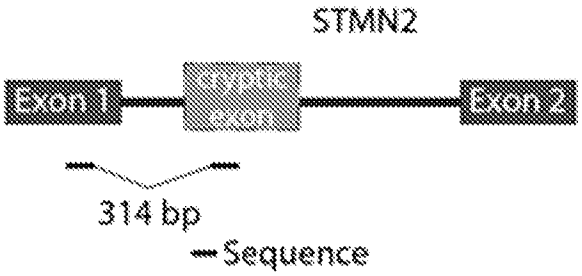
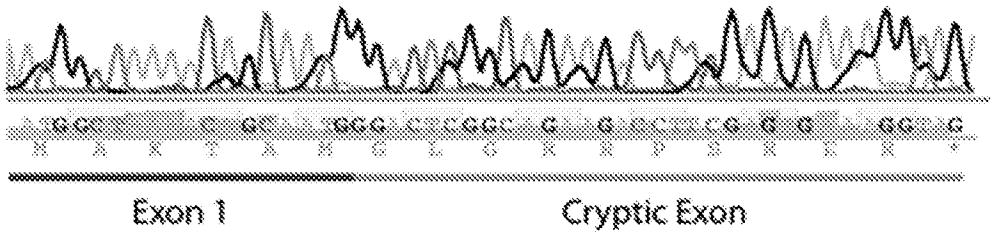


FIG. 15E



SEQ ID NO: 9
SEQ ID NO: 10

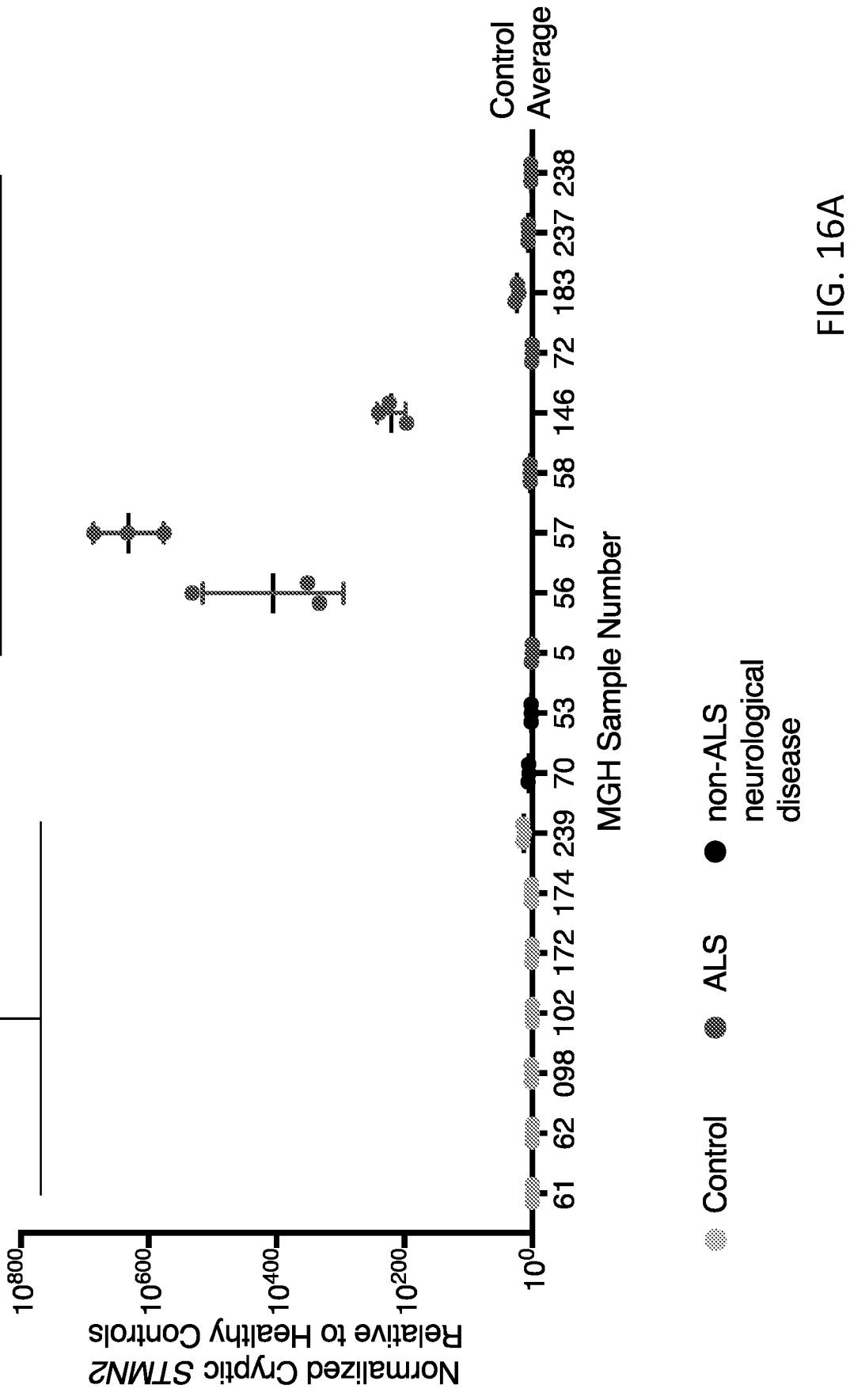

t-test = 0.0016
Normalized Cryptic STMN2
Relative to Healthy Controls
10^800
10^600
10^400
10^200
10^0
61 62 098 102 172 174 239 70 53 5 56 57 58 146 72 183 237 238
Control Average
MGH Sample Number
Control
ALS
non-ALS neurological disease

FIG. 16A

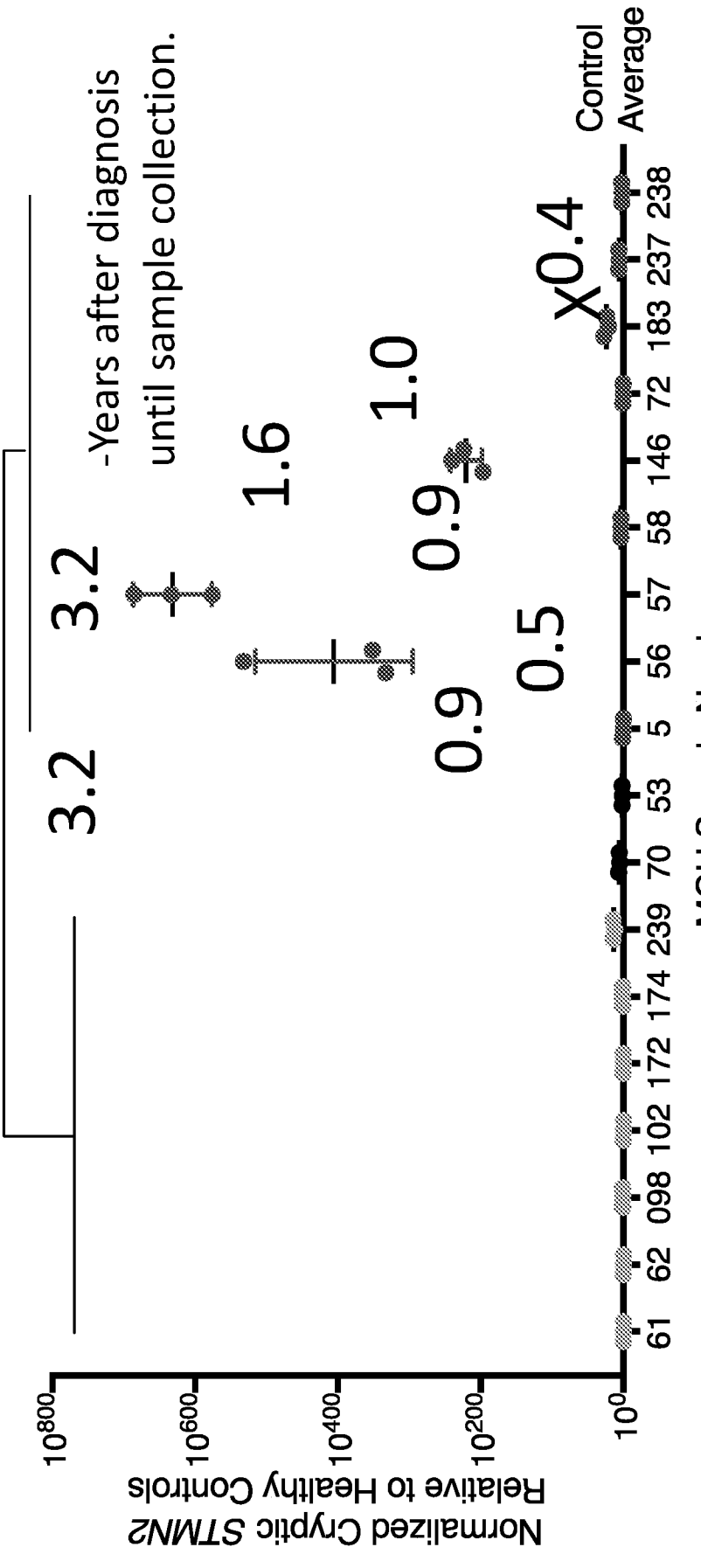

t-test = 0.0016
3.2
3.2
-Years after diagnosis
until sample collection.
1.6
1.0
0.9
0.9
0.5
x0.4
Control
Average
Normalized Cryptic STMN2
Relative to Healthy Controls
10^800
10^600
10^400
10^200
10^0
61 62 098 102 172 174 239 70 53 5 56 57 58 146 72 183 237 238
MGH Sample Number
Control
ALS
non-ALS neurological disease

FIG. 16B

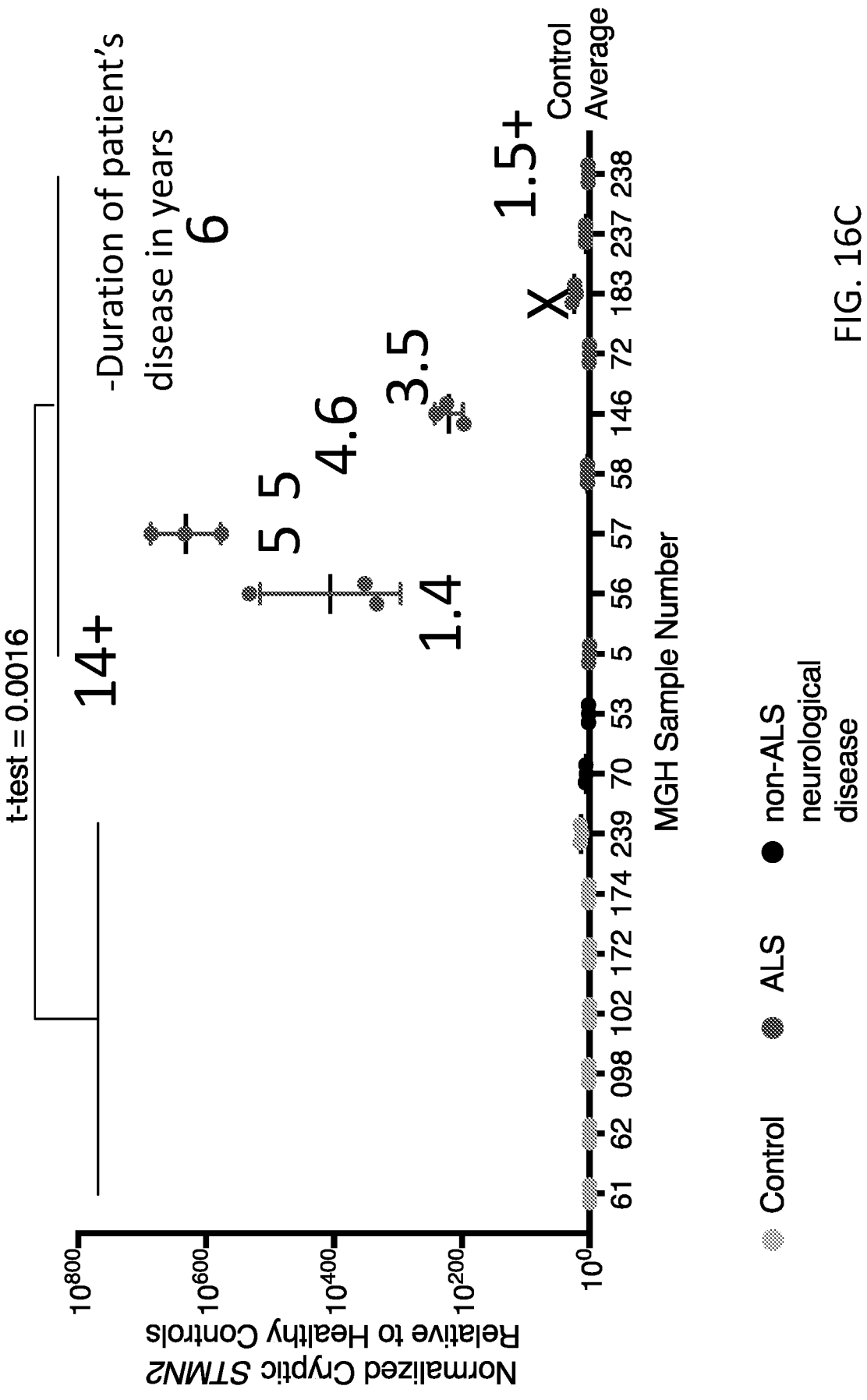

Normalized Cryptic STMN2
Relative to Healthy Controls
10^800
10^600
10^400
10^200
10^0
t-test = 0.0016
14+
-Duration of patient's
disease in years
6
5
5
4.6
3.5
1.4
1.5+
Control
Average
61 62 098 102 172 174 239 70 53 5 56 57 58 146 72 183 237 238
MGH Sample Number
Control
ALS
non-ALS
neurological
disease

FIG. 16C

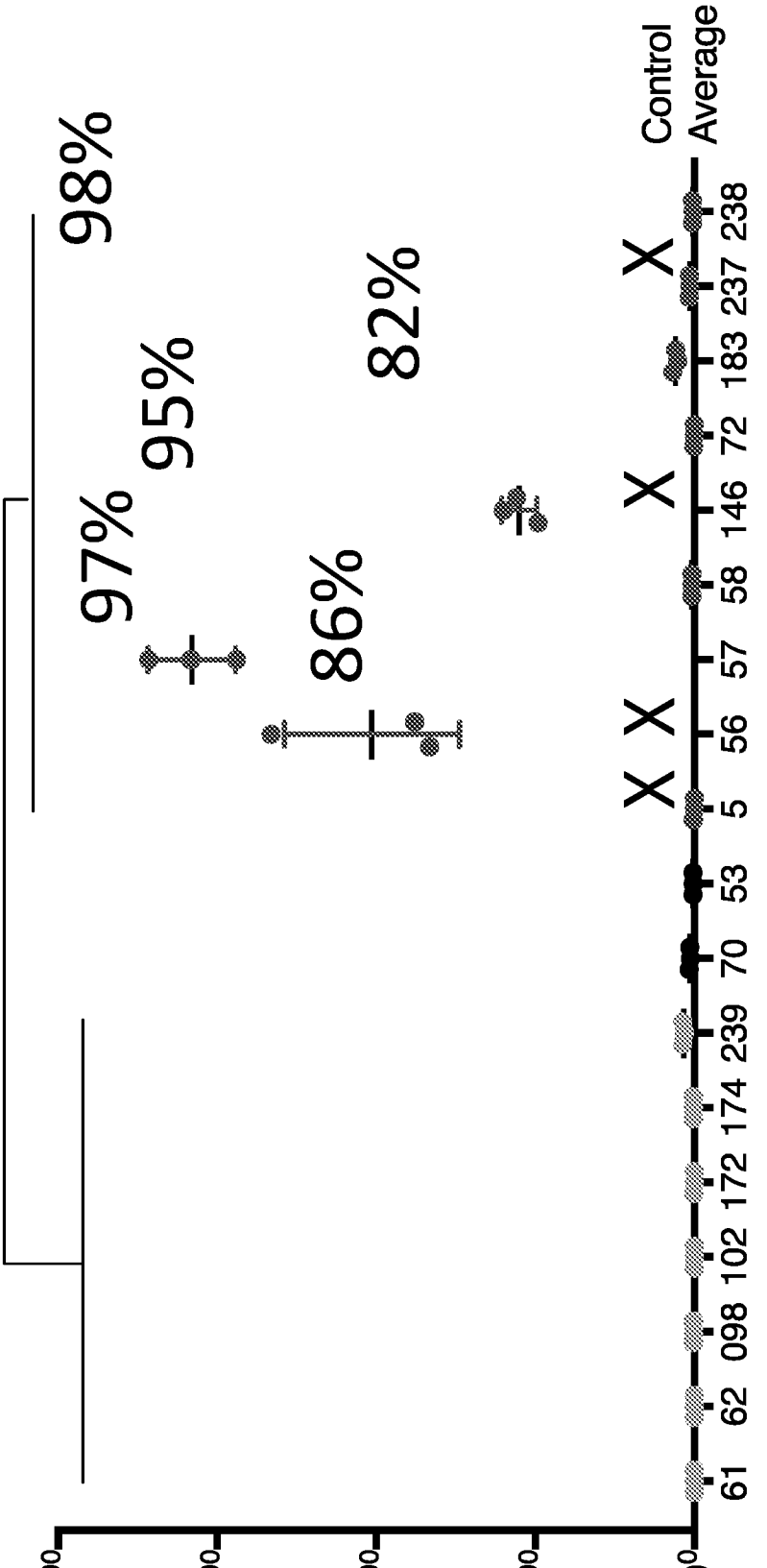

t-test = 0.0016
98%
97%
95%
86%
82%
Control Average
MGH Sample Number
61 62 098 102 172 174 239 70 53 5 56 57 58 146 72 183 237 238
Normalized Cryptic STMN2 Relative to Healthy Controls
10^800
10^600
10^400
10^200
10^0
Control
ALS
non-ALS neurological disease

FIG. 16D

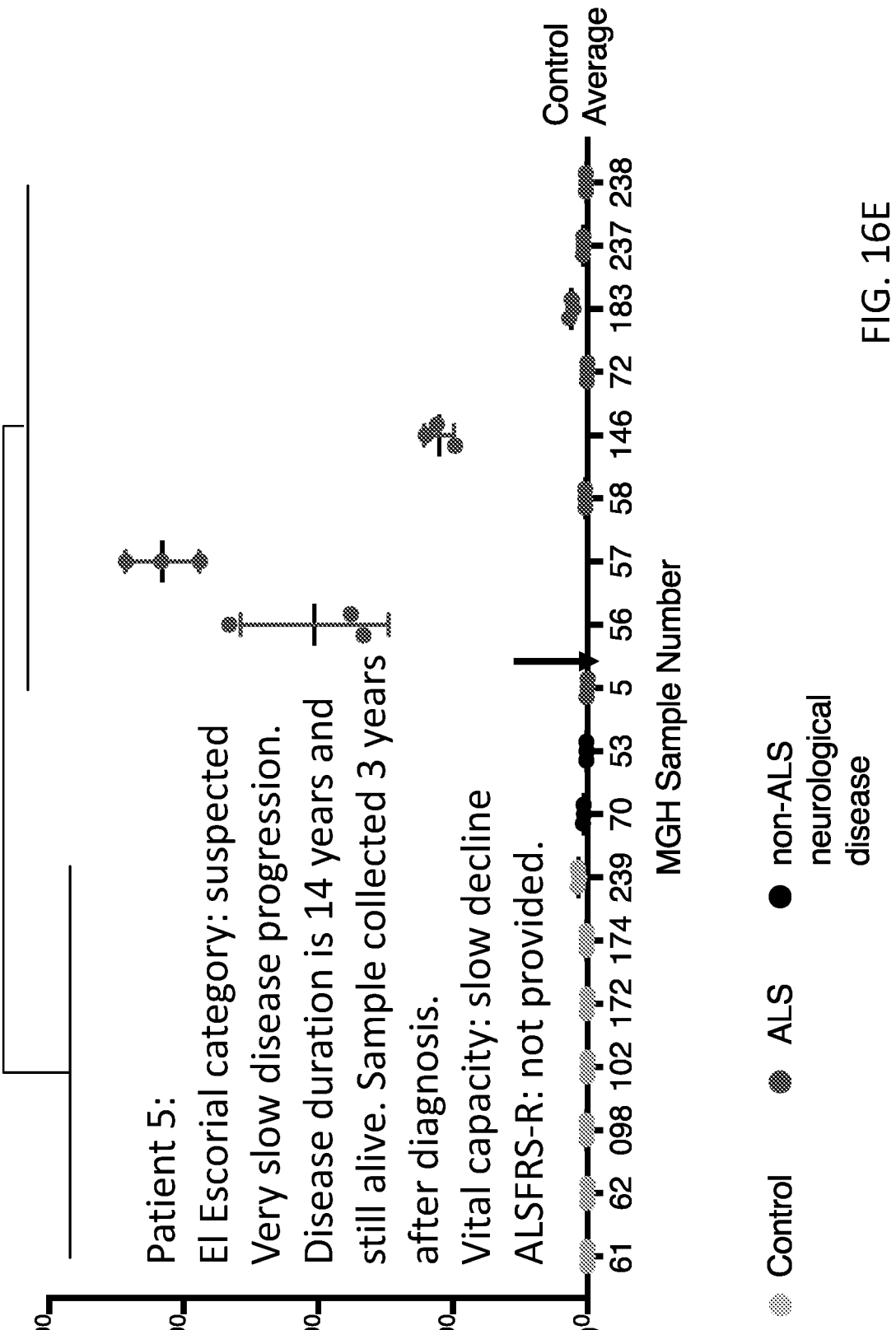

t-test = 0.0016
Patient 5:
El Escorial category: suspected
Very slow disease progression.
Disease duration is 14 years and
still alive. Sample collected 3 years
after diagnosis.
Vital capacity: slow decline
ALSFRS-R: not provided.
Normalized Cryptic STMN2
Relative to Healthy Controls
10^800
10^600
10^400
10^200
10^0
61 62 098 102 172 174 239 70 53 5 56 57 58 146 72 183 237 238
Control Average
MGH Sample Number
Control
ALS
non-ALS neurological disease

FIG. 16E

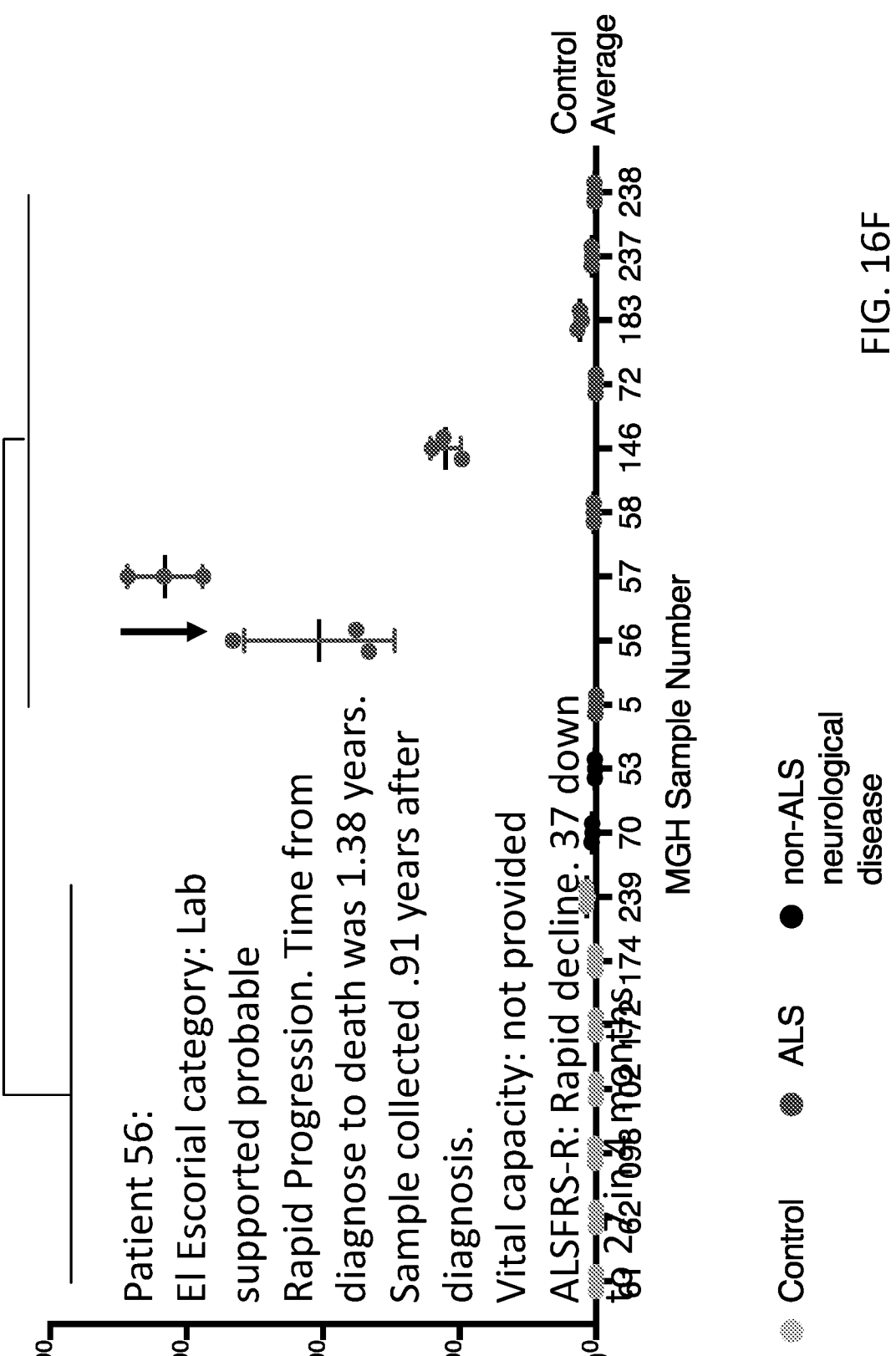

t-test = 0.0016
Patient 56:
El Escorial category: Lab supported probable
Rapid Progression. Time from diagnose to death was 1.38 years.
Sample collected .91 years after diagnosis.
Vital capacity: not provided
ALSFRS-R: Rapid decline. 37 down to 27 in 4 months
Normalized Cryptic STMN2 Relative to Healthy Controls
10^{800}
10^{600}
10^{400}
10^{200}
10^{0}
MGH Sample Number
Control Average
Control
ALS
non-ALS neurological disease

FIG. 16F

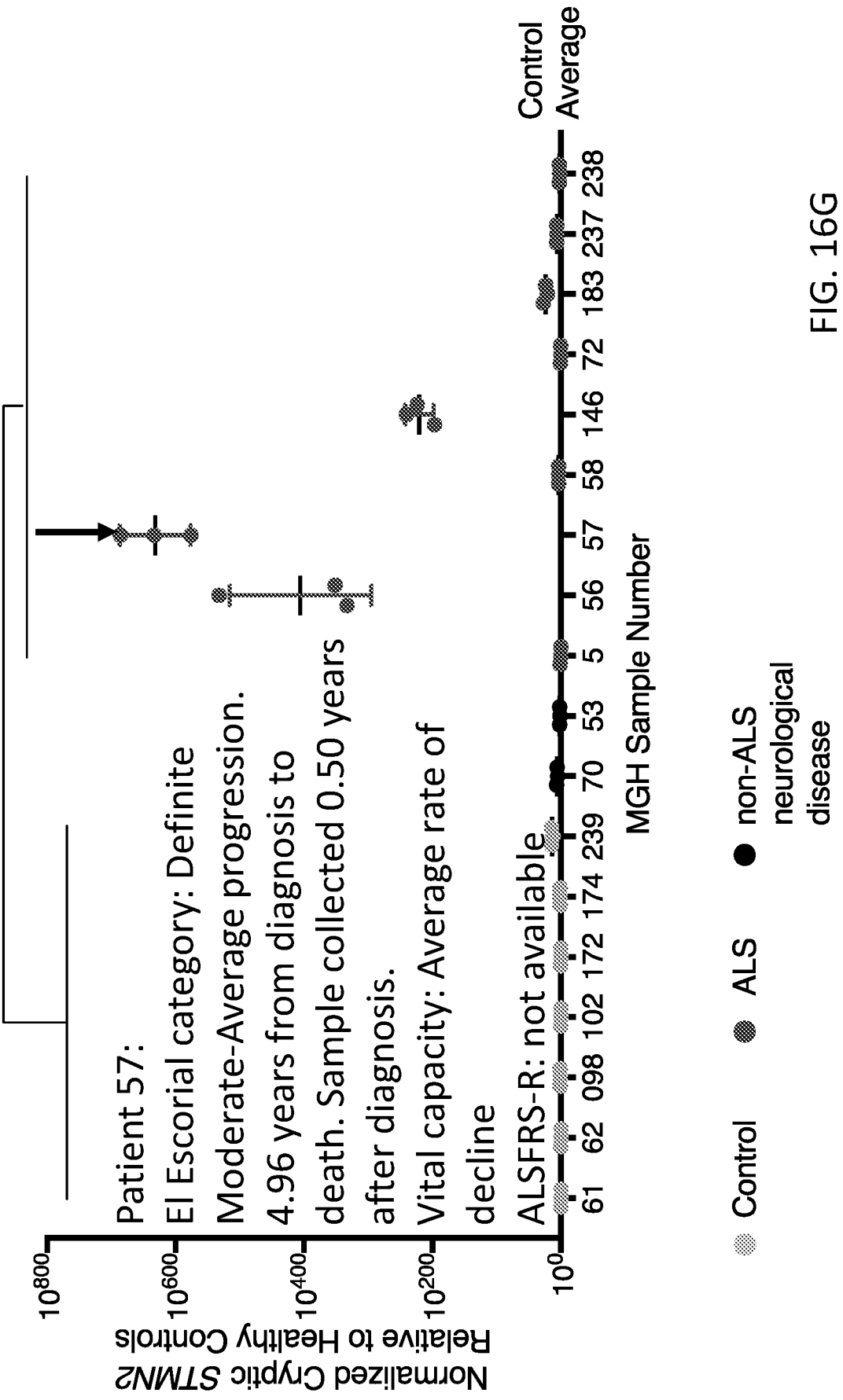

t-test = 0.0016
Patient 57:
El Escorial category: Definite
Moderate-Average progression.
4.96 years from diagnosis to
death. Sample collected 0.50 years
after diagnosis.
Vital capacity: Average rate of
decline
ALSFRS-R: not available
Normalized Cryptic STMN2
Relative to Healthy Controls
10^800
10^600
10^400
10^200
10^0
61 62 098 102 172 174 239 70 53 5 56 57 58 146 72 183 237 238
Control Average
MGH Sample Number
Control
ALS
non-ALS neurological disease

FIG. 16G

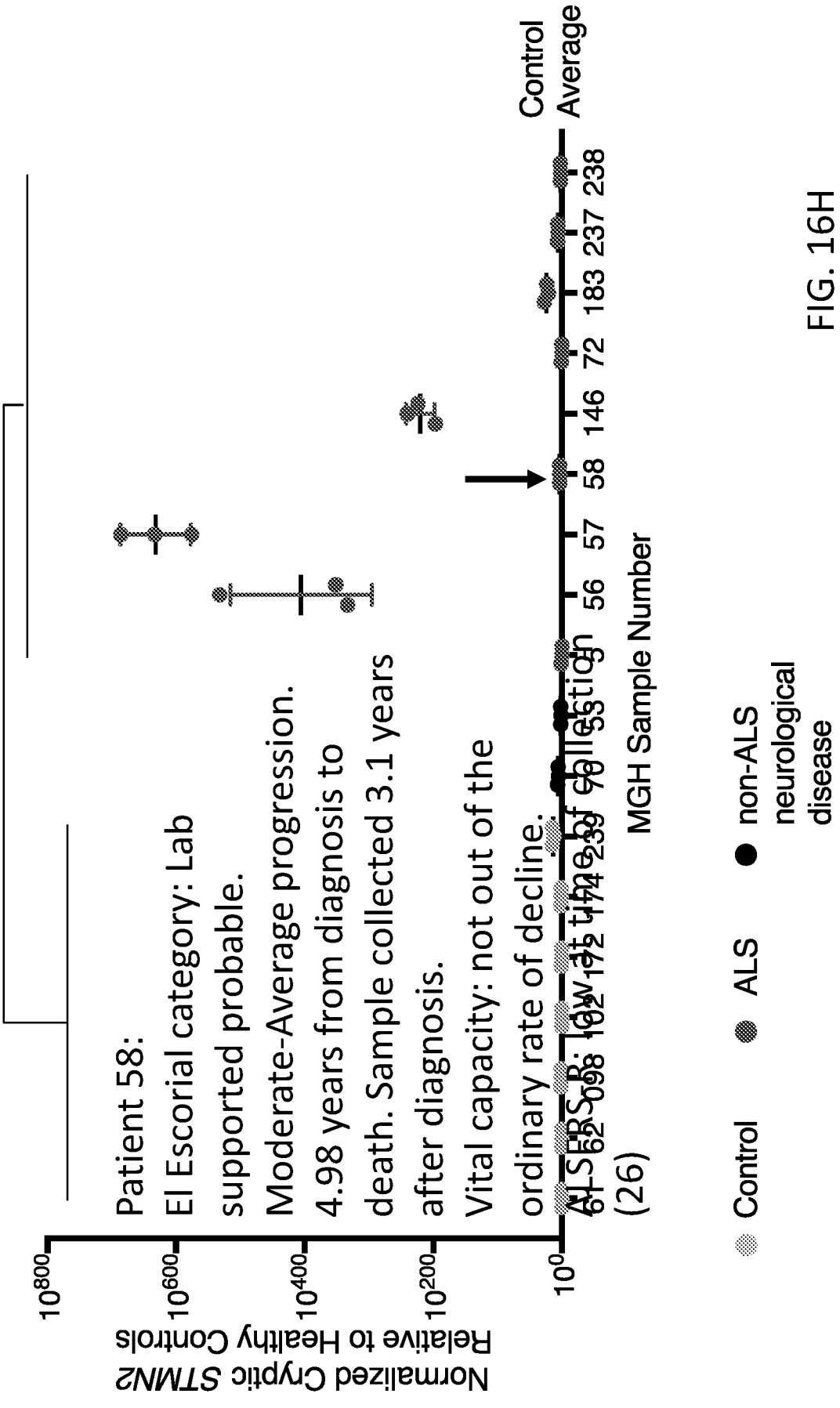

Normalized Cryptic STMN2 Relative to Healthy Controls
10^800
10^600
10^400
10^200
10^0
t-test = 0.0016
Patient 58:
El Escorial category: Lab supported probable.
Moderate-Average progression.
4.98 years from diagnosis to death. Sample collected 3.1 years after diagnosis.
Vital capacity: not out of the ordinary rate of decline.
ALSFRS-R: 40
Time of collection
61 62 98 102 172 174 239 (26)
MGH Sample Number
Control Average
56 57 58 146 72 183 237 238
Control
ALS
non-ALS neurological disease

FIG. 16H

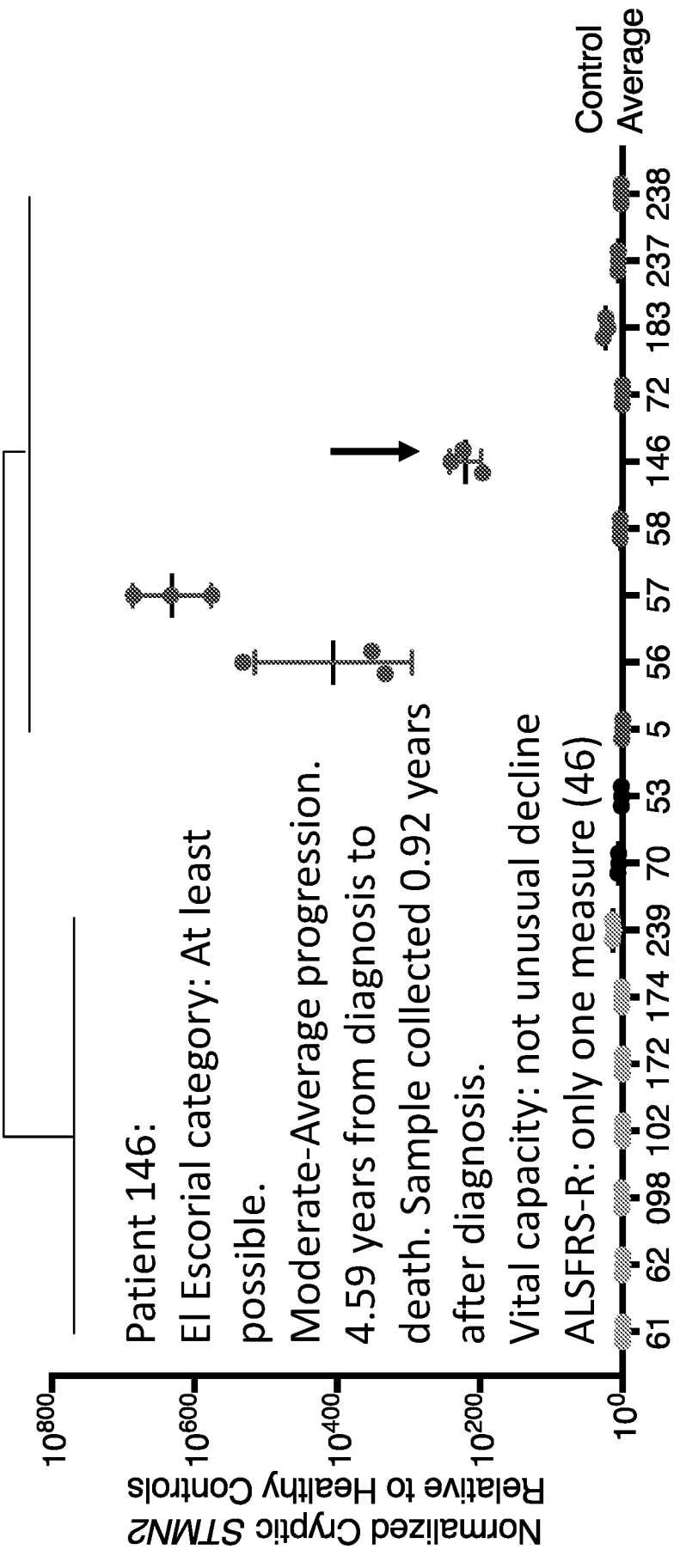

t-test = 0.0016
Patient 146:
El Escorial category: At least possible.
Moderate-Average progression.
4.59 years from diagnosis to death. Sample collected 0.92 years after diagnosis.
Vital capacity: not unusual decline
ALSFRS-R: only one measure (46)
Normalized Cryptic STMN2 Relative to Healthy Controls
10800
10600
10400
10200
100
61 62 098 102 172 174 239 70 53 5 56 57 58 146 72 183 237 238
Control Average
MGH Sample Number
Control
ALS
non-ALS neurological disease

FIG. 16I

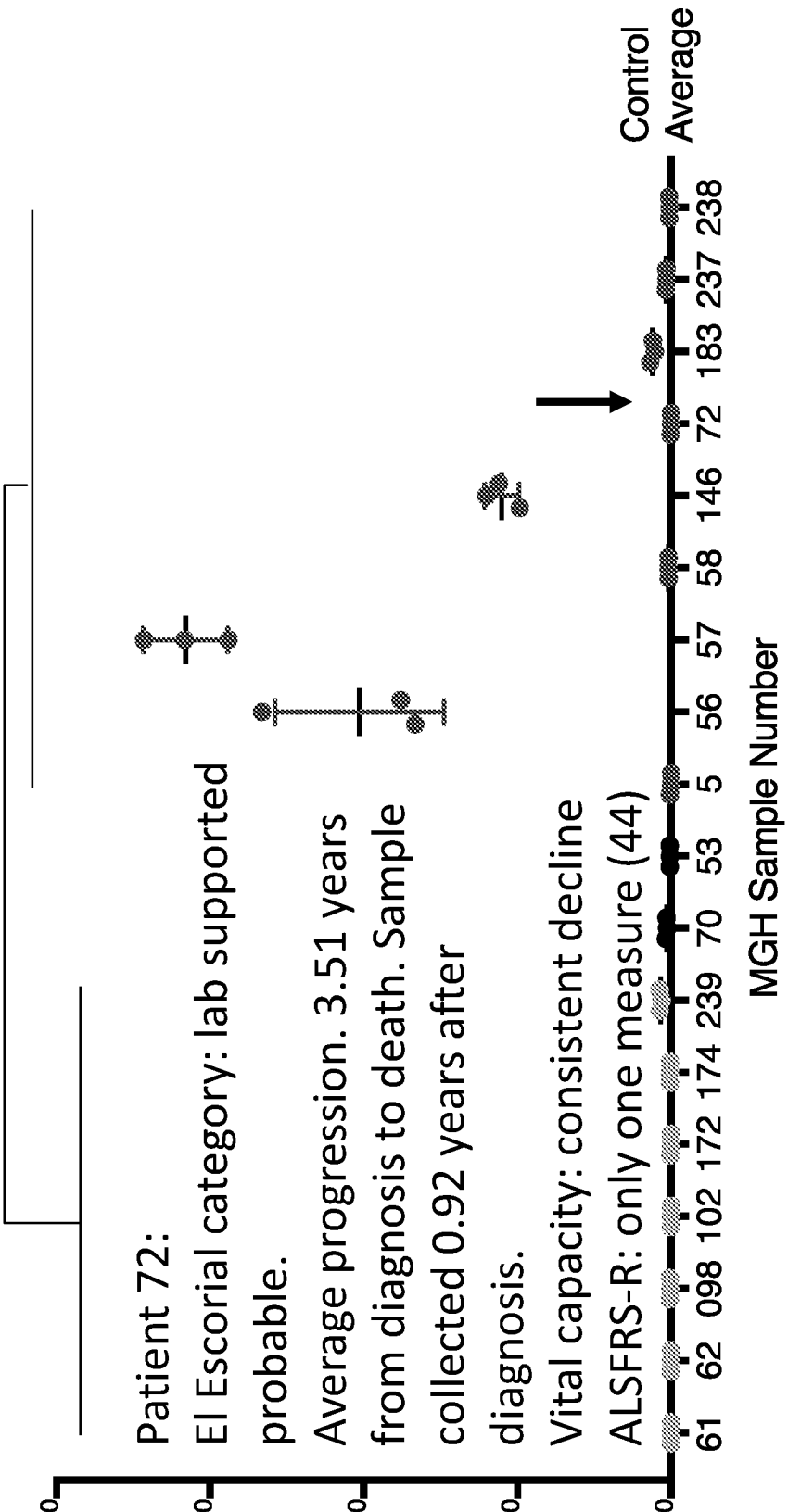

t-test = 0.0016
Patient 72:
El Escorial category: lab supported probable.
Average progression. 3.51 years from diagnosis to death. Sample collected 0.92 years after diagnosis.
Vital capacity: consistent decline
ALSFRS-R: only one measure (44)
Normalized Cryptic STMN2 Relative to Healthy Controls
10^{800}
10^{600}
10^{400}
10^{200}
10^{0}
61 62 098 102 172 174 239 70 53 5 56 57 58 146 72 183 237 238
Control Average
MGH Sample Number
Control
ALS
non-ALS neurological disease

FIG. 16J

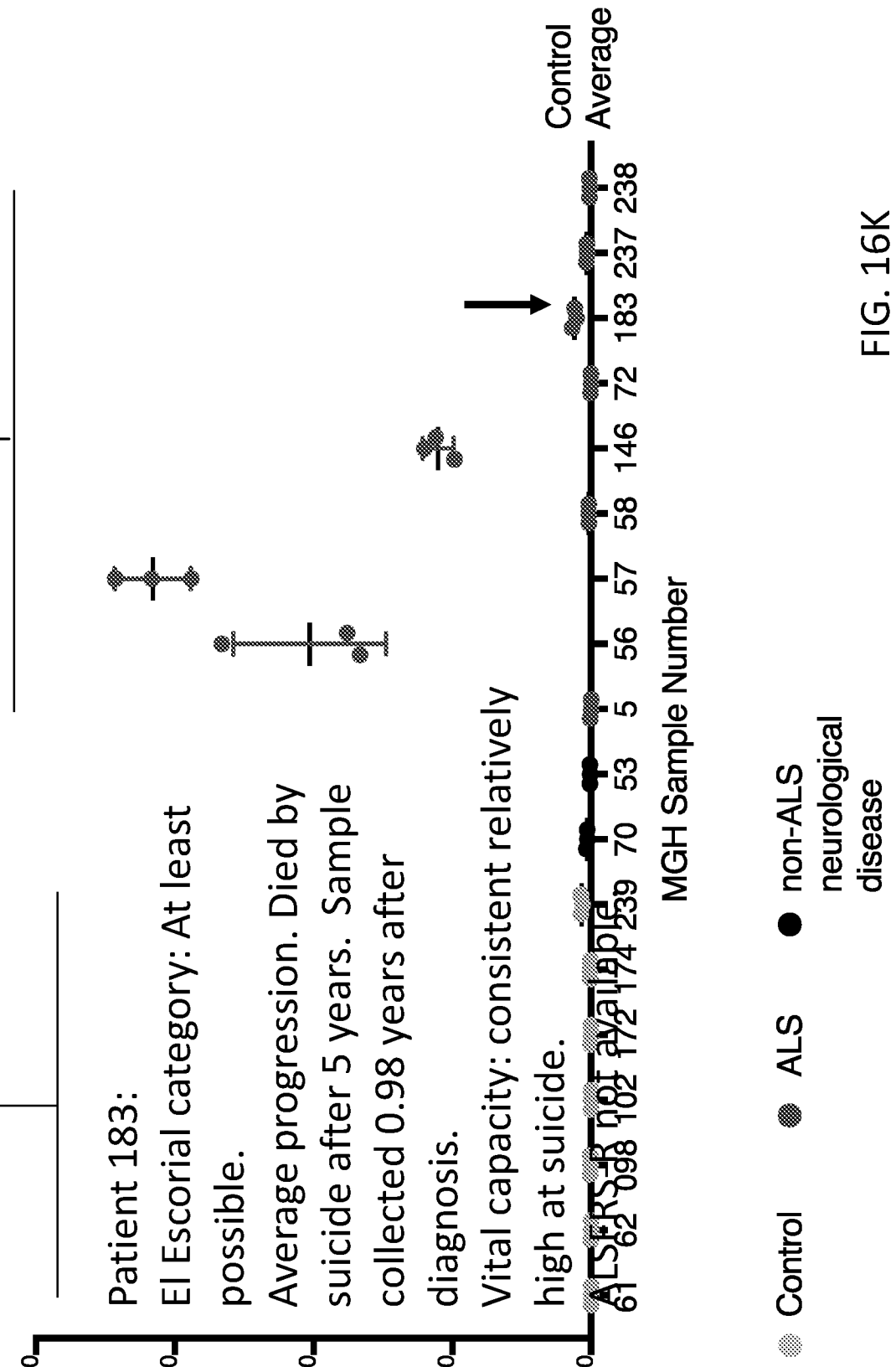

Normalized Cryptic STMN2 Relative to Healthy Controls
10^800
10^600
10^400
10^200
10^0
t-test = 0.0016
Patient 183:
El Escorial category: At least possible.
Average progression. Died by suicide after 5 years. Sample collected 0.98 years after diagnosis.
Vital capacity: consistent relatively high at suicide.
ALS-FRS-R not available
61 62 98 102 172 174 239 70 53 5 56 57 58 146 72 183 237 238
Control Average
MGH Sample Number
Control
ALS
non-ALS neurological disease

FIG. 16K

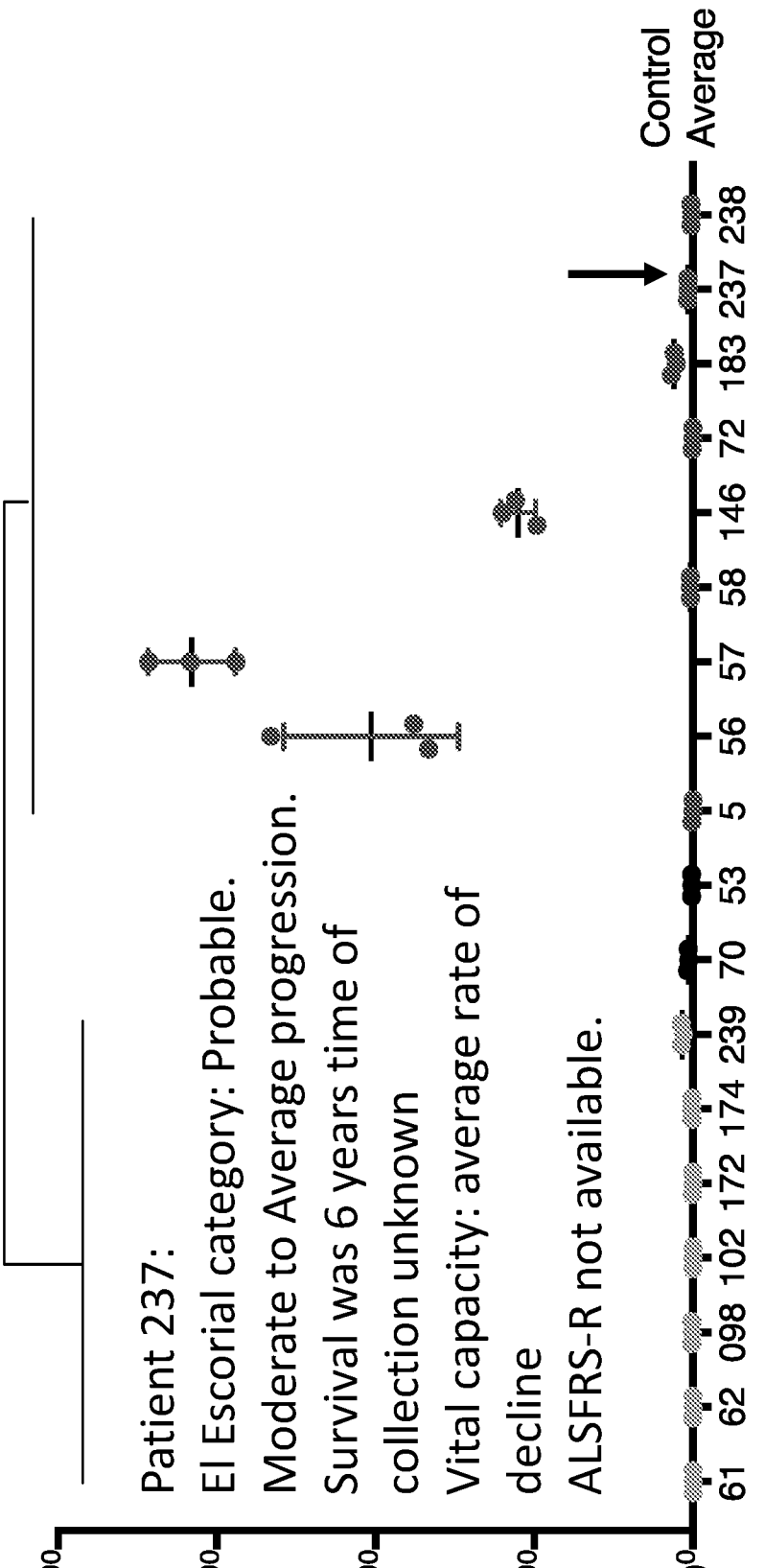

Normalized Cryptic STMN2 Relative to Healthy Controls
10^800
10^600
10^400
10^200
10^0
t-test = 0.0016
Patient 237:
El Escorial category: Probable.
Moderate to Average progression.
Survival was 6 years time of collection unknown
Vital capacity: average rate of decline
ALSFRS-R not available.
61 62 098 102 172 174 239 70 53 5 56 57 58 146 72 183 237 238
Control Average
MGH Sample Number
Control
ALS
non-ALS neurological disease

FIG. 16L

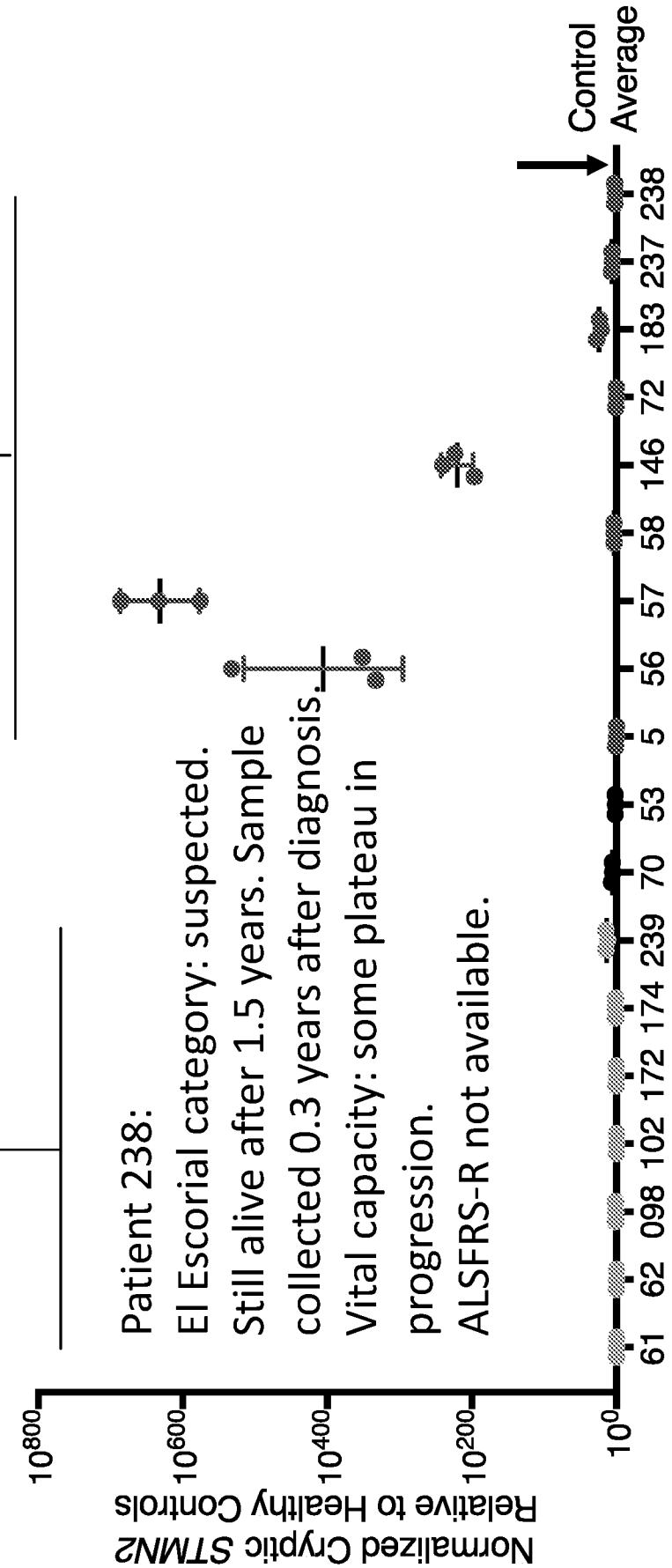

t-test = 0.0016
Patient 238:
El Escorial category: suspected.
Still alive after 1.5 years. Sample collected 0.3 years after diagnosis.
Vital capacity: some plateau in progression.
ALSFRS-R not available.
Normalized Cryptic STMN2 Relative to Healthy Controls
10^800
10^600
10^400
10^200
10^0
61 62 098 102 172 174 239 70 53 5 56 57 58 146 72 183 237 238
MGH Sample Number
Control Average
Control
ALS
non-ALS neurological disease
ALSFRS-R at time of sample collection:

FIG. 16M

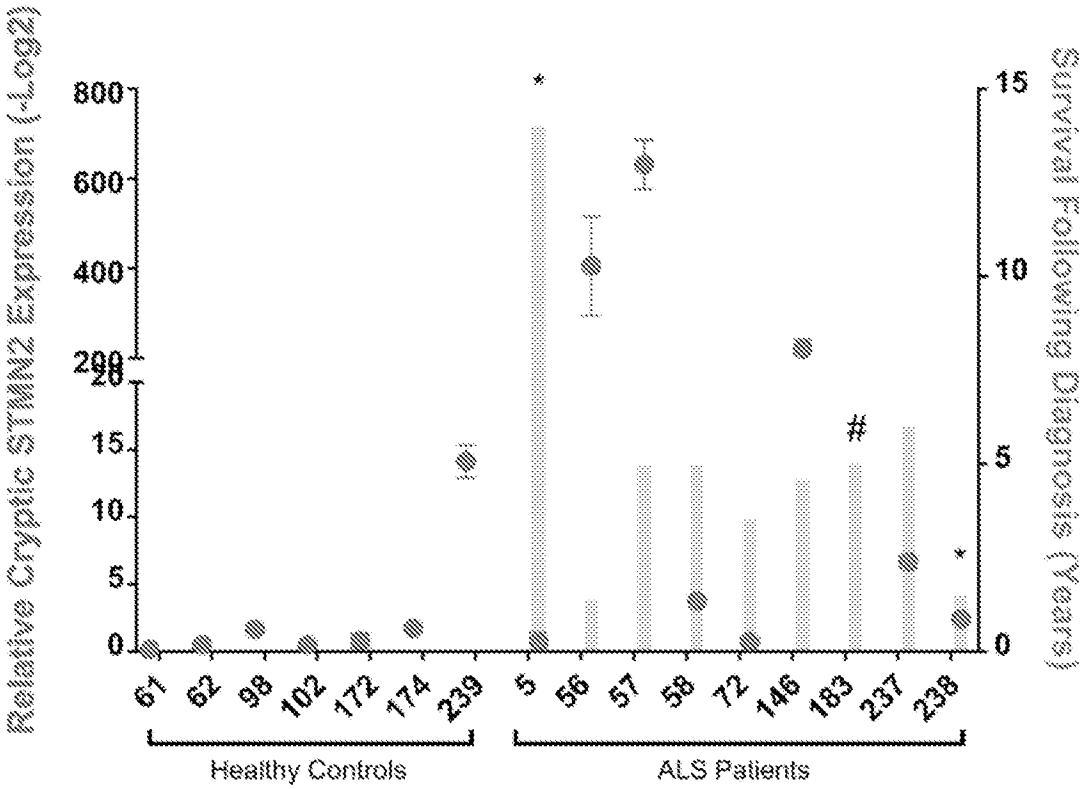


FIG. 16N

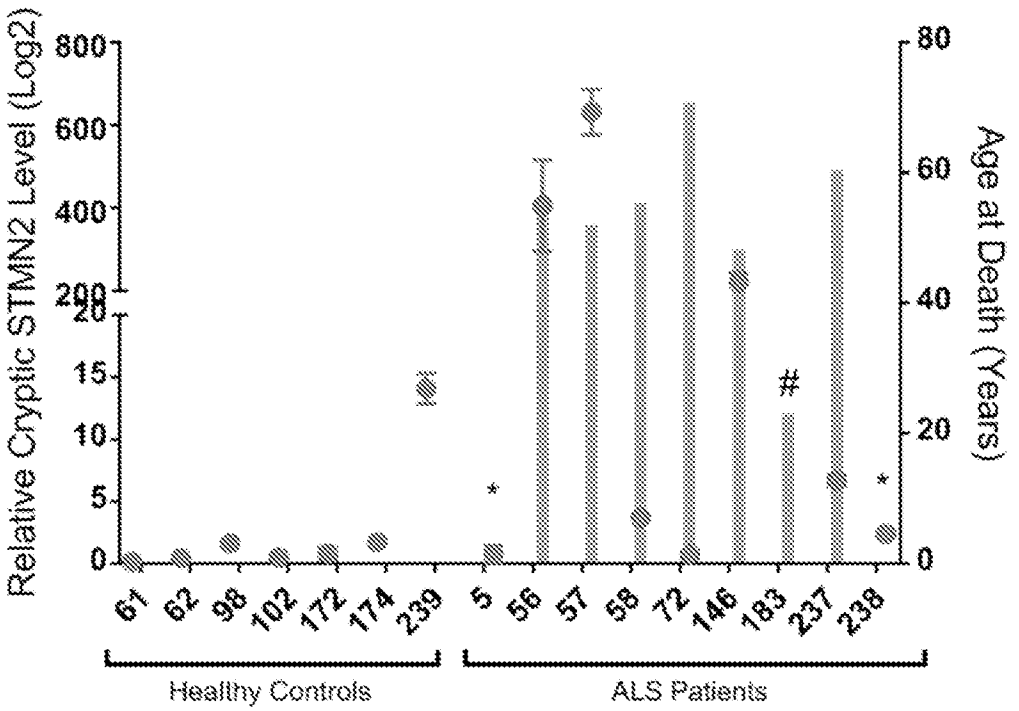
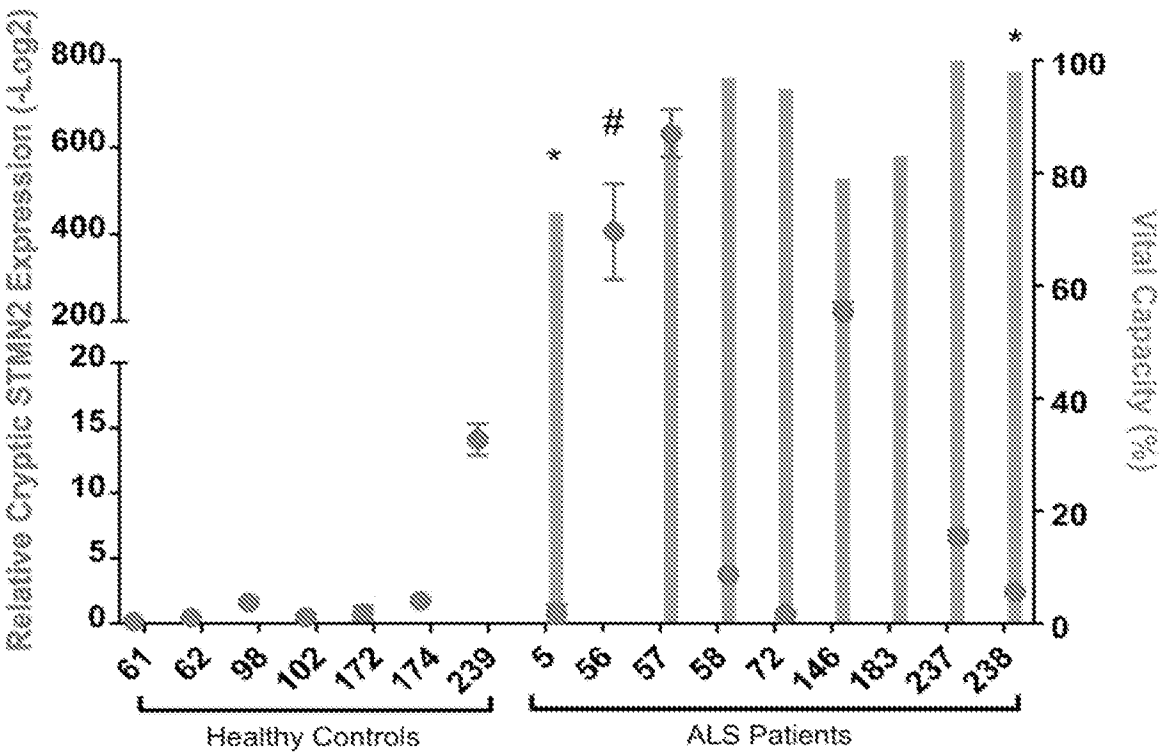


FIG. 16O

* Patient is alive
# Data not available



* Patient is alive
# Data not available

FIG. 16P

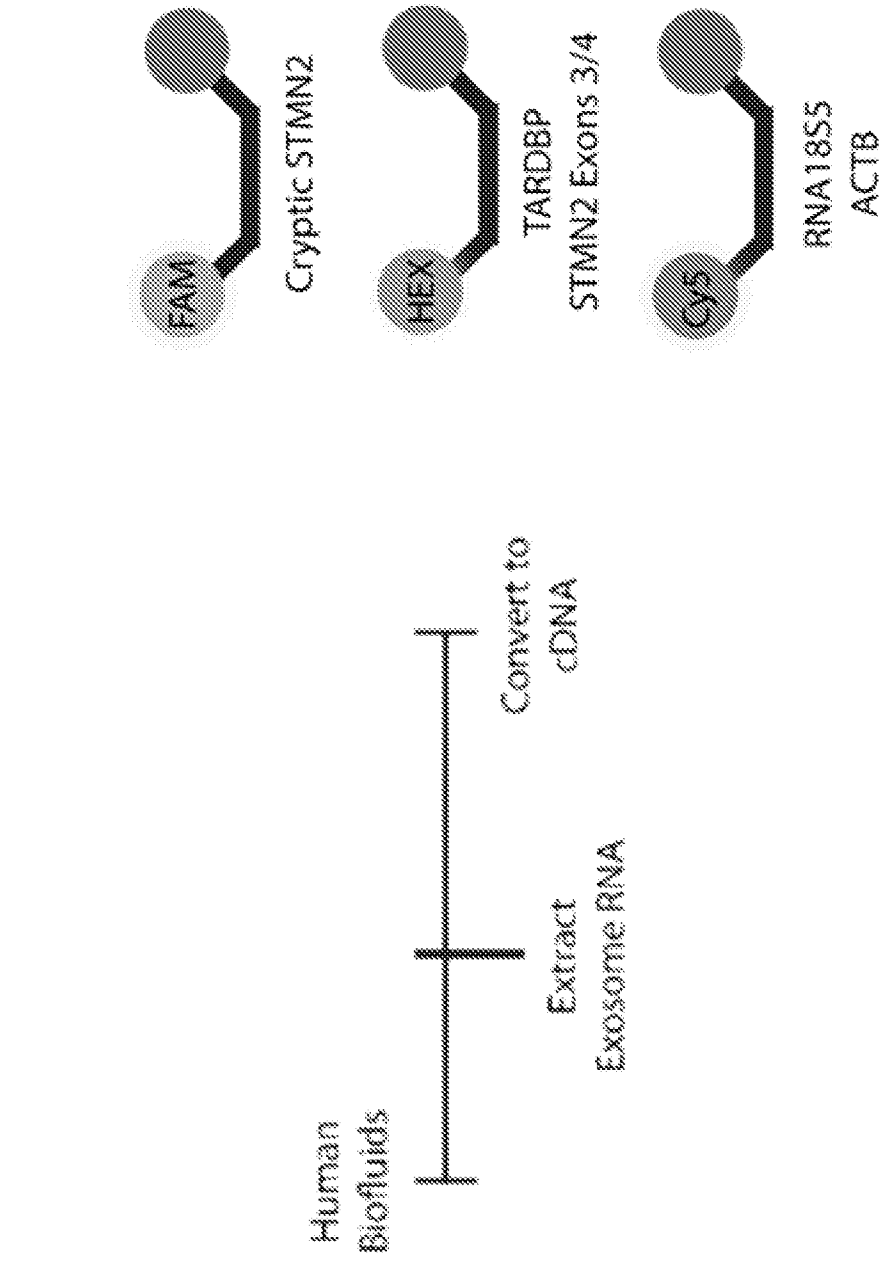

Human Biofluids
Extract Exosome RNA
Convert to cDNA
FAM
Cryptic STMN2
HEX
TARDBP STMN2 Exons 3/4
Cy5
RNA18S5 ACTB

FIG. 17A

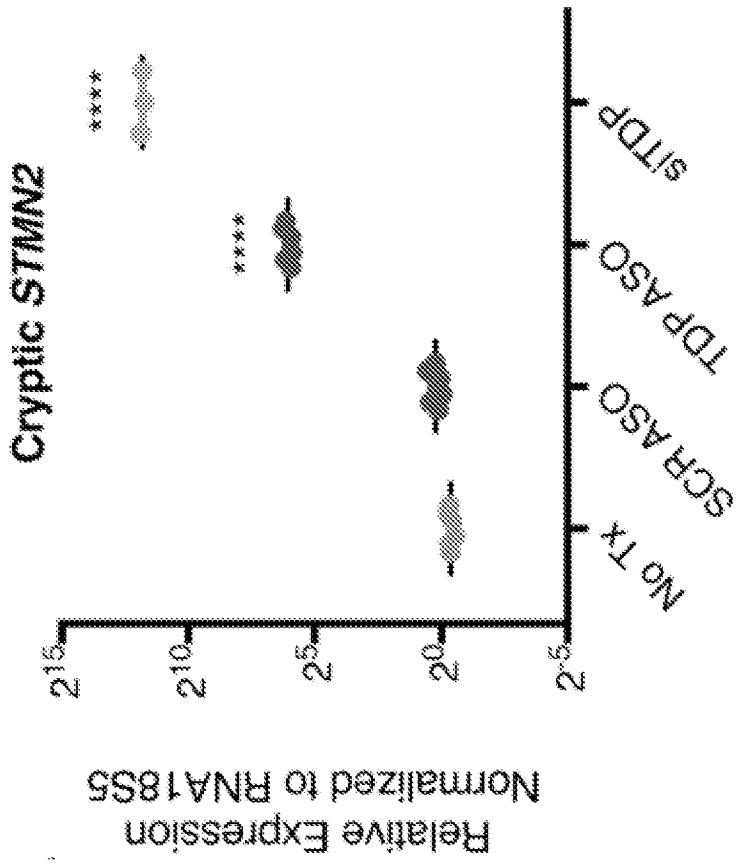

Cryptic STMN2
Relative Expression
Normalized to RNA18S5
2^{15}
2^{10}
2^{5}
2^{0}
2^{-5}
****
****
No Tx
SCR ASO
TDP ASO
siTDP

FIG. 17B

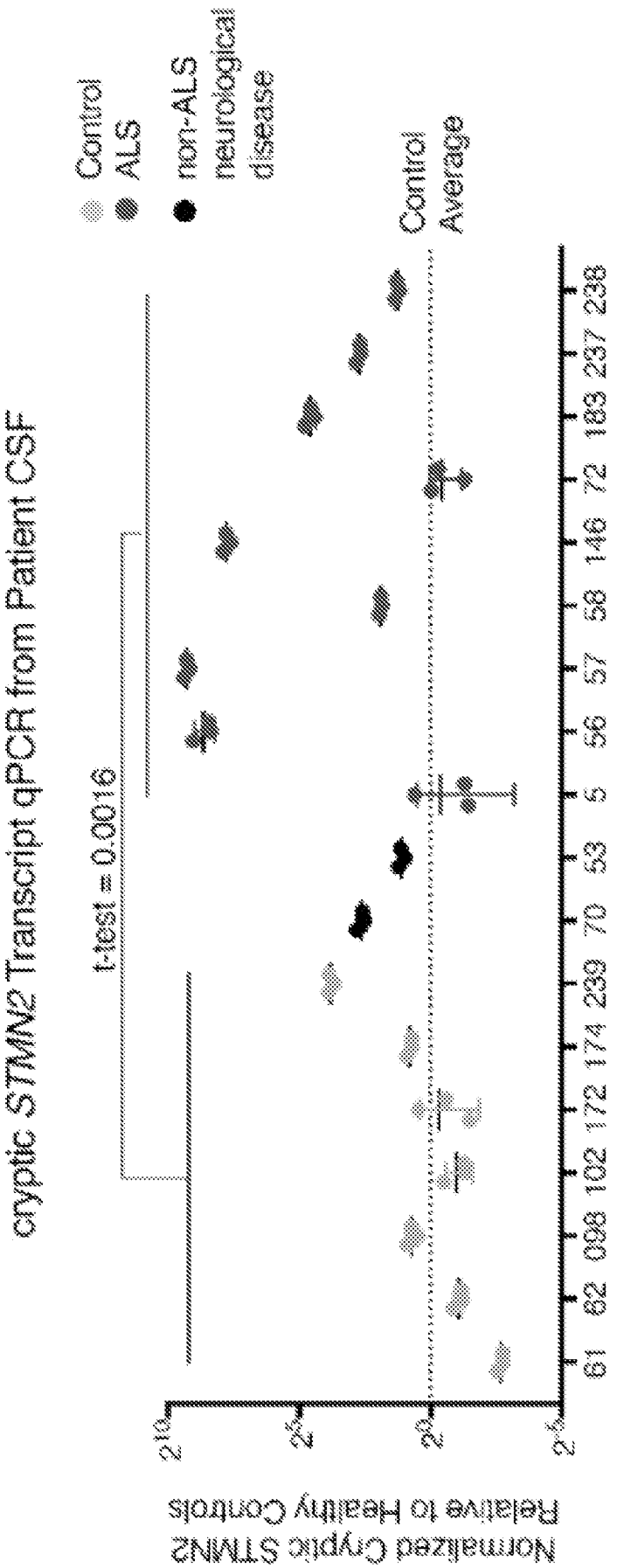

cryptic STMN2 Transcript qPCR from Patient CSF
t-test = 0.0016
Control
ALS
non-ALS neurological disease
Control Average
Normalized Cryptic STMN2 Relative to Healthy Controls
MGH Sample Number
61 82 098 102 172 174 239 70 53 5 56 57 58 146 72 183 237 238

FIG. 17C

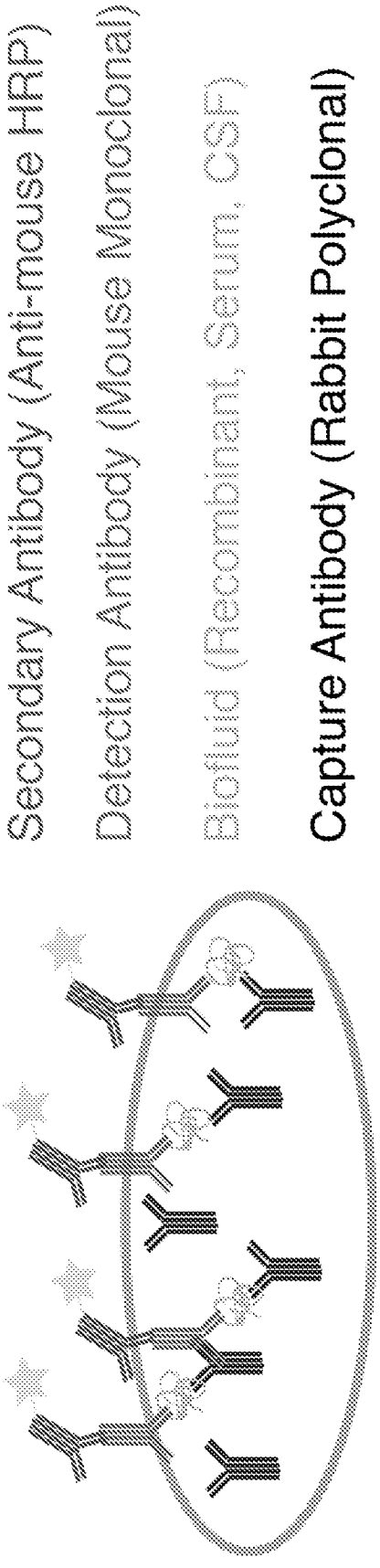

Secondary Antibody (Anti-mouse HRP)
Detection Antibody (Mouse Monoclonal)
Biofluid (Recombinant, Serum, CSF)
Capture Antibody (Rabbit Polyclonal)

FIG. 18A

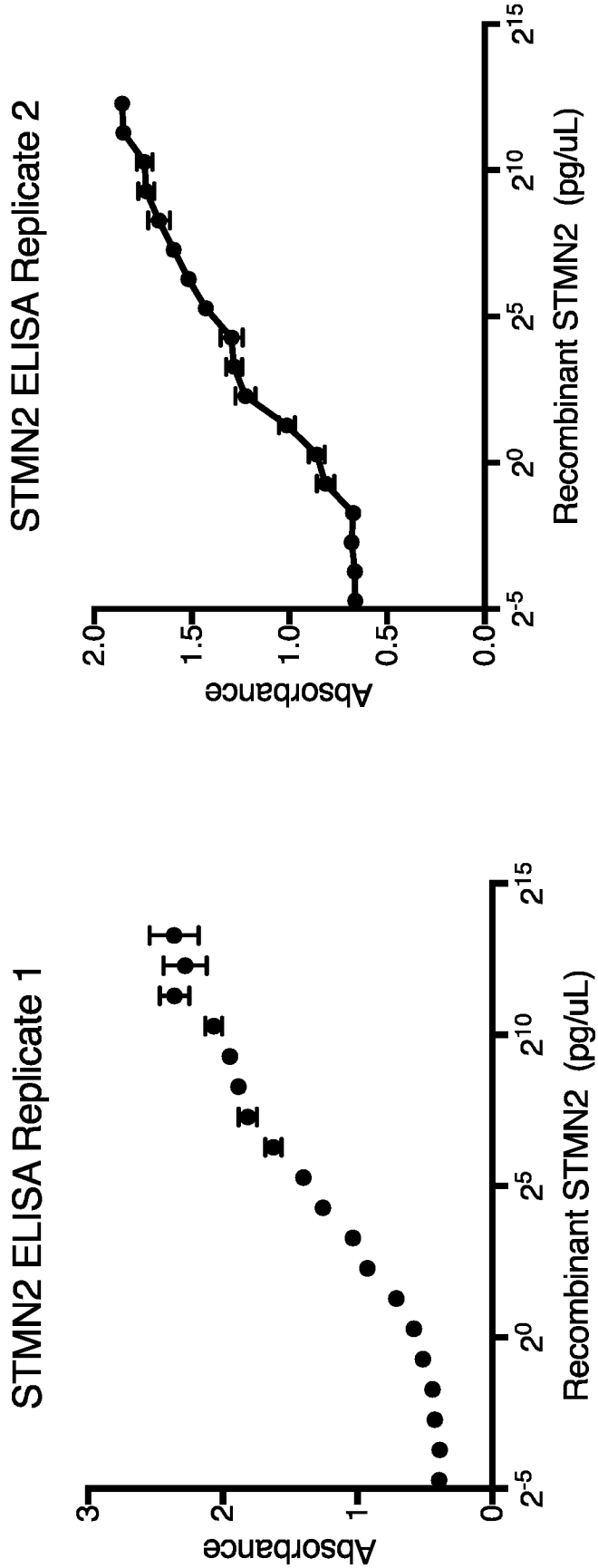

STMN2 ELISA Replicate 2
Absorbance
2.0
1.5
1.0
0.5
0.0
2^{-5}
2^{0}
2^{5}
2^{10}
2^{15}
Recombinant STMN2 (pg/uL)
STMN2 ELISA Replicate 1
Absorbance
3
2
1
0
2^{-5}
2^{0}
2^{5}
2^{10}
2^{15}
Recombinant STMN2 (pg/uL)

FIG. 18B

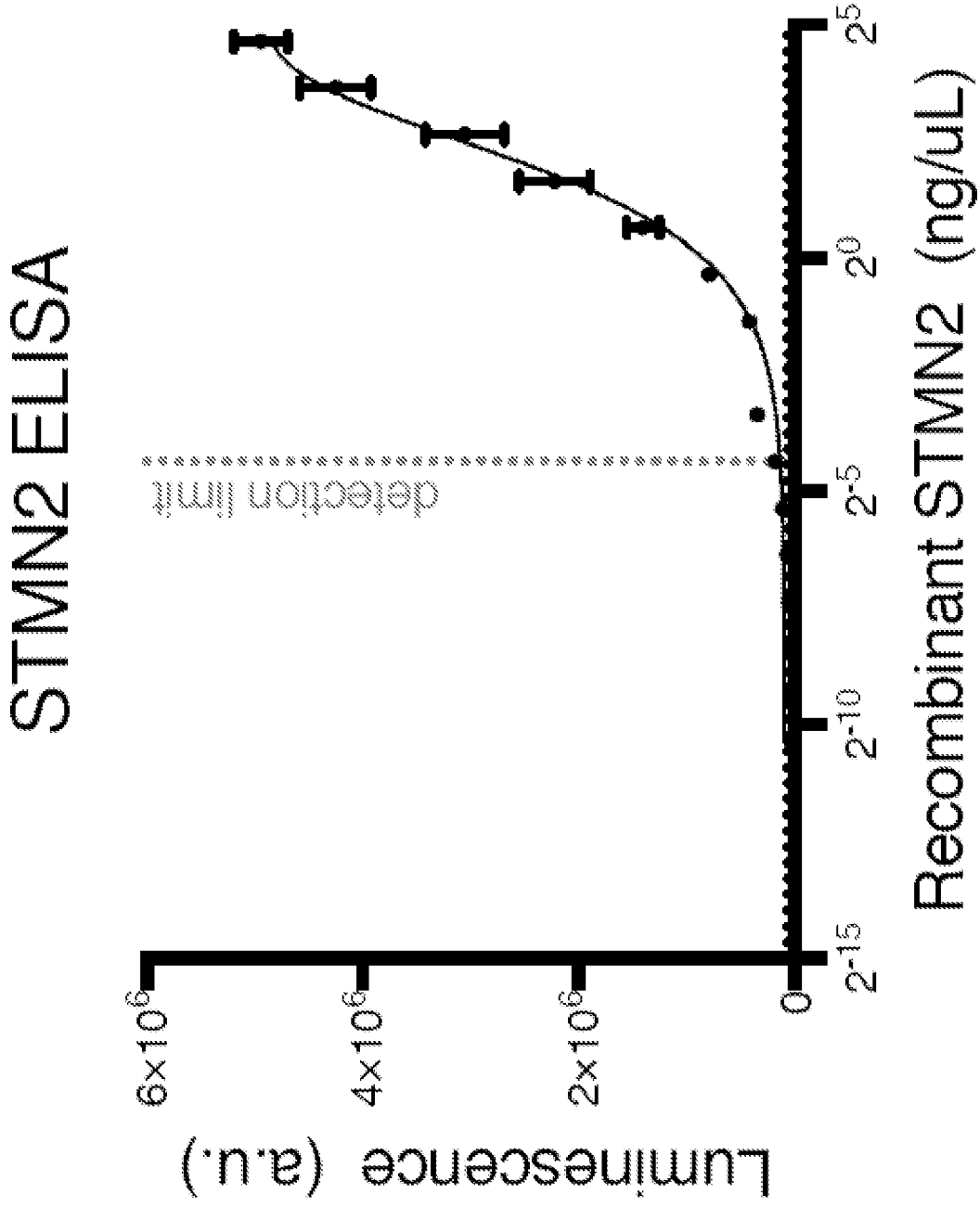

STMN2 ELISA
detection limit
Luminescence (a.u.)
6×10^6
4×10^6
2×10^6
0
Recombinant STMN2 (ng/uL)
2^-15
2^-10
2^-5
2^0
2^5

FIG. 18C

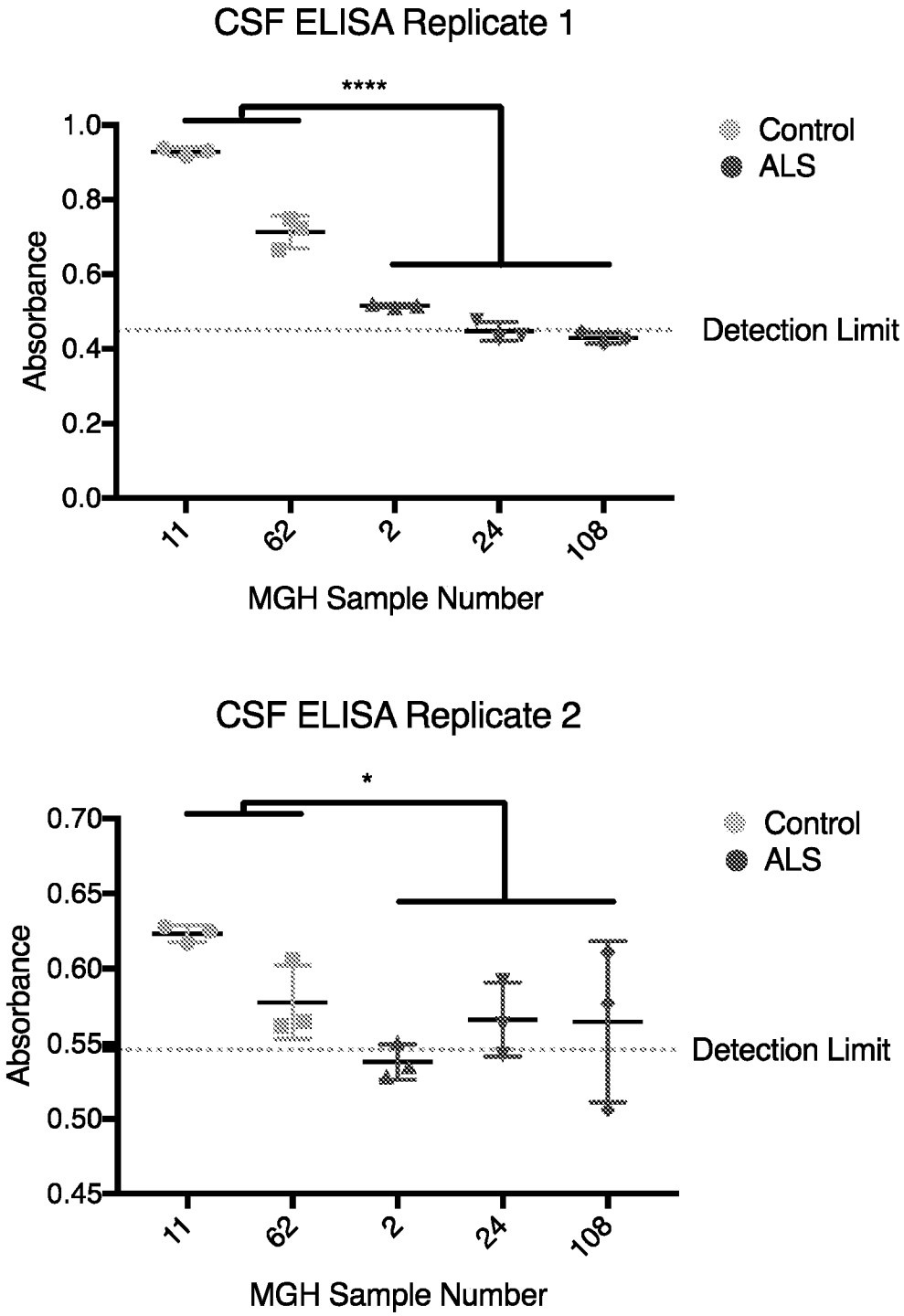
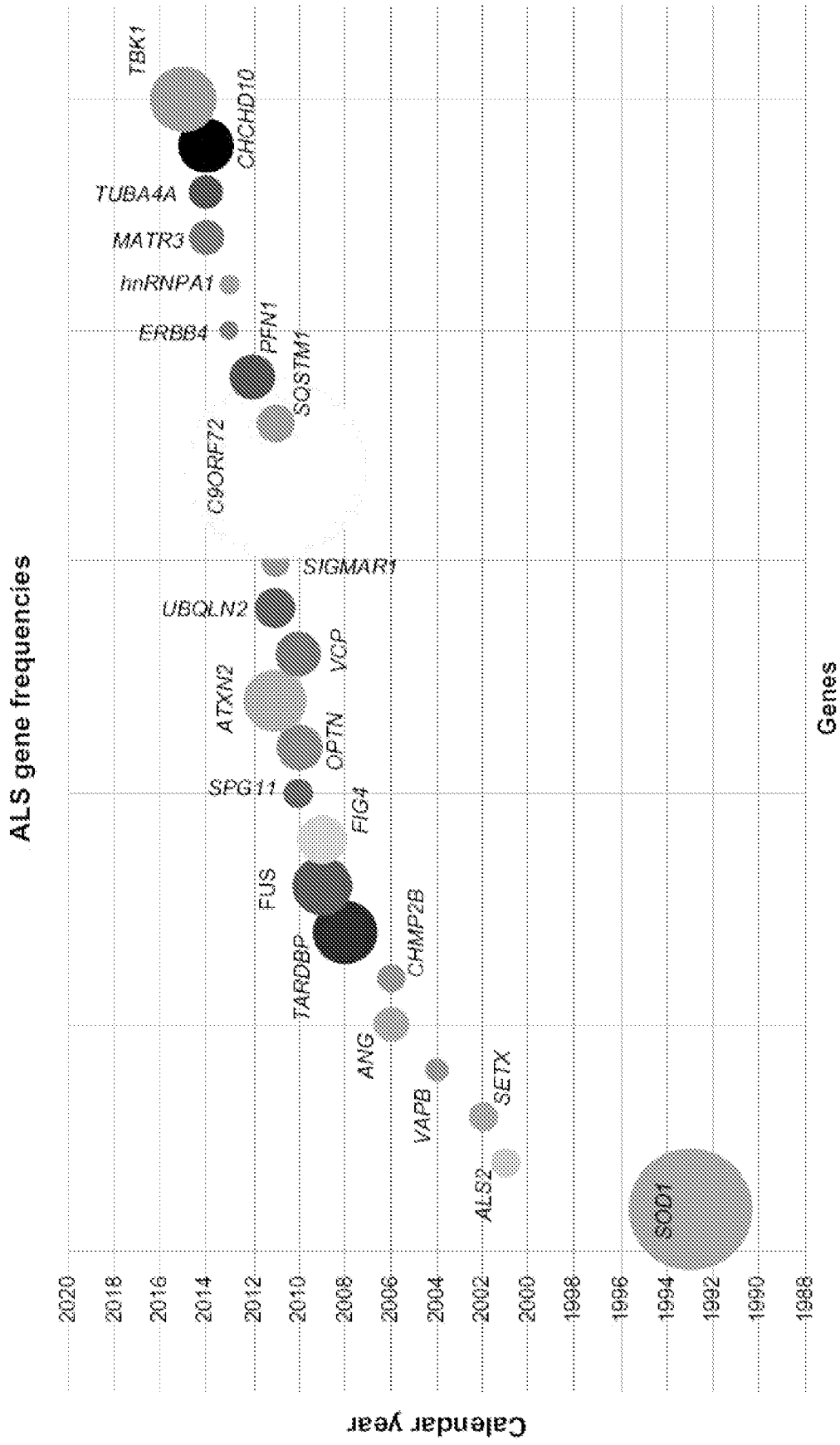
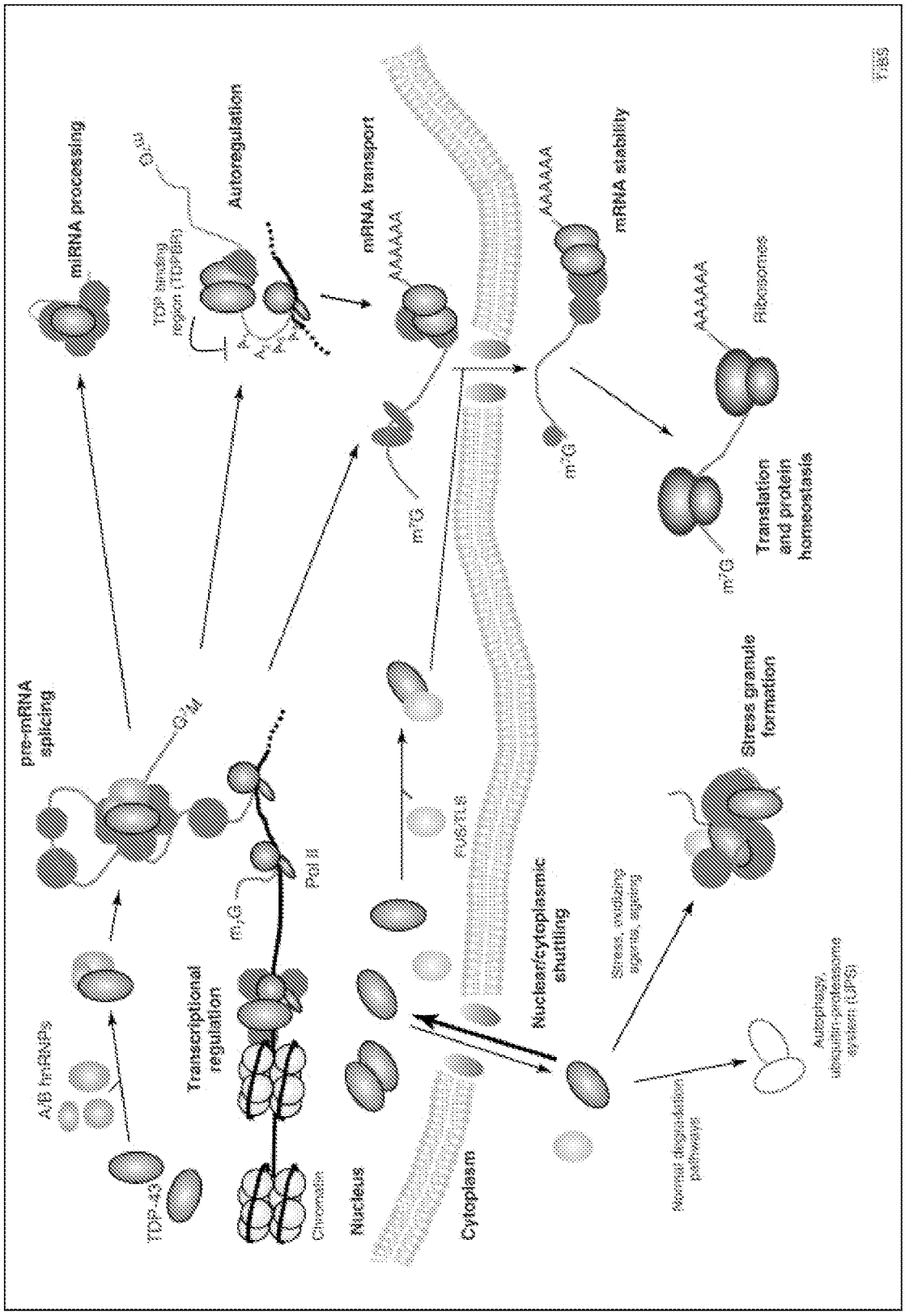

CSF ELISA Replicate 1
****
Absorbance
1.0
0.8
0.6
0.4
0.2
0.0
Control
ALS
Detection Limit
11
62
2
24
108
MGH Sample Number
CSF ELISA Replicate 2
*
Absorbance
0.70
0.65
0.60
0.55
0.50
0.45
Control
ALS
Detection Limit
11
62
2
24
108
MGH Sample Number

FIG. 18D



Alsultan et al. *Degenerative Neurological and Neuromuscular Disease*. **2016**, *6*, 49-64.

FIG. 19



Buratti and Baralle *Trends in Biochem. Sci.*. **2012**, *6*, 237-247.

FIG. 20

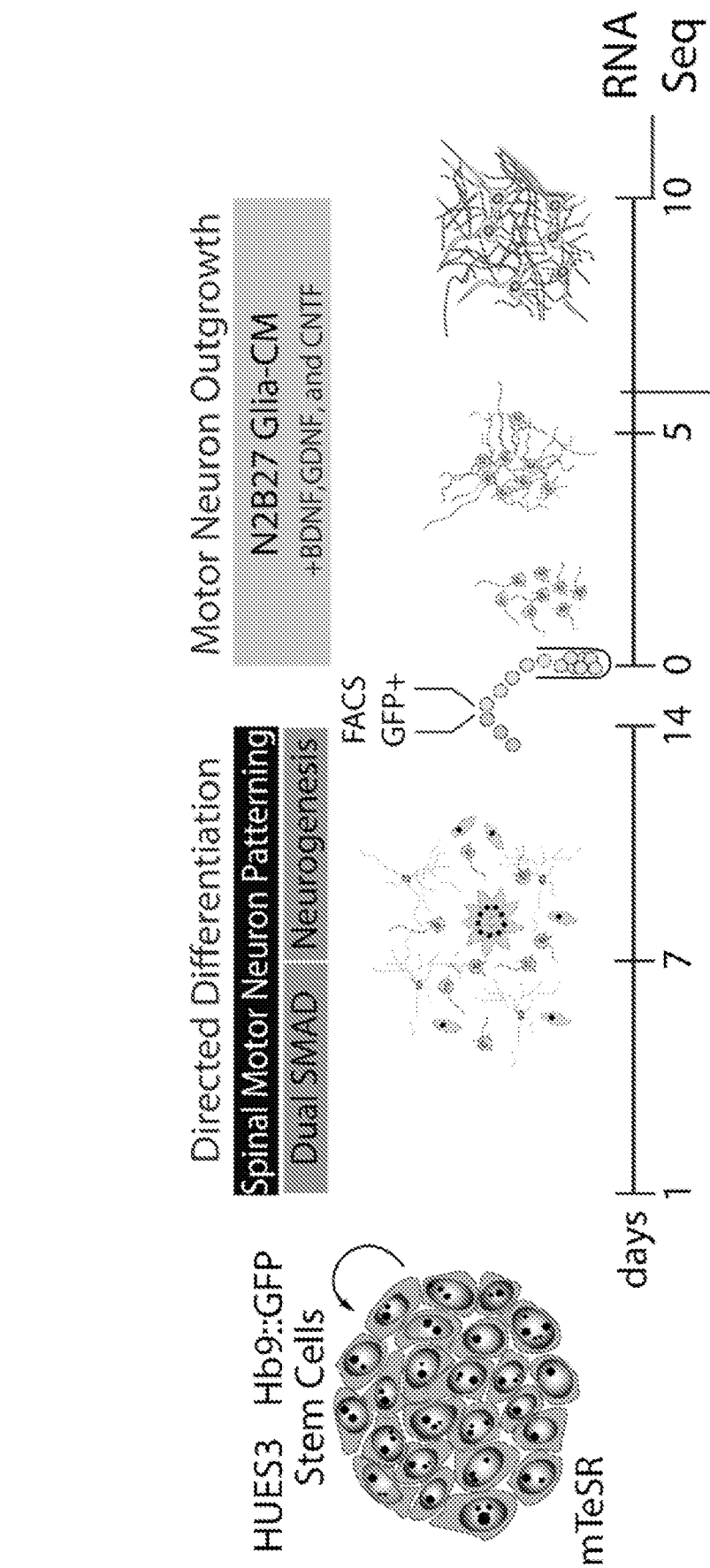
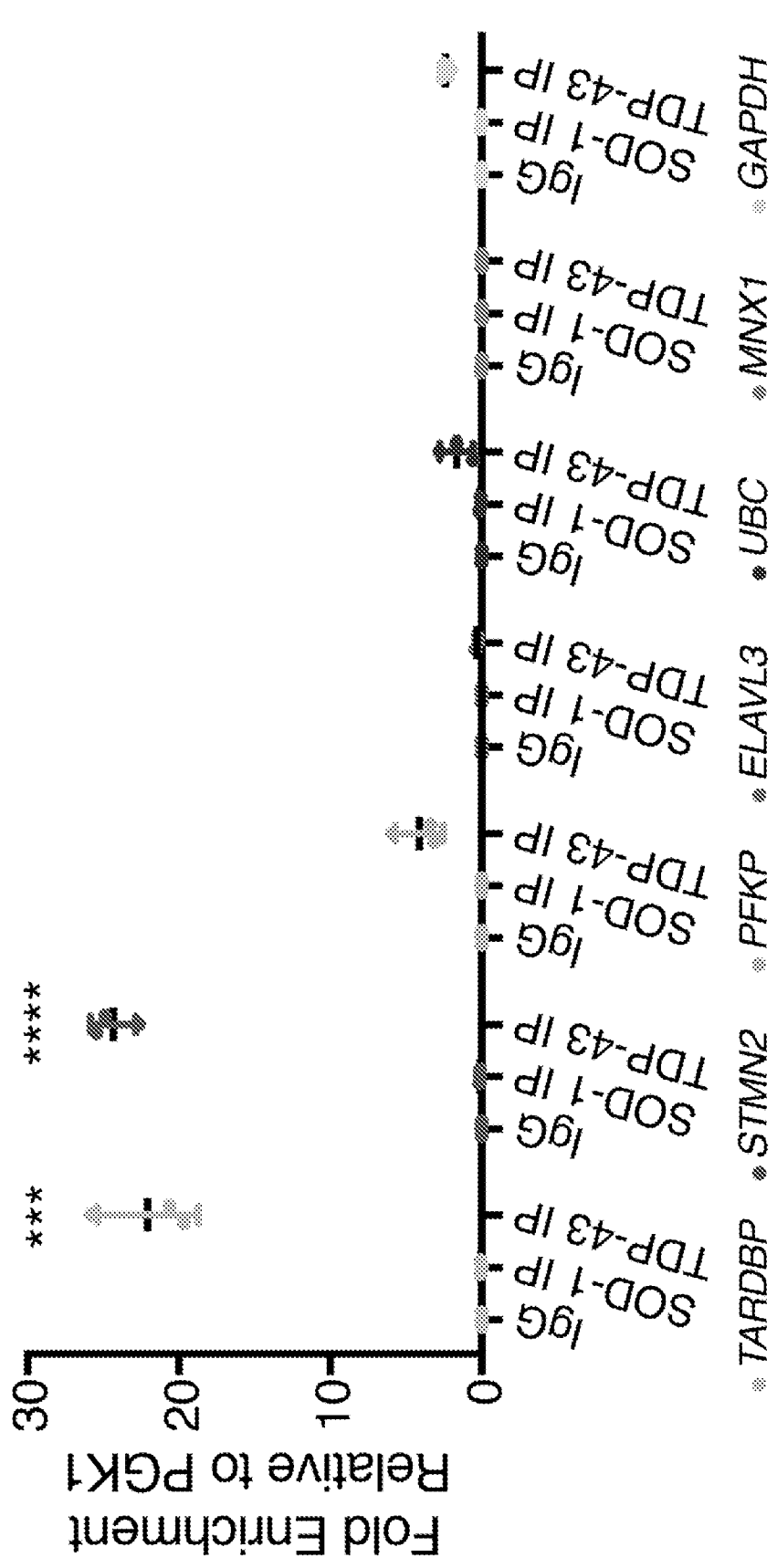

HUES3 Hb9::GFP Stem Cells
mTeSR
Directed Differentiation
Spinal Motor Neuron Patterning
Dual SMAD
Neurogenesis
FACS
GFP+
Motor Neuron Outgrowth
N2B27 Glia-CM
+BDNF,GDNF, and CNTF
days
1
7
14
0
5
10
RNA Seq
siRNA Treatments
No Tx
siRED
siSCR
siTDP43

FIG. 21



Klim et al. *Nature Neuroscience* vol. 22, pages 167–179 (2019)

FIG. 22

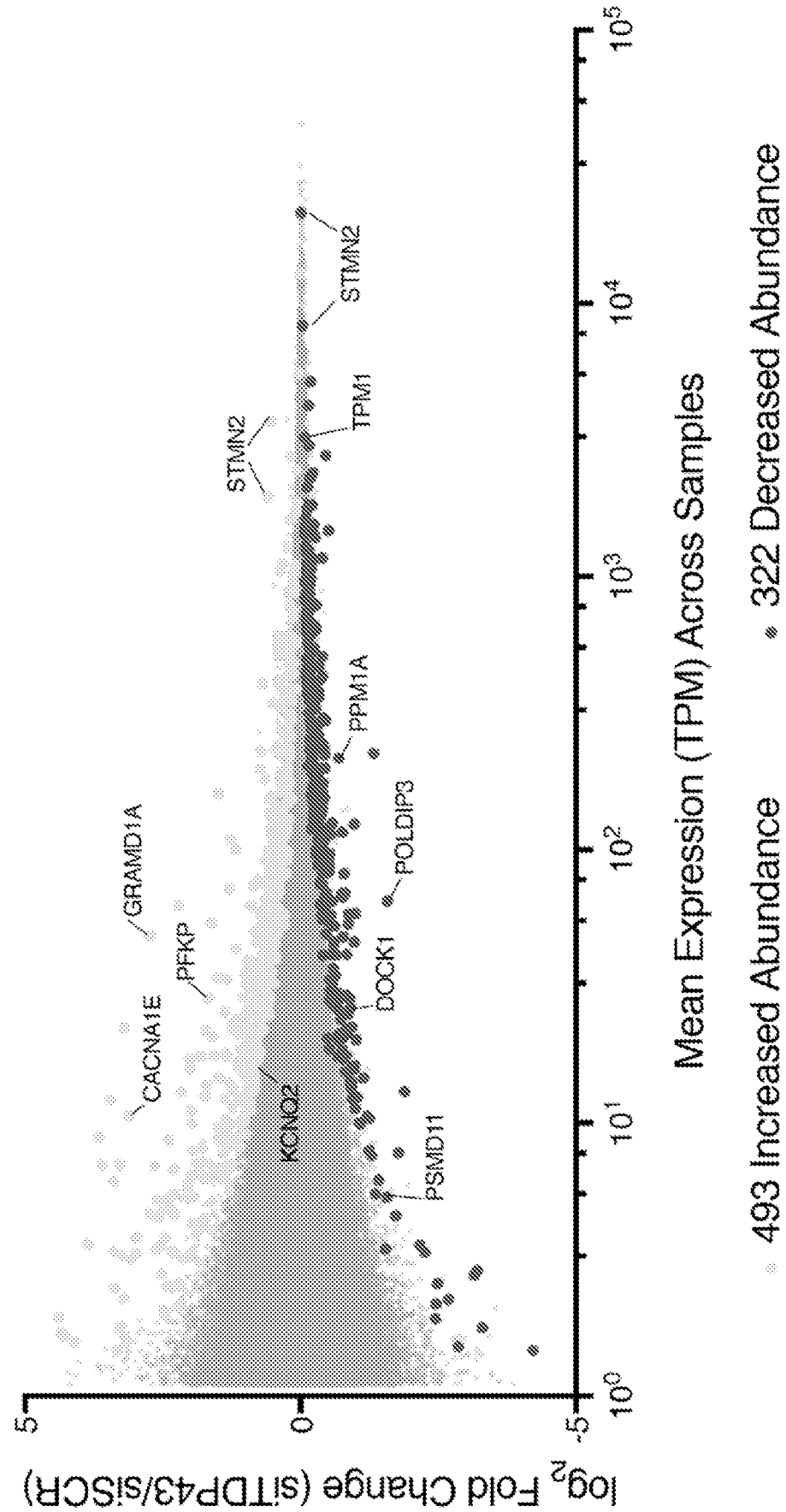

log2 Fold Change (siTDP43/siSCR)
5
0
-5
Mean Expression (TPM) Across Samples
10^0
10^1
10^2
10^3
10^4
10^5
493 Increased Abundance
322 Decreased Abundance
GRAMD1A
PFKP
CACNA1E
KCNQ2
PSMD11
DOCK1
POLDIP3
PPM1A
STMN2
TPM1
STMN2

FIG. 23

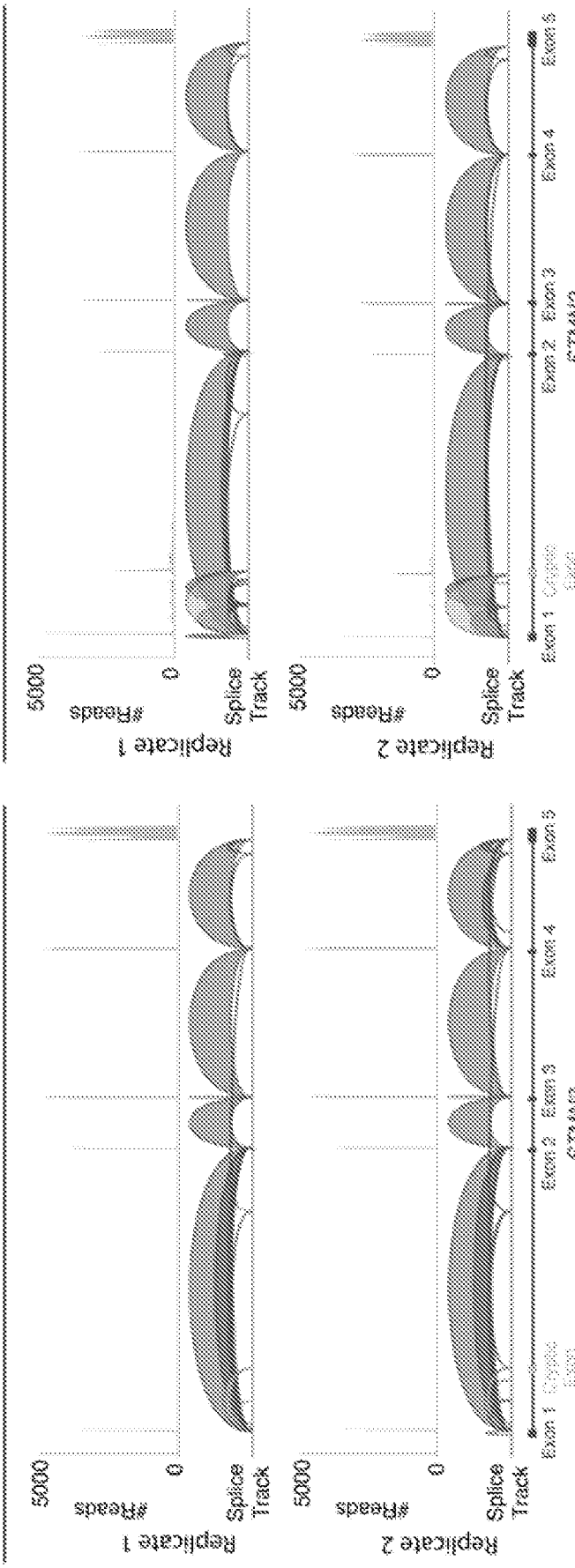

siTDP-43
siSCR
Replicate 1
Replicate 2
#Reads
5000
0
Splice Track
STMN2
Exon 1
Exon 2
Exon 3
Exon 4
Exon 5

FIG. 24

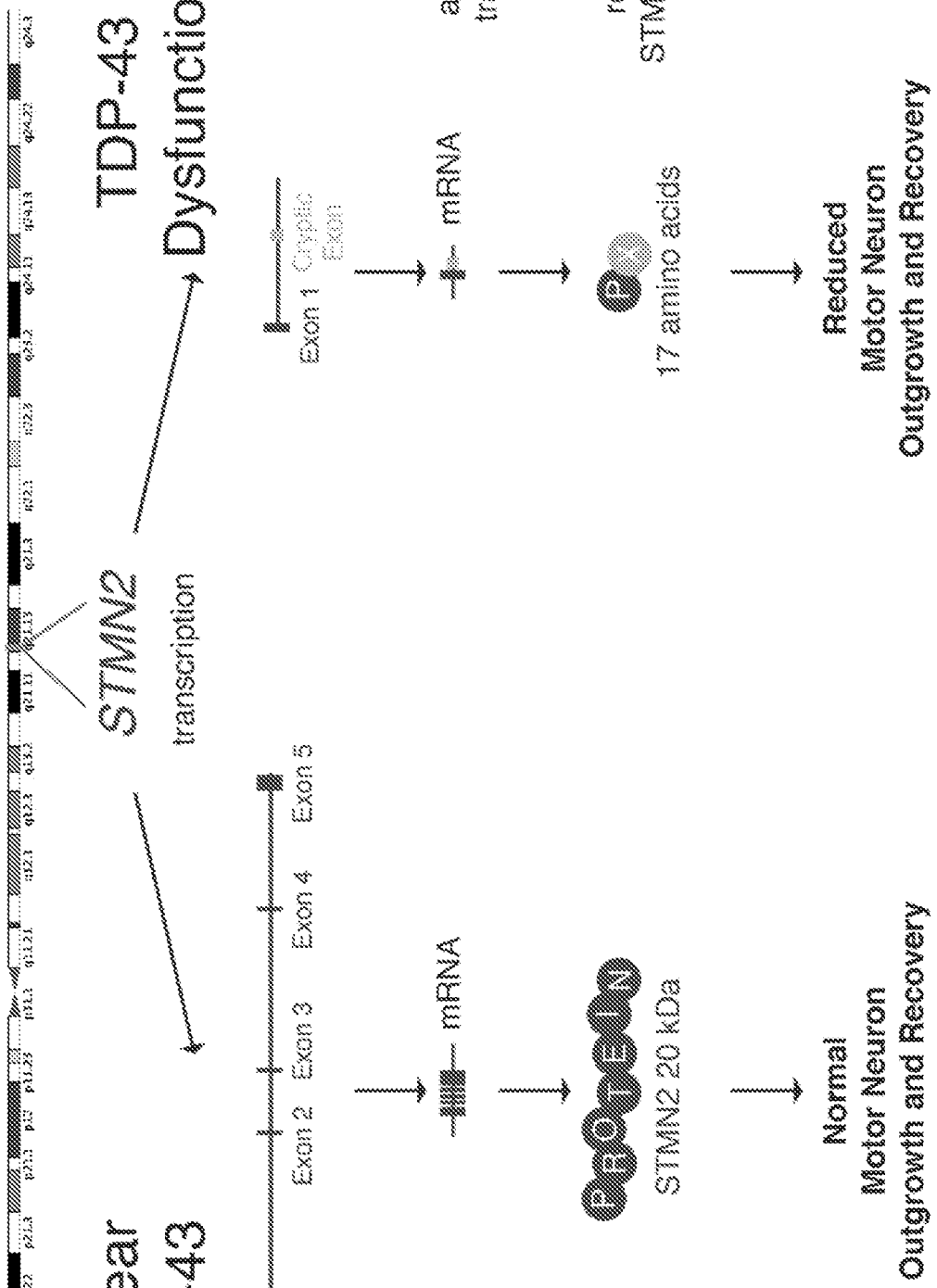

Nuclear
TDP-43
STMN2
transcription
TDP-43
Dysfunction
Exon 1 Cryptic Exon
Exon 2
Exon 3
Exon 4
Exon 5
splicing
mRNA
translation
PROTEIN
STMN2 20 kDa
cellular function
Normal
Motor Neuron
Outgrowth and Recovery
Exon 1 Cryptic Exon
mRNA
aberrant transcript
P
17 amino acids
reduced STMN2 protein
Reduced
Motor Neuron
Outgrowth and Recovery

FIG. 25

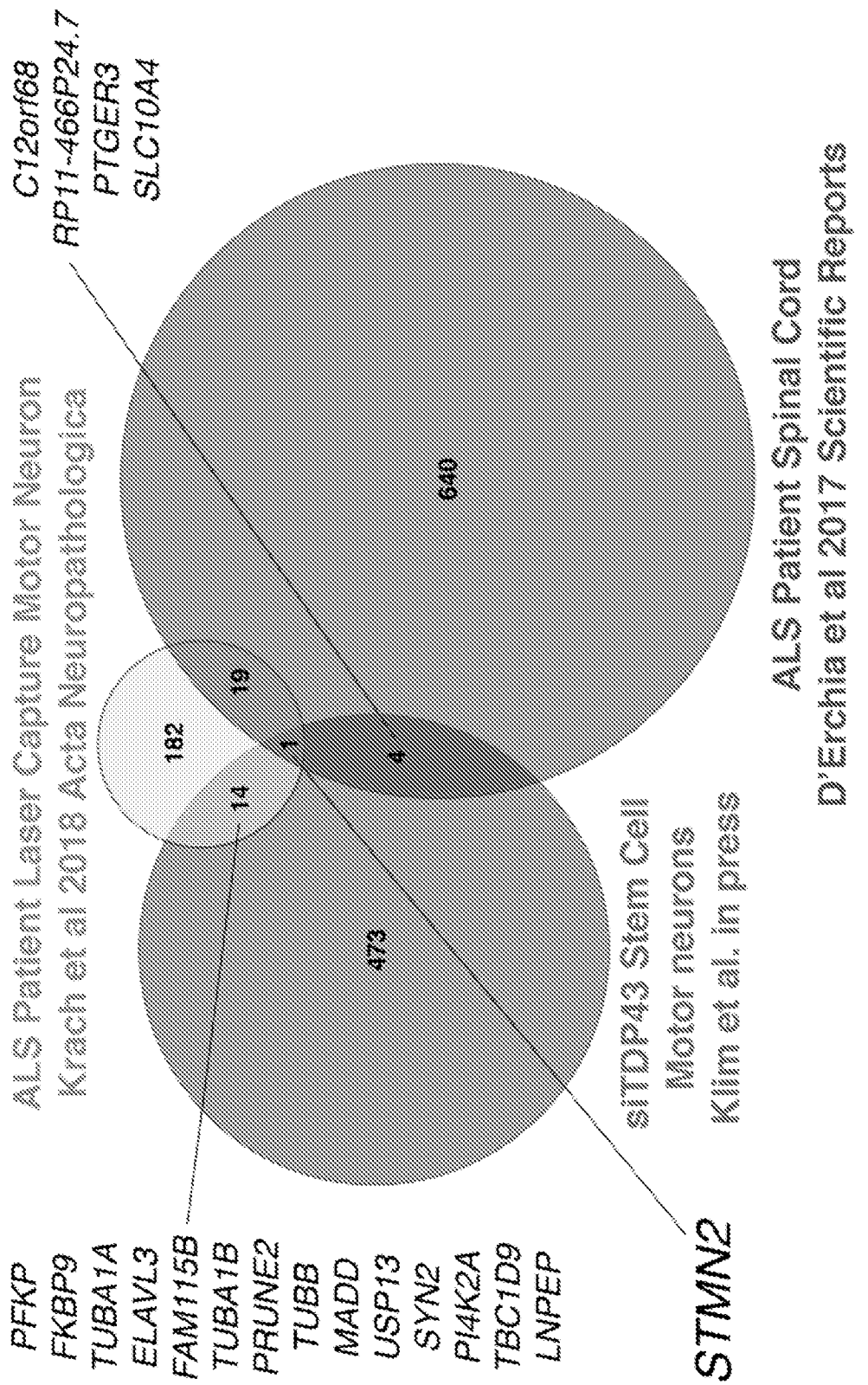

ALS Patient Laser Capture Motor Neuron
Krach et al 2018 Acta Neuropathologica
182
19
14
1
4
640
473
ALS Patient Spinal Cord
D'Erchia et al 2017 Scientific Reports
siTDP43 Stem Cell
Motor neurons
Klim et al. in press
C12orf68
RP11-466P24.7
PTGER3
SLC10A4
PFKP
FKBP9
TUBA1A
ELAVL3
FAM115B
TUBA1B
PRUNE2
TUBB
MADD
USP13
SYN2
PI4K2A
TBC1D9
LNPEP
STMN2

FIG. 26

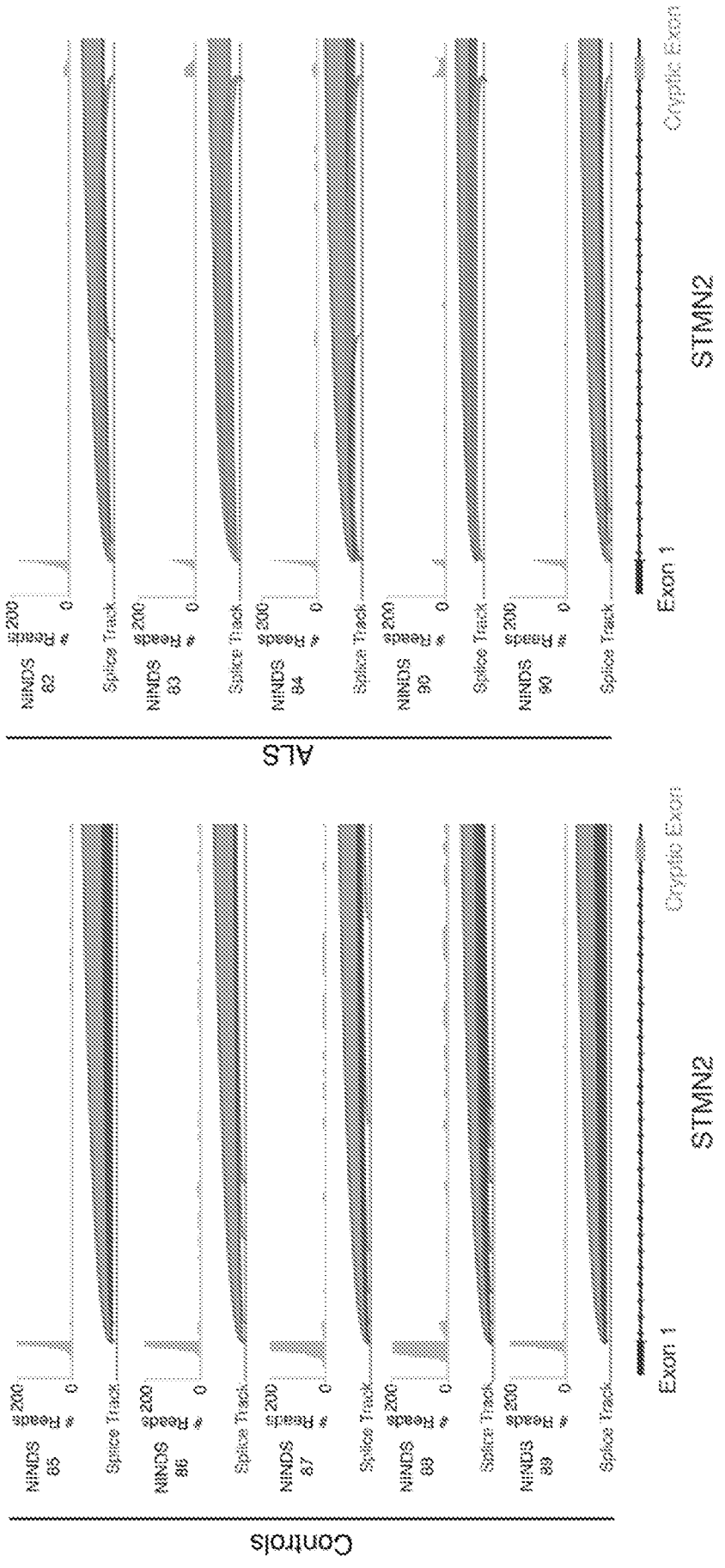

ALS
Controls
NMDS 62
NMDS 63
NMDS 64
NMDS 90
NMDS 90
NMDS 65
NMDS 66
NMDS 67
NMDS 68
NMDS 69
Reads
200
0
Splice Track
Exon 1
STMN2
Cryptic Exon

FIG. 27

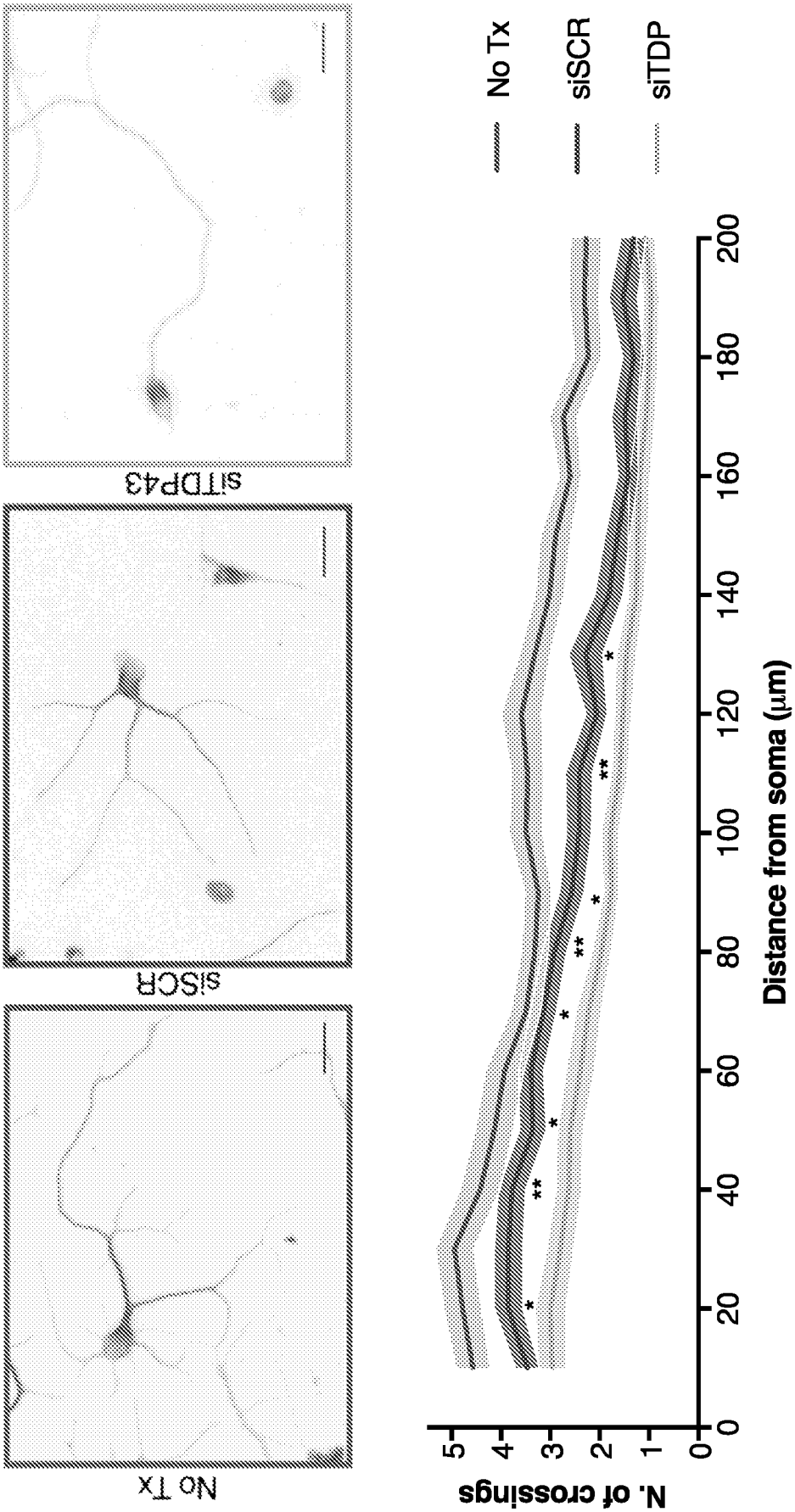

No Tx
siSCR
siTDP43
No Tx
siSCR
siTDP
N. of crossings
Distance from soma (μm)
0
1
2
3
4
5
0
20
40
60
80
100
120
140
160
180
200
*
**
*
**
*
**
*

FIG. 28



FIG. 29

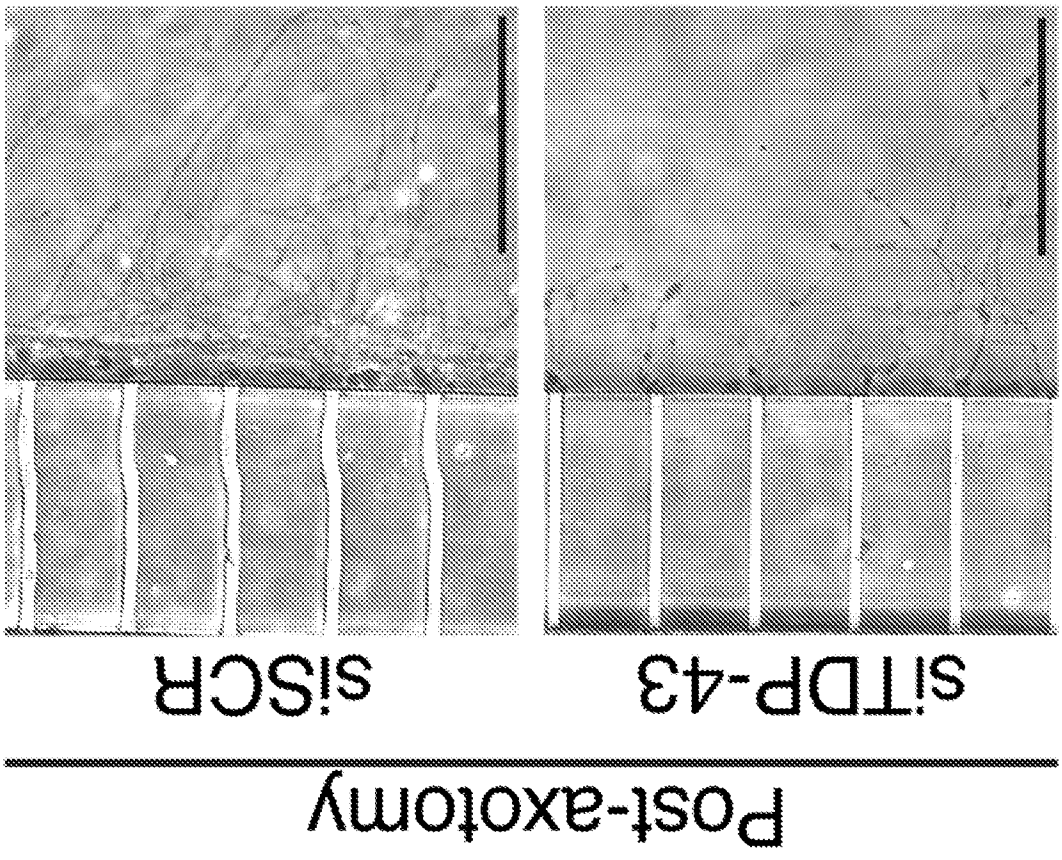


FIG. 30A

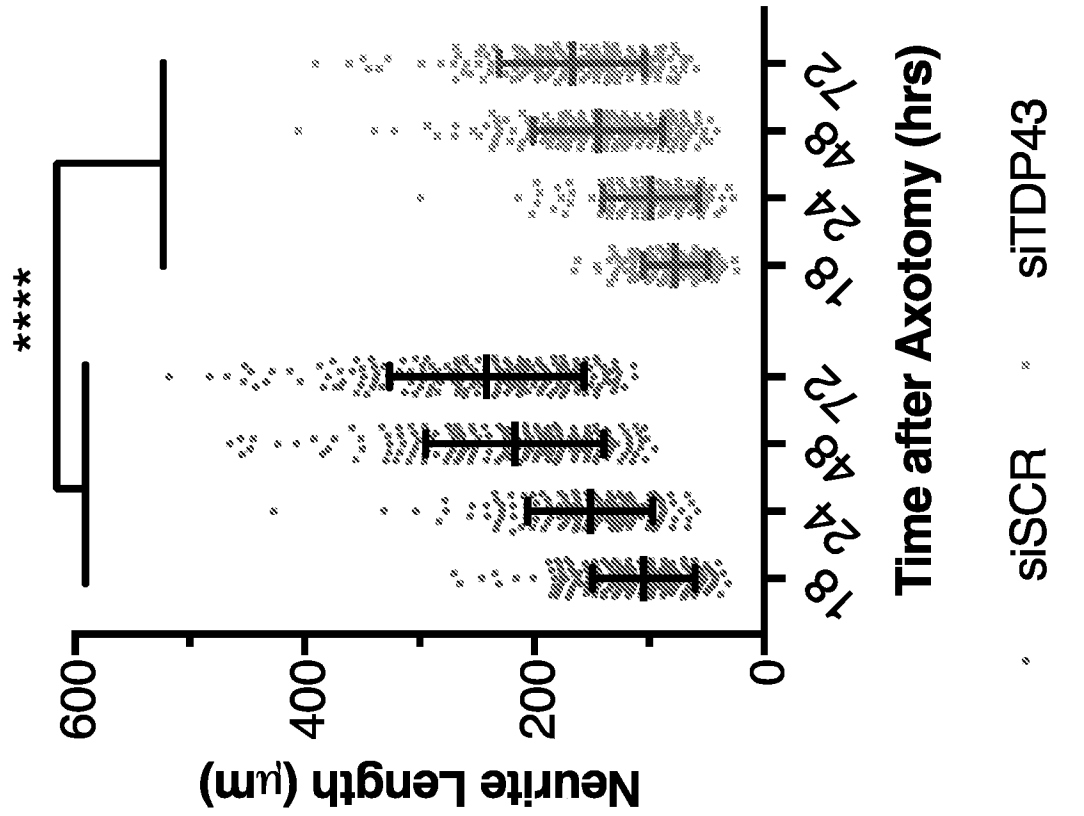
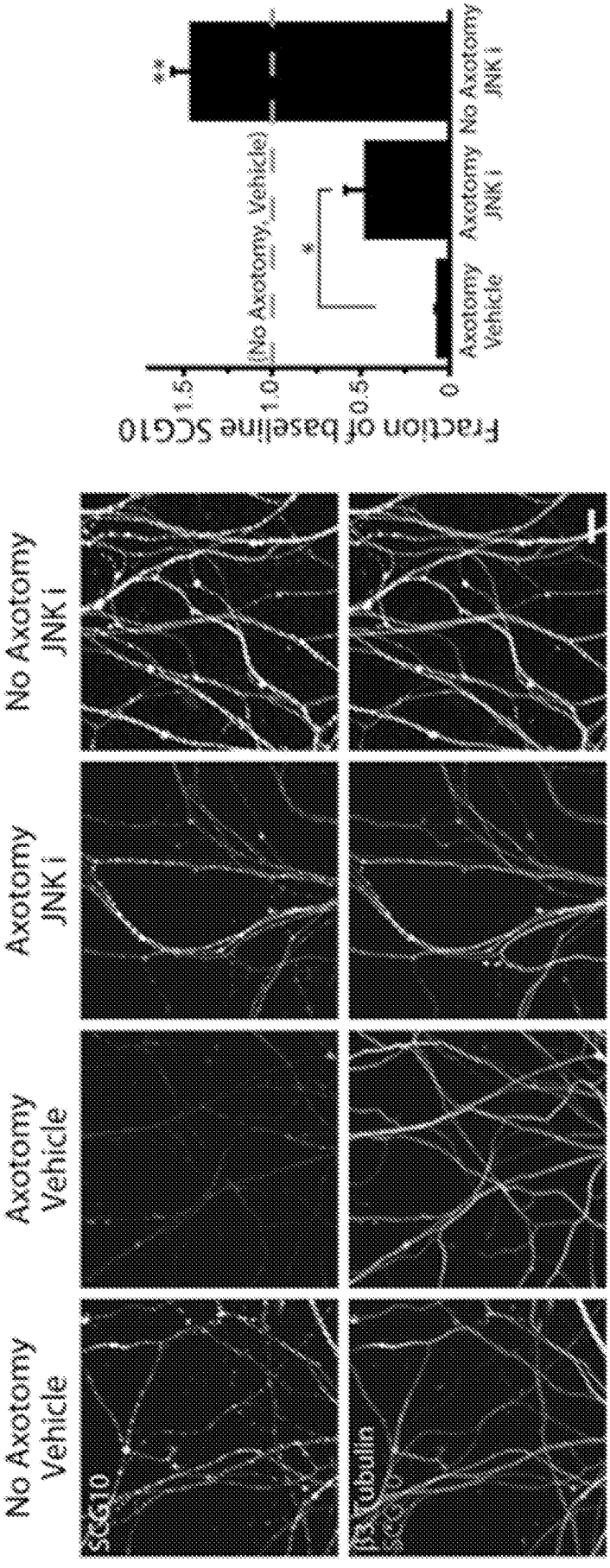
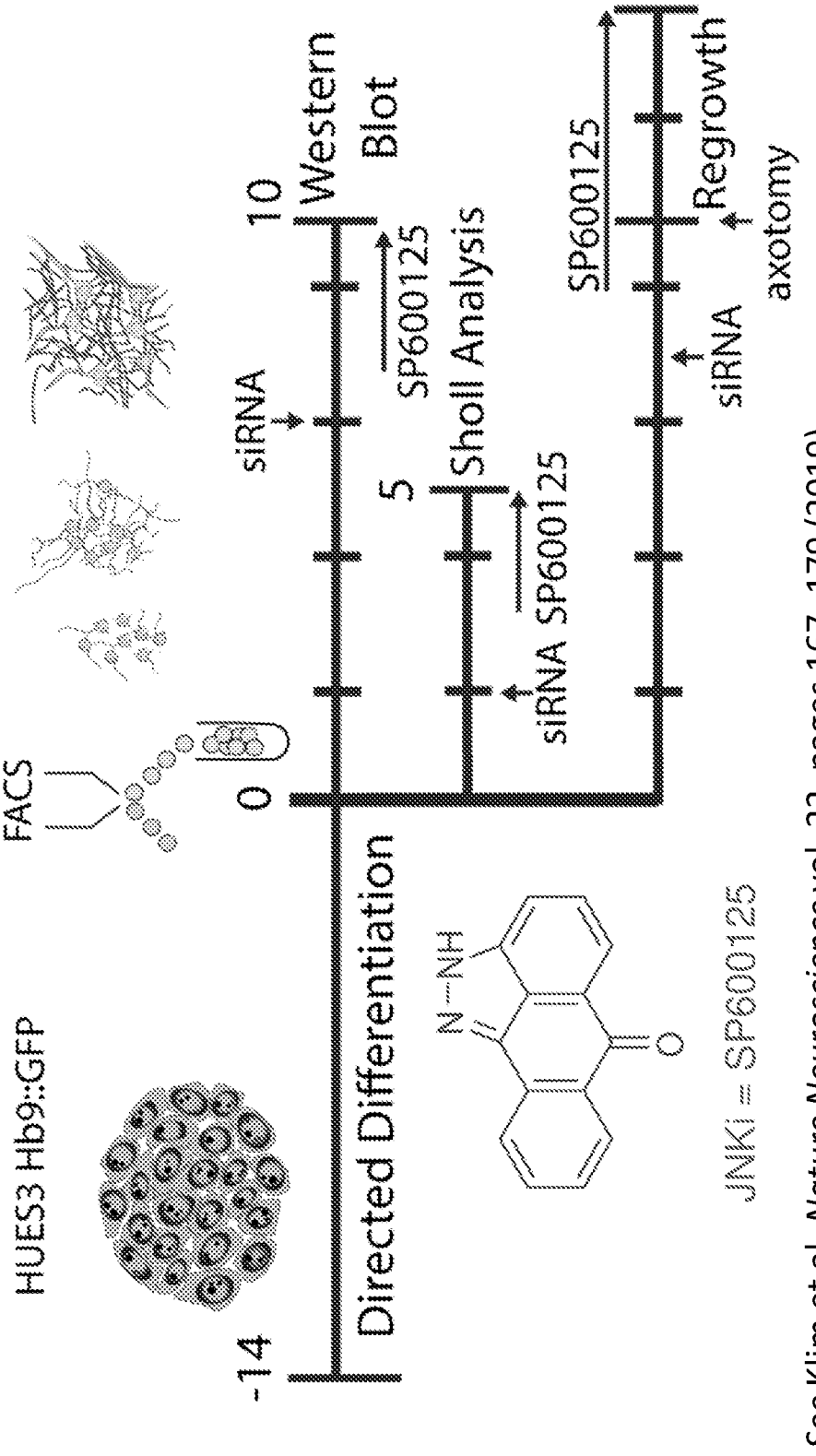


FIG. 30B



J. Eun Shin et al. *PNAS* **2012**, *109*, E3696-3705.

FIG. 31



See Klim et al. *Nature Neuroscience* vol. 22, pages 167–179 (2019).

FIG. 32

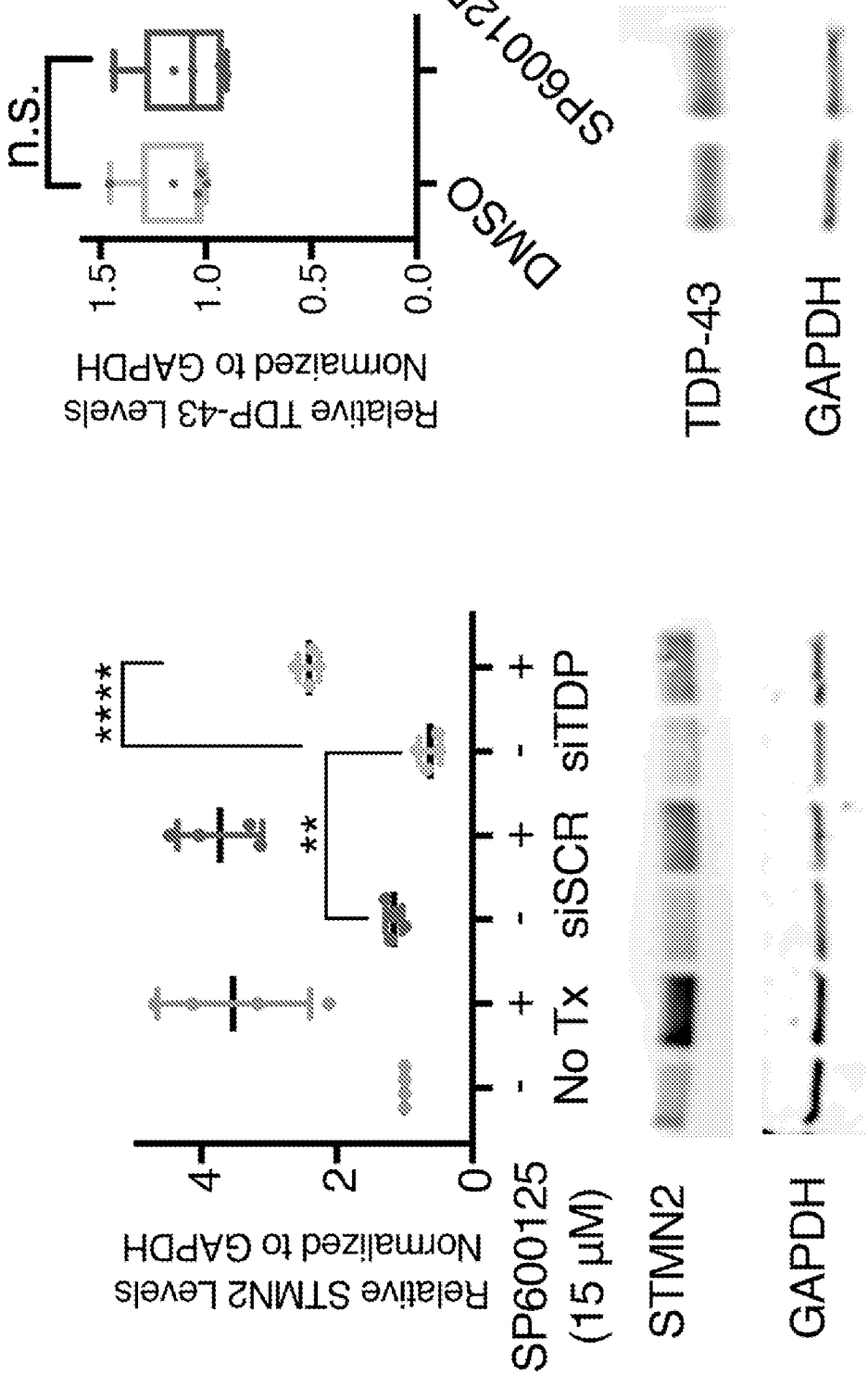

Relative TDP-43 Levels
Normalized to GAPDH
1.5
1.0
0.5
0.0
n.s.
DMSO
SP600125
TDP-43
GAPDH
Relative STMN2 Levels
Normalized to GAPDH
4
2
0
****
**
SP600125 (15 μM) - + - + - +
No Tx siSCR siTDP
STMN2
GAPDH

FIG. 33

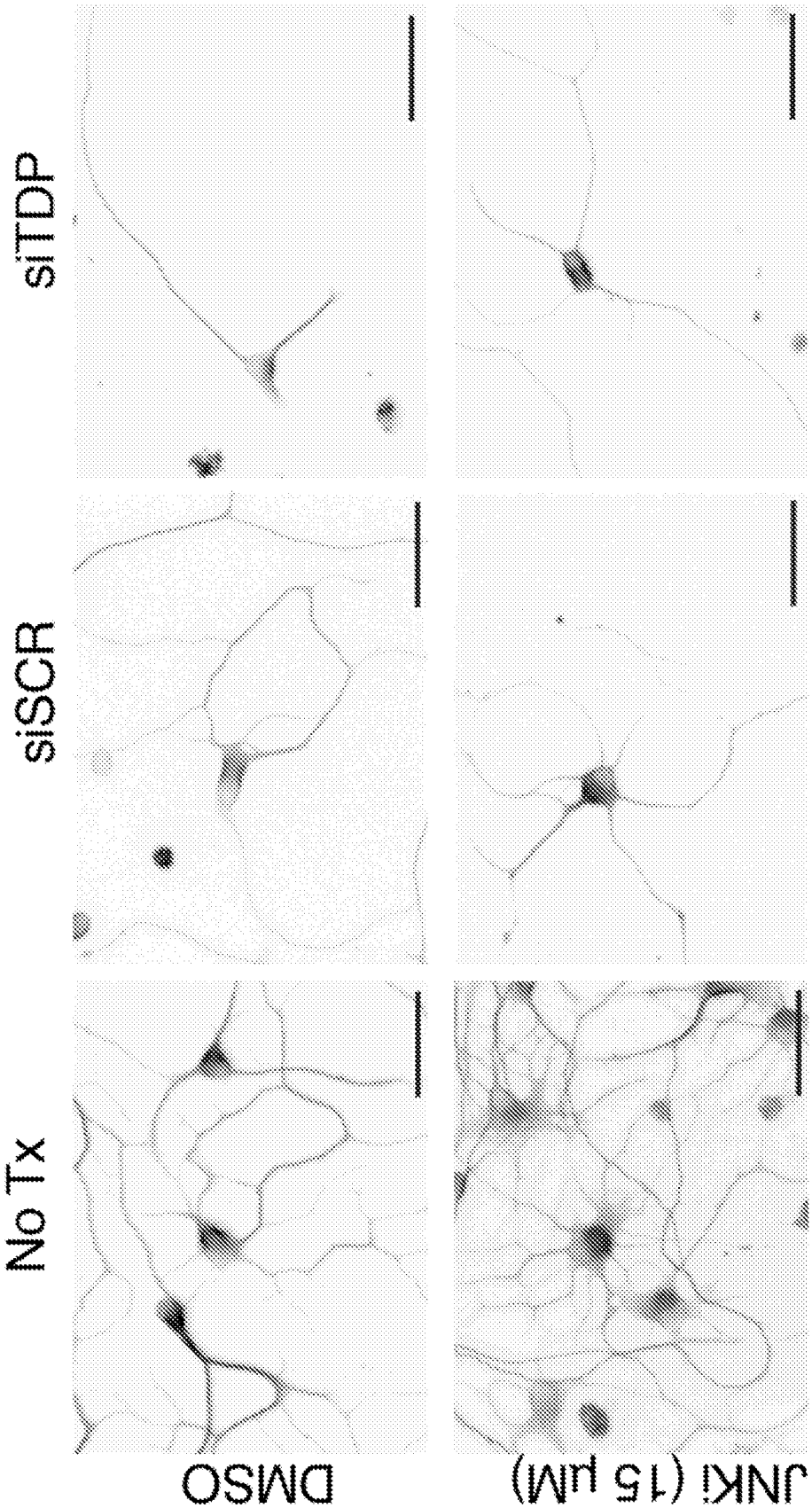


FIG. 34

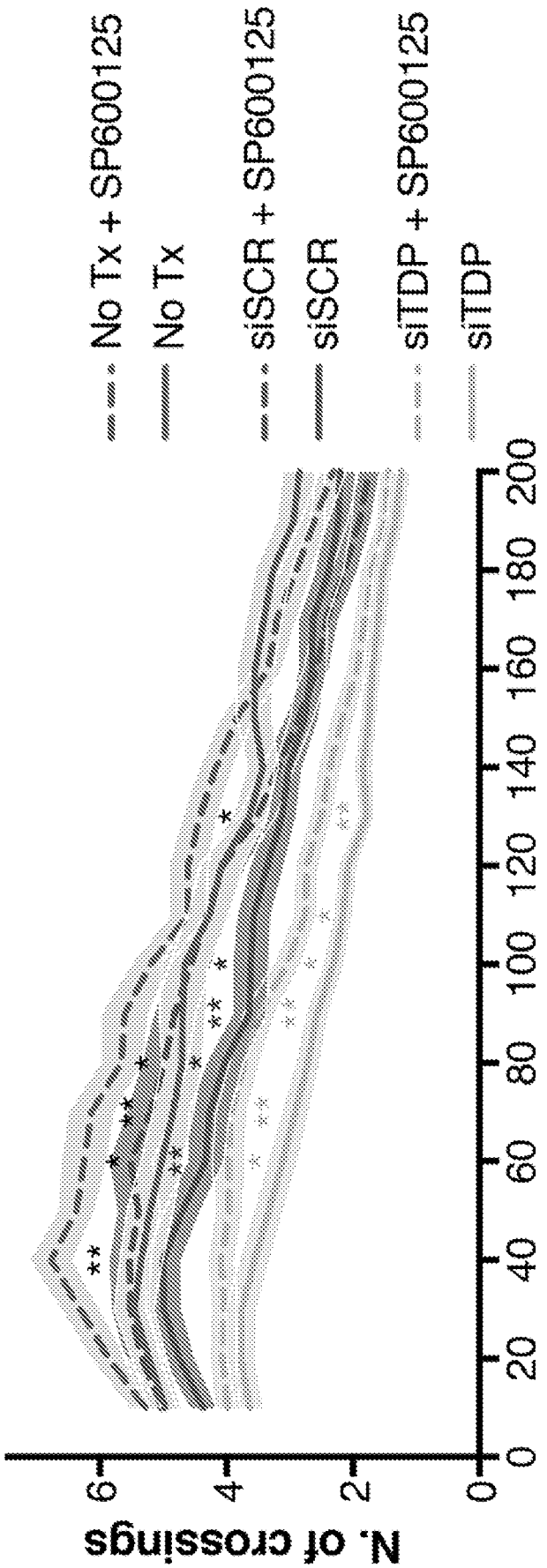

No Tx + SP600125
No Tx
siSCR + SP600125
siSCR
siTDP + SP600125
siTDP
N. of crossings
0
2
4
6
Distance from soma (μm)
0
20
40
60
80
100
120
140
160
180
200

FIG. 35

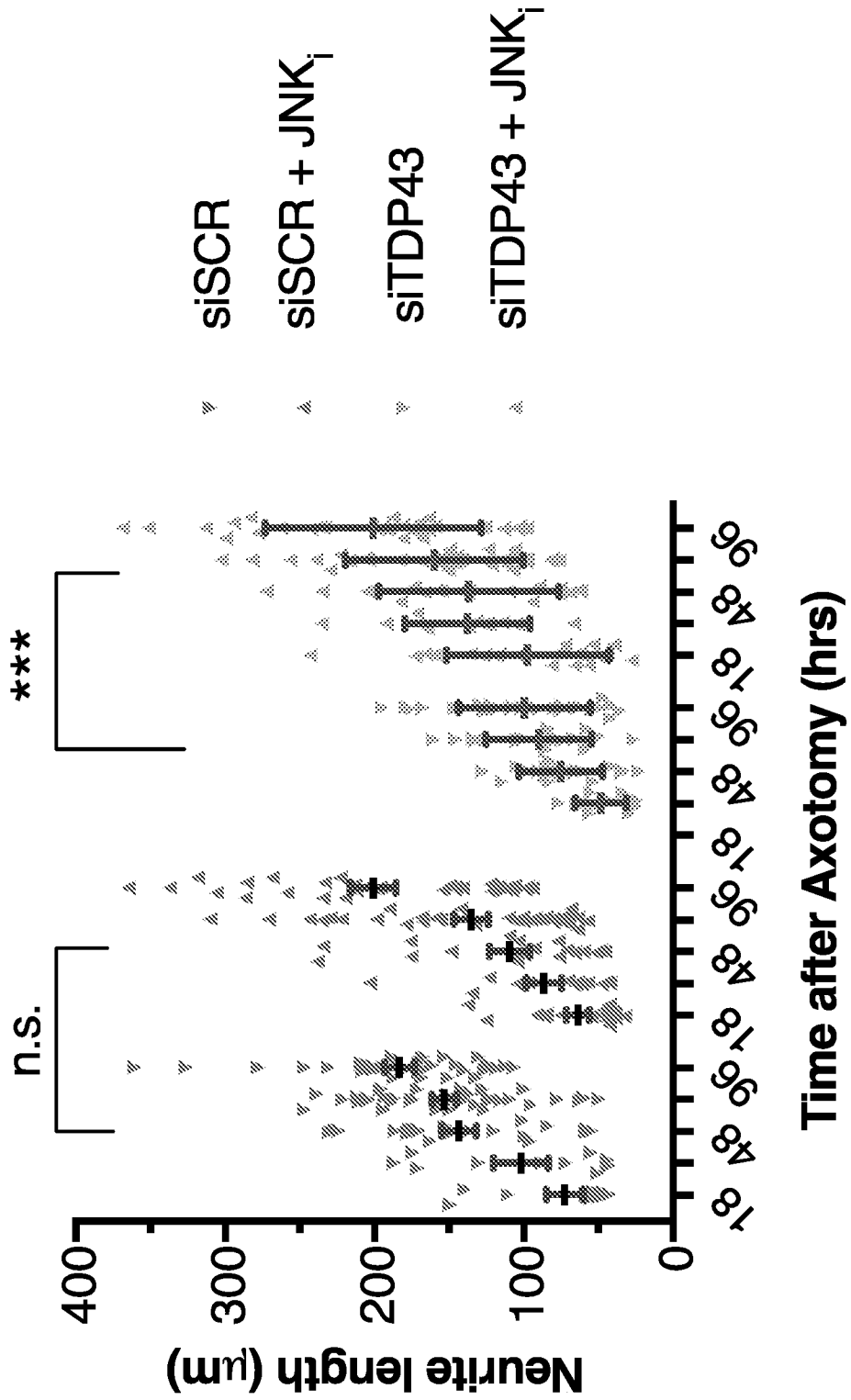

siSCR
siSCR + JNKi
siTDP43
siTDP43 + JNKi
***
n.s.
Neurite length (μm)
0
100
200
300
400
18
48
96
Time after Axotomy (hrs)

FIG. 36

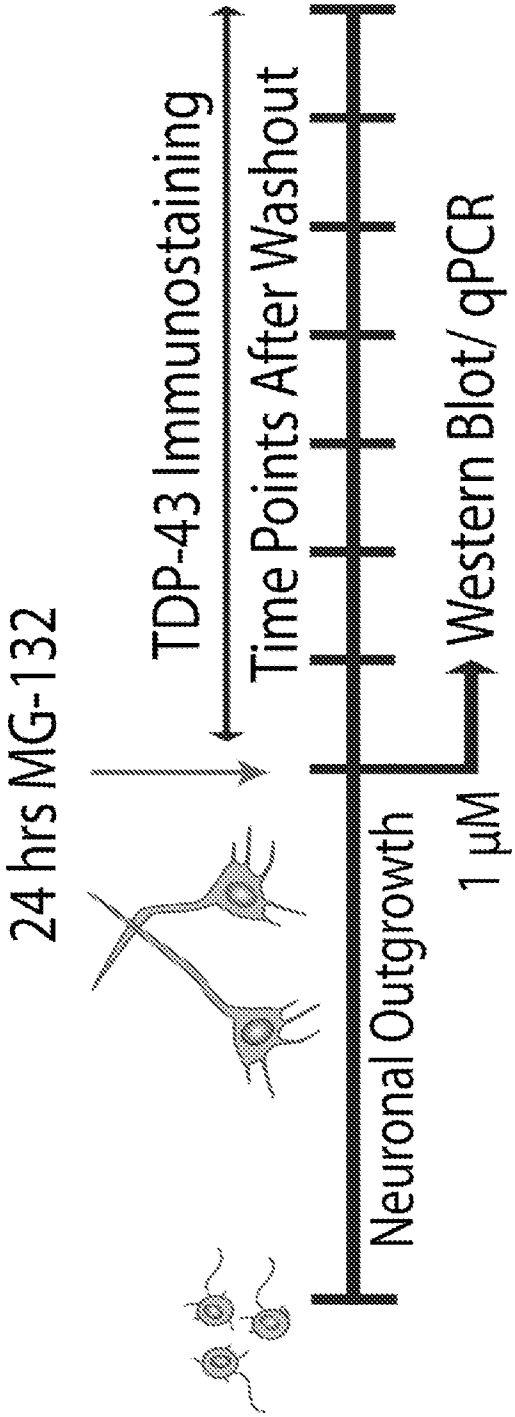

24 hrs MG-132
TDP-43 Immunostaining
Time Points After Washout
Neuronal Outgrowth
1 µM
Western Blot/ qPCR

FIG. 37

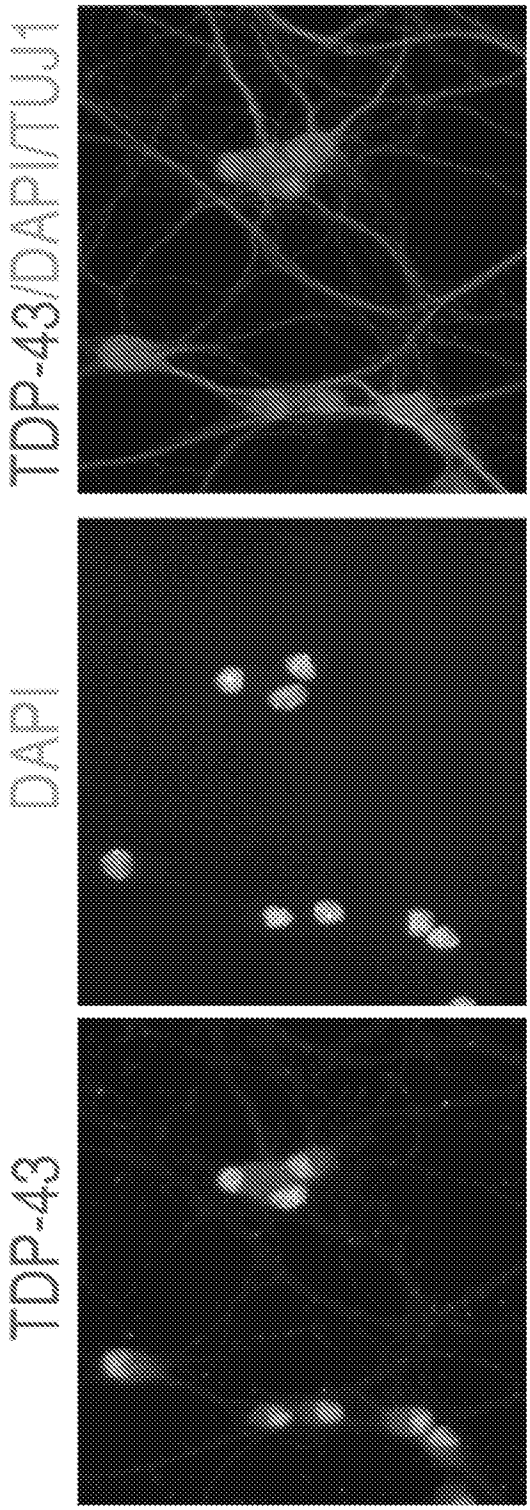


FIG. 38A

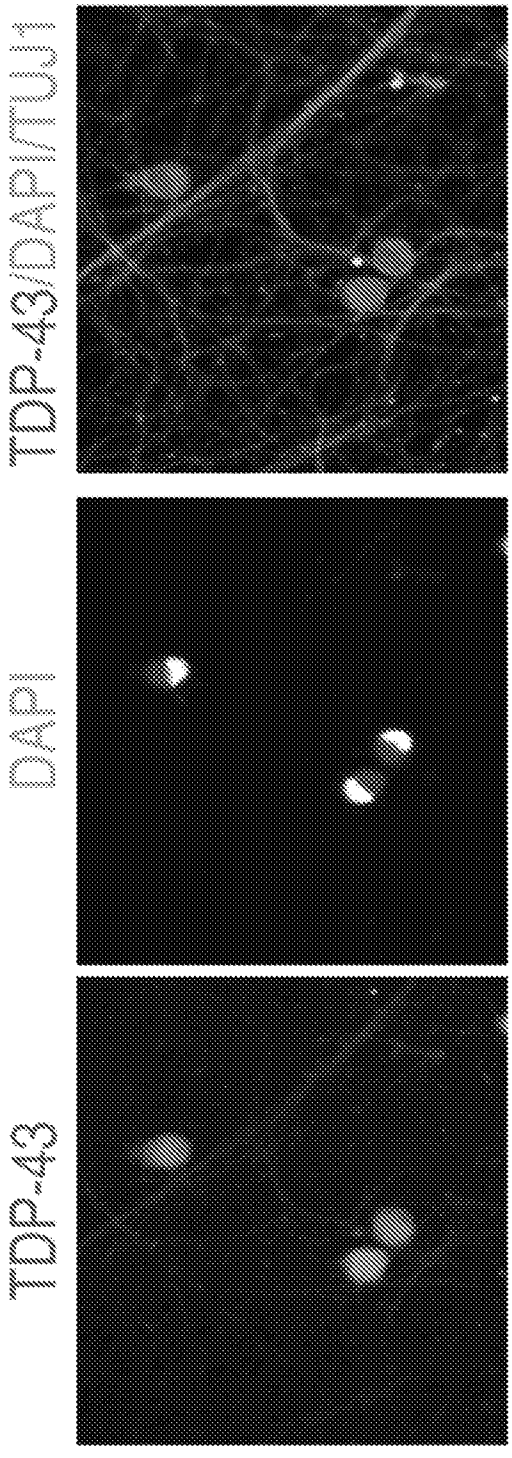


FIG. 38B

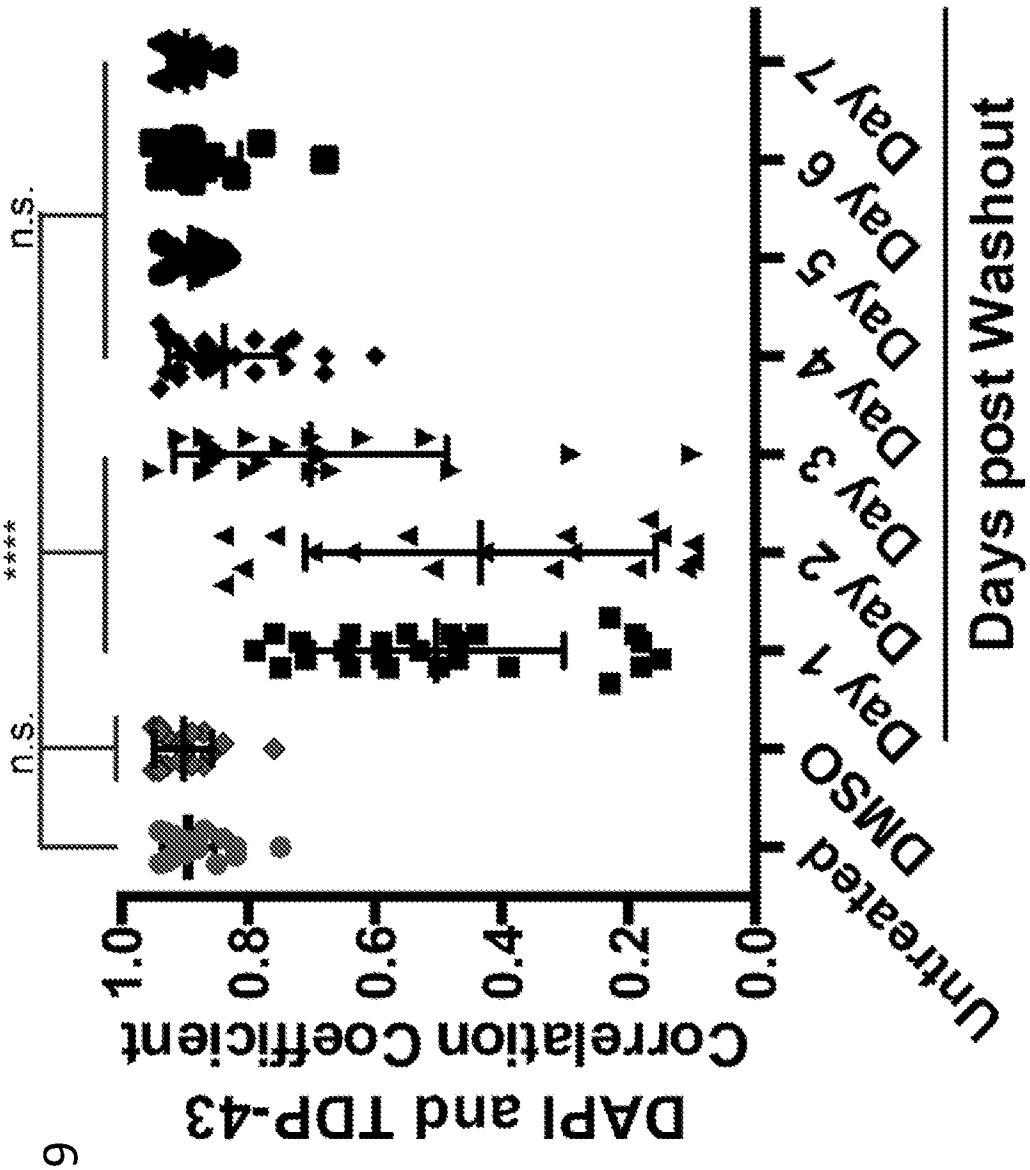
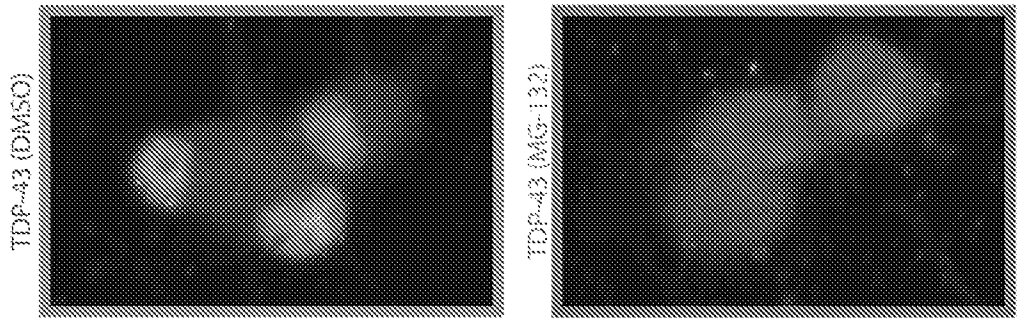

DAPI and TDP-43
Correlation Coefficient
1.0
0.8
0.6
0.4
0.2
0.0
n.s.
****
n.s.
Untreated
DMSO
Day 1
Day 2
Day 3
Day 4
Day 5
Day 6
Day 7
Days post Washout

FIG. 39


TDP-43 (DMSO)
TDP-43 (MG-132)

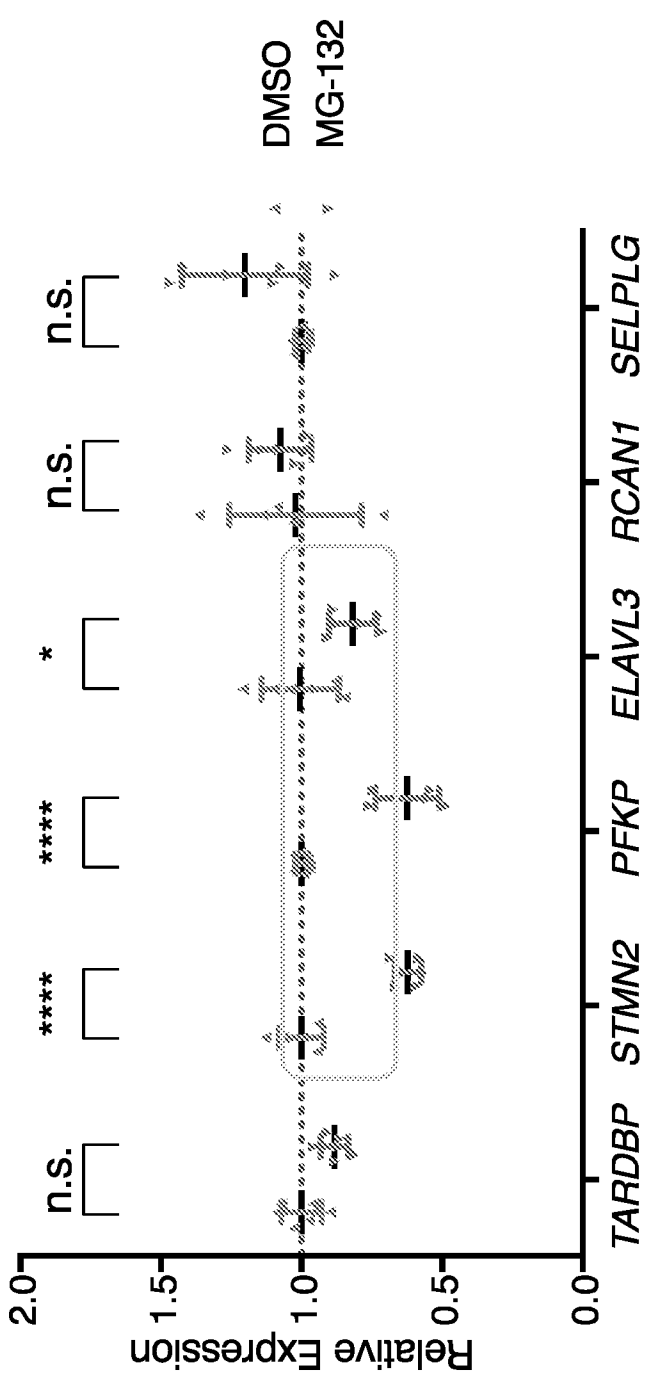

DMSO
MG-132
n.s.
n.s.
*
****
****
n.s.
Relative Expression
2.0
1.5
1.0
0.5
0.0
TARDBP
STMN2
PFKP
ELAVL3
RCAN1
SELPLG

FIG. 40

Gene	Locus	Inheritance	Level of evidence[a]	Mutation frequency							TDP-43 pathology	Implicated protein pathway
				Gene ALS (%)	Familial ALS (%)	Sporadic ALS (%)	Overall FTD (%)	Familial FTD (%)	Sporadic FTD (%)	ALS-FTD (%)		
TBK1[b]	12q14.2	AD[c]	Established	1.3	3	<1	<1	2	1	3–4	+	Autophagy, inflammation
C9ORF72	22q11.23	AD	Established	<1	2	<1	<1	<1	<1	<1	+	Mitochondria dysfunction, synaptic integrity
TUBA4A	2q35	AD	To be validated	<1	1	<1	<1	<1	~	~	+	Cytoskeletal dynamics, axonal transport
MATR3	5q31.2	AD	Established	<1	1–2	1	~	~	~	~	+	RNA metabolism
CCNF	16p13.3	AD	Established	<1	0.6–3.3	<1	4[d]	~	~	~	+	Proteostasis
MERTK[b]	4q33	n.d.[c]	To be validated	1	1–2	<1	~	~	~	~	n.d.	DNA damage responses, cell cycle control, cytoskeletal organization, mitochondrial membrane regulation
C21orf2[b]	21q22.3	n.d.	To be validated	<1	~	~	~	~	~	~	n.d.	DNA damage response, cytoskeletal organization
ANXA11	10q22.3	AD	To be validated	1.1	1	1.7	~	~	~	~	+	Proteostasis
TIA1	2p13.3	AD	To be validated	<1	2.2	<1	~	~	~	<1	+	RNA metabolism

-Nguyen, et al., Trends in Genetics, 2018

FIG. 41

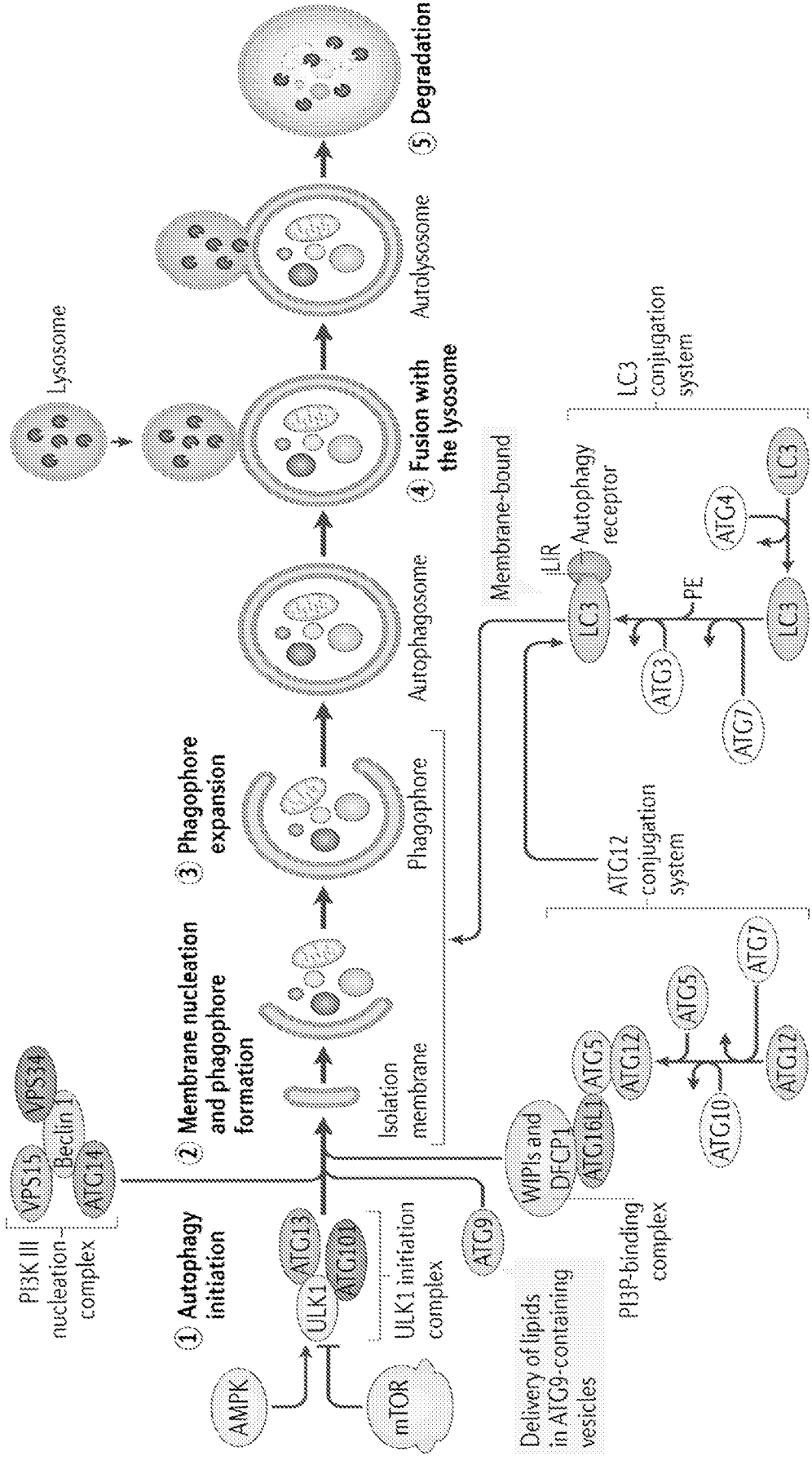


FIG. 42

--Hansen, et, al,. Nature Reviews Molecular Cell Biology. 2018

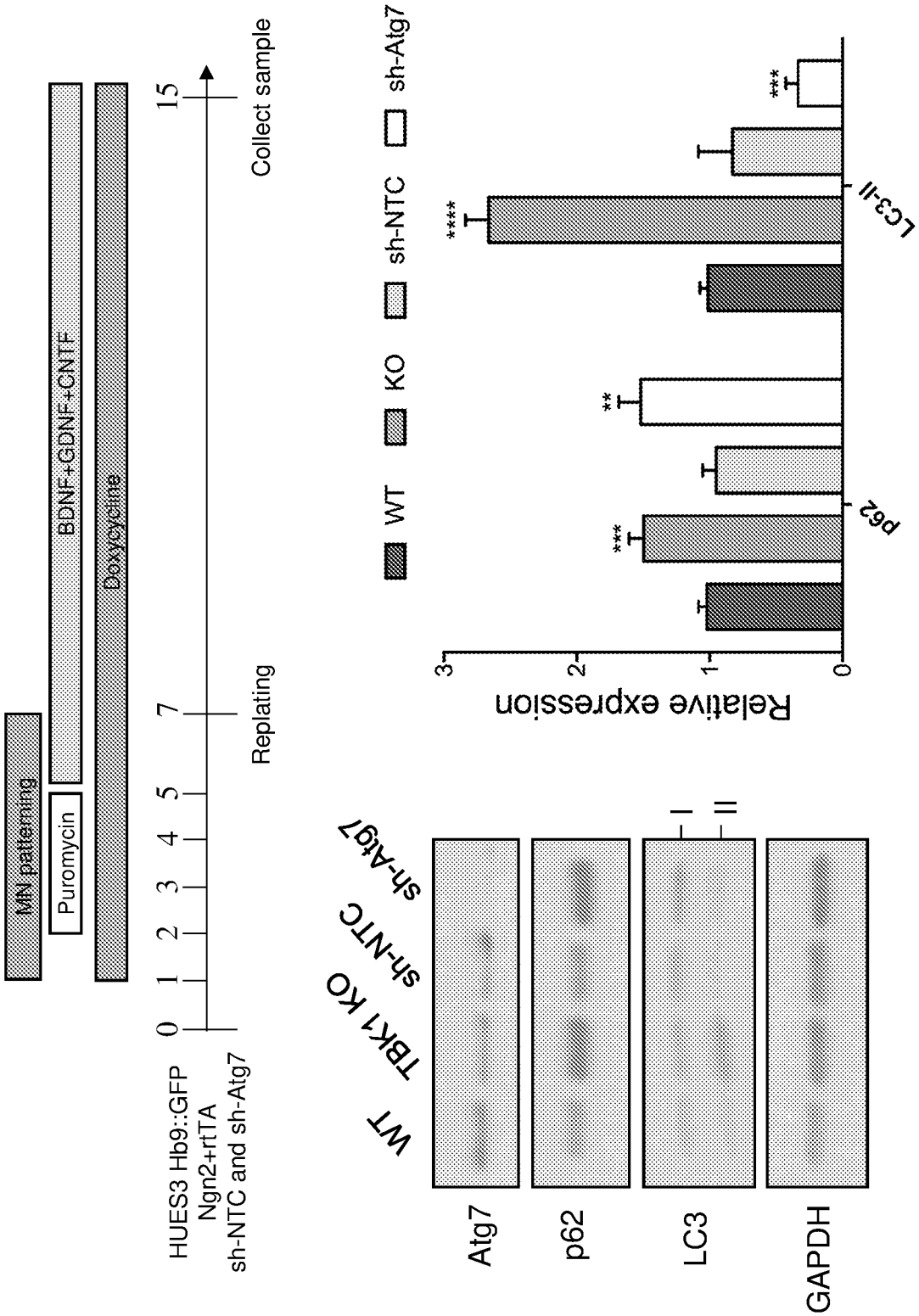

MN patterning
Puromycin
BDNF+GDNF+CNTF
Doxycycline
0 1 2 3 4 5 7 15
Replating
Collect sample
HUES3 Hb9::GFP
Ngn2+rtTA
sh-NTC and sh-Atg7
WT
TBK1 KO
sh-NTC
sh-Atg7
Atg7
p62
LC3
GAPDH
I
II
WT
KO
sh-NTC
sh-Atg7
Relative expression
0
1
2
3
p62
LC3-II
***
**
****
***

FIG. 43

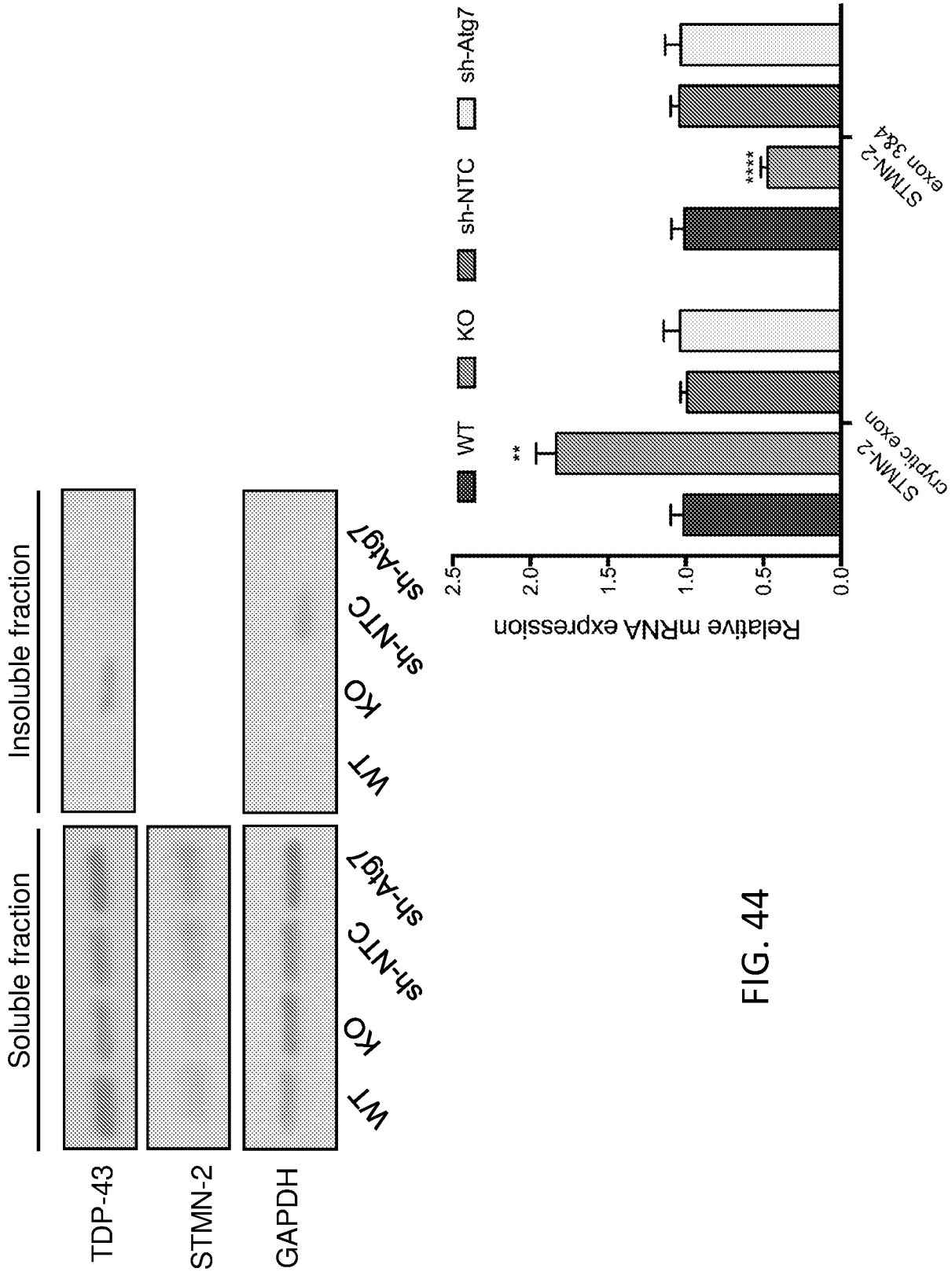

Soluble fraction
Insoluble fraction
TDP-43
STMN-2
GAPDH
WT
KO
sh-NTC
sh-Atg7
Relative mRNA expression
2.5
2.0
1.5
1.0
0.5
0.0
**
****
STMN-2 cryptic exon
STMN-2 exon 3&4

FIG. 44

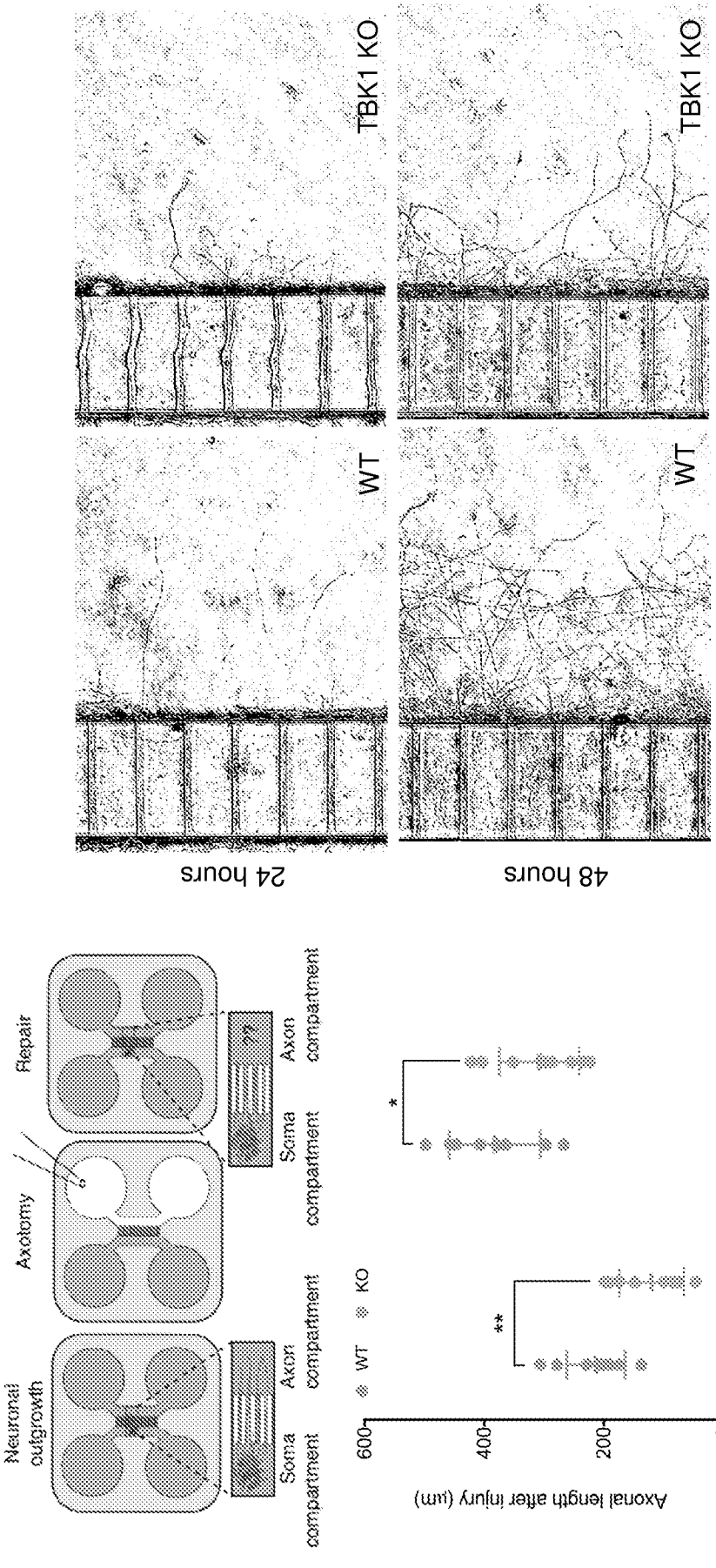

24 hours
48 hours
WT
TBK1 KO
WT
TBK1 KO
Neuronal outgrowth
Soma compartment
Axon compartment
Axotomy
Soma compartment
Axon compartment
Repair
WT
KO
Axonal length after injury (µm)
600
400
200
0
**
*
24 h
48 h

FIG. 45

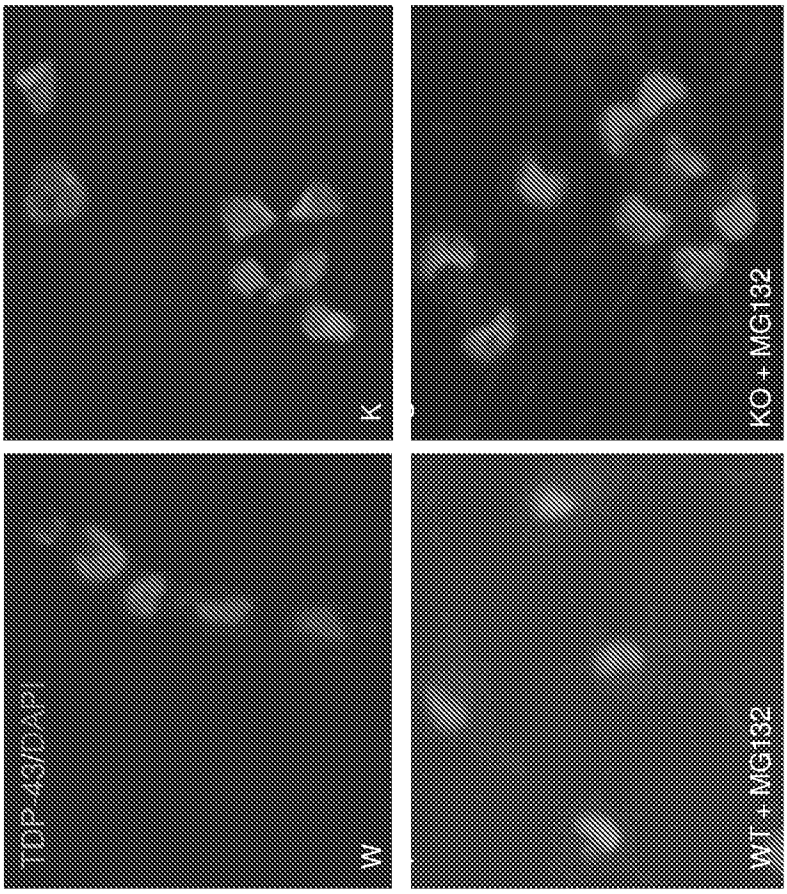


FIG. 46

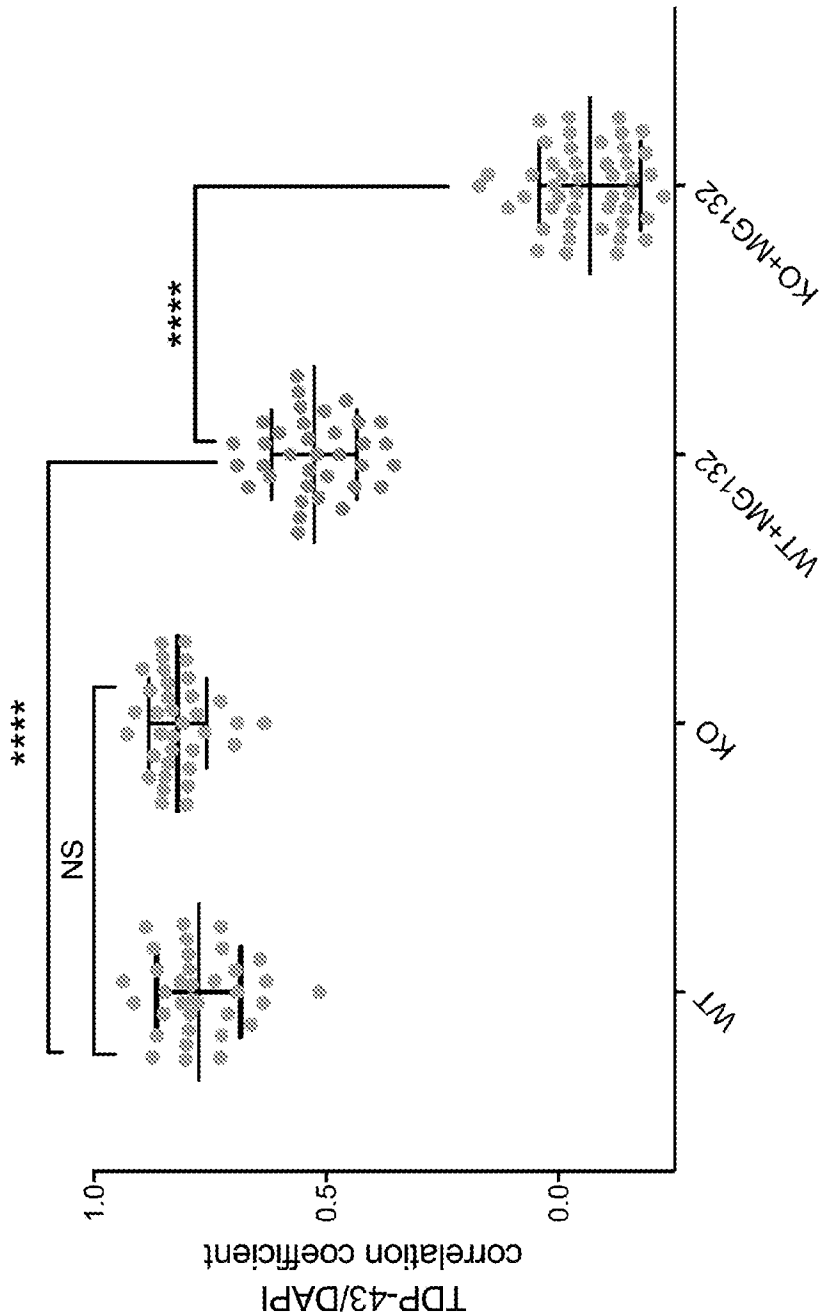

TDP-43/DAPI
correlation coefficient
1.0
0.5
0.0
WT
KO
WT+MG132
KO+MG132
NS
****
****

FIG. 46 cont.

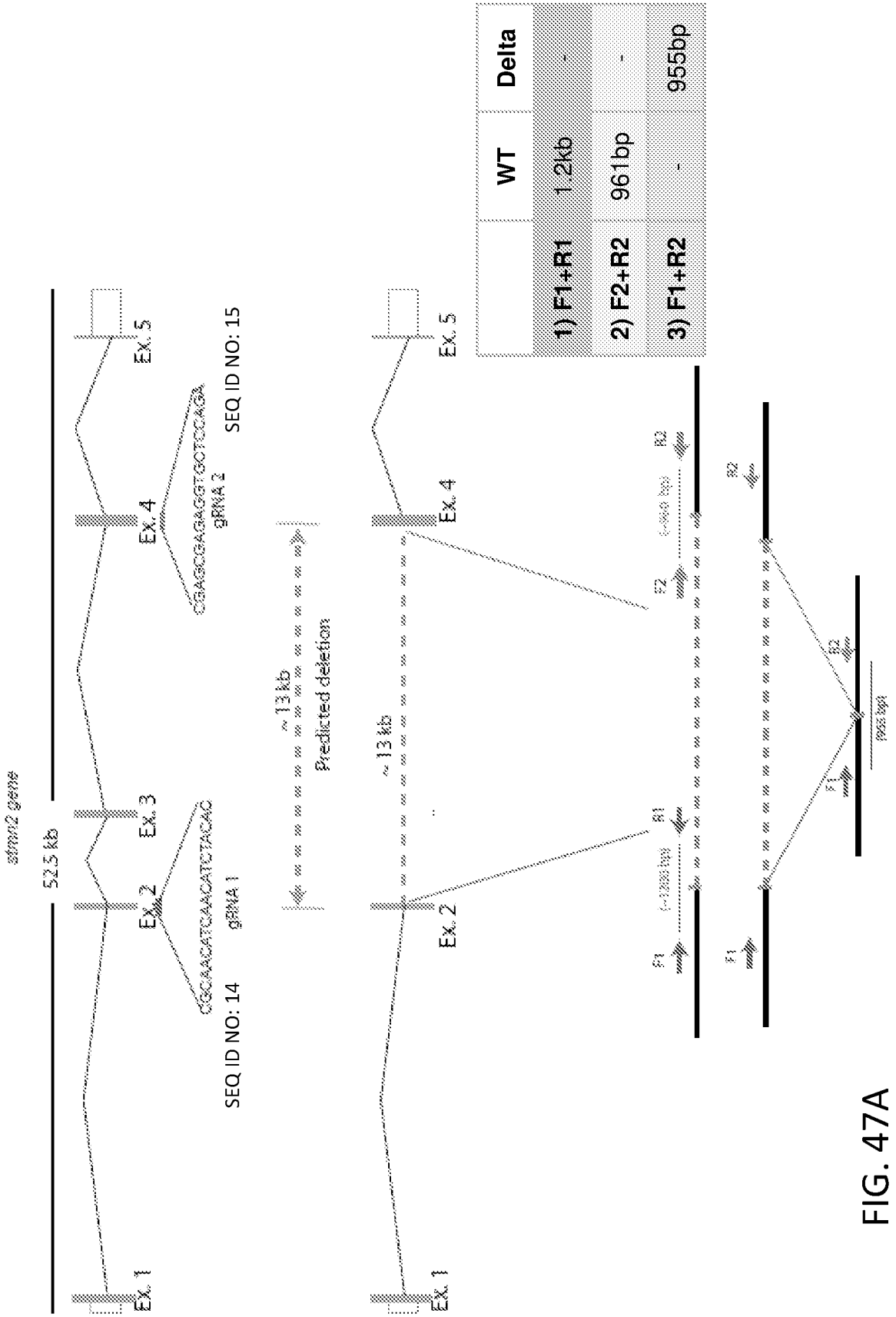

stmn2 gene
52.5 kb
Ex. 1
Ex. 2
Ex. 3
Ex. 4
Ex. 5
CGCAACATCAACATCTACAC
gRNA 1
SEQ ID NO: 14
CGAGCGAGAGGTGCTCCAGA
gRNA 2
SEQ ID NO: 15
~13 kb
Predicted deletion
F1
R1
F2
R2
WT
Delta
1) F1+R1
1.2kb
-
2) F2+R2
961bp
-
3) F1+R2
-
955bp

FIG. 47A

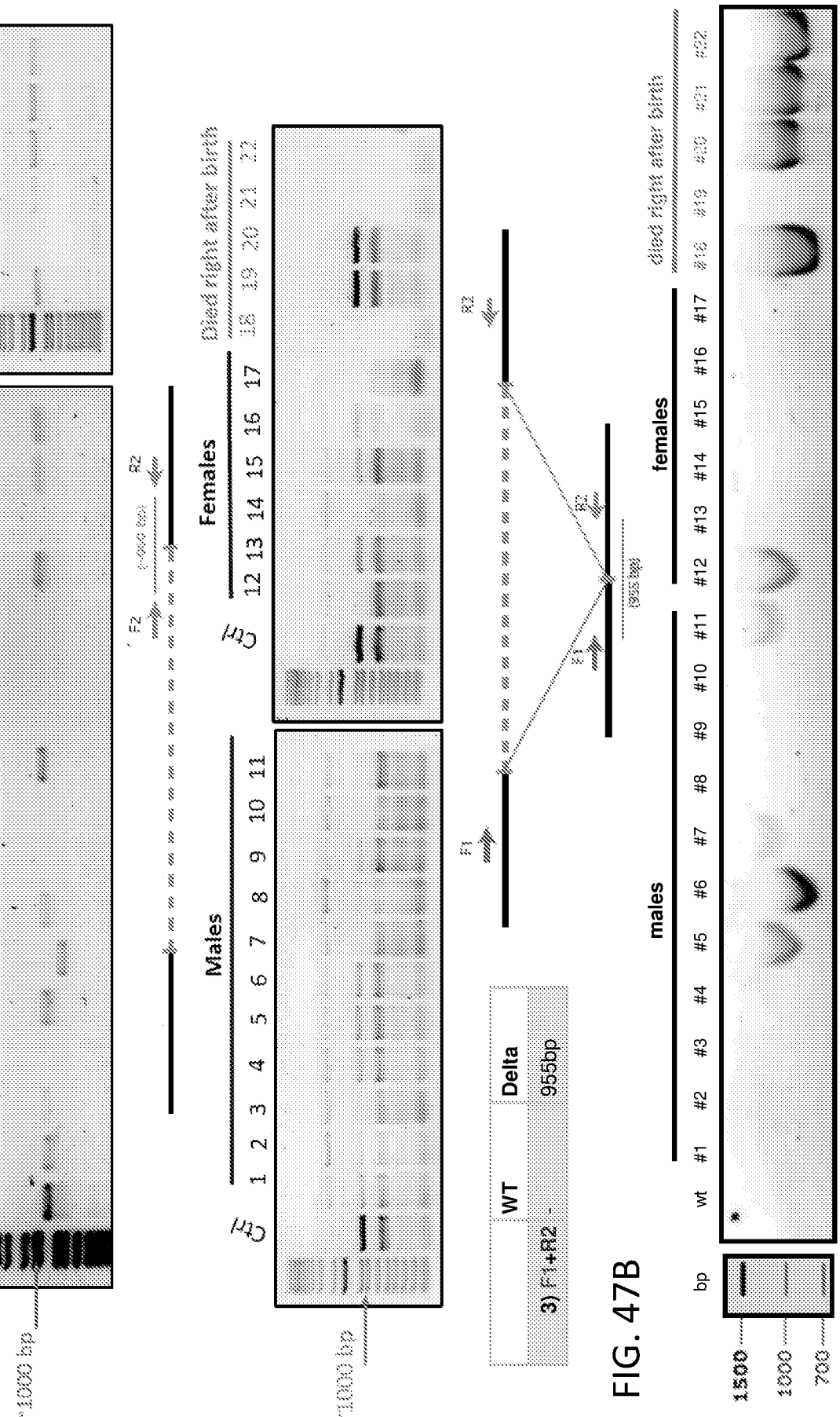

Males
Females
Died right after birth
~1000 bp
F1
F2
R2
WT
Delta
3) F1+R2
955bp
males
females
bp
wt
1500
1000
700

FIG. 47B

Mouse ID and sex	Guide Target Site?	PCR Band Analysis			Sequence analysis		Comments
		WT band	Band shift or no band	13 Kb deletion?	% of WT Sequence	% Indel Frequency	
1 - M	Exon 2	Y				27 (-8 nt) 21 (-3 nt) 18.7 (-1 nt)	
	Exon 4	Y				26 (-14 nt) 28 (-12 nt) 0.40 (-9 nt)	
2 - M	Exon 2	Y				0.84 (+1 nt)	
	Exon 4	Y				0.82 (-12 nt)	
3 - M	Exon 2	N	Y		failed	failed	
	Exon 4	Y			failed	failed	
4 - M	Exon 2	Y				20.4 (-27 nt)[illegible] (-9 nt)	
	Exon 4	Y				0.96 (-12 nt)	
5 - M	Exon 2	N	Y	Y		0	
	Exon 4	Y				0.87 (-1 nt)	
6 - M	Exon 2	Y		Y		0.84 (-17 nt)	
	Exon 4	Y				0.87 (-12 nt)	
7 - M	Exon 2	N	Y	Y	failed	failed	
	Exon 4	Y			failed	failed	
8 - M	Exon 2	Y	Y			58 (-28 nt) 11 (-22 nt) 3 (-3 nt) 0.8 (+26 nt)	
	Exon 4	Y				0.95 (-11 nt)	
9 - M	Exon 2	Y				5.3 65 (+1 nt)	
	Exon 4	Y				38 (-12 nt) 38 (-11 nt) 0.20 (-9 nt)	
10 - M	Exon 2	N	Y		?	?	
	Exon 4	N	Y		?	?	
11 - M	Exon 2	N	Y	Y			
	Exon 4	N	Y				
12 - F	Exon 2	N	Y	Y			
	Exon 4	N	Y				
13 - F	Exon 2	Y	Y			23.72 (+1 nt)	
	Exon 4	N	Y			0.98 (-12 nt)	
14 - F	Exon 2	N	Y			0.55 (-28 nt)[illegible] (-10 nt)[illegible] (+1 nt)	
	Exon 4	Y					
15 - F	Exon 2	Y				0.95 (+1 nt)	
	Exon 4	Y				0.98 (-12 nt)	
16 - F	Exon 2	Y				4 Mixed	
	Exon 4	Y				0.93 (-11 nt)	
17 - F	Exon 2	N	Y				
	Exon 4	N	Y				
18 -	Exon 2	Y		Y		67 -	
	Exon 4	N					
19 -	Exon 2	Y				80.56 (+1 nt)	
	Exon 4	Y				0.96 (-1 nt)	
20 -	Exon 2	Y		Y		0.97 (+2 nt)	
	Exon 4	Y				0.95 (-11 nt)	
21 -	Exon 2	Y		Y		0.95 (-6 nt)	
	Exon 4	Y				0.96 (-11 nt)	
22 -	Exon 2	Y		Y		0.99 (-3 nt)	
	Exon 4	N					

FIG. 47C

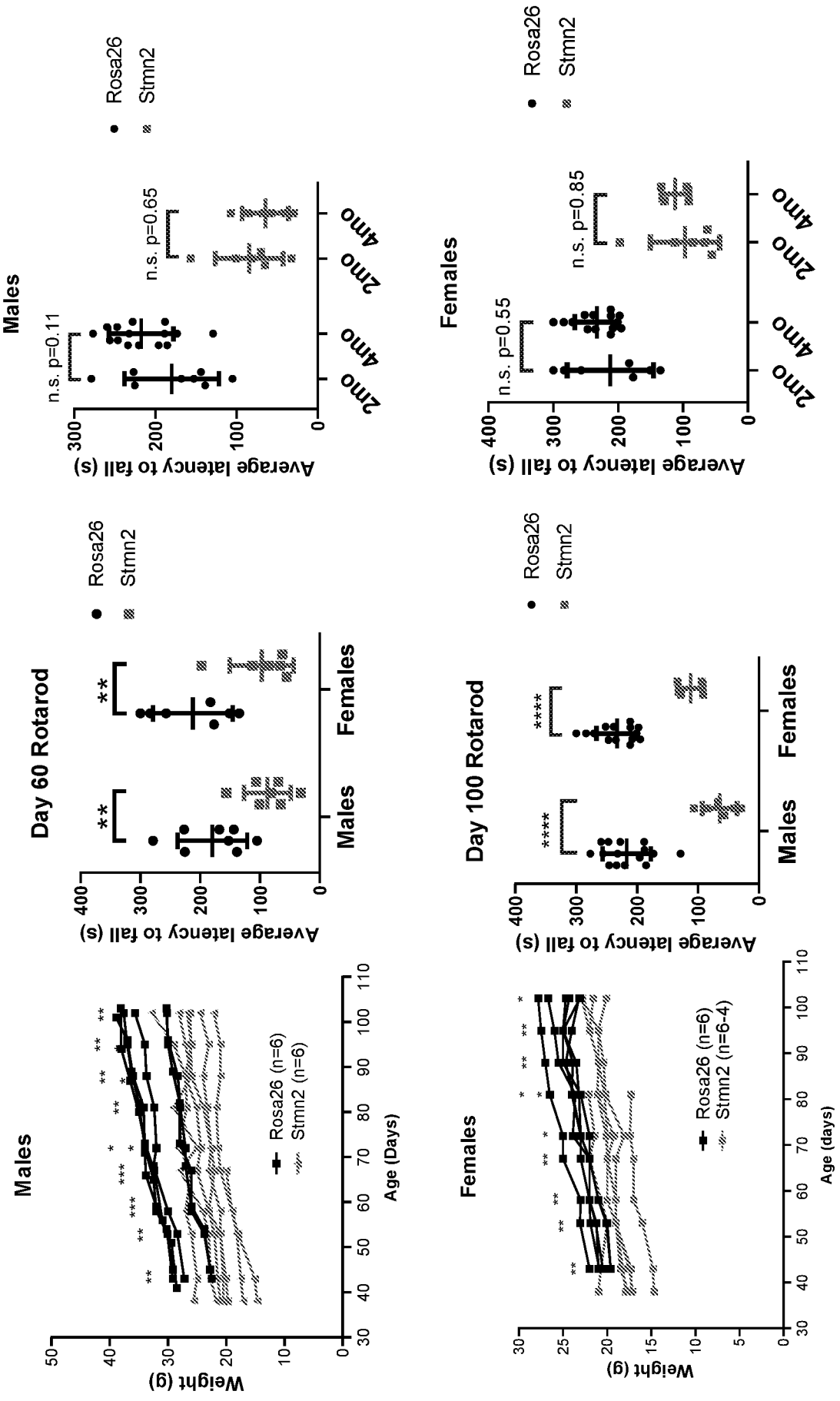

Males
Weight (g)
Age (Days)
Rosa26 (n=6)
Stmn2 (n=6)
Day 60 Rotarod
Average latency to fall (s)
Rosa26
Stmn2
Males
Females
n.s. p=0.11
n.s. p=0.65
2mo
4mo
Females
Weight (g)
Age (days)
Rosa26 (n=6)
Stmn2 (n=6-4)
Day 100 Rotarod
n.s. p=0.55
n.s. p=0.85

FIG. 48

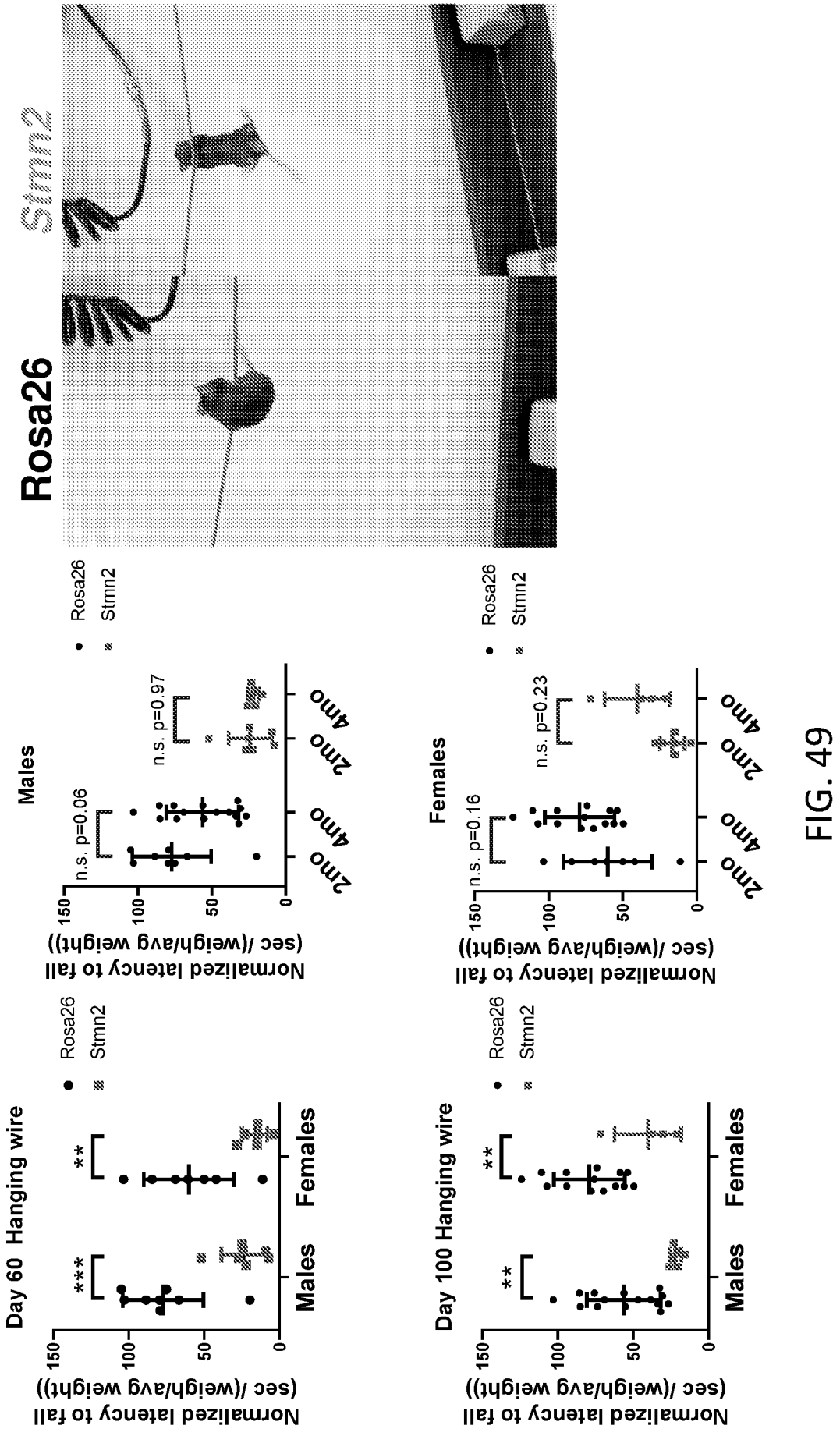

Rosa26
Stmn2
Day 60 Hanging wire
Normalized latency to fall (sec /(weigh/avg weight))
Rosa26
Stmn2
***
**
Males
Females
Males
n.s. p=0.06
n.s. p=0.97
2mo
4mo
2mo
4mo
Day 100 Hanging wire
**
**
Females
n.s. p=0.16
n.s. p=0.23

FIG. 49

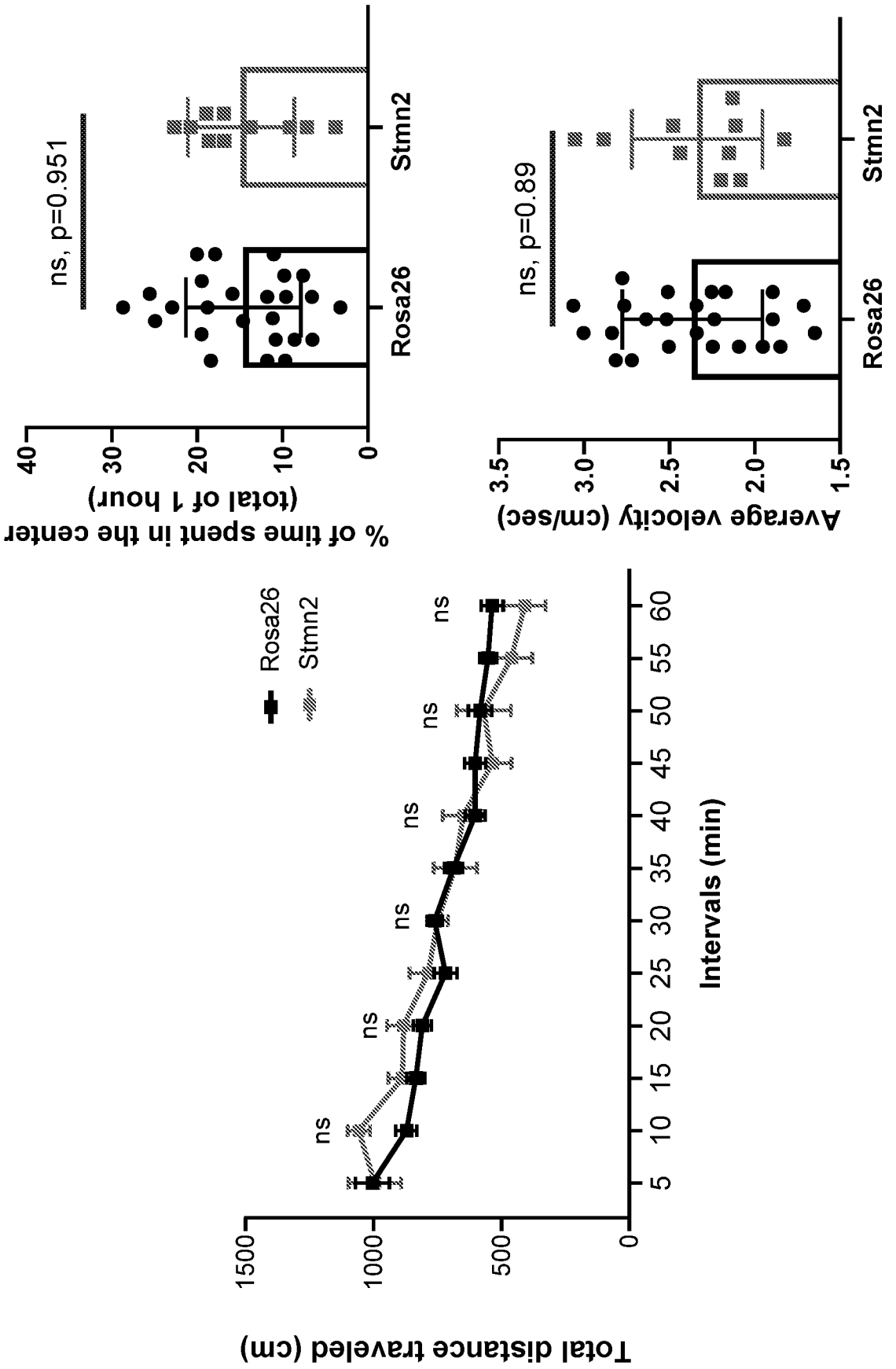
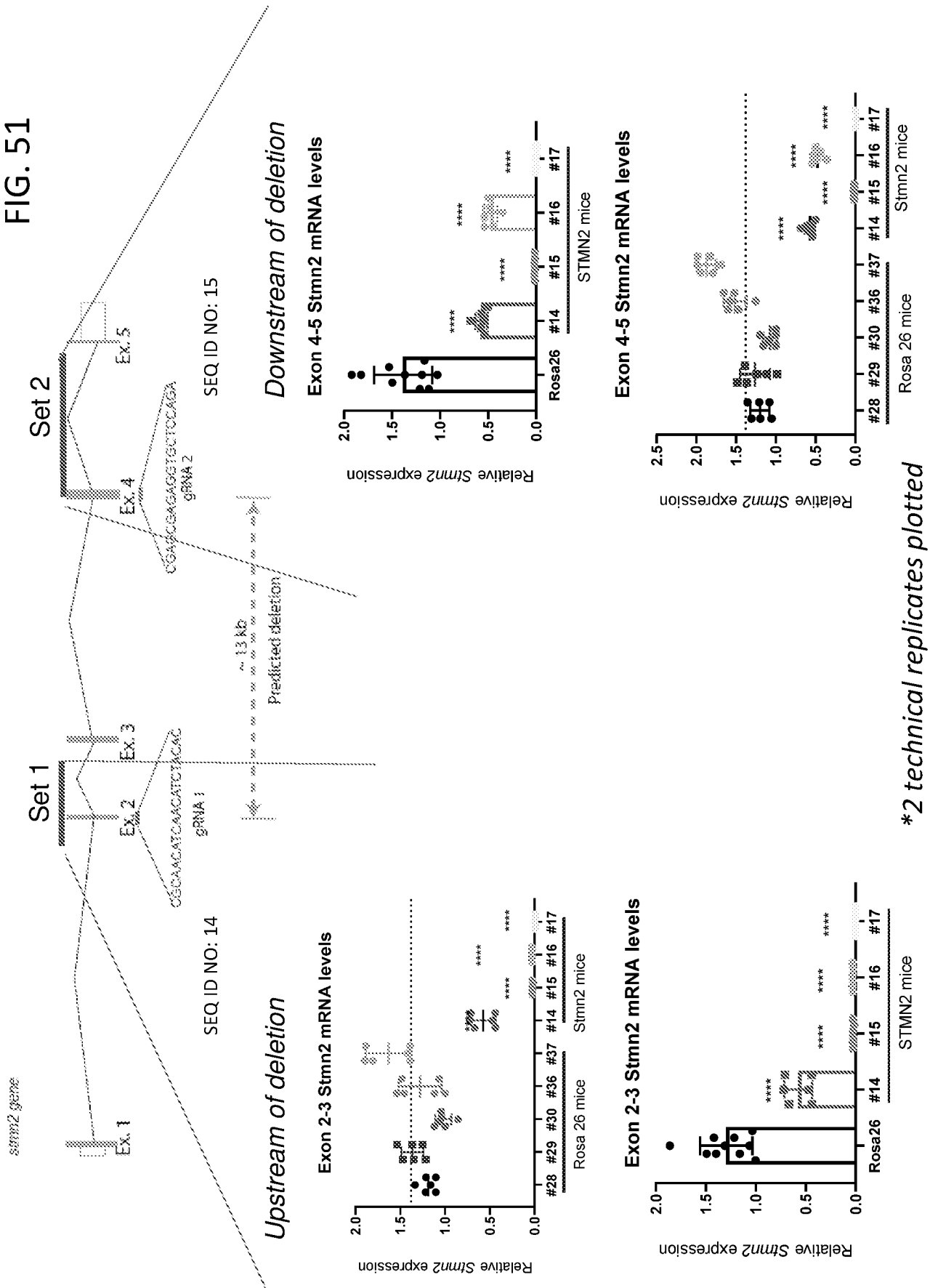

Total distance traveled (cm)
1500
1000
500
0
5 10 15 20 25 30 35 40 45 50 55 60
Intervals (min)
Rosa26
Stmn2
ns
ns
ns
ns
ns
ns
% of time spent in the center (total of 1 hour)
40
30
20
10
0
ns, p=0.951
Rosa26
Stmn2
Average velocity (cm/sec)
3.5
3.0
2.5
2.0
1.5
ns, p=0.89
Rosa26
Stmn2

FIG. 50

FIG. 51


stmn2 gene
Set 1
Set 2
Ex. 1
Ex. 2
Ex. 3
Ex. 4
Ex. 5
CGCAACATCAACATCTACAC
gRNA 1
CGAGCGAGAGGTGCTCCAGA
gRNA 2
SEQ ID NO: 14
SEQ ID NO: 15
~ 13 kb
Predicted deletion
Upstream of deletion
Downstream of deletion
Exon 2-3 Stmn2 mRNA levels
Exon 4-5 Stmn2 mRNA levels
Relative Stmn2 expression
Rosa26 #14 #15 #16 #17
STMN2 mice
#28 #29 #30 #36 #37 #14 #15 #16 #17
Rosa 26 mice
Stmn2 mice
****
*2 technical replicates plotted

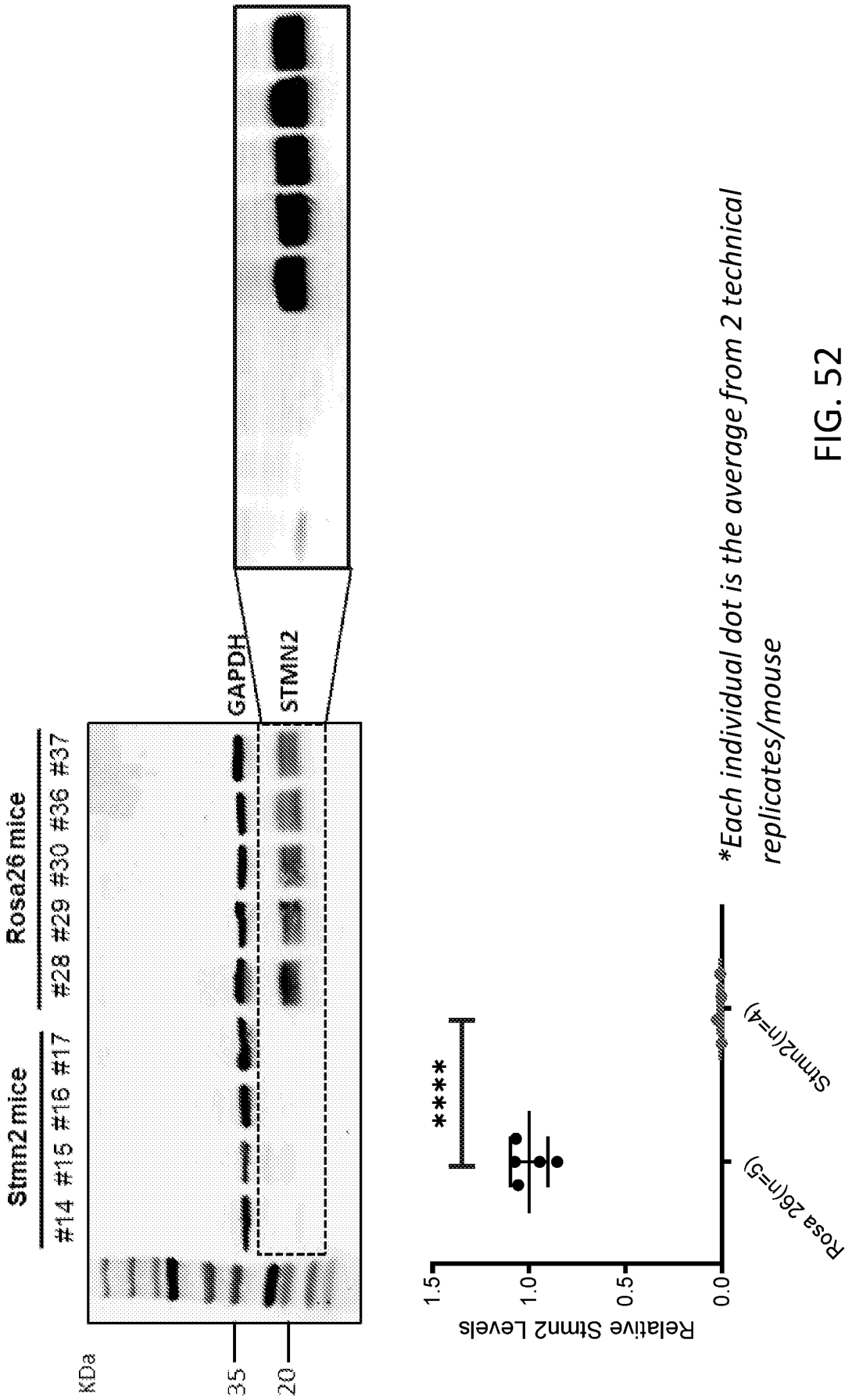

Stmn2 mice
#14 #15 #16 #17
Rosa26 mice
#28 #29 #30 #36 #37
GAPDH
STMN2
KDa
35
20
****
Relative Stmn2 Levels
1.5
1.0
0.5
0.0
Rosa 26(n=5)
Stmn2(n=4)
*Each individual dot is the average from 2 technical replicates/mouse

FIG. 52

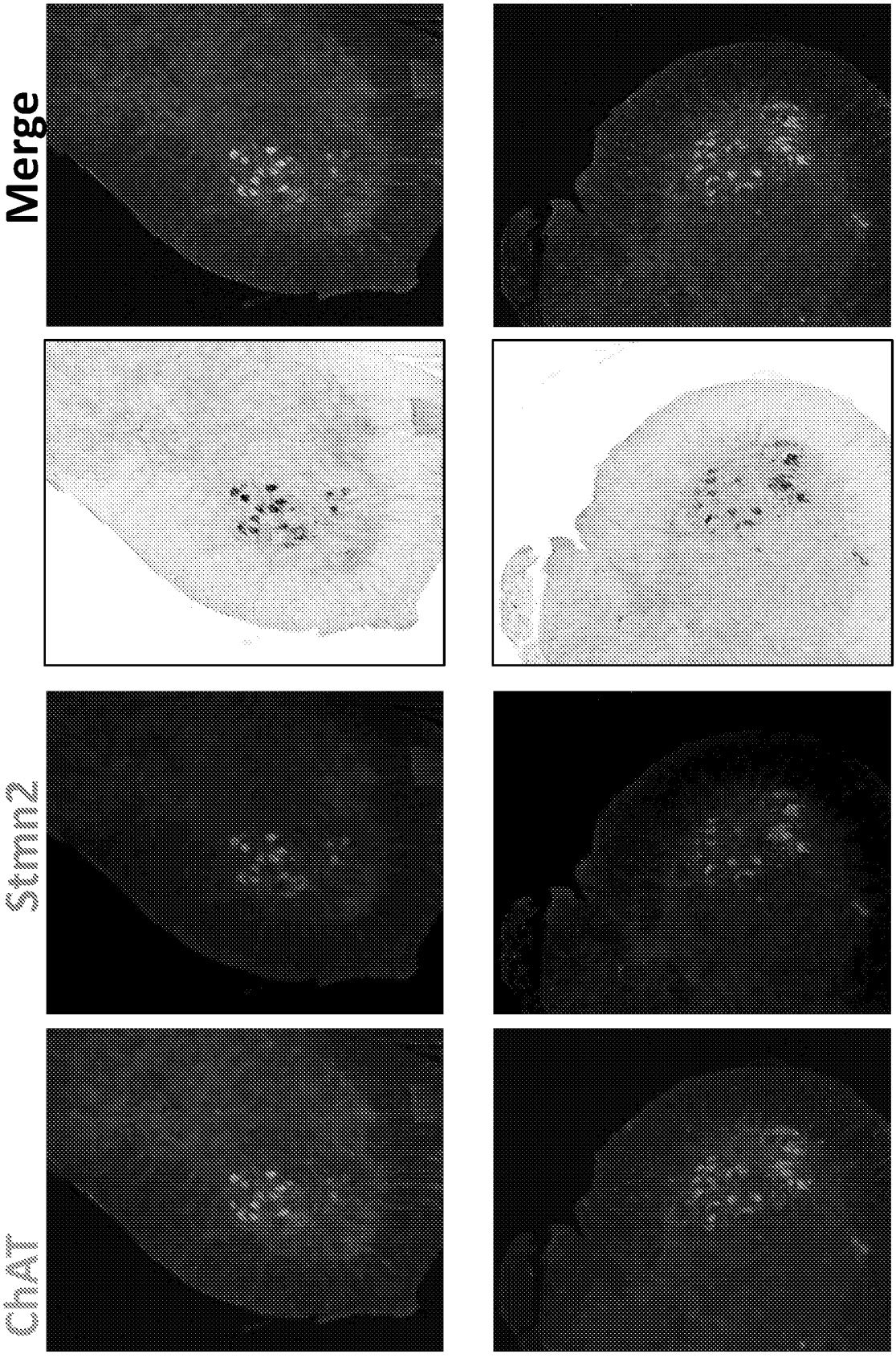


FIG. 53

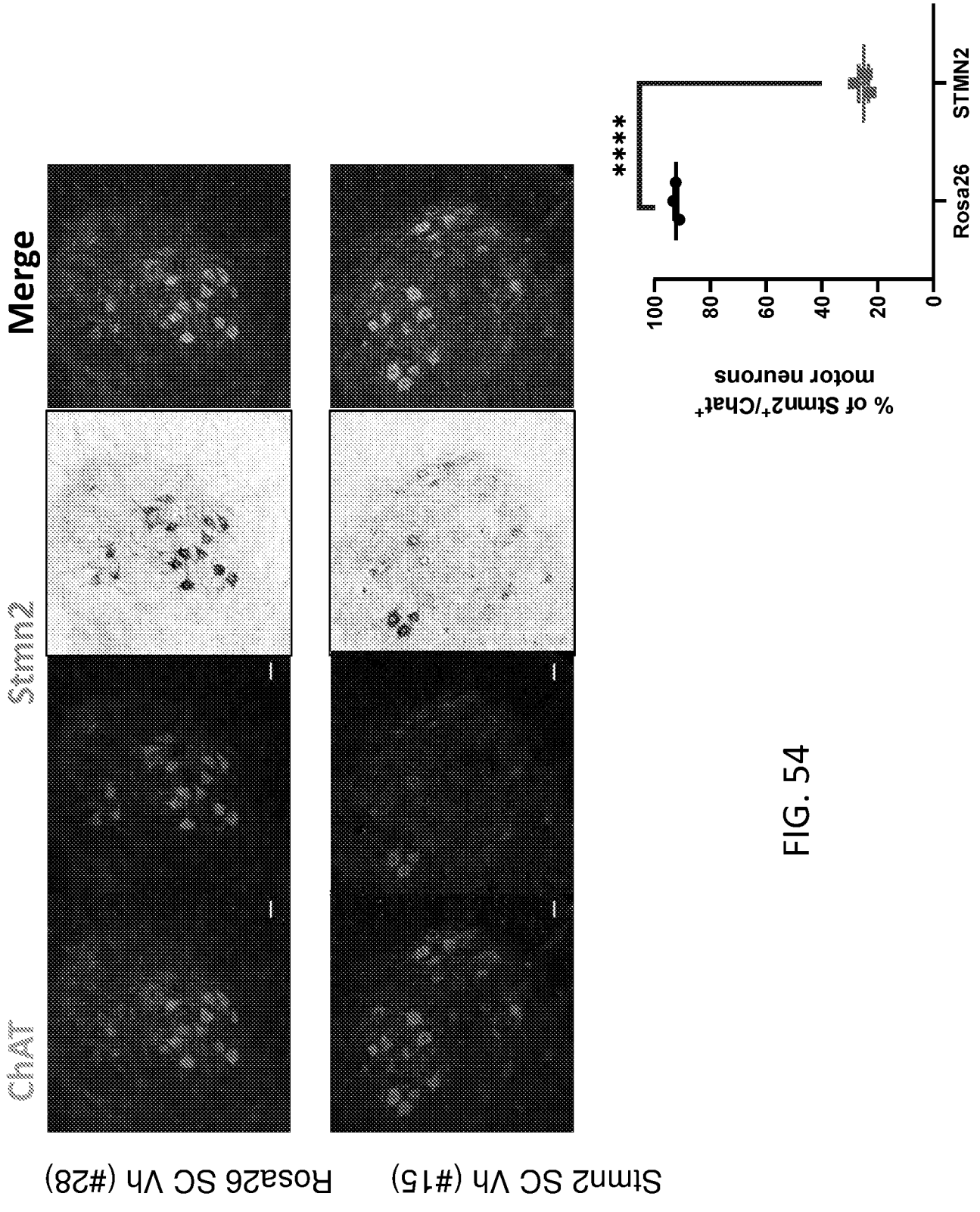

ChAT
Stmn2
Merge
Stmn2 SC Vh (#15)
Rosa26 SC Vh (#28)
****
% of Stmn2+/Chat+ motor neurons
100
80
60
40
20
0
Rosa26
STMN2

FIG. 54

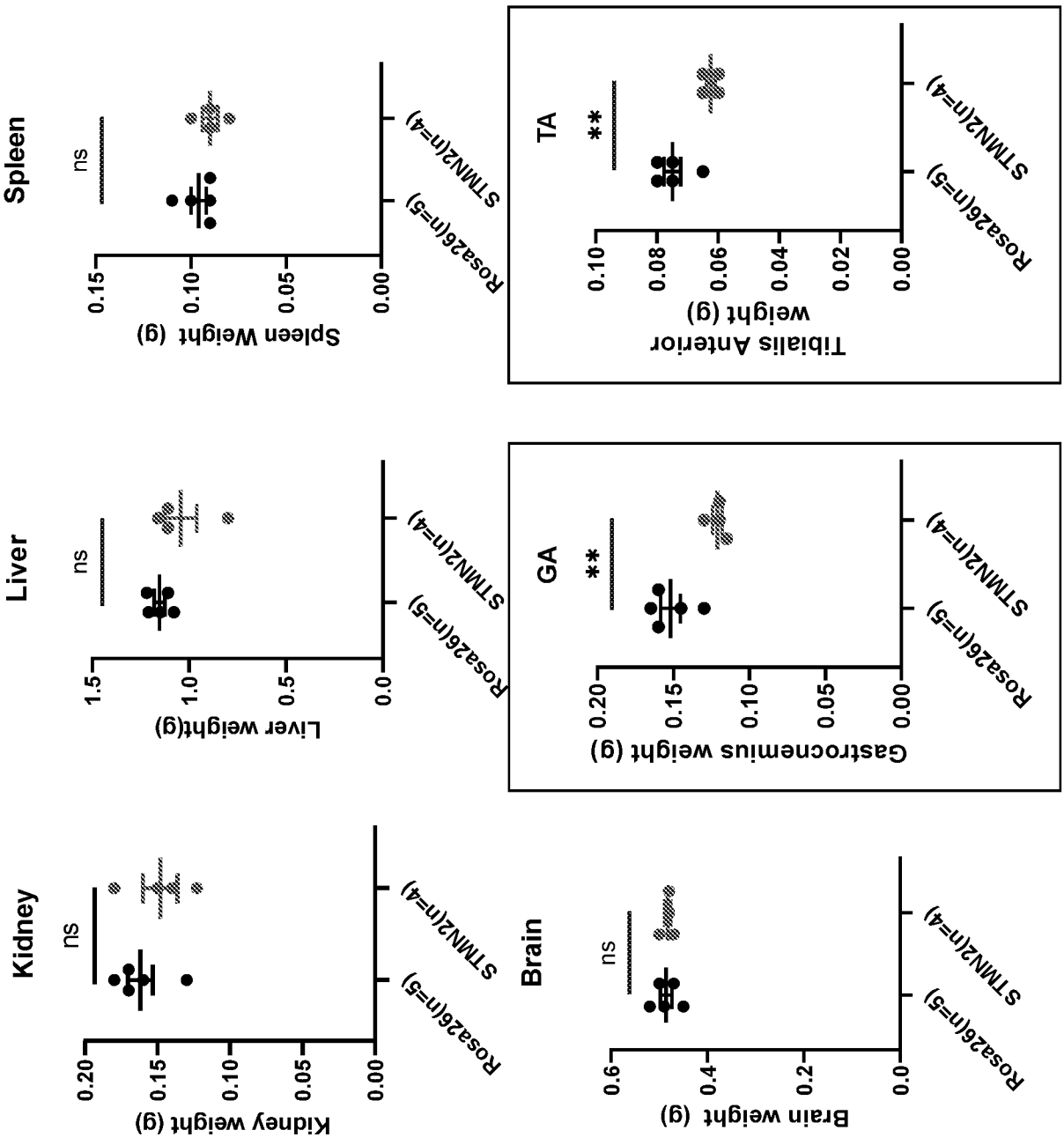

Kidney
ns
Kidney weight (g)
0.20
0.15
0.10
0.05
0.00
Rosa26(n=5)
STMN2(n=4)
Liver
ns
Liver weight(g)
1.5
1.0
0.5
0.0
Rosa26(n=5)
STMN2(n=4)
Spleen
ns
Spleen Weight (g)
0.15
0.10
0.05
0.00
Rosa26(n=5)
STMN2(n=4)
Brain
ns
Brain weight (g)
0.6
0.4
0.2
0.0
Rosa26(n=5)
STMN2(n=4)
GA
**
Gastrocnemius weight (g)
0.20
0.15
0.10
0.05
0.00
Rosa26(n=5)
STMN2(n=4)
TA
**
Tibialis Anterior weight (g)
0.10
0.08
0.06
0.04
0.02
0.00
Rosa26(n=5)
STMN2(n=4)

FIG. 55

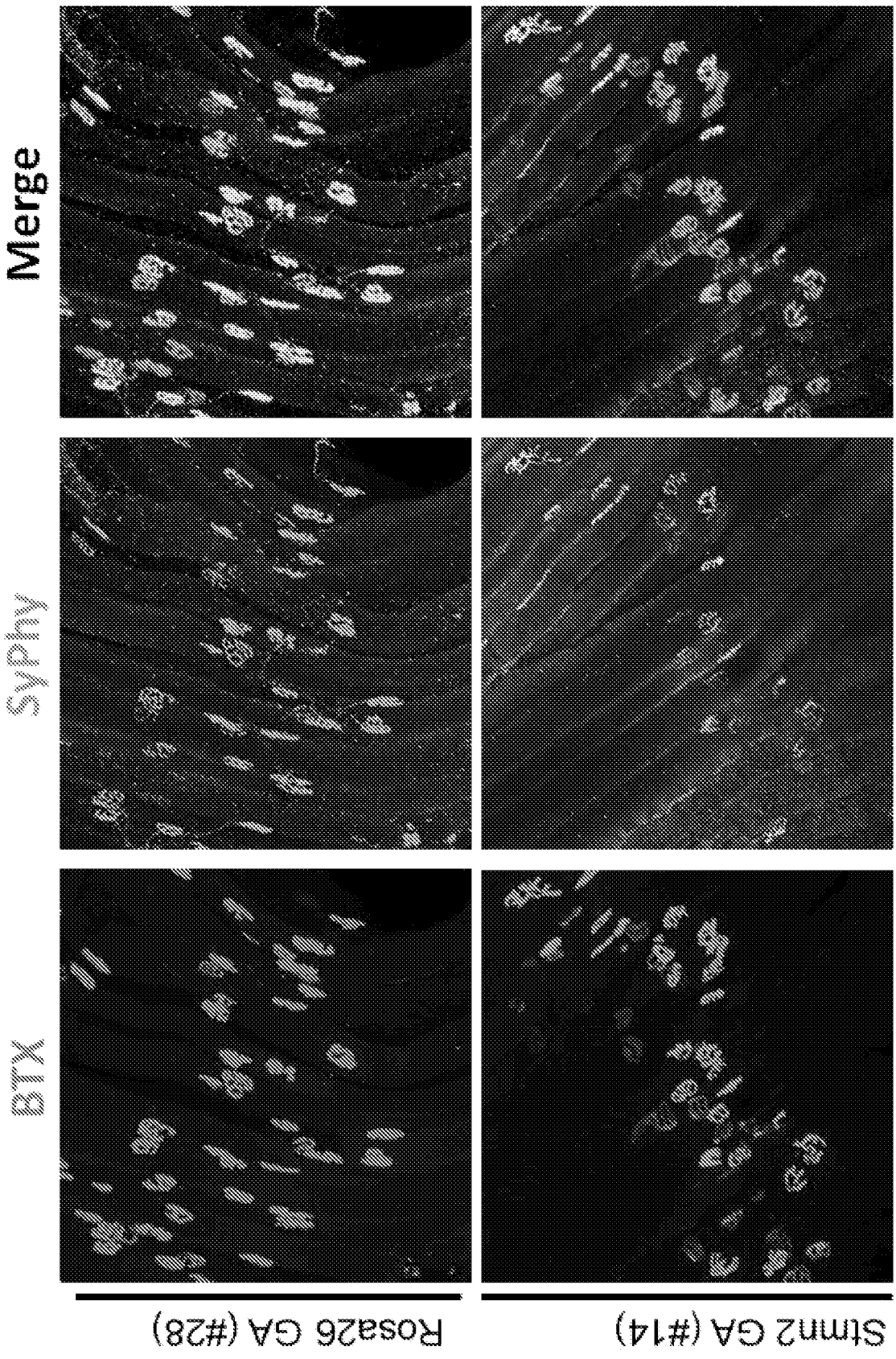


FIG. 56

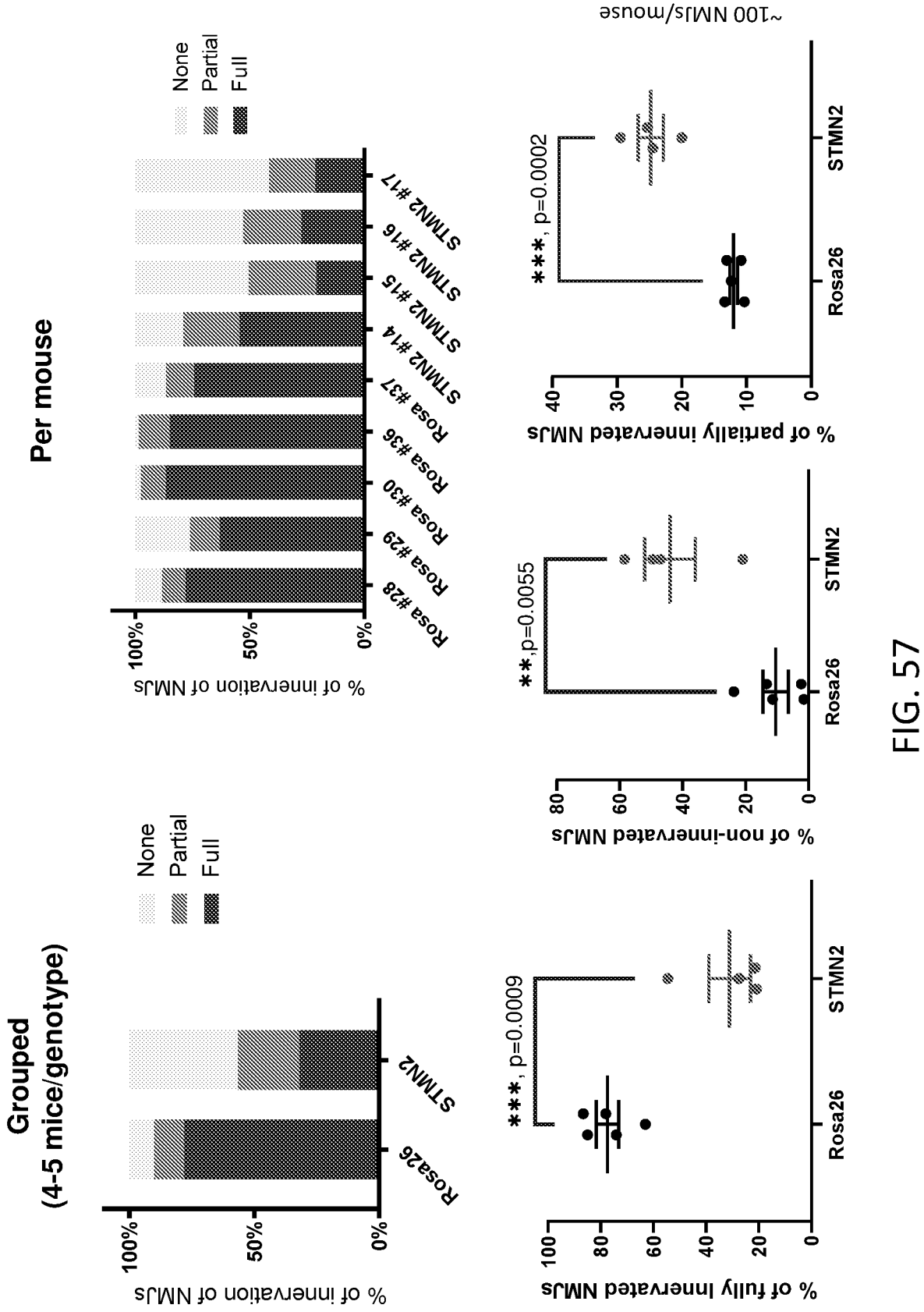

Grouped
(4-5 mice/genotype)
None
Partial
Full
% of innervation of NMJs
100%
50%
0%
Rosa26
STMN2
Per mouse
None
Partial
Full
% of innervation of NMJs
100%
50%
0%
Rosa #28
Rosa #29
Rosa #30
Rosa #36
Rosa #37
STMN2 #14
STMN2 #15
STMN2 #16
STMN2 #17
% of fully innervated NMJs
***, p=0.0009
Rosa26
STMN2
% of non-innervated NMJs
**,p=0.0055
Rosa26
STMN2
% of partially innervated NMJs
***, p=0.0002
Rosa26
STMN2
~100 NMJs/mouse

FIG. 57

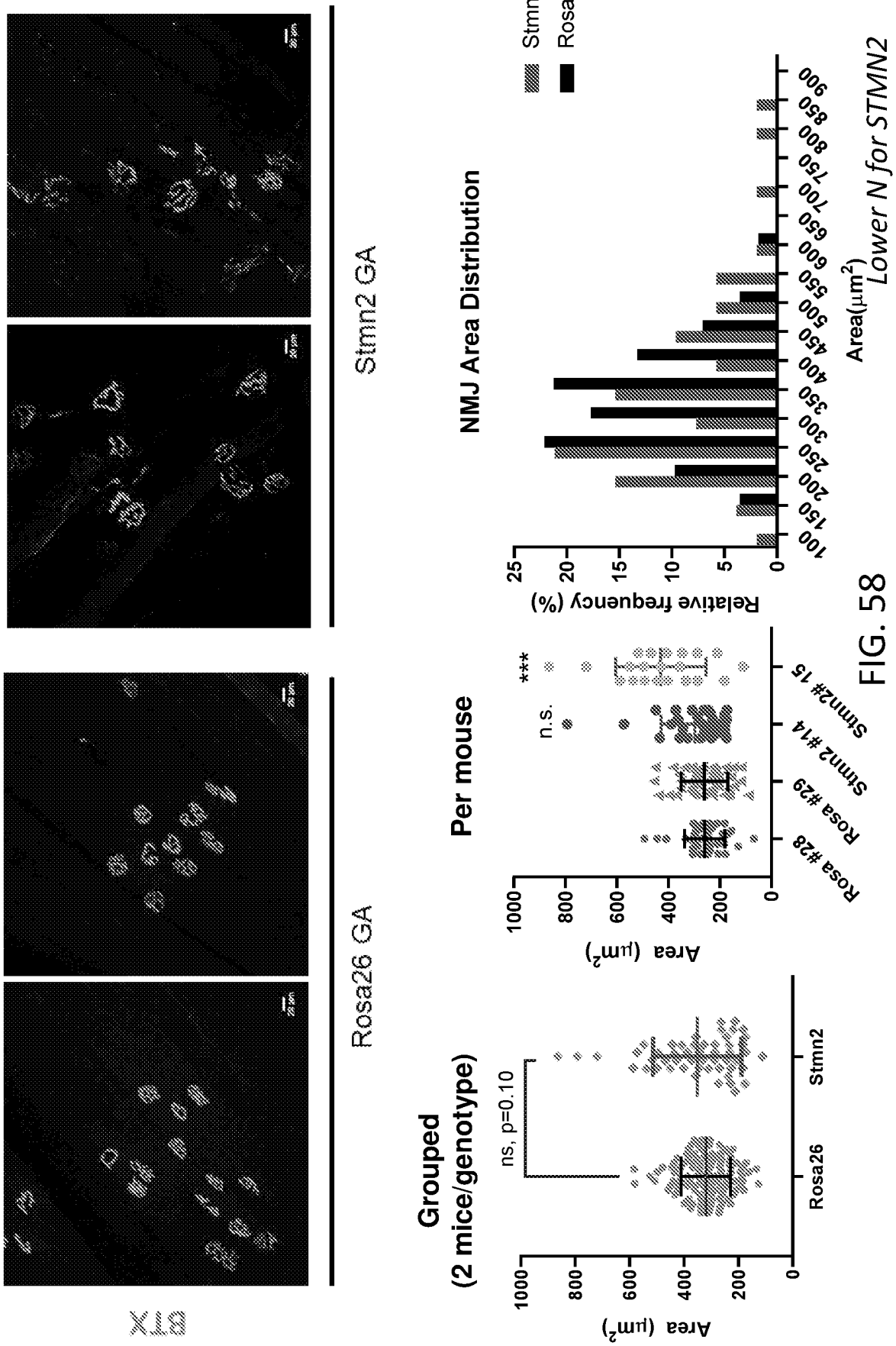

#28
#29
#14
#15
Rosa26 GA
Stmn2 GA
STX
Grouped
(2 mice/genotype)
ns, p=0.10
Area (μm²)
Rosa26
Stmn2
Per mouse
n.s.
***
Rosa #28
Rosa #29
Stmn2 #14
Stmn2# 15
NMJ Area Distribution
Stmn2
Rosa26
Relative frequency (%)
Area(μm²)
Lower N for STMN2

FIG. 58

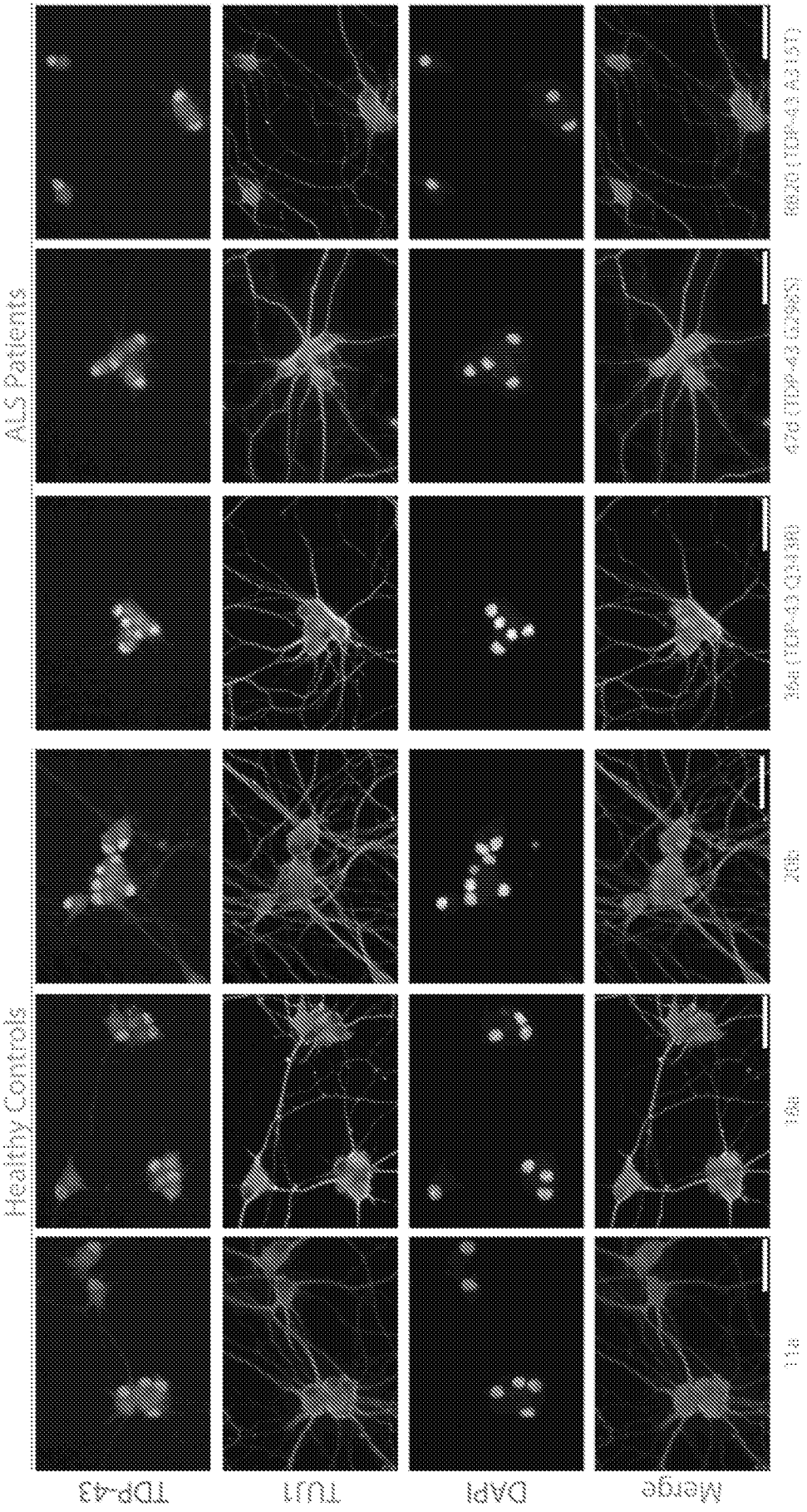

TDP-43
TUJ1
DAPI
Merge
ALS Patients
Healthy Controls
11a
16a
20b
36a (FUS-R521H)
67d (VCP-A232E)
69d (FUS-R495X)

FIG. 59

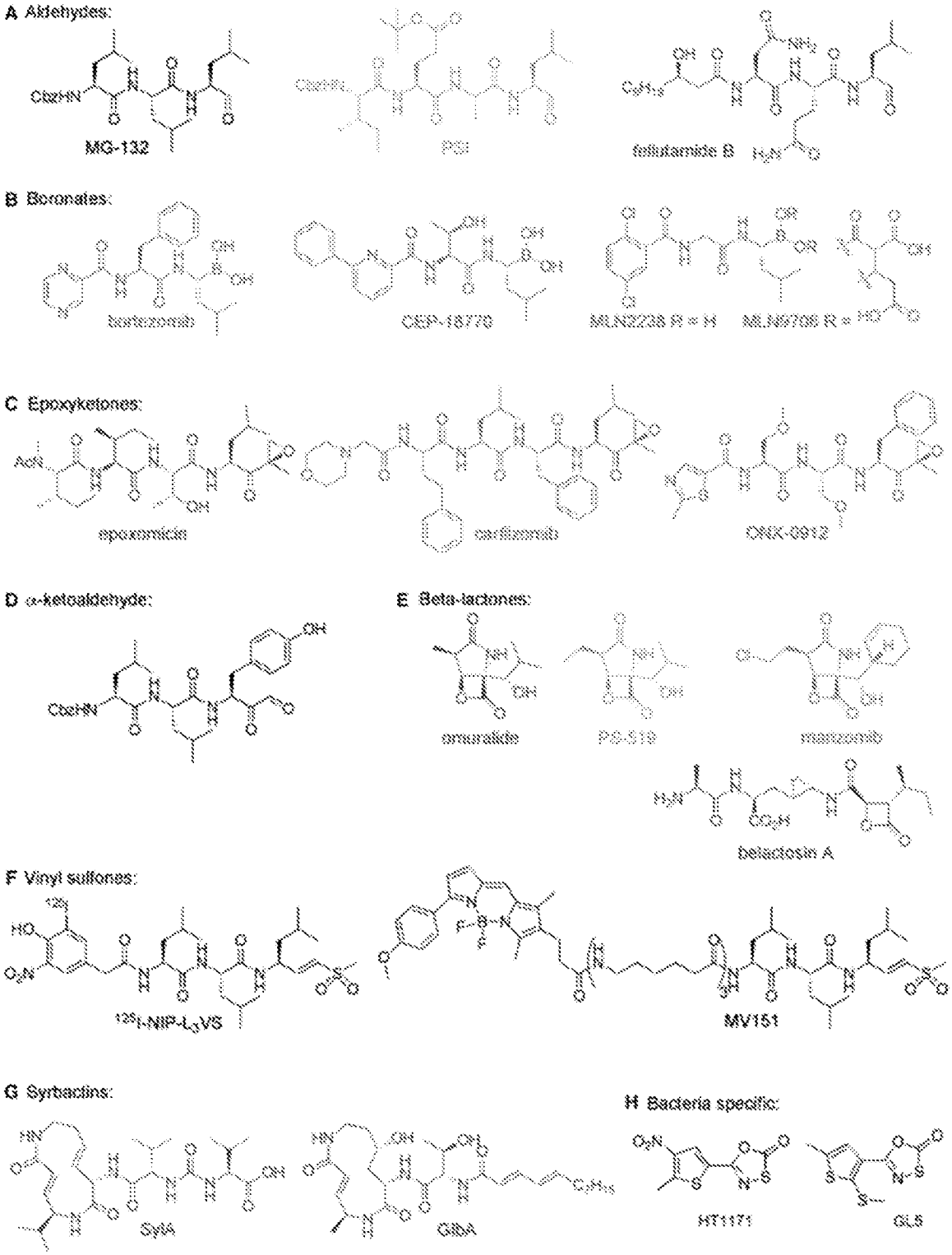

A Aldehydes:
MG-132
PSI
feltamide B
B Boronates:
bortezomib
CEP-18770
MLN2238 R = H
MLN9708 R =
C Epoxyketones:
epoxomicin
carfilzomib
ONX-0912
D α-ketoaldehyde:
E Beta-lactones:
omuralide
PS-519
marizomib
belactosin A
F Vinyl sulfones:
125I-NIP-L3VS
MV151
G Syrbactins:
SyA
GlbA
H Bacteria specific:
HT1171
GL8

FIG. 60

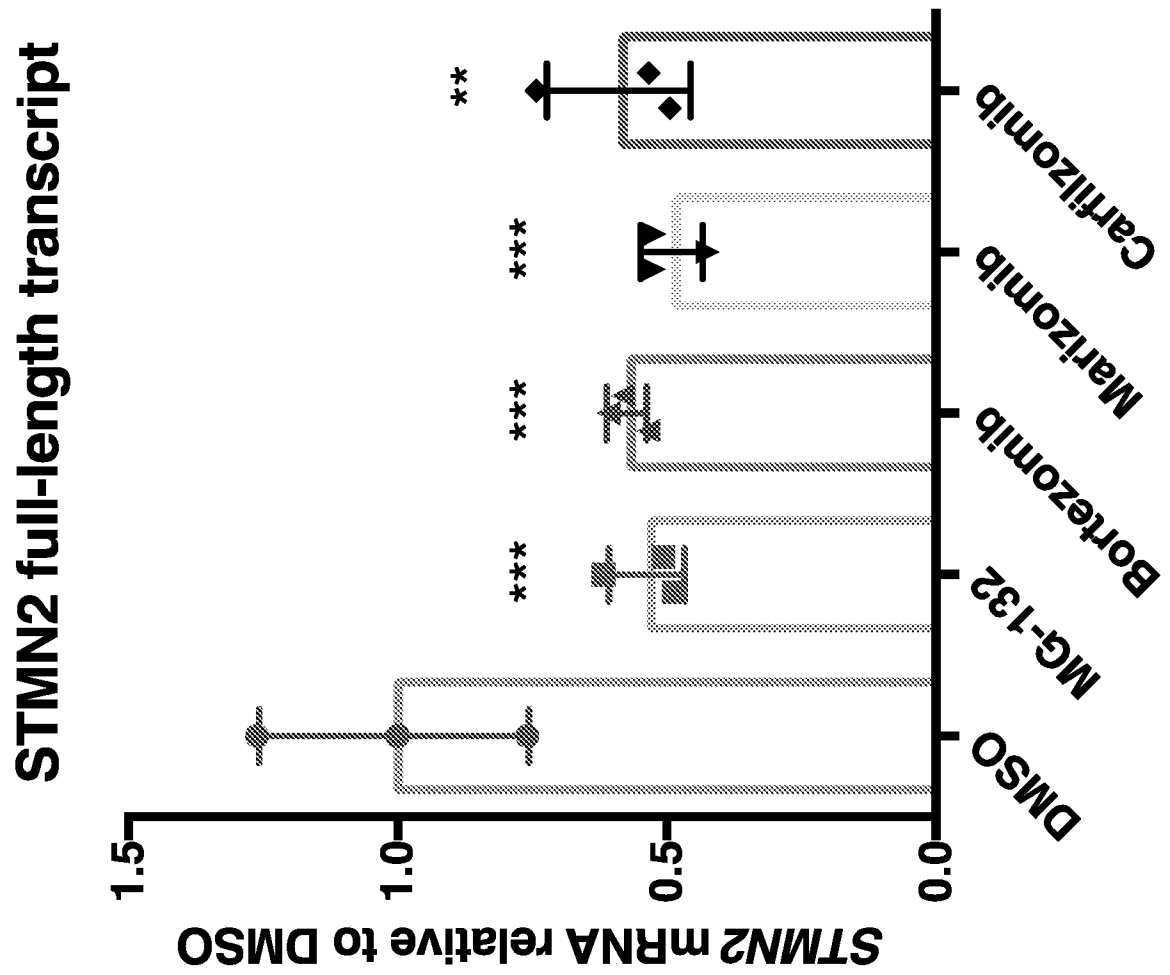

STMN2 full-length transcript
STMN2 mRNA relative to DMSO
1.5
1.0
0.5
0.0
DMSO
MG-132
Bortezomib
Marizomib
Carfilzomib
***
***
***
**

FIG. 61

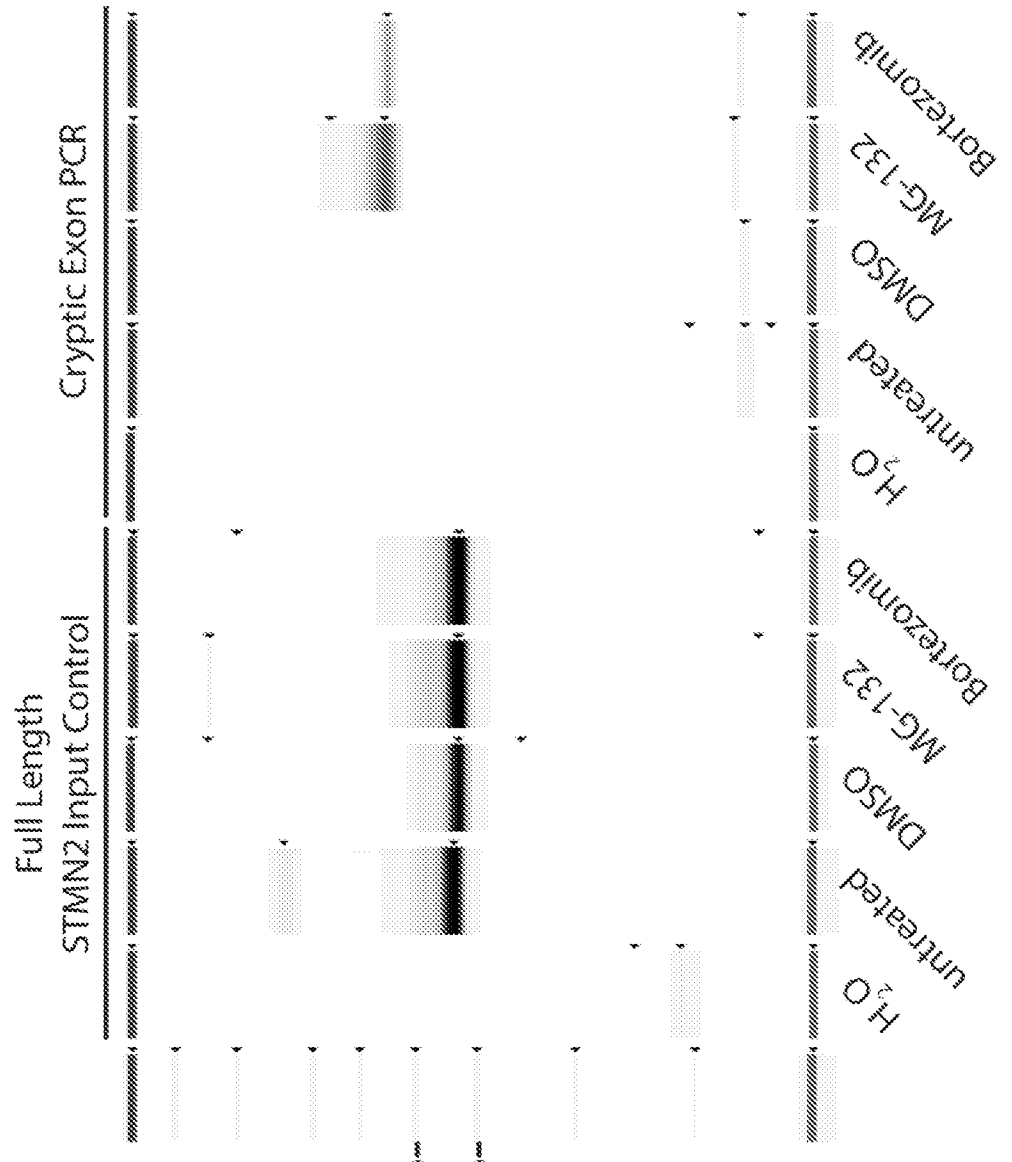

Full Length
STMN2 Input Control
Cryptic Exon PCR
300 bp
200 bp
H2O
untreated
DMSO
MG-132
Bortezomib
H2O
untreated
DMSO
MG-132
Bortezomib

FIG. 62

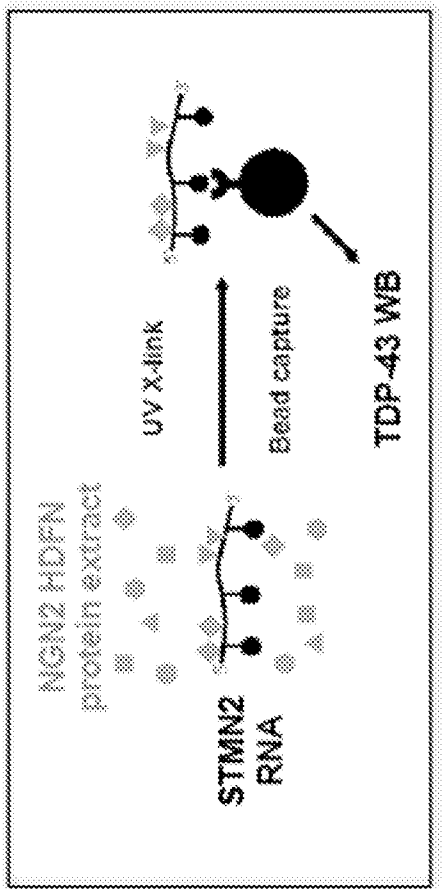


FIG. 63A

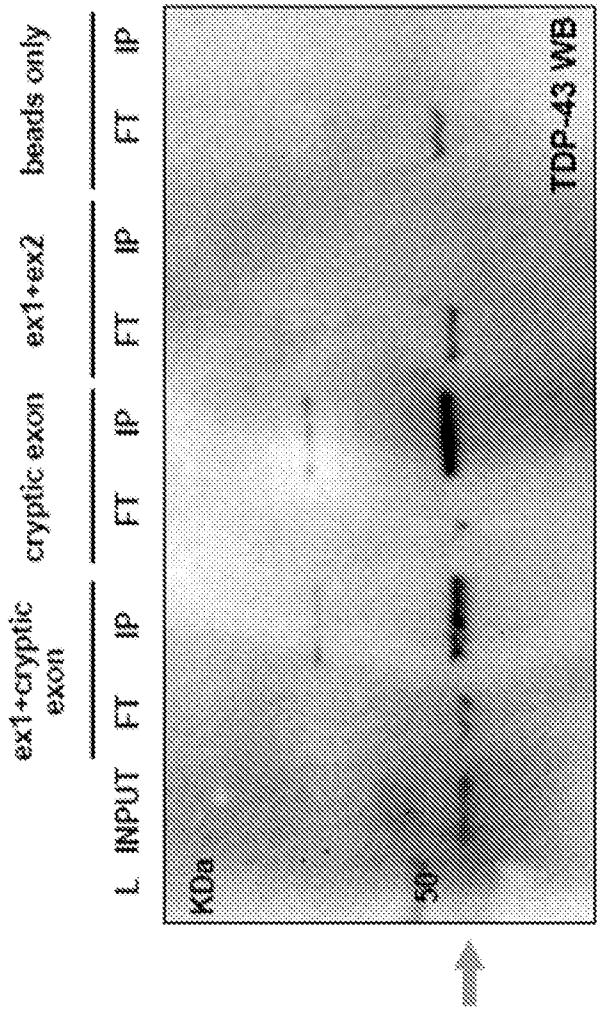


FIG. 63B

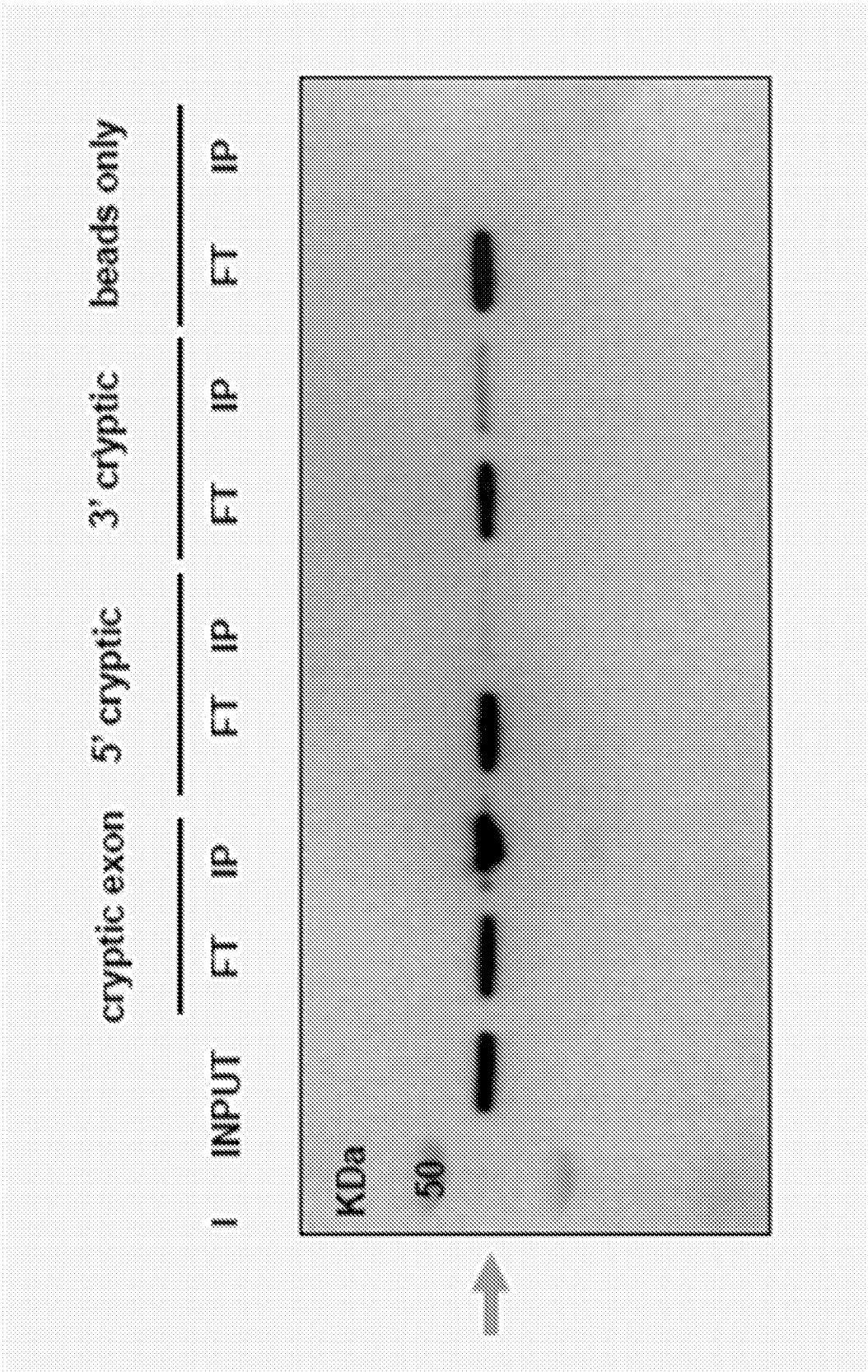

cryptic exon
5' cryptic
3' cryptic
beads only
I INPUT FT IP FT IP FT IP FT IP
KDa
50

FIG. 64

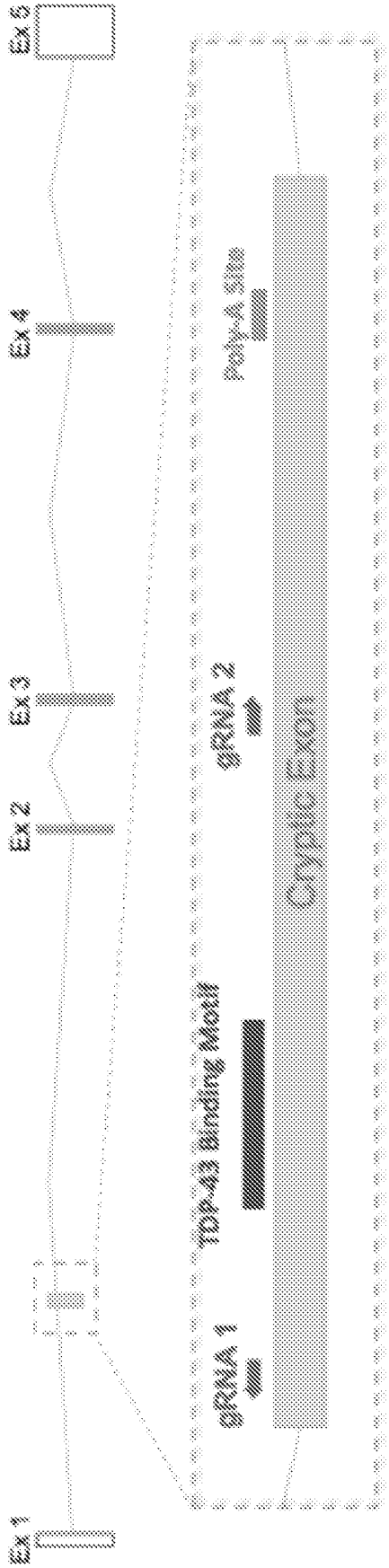
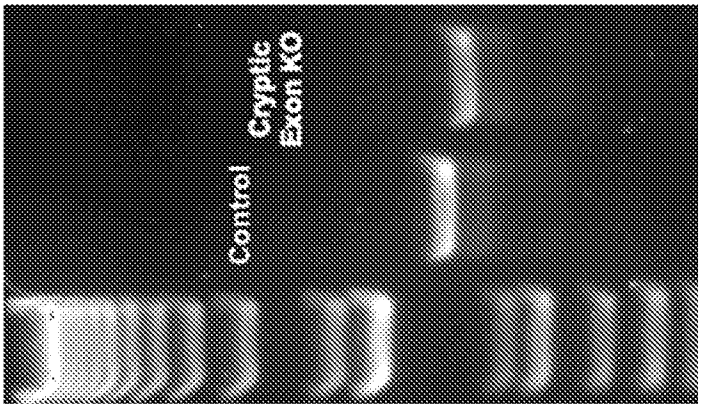

Ex 5
Ex 4
Ex 3
Ex 2
Ex 1
Poly-A Site
gRNA 2
Cryptic Exon
TDP-43 Binding Motif
gRNA 1

FIG. 65



SEQ ID NO: 12

SEQ ID NO: 13

FIG. 66

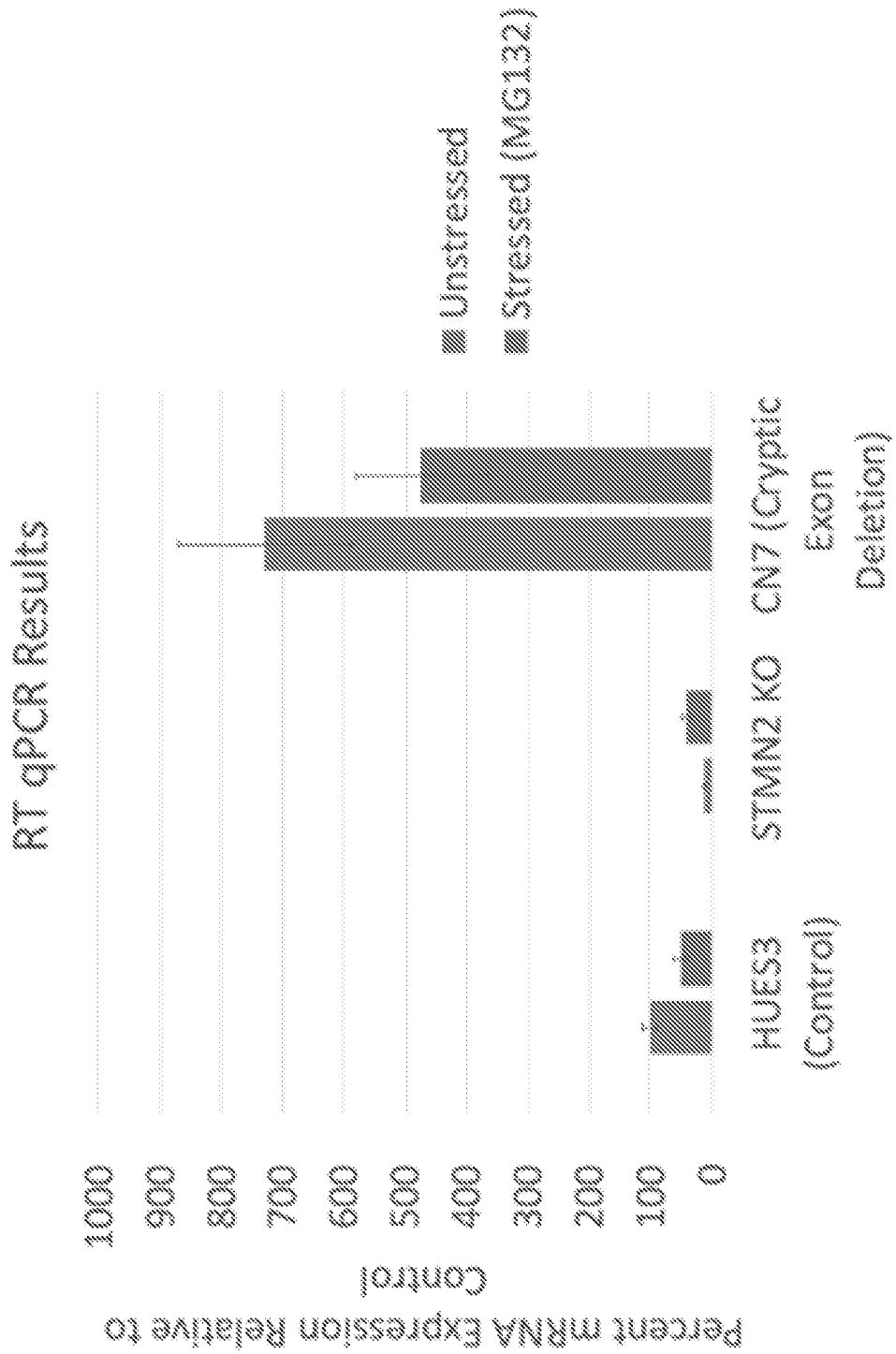

RT qPCR Results
Unstressed
Stressed (MG132)
Percent mRNA Expression Relative to Control
1000
900
800
700
600
500
400
300
200
100
0
HUES3 (Control)
STMN2 KO
CN7 (Cryptic Exon Deletion)

FIG. 67

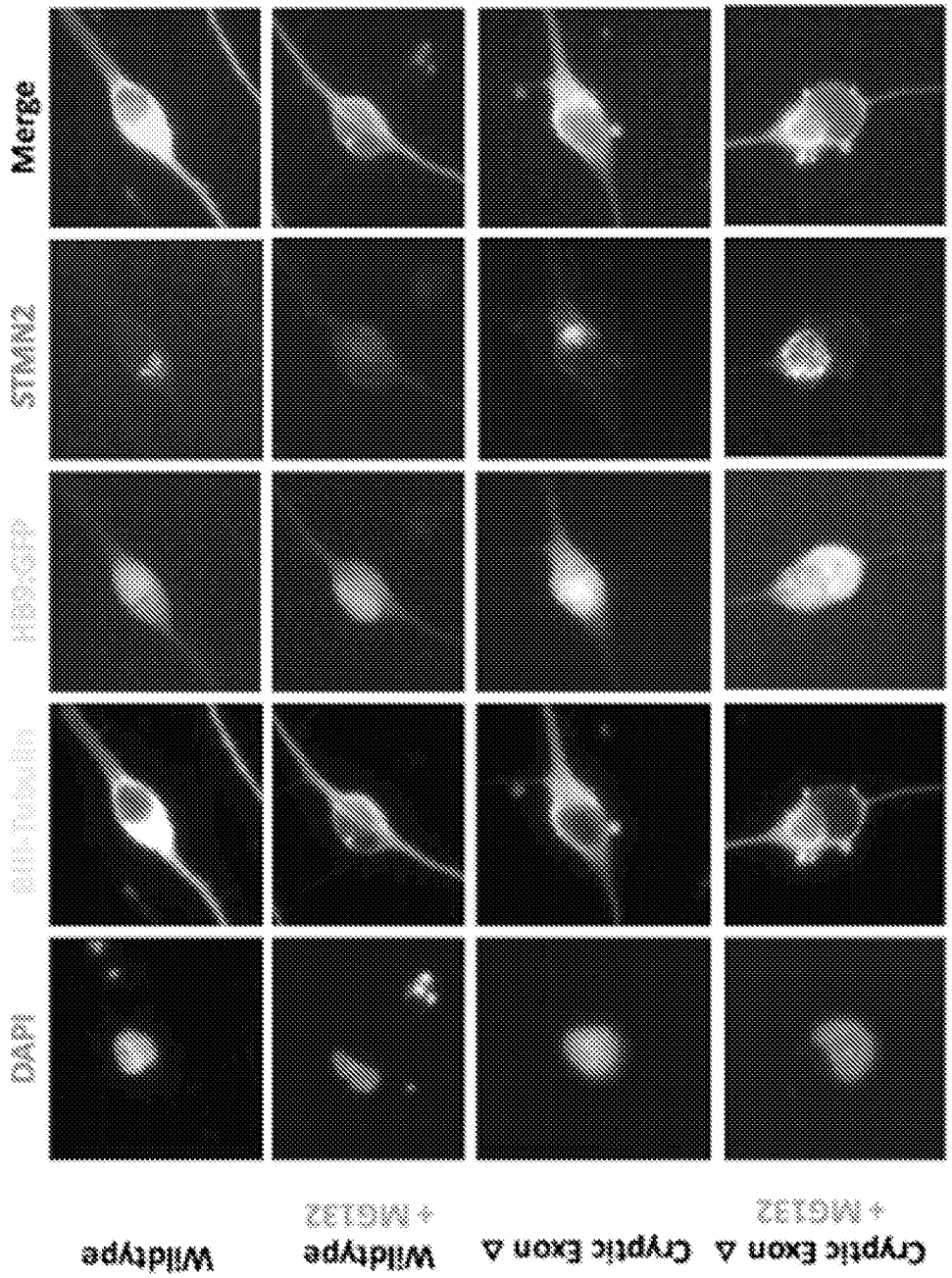

Merge
STMN2
hGDNF
DAPI
Wildtype
Wildtype + MG132
Cryptic Exon Δ
Cryptic Exon Δ + MG132

FIG. 68A

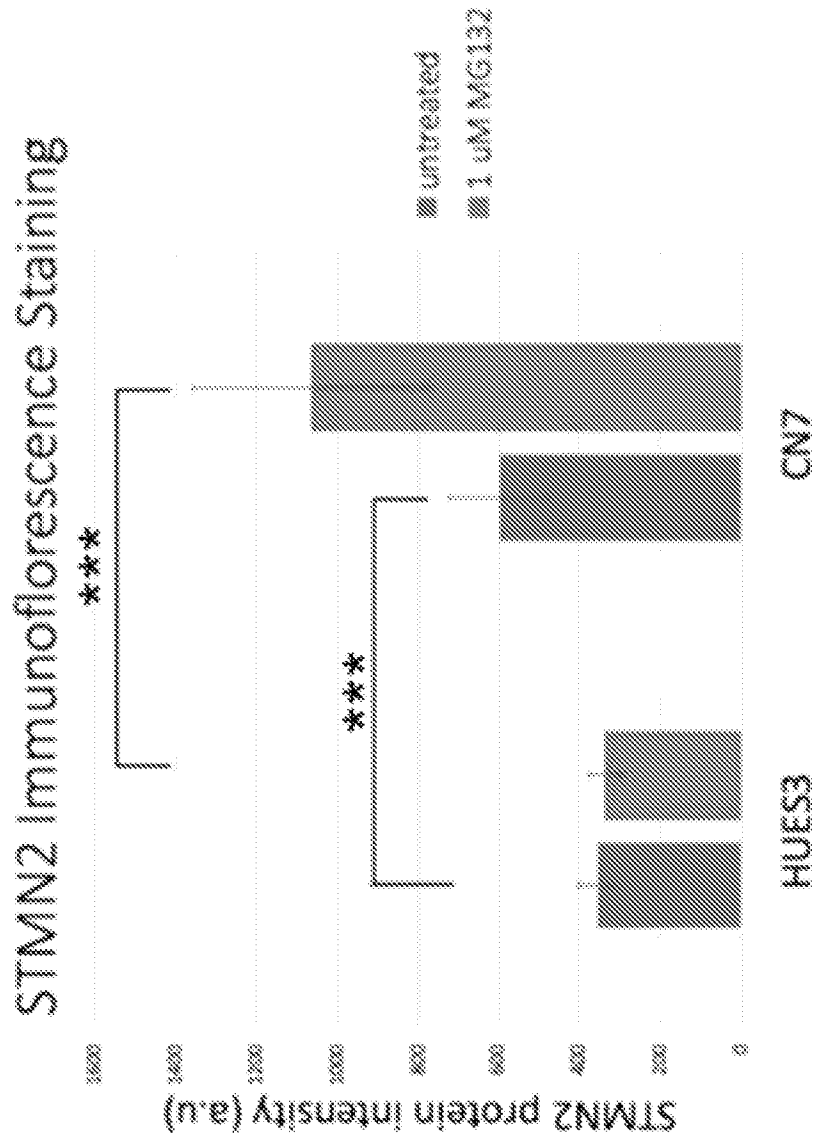

STMN2 Immunoflorescence Staining
untreated
1 uM MG132
***
***
STMN2 protein intensity (a.u)
0
CN7
HUES3

FIG. 68B

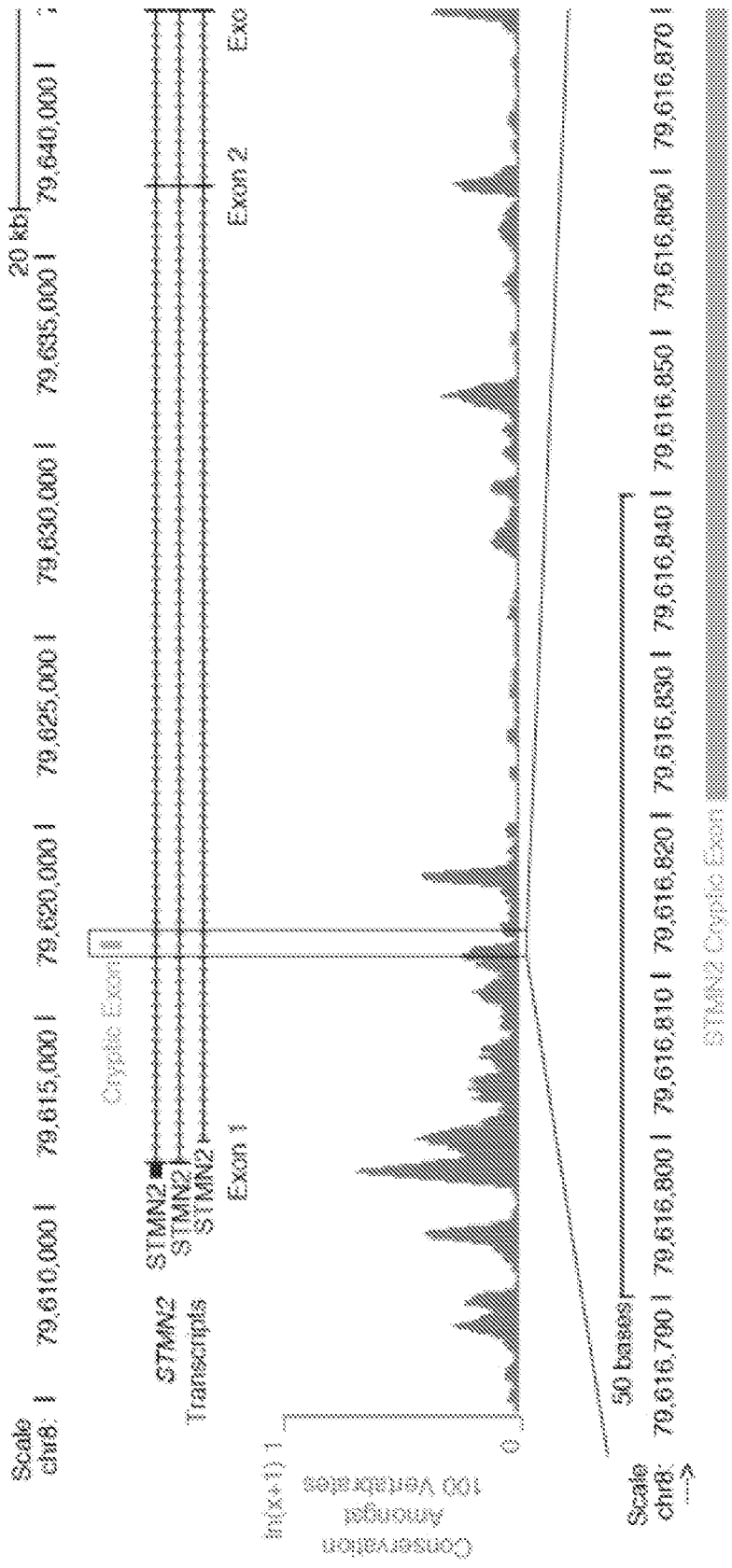

Scale
chr8: 1
79,610,000
79,615,000
79,620,000
79,625,000
79,630,000
79,635,000
20 kb
79,640,000
Cryptic Exon 1
STMN2
Transcripts
STMN2
STMN2
Exon 1
Exon 2
Exo
Conservation
Amongst
100 Vertebrates
log(x+1) 1
0
Scale
chr8:
79,616,790
79,616,800
79,616,810
79,616,820
79,616,830
79,616,840
79,616,850
79,616,860
79,616,870
50 bases
STMN2 Cryptic Exon

FIG. 69A

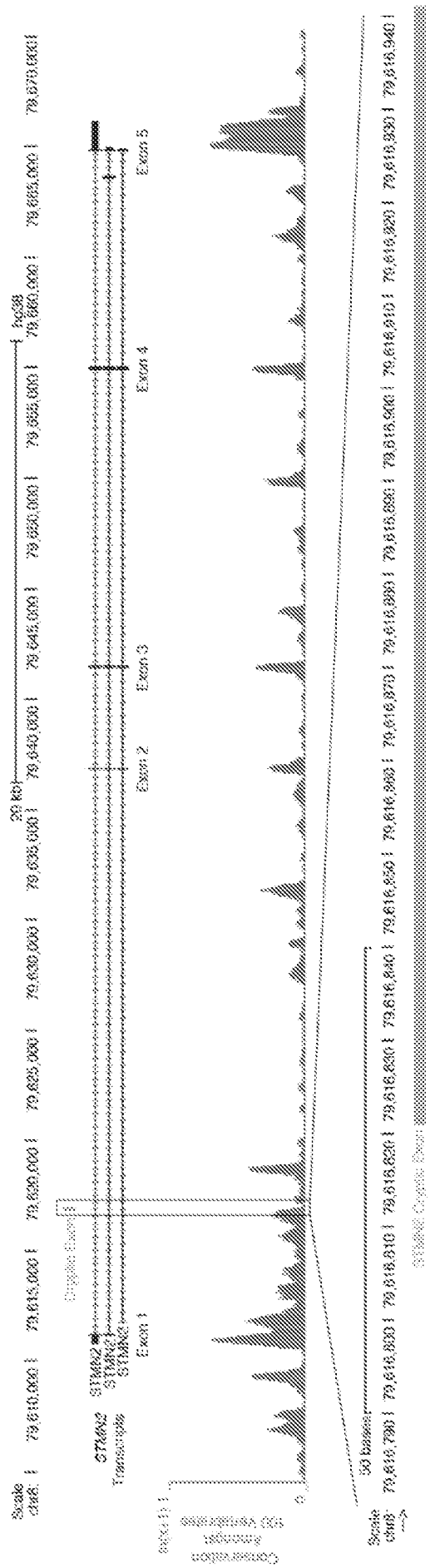

Scale
chr5: 79,615,000 79,620,000 79,625,000 79,630,000 79,635,000 79,640,000 79,645,000 79,650,000 79,655,000 79,660,000 79,665,000 79,670,000
20 kb
hg38
STMN2
Transcripts
STMN2-201
STMN2-1
STMN2
Exon 1
Exon 2
Exon 3
Exon 4
Exon 5
Coverage
50 bases
chr5: 79,616,790 79,616,800 79,616,810 79,616,820 79,616,830 79,616,840 79,616,850 79,616,860 79,616,870 79,616,880 79,616,890 79,616,900 79,616,910 79,616,920 79,616,930 79,616,940

FIG. 69A cont.

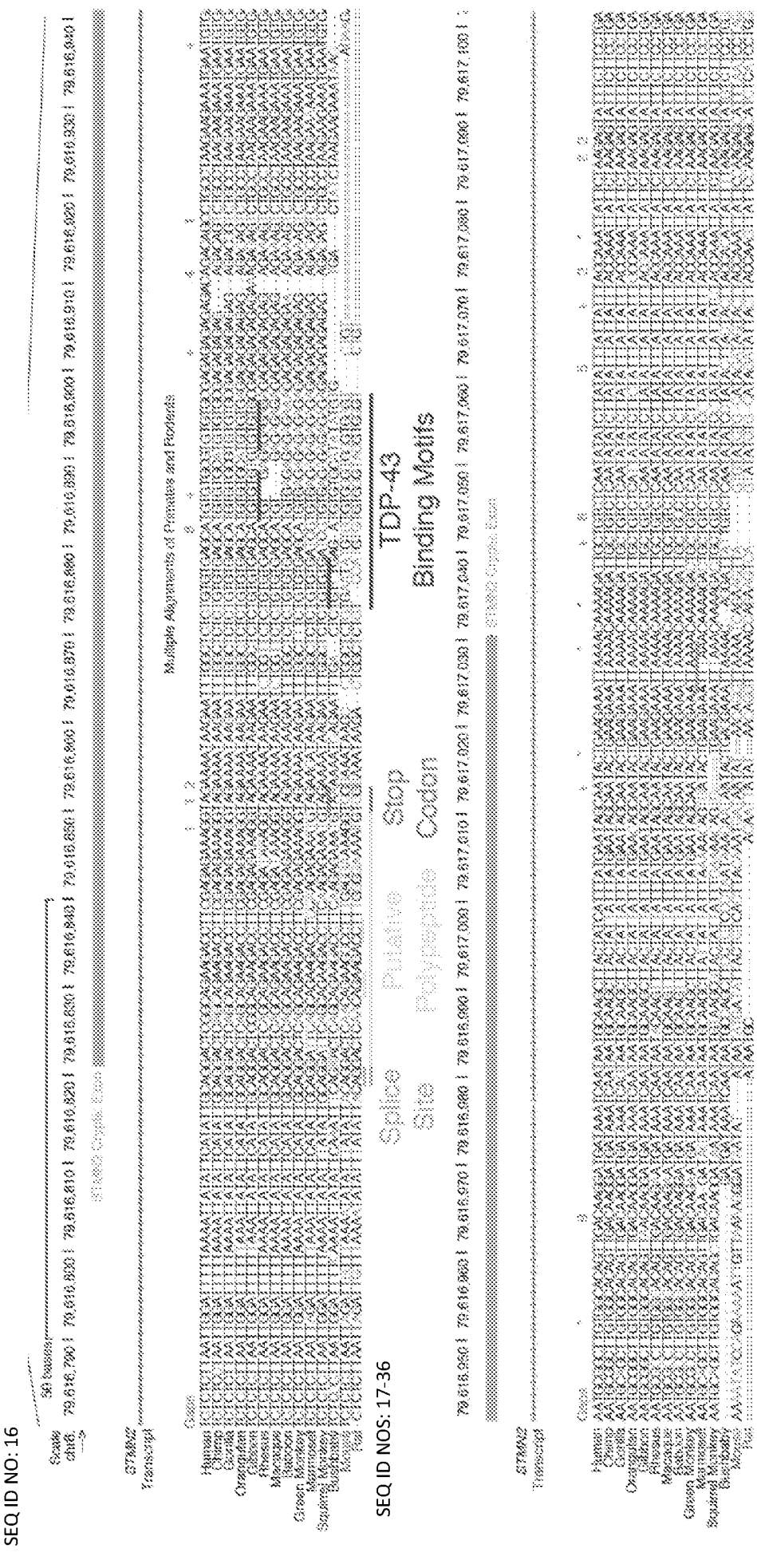

SEQ ID NO: 16
SEQ ID NOS: 17-36
Multiple Alignments of Primates and Rodents
TDP-43
Binding Motifs
Splice Site
Putative Stop Codon
Polypeptide
poly-A Site

FIG. 69B

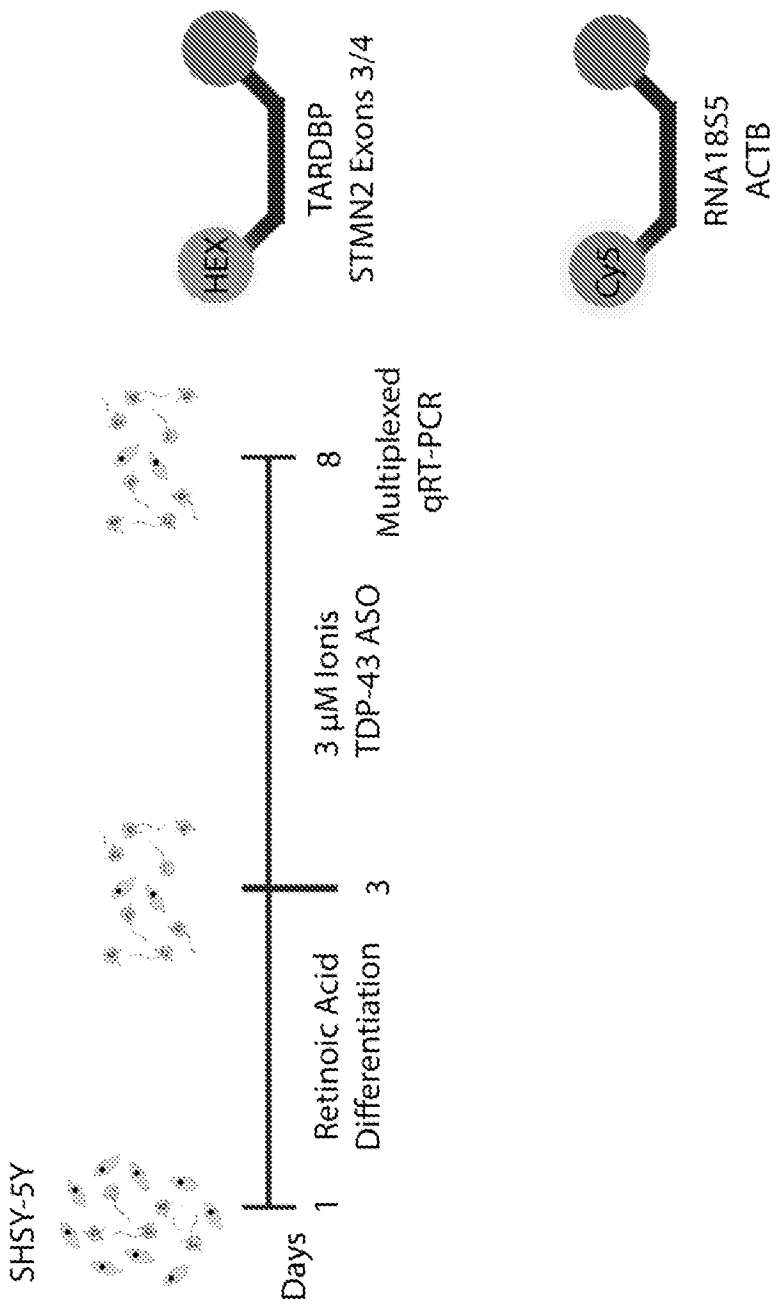

FAM
Cryptic STMN2
HEX
TARDBP
STMN2 Exons 3/4
Cy5
RNA18S5
ACTB
SHSY-5Y
Days
1
Retinoic Acid
Differentiation
3
3 µM Ionis
TDP-43 ASO
8
Multiplexed
qRT-PCR

FIG. 70

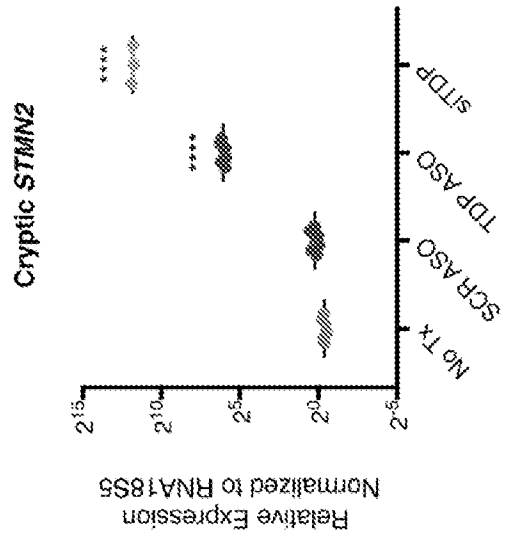


FIG. 71C

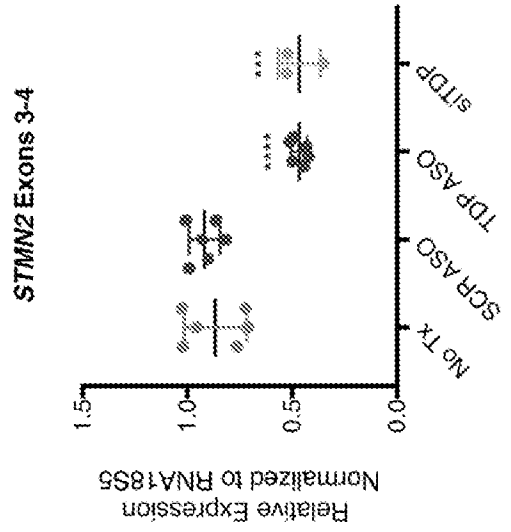


FIG. 71B

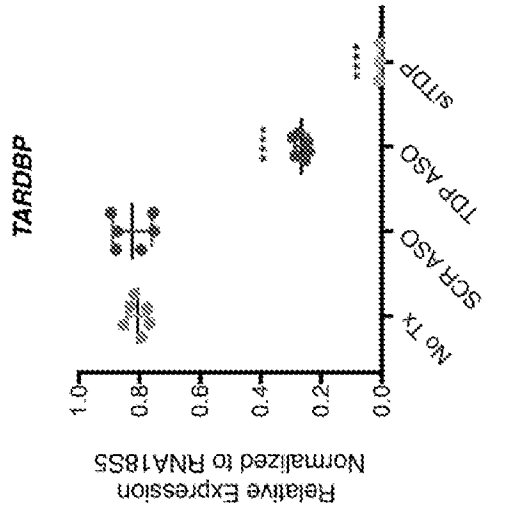


FIG. 71A

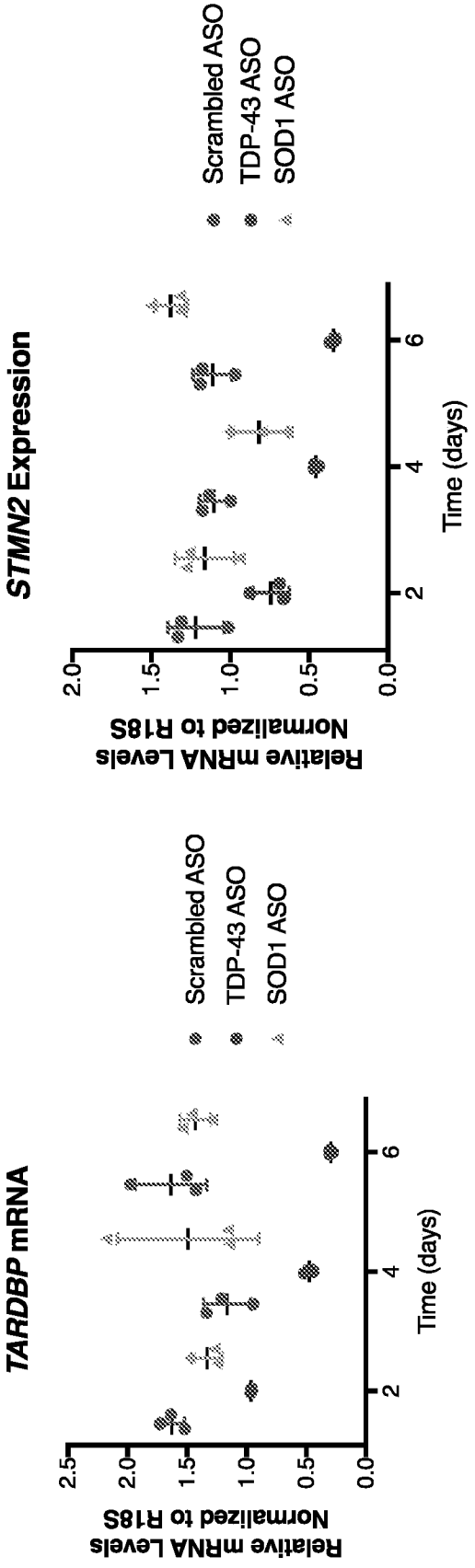


FIG. 72A

FIG. 72B

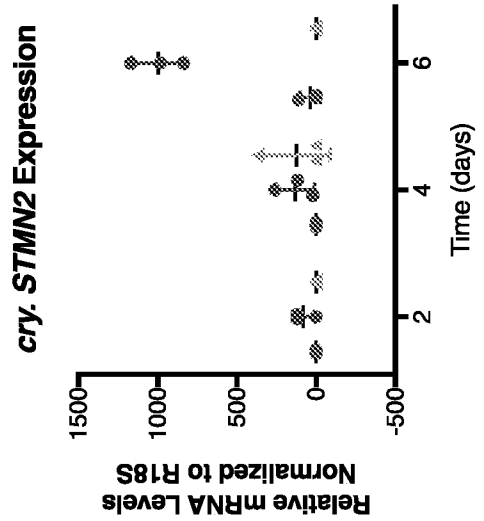


FIG. 72C

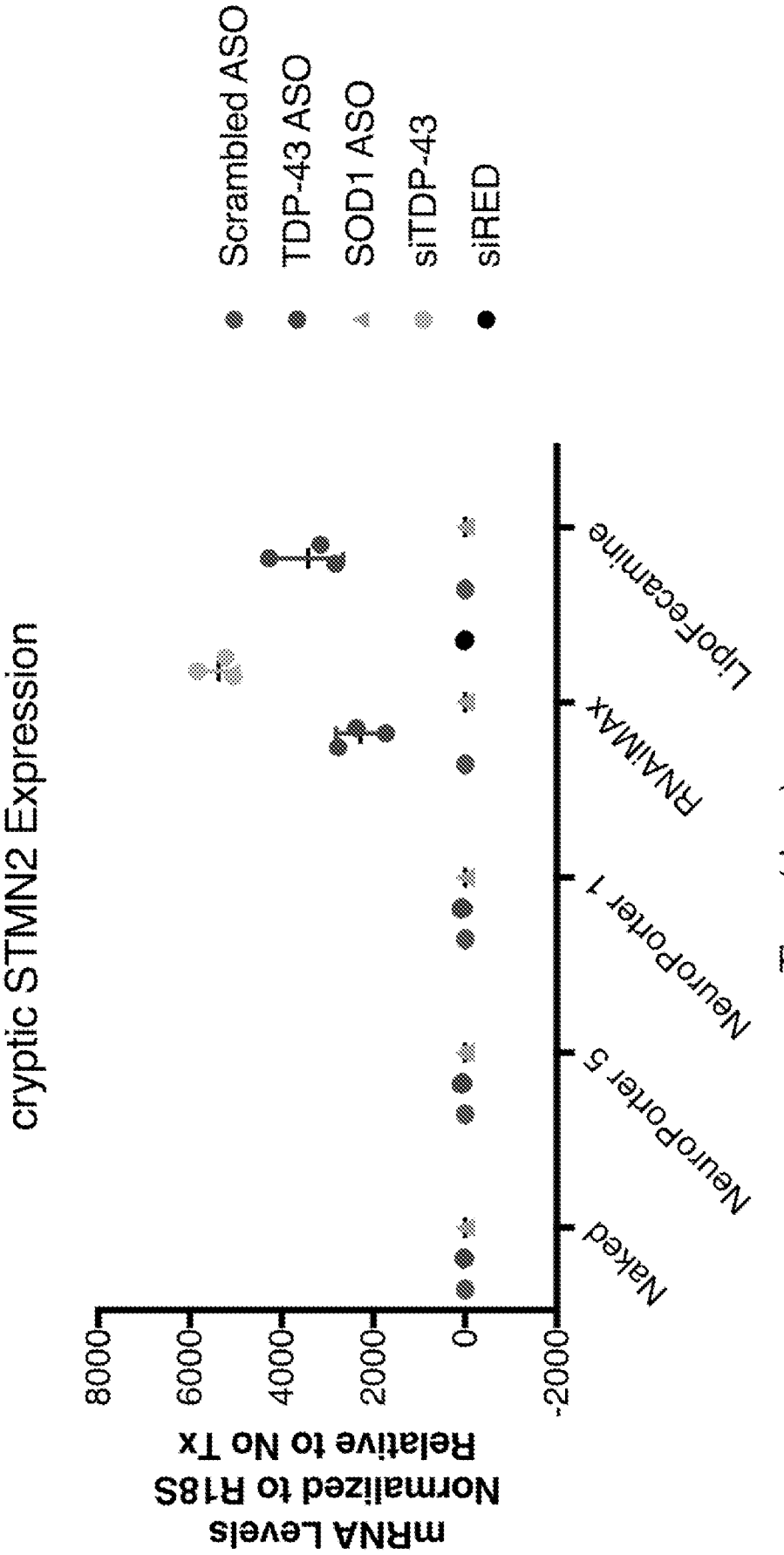

cryptic STMN2 Expression
mRNA Levels
Normalized to R18S
Relative to No Tx
8000
6000
4000
2000
0
-2000
Naked
NeuroPorter 5
NeuroPorter 1
RNAiMAX
LipoFecamine
Time (days)
Scrambled ASO
TDP-43 ASO
SOD1 ASO
siTDP-43
siRED

FIG. 73

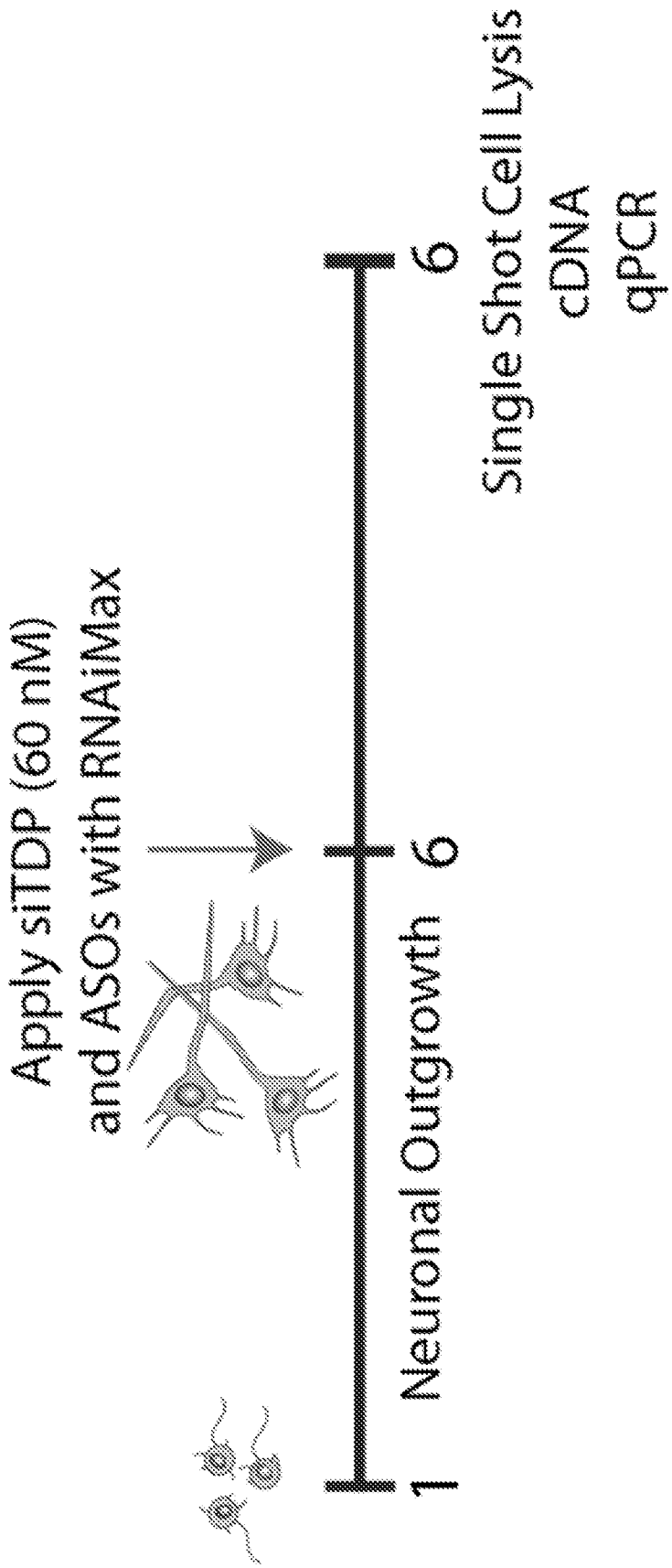

Apply siTDP (60 nM)
and ASOs with RNAiMax
1
Neuronal Outgrowth
6
6
Single Shot Cell Lysis
cDNA
qPCR

FIG. 74

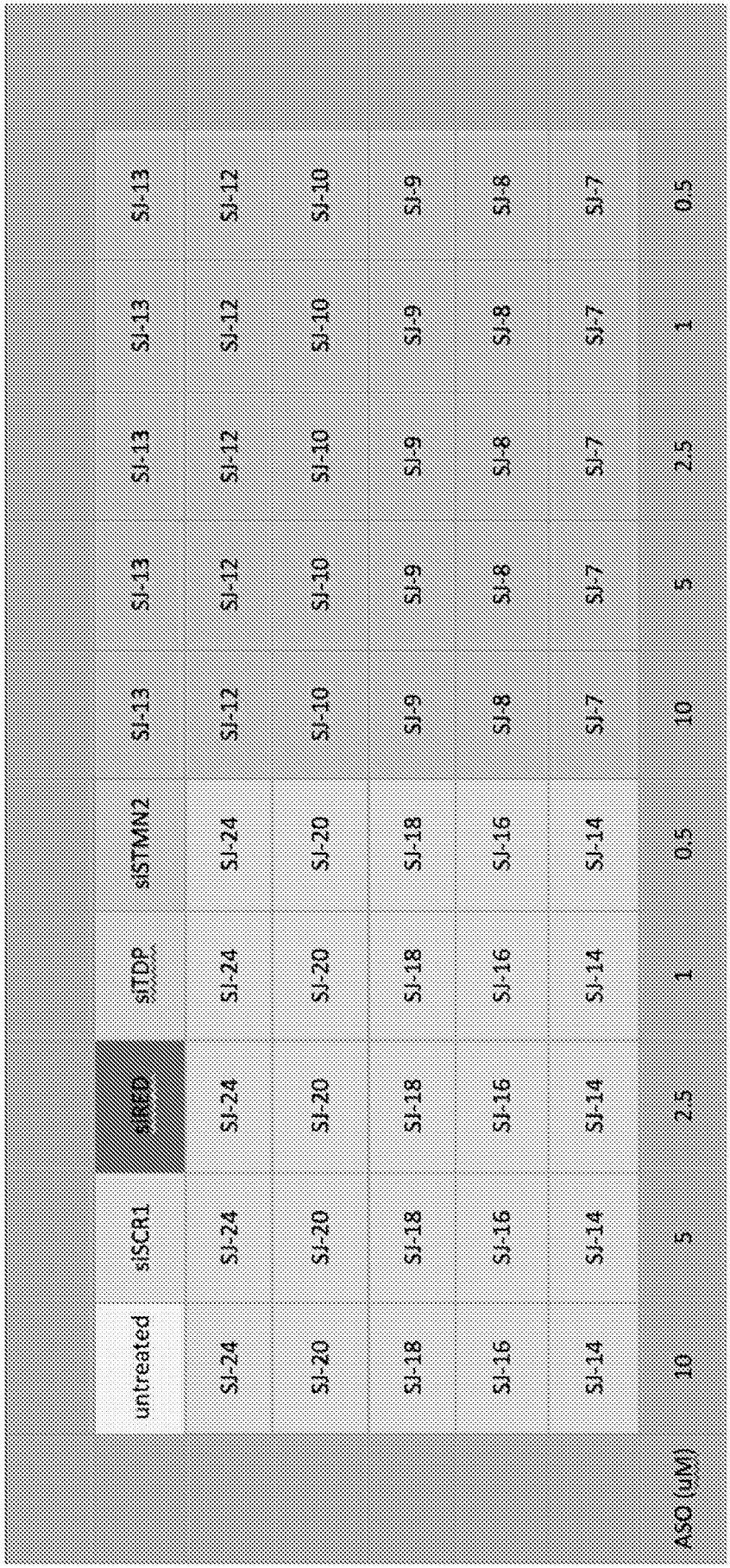

ASO (uM)
10
5
2.5
1
0.5
untreated
siSCR1
siRED
siTDP
siSTMN2
SJ-24
SJ-20
SJ-18
SJ-16
SJ-14
SJ-13
SJ-12
SJ-10
SJ-9
SJ-8
SJ-7

FIG. 75A

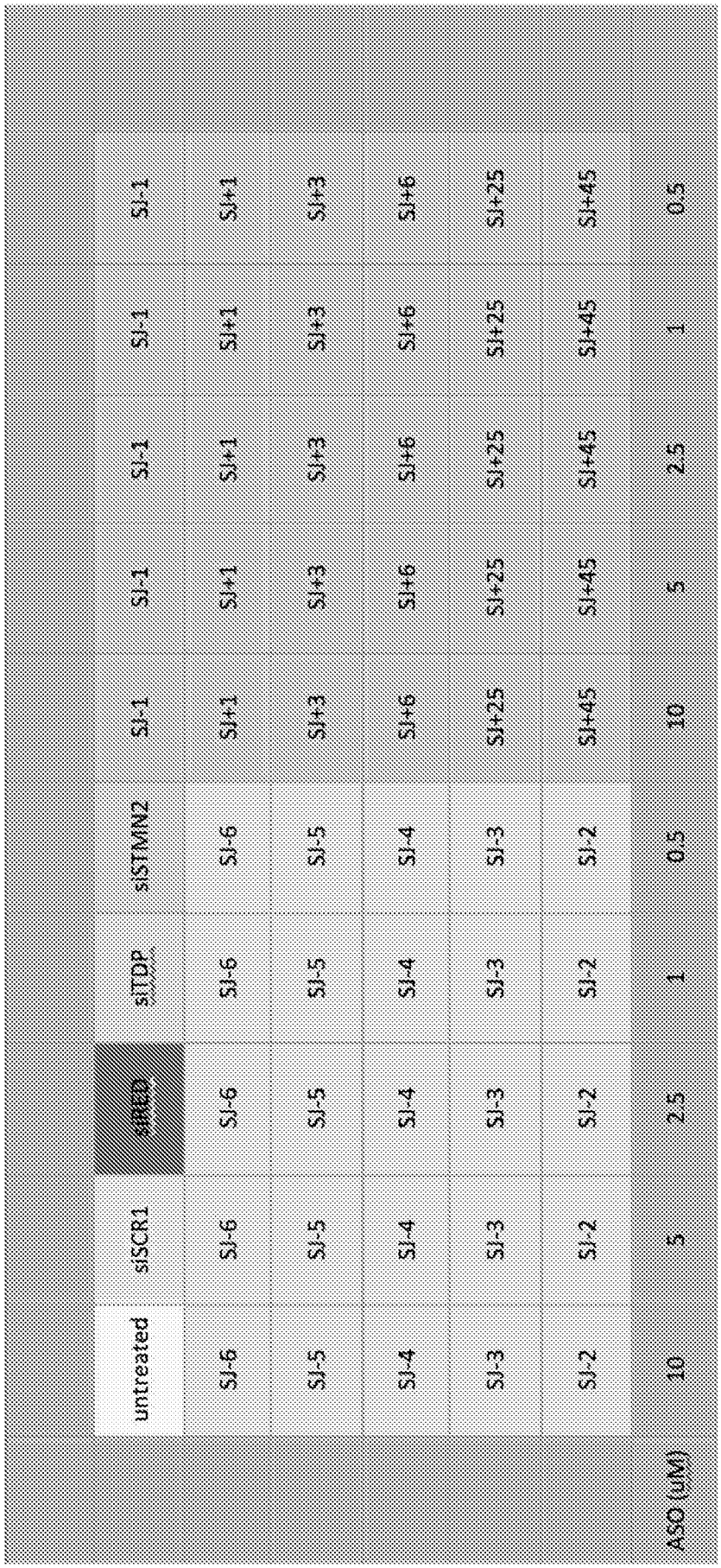

untreated
siSCR1
siRED
siTDP
siSTMN2
SJ-1
SJ+1
SJ+3
SJ+6
SJ+25
SJ+45
SJ-6
SJ-5
SJ-4
SJ-3
SJ-2
ASO (uM)
10
5
2.5
1
0.5

FIG. 75B

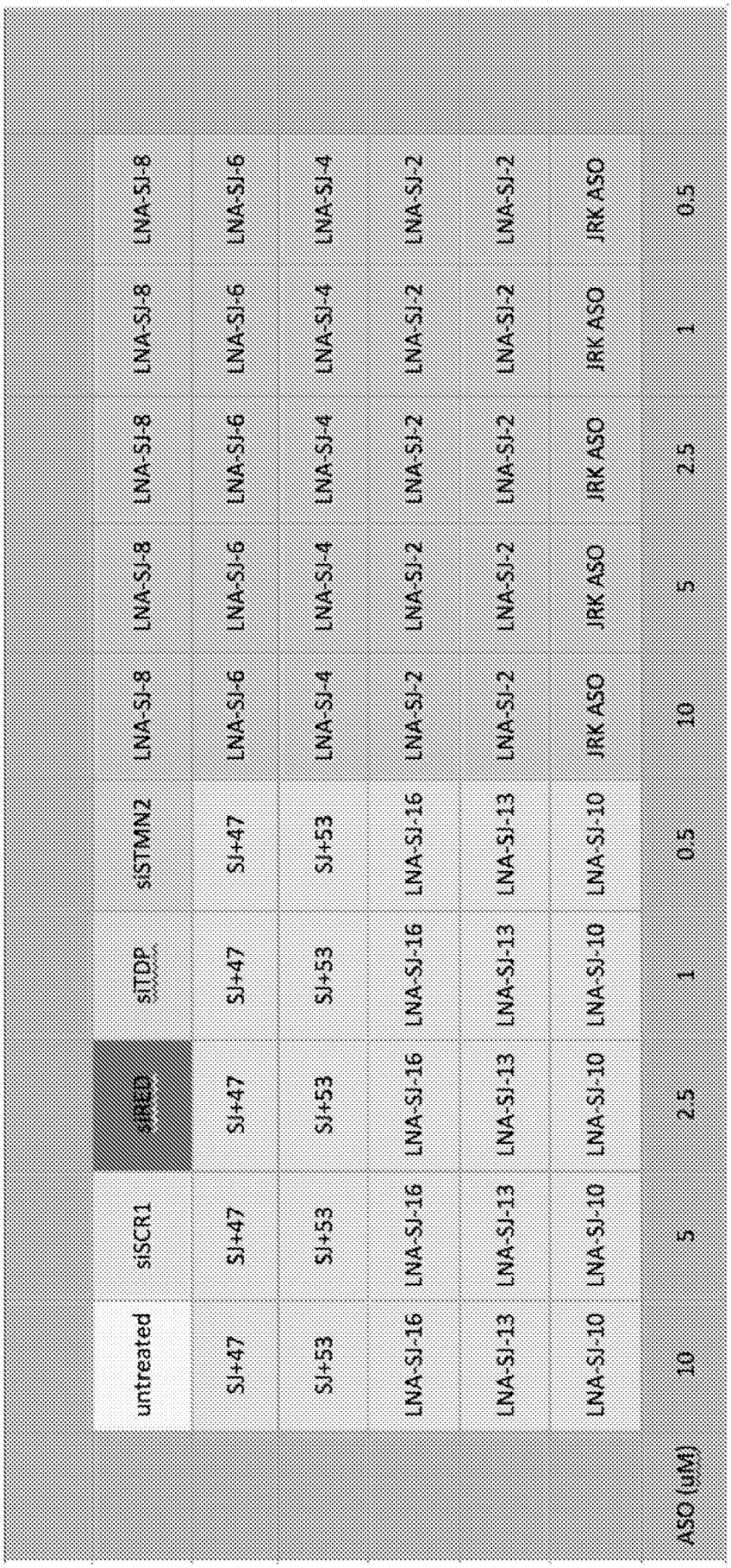

untreated
siSCR1
siRED
siTDP
siSTMN2
LNA-SJ-8
LNA-SJ-6
LNA-SJ-4
LNA-SJ-2
JRK ASO
SJ+47
SJ+53
LNA-SJ-16
LNA-SJ-13
LNA-SJ-10
ASO (uM)
10
5
2.5
1
0.5

FIG. 75C


ASO (uM)
10
5
2.5
1
0.5
NC5
TDP ASO
Tofersen
NTC
Nusinuren
untreated
siSCR1
siRED1
siTDP
siSTMN2

FIG. 75D

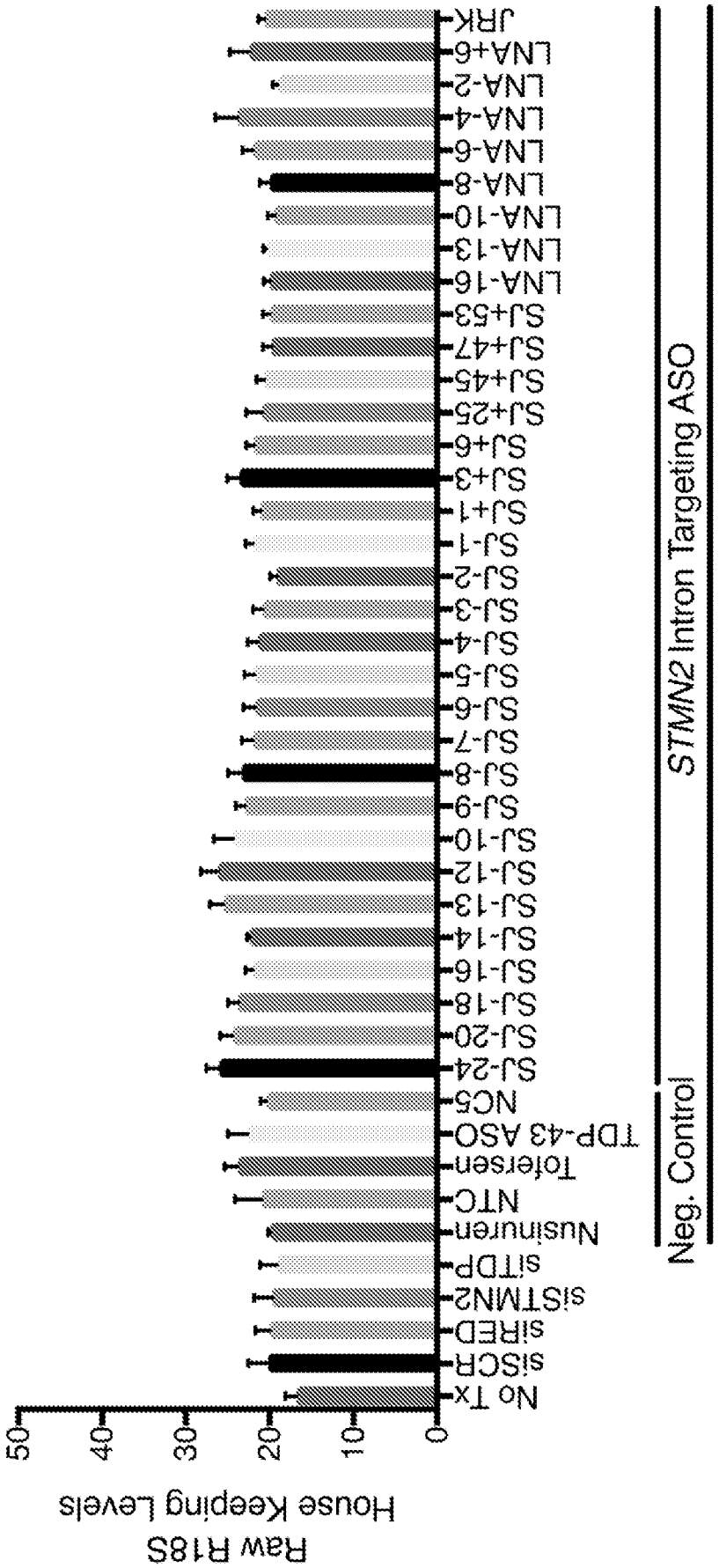

Raw R18S
House Keeping Levels
50
40
30
20
10
0
No Tx
siSCR
siRED
siSTMN2
siTDP
Nusinuren
NTC
Tolerseen
TDP-43 ASO
NC5
SJ-24
SJ-20
SJ-18
SJ-16
SJ-14
SJ-13
SJ-12
SJ-10
SJ-9
SJ-8
SJ-7
SJ-6
SJ-5
SJ-4
SJ-3
SJ-2
SJ-1
SJ+1
SJ+3
SJ+6
SJ+25
SJ+45
SJ+47
SJ+53
LNA-16
LNA-13
LNA-10
LNA-8
LNA-6
LNA-4
LNA-2
LNA+6
JRK
Neg. Control
STMN2 Intron Targeting ASO
siTDP-43 +

FIG. 76

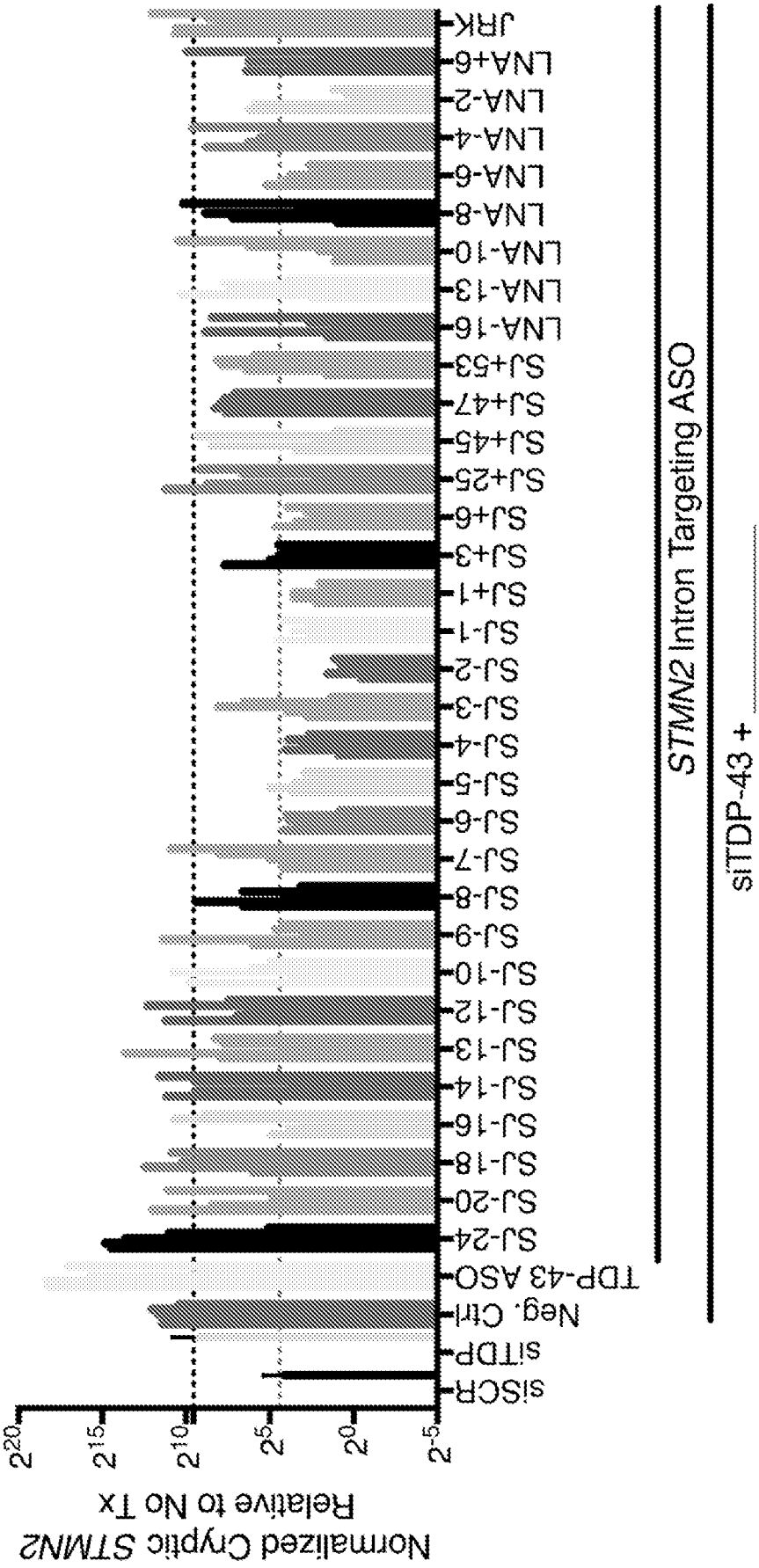

Normalized Cryptic STMN2
Relative to No Tx
2^20
2^15
2^10
2^5
2^0
2^-5
siSCR
siTDP
Neg. Ctrl
TDP-43 ASO
SJ-24
SJ-20
SJ-18
SJ-16
SJ-14
SJ-13
SJ-12
SJ-10
SJ-9
SJ-8
SJ-7
SJ-6
SJ-5
SJ-4
SJ-3
SJ-2
SJ-1
SJ+1
SJ+3
SJ+6
SJ+25
SJ+45
SJ+47
SJ+53
LNA-16
LNA-13
LNA-10
LNA-8
LNA-6
LNA-4
LNA-2
LNA+6
JRK
STMN2 Intron Targeting ASO
siTDP-43 +

FIG. 77

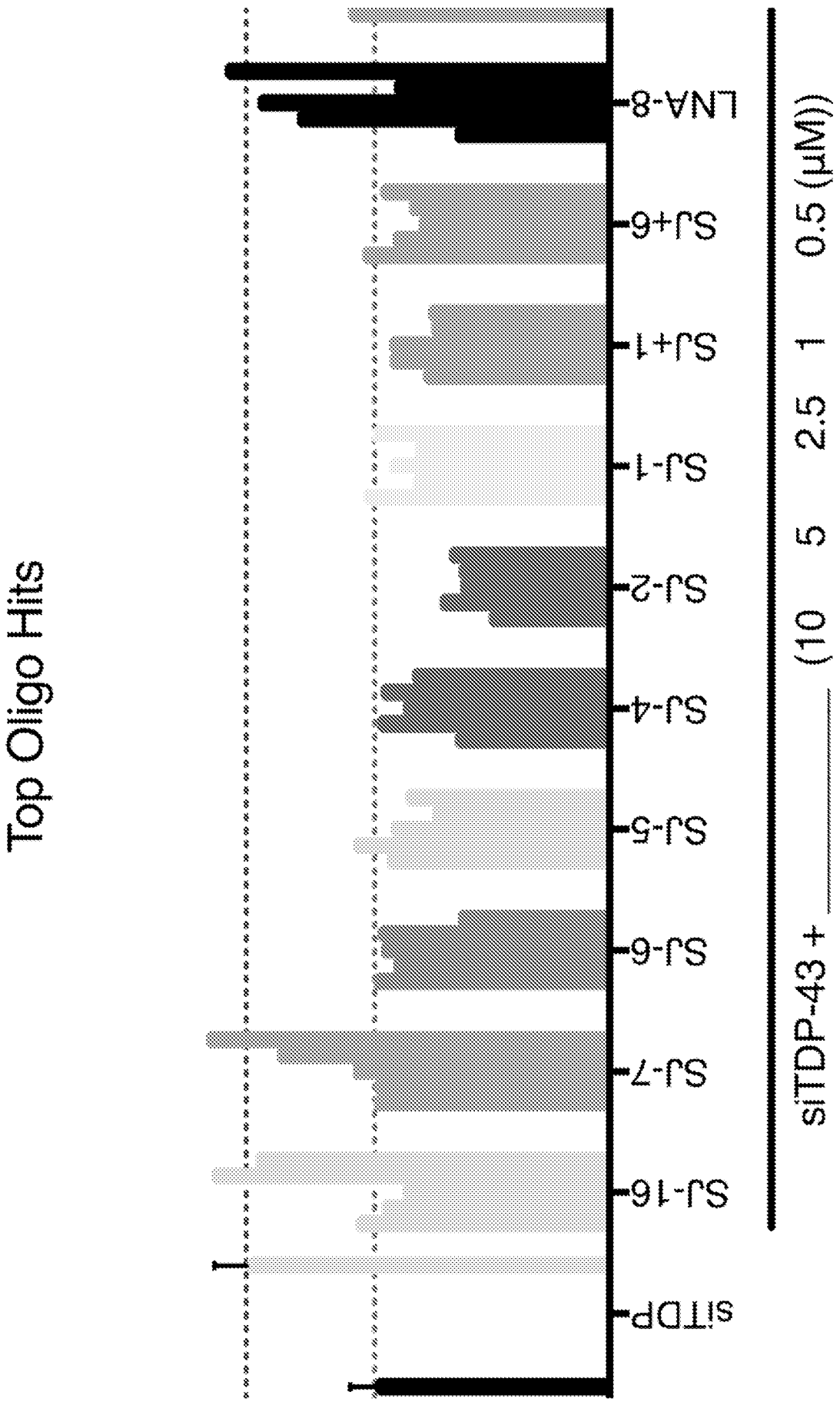

Top Oligo Hits
siTDP
SJ-16
SJ-7
SJ-6
SJ-5
SJ-4
SJ-2
SJ-1
SJ+1
SJ+6
LNA-8
siTDP-43 + _____ (10 5 2.5 1 0.5 (μM))

FIG. 78

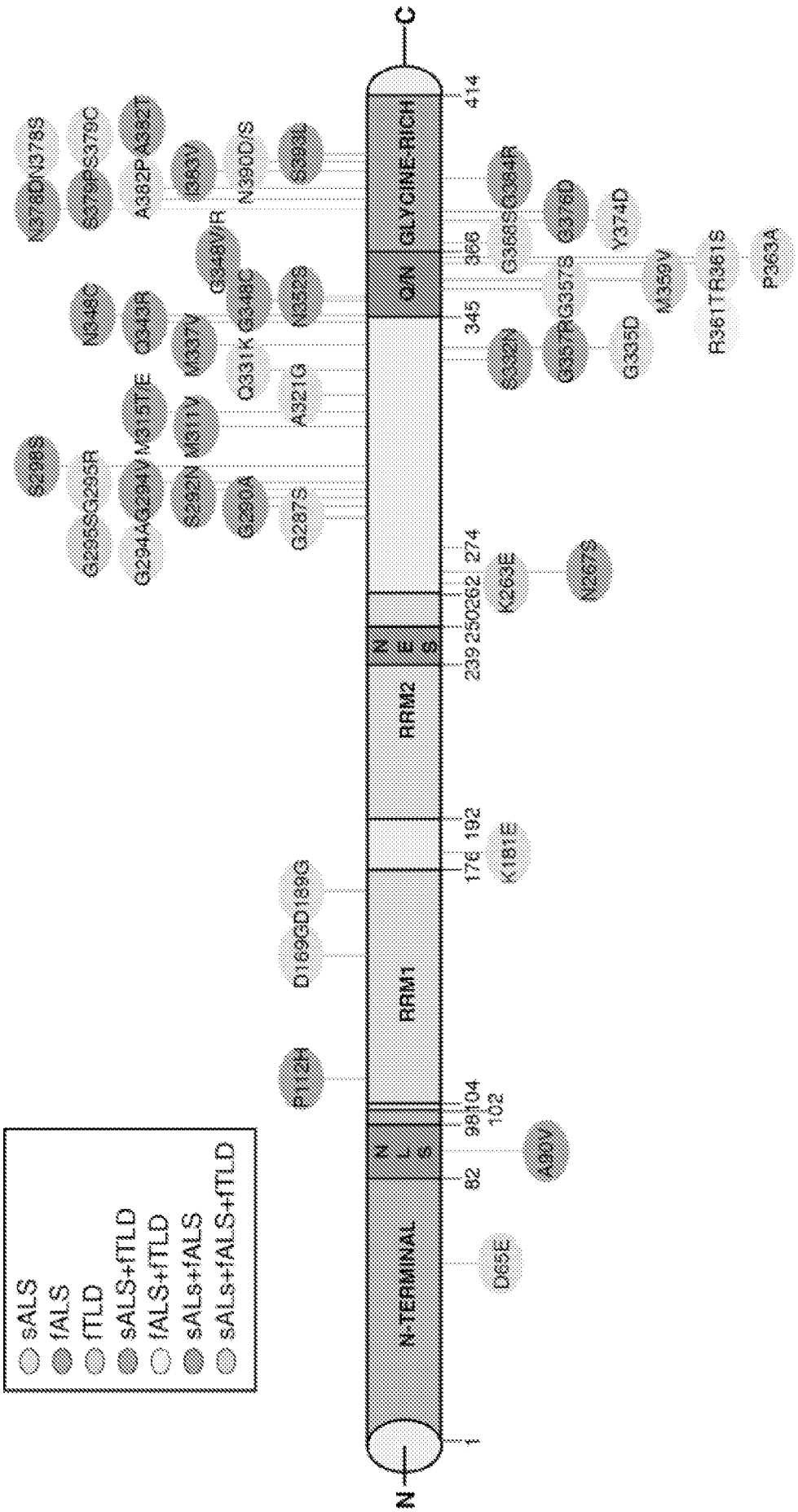

sALS
fALS
fTLD
sALS+fTLD
fALS+fTLD
sALS+fALS
sALS+fALS+fTLD
N-TERMINAL
RRM1
RRM2
GLYCINE-RICH
N
C
1
82
98
104
102
176
192
239
250
262
274
345
368
414
D65E
A90V
P112H
D169G
D169G
K181E
K263E
M292V
G294A
G294V
S295R
S298S
M311V
M311L
Q331K
G335D
G336D
A321G
G348C
G348V
N390D
S393L
A382P
A382T
D378H
S379C
S379P
Y374D
G368A
G368D
G376D
M359V
R361S
R361T
P363A
G287S
G290A
G298S
G335S
G337R
G337S
G332R
G332S
M267I

FIG. 79A

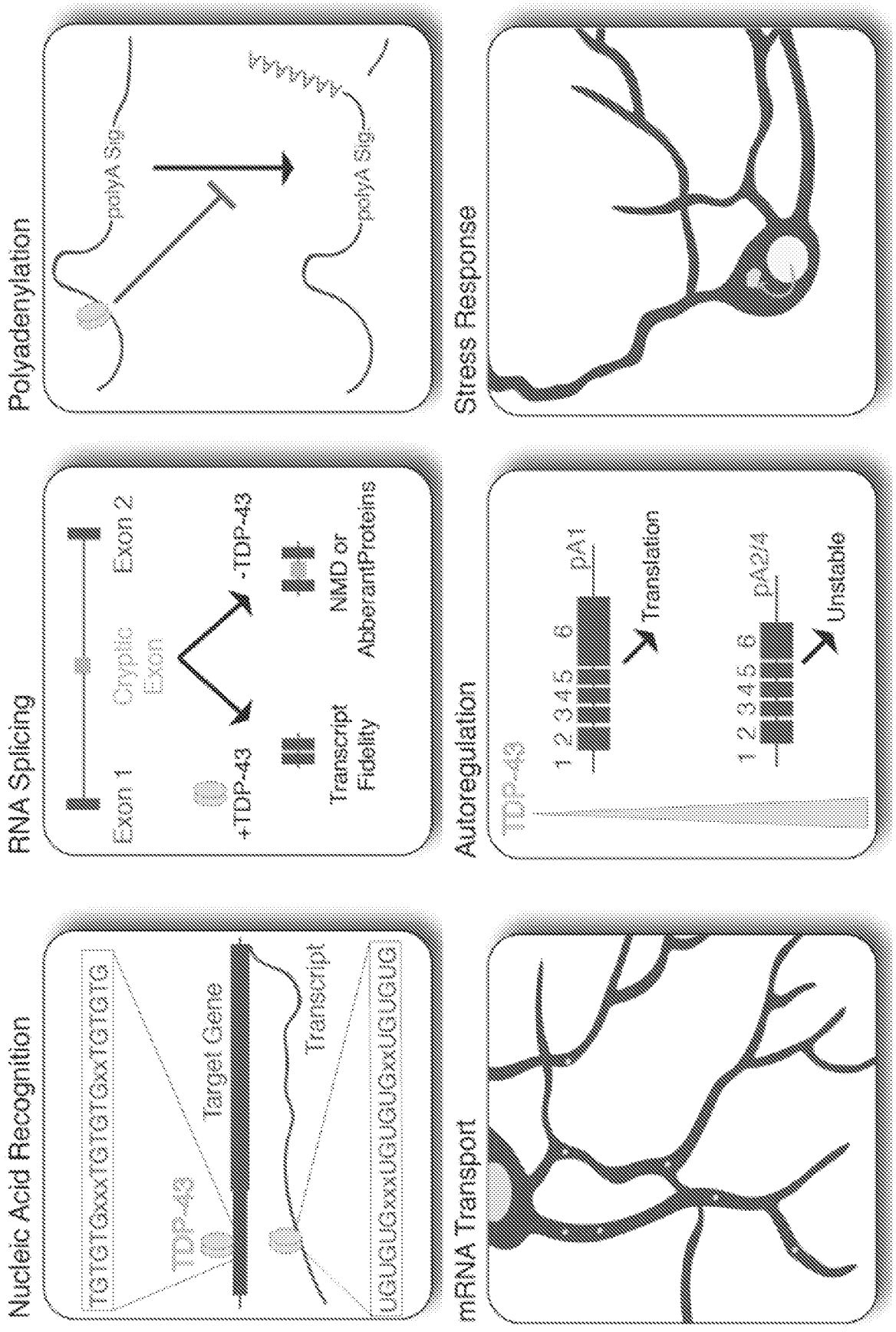

Nucleic Acid Recognition
TGTGTGxxxTGTGTGxxTGTGTG
TDP-43
Target Gene
Transcript
UGUGUGxxxUGUGUGxxUGUGUG
RNA Splicing
Exon 1
Cryptic Exon
Exon 2
+TDP-43
-TDP-43
Transcript Fidelity
NMD or AbberantProteins
Polyadenylation
polyA Sig
AAAAAA
polyA Sig
Stress Response
mRNA Transport
Autoregulation
TDP-43
1 2 3 4 5 6
pA1
Translation
1 2 3 4 5 6
pA2/4
Unstable

FIG. 79B

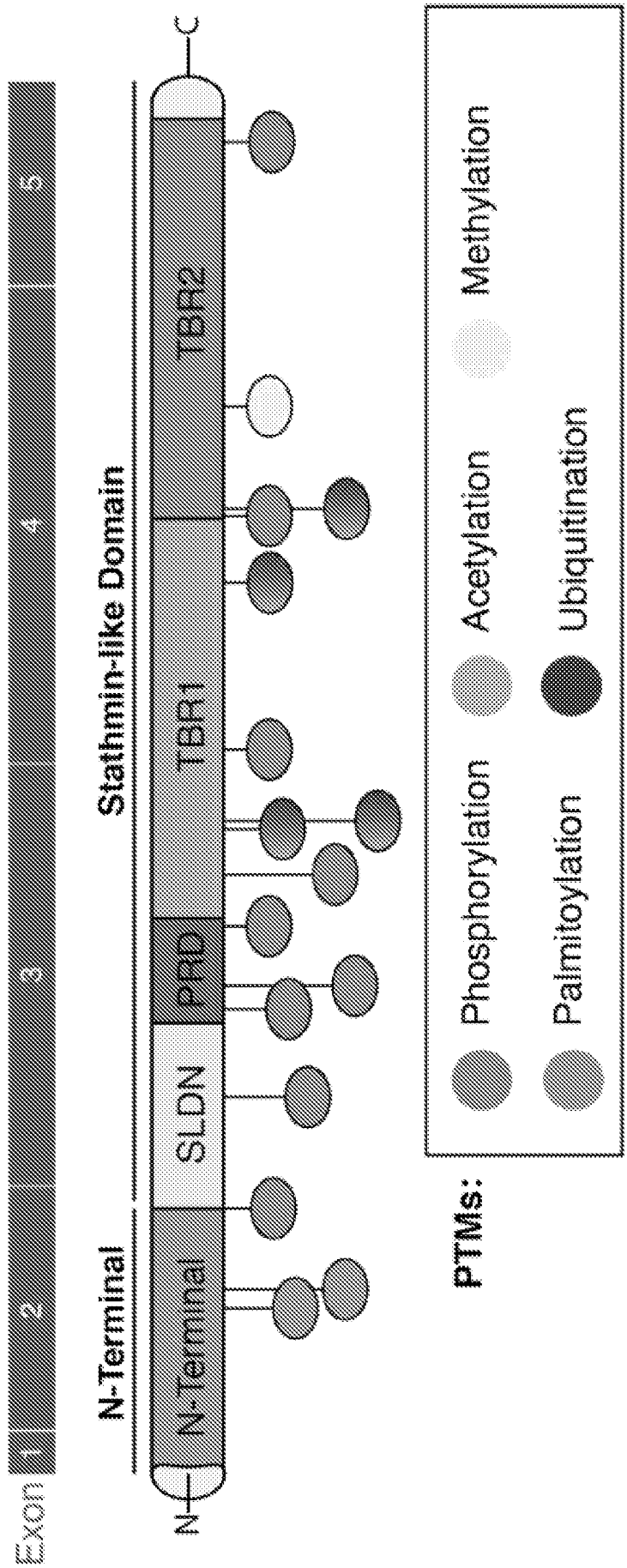

Exon
1
2
3
4
5
N-Terminal
Stathmin-like Domain
N
N-Terminal
SLDN
PRD
TBR1
TBR2
C
PTMs:
Phosphorylation
Acetylation
Methylation
Palmitoylation
Ubiquitination

FIG. 80A

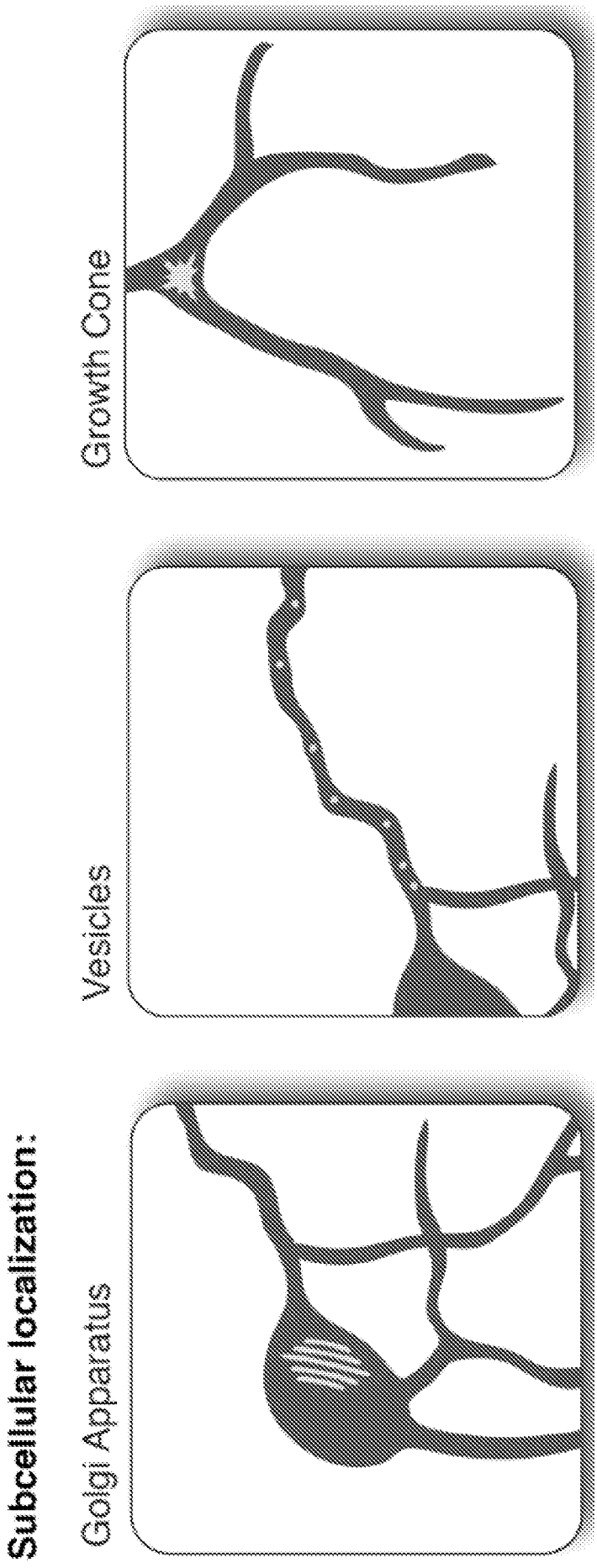

Subcellular localization:
Golgi Apparatus
Vesicles
Growth Cone

FIG. 80B

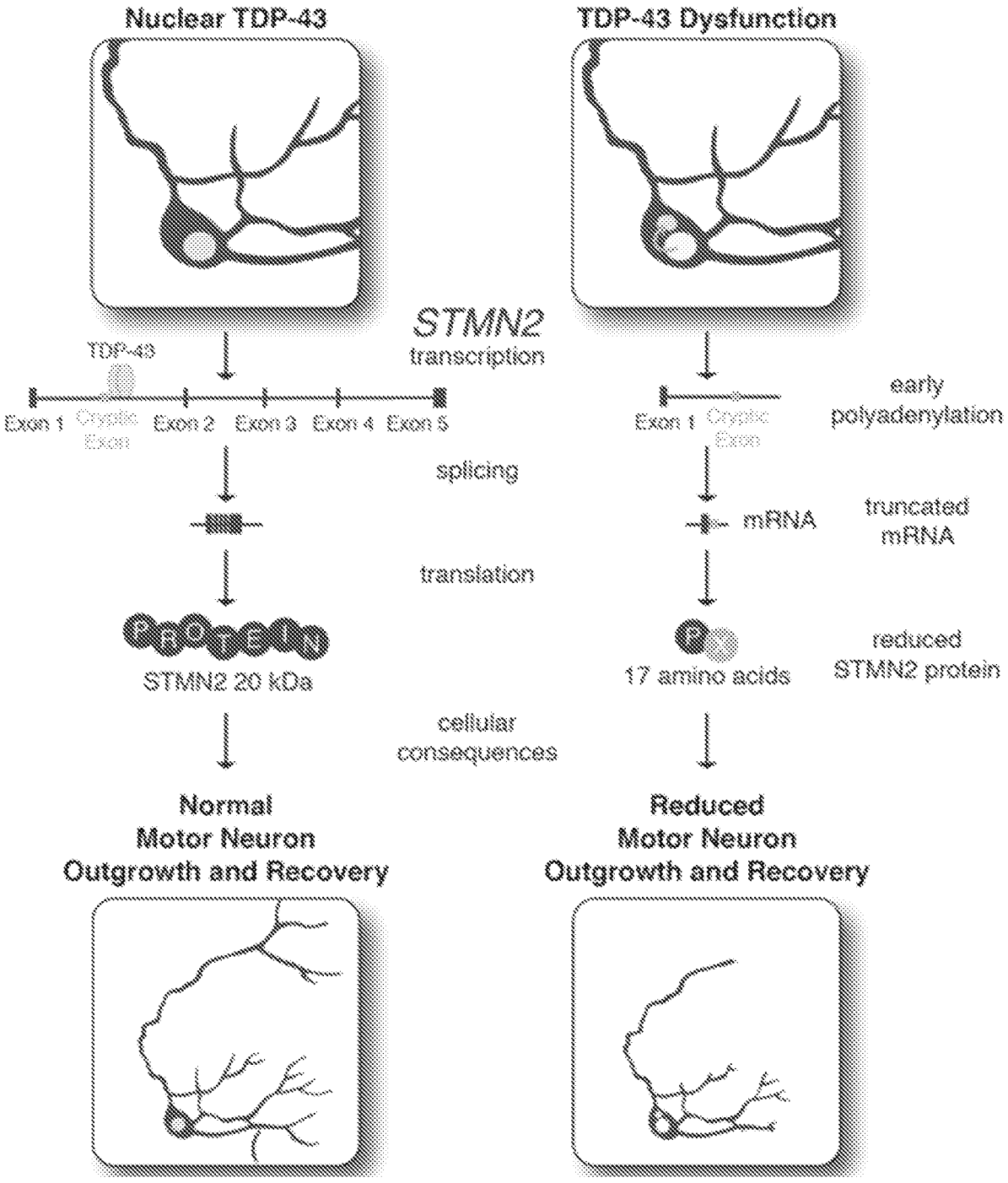

Nuclear TDP-43
TDP-43 Dysfunction
STMN2
transcription
TDP-43
Exon 1
Cryptic Exon
Exon 2
Exon 3
Exon 4
Exon 5
Exon 1
Cryptic Exon
early polyadenylation
splicing
mRNA
truncated mRNA
translation
PROTEIN
STMN2 20 kDa
17 amino acids
reduced STMN2 protein
cellular consequences
Normal Motor Neuron Outgrowth and Recovery
Reduced Motor Neuron Outgrowth and Recovery

FIG. 81

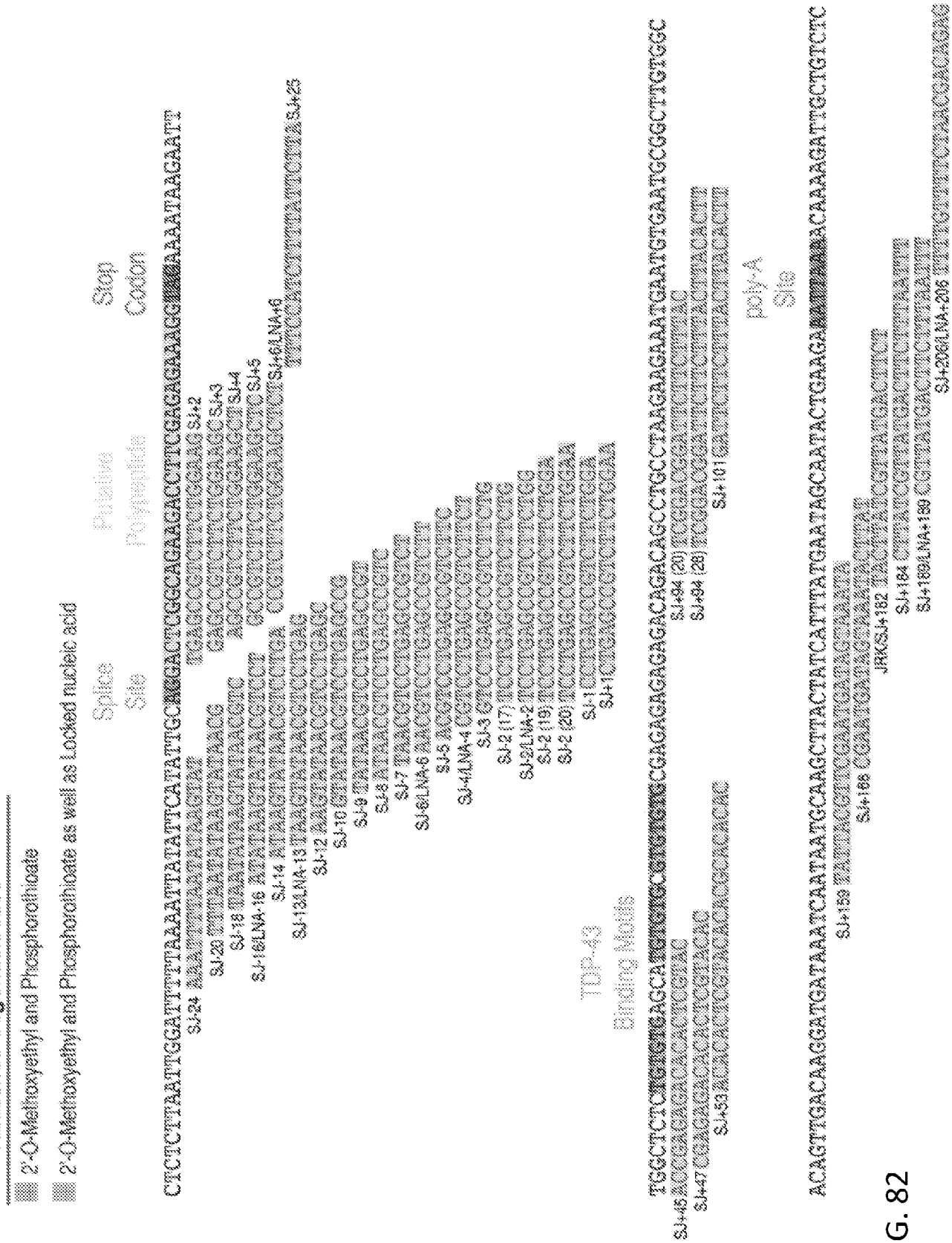

Antisense Oligonucleotides
2'-O-Methoxyethyl and Phosphorothioate
2'-O-Methoxyethyl and Phosphorothioate as well as Locked nucleic acid
Splice Site
Putative Polyamide
Stop Codon
CTCTCTTAATTGGATTTTTTAAAATTTATATTCATATTGCAGACTCGGCAGAAGACCTTCGAGAGAAAGGTTAAAATAAGAATT
SJ-24 AAATTTTATATTAAGTAT TCGAGCCGTCTTCTTCGAAG SJ-2
SJ-23 TTTAATTATAAGTATTAACG GAGCCGTCTTCTTCGAAGC SJ-3
SJ-18 TAATTATAAGTATTAACGTC AGCCGTCTTCTTCGAAGCT SJ-4
SJ-16LNA-16 ATATTAAGTATTAACGTCTT GCCGTCTTCTTCGAAGCTC SJ-5
SJ-14 ATTAAGTATTAACGTCTTCT CCGTCTTCTTCGAAGCTCTT SJ-6LNA+6
SJ-12LNA-13 TAAGTATTAACGTCTTCGAG TTTCGAAGCTCTTTAATTCTTTA SJ-25
SJ-12 AAGTATTAACGTCTTCGAGC
SJ-10 GTATTAACGTCTTCGAGCCG
SJ-9 TATTAACGTCTTCGAGCCGT
SJ-8 ATTAACGTCTTCGAGCCGTC
SJ-7 TTAACGTCTTCGAGCCGTCT
SJ-6LNA-6 AACGTCTTCGAGCCGTCTT
SJ-5 ACGTCTTCGAGCCGTCTTC
SJ-4LNA-4 CGTCTTCGAGCCGTCTTCT
SJ-3 GTCTTCGAGCCGTCTTCTG
SJ-2 (17) TCTTCGAGCCGTCTTCTG
SJ-2LNA-2 TCTTCGAGCCGTCTTCTG
SJ-2 (19) TCTTCGAGCCGTCTTCTGA
SJ-2 (20) TCTTCGAGCCGTCTTCTGAA
SJ-1 CTTCGAGCCGTCTTCTGA
SJ-1CTCGAGCCGTCTTCTGAA
TDP-43 Binding Motifs
TGGCTCTCTGTGTGAGCATGTCTCCTCTCGAGAGAGAGACAGACAGCCTGCCTAAGAAGAAATGAATGTGAATGCGGCTTGTGTGC
SJ-45 ACCGACAGACACACTCGTAC SJ-49 (20) TCGGACCGAATTCTTCTTACTTACACTT
SJ-47 CGAGACAGACACACTCGTACAC SJ-49 (28) TCGGACCGAATTCTTCTTACTTACACTTT
SJ-53 ACAGACACTCGTACACACCACACAC SJ-101 GAATTCTTCTTACTTACACTTT
poly-A Site
ACAGTTGACAAGGATGATAAATCAATAATGCAAGCTTACTATCATTTATGAATAGCAATACTGAAGAAAAAAAAAACAAAAGATTGCTGTCTC
SJ-159 TATTACCTTCCGATCATTAGTTAAATA
SJ-160 CGATCATTAGTTAATACTTAAT
JRKSJ-4182 TACTTATCGTTAATGACTTCT
SJ-184 CTTATCGTTAATGACTTCTTTAATTT
SJ-180LNA+189 CGTTAATGACTTCTTTAATTT
SJ-206LNA+206 TTTTGTTTTCTTAACGACAGAG

FIG. 82

CTCTTAATTGGATTTTTTAAAAATTATATTCATATTGCAGGACTCGGCAGAAGACCTTCGAGAGAA
AGGTAGAAAATAAGAATTTGGCTCTCTGTGTGAGGCATGTGTGGCGTGTGCGAGAGAGAGGAGAC
AGACAGCCTGCCTAAGAAGAAATGAATGTGAATGCGGCTTGTGGCACACAGTTGACAAGGATGATA
AATCAATAATGCAAGCTTACTATCATTTATGAATAGCAATACTGAAGAAATTAAAAACAAAAAGAT
TGCTGTCTCAATATATCTTATATTTATTTACCAAATTA

Color codes for sequence annotation:

Nucleotides flanking the cryptic splice site

Predicted TDP-43 binding site

Predicted dynamic region just downstream of TDP-43 binding site

Putative premature polyadenylation signal

Nucleotides not included in the truncated RNA isoform

FIG. 83A

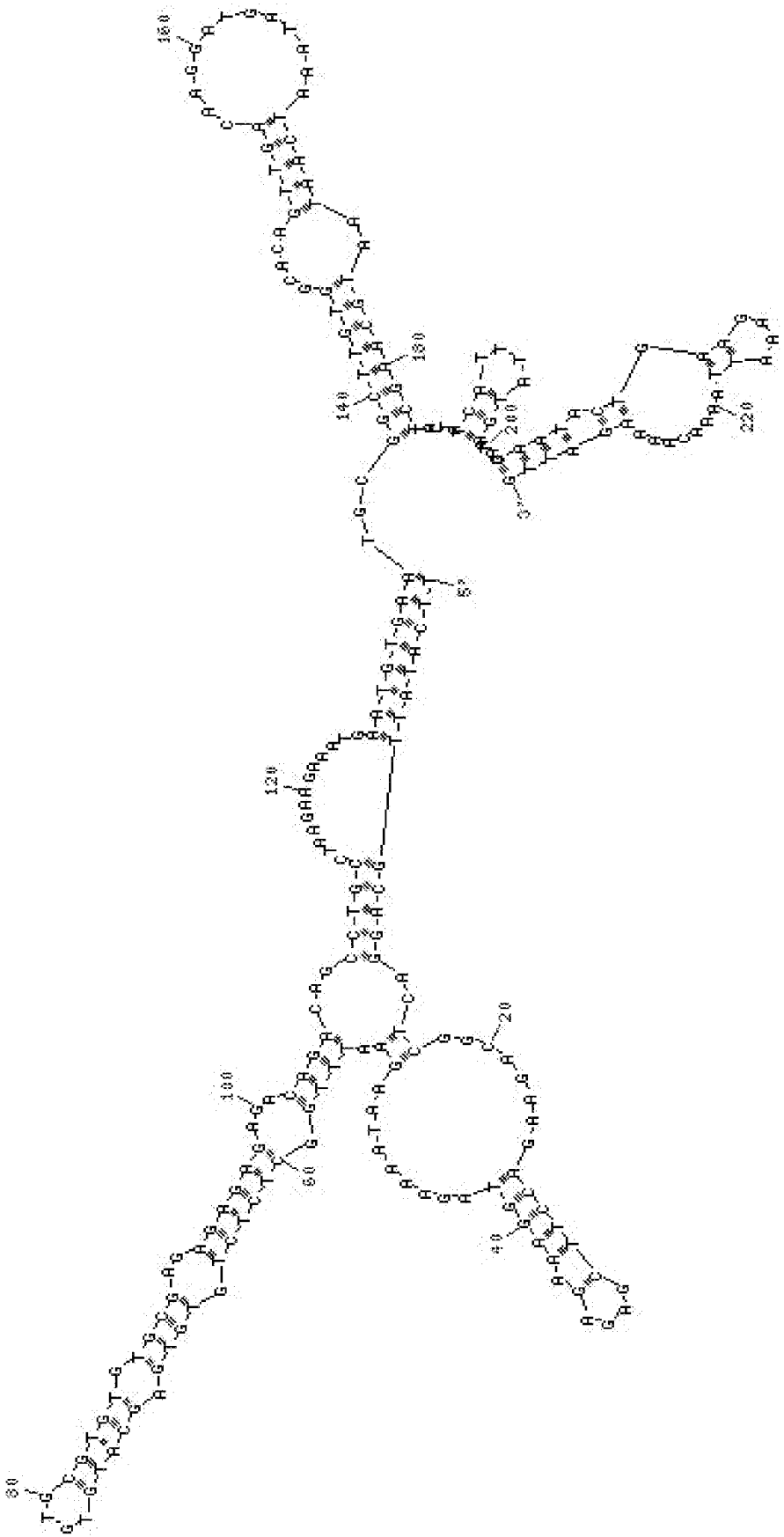


FIG. 83B

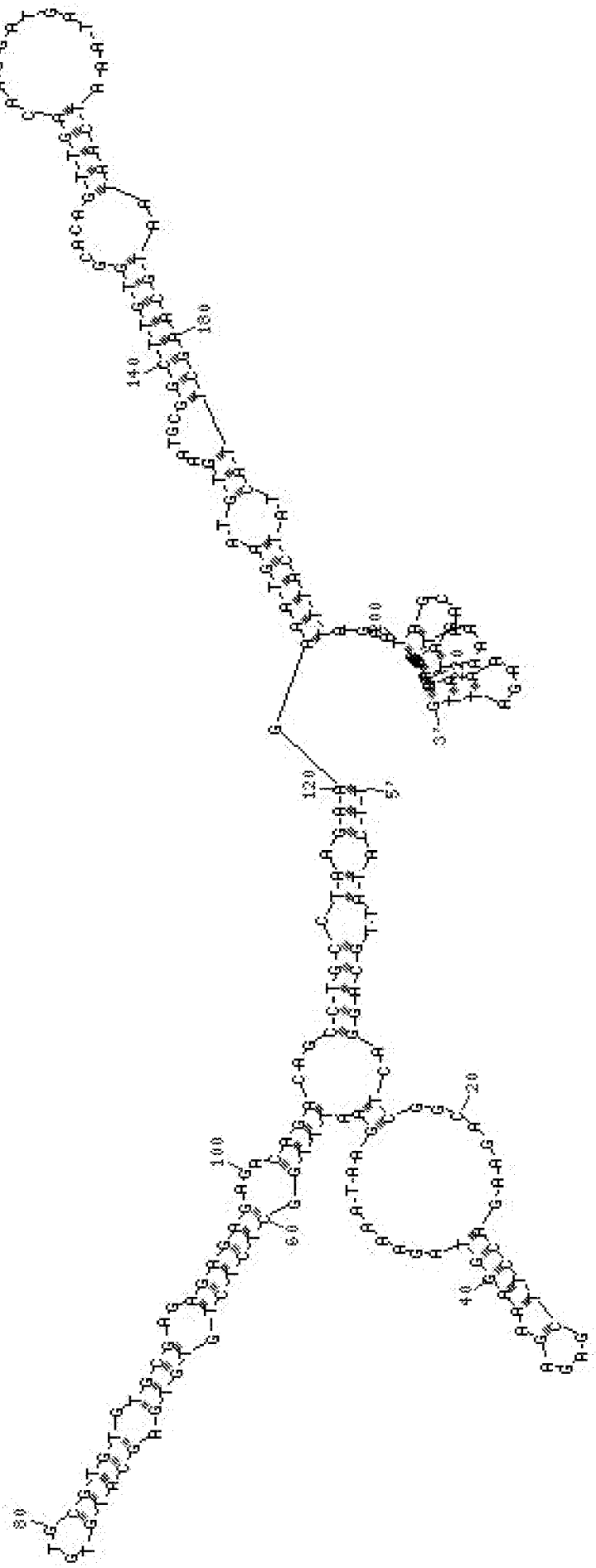


FIG. 83C

FIG. 84B

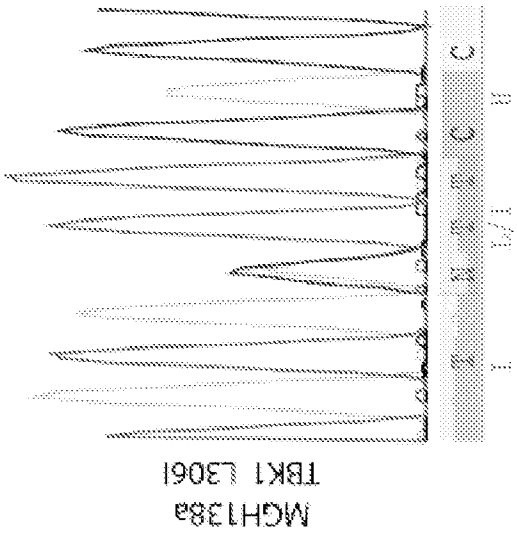
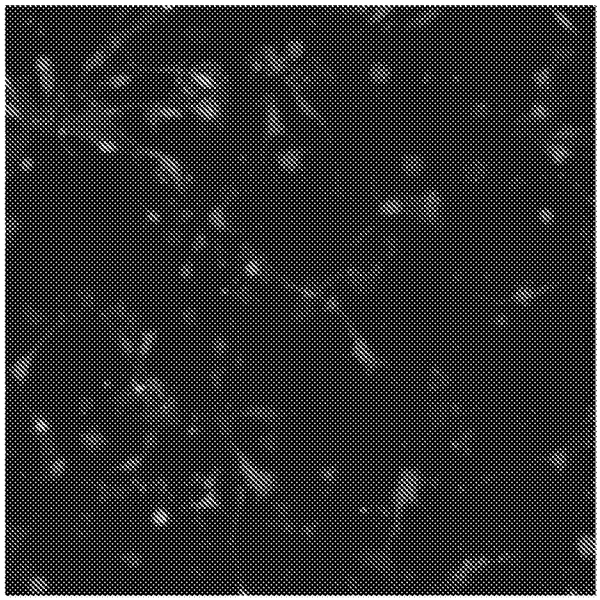


FIG. 84D



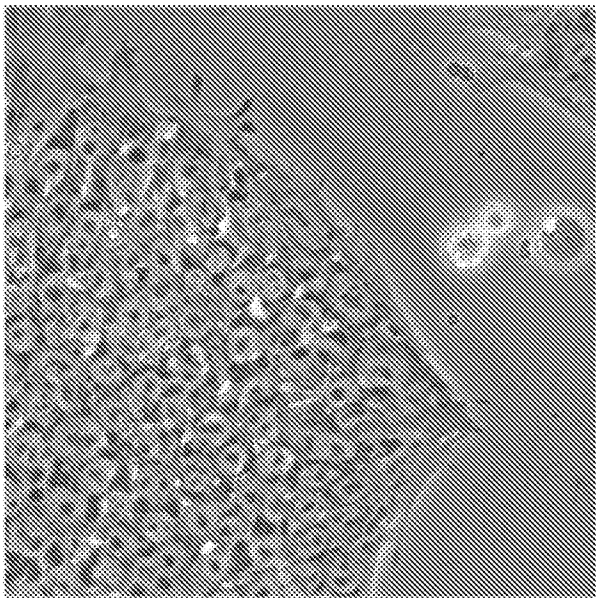


FIG. 84A

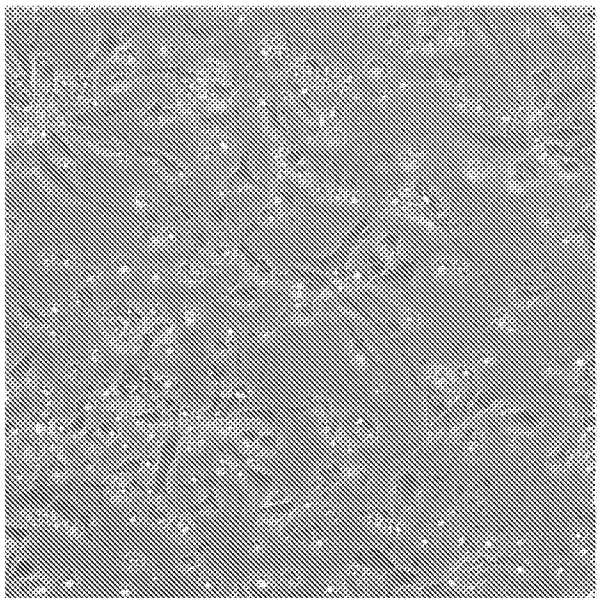


FIG. 84C

FIG. 85A

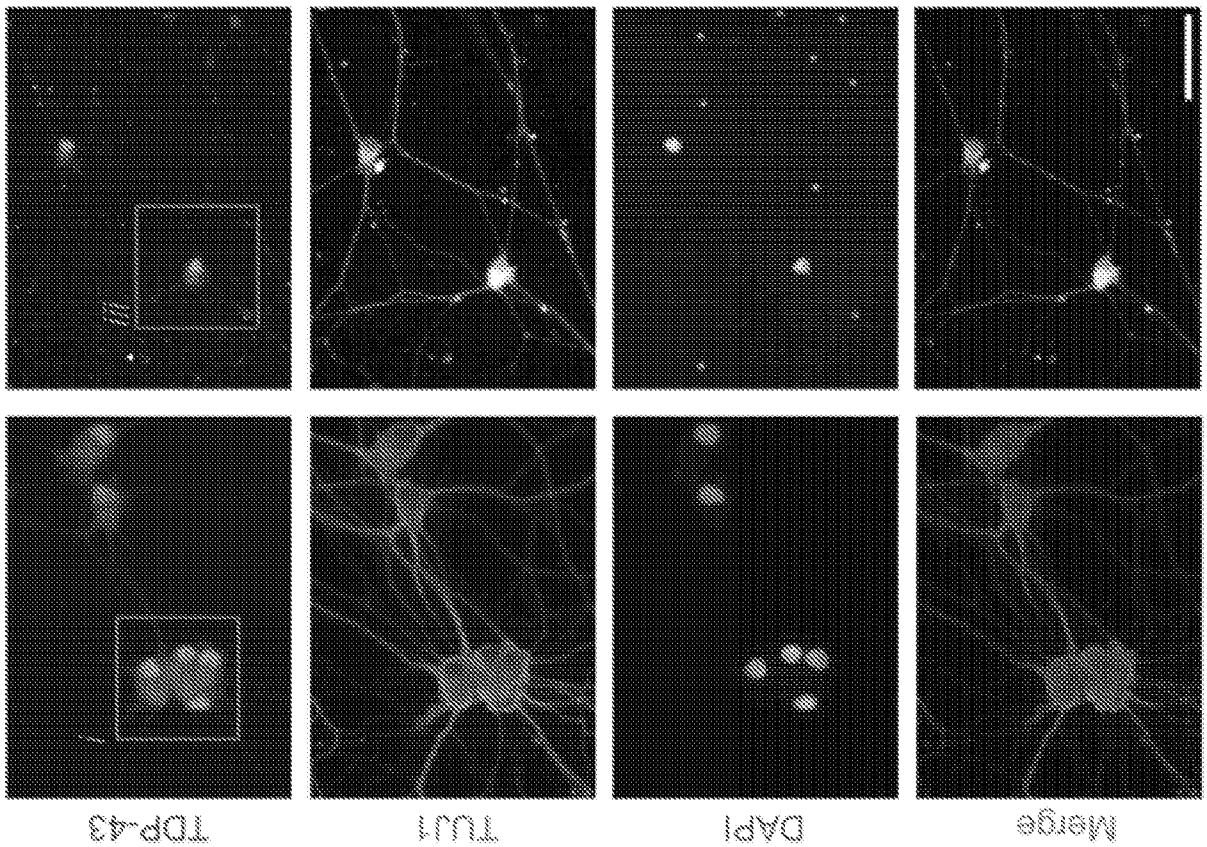
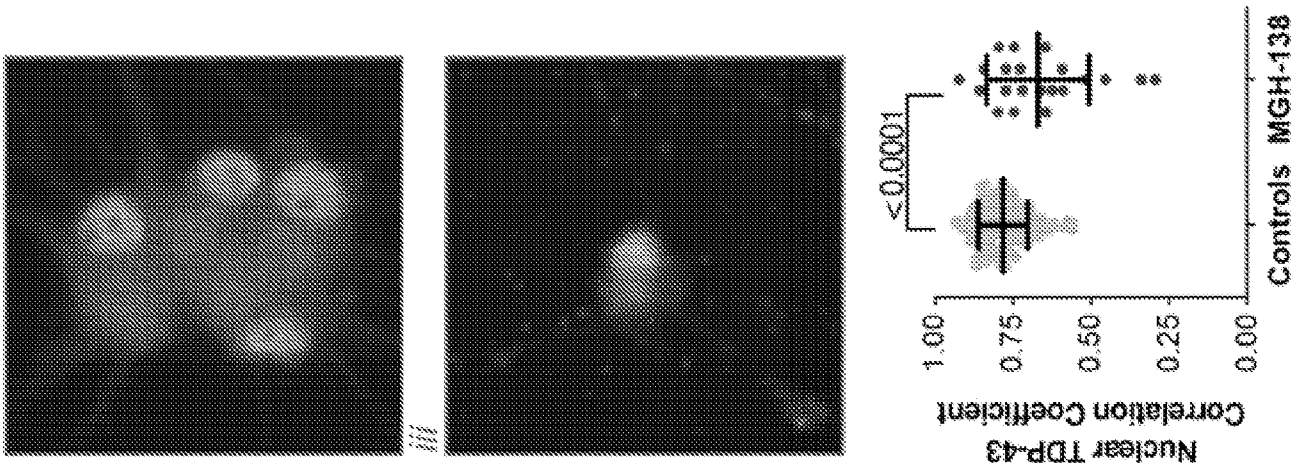


FIG. 85B



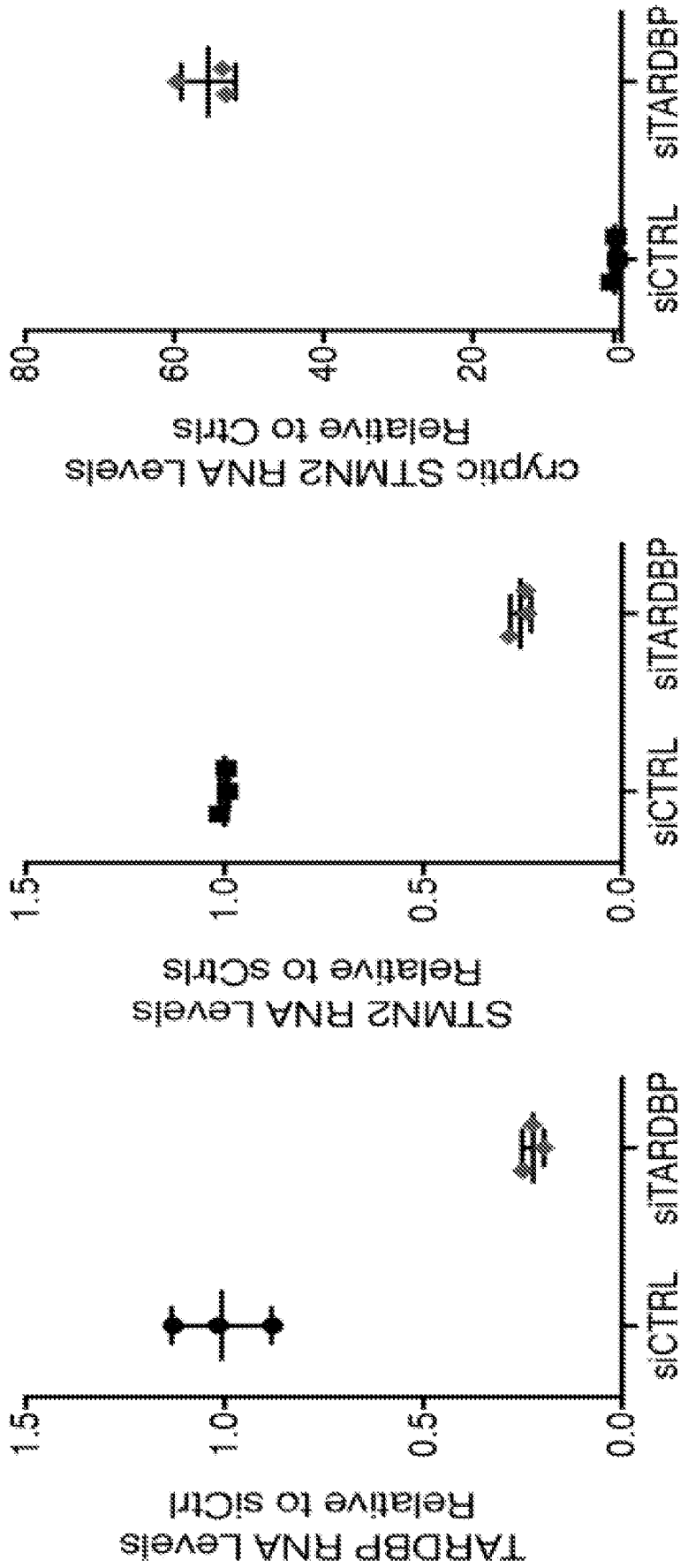


FIG. 86A

FIG. 86B

FIG. 86C

```
STMN2 Ref.  GCTGATTCTGACCACTAAACACATCAGTTTTAGGGATATTAACTTGTAATATACAGGTAT  60
MGH-138a    GCTGATTCTGACCACTAAACACATCAGTTTTAGGGATATTAACTTGTAATATACAGGTAT  60
            ************************************************************

STMN2 Ref.  CCCTCCTGGTAAGCTCTGGTATTATGTCTTAACATTTTTAAATCTATGGTAATCTTTACA 120
MGH-138a    CCCTCCTGGTAAGCTCTGGTATTATGTCTTAACATTTTTAAATCTATGGTAATCTTTACA 120
            ************************************************************

STMN2 Ref.  AAATATTTTACTTCCGAACTCATATACCTGGGGATTTTATTACTCTGGAATTATGTGTT 180
MGH-138a    AAATATTTTACTTCCGAACTCATATACCTAGGGATTTTATTACTCTGGAATTATGTGTT 180
            ****************************** ******************************

STMN2 Ref.  CTGCCCCATCACTCTCTCTTAACTGCATTTTTAAAATTATATTCATATTGCAGGACTCGG 240
MGH-138a    CTGCCCCATCACTCTCTCTTAATTGCATTTTTAAAATTATATTCATATTGCAGGACTCGG 240
            ************************************************************
ASO Targeted Region
STMN2 Ref.  CAGAAGACCTTCGAGAGAAGGTAGAAATAAGAATTGGCTCTCTGTGTGAGCATGTGT 300
MGH-138a    CAGAAGACCTTCGAGAGAAGGTAGAAATAAGAATTGGCTCTCTGTGTGAGCATGTGT 300
            ************************************************************

STMN2 Ref.  GCGTGTGTGCGAGAGAGAGACAGACAGCCTGCCTAAGAAGAAATGAATGTGAATGCGG 360
MGH-138a    GCGTGTGTGCGAGAGAGAGACAGACAGCCTGCCTAAGAAGAAATGAATGTGAATGCGG 360
            ************************************************************

STMN2 Ref.  CTTGTGGCACAGTTGACAAGGATGATAAATCAATAATGCAAGCTTACTATCATTTATGAA 420
MGH-138a    CTTGTGGCACAGTTGACAAGGATGATAAATCAATAATGCAAGCTTACTATCATTTATGAA 420
            ************************************************************

STMN2 Ref.  TAGCAATACTGAAGAAATTAAAACAAAAGATTGCTGTCTCAATATATCTTATATTTATTA 480
MGH-138a    TAGCAATACTGAAGAAATTAAAACAAAAGATTGCTGTCTCAATATATCTTATATTTATTA 480
            ************************************************************

STMN2 Ref.  TTTACCAAATTATTCTAAGAGTATTTCTTCCTGAATACCATGTGAGAAAATTCTTAAGAA 540
MGH-138a    TTTACCAAATTATTCTAAGAGTATTTCTTCCTGAATACCATGTGAGAAAATTCTTAAGAA 540
            ************************************************************

STMN2 Ref.  TTTATTGAGTATGACTGTATATTTGAAAAGAGTGTTTTCTTCTGCTTATCTAAGCCAATA 600
MGH-138a    TTTATTGAGTATGACTGTATATTTGAAAAGAGTGTTTTCTTCTGCTTATCTAAGCCAATA 600
            ************************************************************

STMN2 Ref.  AAGGATCTTCATTATTCAATTCTAACTTTCTAAGGAAGTCAACCTACAGATCAGAAAGAG 660
MGH-138a    AAGGATCTTCATTATTCAATTCTAACTTTCTAAGGAAGTCAACCTACAGATCAGAAAGAG 660
            ************************************************************

STMN2 Ref.  GATCTTCAAGGAATAGCATCAAAGACATAGTCAGGTCTCCCATGCACTGACTGGCTGACC 720
MGH-138a    GATCTTCAAGGAATAGCATCAAAGACATAGTCAGGTCTCCCATGCACTGACTGGCTGACC 720
            ************************************************************

STMN2 Ref.  ATGCAGCCATTACCACCTTTCTGGAAATATTATGCTGCAAAAAT 764
MGH-138a    ATGCAGCCATTACCACCTTTCTGGAAATATTATGCTGCAAAAAT 764
            *********************************************
```

FIG. 87A

FIG. 87B

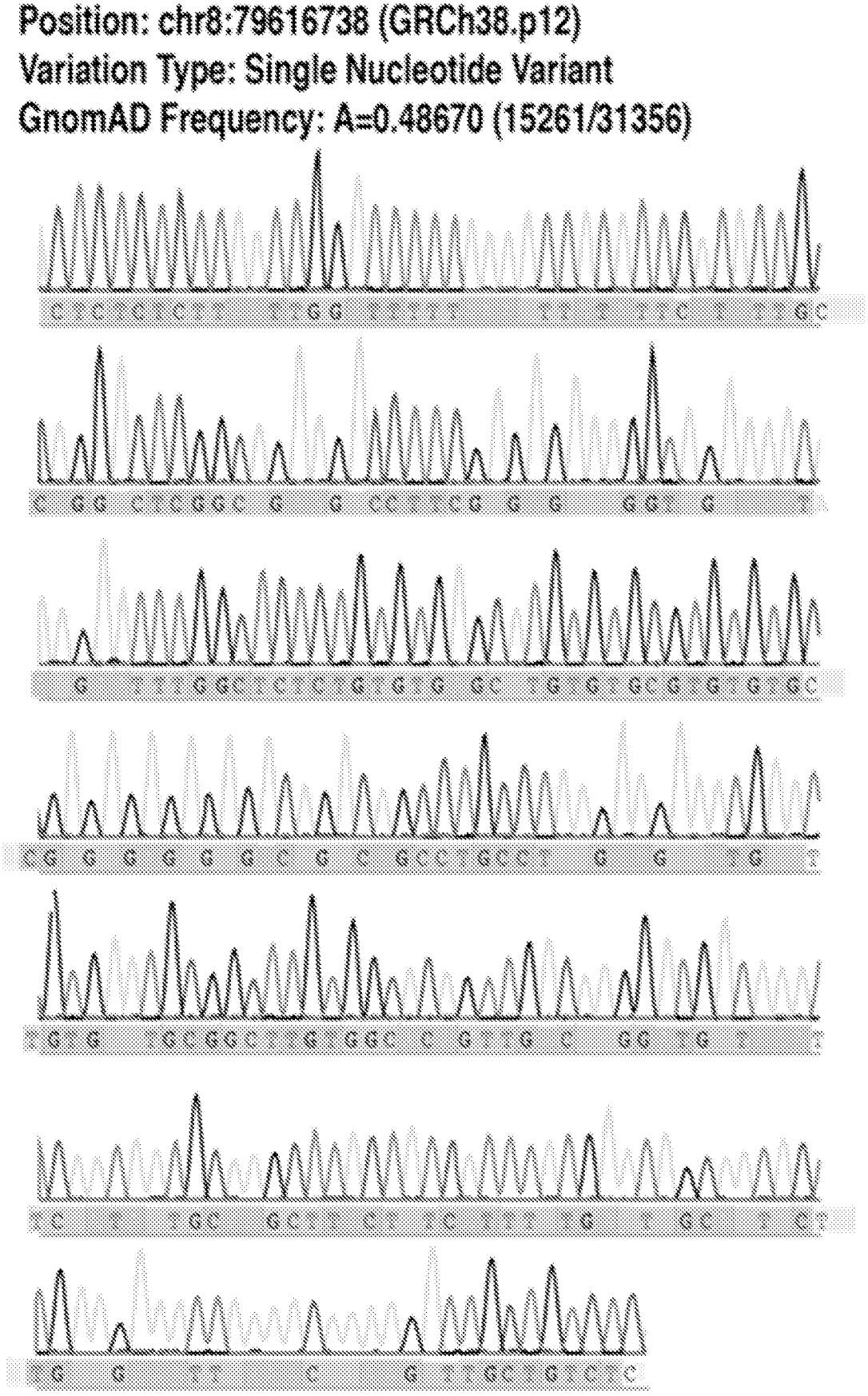


FIG. 87C

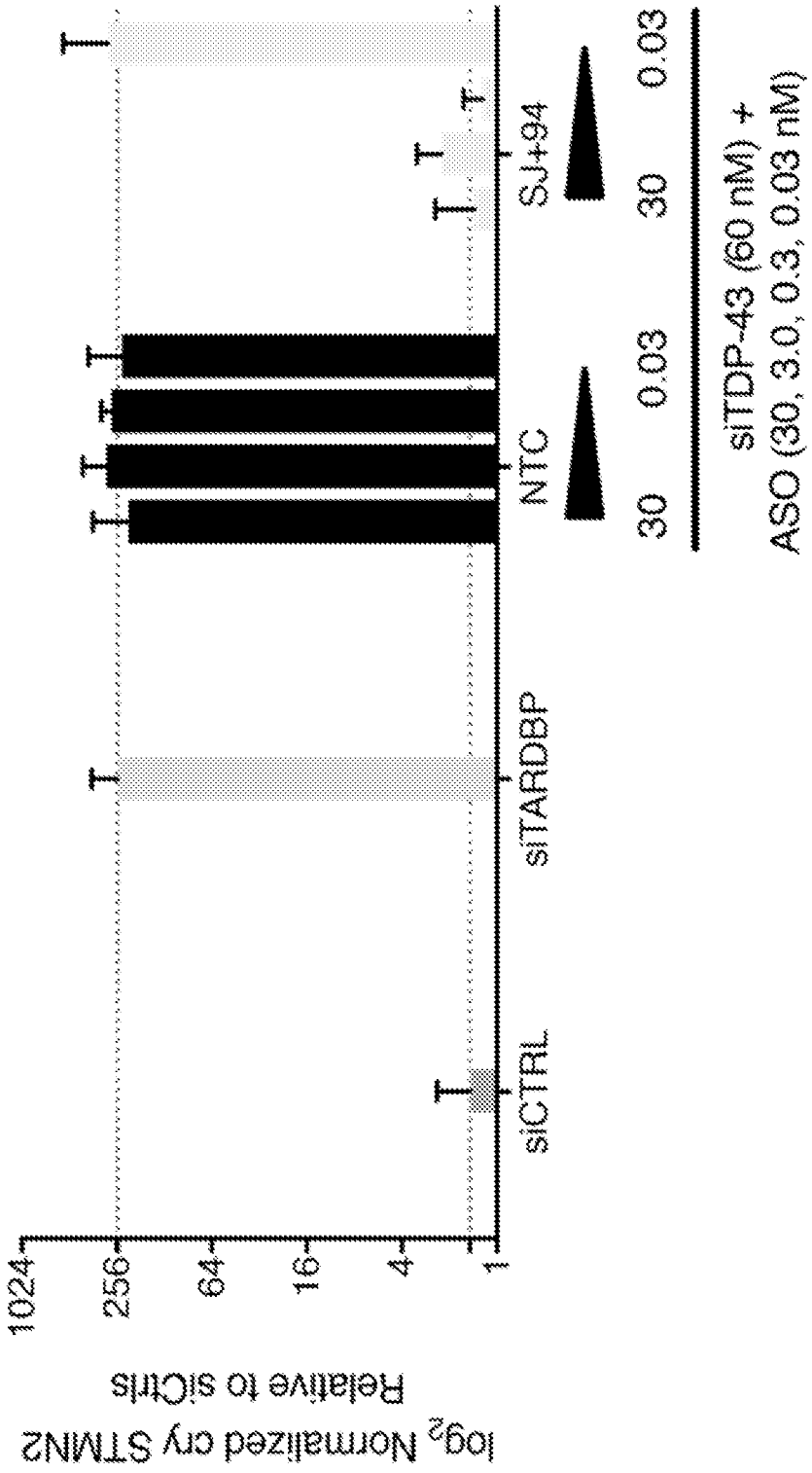

log2 Normalized cry STMN2
Relative to siCtrls
1024
256
64
16
4
1
siCTRL
siTARDBP
NTC
SJ+94
30
0.03
30
0.03
30
siTDP-43 (60 nM) +
ASO (30, 3.0, 0.3, 0.03 nM)

FIG. 88A

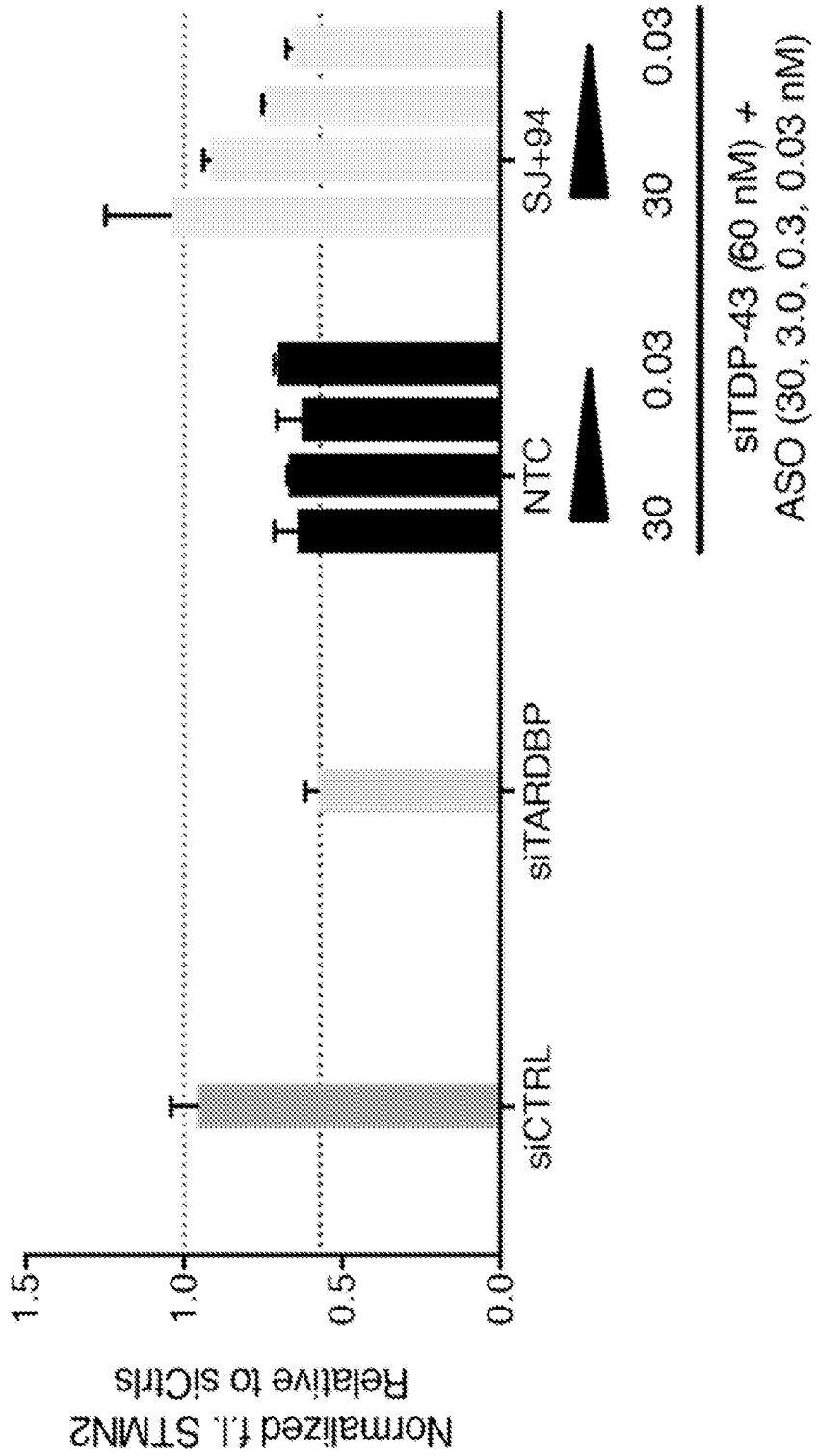

Normalized f.l. STMN2
Relative to siCtrls
1.5
1.0
0.5
0.0
siCTRL
siTARDBP
NTC
SJ+94
30
0.03
30
0.03
siTDP-43 (60 nM) +
ASO (30, 3.0, 0.3, 0.03 nM)

FIG. 88B

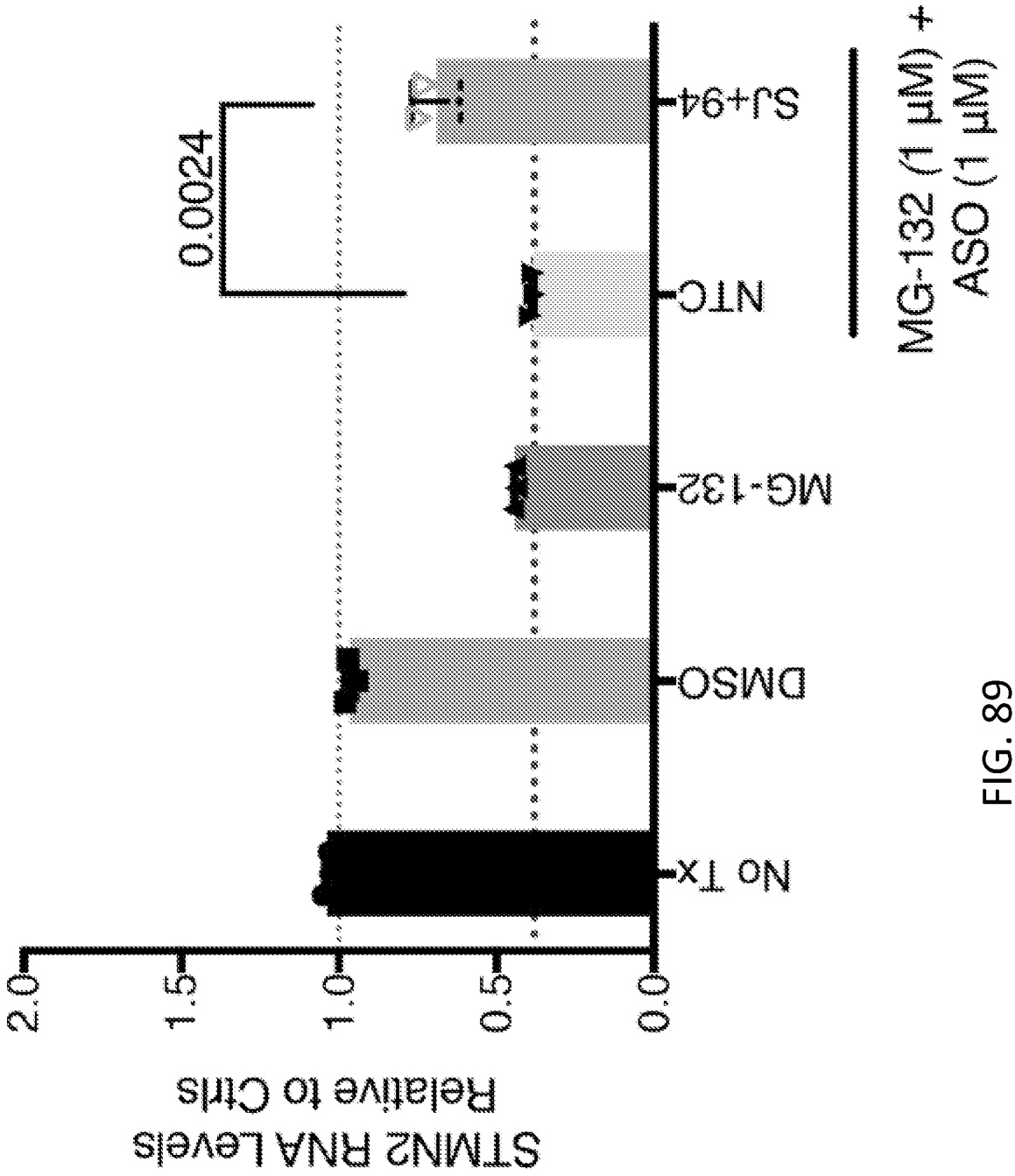

STMN2 RNA Levels
Relative to Ctrls
2.0
1.5
1.0
0.5
0.0
No Tx
DMSO
MG-132
NTC
SJ+94
0.0024
MG-132 (1 μM) +
ASO (1 μM)

FIG. 89

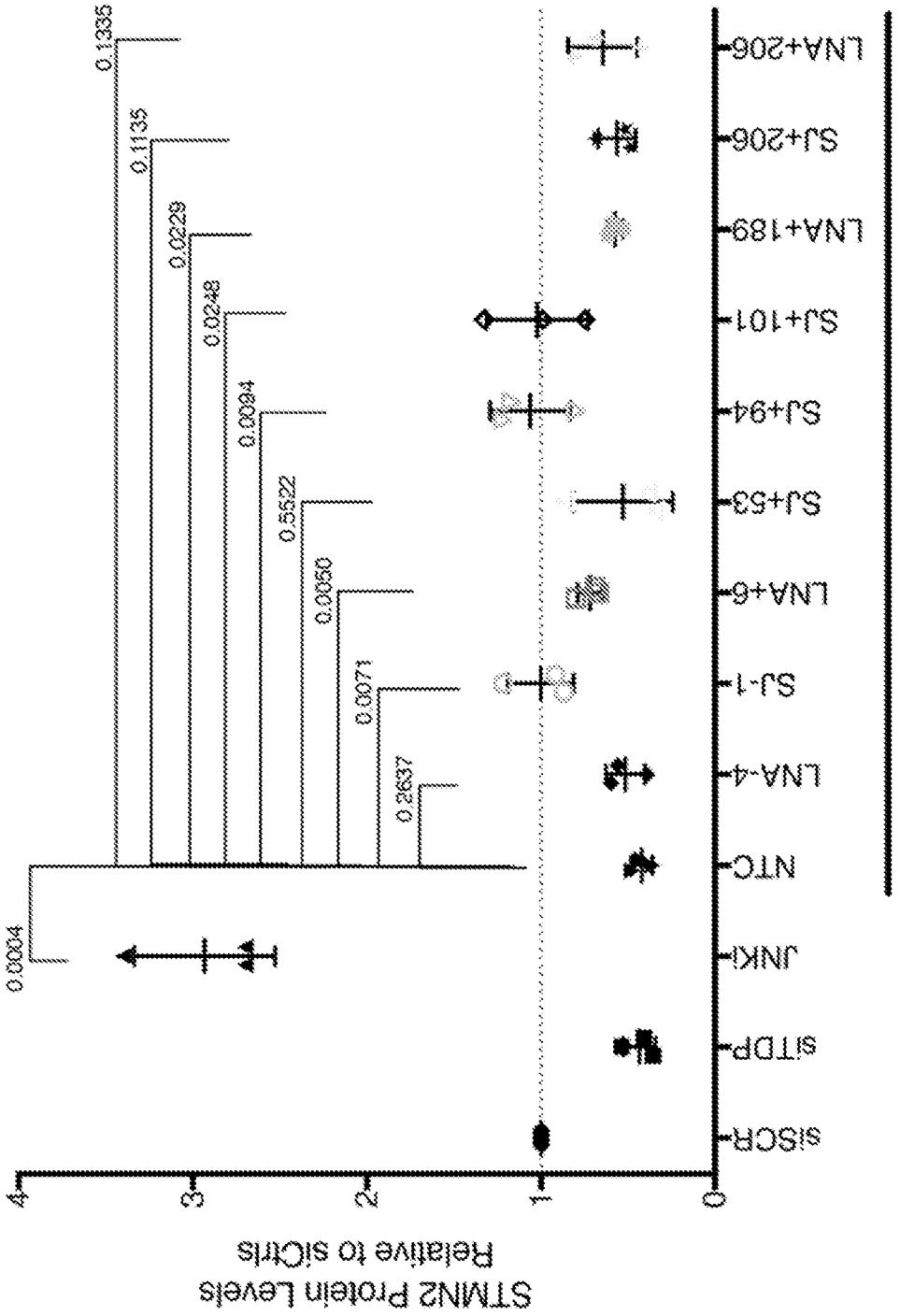

siSCR
siTDP
JNK1
NTC
LNA-4
SJ-1
LNA+6
SJ+53
SJ+94
SJ+101
LNA+189
SJ+206
LNA+206
0.1335
0.1135
0.0229
0.0248
0.0094
0.5522
0.0050
0.0071
0.2637
0.0004
0
1
2
3
4
STMN2 Protein Levels
Relative to siCtrls

FIG. 90

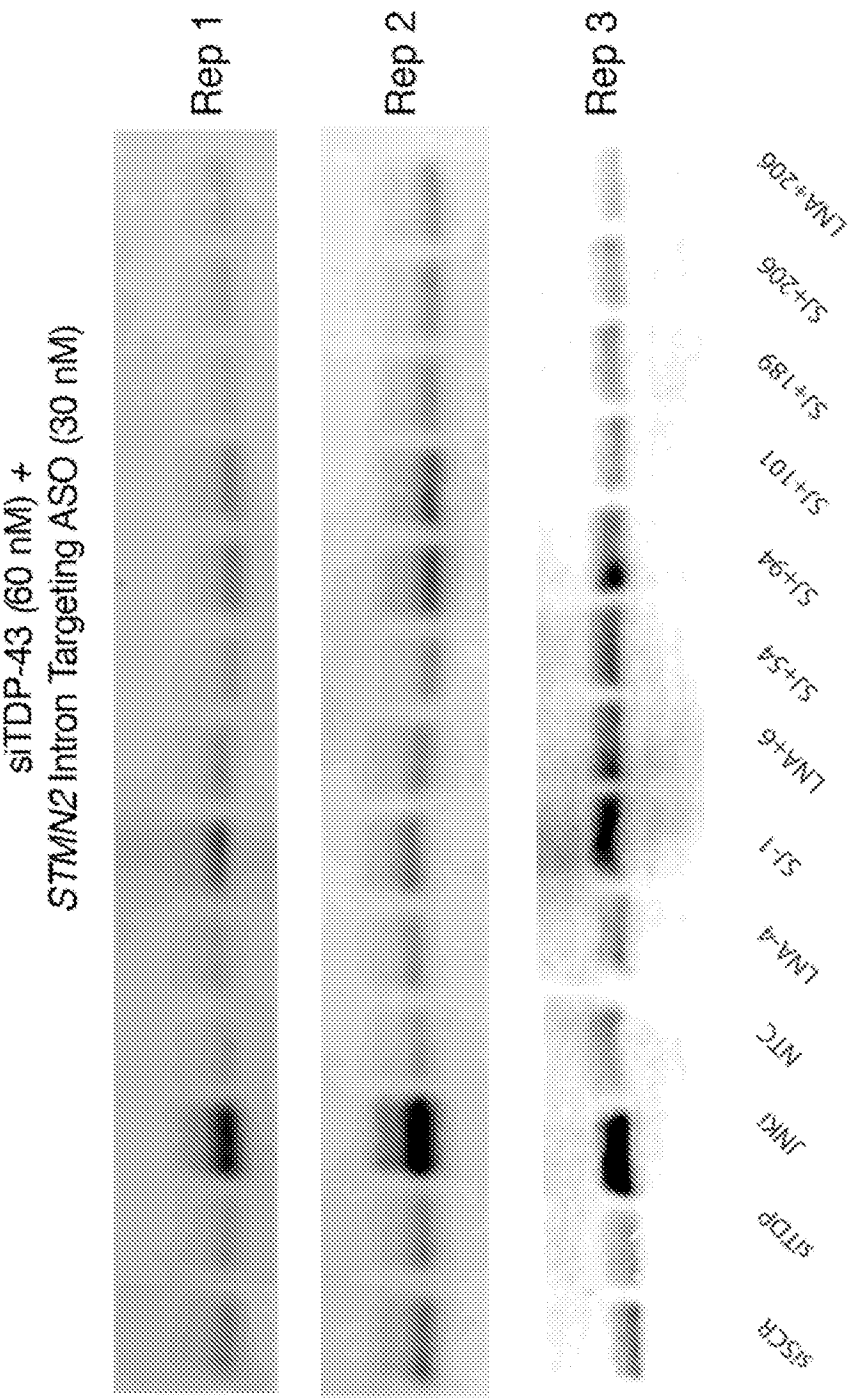

siTDP-43 (60 nM) +
STMN2 Intron Targeting ASO (30 nM)
Rep 1
Rep 2
Rep 3
siSCR
siTDP
JNK1
NTC
LNA-4
SJ-1
9+LNA
5+5
6+5
10+5
18+5
20+5
LNA+20

FIG. 90 cont.

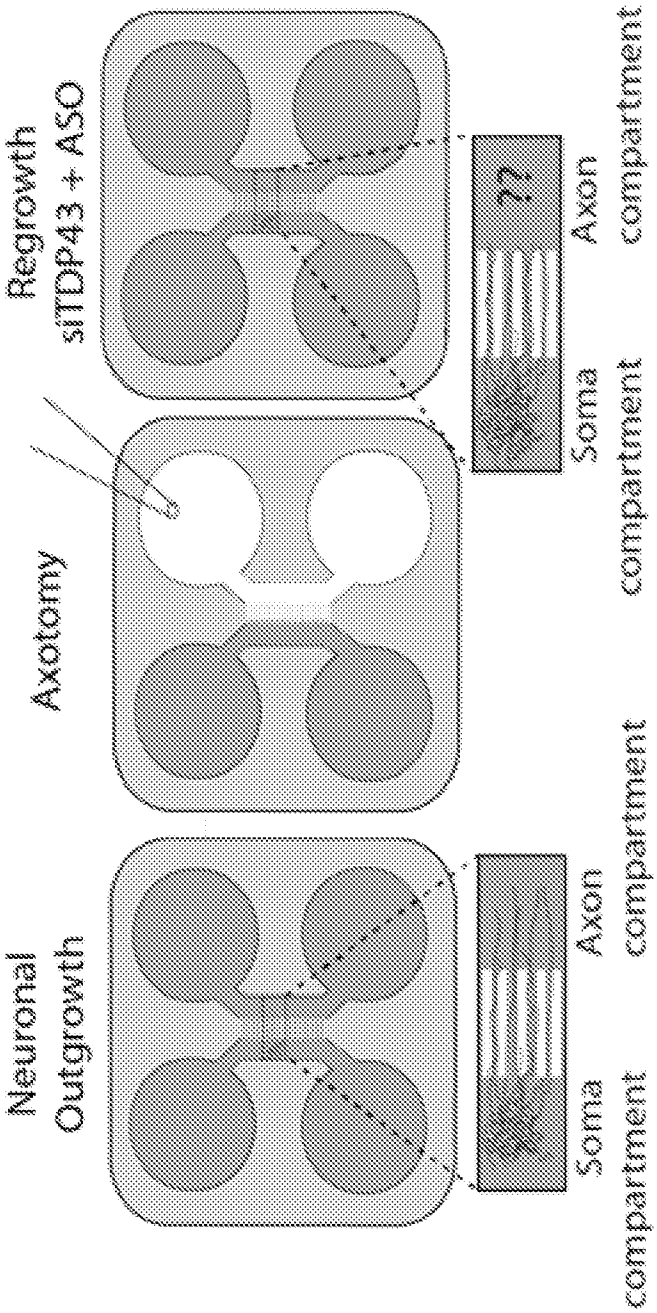

Neuronal Outgrowth
Axotomy
Regrowth siTDP43 + ASO
Soma compartment
Axon compartment
??
Soma compartment
Axon compartment

FIG. 91A

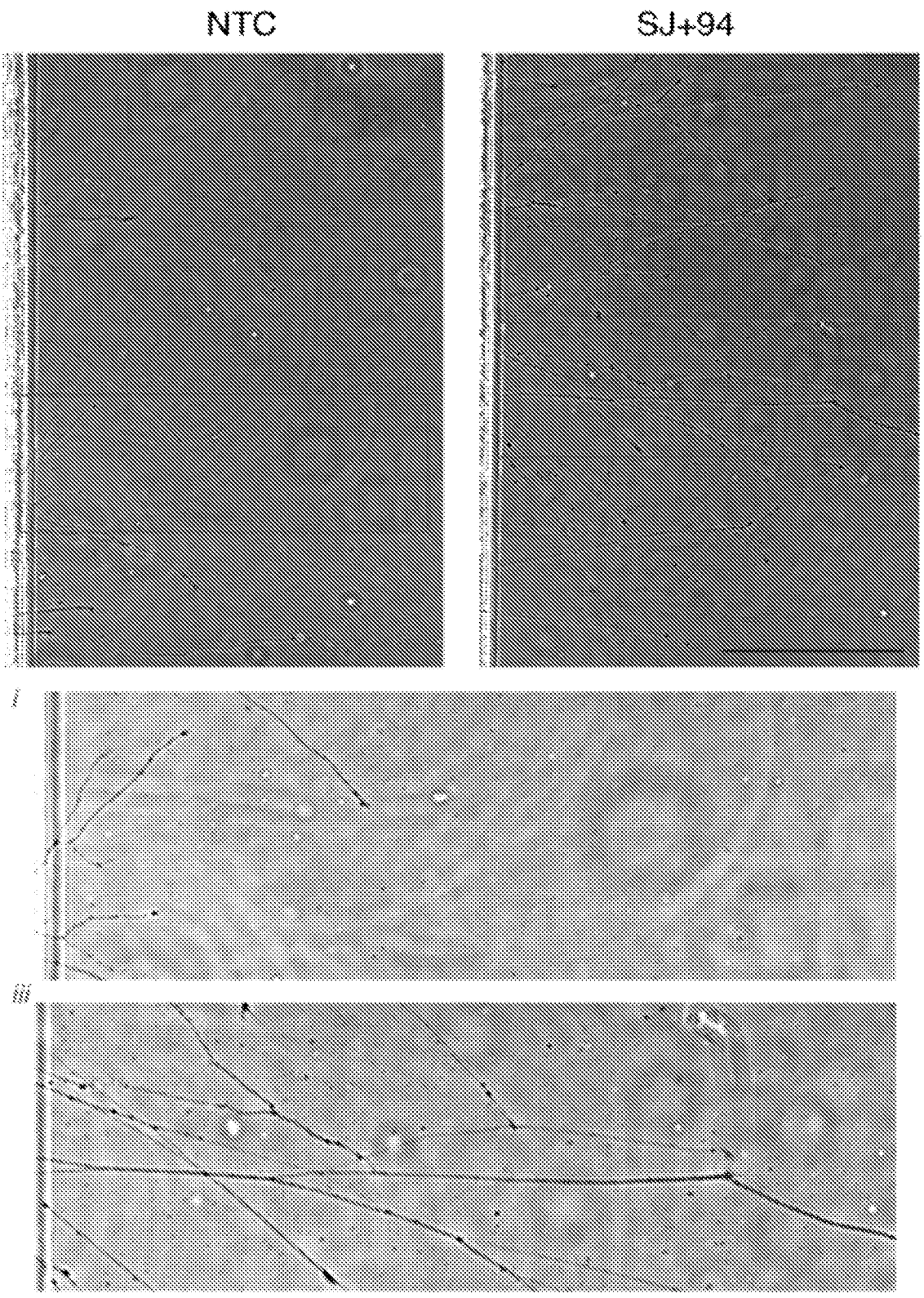


FIG. 91B

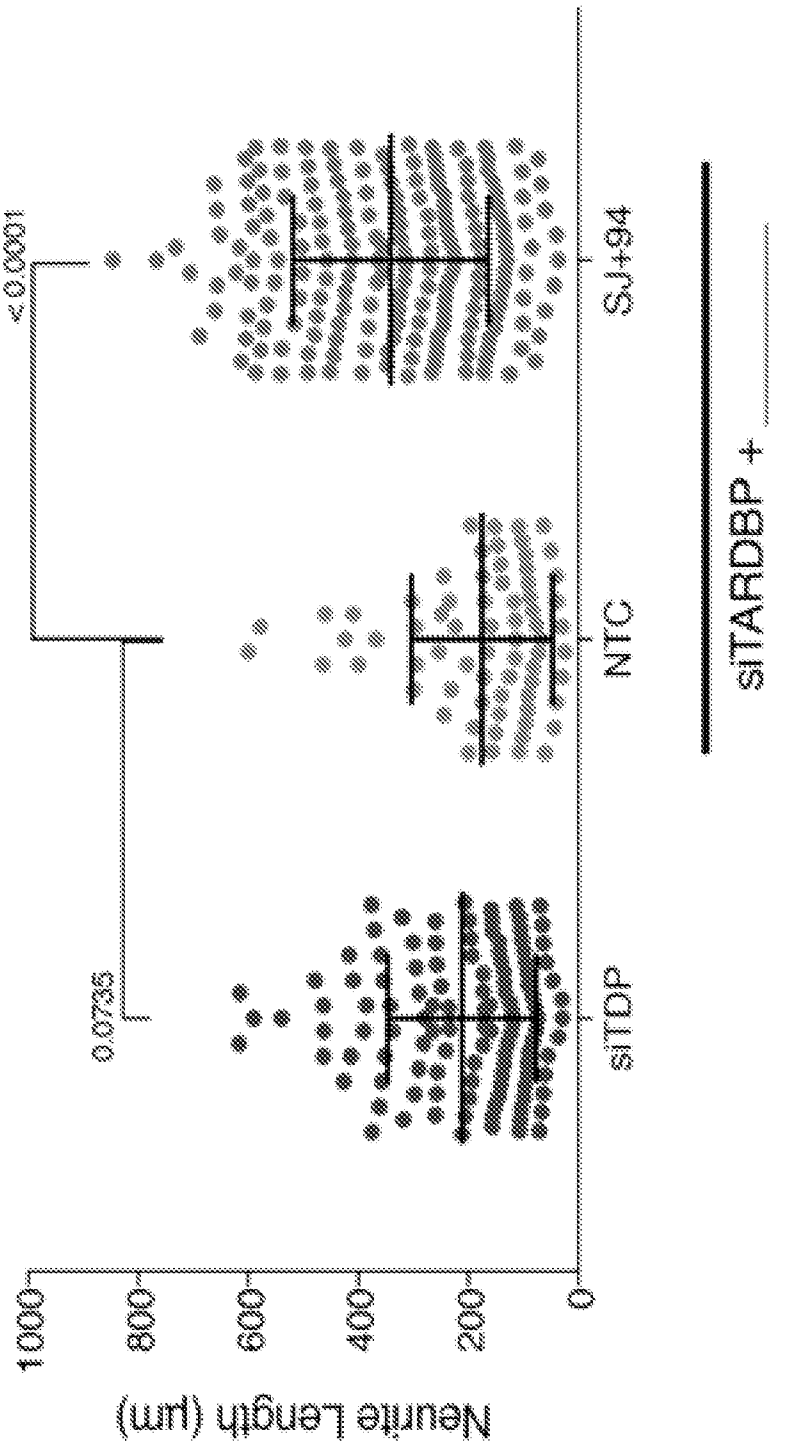

Neurite Length (µm)
1000
800
600
400
200
0
siTDP
NTC
SJ+94
0.0735
<0.0001
siTARDBP +

FIG. 91C

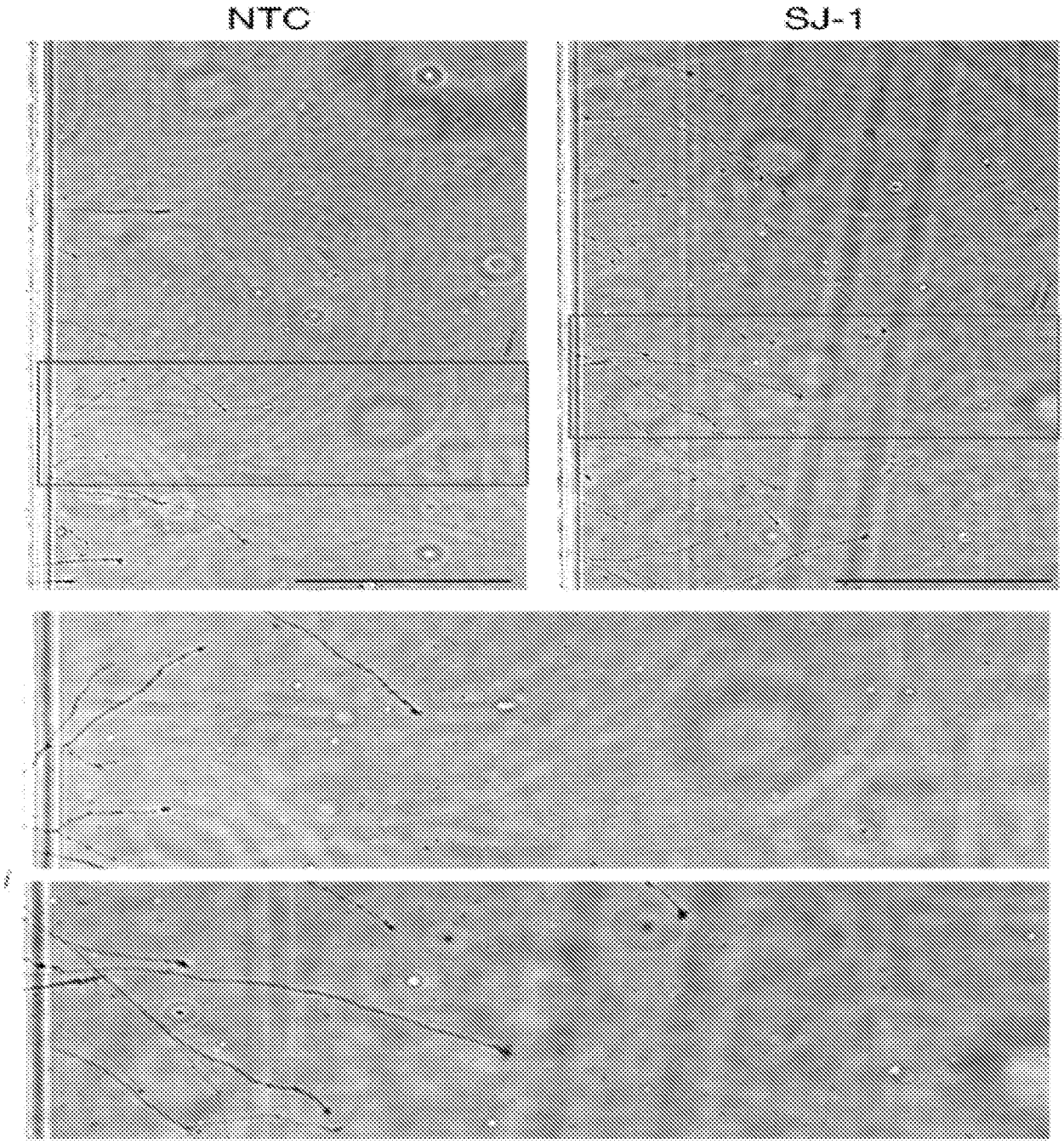


FIG. 91D

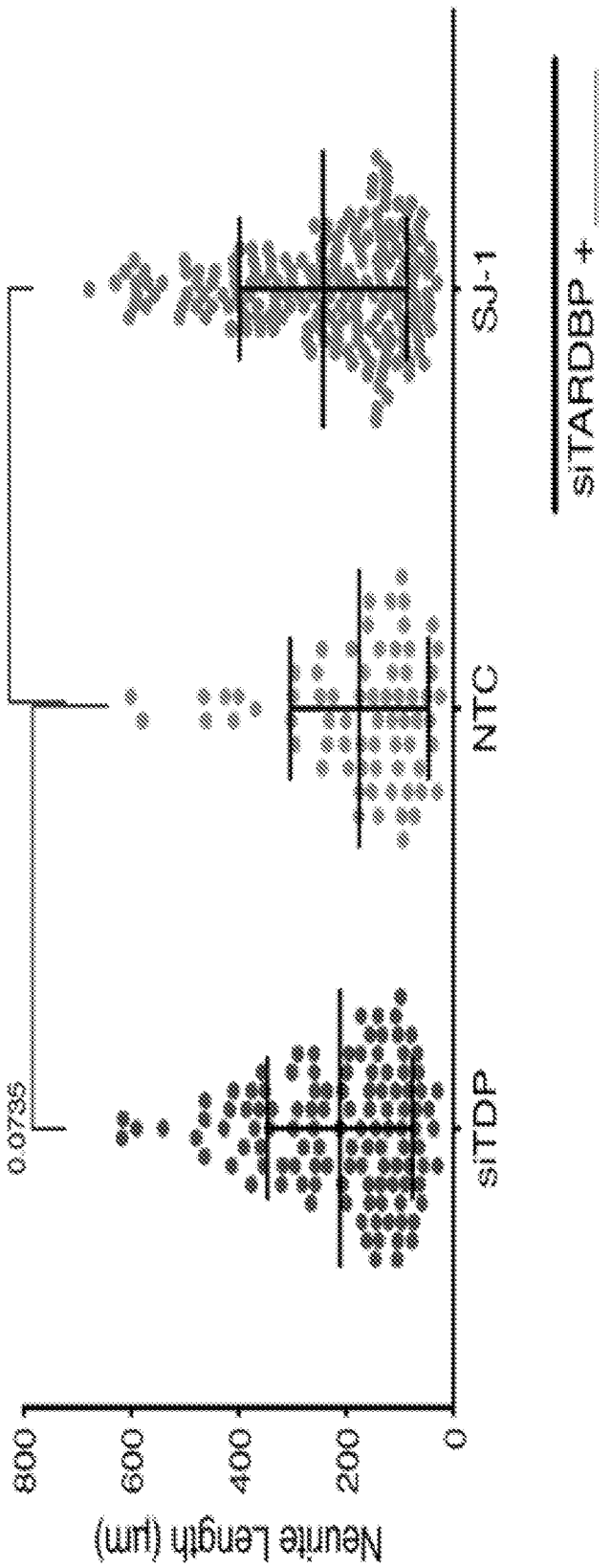

Neurite Length (µm)
800
600
400
200
0
0.0735
0.0014
siTDP
NTC
SJ-1
siTARDBP +

FIG. 91E

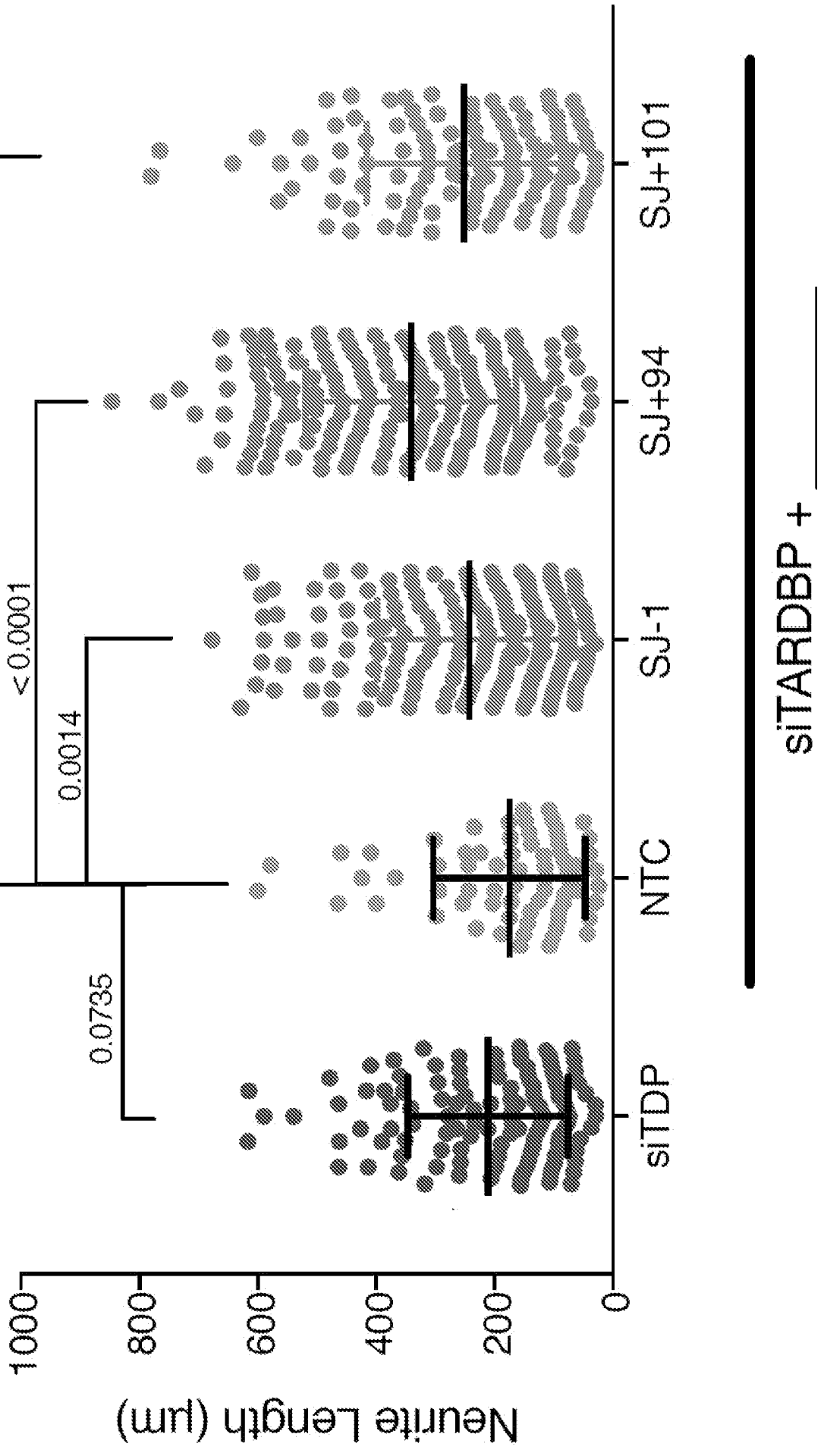

Neurite Length (µm)
1000
800
600
400
200
0
siTDP
NTC
SJ-1
SJ+94
SJ+101
0.0735
0.0014
<0.0001
0.0010
siTARDBP +

FIG. 92

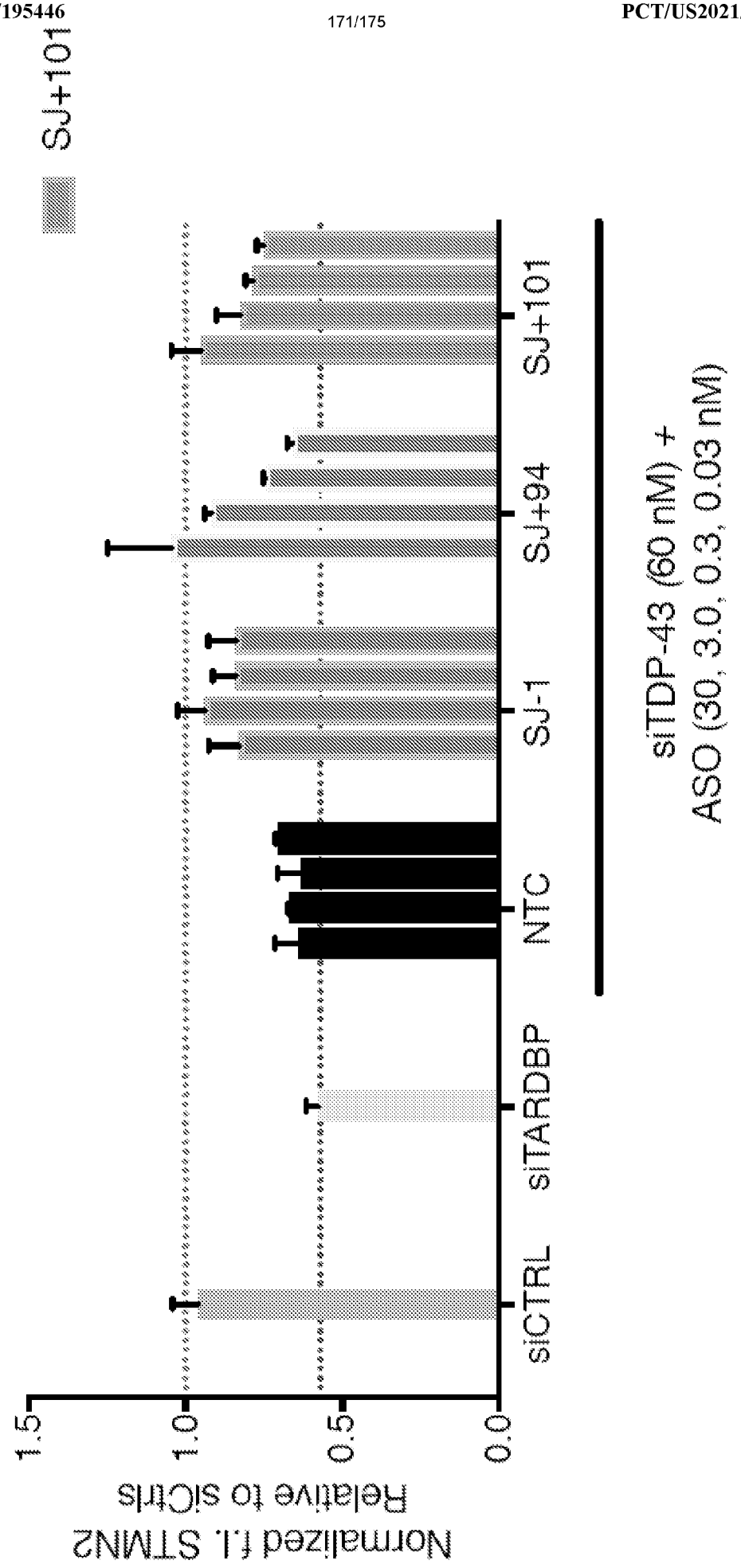

SJ+101
Normalized f.l. STMN2
Relative to siCtrls
1.5
1.0
0.5
0.0
siCTRL
siTARDBP
NTC
SJ-1
SJ+94
SJ+101
siTDP-43 (60 nM) +
ASO (30, 3.0, 0.3, 0.03 nM)

FIG. 93

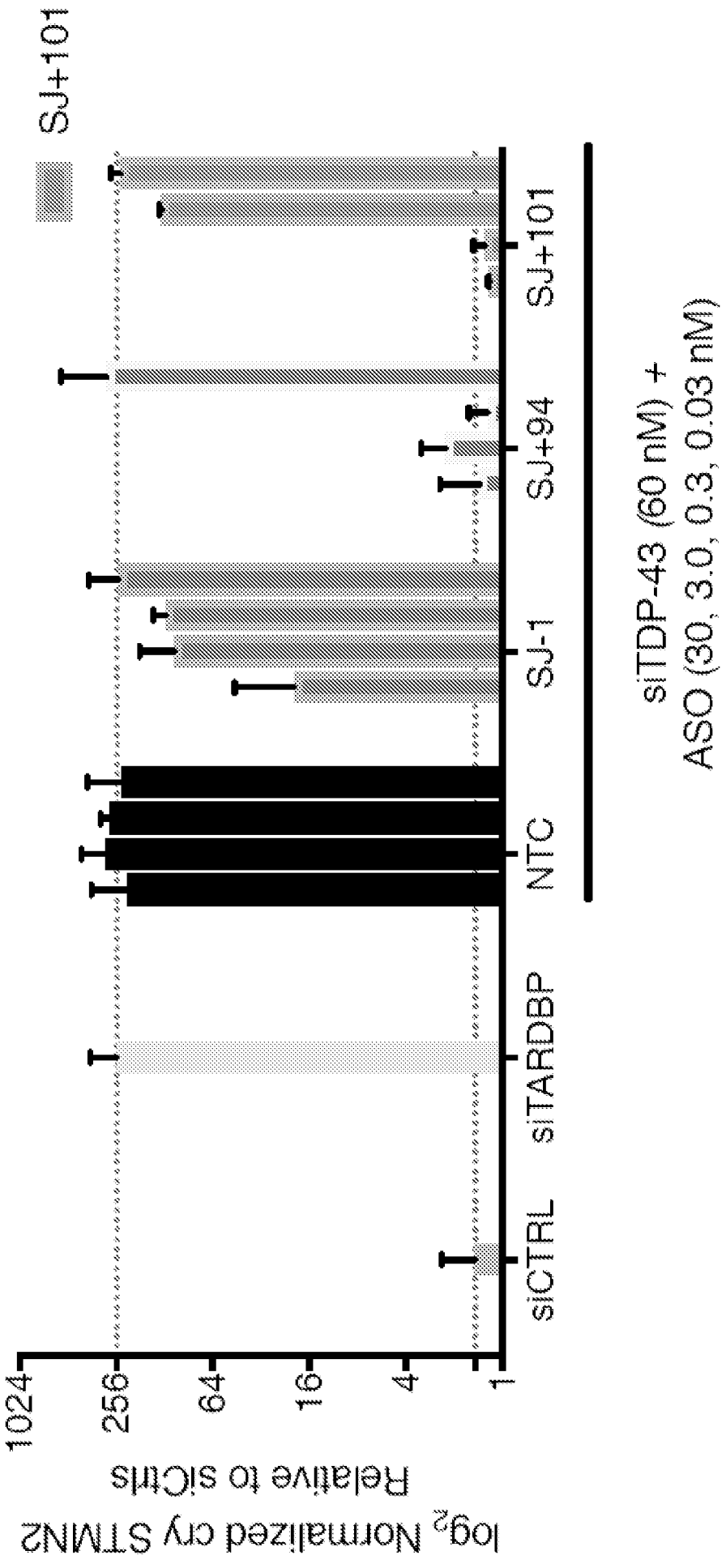

log2 Normalized cry STMN2
Relative to siCtrls
1024
256
64
16
4
1
siCTRL
siTARDBP
NTC
SJ-1
SJ+94
SJ+101
SJ+101
siTDP-43 (60 nM) +
ASO (30, 3.0, 0.3, 0.03 nM)

FIG. 94

FIG. 95A

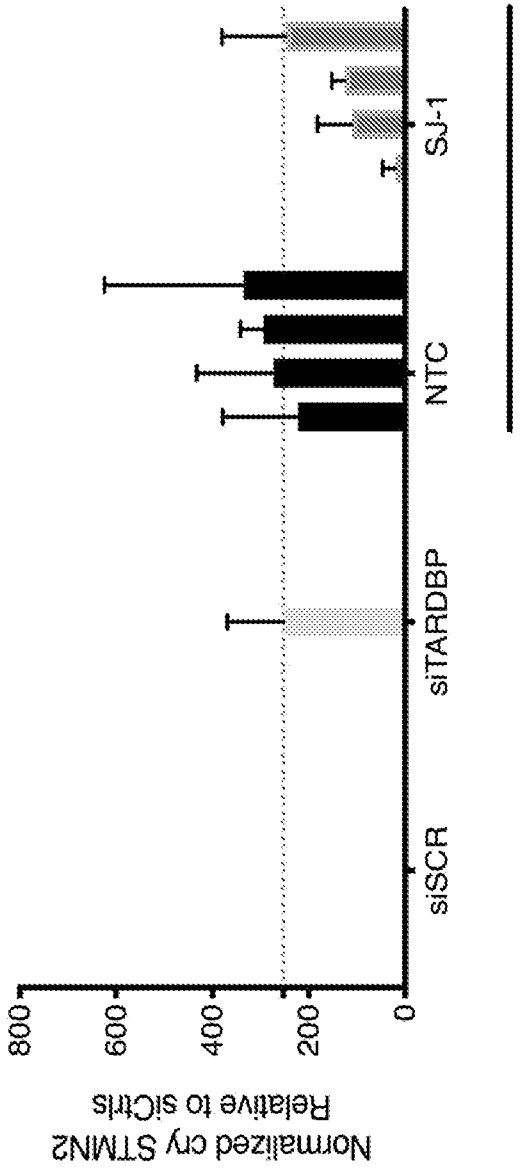
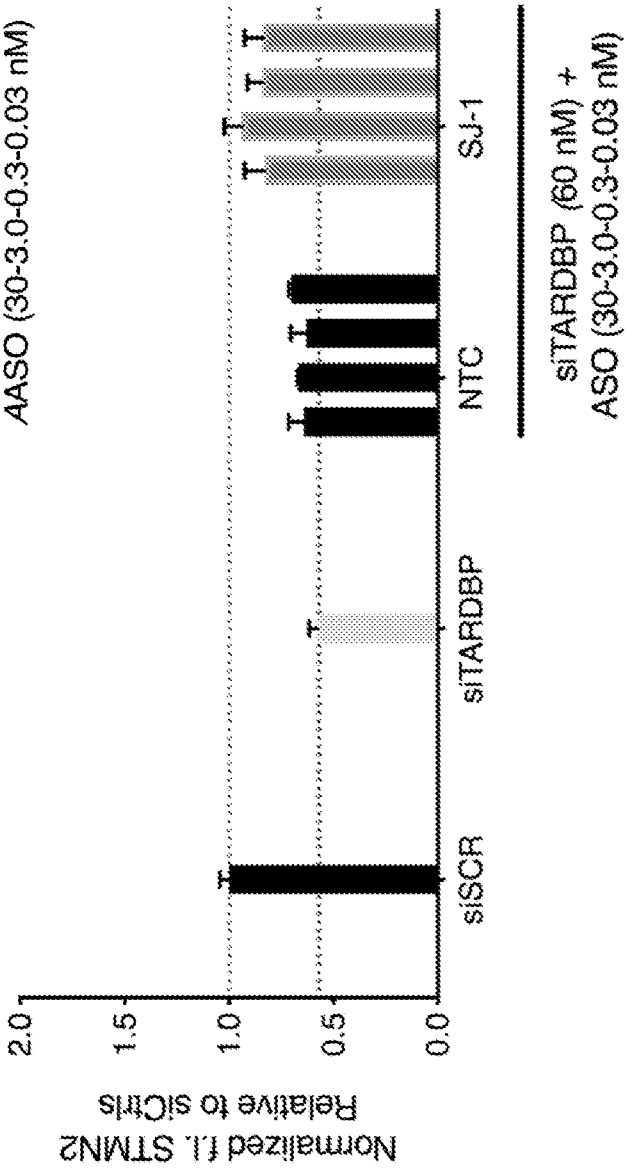


FIG. 95B



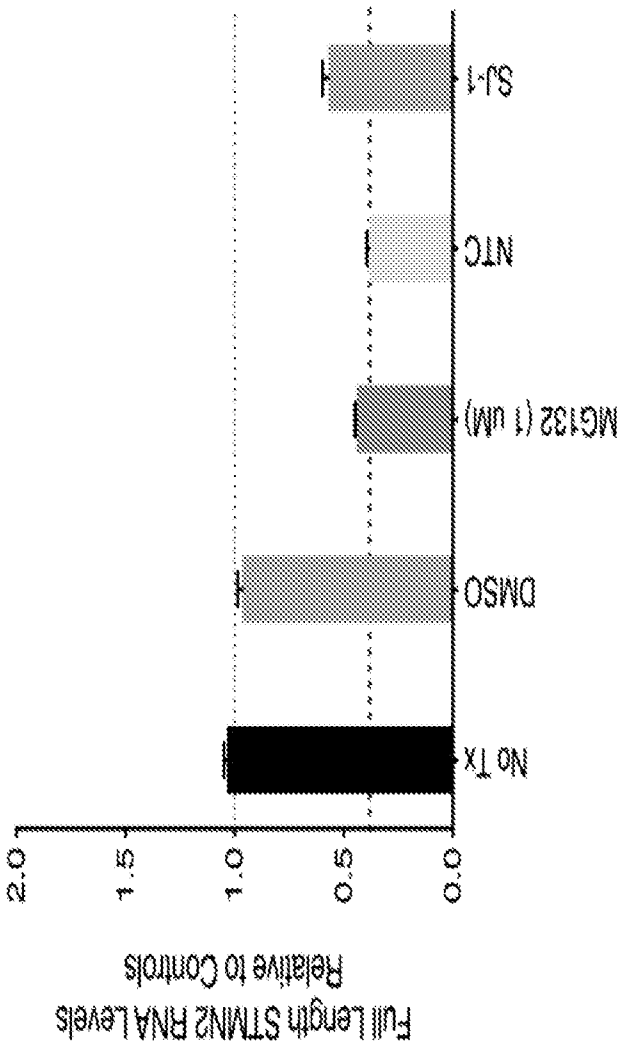

Full Length STMN2 RNA Levels
Relative to Controls
2.0
1.5
1.0
0.5
0.0
No Tx
DMSO
MG132 (1 uM)
NTC
SJ-1

FIG. 96

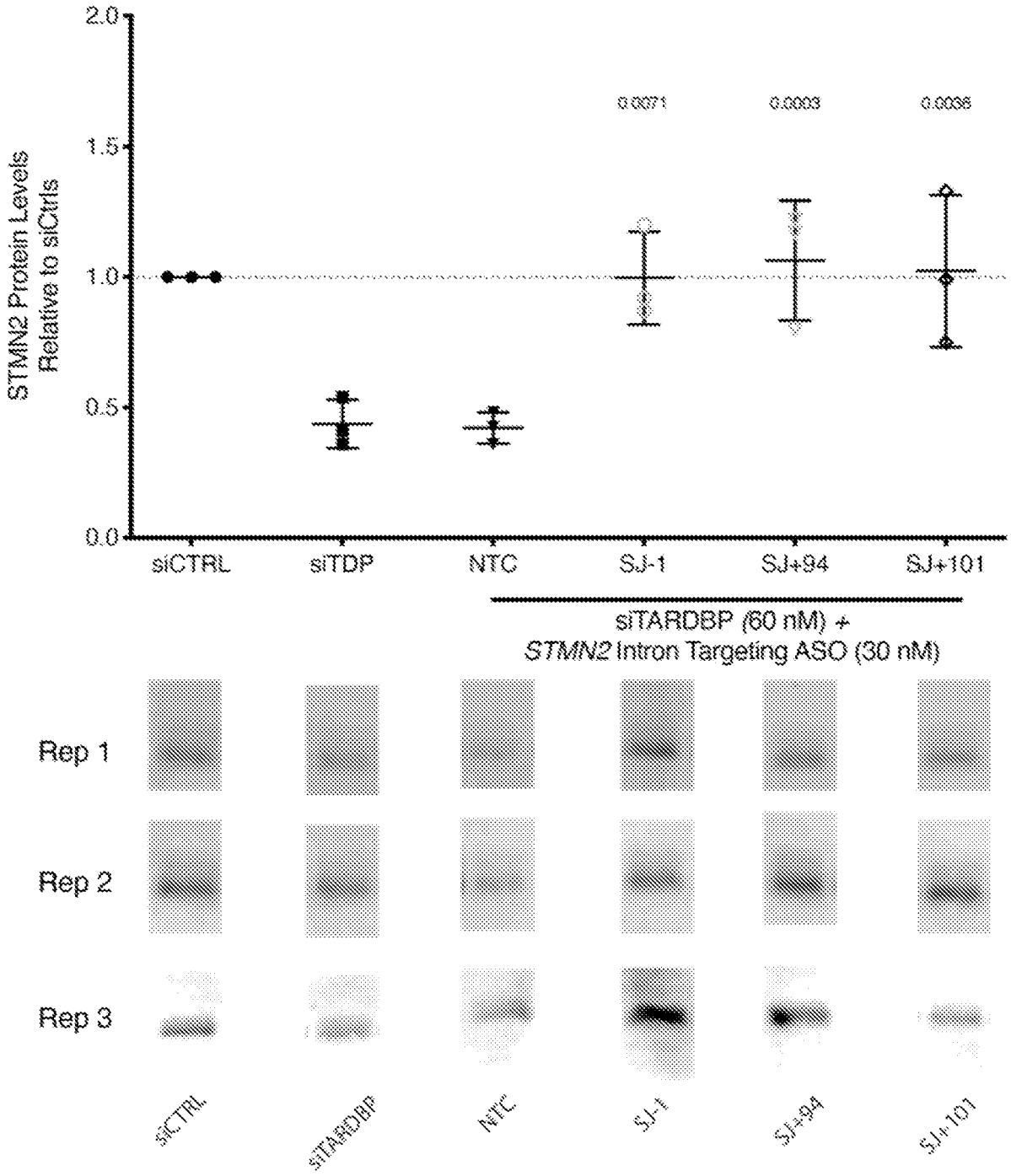

STMN2 Protein Levels
Relative to siCtrls
2.0
1.5
1.0
0.5
0.0
0.0071
0.0003
0.0036
siCTRL
siTDP
NTC
SJ-1
SJ+94
SJ+101
siTARDBP (60 nM) +
STMN2 Intron Targeting ASO (30 nM)
Rep 1
Rep 2
Rep 3
siCTRL
siTARDBP
NTC
SJ-1
SJ+94
SJ+101

FIG. 97